frontiers | Research Topics

# Multiple stressors and ecological response in marine fishery ecosystems

**Edited by**
Jun Xu, Ying Xue and Binhe Gu

**Published in**
Frontiers in Marine Science

ISSN 1664-8714
ISBN 978-2-83251-362-0
DOI 10.3389/978-2-83251-362-0

## About Frontiers

Frontiers is more than just an open access publisher of scholarly articles: it is a pioneering approach to the world of academia, radically improving the way scholarly research is managed. The grand vision of Frontiers is a world where all people have an equal opportunity to seek, share and generate knowledge. Frontiers provides immediate and permanent online open access to all its publications, but this alone is not enough to realize our grand goals.

## Frontiers journal series

The Frontiers journal series is a multi-tier and interdisciplinary set of open-access, online journals, promising a paradigm shift from the current review, selection and dissemination processes in academic publishing. All Frontiers journals are driven by researchers for researchers; therefore, they constitute a service to the scholarly community. At the same time, the *Frontiers journal series* operates on a revolutionary invention, the tiered publishing system, initially addressing specific communities of scholars, and gradually climbing up to broader public understanding, thus serving the interests of the lay society, too.

## Dedication to quality

Each Frontiers article is a landmark of the highest quality, thanks to genuinely collaborative interactions between authors and review editors, who include some of the world's best academicians. Research must be certified by peers before entering a stream of knowledge that may eventually reach the public - and shape society; therefore, Frontiers only applies the most rigorous and unbiased reviews. Frontiers revolutionizes research publishing by freely delivering the most outstanding research, evaluated with no bias from both the academic and social point of view. By applying the most advanced information technologies, Frontiers is catapulting scholarly publishing into a new generation.

## What are Frontiers Research Topics?

Frontiers Research Topics are very popular trademarks of the *Frontiers journals series*: they are collections of at least ten articles, all centered on a particular subject. With their unique mix of varied contributions from Original Research to Review Articles, Frontiers Research Topics unify the most influential researchers, the latest key findings and historical advances in a hot research area.

Find out more on how to host your own Frontiers Research Topic or contribute to one as an author by contacting the Frontiers editorial office: frontiersin.org/about/contact

# Multiple stressors and ecological response in marine fishery ecosystems

**Topic editors**

Jun Xu — Institute of Hydrobiology, Chinese Academy of Sciences (CAS), China

Ying Xue — Ocean University of China, China

Binhe Gu — University of Florida, United States

**Topic coordinator**

Guohuan Su — Center for Advanced Systems Understanding, Helmholtz Center Dresden-Rossendorf, Helmholtz Association of German Research Centers (HZ), Germany

**Citation**

Xu, J., Xue, Y., Gu, B., eds. (2023). *Multiple stressors and ecological response in marine fishery ecosystems*. Lausanne: Frontiers Media SA.

doi: 10.3389/978-2-83251-362-0

# Table of contents

frontiers | Frontiers in Marine Science

TYPE Editorial
PUBLISHED 04 January 2023
DOI 10.3389/fmars.2022.1122772



OPEN ACCESS

EDITED AND REVIEWED BY
Angel Borja,
Technology Center Expert in Marine and Food Innovation (AZTI), Spain

*CORRESPONDENCE
Guohuan Su
guohun.su@gmail.com
Jun Xu
junxu@ihb.ac.cn

SPECIALTY SECTION
This article was submitted to Marine Ecosystem Ecology, a section of the journal Frontiers in Marine Science

RECEIVED 13 December 2022
ACCEPTED 21 December 2022
PUBLISHED 04 January 2023

CITATION
Su G and Xu J (2023) Editorial: Multiple stressors and ecological response in marine fishery ecosystems.
*Front. Mar. Sci.* 9:1122772.
doi: 10.3389/fmars.2022.1122772



# Editorial: Multiple stressors and ecological response in marine fishery ecosystems

Guohuan Su[1,2*] and Jun Xu[2*]

[1]Center for Advanced Systems Understanding (CASUS), Helmholtz-Zentrum Dresden-Rossendorf (HZDR), Görlitz, Germany, [2]Institute of Hydrobiology, Chinese Academy of Sciences, Wuhan, China

KEYWORDS

**fishery management policy, trophic niche, climate change, artificial reefs, human disturbance**

Editorial on the Research Topic
Multiple stressors and ecological response in marine fishery ecosystems

In 2018, global capture fisheries production was over 96 million tonnes with marine fisheries contributions of about 88% (FAO, 2020). Fisheries provided more than 3.3 billion people with 20% of per capita animal protein intake and supported the livelihoods of 10% of the world's population in 2017 (FAO, 2020). However, over the past few decades, we have witnessed continued and dramatic declines in global marine fish stocks, with 34% of stocks currently considered unsustainable. (FAO, 2020, but see Zimmermann and Werne, 2019; Juan-Jordá et al., 2022), highlighting the urgency to effectively develop sustainable marine fisheries and ecosystems.Multiple stressors, including poor management measures, unharmonious national fisheries policies, and the joint effect of biotic and abiotic factors (e.g., overfishing, climate change) affect the recovery of fishery resources and sustainability of the marine ecosystem functions (Breitburg & Riedel, 2005; Oguz, 2017; Barange et al., 2018). However, how these stressors interact to affect ecosystems remains poorly understood. Therefore, disentangling the impact of these stressors on marine fisheries and ecosystems will help us better understand the synergies and dependencies of fishery resources, diversity, nutrient cycles, ecosystem threats, and management practices. More importantly, it will provide managers and decision-makers with a solid scientific basis for management to protect marine biodiversity and restore fishery resources.In this Research Topic, we collected seventeen research papers linked to this topic about marine fisheries and ecosystems. These papers covered multiple marine biomes, as well as different ecosystem components, such as fish, zooplankton, or invertebrates, and used various algorithms to analyze the collected data, such as stable isotope, mass models, DNA-based analyses, etc. For instance, an investigation study conducted by Xu et al. (2022) identified the species diversity and distribution of crustacean larvae in the Zhongsha Islands waters, South China Sea by using DNA barcoding and molecular species identification approach, revealing that the crustacean diversity in the islands had been seriously underestimated before.

Fisheries management policies have received considerable critical attention for their conservation effects on resource recoveries. Compared the carbon transfer efficiency of the three large marine ecosystems around China to other ecosystems, Chen et al. (2022) revealed

that without proper fisheries management, the fisheries in the ecosystems were likely to collapse with an increasing carbon transfer efficiency. Indeed, effective fisheries management considering other relevant factors that may affect marine ecosystems is imminent and worth exploring. Based on two mass balance models, Xu et al. (2022) revealed that the implementation of fisheries management policies, especially seasonal fishing moratorium, had positive effects on fishery resources recovery, especially commercial fish in the East China Sea. Thus, they suggested that fishery management in the East China Sea needs to be strengthened by extending the seasonal fishing moratorium and reducing fishing pressure afterward.

Climate change is another factor significantly altering marine fisheries and ecosystems over the world. Here, three studies were conducted to explore the role of climate change in affecting specific marine fishery species. Hou et al. (2022) analyzed the relationship between climate variability and the Skipjack tuna fishery in the Northwest Pacific region, suggesting managing the Skipjack tuna fishery by incorporating the trans-basin climatic variation. Zhang et al. (2022) revealed that climate change might have a large influence on the distribution of small yellow croaker by affecting sea surface temperature and salinity in the China Seas. Meanwhile, Han et al. (2022) reported that the biomass-density hotspots of small yellow croaker in both spring and summer seasons had shrunk or disappeared over the past 40 years by multiple pressures (e.g., climate change, human activity), highlighting the importance of developing targeted spatial conservation measures. These studies provide essential implications and references for predicting and managing marine fisheries by incorporating the climate index. In addition, under the context of climate change, Zhao et al. (2022) underlined the need to implement specific climate-adaptive functional diversity conservation measures and sustainable fisheries management in diverse marine ecosystems.

Moreover, investigating the trophic niches of particularly important commercial fish is also critical to the conservation and management of fishery resources. Stable isotope analysis has been widely used in the past decades in the field. In this topic, Wang et al. (2022) and Jiang et al. (2022) applied the stable isotope analysis to disentangle the trophic interactions of key fisheries species (Sciaenidae and *Thunnus*) in the Solomon Islands and Zhoushan Islands, respectively. They both found that niche overlap existed to some extent between the focal species reflecting the similarity of resources used and prey competition between them. Nonetheless, the differentiation in habitats, migration routes, or body size allows their coexistence in an ecosystem in the same area.

Nearshore species, estuaries, and bay ecosystems are more vulnerable to human disturbance than other marine species and ecosystems. Zeng et al. (2022) investigated the impacts of human disturbances on the species and functional dynamics of the demersal fish community in the Pearl River Estuary, highlighting the complicated interactions between the demersal fish community and disturbances. Ke et al. (2022) revealed that high anthropogenic nutrient loading might reduce the difference in trophic niches among zooplankton groups. They provided detailed information on the distribution of zooplankton $\delta^{13}C$ and $\delta^{15}N$ in Jiaozhou Bay, China, which would be useful for understanding the anthropogenic influence on the ecosystem structure and functions. Du et al. (2022) also found that long-term changes existed in zooplankton composition in the Changjiang estuary due to human disturbance and water temperature rise.

Besides focusing on the taxonomic species groups, two studies assessed the functioning of marine ecosystems with artificial reefs using Ecopath models. Wang et al. (2022) provided a dynamic model framework to alternatively estimate the ecological carrying capacity for stock enhancement practices in the development of marine ranching ecosystems. In contrast, Zhang et al. (2022) revealed that the current artificial system had formed complicated interspecies relations and high-level stability, which could be a way to alleviate the current natural coral reef crisis. These two studies used a similar approach to illustrate the functioning evolvement of established artificial reefs and provide the scientific basis for the improvement of marine fishery production and management.

Overall, this Research Topic has made a significant contribution to improving our understanding of the impact of multiple stressors on the marine ecosystems and the recovery of fishery resources and sustainability. Papers on this topic either revealed the impact mechanism of various stressors from different aspects, or provided new insights for improving marine fishery management. Nevertheless, research on this topic is still far from enough, further actions should be made to develop sustainable fishery management and mitigate the decline of fisheries resources.

## Author contributions

All authors listed have made a substantial, direct, and intellectual contribution to the work and approved it for publication.

## Acknowledgments

This work was supported by the National Key R&D Program of China (Grant No. 2018YFD0900904), the International Cooperation Project of the Chinese Academy of Sciences (Grant No. 152342KYSB20190025) and the National Natural Science Foundations of China (Grant No. 31872687).

## Conflict of interest

The authors declare that the research was conducted in the absence of any commercial or financial relationships that could be construed as a potential conflict of interest.

## Publisher's note



## References

Barange, M., Bahri, T., Beveridge, M.C.M., Cochrane, K. L., Funge-Smith, S., and Poulain, F. (2018). *Impacts of climate change on fisheries and aquaculture* Vol. 12 (United Nations' Food and Agriculture Organization), 628–635.

Breitburg, D. L., and Riedel, G. F. (2005). Multiple stressors in marine systems. *Mar. Conserv. Biology: the Science of Maintaining the Sea's Biodiversity,* edited by Norse, E. A., and Crowder, L. B. 167–182. Washington, D.C.: Island Press.

FAO (2020). *The state of world fisheries and aquaculture 2020: Sustainability in action* (Food and Agriculture Organization of the United Nations).

Juan-Jordá, M. J., Murua, H., Arrizabalaga, H., Merino, G., Pacoureau, N., and Dulvy, N. K. (2022). Seventy years of tunas, billfishes, and sharks as sentinels of global ocean health. *Science* 378 (6620), eabj0211.

Oguz, T. (2017). Controls of multiple stressors on the black Sea fishery. *Front. Mar. Sci.* 4, 110.

Zimmermann, F., and Werner, K. M. (2019). Improved management is the main driver behind recovery of northeast Atlantic fish stocks. *Front. Ecol. Environ.* 17 (2), 93–99.

frontiers | Frontiers in Marine Science

ORIGINAL RESEARCH
published: 11 May 2022
doi: 10.3389/fmars.2022.911714

# Using Ecopath Models to Explore Differences in Ecosystem Characteristics Between an Artificial Reef and a Nearby Natural Reef on the Coast of the North Yellow Sea, China

*Rongliang Zhang[1,2], Qianqian Zhang[3], Jianmin Zhao[3], Zhongxin Wu[4], Hui Liu[3]*, Lu Shou[1,2]*, Yibo Liao[1,2], Qinghe Liu[1,2], Yanbin Tang[1,2] and Jiangning Zeng[1,2]*

*[1] Key Laboratory of Marine Ecosystem Dynamics, Second Institute of Oceanography, Ministry of Natural Resources, Hangzhou, China, [2] Observation and Research Station of Yangtze River Delta Marine Ecosystems, Ministry of Natural Resources, Zhoushan, China, [3] Key Laboratory of Coastal Biology and Biological Resources Utilization, Yantai Institute of Coastal Zone Research Chinese Academy of Sciences, Yantai, China, [4] Center for Marine Ranching Engineering Science Research of Liaoning, Dalian Ocean University, Dalian, China*

OPEN ACCESS

**Edited by:**
*Ying Xue,*
*Ocean University of China, China*

**Reviewed by:**
*Yunkai Li,*
*Shanghai Ocean University, China*
*Chongliang Zhang,*
*Ocean University of China, China*

***Correspondence:**
*Hui Liu*
*huiliu@yic.ac.cn*
*Lu Shou*
*shoulu981@sio.org.cn*

**Specialty section:**
*This article was submitted to Marine Ecosystem Ecology, a section of the journal Frontiers in Marine Science*

**Received:** *03 April 2022*
**Accepted:** *12 April 2022*
**Published:** *11 May 2022*

**Citation:**
*Zhang R, Zhang Q, Zhao J, Wu Z, Liu H, Shou L, Liao Y, Liu Q, Tang Y and Zeng J (2022) Using Ecopath Models to Explore Differences in Ecosystem Characteristics Between an Artificial Reef and a Nearby Natural Reef on the Coast of the North Yellow Sea, China. Front. Mar. Sci. 9:911714. doi: 10.3389/fmars.2022.911714*

The comparison of trophic structure and energy flow between natural and artificial reefs is imperative to evaluate whether these man-made structures work similarly to comparable natural reefs. Here, to characterize the potential difference in functioning between two types of reef ecosystems, two trophic models (Ecopath) at an artificial reef and an adjacent natural reef on the coast of the north Yellow Sea, China, were established. Both Ecopath models were divided into 18 functional groups from primary producers (algae and phytoplankton) and detritus to predatory species (e.g., *Sebastes schlegelii*). Model outputs showed that the ecosystem scale was smaller in the artificial reef (total system throughput (TPP) = 6,455.47 $t{\cdot}km^{-2}{\cdot}year^{-1}$) relative to its natural counterpart (TPP = 9,490.48 $t{\cdot}km^{-2}{\cdot}year^{-1}$). At both reef types, a large proportion of energy occurred at trophic levels I and II, and most of the primary production was utilized through a detritus pathway. This result implies a bottom-up energy flow control for both cases. However, two types of reef systems were behaving in a reasonable manner, as mean transfer efficiencies were similar to the Lindeman efficiency (10%). The ecosystem maturity of the artificial reef is not comparable to that of the natural reef for its inferior value of total primary production/total respiration (TPP/TR). Moreover, both the connectance index (CI) and system omnivory index (SOI) were slightly higher at the artificial reef relative to the natural reef as well as other coastal systems with parallel latitudes, suggesting that the current artificial system has formed complicated interspecies relations and high-level stability. This work updates our knowledge about the functioning evolvement of established artificial reefs and provides a baseline for the efficient management of coastal zones and further investigations.

**Keywords: artificial reefs, natural reefs, Ecopath, trophic structure, energy flow**

# 1 INTRODUCTION

As marine habitat loss and degradation become major threats to biodiversity and fishery reduction, the establishment of artificial reefs has become an effective way to alleviate habitat stressors (McCauley et al., 2015; Lima et al., 2019). A small scale biosphere reserve will arise *in situ* after the deployment of artificial reefs, where various organisms can find shelters (e.g., fish) or attachment bases (e.g., algae and filter feeders), leading to gathering effects on marine organisms (Bohnsack, 1989; Brickhill et al., 2005; Raj et al., 2020). Moreover, the upwelling generated around the reef will promote nutrient recycling and subsequently be conducive to primary production (Liu et al., 2013). As a result, these submerged structures facilitate populations of living marine resources and enhance biodiversity *in situ* with time extending.

Ecological succession around newly deployed reefs is not only characterized by the change of biological community but also accompanied by the evolvement of ecosystem functions (Nicoletti et al., 2007; Toledo et al., 2020). As artificial reefs have been deliberately constructed or placed to emulate some functions of natural reefs (United Nations Environment Programme, 2009), comparative biological surveys between two types of reefs are essential and have been performed worldwide (Paxton et al., 2020). Revealing similarities and differences in terms of community composition and biodiversity have brought insights into the performance of newly deployed reefs. However, current knowledge has rarely concerned the characteristics of trophic structure and energy flow, which allows for the performance evaluation of artificial reefs in ecosystem functioning. It has been widely accepted that energy sources and pathways play crucial roles in the functions of the artificial reef ecosystem (Brickhill et al., 2005). Thus, uncovering the trophic characteristics will shed light on the mechanism of these man-made structures involved in habitat restoration and fishery conservation and facilitate ecosystem-based approaches to fisheries finally.

As a common tool in depicting the characteristics of aquatic ecosystems, Ecopath with Ecosim (EwE) is now generally applied in assessing the sustainability, productivity, and resilience of an ecosystem (Polovina, 1984; Colléter et al., 2015; Abdou et al., 2020) and tracking the effects of anthropogenic and environmental stressors on ecosystems (Shin and Shannon, 2010; Reed et al., 2017). This model considers both the fishing impacts on target and non-target species and interactions between ecosystem components, thus providing a better understanding of implementing an ecosystem-based approach to fisheries management. In China, the application of EwE has extended to the artificial reef ecosystems over the years, such as Lidao (Wu et al., 2016), Laoshan Bay (Liu et al., 2019), and Laizhou Bay (Xu et al., 2019). Relevant studies analyzed trophic interactions and energy transfer between different functional groups and assessed the impact of artificial reefs on the original ecosystem functions in detail, which supplies important data and theories for the establishment of artificial reefs subsequently. Nevertheless, comparative studies on artificial reefs before and after deployments, and on ecosystems between artificial reefs and natural reefs remain limited (Lee and Zhang, 2018; Xu et al., 2019), which hinders our further evaluation of how well an artificial reef system performs after years' development, especially when compared to its natural counterpart.

Over the past dozen years, to cope with coastal pollution (such as nutrition overloading) caused by anthropogenic activities and prevent bottom trawling, along with supporting habitat as well as marine aquatic resources rehabilitation, artificial reefs were deployed extensively in the coastal Yellow Sea, China. Accordingly, to assess the ecological and economic values brought by these man-made reefs and check whether their goals are achieved, a large amount of empirical data were collected based on the community composition and biodiversity (Wu et al., 2019; Zhou et al., 2019; Yu et al., 2020). Relevant studies generally underlined the higher biodiversity and fishery abundance after the reef was constructed, and they have pointed out that the reef design, submersion period, and environmental conditions also had an impact on the biological communities. Yet whether these artificial structures evolve to be identical to the natural reefs in terms of ecosystems functions remains unclear and warrants comparative research. In the current study, we characterized the potential difference in trophic structure and energy flow between an established artificial reef located on the coast of the Yellow Sea, China, and an adjacent natural reef ecosystem based on the Ecopath model. We aimed to illustrate how an artificial ecosystem developed after years' deployment by comparing the trophic characteristics of two reef types. Our results are expected to provide reference cases and data support for the artificial reef establishment in the future.

# 2 MATERIAL AND METHODS

## 2.1 Study Area

This study was conducted on the coast of the Yellow Sea, China (**Figure 1**). The artificial reef was constructed in 2009 and distributed over an area of approximately 1,200 $km^2$. All the reef modules were made of rocks or concrete cubes with holes (3 m × 3 m × 3 m) and had a depth of 10–20 m on soft sediment bottom. The natural reef, ca. 18 km west of the artificial reef, situates close to Yangma Island and is composed mainly of rocky stone. This natural rocky area is also interspersed with sediment bottoms, extending toward the offshore and reaching a maximum depth of 20 m.

## 2.2 Ecopath Models

EwE 6.5 software (Christensen and Walters, 2004; Christensen et al., 2008) was used as the construction platform for the Ecopath model here. The Ecopath model is composed of multiple interrelated functional groups, which must be qualified to represent the biological components in the ecosystem. All functional groups need to cover the entire process of energy flow in the ecosystem, and the oval

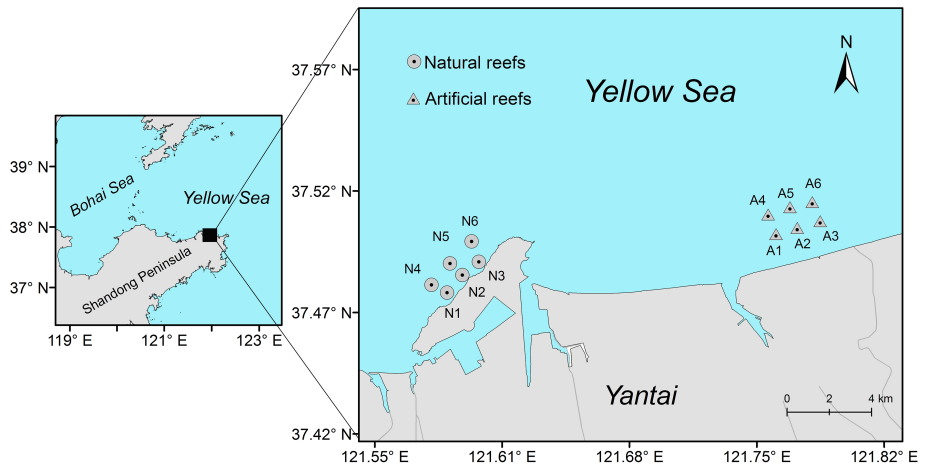


**FIGURE 1** | Study locations of artificial reefs and natural reefs on the coast of Yellow Sea, China.

operation process complies with the following equation:

$$B_i \times (\frac{P}{B})_i \times EE_i = \sum_{j=1}^{j} B_j \times \left(\frac{Q}{B}\right)_j \times DC_{ij} + Y_i + BA_i + E_i$$

where $B_i$ is the biomass ($t \cdot km^{-2}$) of functional group $i$, $B_j$ is the biomass of the consumer group $j$, $(P/B)_i$ is the production/biomass ratio of group $i$, $(Q/B)_j$ is the consumption to biomass ratio for the group $j$, $EE_i$ is the ecotrophic efficiency (the utilized proportion of the production in the ecosystem), $DC_{ij}$ is the proportion of prey $i$ in the diet of predator $j$, $Yi$ is the fishery catch rate of group $i$, $BAi$ is the biomass accumulation of group $i$, and $Ei$ is the net migration rate of group $i$. Here in the model, the simulation duration at 1 year was set, and the ecosystem was assumed in a stable state based on the literature suggestion (Christensen et al., 2008; Heymans et al., 2016), that is, $BA_i = 0$, $E_i = 0$ for both artificial and natural cases.

### 2.2.1 Data Sources

Based on similarities in biological characteristics, feeding strategies, and ecological functions, the species included were clustered into 18 functional groups for both artificial and natural models, respectively (**Table 1**). And considering dominant species (measured from bottom fishery surveys) all year round coupled with their ecological and economic values, each of Korean Rockfish *Sebastes schlegelii*, Fat Greenlings *Hexagrammos otakii*, Japanese swimming crab *Charybdis japonica*, Pacific Oysters *Crassostrea gigas*, and Fang's blenny *Enedrias fangi* was divided into a functional group separately.

As for input parameters (B, P/B, Q/B, diet matrix DC, and catches Y) required in the model, empirical data wherever possible were used; otherwise, references and estimates from the model equations were used. Field samplings were undertaken in February, May, August, and November 2019, and the mean value of corresponding parameters was included in the models. For bottom fishery organisms, trap nets and trawl nets were used in or around both reef types. Sessile organisms (i.e., bivalves and macroalgae) were collected and measured by using 0.5 × 0.5 m quadrats by scuba diving, with at least three replicates at each station seasonally. The macrobenthos was sampled by box dredger with a 0.1-$m^2$ area, and the zooplankton was obtained by plankton net with 505-μm mesh size. The biomass of phytoplankton was measured by converting the average annual chlorophyll concentration ($mg/m^3$) to biomass (Sandu et al., 2003). For the biomass of each functional group input in the Ecopath model at both reef types, the details are shown in **Table 2**.

The P/B and Q/B ratios of fish and other functional groups, as well as the production and biomass of heterotrophic bacteria and detritus in water, were obtained from FishBase (www.fishbase.org), and relevant publications were carried out in areas nearby or with the same latitude worldwide (Okey et al., 2004; Ouyang and Guo, 2010; Wu et al., 2016; Xu et al., 2019). The input B value of each functional group was the sum of a weighted average of its internal members' biomass, and the weights of each member were mainly based on their biomass ratio in the functional group (**Table 2**). The diet composition matrix (**Table 3**) was mainly from the result of our previous studies (Zhang et al., 2021a; Zhang et al., 2021b), together with published literature on feeding ecology in nearby areas (Yang, 2001a; Yang, 2001b; Zhang et al., 2012; Zhang, 2018) and FishBase. As biomass and diet composition were usually the most uncertain parameters among that input, they were slightly adjusted to achieve mass balance of the model whenever necessary.

### 2.2.2 Model Balancing and Ecological Indicators

The Ecopath model was debugged according to Heymans et al. (2016), until balanced. Before the model was run, it was checked whether the parameter values had biological credibility. After the model parameters were initialized, the $0 < EE \leq 1$ and $P/Q < 0.5$ of each functional group were adjusted to ensure the model balance. Considering the reliability and accuracy of model parameters are the main factors affecting model quality, the pedigree index (p-value) was calculated to reflect the sensitivity of the model and quantify the uncertainty of the input

**TABLE 1** | Species composition of functional groups in the nearshore artificial and the natural reefs of Yellow Sea, China.

| Area | Functional group | Taxon |
|---|---|---|
| Artificial reefs | Shellfish-killers | *Asterias amurensis*, *Asteri pectinifera*, *Luidia quiria*, *Rapa venosa* |
| | *Hexagrammos otakii* | *H. otakii* |
| | Benthivores | *Acanthopagrus schlegelii*, *Apogon lineatus*, *Argyrosomus argentatus*, *Chirolophis japonicus*, *Conger myriaster*, *Ernogrammus hexagrammus*, *Eupleurogrammus muticus*, *Konosirus punctatus*, *Larimichthys polyactis*, *Liparis takae*, *Liza haematocheila*, *Paralichthys olivaceus*, *Platycephalus indicus*, *Pseudopleuronectes yokohamae*, *Sebastes marmoratus*, *Sillago sihama* |
| | *Enedrias fangi* | *E. fangi* |
| | Planktivores | *Ammodytes persotus*, *Engraulis japonicus*, *Sardinella zusi*, *Thryssa kammalensis* |
| | *Crustacean* | *Alpheus distinguendus*, *Alpheus japonicus*, *Carcinoplax vestitus*, *Crangon affinis*, *Eualus sinensis*, *Heptacarpus futilirostries*, *Litopenaeus vannamei*, *Oratosquilla oratoria*, Paguridae, *Palaemon gravieri*, *Palaemon ortmanni*, *Portunus trituberculatus*, *Pugettia quadridens*, *Trachysalambria curvirostris* |
| | *Charybdis japonica* | *C. japonica* |
| | Gastropoda | *Tectonatica janthostomoides*, *Neverita didyma*, *Pleurobracheaea novaezealandiae* |
| | Cephalopoda | *Loligo japonica*, *Octopus ocellatus*, *Octopus variabilis*, *Sepiola birostrata* |
| | Gobiidae | *Acanthogobius flavimanus*, *Acanthogobius ommaturus*, *Amblychaeturichthys hexanema*, *Chaemrichthys stigmatias*, *Myersi filifer*, *Pterogobius zacalles*, *Tridentiger barbatus*, *Tridentiger trigonocephalus* |
| | *Sebastes schlegelii* | *S. schlegelii* |
| | Piscivores | *Lateolabrax japonicus*, *Pneumatophorus japonicus*, *Saurida elongata*, *Scomberomorus niphonius* |
| Natural reefs | Shellfish-killers | *A. amurensis*, *A. pectinifera*, *L. quiria*, *R. venosa* |
| | *H. otakii* | *H. otakii* |
| | Benthivores | *A. schlegelii*, *A. lineatus*, *A. argentatus*, *Chelidonichthys spinosus*, *C. japonicus*, *C. myriaster*, *E. hexagrammus*, *E. muticus*, *K. punctatus*, *L. polyactis*, *L. takae*, *L. haematocheila*, *P. olivaceus*, *P. indicus*, *P. yokohamae*, *S. marmoratus*, *S. sihama*, *Takifugu vermicularis*, *Takifugu xanthopterus*, *Thamconus modestus* |
| | *E. fangi* | *E. fangi* |
| | Planktivores | *A. persotus*, *E. japonicus*, *S. zusi*, *Setipin tenuifilis*, *T. kammalensis* |
| | *Crustacean* | *A. distinguendus*, *A. japonicus*, *C. vestitus*, *C. affinis*, *H. futilirostries*, *O. oratoria*, Paguridae, *P. gravieri*, *P. ortmanni*, *Peeus monodon*, *P. trituberculatus*, *P. quadridens*, *T. curvirostris* |
| | *C. japonica* | *C. japonica* |
| | Gastropoda | *N. didyma*, *P. novaezealandiae* |
| | Cephalopoda | *L. japonica*, *O. ocellatus*, *O. variabilis* |
| | Gobiidae | *A. ommaturus*, *A. hexanema*, *C. stigmatias*, *M. filifer*, *P. zacalles*, *T. barbatus*, *T. trigonocephalus* |
| | *S. schlegelii* | *S. schlegelii* |
| | Piscivores | *L. japonicus*, *P. japonicus*, *S. elongata*, *S. niphonius*, *Sphyrae pinguis* |

parameters (Christensen and Walters, 2004). The p-value of each functional group was finally integrated and unified into the overall P index, to evaluate the overall quality of the Ecopath model. Besides, sensitivity analyses were performed on both Ecopath models to test the effects of input parameter variation (−50% to 50%) on the estimated parameters. A mixed trophic impact (MTI) analysis was also conducted to assess the direct and indirect trophic interactions among compartments, including impacts of fishery practices throughout the system (Ulanowicz and Puccia, 1990; Christensen et al., 2008). This routine would evaluate the influence of small biomass increases of one group on the biomass of other groups, thus providing a manner of sensitivity analysis.

Ecological indicators were calculated based on network analysis (Ulanowicz, 1986). Specifically, the total system throughput (TST) was considered, which is consist of total consumption (TC), total exports (TEX), total respiration (TR), and total flows into detritus (TDET), to measure the ecological size of a system (Finn, 1976) and its metabolism (Ortiz et al., 2015). More descriptive indicators, such as total primary production (TPP) and total biomass (TB), characterize the overall activity and the size of the ecosystem (Latham, 2006; Ortiz et al., 2015). Net system production (NSP), the difference value between TPP and TR, represents the sum of the productivity of all producers. TPP/TR describes system maturity (Odum, 1969; Christensen, 1995). Mean transfer efficiency (MTE) within trophic levels (TLs), measures the efficiency of energy utilization of each TL in the system (Christensen et al., 2008). Connectance index (CI) and system omnivory index (SOI) reflect the complexity of the system's internal connections (Christensen and Walters, 2004; Libralato, 2013).

# 3 RESULT

## 3.1 Overall Characteristics of Ecosystem Energy Flow

The P index in each model was 0.469, which sits in the middle of those values obtained from more than 150 Ecopath models worldwide (Morissete et al., 2006), indicating the input and statistics data quality were of good reliability and credibility to a certain degree. The sensitivity of the estimated parameters to

**TABLE 2 |** Initial input and estimated parameters (in bold) in the Ecopath models of the artificial and natural reefs on the coast of Yellow Sea, China.

| Area | No. | Functional group | Trophic level | Biomass (t/km²) | Production/biomass | Q/B | EE |
|---|---|---|---|---|---|---|---|
| Artificial reefs | 1 | Planktivores | 2.6 | 0.18 | 2.37 | 8.98 | **0.143** |
| | 2 | Piscivores | 3.65 | 0.03 | 0.8 | 4.5 | **0** |
| | 3 | *Sebastes schlegelii* | 3.94 | 0.73 | 1.01 | 5.3 | **0.002** |
| | 4 | *Hexagrammos otakii* | 3.7 | 0.33 | 0.92 | 4.95 | **0** |
| | 5 | Benthivores | 3.51 | 1.2 | 2.6 | 4.95 | **0.743** |
| | 6 | *Enedrias fangi* | 2.97 | 1.36 | 2.79 | 9.97 | **0.685** |
| | 7 | Gobiidae | 3.36 | 2.06 | 1.98 | 5.7 | **0.924** |
| | 8 | Cephalopoda | 3.72 | 0.59 | 3.3 | 11.2 | **0.318** |
| | 9 | *Charybdis japonica* | 3.19 | 1.69 | 1.5 | 9.6 | **0.915** |
| | 10 | Crustacean | 2.77 | 3.22 | 5.6 | 15.9 | **0.996** |
| | 11 | Gastropoda | 2.11 | **1.58** | 4.43 | 17.2 | 0.8 |
| | 12 | Shellfish-killers | 3 | 1.56 | 0.8 | 2.82 | **0.166** |
| | 13 | *Crassostrea gigas* | 2 | 28.59 | 6 | 10.5 | **0.045** |
| | 14 | Infauna | 2.11 | **17.08** | 1.67 | 8.35 | 0.96 |
| | 15 | Zooplankton | 2 | 13.98 | 25 | 122.1 | **0.107** |
| | 16 | Phytoplankton | 1 | 16.7 | 106.2 | | **0.861** |
| | 17 | Algae | 1 | 63.13 | 9.88 | | **0.08** |
| | 18 | Detritus | 1 | 24.87 | | | **0.345** |
| Natural reefs | 1 | Planktivores | 2.61 | 0.21 | 2.37 | 8.98 | **0.154** |
| | 2 | Piscivores | 3.66 | 0.05 | 0.8 | 4.5 | **0** |
| | 3 | *S. schlegelii* | 3.96 | 0.46 | 1.01 | 5.3 | **0.004** |
| | 4 | *H. otakii* | 3.74 | 0.41 | 0.92 | 4.95 | **0** |
| | 5 | Benthivores | 3.5 | 1.54 | 2.6 | 4.95 | **0.921** |
| | 6 | *E. fangi* | 2.98 | 2.28 | 2.79 | 9.97 | **0.358** |
| | 7 | Gobiidae | 3.36 | 5.3 | 1.59 | 5.7 | **0.602** |
| | 8 | Cephalopoda | 3.71 | 0.65 | 3.3 | 11.2 | **0.589** |
| | 9 | *C. japonica* | 3.18 | 1.98 | 1.5 | 9.6 | **0.872** |
| | 10 | Crustacean | 2.76 | 4.45 | 7.6 | 26.9 | **0.981** |
| | 11 | Gastropoda | 2.11 | **2.47** | 4.43 | 17.2 | 0.8 |
| | 12 | Shellfish-killers | 3 | 1.58 | 1.3 | 4.7 | **0.334** |
| | 13 | *C. gigas* | 2 | 65.19 | 6 | 27 | **0.029** |
| | 14 | Infauna | 2.11 | **35.33** | 1.67 | 8.35 | 0.96 |
| | 15 | Zooplankton | 2 | 11.8 | 25 | 122.1 | **0.249** |
| | 16 | Phytoplankton | 1 | 19.41 | 106.2 | | **0.996** |
| | 17 | Algae | 1 | 121.17 | 9.88 | | **0.086** |
| | 18 | Detritus | 1 | 52 | | | **0.567** |

changes in input parameters of different functional groups depends on the degree of trophic linkages between these functional groups. Results showed that the resulting change in the estimated parameter ranged from −39.8% to 194.3%. The first six most sensitive estimated parameters were extracted in each model and visualized in **Figure 2**. Apart from two groups exhibiting a remarkable change in the estimated parameters, i.e., effects of Gastropoda (P/B) on Gastropoda (B) and effects of Infanna (EE) on Infauna (B), the other five groups of input parameters in both artificial and natural Ecopath models had a slight effect on the estimated parameters. The change in P/B value for the Gastropoda group had a great influence on the corresponding biomass estimation. When P/B decreased by 50%, the estimated biomass of Gastropoda increased by 194.3%. When EE of other benthic animals decreased by 50%, the estimation of corresponding biomass changed by 100% (**Figure 2**). The sensitivity analysis indicated that most estimated parameters were insensitive to changes in input parameters in both reef models.

The aggregated summary statistics and indicators of network flow and ecosystem structure for each model are listed in **Table 4**. For the artificial system, the TST was 9,490.48 $t{\cdot}km^{-2}{\cdot}year^{-1}$, comprising percentage contributions of TC (39.6%), TR (23.07%), TEX (11.28%), and TDET (26.05%). For the natural system, TST was 6,455.47 $t{\cdot}km^{-2}{\cdot}year^{-1}$, of which 35.53% was consumed, 19.24% was respired, 17.91% was exported, and 27.32% flowed to detritus. TDET values accounted for over 26% of the TST for both cases, indicating that re-entering the ecosystem and recycling subsequently were the main ways of energy utilization for both reef systems, and energy underutilization occurred in each case. The TPP/TR and CI values were higher in the artificial system relative to its natural counterpart, while SOI values were similar for both cases (**Table 4**).

## 3.2 Trophic Levels and Energy Distribution

In each balanced model, the highest TL emerged in *S. schlegelii* (3.94 and 3.96 in the artificial and natural systems, respectively) among fish groups, followed by *H. otakii* (3.70 and 3.74 in the artificial and natural reef systems, respectively). Similarly, Cephalopods displayed the highest TL among invertebrates, with 3.72 and 3.71 in the artificial and natural models, respectively. Overall, the biomass at both reef types complies with the "pyramid" law, where low TL species accounted for a

**TABLE 3 |** Diet matrix imported into the Ecopath models of the artificial and natural reefs on the coast of Yellow Sea, China.

| Area | No. | Functional group | 1 | 2 | 3 | 4 | 5 | 6 | 7 | 8 | 9 | 10 | 11 | 12 | 13 | 14 | 15 |
|---|---|---|---|---|---|---|---|---|---|---|---|---|---|---|---|---|---|
| Artificial reefs | 1 | Planktivores | | 0.37 | | | 0 | | | | | | | | | | |
| | 2 | Piscivores | | | | | | | | | | | | | | | |
| | 3 | *Sebastes schlegelii* | | 0.01 | | | | | | | | | | | | | |
| | 4 | *Hexagrammos otakii* | | | | | | | | | | | | | | | |
| | 5 | Benthivores | | 0.03 | | | 0.03 | | 0.03 | 0.03 | 0.06 | 0.01 | | | | | |
| | 6 | *Enedrias fangi* | | 0.22 | 0.36 | | 0.09 | | | 0.05 | 0.02 | | | | | | |
| | 7 | Gobiidae | | 0.09 | 0.16 | 0.24 | 0.15 | | 0.03 | 0.05 | 0.04 | 0.01 | | | | | |
| | 8 | Cephalopoda | | 0 | 0 | 0 | 0 | | | 0 | 0 | 0.01 | | | | | |
| | 9 | *Charybdis japonica* | | | | | 0.03 | | | 0.32 | | | | | | | |
| | 10 | Crustacean | 0.06 | 0.05 | 0.47 | 0.5 | 0.26 | 0.11 | 0.29 | 0.02 | 0.16 | 0.12 | | | | | |
| | 11 | Gastropoda | | 0 | | | 0.05 | | | | 0.14 | 0.03 | 0.05 | | | | |
| | 12 | Shellfish-killers | | | | | 0.04 | | | | | | | | | | |
| | 13 | *Crassostrea gigas* | | | | | | | | | 0.2 | | | 1 | | | |
| | 14 | Infauna | | | 0.01 | 0.13 | 0.16 | 0.2 | 0.46 | 0.06 | 0.23 | 0.27 | | | | | |
| | 15 | Zooplankton | 0.5 | 0.24 | | 0.1 | 0.07 | 0.57 | 0.19 | 0.26 | | 0.14 | 0.05 | | | 0.11 | |
| | 16 | Phytoplankton | 0.2 | | | | 0.03 | | | | | | 0.2 | | 0.5 | 0.04 | 0.8 |
| | 17 | Algae | | | | 0.03 | | | | | | 0.17 | 0.2 | | | 0.25 | |
| | 18 | Detritus | 0.24 | | | | 0.1 | 0.13 | | | 0.15 | 0.24 | 0.5 | | 0.5 | 0.6 | 0.2 |
| Natural reefs | 1 | Planktivores | | 0.37 | | | 0 | | | | | | | | | | |
| | 2 | Piscivores | | | | | | | | | | | | | | | |
| | 3 | *S. schlegelii* | | 0.01 | | | | | | | | | | | | | |
| | 4 | *H. otakii* | | | | | | | | | | | | | | | |
| | 5 | Benthivores | | 0.03 | | | 0.03 | | 0.03 | 0.03 | 0.06 | 0.01 | | | | | |
| | 6 | *E. fangi* | | 0.22 | 0.33 | 0 | 0.09 | | | 0.05 | 0.02 | | | | | | |
| | 7 | Gobiidae | | 0.09 | 0.18 | 0.13 | 0.15 | | 0.03 | 0.05 | 0.04 | 0.01 | | | | | |
| | 8 | Cephalopoda | | 0 | 0.02 | 0.01 | 0 | | | 0 | 0 | 0.01 | | | | | |
| | 9 | *C. japonica* | | | | | 0.03 | | | 0.32 | | | | | | | |
| | 10 | Crustacean | 0.06 | 0.05 | 0.47 | 0.74 | 0.26 | 0.11 | 0.29 | 0.02 | 0.16 | 0.12 | | | | | |
| | 11 | Gastropoda | | 0 | | | 0.05 | | | | 0.14 | 0.03 | 0.05 | | | | |
| | 12 | Shellfish-killers | | | | | 0.04 | | | | | | | | | | |
| | 13 | *C. gigas* | | | | | | | | | 0.2 | | | 1 | | | |
| | 14 | Infauna | | | 0 | 0.08 | 0.16 | 0.2 | 0.46 | 0.06 | 0.23 | 0.27 | | | | | |
| | 15 | Zooplankton | 0.5 | 0.24 | | | 0.07 | 0.57 | 0.19 | 0.26 | | 0.14 | 0.05 | | | 0.11 | |
| | 16 | Phytoplankton | 0.2 | | | | 0.03 | | | | | | 0.2 | | 0.5 | 0.04 | 0.8 |
| | 17 | Algae | | | | 0.03 | | | | | | 0.17 | 0.2 | | | 0.25 | |
| | 18 | Detritus | 0.24 | | | | 0.1 | 0.13 | | | 0.15 | 0.24 | 0.5 | | 0.5 | 0.6 | 0.2 |

large portion, and the biomass reduced gradually with increasing TL (**Figure 3**).

Energy flows in both models were derived directly from detritus or indirectly from primary production by detritus- or grazing-based food chains, respectively (**Figure 3**). The majority of energy flows converged between integrated TLs I, II, and III for each reef system, collectively accounting for over 95% of TST for both cases (**Figure 4**). The total energy flowing into the detritus was 1,484 and 1,932 $t{\cdot}km^{-2}{\cdot}year^{-1}$ in the artificial and natural systems, respectively, to which principally contributed by primary producers (55.25% and 57.03% in artificial and natural models, respectively) and TL II taxa (43.7% and 41.46% in artificial and natural models, respectively), mainly zooplankton and benthic invertebrates. The TPP of artificial and natural systems was 2,396.8 and 3,258.4 $t{\cdot}km^{-2}{\cdot}year^{-1}$, respectively, of which 65.8% and 66.16% flow into TL II, respectively. Besides, the consumption of detritus by TL II was also high in each model (**Figure 4**).

Overall, the MTE in the artificial model (10.56%) was similar to that in the natural system (10.21%), both of which were in proximity to the desired Lindeman efficiency of 10% (Lindeman, 1991). In the natural system, the MTE from the detritus (10.36%) was nearly the same as that of primary producers (10.11%), but in the artificial system, the MTE from the detritus (9.86%) was lower than that from the primary producers (12.03%). Moreover, the highest transfer efficiency from primary producers (19.26%) and detritus (19.64%) occurred in TL III in the artificial model, while these two parameters (16.23% and 16.28%, respectively) peaked at TL IV in the natural model.

## 3.3 Mixed Trophic Impact Analysis

Direct and indirect trophic interactions in both systems are revealed based on MTI analysis (**Figure 5**). Overall, the bait groups had positive effects on their predators, while the predator groups posed a direct or indirect negative effect on other groups, such as the planktonic group and piscivorous group, *E. fangi* and *S. schlegelii*. The diagonal line indicating negative effects also represents the interspecific competition in diet (**Figure 5**). No significant correlation was detected between two top predators, *S. schlegelii* and *H. otakii*, indicating that there is no fierce predation or competition between them. Moreover, as basal food sources, the algae, phytoplankton, and detritus displayed positive impacts on most functional groups.

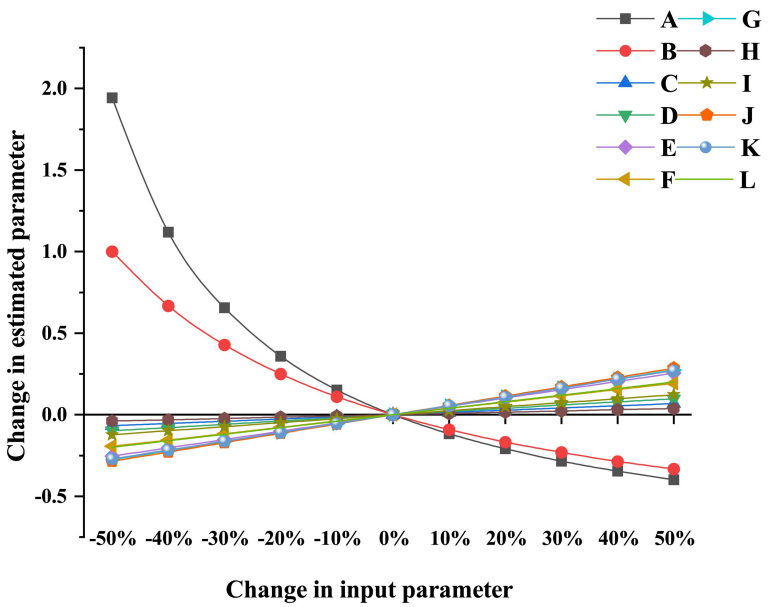


**FIGURE 2** | Partial sensitivity analysis of Ecopath model for artificial reef and natural reef ecosystems. **(A)** Effects of Gastropoda (P/B) on Gastropoda (B) of Ecopath model for artificial reef and natural reef ecosystems. **(B)** Effects of Infauna (EE) on Infauna (B) of Ecopath model for artificial reef and natural reef ecosystems. **(C)** Effects of *Charybdis japonica* (B) on Infauna (B) of Ecopath model for artificial reef ecosystem. **(D)** Effects of Gobiidae (B) on Infauna (B) of Ecopath model for artificial reef ecosystem. **(E)** Effects of Crustacean (B) on Infauna (B) of Ecopath model for artificial reef ecosystem. **(F)** Effects of Crustacean (B) on Gastropoda (B) of Ecopath model for artificial reef ecosystem. **(G)** Effects of *C. japonica* (B) on Gastropoda (B) of Ecopath model for artificial reef ecosystem. **(H)** Effects of *C. japonica* (B) on Infauna (B) of Ecopath model for natural reef ecosystem. **(I)** Effects of Gobiidae (B) on Infauna (B) of Ecopath model for Natural Reef ecosystem. **(J)** Effects of Crustacean (B) on Infauna (B) of Ecopath model for Natural Reef ecosystem. **(K)** Effects of Crustacean (B) on Gastropoda (B) of Ecopath model for natural reef ecosystem. **(L)** Effects of *C. japonica* (B) on Gastropoda (B) of Ecopath model for natural reef ecosystem.

# 4 DISCUSSION

## 4.1 Model Quality Evaluation

The Ecopath model synthesizes existing knowledge into a quantitative relationship that explains the overall ecosystem functioning and allows comparisons of organic matter input and transfer along with the food-web dynamics between the artificial and natural systems. The p-values in each model were not at a very high level, implying that our models may be not sufficiently time-sensitive and that the applicability of the conclusions still needs the supplement of new empirical data. Due to the limitations of geographical conditions *in situ* and the restrictions on sampling methods (for instance, the scattered fishing activities in the local area made the fishery catches hard to estimate; the bottom trawling

**TABLE 4** | Comparisons of ecosystem attributes estimated by balanced Ecopath model between the nearshore artificial reef (AR) and the natural reef (NR) in Yellow Sea, China, and other costal reef areas.

| Locations | This study | | LZB | LSB | ZZD | LD | SS | ZW | GQD | GA |
|---|---|---|---|---|---|---|---|---|---|---|
| **Reef types** | **ARs** | **NRs** | **ARs** | **ARs** | **ARs** | **ARs** | **ARs** | **ARs** | **Kelp bed** | **NRs** |
| Total consumption, TC | 2,293.68 | 3,758.46 | 1,675.48 | 5,928.58 | 13,768.62 | — — | 2,249.94 | 1,839.5 | 12,307.12 | 51600 |
| Total export, TEX | 1,155.9 | 1,070.26 | 309.68 | 400.77 | 7,962.42 | — — | 481.92 | 34.99 | 2,060.81 | -5412 |
| Total respiration, TR | 1,242.18 | 2,189.62 | 836.73 | 3,166.59 | 6,622.08 | — — | 1,249.06 | 991.91 | 7,126.78 | 27638 |
| Total flows into detritus, TDET | 1,763.71 | 2,472.15 | 1,102.61 | 9,694.43 | 9,872.45 | 4,552.64 | 1,179.14 | 523.73 | 6,524.31 | 21024 |
| Total system throughput, TST | 6,455.47 | 9,490.48 | 3,924.49 | 14,256.51 | 18,939.09 | 11104 | 5160 | 3,390.13 | 28019 | 94850 |
| Total production, TP | 2,989.53 | 4,075.55 | 855.32 | 3,657.35 | 14,546.27 | 4,990.3 | 2282 | 1,506.59 | 11604 | 17337 |
| Net system production, NSP | 1,154.58 | 1,068.78 | 556.2 | | — — | 1,865.2 | 480.89 | 34.99 | 8,883.74 | 13250 |
| Total biomass, TB (excluding detritus) | 154.01 | 274.26 | 176.88 | 262.2 | 986.98 | 620.2 | 61.77 | 1,506.59 | | 2620 |
| Mean transfer efficiency, MTE | 10.56% | 10.21% | 15.09% | 10.80% | 14.50% | 11.70% | 13.60% | 12.80% | 12.70% | — — |
| Total primary production/total respiration, TPP/TR | 1.93 | 1.49 | 0.67 | 1.13 | 2.2 | 1.84 | 1.39 | 1.04 | 1.25 | 0.48 |
| Connectance index, CI | 0.3 | 0.27 | 0.236 | 0.293 | 0.2 | 0.32 | | 0.444 | 0.331 | 0.16 |
| System omnivory index, SOI | 0.2 | 0.19 | 0.188 | 0.333 | 0.12 | 0.14 | | 0.36 | 0.222 | 0.25 |

*LZB, Laizhou Bay (Xu et al., 2019); LSB, Laoshan Bay (Liu et al., 2019); ZZD, Zhangzidao (Xu et al., 2016); LD, Lidao (Wu et al., 2016); SS, Shengsi (Li et al., 2007); ZW, Zhuwang, Laizhou Bay (Yang et al., 2016); GQD, Gouqidao (Zhao et al., 2010); GA, Galapagos Archipelago (Okey et al., 2004).*

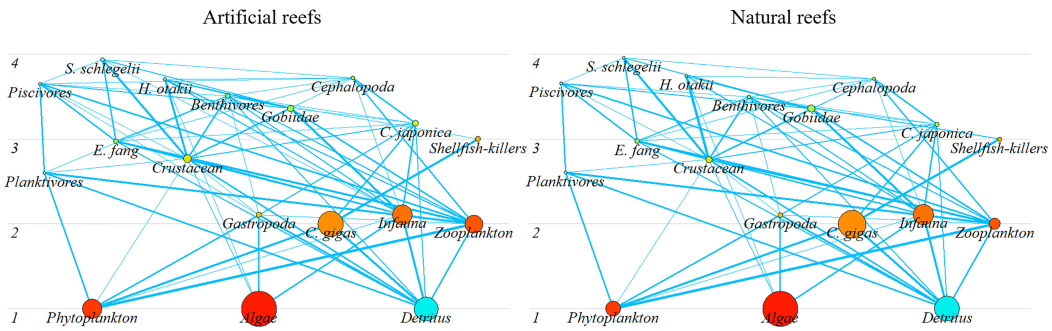


**FIGURE 3** | Trophic structure of the artificial and natural reef ecosystems on the coast of Yellow Sea, China. Circle size represents the biomass proportion.

could only be executed in an adjacent area other than in reef area), the model precision is unguaranteed generally. Furthermore, uncertainties in input parameters (e.g., dietary composition, P/B, and Q/B) for some functional groups also increased the difficulties in the model construction. To overcome the disadvantages, we kept consistent the survey methods, sampling time, and post-data processing procedures at both reef types during the model construction to guarantee that the "distortion" degree in the two models is comparable. As this study aimed to emphasize the comparison of energy flow characteristics, detecting the "potential gap" on the same parameters to reflect the difference in structure and function between two types of reef systems was more

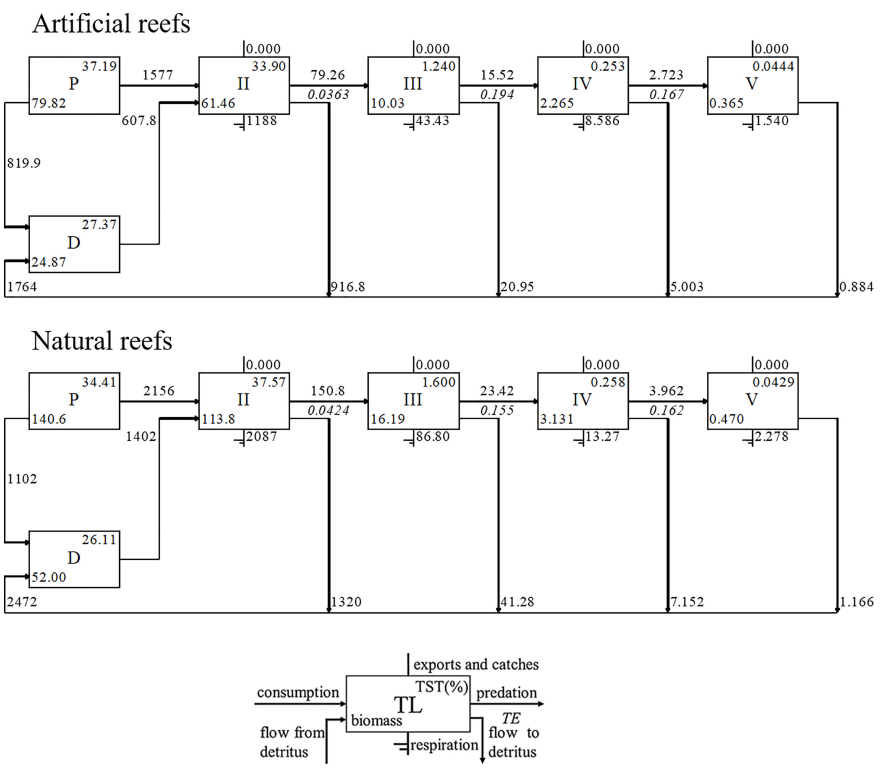


**FIGURE 4** | Lindeman spine diagram at the artificial and natural reef ecosystems on the coast of Yellow Sea, China.

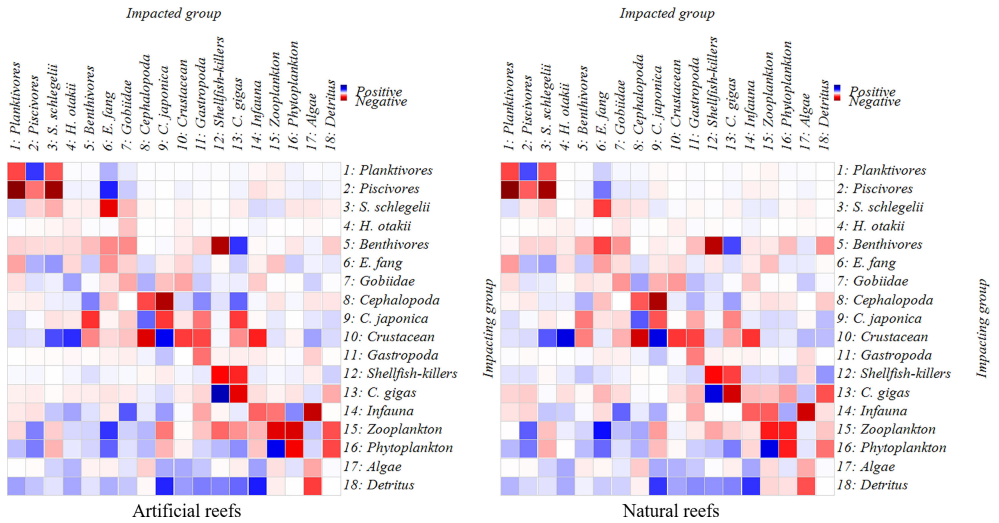


**FIGURE 5** | Mix trophic impacts analysis for the artificial and natural reef ecosystems on the coast of Yellow Sea, China. Positive impacts are denoted in blue rectangles while negative impacts in red rectangles, and the color concentration represents the impact strength.

underlined. Insufficiency or difficulties in quantifying the biological resource also indicate new requirements for future research in reef areas, where optimizing the experimental plan and improving survey methods should be paid more attention.

## 4.2 Overall System Characteristics

Both types of reef ecosystems were characterized by high biomass of algae, filter-feeding shellfish (*C. gigas*), and crustaceans (**Table 2**). The dominance of consumers with lower TLs probably results from the high productivity and standing crop of benthic macroalgae in each area, which has also been documented previously in other coastal systems (Okey et al., 2004; Wu et al., 2016). As representing organisms in reef areas, *S. schlegelii* and *H. otakii* occupied the top two positions in biomass and TLs in both models, which once again confirms that the artificial reefs could support the aggregation of reef fishes (Streich et al., 2017; Cresson et al., 2019).

The TPP of the artificial reef system was lower relative to its natural counterpart, generally indicating that there remains plenty of scope for the artificial ecosystem in scale. Apart from the disparity of the development duration, this can be explained by the smaller area of the artificial reef, supporting less colonization of sessile filter feeders (e.g., *C. gigas*) and benthic micro- and macroalgae when compared to the natural reef. Additionally, man-made modules were arranged in a regular manner, leading to a more homogeneous habitat. This pattern may only attract reef-associated species and will confine the development of the biodiversity even if the whole ecosystem has been formed for a long term. Previous studies have also implied that other conservation actions could impact the development of the artificial reef, such as establishing marine protected areas and reducing overfishing and unsustainable fishing practices (Baine, 2001; Lima et al., 2019). Hence, long-term monitoring in conjunction with conservation actions is advised to estimate the scale of developing the artificial reef.

Compared with other identical reef ecosystems in China and Galapagos, Ecuador (**Table 4**), the scales of both artificial and natural reef systems in this study stay at a medium level, with the TPPs merely higher than those of Laizhou Bay (Xu et al., 2019) and Shengsi (Li et al., 2007) but lower than those of Laoshan Bay (Liu et al., 2019), Zhangzidao (Xu et al., 2016), Zhuwang, Laizhou Bay (Yang et al., 2016), Lidao (Wu et al., 2016), Gouqidao (Zhao et al., 2010), and Galapagos Archipelago (Okey et al., 2004). The aforementioned differences can be explained by the spatial heterogeneity of the ecological environment in different study areas, where the nutrient richness, current condition, and chlorophyll-*a* content would directly affect the primary productivity, while differences in the substrate environment may also cause geographical differences in community structures (Mills et al., 2017). In addition, differences in data collection and model debugging during the model building could also be non-negligible factors.

## 4.3 Energy Flow and Transfer Efficiency Between Trophic Levels

The overall energy flow distribution showed a gradual decrease from low TL to high TL, which is in line with the energy "pyramid" principle. Both the intake proportion of TL I and the TPP proportion of TL I and II in the two models were high, indicating that low TLs composed mainly of macroalgae, phytoplankton, and detritus are the main energy sources in both reef ecosystems. Based on the energy proportion of each TL flowing into the detritus, both TL I and TL II were underutilized, while those above were more utilized for each case, which is in agreement with the conclusion that the detritus-based pathway dominates in the temperate reef

ecosystem (Pinkerton et al., 2008). Energy derived from TLs I and II was blocked up to the classical food chain, which probably is attributed to the insufficient biomass of consumers. For example, grazing groups (such as sea urchins and abalone) in both areas were nearly absent, which cannot effectively transfer the amount of primary productivity to the next TL directly.

Studies have found that a considerable part of macroalgae will decay and settle on the seafloor, which will firstly be decomposed by bacteria and then enter the debris channel to provide energy for other TLs indirectly (Schaal et al., 2010). According to Krumhansl and Scheibling (2012), the global average rate of detritus derived from kelps accounts for ca. 82% of the annual kelp productivity. As the energy of TL I flowing to the detritus is lower in the artificial system than in the natural system here, this is probably related to the spatial difference in algae provision. Overall, the natural reef covers a larger area than the artificial reef and may across multiple water columns, thus facilitating the colonization and growth of more macroalgae. Alternatively, the natural reef area is located near an island, where abundant algae detritus in the intertidal zone would inevitably flow into the natural system and provides significant energy subsidies for the enhancement of benthos stock. Conversely, most of the reef structures were deployed at a depth of no less than 15 m, where sunshine penetration was lower, thus weakening the production of algae. Furthermore, the surroundings of the artificial reef featured sediment mixed with sand, and the external input of detritus was lower.

Based on **Figure 4**, we observed that the highest transfer efficiency occurred differently in both reef ecosystems. The highest transfer efficiency in the artificial reef occurred in TL III, above which the transfer efficiency went down dramatically. This reflects the pivotal roles of invertebrates, especially crustaceans and other functional groups with low TLs, in the artificial reef food web. In contrast, the highest transfer efficiency went to the TL IV in the natural reef, indicating that higher TLs still had an obvious regulation on the food web. This difference is probably related to the development time of the ecosystem. For a newly established ecosystem, the ecosystem functioning depends on the phase of community succession, which means the network of energy, nutrients, and organic matter fluxes will be incomplete prior to the community being mature, and this process always undergoes long periods. Previous studies have observed that artificial reefs with similar structural features supported fish communities similar to those found on natural reefs, after several years' deployment (Perkol-Finkel et al., 2006; Granneman and Steele, 2015; Paxton et al., 2020). However, the recovery of the community metrics does not mean a function recovery, since the latter will take more time than the former (James et al., 2020). The geographical difference could be another reason for the difference above. For instance, the hydrological condition and the complexity of substrate structure would impose on the habitat diversity, which will have an effect on the biodiversity and the ecosystem functions at last. The average transfer efficiency in both natural and artificial reef systems was similar to the Lindeman efficiency (10%) (Lindeman, 1942) and the average result from 48 global aquatic ecosystems (10.1%) (Pauly and Christensen, 1995), and this result suggests not only the characteristics of temperate coastal ecosystems but also the overall health of both reef ecosystems in energy flow.

## 4.4 System Maturity and Stability

Usually, the TPP/TR ratio is used to indicate the maturity of an ecosystem (Odum, 1969). As one of the principal features of mature ecosystems, TPP/TR close to 1 implies that all primary production is used for respiration with no residual production left. In the early stage of an ecosystem, TPP/TR ratio tends to be greater than 1, because the structure of the food web's incomplete, and the primary production cannot be fully utilized. Later on, the ecosystem gets fully matured with the development of the system when the TB tends to be the maximum, and the corresponding TPP/TR ratio will get smaller. In the current study, the TPP/TR ratio in natural and artificial reef systems was slightly higher than that in Zhuwang, Laizhou Bay (Yang et al., 2016), Shengsi (Li et al., 2007), and Laoshan Bay (Liu et al., 2019) when compared to other similar ecosystems with parallel latitudes, reflecting the maturity difference caused by spatial and temporal variation. CI and SOI are indices elucidating the ecosystem complexity, as their higher values indicate more complex population interactions. Here, the CI and SOI values in the artificial reef system were slightly higher than those in the natural reef system and were not significantly different from other ecosystems with identical latitudes. Therefore, it can be concluded that excess production can be reutilized in artificial systems than its natural counterpart. This indicates that the artificial reef system is less mature than the natural reef, even though it has formed a relatively complex interspecific relationship and high stability. Using the Ecopath model, Pitcher et al. (2002) proposed that it would take 10 to 25 years for artificial reefs to have a significant positive effect on local biological resources, and they highlighted the necessity to extend the fishing moratorium to magnify the post-reef effect. In the present study, the artificial reef is less than 10 years old, and the changes in ecological functions of which during the developing time still need to be further tracked and monitored. On the other hand, we notice that the natural reef system seemed to be inadequate compared to other ecosystems with parallel latitudes in terms of maturity (**Table 4**). This could be owing to the marine aquaculture and other fishery activities around the natural reefs, which would probably interfere with the normal ecosystem functioning and weaken its maturity if the variation was not caused by geographical heterogeneity. This also reminds us to strengthen the restoration and protection of islands and reefs in the future, by regulating the development and utilization activities, to maintain or restore their original ecological functions gradually.

Our work compares the system characteristics including trophic structures and energy flow between the artificial and natural reef ecosystems. However, regional-scale heterogeneity in initial environment characteristics (e.g., currents, nutrients, and

terrigenous inputs) was not included here due to inadequate data recording, which may interfere with the comparison and weaken the robustness of conclusions. Theoretically, comparisons between two types of reefs should be performed in areas with comparable environmental conditions initially, to underscore the ecosystem changes *in situ* with the deployed ages of artificial reefs. Yet areas with optimal conditions are hard to find practically, which probably explains why studies of interest are relatively few. With results of the present study as a base, future work on artificial reefs could be directed toward a better data recording prior to and after artificial reef projects, to provide more information about not only the successional process of biota communities but also more complete trajectories of the ecosystem functioning development.

## 5 CONCLUSIONS

With the establishment of Ecopath models at two types of the reef on the coast of the Yellow Sea, China, this study performed comparisons of trophic structure and energy flow between artificial and natural reef systems. The TPP was estimated to be lower in the artificial system than in the natural reef system, indicating that there is still development potential for the artificial reef. A large proportion of energy was occupied by medium and low TLs in each system, reflecting that the primary production (macroalgae and phytoplankton) and detritus were the main energy sources driving both systems, and the detritus-based channel played a dominant role. Both systems were highly consistent in terms of the energy transfer efficiency, which was close to the Lindeman efficiency (10%), reflecting the good operation of the energy flow for both reef systems. Moreover, the models estimated that there is still a gap between the artificial and natural systems with regard to maturity, but the former has developed relatively complex interspecific interaction and high stability.

## DATA AVAILABILITY STATEMENT

The original contributions presented in the study are included in the article/supplementary materials, further inquiries can be directed to the corresponding authors.

## AUTHOR CONTRIBUTIONS

RZ: formal analysis and original draft writing. QZ and JZ: writing—review and editing. ZW: data curation and validation. HL and LS: funding acquisition and writing—review and editing. YL, QL, YT, and JZ: writing—review and editing.

## ACKNOWLEDGMENTS

This research was jointly supported by the Strategic Pilot Project of Chinese Academy of Sciences (XDA23050303), National Natural Science Foundation of China (41806150), and the Youth Innovation PromotionAssociation, Chinese Academy of Sciences (No. 2019216). We also address special thanks to those who gave supports in field surveys and laboratory works, provided suggestions for data analysis, or facilitated access to the paper writing.

## REFERENCES

Abdou, K., Le Loc'h, F., Gascuel, D., Romdhane, M. S., Aubin, J., Ben RaisLasram, F., et al. (2020). Combining Ecosystem Indicators and Life Cycle Assessment for Environmental Assessment of Demersal Trawling in Tunisia. *Int. J. Life Cycle Ass.* 25, 105–119. doi: 10.1007/s11367-019-01651-5

Baine, M. (2001). Artificial Reefs: A Review of Their Design, Application, Management and Performance. *Ocean. Coast. Manag.* 44, 241–259. doi: 10.1016/S0964-5691(01)00048-5

Bohnsack, J. A. (1989). Are High-Densities of Fishes at Artificial Reefs the Result of Habitat Limitation or Behavioral Preference. *B Mar. Sci.* 44, 631–645. doi: 10.1515/botm.1989.32.2.181

Brickhill, M. J., Lee, S. Y., and Connolly, R. M. (2005). Fishes Associated With Artificial Reefs: Attributing Changes to Attraction or Production Using Novel Approaches. *J. Fish. Biol.* 67, 53–71. doi: 10.1111/j.0022-1112.2005.00915.x

Christensen, V. (1995). Ecosystem Maturity — Towards Quantification. *Ecol. Modell.* 77, 3–32. doi: 10.1016/0304-3800(93)E0073-C

Christensen, V., and Walters, C. J. (2004). Ecopath With Ecosim: Methods, Capabilities and Limitations. *Ecol. Modell.* 172, 109–139. doi: 10.1016/j.ecolmodel.2003.09.003

Christensen, V., Walters, C. J., Pauly, D., et al. (2008). Ecopath With Ecosim Version 6 User Guide Vancouver, Canada: Fisheries Center Univ. of BritishColumbia, p. 1–235.

Colléter, M., Valls, A., Guitton, J., Gascuel, D., Pauly, D., Christensen, V., et al. (2015). Global Overview of the Applications of the Ecopath With Ecosim Modeling Approach Using the EcoBase Models Repository. *Ecol. Modell.* 302, 42–53. doi: 10.1016/j.ecolmodel.2015.01.025

Cresson, P., Le Direach, L., Rouanet, E., Goberville, E., Astruch, P., Ourgaud, M., et al. (2019). Functional Traits Unravel Temporal Changes in Fish Biomass Production on Artificial Reefs. *Mar. Environ. Res.* 145, 137–146. doi: 10.1016/j.marenvres.2019.02.018

Finn, J. T. (1976). Measures of Ecosystem Structure and Function Derived From Analysis of Flows. *J. Theor. Biol.* 56, 363–380. doi: 10.1016/S0022-5193(76)80080-X

Granneman, J. E., and Steele, M. A. (2015). Effects of Reef Attributes on Fish Assemblage Similarity Between Artificial and Natural Reefs. *Ice. J. Mar. Sci.* 72, 2385–2397. doi: 10.1093/icesjms/fsv094

Heymans, J. J., Coll, M., Link, J. S., Mackinson, S., Steenbeek, J., Walters, C., et al. (2016). Best Practice in Ecopath With Ecosim Food-Web Models for Ecosystem-Based Management. *Ecol. Modell.* 331, 173–184. doi: 10.1016/j.ecolmodel.2015.12.007

James, W. R., Lesser, J. S., Litvin, S. Y., and Nelson, J. A. (2020). Assessment of Food Web Recovery Following Restoration Using Resource Niche Metrics. *Sci. Tot. Env.* 711, 134801. doi: 10.1016/j.scitotenv.2019.134801

Krumhansl, K. A., and Scheibling, R. E. (2012). Production and Fate of Kelp Detritus. *Mar. Ecol. Prog. Ser.* 467, 281–302. doi: 10.3354/meps09940

Latham, L. G. (2006). Network Flow Analysis Algorithms. *Ecol. Modell.* 192, 586–600. doi: 10.1016/j.ecolmodel.2005.07.029

Lee, S. I., and Zhang, C. I. (2018). Evaluation of the Effect of Marine Ranching Activities on the Tongyeong Marine Ecosystem. *Ocean. Sci. J.* 53, 557–582. doi: 10.1007/s12601-018-0045-8

Libralato, S. (2013). System Omnivory Index. *Encycloped. Ecol.* 4, 3472–3477. doi: 10.1016/B978-0-12-409548-9.00605-9

Lima, J. S., Zalmon, I. R., and Love, M. (2019). Overview and Trends of Ecological and Socioeconomic Research on Artificial Reefs. *Mar. Environ. Res.* 145, 81–96. doi: 10.1016/j.marenvres.2019.01.010

Lindeman, R. L. (1942). The Trophic-Dynamic Aspect of Ecology. *Ecology.* 23, 399–418. doi: 10.2307/1930126

Lindeman, R. L. (1991). The Trophic-Dynamic Aspect of Ecology. *Bull. Math. Biol.* 53, 167–191. doi: 10.1016/S0092-8240(05)80045-X

Liu, H. Y., Yang, C. J., Zhang, P. D., Li, W. T., and Zhang, X. M. (2019). An Ecopath Evaluation of System Structure and Function for the Laoshan Bay Artificial Reef Zone Ecosystem. *Acta Ecol. Sinica.* 39, 3926–3936. doi: 10.5846/stxb201805301193

Liu, Y., Zhao, Y. P., Dong, G. H., Guan, C. T., Cui, Y., and Xu, T. J. (2013). A Study of the Flow Field Characteristics Around Star-Shaped Artificial Reefs. *J. Fluid. Struct.* 39, 27–40. doi: 10.1016/j.jfluidstructs.2013.02.018

Li, Y. G., Wang, Z. H., and Zhang, S. Y. (2007). A Prelmi Inary Approach on the Ecosystem Model of the Artificial Reef in Shengsi. *Mar. Fish.* 29, 226–234. doi: 10.3969/j.issn.1004-2490.2007.03.006

McCauley, D. J., Pinsky, M. L., Palumbi, S. R., Estes, J. A., Joyce, F. H., and Warner, R. R. (2015). Marine Defaunation: Animal Loss in the Global Ocean. *Science.* 347, 1255641. doi: 10.1126/science.1255641

Mills, K. A., Hamer, P. A., and Quinn, G. P. (2017). Artificial Reefs Create Distinct Fish Assemblages. *Mar. Ecol. Prog. Ser.* 585, 155–173. doi: 10.3354/meps12390

Morissete, L., Hammill, M. O., and Savenkoff, C. (2006). The Trophic Role of Marine Mammals in the Northern Gulf of StLawrence. *Mar. Mamm. Sci.* 22, 74–103. doi: 10.1111/j.1748-7692.2006.00007.x

Nicoletti, L., Marzialetti, S., Paganelli, D., and Ardizzone, G.D. (2007). Long-Term Changes in a Benthic Assemblage Associated With Artificial Reefs. *Hydrobiologia.* 580, 233–240. doi: 10.1007/s10750-006-0450-3

Odum, E. P. (1969). The Strategy of Ecosystem Development. *Science.* 164, 262–270. doi: 10.1126/science.164.3877.262

Okey, T. A., Banks, S., Born, A. R., Bustamante, R. H., Calvopina, M., Edgar, G. J., et al. (2004). A Trophic Model of a Galapagos Subtidal Rocky Reef for Evaluating Fisheries and Conservation Strategies. *Ecol. Modell.* 172, 383–401. doi: 10.1016/j.ecolmodel.2003.09.019

Ortiz, M., Berrios, F., Campos, L., Uribe, R., Ramirez, A., Hermosillo-Núñez, B., et al. (2015). Mass Balanced Trophic Models and Short-Term Dynamical Simulations for Benthic Ecological Systems of Mejillones and Antofagasta Bays (SE Pacific): Comparative Network Structure and Assessment of Human Impacts. *Ecol. Modell.* 309-310, 153–162. doi: 10.1016/j.ecolmodel.2015.04.006

Ouyang, L. J., and Guo, X. W. (2010). Studies on the Q/B Values and Food Consumption of Major Fishes in the East China Sea and the Yellow Sea. *Prog. Fish. Sci.* 31, 23–29.

Pauly, D., and Christensen, V. (1995). Primary Production Required to Sustain Global Fisheries. *Nature.* 374, 255–257. doi: 10.1038/374255a0

Paxton, A. B., Shertzer, K. W., Bacheler, N. M., Kellison, G. T., Riley, K. L., and Taylor, J. C. (2020). Meta-Analysis Reveals Artificial Reefs can be Effective Tools for Fish Community Enhancement But Are Not One-Size-Fits-All. *Front. Mar. Sci.* 7, 282. doi: 10.3389/fmars.2020.00282

Perkol-Finkel, S., Shashar, N., and Benayahu, Y. (2006). Can Artificial Reefs Mimic Natural Reef Communities? The Roles of Structural Features and Age. *Mar. Environ. Res.* 61, 121–135. doi: 10.1016/j.marenvres.2005.08.001

Pinkerton, M. H., Lundquist, C. J., Duffy, C. A. J., and Freeman, D. J. (2008). Trophic Modelling of a New Zealand Rocky Reef Ecosystem Using Simultaneous Adjustment of Diet, Biomass and Energetic Parameters. *J. Exp. Mar. Biol. Ecol.* 367, 189–203. doi: 10.1016/j.jembe.2008.09.022

Pitcher, T. J., Buchary, E. A., and Hutton, T. (2002). Forecasting the Benefits of No-Take Human-Made Reefs Using Spatial Ecosystem Simulation. *Ice. J. Mar. Sci.* 59, S17–S26. doi: 10.1006/jmsc.2002.1185

Polovina, J. J. (1984). Model of a Coral-Reef Ecosystem. *Coral. Reef.* 3, 1–11. doi: 10.1007/Bf00306135

Raj, K. D., Mathews, G., and Edward, J. K. P. (2020). Long-Term Benefits of Artificial Reef Modules for Reef Recovery in Gulf of Mannar, Southeast India. *J. Coast. Conserv.* 24, 53. doi: 10.1007/s11852-020-00773-5

Reed, J., Shannon, L., Velez, L., Akoglu, E., Bundy, A., Coll, M., et al. (2017). Ecosystem Indicators—Accounting for Variability in Species' Trophic Levels. *Ice. J. Mar. Sci.* 74, 158–169, fsw150. doi: 10.1093/icesjms/fsw150

Sandu, C., Iacob, R., and Nicolescu, N. (2003). Chlorophyll-*A* Determination - A Reliable Method for Phytoplankton Biomass Assessment. *Acta Bot. Hung.* 45, 389–397. doi: 10.1556/ABot.45.2003.3-4.13

Schaal, G., Riera, P., and Leroux, C. (2010). Trophic Ecology in a Northern Brittany (Batz Island, France) Kelp (*Laminaria Digitata*) Forest, as Investigated Through Stable Isotopes and Chemical Assays. *J. Sea. Res.* 63, 24–35. doi: 10.1016/j.seares.2009.09.002

Shin, Y.-J., and Shannon, L. J. (2010). Using Indicators for Evaluating, Comparing, and Communicating the Ecological Status of Exploited Marine Ecosystems. *1. IndiSea. Proj. Ice. J. Mar. Sci.* 67, 686–691. doi: 10.1093/icesjms/fsp273

Streich, M. K., Ajemian, M. J., Wetz, J. J., Williams, J. A., Shipley, J. B., and Stunz, G.W. (2017). A Comparison of Size Structure, Age, and Growth of Red Snapper From Artificial and Natural Habitats in the Western Gulf of Mexico. *T. Am. Fish. Soc* 146, 762–777. doi: 10.1080/00028487.2017.1308884

Toledo, M. I., Torres, P., Diaz, C., Zamora, V., López, J., and Olivares, G. (2020). Ecological Succession of Benthic Organisms on Niche-Type Artificial Reefs. *Ecol. Proc.* 9, 38. doi: 10.1186/s13717-020-00242-9

Ulanowicz, R. E. (1986). *Growth and Development: Ecosystems Phenomenology*. New York, NY: Springer-Verlag, XF2006293306.11. doi: 10.2307/1351721

Ulanowicz, R., and Puccia, C. (1990). Mixed Trophic Impacts Ecosystems. *Coenoses* 5, 7–16.

United Nations Environment Programme (2009). *London Convention and Protocol/UNEP Guidelines for the Placement of Artificial Reefs* (London: United Nations Environment Programme (UNEP).

Wu, Z., Tweedley, J. R., Loneragan, N. R., and Zhang, X. (2019). Artificial Reefs Can Mimic Natural Habitats for Fish and Macroinvertebrates in Temperate Coastal Waters of the Yellow Sea. *Ecol. Eng.* 139, 105579. doi: 10.1016/j.ecoleng.2019.08.009

Wu, Z., Zhang, X., Lozano-Montes, H. M., and Loneragan, N. R. (2016). Trophic Flows, Kelp Culture and Fisheries in the Marine Ecosystem of an Artificial Reef Zone in the Yellow Sea. *Estuar. Coast. Shelf. Sci.* 182, 86–97. doi: 10.1016/j.ecss.2016.08.021

Xu, Z. X., Chen, Y., Tian, T., Liu, Y. H., Yin, Z. Q., and Liu, H. C. (2016). Structure and Function of an Artificial Reef Ecosystem in Zhangzi Island Based on Ecopath Model. *J. Dalian. Ocean. Univ.* 31, 85–94. doi: 10.16535/j.cnki.dlhyxb.2016.01.015

Xu, M., Qi, L., Zhang, L., Zhang, T., Yang, H., and Zhang, Y. (2019). Ecosystem Attributes of Trophic Models Before and After Construction of Artificial Oyster Reefs Using Ecopath. *Aquacult. Env. Interac.* 11, 111–127. doi: 10.3354/aei00284

Yang, J. M. (2001a). A Study on Food and Trophic Levels of Bohai Sea Fish. *Modern. Fish. Info.* 16, 10–19.

Yang, J. M. (2001b). A Study on Food and Trophic Levels of Bohai Sea Invertebrates. *Modern. Fish. Info.* 16, 8–16. doi: 10.3969/j.issn.1004-8340.2001.09.002

Yang, C. J., Wu, Z. X., Liu, H. Y., Zhang, P. D., Li, W. T., Zeng, X.Q., et al. (2016). The Fishing Strategy of *Charybdis Japonica* and *Rapana Venosa* and the Carrying Capacity of *Apostichopus Japonucus* in Zhuwang, Laizhou Artificial Reef Ecosystems Based on Ecopath Model. *Periodic. Ocean. Univ. China.* 46, 168–177. doi: 10.16441/j.cnki.hdxb.20160112

Yu, H., Yang, W., Liu, C., Tang, Y., Song, X., and Fang, G. (2020). Relationships Between Community Structure and Environmental Factors in Xixiakou Artificial Reef Area. *J. Ocean. U. China.* 19, 883–894. doi: 10.1007/s11802-020-4298-3

Zhang, B. (2018). Feeding Ecology of Fishes in the Bohai Sea. *Prog. Fish. Sci.* 39, 11–22. doi: 10.19663/j.issn2095-9869.20171103001

Zhang, B., Li, Z. Y., and Jin, X. S. (2012). Functional Groups of Fish Assemblages and Their Major Species in the Bohai Sea. *J. Fish. China.* 36, 64–72. doi: 10.3724/SP.J.1231.2012.27617

Zhang, R. L., Liu, H., Zhang, Q. Q., Zhang, H., and Zhao, J. M. (2021a). Trophic Interactions of Reef-Associated Predatory Fishes (*Hexagrammos Otakii* and *Sebastes Schlegelii*) in Natural and Artificial Reefs Along the Coast of North Yellow Sea, China. *Sci. Tot. Environ.* 791, 148250. doi: 10.1016/j.scitotenv.2021.148250

Zhang, R. L., Zhang, H., Liu, H., and Zhao, J. M. (2021b). Differences in Trophic Structure and Trophic Pathways Between Artificial Reef and Natural Reef Ecosystems Along the Coast of the North Yellow Sea, China, Based on Stable Isotope Analyses. *Ecol. Indic.* 125, 107476. doi: 10.1016/j.ecolind.2021.107476

Zhao, J., Zhang, S. Y., and Xu, M. (2010). The Primary Research of the Energy Flow in Gouqi Kelp Bed Ecosystem. *J. Shanghai. Ocean. Univ.* 19, 98–104.

Zhou, X., Zhao, X., Zhang, S., and Lin, J. (2019). Marine Ranching Construction and Management in East China Sea: Programs for Sustainable Fishery and Aquaculture. *Water*. 11, 1237. doi: 10.3390/w11061237

**Conflict of Interest:** The authors declare that the research was conducted in the absence of any commercial or financial relationships that could be construed as a potential conflict of interest.

**Publisher's Note:** All claims expressed in this article are solely those of the authors and do not necessarily represent those of their affiliated organizations, or those of the publisher, the editors and the reviewers. Any product that may be evaluated in this article, or claim that may be made by its manufacturer, is not guaranteed or endorsed by the publisher.

frontiers | Frontiers in Marine Science

ORIGINAL RESEARCH
published: 03 June 2022
doi: 10.3389/fmars.2022.890219

# Otolith Marking With Strontium for Stock Assessment in *Coilia nasus*

*Ming-Zhi Liu*[1,2,3,4], *Ri-jin Jiang*[2,3,4]*, *Hui Zhang*[5,6], *Fan Yang*[1,2,3,4], *Xia-Fang Li*[1,2,3,4], *Guang-Peng Feng*[6], *Rui Yin*[2,3,4] *and Feng Chen*[2,3,4]

[1] Marine and Fisheries Research Institute, Zhejiang Ocean University, Zhoushan, China, [2] Zhejiang Marine Fisheries Research Institute, Zhoushan, China, [3] Scientific Observation and Experimental Station of Fishery Resources of Key Fishing Grounds, Ministry of Agriculture and Rural Affairs of the People's Republic of China, Zhoushan, China, [4] Key Laboratory of Sustainable Utilization of Technology Research for Fishery Resources of Zhejiang Province, Zhoushan, China, [5] Key Laboratory of East China Sea and Oceanic Fishery Resource Exploitation, Ministry of Agriculture, Shanghai, China, [6] East China Sea Fisheries Research Institute, Chinese Academy of Fishery Science, Shanghai, China

OPEN ACCESS

**Edited by:**
Jun Xu,
Institute of Hydrobiology (CAS), China

**Reviewed by:**
Xiujuan Shan,
Chinese Academy of Fishery Sciences (CAFS), China
Aafaq Nazir,
Indian Institute of Science (IISc), India

***Correspondence:**
Ri-jin Jiang
jiangridge@163.com

**Specialty section:**
This article was submitted to Marine Ecosystem Ecology, a section of the journal Frontiers in Marine Science

**Received:** 05 March 2022
**Accepted:** 06 May 2022
**Published:** 03 June 2022

**Citation:**
Liu M-Z, Jiang R-j, Zhang H, Yang F, Li X-F, Feng G-P, Yin R and Chen F (2022) Otolith Marking With Strontium for Stock Assessment in Coilia nasus. Front. Mar. Sci. 9:890219. doi: 10.3389/fmars.2022.890219

Mass stock enhancement and release are excellent ways to recover *Coilia nasus* resources. However, it is challenging to evaluate stock enhancement effectively, and it is important to establish a method suitable for estimating *C. nasus* populations. We explored the effectiveness of marking otoliths in these fish with strontium by immersing *C. nasus* in hexahydrate strontium chloride solutions. We used laser ablation inductively coupled plasma mass spectrometry to measure the strontium content of otoliths and fish bodies. The larvae (40 d post hatch) were reared in five different concentrations of strontium (0, 12, 24, 48, and 60 mg/L) for 7 d, followed by treatment in non-additive water for 3 wk. The results showed that the cumulative mortality rate was not significantly different between treatment and control groups ($P>0.05$), except in the group treated with 24 mg/L strontium. The swimming and feeding behaviors did not change significantly, indicating that strontium did not negatively affect survival in this species. The strontium/calcium ratios of otoliths in the control group were stable (1.78–2.32 mmol/mol), whereas those of the experimental (marked) groups ranged widely (4.47–61.02 mmol/mol). The strontium/calcium ratios increased with increasing strontium concentration, but gradually returned to baseline values, resulting in a 100% success rate of marking with strontium. Following immersion in 12 mg/L strontium, strontium levels in the body returned to normal after 24 d. In summary, a treatment of 12 mg/L strontium for 4 d was identified as viable for marking. We confirmed the feasibility of strontium marking for the mass marking and release of *C. nasus*. This marking method does not affect the physiology of the fish and may provide a new approach for reasonable and scientific stock assessment of *C. nasus* post hatch.

**Keywords: *Coilia nasus*, otolith, strontium marking, enhancement and release, stock assessment**

## INTRODUCTION

*Coilia nasus* is an estuarine migratory fish belonging to the family *Engraulidae* of the order *Clupeiformes*. Previously, it was one of the most economically important fish species in China and was widely distributed in the East China Sea. However, the species is now threatened by overexploitation and loss of habitat that has devastated its population. Accordingly, catch sizes have decreased substantially, and it is difficult to establish a fishing season (**Figure 1**). Moreover, the majority of fish are caught at a younger age and reach sexual maturity earlier than they did before the 1970s (Zhang et al., 2005).

Enhancement and release initiatives are an effective way of restoring fishery resources (He et al., 2011; Yan et al., 2015), but evaluating the results is essential for protecting and using fishery resources. At present, there are several practical methods for assessing stock conditions, including external (fin-clipping and cold-branding) and internal (fluorescence marking) marking techniques. However, these may cause issues such as high mortality and difficult recognition (Nielsen, 1992; Yang et al., 2013). Therefore, there is an urgent need to explore a method of stock assessment that is suitable for releasing *C. nasus*.

Some studies have reported that the strontium content of otoliths is associated with seawater strontium content, and strontium marking technology has been applied in several released species (Pollard et al., 1999; Schroder et al., 2001). For example, strontium has been used successfully to mark *Aristichthys nobilis, Cyprinus carpio*, and *Sparus macrocephalus* (Li et al., 2017; Zhang et al., 2018; Qiu et al., 2019b). Researchers have reported the steady deposition of a given concentration of strontium in otoliths through a complex metabolic process with demonstrable reliability. Moreover, deposition is not assimilated by the body. However, to our knowledge, no studies have reported the application of this marking technique in *Clupeiformes*. Therefore, we investigated the optimal strontium concentration and treatment duration for marking in *C. nasus*. In this study, we evaluated a marking technique and providing a theoretical basis for its application in enhancement and release practices.

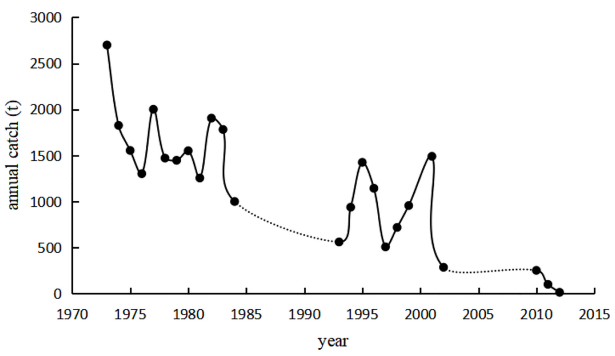


**FIGURE 1** | Annual catch of Coilia nasus in the lower reaches of the Yangtze River. The data for 1973–1984, 1993–2002, and 2010–2012 are from Yuan (1988); Zhang et al. (2005), and Liu et al. (2012), respectively. The dashed lines indicate where data was not available.

## MATERIALS AND METHODS

### Experimental Design

Larvae were cultivated by the Fisheries Research Institute, Shanghai, China. We directly collected the samples at 40 d post hatch. Hexahydrate strontium chloride was obtained from China, Sinopharm Chemical Reagent Co., Ltd (batch number is 20210114). The reagent was dissolved in fresh water. Four strontium concentrations (12, 24, 48, and 60 mg/L) were tested according to the strontium content of seawater. A total of 15 containers (300 L) were installed with 150 samples per container. There were three containers for each experimental group, and the remaining containers were regarded as the control group. Fresh water for cultures was obtained from the institute. All containers were stored at 27.5–28°C and the water salinity was maintained at 1.3‰–1.4‰. Blackout fabric was installed to prevent exposure to sun and light, as these impact water temperature and larval survival. The tanks were cleaned, and half of the water was changed daily.

The experiment was divided into three phases. In the first phase, all samples were kept for 1 d in containers equipped with an oxygenation device composed of an aerator and an air-transporting soft pipe. None of the groups were fed during this period. In the second phase, cultivation with added strontium lasted for 7 d. The fish larvae were fed *Cladoceran* prey twice per day. In the third phase, the immersed groups were transferred to water without added strontium for 3 wk and cultured as above. The activity and number of larvae were monitored daily.

### Sample Analysis

To evaluate the effect of strontium deposition in fish, 30 samples were collected from each concentration group every 3 d during the second phase, and 30 samples were collected from the experimental (12 mg/L) group every 7 d during the third phase. After the marking process, specimens from experimental and control groups were collected for the analysis of body length (accurate to 0.01 mm) and weight (accurate to 0.001 g) (**Table 1**). Body length was defined as the distance from the rostral side to the end of the tail fin. An electronic balance was used for weighing (Mettler Toledo PL403). Before weighing, blotting paper was used to remove water from the fish bodies to minimize error.

We attempted to collect three pairs of otoliths (sagittaes, asteriscus, and lapillus) for the analyses; however, only sagittaes could be used as experimental materials because of their size. Laser ablation- inductively coupled plasma-mass spectrometry (LA-ICP-MS) (Thermo X Series II, Thermo Fisher Scientific, Bremen, Germany) was used to measure the strontium and calcium concentrations in the otoliths and fish bodies

**TABLE 1** | Parameter values of the equation ($W = aL^b$) fitted to body length and body weight in *Coilia nasus* larvae in the marked and control groups.

| Group | Sample size | *a* | *b* | *R* |
|---|---|---|---|---|
| Marked group | 149 | $0.3524\times10^{-5}$ | 2.8915 | 0.8756 |
| Control group | 141 | $1.1641\times10^{-5}$ | 2.5758 | 0.8638 |

*W and L are the body weight and body length, respectively; a and b are the parameters of the power function; R is the regression coefficient.*

(Zhang et al., 2013; Zhang et al., 2019). The LA system was equipped with an excimer laser operating at 213 nm. The otoliths were analyzed using a spot size of 32 μm and a laser repetition rate of 2 μm/s. The measurements were conducted under conditions of pure helium (He) to minimize the re-deposition of ablated material, and the samples were entrained into the argon (Ar) carrier gas flow to the ICP-MS. We used Plasmalab (Thermo Fisher Scientific, Bremen, Germany) to complete sensor calibration to achieve the best performance indicators. Based on Warren-Myers et al. (2014), making success was determined with 100% accuracy when the mean in the marking area was 3.3 times that of the control group.

## Statistical Analysis

The power function was tested to examine the growth pattern of *C. nasus* during its early life stages as follows (Zhan, 1995):

$$W = aL^b$$

where $W$ (g) and $L$ (mm) are the body weight and body length, respectively; and $a$ and $b$ are the parameters of the power function. Statistical analysis was performed using Excel 2019 (Microsoft Corp., Redmond, WA, USA) and IBM SPSS Statistics v.24.0 (IBM Corp., Armonk, NY, USA).

# RESULTS

## Survival in Different Strontium Concentrations

Mortality occurred in each group throughout the experiment but was relatively low overall (**Figure 2**). During the second phase, mortality was the highest at a strontium concentration of 24 mg/L. A paired sample *t*-test showed a significant difference between the control and 24 mg/L groups ($P < 0.05$); however, no significant differences were observed between the other experimental and control groups groups ($P > 0.05$). Mortality was not significantly different between groups in the third phase ($P > 0.05$). Additionally, swimming and feeding behaviors were not observed to be significantly different between groups, indicating that the treatment was safe. The mortality rate was the highest when the concentration was 24 mg/L; however, this may have been due to improper suction of sewage. The cumulative mortality increased with time, probably due to increasing ammonia and nitrogen and human operational mistakes.

To analyze the growth patterns of fish cultivated in different strontium concentrations, we used the body length and weight of 7 d-immersed larvae (**Figure 3**). The body length and weight were 43.19 ± 6.89 mm and 0.02 ± 0.08 g in the marked groups and 39.46 ± 9.39 mm and 0.17 ± 0.09 g in the control groups, respectively.

The parameters of power equation were estimated using the linear least square method (**Table 1**). The $b$ parameters of the fitted function in the marked and control groups were below 3. This indicates that populations showed allometric growth. One-way analysis of variance (ANOVA) and Duncan's test indicated no differences in the growth parameters among groups ($P > 0.05$), indicating that strontium had little effect on the growth of fish. These findings suggested that the results of strontium marking in *C. nasus* were reliable.

## Quantitative Analysis of Otolith Marking

Strontium-to-calcium (Sr/Ca) ratios were used for quantitative analysis of the marking process. The ratio in otoliths in the control group was stable (1.78–2.32 mmol/mol), and the range did not fluctuate significantly during the experiment. However, the Sr/Ca ratios varied widely in the experimental groups (4.47–61.02 mmol/mol; **Table 2**) and were 3.3 times the value in the control group.The Sr/Ca ratios from the core to the edge of the otoliths (0.37–0.57 mm) increased after 1 d after marking and stabilized after 3 d. The distances varied between samples

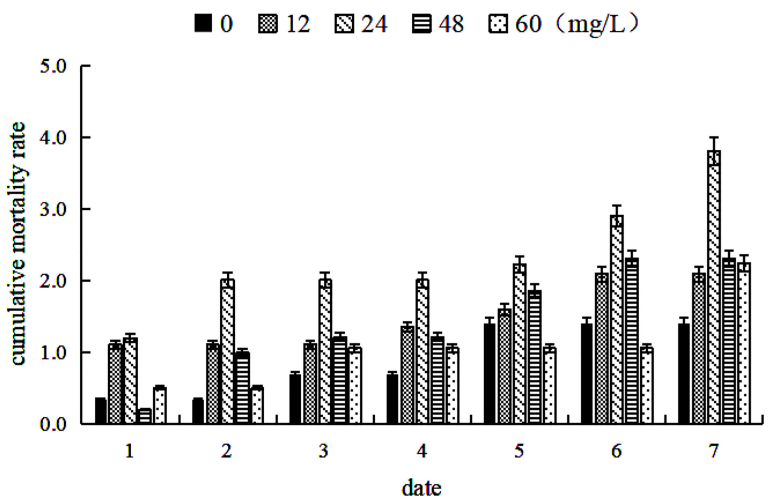


**FIGURE 2** | Cumulative mortality of Coilia nasus larvae in the second phase (cultivation with added strontium for 7 d) with different strontium concentrations. Cumulative mortality refers to the sample death as a percentage of total sample size.

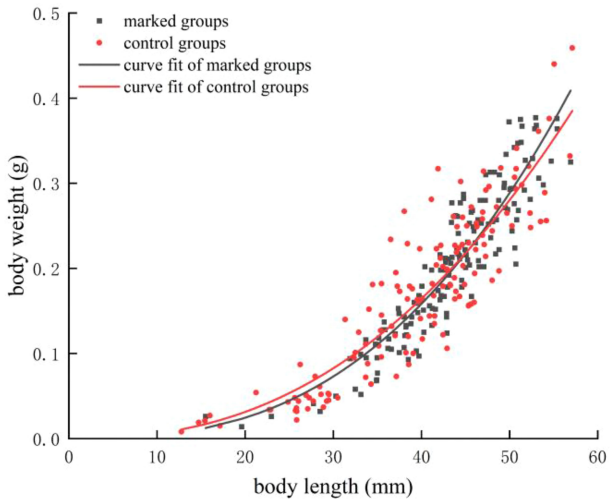


**FIGURE 3** | Body length and body weight of Coilia nasus larvae in the marked and control groups.

because of the difference in the sizes of otoliths (**Figure 4**). In areas with significant differences in Sr/Ca ratios, the ratios increased with increased strontium concentration. There were significant differences in Sr/Ca ratios between experimental and control groups, as indicated by paired sample *t*-tests ($P < 0.01$).

During the third phase, the Sr/Ca ratio in the experimental groups reflected crests with a width of approximately 0.11 mm (0.42–0.54 mm from the edge of otoliths). For the groups cultivated in 12 mg/L strontium for 14, 21, and 28 d, the Sr/Ca ratios were 10.87 ± 5.65, 11.86 ± 6.15, and 12.32 ± 5.44 (mmol/mol), respectively. Subsequently, the ratios returned to baseline levels. The marking rate was significantly higher than the of non-marking rate (**Figure 5**), indicating a 100% success rate of marking by exogenous strontium treatment.

## Changes in the Strontium Content of Fish

The otolith samples were below the minimum weight required for detection with LA-ICP-MS; therefore, we used the whole body as a testing material. Paired sample *t*-tests revealed no significant differences in strontium content in phase one ($P > 0.05$). However, strontium levels increased significantly in the second phase ($P < 0.05$), and then decreased gradually until the end of the treatment period (**Figure 6**). The strontium content in the marking

**TABLE 2** | Sr/Ca ratios in the strontium-marked otoliths of *Coilia nasus* larvae in different treatment groups.

| $Sr^{2+}$ concentration | Sr/Ca ratios in otoliths (mmol/mol) | | |
|---|---|---|---|
| | 1 d | 4 d | 7 d |
| 0 mg/L | 1.78 ± 0.55 | 2.01 ± 0.47 | 2.32 ± 0.48 |
| 12 mg/L | 4.47 ± 0.86 | 11.89 ± 7.68 | 13.47 ± 7.95 |
| 24 mg/L | 7.78 ± 3.36 | 20.36 ± 12.54 | 23.59 ± 13.97 |
| 48 mg/L | 8.20 ± 5.27 | 39.11 ± 26.97 | 61.02 ± 24.02 |
| 60 mg/L | 12.66 ± 6.55 | 43.76 ± 26.72 | 57.63 ± 37.66 |

*Mean ± standard deviation of 150 samples is shown.*

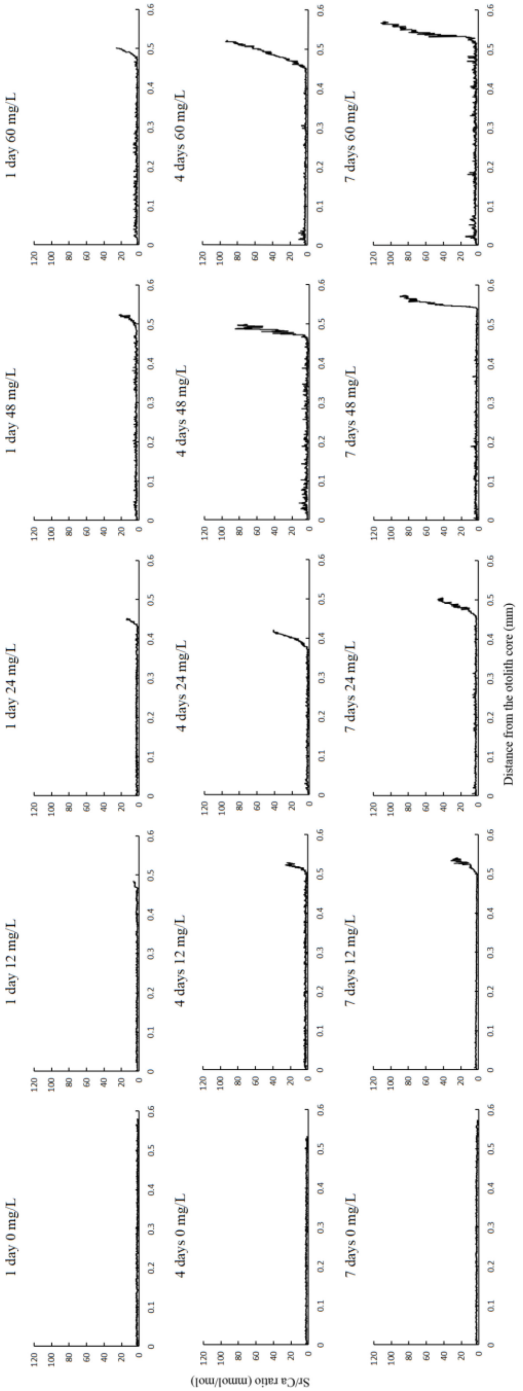


**FIGURE 4** | Fluctuations in strontium-to-calcium (Sr/Ca) ratios along a line transect from the core (0 mm) to the edge of otoliths in Coilia nasus larvae cultivated at different strontium concentrations (0, 12, 24, 48, and 60 mg/L) for 1, 4, and 7 d in the second phase (cultivation with added strontium for 7 d).

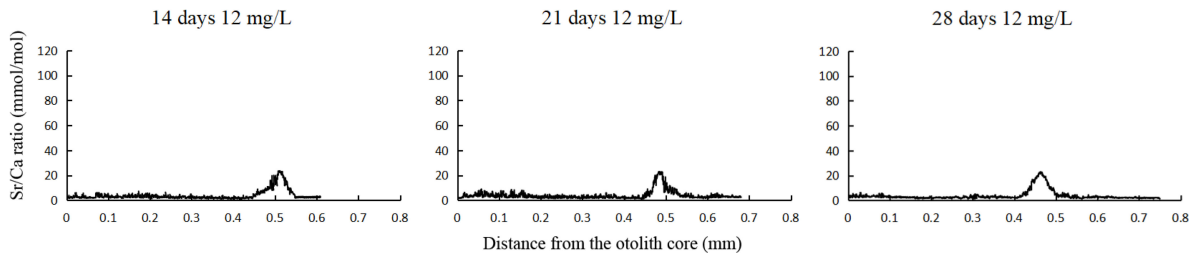


**FIGURE 5** | Fluctuations in Sr/Ca ratios along a line transect from the core (0 mm) to the edge of otoliths in Coilia nasus larvae cultivated under different immersion durations (14, 21, and 28 d) at a 12 mg/L concentration of strontium in the third phase (groups were transferred to water without added strontium for 3 wk).

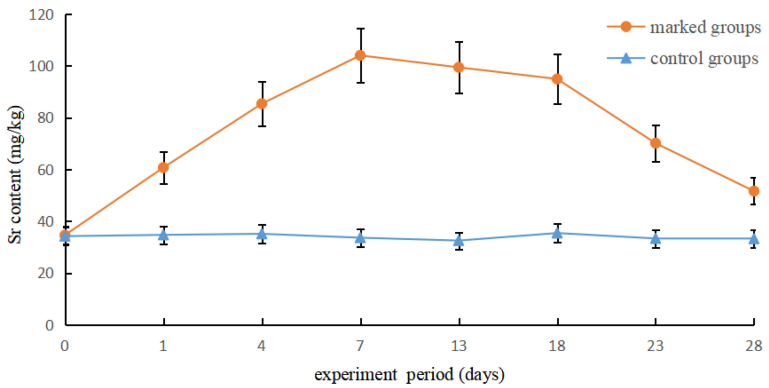


**FIGURE 6** | Variation in Sr concentrations between the marked and control groups of Coilia nasus larvae.

group was approximately twice that of the control group. From 7–28 d, the variation in strontium content fit the following formula:

$$Y = -0.1363x^2 + 2.2174x + 95.095$$

where $x$ represents the experimental period and $y$ axis represents the Strontium levels in the body returned to baseline levels similar to that of the control group at approximately 31 d.

# DISCUSSION

## Feasibility of Strontium Marking in *C. nasus*

Strontium commonly exists in natural water. A literature survey reported that average Sr/Ca ratios (molar ratio) are 2.7 ± 1.5 in freshwater, 5.6 ± 1.1 in estuarine water, and 8.3 ± 4.5 in seawater (Yang et al., 2011). The Environmental Protection Agency (USA) stipulates that the level of strontium ions in standard public drinking water should have an upper limit of 4 mg/L (ATSDR, 2004); in China, the limit is 0.2–5 mg/L. As a necessary trace element, strontium plays an important role in the growth and development of organisms (Buehler et al., 2001; Dahl et al., 2001) by promoting the growth and formation of bone cells and enhancing bone strength (Caverzasio, 2008). Strontium strongly inhibits calcium absorption in the early life stages of fish (Chowdhury and Blust, 2002), and high levels of strontium can cause larval and juvenile mortality in rainbow trout (Birge et al., 1981). Pyle et al. (2002) found that $Sr^{2+}$ ions in the fresh water did not cause substantial mortality in larvae but caused a decline in egg hatching rates. A study on chum salmon showed that $Ca^{2+}$-ATPase activity and growth indices were the highest at a strontium mass concentration of 10 mg/L, and that mortality increased with an increase in $Sr^{2+}$ concentration (Song, 2013). At a strontium mass concentration of 50 mg/L, sedimentation values of an experimental group were 50 times that of the control group (accompanied by a strong marking effect), although the growth and feeding statuses remained unchanged (Wang et al., 2015). These findings indicate that an appropriate concentration of $Sr^{2+}$ can promote the development of fish, whereas outlier values are not conducive to growth. Thus, when exogenous strontium exceeds optimal levels, it affects the enrichment of otolith elements. Different populations exhibit differing ranges of adaptation to strontium. Strontium marks in otoliths were confirmed to exist for at least 20 mo in *C. carpio* (Qiu et al., 2021). In the current study, we evaluated the effects of immersion in concentrations of 0, 12, 24, 48, and 60 mg/L of strontium, nearly 2–10 times the levels found in natural seawater. These concentrations were used because it is usually difficult to distinguish between conditions at release and in the wild. However, the concentrations had no negative effect on the development of fish, indicating that they would not cause a toxic response and were safe and reliable.

## Strontium Marking of Otoliths

To recover from a decline in fishery resources, it is important to develop strategies for stock enhancement and release. Accurately distinguishing between release and catches and evaluating the associated responses have become urgent scientific problems. To this end, several methods have been employed, including marking techniques such as fin-clipping and scutcheon-tagging (Pan et al., 2010). However, these traditional methods often involve a heavy workload, and the markers may fall off or make identification difficult; therefore, these methods are unsuitable for large-scale use.

*Coilia nasus* exhibit high sensitivity and die immediately in the absence of water (Wang, 2015), because of which some common marking methods are inapplicable in this species. Otoliths are used as a natural indicator of the ontogeny of fish, and strontium is a biomarker used to track and reconstruct habitat events (Melancon et al., 2009). Combining these factors provides a new approach for mark–release technologies. Owing to anthropogenic factors that increase the strontium content in water bodies, strontium is expected to be deposited in otoliths. In this study, most of the Sr/Ca ratios measured in the experimental group were 3.3 times the values in the control group. The results of otolith marking with strontium showed that specific peaks were formed under different strontium concentration and immersion duration conditions, with a 100% success rate. A slight curve was detected in Sr/Ca ratios when the concentration was 24 mg/L or after immersion for 1 d. The Sr/Ca ratios were higher on day four than on day one and higher on day seven than on day four. This is because the marking process operated at near capacity for the first 4 d. The fitted function indicates that 4 d is an appropriate duration for marking. Of the various concentrations at which the Sr/Ca ratio could be measured, 12 mg/L strontium was chosen based on economic feasibility. Strontium is a long-lasting trace element that is not lost over time (even during the third phase of this experiment). Accordingly, its persistence is positively correlated with immersion time and concentration. Remarkably, there was no time lag for marking in *C. nasus*, contrary to the results of Qiu et al. (2019a), which can be explained by the different detection principles of the two instruments. However, further studies are needed to test whether its deposition has any lingering effects.

## Effects of Strontium-Enriched Water on Strontium Content in the Body of *C. nasus*

Experimental samples are occasionally caught by fishermen after the large-scale release of marked individuals. Although strontium has low toxicity (Qin and Pan, 2001), it may still cause food safety issues. If the strontium content in the fish body is not fully absorbed and metabolized over time, excessive consumption of strontium may have adverse effects on the physical health of consumers, including nausea, digestive upsets, and other phenomena (Wu, 2012). Therefore, we analyzed the metabolic rate of strontium to avert potential side-effects of marking practices. The levels of $Sr^{2+}$ increased considerably after immersion in 12 mg/L strontium for 7 d, and decreased gradually thereafter (**Figure 5**). Statistical analysis revealed that the strontium levels of marked groups decreased to baseline levels after 24 d. Therefore, we recommend that after large-scale marking, fish should be cultured in natural water to ensure the removal of excess strontium and avoid its side effects.

# CONCLUSION

The paper reported that strontium has little impact on *Coilia nasus* larvae in different marked groups, and strontium can deposit on otoliths stably. Moreover, the level of strontium also toward lower with body's metabolism. Strontium can be used as a natural biomarker to evaluate the effect of stock enhancement. According to the strontium marking of otoliths in the early stages, the released populations can be identified through mark-recapture, and the length of released fish can be determined according to the growth equation. The ratio of strontium and calcium can be used to distinguish wild fish from the released population. The effect of the release can be analyzed according to the recapture rate; for rapidly declining fish species, this method can be used to artificially increase stock.

# DATA AVAILABILITY STATEMENT

The original contributions presented in the study are included in the article/supplementary material. Further inquiries can be directed to the corresponding author.

# ETHICS STATEMENT

The animal study was reviewed and approved by Zhejiang Marine Fisheries Research Institute.

# AUTHOR CONTRIBUTIONS

M-ZL wrote the paper; HZ performed the experiment; FY helped with the analysis and discussions; X-FL assisted in the experiment; G-PF coordinated the sampling; RY adjusted and tested equipment; FC offered technical support; R-jJ contributed to the conception of the study. All authors contributed to the article and approved the submitted version.

# FUNDING

This study was supported by grants from the Chinese Ministry of Science and Technology through the National Key Research and Development Program of China (2020YFD0900805), and the Public Welfare Technology Application Research Project of Zhejiang Province (LGN20C190012).

# ACKNOWLEDGMENTS

We thank HZ and the technical staff of the East China Sea Fisheries Research Institute of the Chinese Academy of Fishery Sciences, who assisted with LA-ICP-MS analyses.

## REFERENCES


Agency for Toxic Substances and Disease Registry (ATSDR) (2004) *Toxicological Profile for Strontium* (Atlanta: US Department of Health and Human Services, Public Health Service). Available at: https://wwwn.cdc.gov/TSP/ToxProfiles/ToxProfiles.aspx?id=656&tid=120 (Accessed May 4, 2022).

Birge, W. J., Black, J. A., and Ramey, B. A. (1981). "The Reproductive Toxicology of Aquatic Contaminants," in *Hazard Assessment of Chemicals: Current Developments*. Eds. J. Saxena and F. Fisher (New York: Academic Press), 59–115.

Buehler, J., Chappuis, P., Saffar, J. L., Tsouderos, Y., and Vignery, A. (2001). Strontium Ranelate Inhibits Bone Resorption While Maintaining Bone Formation in Alveolar Bone in Monkeys (*Macaca Fascicularis*). *Bone.* 29, 176–179. doi: 10.1016/s8756-3282(01)00484–7

Caverzasio, J. (2008). Strontium Ranelate Promotes Osteoblastic Cell Replication Through at Least Two Different Mechanisms. *Bone.* 42, 1131–1136. doi: 10.1016/j.bone.2008.02.010

Chowdhury, M. J., and Blust, R. (2002). Bioavailability of Waterborne Strontium to the Common Carp, *Cyprinus Carpio*, in Complexing Environments. *Aquat. Toxicol.* 58, 215–227. doi: 10.1016/S0166–445X(01)00230–2

Dahl, S. G., Allain, P., Marie, P. J., Mauras, Y., Boivin, G., and Ammann, P. (2001). Incorporation and Distribution of Strontium in Bone. *Bone.* 28, 446–453. doi: 10.1016/s8756–3282(01)00419–7

He, J., Gu, X. H., and Zhang, X. Z. (2011). Study on Structural Characteristics and Driving Mechanism of Natural Fishery in Taihu Lake. *J. Jiangsu. Agric. Sci.* 39, 287–291. doi: 10.3969/j.issn.1002-1302.2011.03.116

Li, X. Q., Cong, X. R., and Shi, J. H. (2017). Feasibility Analysis of Releasing Individuals of *Aristichthys Nobilis* Identification Based on Otolith Sr Markers. *J. Lake. Sci.* 29, 914–922. doi: 10.18307/2017.0415

Liu, K., Duan, J. R., Zhang, M. Y., Fang, D. A., Shi, D. A., and Shi, W. G. (2012). Present Situation of *Coilia Nasus* Population Features and Yield in Yangtze River Estuary Waters in Fishing Season. *Chin. J. Ecol.* 12, 3138–3143. doi: 10.13292/j.1000-4890.2012.0407

Melancon, S., Fryer, B. J., and Markham, J. L. (2009). Chemical Analysis of Endolymph and the Growing Otolith: Fractionation of Metals in Freshwater Fish Species. *Environ. Toxicol. Chem.* 28, 1279–1287. doi: 10.1897/08–358.1

Nielsen, L. A. (1992). *Methods of Marking Fish and Shellfish* (New York: American Fisheries Society Special Publication).

Pan, X. W., Yang, L. L., Ji, L. L., and Liu, Z. L. (2010). Research Progress on Technique of Fish Stock Enhancement. *Jiangsu. Agric. Sci.* 4, 263–240. doi: 10.15889/j.issn.1002-1302.2010.04.151

Pollard, M. J., Kingsford, M. J., and Battaglene, S. C. (1999). Chemical Marking of Juvenile Snapper, *Pagrus Auratus* (Sparidae), by Incorporation of Strontium Into Dorsal Spines. *Fish. Bull.* 97, 118–131.

Pyle, G. G., Swanson, S. M., and Lehmkuhl, D. M. (2002). Toxicity of Uranium Mine Receiving Waters to Early Life Stage Fathead Minnows (*Pimephales Promelas*) in the Laboratory. *Environ. Pollut.* 116, 243–255. doi: 10.1016/s0269–7491(01)00130–0

Qin, J. F., and Pan, W. Q. (2001). Limited Amount Index of Sr in Drinking Nature Mineral Water. Guangdong Trace Elem. *Science* 1, 16–23. doi: 10.16755/j.cnki.issn.1006-446x.2001.01.003

Qiu, C., Jiang, T., Chen, X. B., Liu, H. B., and Yang, J. (2019a). Characteristics of Otolith Strontium Marking and its Time Lags of Larval *Cyprinus Carpio*. *Oceanologia. Limnol. Sin.* 50, 903–912.

Qiu, C., Jiang, T., Chen, X. B., Liu, H. B., and Yang, J. (2019b). Effectiveness of Otolith Strontium Marking for Juvenile *Cyprinus Carpio*. *Chin. J. Appl. Ecol.* 30, 2093–2100. doi: 10.13287/j.1001–9332.201906.027

Qiu, C., Jiang, T., Chen, X. B., Liu, H. B., and Yang, J. (2021). Persistence Evaluation of Strontium Marking on Otoliths in Larvae Common Carp (*Cyprinus Carpio*). *Hubei. Agric. Sci.* 60, 114–117. doi: 10.14088/j.cnki.issn0439-8114.2021.08.023

Schroder, S. L., Volk, E. C., and Hagen, P. (2001). Marking Salmonids With Strontium Chloride at Various Life History Stages. *NPAFC. Tech. Rep.* 3, 9–10.

Song, H. J. (2013). *Allometric Growth of Chum Salmon Larvae and Effects of Strontium on Physiological Indices of Their Juveniles* (Harbin, IL: Northeast Agricultural University).

Wang, Y. (2015). *Effects of Acute Handling Stress on Coilia Nasus. [Master's Thesis]* Hainan (IL: University of Hainan). doi: 10.13287/j.1001-9332.20150921.033

Wang, C., Liu, W., Zhan, P. R., Wang, J. L., and Li, P. L. (2015). Exogenous Sr2+ Sedimentation on Otolith of Chum Salmon Embryos. *Chin. J. Appl. Ecol.* 26, 3189–3194.

Warren–Myers, F., Dempster, T., Fjelldal, P. G., Hansen, T., Jensen, A. J., and Swearer, S. E. (2014). Stable Isotope Marking of Otoliths During Vaccination: A Novel Method for Mass-Marking Fish. *Aquacult. Environ. Interact.* 5, 143–154. doi: 10.3354/aei00103

Wu, M. J. (2012). The Relationship Between Strontium and Human Health. *Stud. Trace Elem. Health* 29, 66–67. doi: 10.3969/j.issn.1005-5320.2007.01.030

Yang, J., Jiang, T., and Liu, H. (2011). Are There Habitat Salinity Markers of the Sr: Ca Ratio in the Otolith of Wild Diadromous Fishes? A Literature Survey. *Ichthyol. Res.* 58, 291–294. doi: 10.1007/s10228–011–0220–8

Yang, X. J., Pan, X. F., Chen, X. Y., Wang, X. A., Zhao, Y. P., and Li, J. Y. (2013). Overview of the Artificial Enhancement and Release of Endemic Freshwater Fish in China. *Zool. Res.* 34, 267–280. doi: 10.11813/j.issn.0254–5853.2013.4.0267

Yan, C. M., Zheng, W., and Zhang, Y. B. (2015). Study on Germplasm Identification and Resource Restoration of *Cyprinus Carpio* Linnaeus. *Fish. Sci. Technol. Inf.* 42, 30–35. doi: 10.16446/j.cnki.1001-1994.2015.01.007

Yuan, C. M. (1988). Changes of Resources and Population Composition of *Coilia Nasus* in the Middle and Lower Reaches of the Yangtze River and its Causes. *J. Zool.* 03, 12–15. doi: 10.13859/j.cjz.1988.03.005

Zhan, B. Y. (1995). *Fisheries Stock Assessment* (Beijing: China Agriculture Press).

Zhang, Y., Jiang, Y. Z., Xu, K. D., Jiang, H. L., Jiao, H. F., Zhang, H., et al. (2018). Evaluation on Effectiveness of Marking Juvenile Sparus Macrocephalus Otoliths With Strontium. *Mar. Fish.* 40, 171–178. doi: 10.3969/j.issn.1004-2490.2018.02.006

Zhang, H., Jiang, Y. Z., Yuan, X. W., Zhang, Y., Jiang, H. L., Jiao, H. F., et al. (2019). Effects of Strontium-Enriched Water on Strontium Content in the Otolith and Body of Hatchery–Reared *Larimichthys Crocea*. *Mar. Fish.* 41, 338–345. doi: 10.13233/j.cnki.mar.fish.2019.03.009

Zhang, Y., Li, Y. X., Xu, X. M., Huang, J. H., Gao, Y. S., Xu, H., et al. (2013). Effects of Environmental Factors on Otolith Sr Incorporation in Juvenile *Larimichthys Crocea*. *Mar. Fish.* 35, 278–288. doi: 10.3969/j.issn.1004-2490.2013.03.004

Zhang, M. Y., Xu, D. P., Kai, L., and Shi, W. G. (2005). Studies on Biological Characteristics and Change of Resource of *Coilia Nasus* Schlegel in the Lower Reaches of the Yangtze River. *Resour. Environ. Yangtze. Basin.* 6, 22–26. doi: 10.3969/j.issn.1004-8227.2005.06.005


**Conflict of Interest:** The authors declare that the research was conducted in the absence of any commercial or financial relationships that could be construed as a potential conflict of interest.

frontiers | Frontiers in Marine Science

ORIGINAL RESEARCH
published: 09 June 2022
doi: 10.3389/fmars.2022.865645

# Estimating the Impact of a Seasonal Fishing Moratorium on the East China Sea Ecosystem From 1997 to 2018

*Lingyan Xu[1,2†], Puqing Song[2†], Yuyu Wang[3], Bin Xie[2], Lingfeng Huang[4], Yuan Li[2], Xinqing Zheng[2,5*] and Longshan Lin[2*]*

*[1] College of Marine Sciences, Shanghai Ocean University, Shanghai, China, [2] Third Institute of Oceanography, Ministry of Natural Resources, Xiamen, China, [3] School of Ecology and Nature Conservation, Beijing Forestry University, Beijing, China, [4] College of the Environment and Ecology, Xiamen University, Xiamen, China, [5] Observation and Research Station of Island and Coastal Ecosystems in the Western Taiwan Strait, Ministry of Natural Resources, Xiamen, China*

OPEN ACCESS

**Edited by:**
*Jun Xu,*
*Institute of Hydrobiology (CAS), China*

**Reviewed by:**
*Zhongxin Wu,*
*Dalian Ocean University, China*
*Chongliang Zhang,*
*Ocean University of China, China*

***Correspondence:**
*Xinqing Zheng*
*zhengxinqing@tio.org.cn*
*Longshan Lin*
*lslin@tio.org.cn*

*[†]These authors have contributed equally to this work and share first authorship*

**Specialty section:**
*This article was submitted to Marine Ecosystem Ecology, a section of the journal Frontiers in Marine Science*

**Received:** *30 January 2022*
**Accepted:** *20 April 2022*
**Published:** *09 June 2022*

**Citation:**
*Xu L, Song P, Wang Y, Xie B, Huang L, Li Y, Zheng X and Lin L (2022) Estimating the Impact of a Seasonal Fishing Moratorium on the East China Sea Ecosystem From 1997 to 2018. Front. Mar. Sci. 9:865645. doi: 10.3389/fmars.2022.865645*

Fisheries management policies (FMPs) have been implemented in coastal countries to ensure a sustainable supply of seafood and the recovery of species diversity. Because of the depletion of fishery stocks, China has introduced a series of FMPs since 1995, including a seasonal fishing moratorium (SFM), a zero-growth strategy, and a minimum mesh size for fishing nets. Here, we built two mass balance models for 1997–2000 (M1997) and 2018–2019 (M2018) using Ecopath with Ecosim 6.6 to illustrate the interannual changes over the past two decades in the East China Sea (ECS). We then simulated two dynamic scenarios from 1997 to 2018, SFM ($M2018_{SFM}$) and no SFM ($M2018_{no\text{-}SFM}$), to test the role of the SFM under fishing pressure in the ECS. Ecopath showed that the ECS ecosystem is becoming more mature, although it is still unstable, featuring lower total primary production/total respiration, longer cycles, faster organic material circulation speed, and a higher omnivorous degree. This suggests a slow recovery for the ECS ecosystem in the past two decades. The biomass of fish in the ECS—especially the planktivores, dominated by small-sized *Benthosema pterotum*—significantly increased in M2018 versus M1997, but there were fewer medium- and large-sized fish. The keystone species switched from the planktivores/piscivores dominated by *Decapterus maruadsi* in M1997 to planktivores in M2018. Ecosim illustrated that the SFM has positive effects on fishery resources recovery, especially for commercial fishes (i.e., large yellow croakers and hairtails), as reflected by the significantly higher predicted biomass of fish in $M2018_{SFM}$ compared to $M2018_{no\text{-}SFM}$ and M1997, although the bioaccumulation was consumed by the intense fishing pressure after the SFM. However, the $M2018_{SFM}$ prediction for nektons was still lower than the actual value, especially for planktivores, which display a sharp increase in biomass. This should be partly attributable to the policy of the minimum mesh size (<5 cm was banned), which benefits *B. pterotum* due to its 3.5 cm maximum body size. Therefore, a series of FMPs,

rather than only the SFM, functioned together in the ECS ecosystem. However, the mixed trophic impact indicated a negative impact if the fisheries were further developed. Fishery management in the ECS needs to be strengthened by extending the SFM and reducing fishing pressure after the SFM.

**Keywords: Ecopath with Ecosim, East China Sea, seasonal fishing moratorium, commercial fish, fisheries management policies**

# 1 INTRODUCTION

Aquatic products are a primary protein source for humans (Lira et al., 2021). As such, global marine capture production had reached 92.51 million tons by 2017, with an average increase of 10-fold relative to 1950, resulting in the catch per unit effort declining by 50% to 80% (Zhou et al., 2015; Link and Watson, 2019). Therefore, to ensure a sustainable supply of seafood and the recovery of species diversity, fisheries management policies (FMPs) such as total allowable catches, individual transferable quotas, seasonal and area closures, and stock assessments have been widely implemented by coastal countries (Bromley, 2005; Fulton et al., 2014). Similarly, China has introduced a series of FMPs since 1995 that include zero and minus growth targets, a seasonal fishing moratorium (SFM), a minimum mesh size for fishing nets, and a minimum catch size for fishing targets (Cao et al., 2017). There has also been a ban on destructive fishing methods, the construction of artificial fish reefs, and the release of some commercial fish (i.e., *Larimichthys crocea*) to restore the disturbed marine ecosystem (Han, 2018; Xin et al., 2020).

Fisheries management policies (FMPs) have received considerable critical attention for their protective effect on resource recoveries. Many studies have reported the positive effects of FMPs. For example, Yue et al. (2015) found that after the SFM, the catch increased in the East China Sea (ECS) and the South China Sea. Wang et al. (2020) found that the reduction of fishermen, fishing vessels, and catches all had a positive effect on the recovery of fishery stocks in the Pearl River Delta. Lee and Midani (2014) also showed that the catch per unit effort of sandfish nearly doubled from 2005 to 2011 in the East Sea of Korea after the implementation of a fishing stock-rebuild plan. However, some studies have found that the effectiveness of these fishery strategies had a spatiotemporal limit. Yan et al. (2019a) concluded that in the ECS, the accumulation of biomass during the SFM was rapidly removed by the subsequent intense fishing pressure. In addition, the Fujian fishery statistical yearbook shows that the landing of large yellow croaker (*L. crocea*) has been maintained at a low level since 2000, although millions of *L. crocea* larvae have been released (Wu et al., 2021). Di Franco et al. (2009) also reported no differences in the fish assemblages between partially protected areas and a location outside the marine protected area in northeast Sardinia (Italy).

The ECS is one of the most important fishing areas, providing about 40% of the total catch in China (Zhang et al., 2018). In the 1990s, the number of fishing vessels in this region exceeded 100,000 and accounted for nearly half of the total fishing vessels in the China Sea (Shi, 1995). Under such intense fishing pressure, the ECS ecosystem had already been overloaded. Many traditional commercial fish stocks such as the large yellow croaker were exhausted, and the length of the fishing season has declined in some fishing grounds (Liu et al., 2012; Mei, 2019; Xu et al., 2021). Similarly, much uncertainty remains about whether the FMPs in the ECS work in the long term. For the ECS ecosystem, FMPs such as the minimum mesh size (Tokai et al., 2019), zero and minus growth targets (Ye and Rosenberg, 1991), SFM (Cheng et al., 2004), and release enhancement (Lü et al., 2008) have been recognized to be the major drivers rebuilding the fishery resources (Shih et al., 2009; Shen and Heino, 2014; Zhou et al., 2019). However, the previous evaluations of FMPs in the ECS have been focused at the short-term (Yan et al., 2019b), single-policy (Liu and Cheng, 2015; Yue et al., 2015), or species level (Xu and Liu, 2007) rather than at the long-term, multiple-policy, or ecosystem level. Therefore, whether or not FMPs, especially the SFM and reduced fishing pressure, drove the variances in the structure and function of the ECS ecosystem over the last 20 years needs to be further verified.

Ecopath with Ecosim (EwE), a widely used tool to support ecosystem-based fisheries management, prioritizes the ecosystem rather than a single species population (Pikitch et al., 2004; Halpern et al., 2008; Surma et al., 2019; Reum et al., 2021), and it can explore the long-term performances of multiple FMPs under different scenarios (Li, 2009; Russo et al., 2017; Papapanagiotou et al., 2020; Wang et al., 2020; Paradell et al., 2021). Therefore, to verify the hypothesis on FMPs' effects, this work attempted to estimate the interannual variation of the ECS ecosystem from 1997 to 2018 with EwE and explored the long-term effects of the SFM under the actual fishing pressures present during the two decades. We constructed two mass balance models for 1997–2000 (referred to as M1997) and 2018–2019 (referred to as M2018) in the ECS, to depict the variation in the ecosystem's structure and function over the past two decades. We further conducted scenario simulations based on the M1997 model to evaluate the contribution of the SFM under fishing pressure to the variations of the ECS ecosystem during the two decades. These results reveal the combined effects of the SFM and fishing pressures on the rehabilitation of the structure and function of the ECS ecosystem and offer advice on the management of fishery resources in the ECS for governmental policymakers.

# 2 MATERIALS AND METHODS

## 2.1 Study Area

The ECS is located in the western Pacific Ocean and is connected with the Sea of Japan through the Tsushima Strait and with the

South China Sea through the Taiwan Strait (**Figure 1**; Li and Zhang, 2012). It is influenced by the Kuroshio Current and dilute water from the Yangtze River. The ECS is one of the most productive regions globally, leading to many important fishing grounds such as the Zhoushan and Minzhong (Liu, 2013). The ECS has experienced three periods associated with dramatically increased fishing equipment and changes in fishing methods: slow growth (1951 to the 1990s), rapid growth (1991 to the 2000s), and high yield (after the 2000s; Chen et al., 1997; Mei, 2019). High-intensity fishing pressure has brought immense economic benefits, but it has also driven a great change in the catch composition from the ECS (Chen et al., 2004).

The SFM, which can offer a suitable time for adult spawning and larvae growth, is considered the utmost protection to rebuild fish stocks (Su et al., 2019). Initially, it was implemented in the northern ECS (27°N to 35°N) from 1 June to 31 August in 1995. During this period, only the trawl and sailing nets were banned. In 2017, all fishing gear with the exception of hooks and lines was banned in the ECS from noon on 1 May to noon on 16 September (Yan et al., 2019a). A minimum mesh size for nets was implemented in 2004 to protect recruitment. In 2017, the Ministry of Agriculture and Rural Affairs announced a minimum allowable size for 15 marine economic fish species. A series of FMPs were also introduced to reduce the fishing pressure, including zero and minus growth targets, a licensing system, a vessel buyback program, dual control, and a fishermen relocation program. The Ministry of Agriculture designed the zero and minus growth system in 1999 and the fishing quota management system based on the maximum sustainable yield in 2000. In 2017, species quota fishing was implemented in the Zhejiang and Shandong provinces (Mei, 2019). The licensing system, vessel buyback program, dual control, and fishermen relocation program were also implemented after 2002 (Cao et al., 2017).

## 2.2 Ecopath Model Construction and Parameterization

Ecopath offers a static snapshot that reflects the structure and function of the ecosystem at a specific time. The Ecopath model is based on a set of linear equations for each function group in the system. It is formed by the food consumption equation and energy theory (Polovina, 1984; Ulanowicz, 1986). Ecopath needs the following input parameters: biomass (B), the production/biomass ratio (P/B), the consumption/biomass ratio (Q/B), diet composition (DC), and ecotrophic efficiency (EE). Usually, only three of the four groups of parameters need to be entered, and the model can then automatically obtain the fourth parameter. The EE is difficult to obtain, and thus, the other three parameters are usually entered (Christensen et al., 2005).

The basic equation is

$$B_i \cdot (P/B)_i = \sum_{j=1}^{n} B_j \cdot (Q/B)_j \cdot DC_{ji} + (P/B)_i \cdot B_i \cdot (1 - EE_i) + Y_i + E_i + BA_i,$$

where $(P/B)_i$ and $B_i$ are the production/biomass ratio and biomass of group $i$, respectively; $(Q/B)_j$ is the consumption/biomass ratio of group $j$, $DC_{ji}$ is the proportion of the diet that

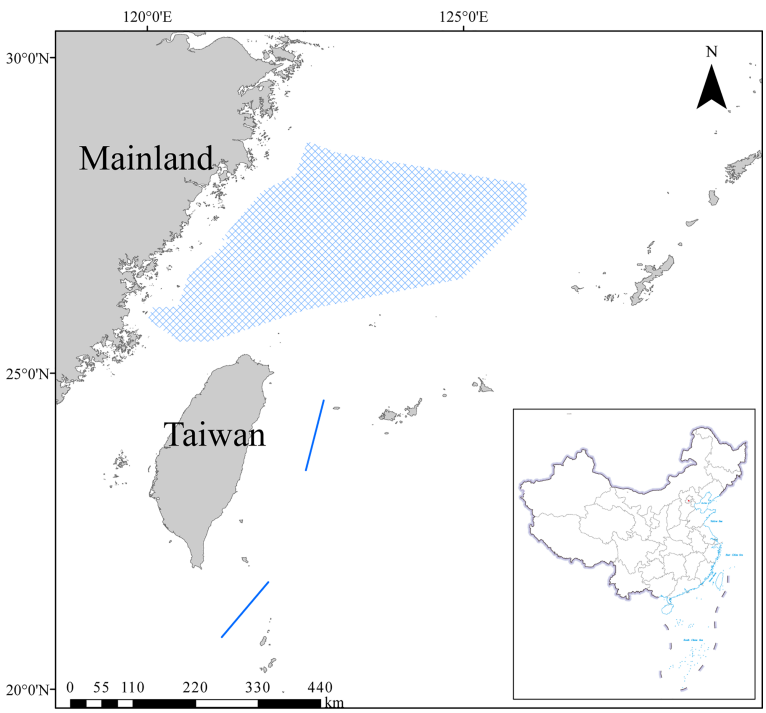


**FIGURE 1** | The study area in the East China Sea.

predator group $i$ obtains from prey group $j$, $EE_i$ is the ecotrophic efficiency, $B_i$ (1 - $EE_i$) is other mortality, $Y_i$ is the catch of group $i$, $E_i$ is the net migration of group $i$, and $BA_i$ is the biomass accumulation rate for $i$.

To simplify the trophic structure of the ecosystem, species with a similar ecological niche were aggregated in one function group (Christensen et al., 2005). The function group can also be composed of a single species or the different age structures of a species (Zheng et al., 2020; Lin et al., 2021). There were 24 function groups in the ECS ecosystem, including phytoplankton, zooplankton, polychaetes, mollusks, benthic crustaceans, echinoderms, other invertebrates, crabs, shrimps, cephalopods, planktivores, benthivores, piscivores, planktivores/piscivores, planktivores/benthivores, benthivores/piscivores, omnivores, sharks, marine mammals, and detritus (**Table S1**). In addition, large yellow croakers, small yellow croakers, hairtails, and Bombay duck were treated as separate function groups due to their high economic values and resources.

The biomass data were collected from field surveys and published literature. Data for the first model was from a 1997–2000 marine living resources supplementary survey and resource evaluation. The second model data were from a joint survey in the ECS in the autumn of 2018 and the spring of 2019. The P/B and Q/B values were obtained using empirical equations and from published literature (Palomares and Pauly, 1989; Pauly et al., 1990; Christensen et al., 2005; Cheng et al., 2009; OuYang and Guo, 2010; Li and Zhang, 2012). The diet data were estimated based on stomach content analyses in the published literature (**Tables S2**, **S3**). The food matrix of the function groups was calculated based on the biomass weight of each species in the function group. We used similar diet matrices in the M1997 and M2018 models but made slight changes in several groups, e.g., hairtails, piscivores, and planktivores. Information on catch was obtained from the China Fishery Statistical Yearbook (CFSY), but there was no discard data in the two models due to a lack of data.

### 2.2.1 Ecological Indicators

Ecological indicators, which can be used as measures to assess ecosystem status, are included and presented along with other Chinese models and models at similar latitudes. The Finn's cycling index indicates the speed of organic material circulation in the ecosystem, and the mean path length represents the total number of trophic links divided by the number of pathways (Finn, 1976; Christensen et al., 2005). The connectivity index reveals the interaction between species in terms of predation, and the system omnivory index (SOI) is defined as the average omnivorous degree of the consumers (Nee, 1990; Pauly and Christensen, 1993). These indicators are linked with the maturity of the ecosystem (Ulanowicz, 2012). Total system throughput (TST) sums all flows in this model according to Ulanowicz (2012). Mixed trophic impact (MTI) can reveal a direct or indirect influence of one function group on another function group, which can explain the relationship between groups in the ecosystem (Ulanowicz and Puccia, 1990). The keystone index can identify the key species of the ecosystem by selecting indexes greater than zero. The keystones play a primary role in maintaining stability and complexity and have a disproportionate impact on biomass (Libralato et al., 2006).

### 2.2.2 Model Balance and Sensitivity Analysis

After all data were input, the EE should be below 1, and most of the gross efficiency values should be between 0.1 and 0.3, with the exception of some fast-growing organisms (Christensen et al., 2005). Pedigree and a sensitivity analysis were used to verify the reliability of the model. The pedigree can mark the source and calculate the credibility of the input data (Majkowski, 1982; Funtowicz and Ravetz, 1990). It is also the reference used to adjust the parameters of the model. The parameter with the lowest confidence would thus be adjusted when the model is unbalanced (Funtowicz and Ravetz, 1990). The sensitivity analysis can evaluate the uncertainty of the output data of the model when the input data fluctuate. The sensitive analysis routine was set to ±20% uncertainty for all input parameters (Han et al., 2017).

## 2.3 Dynamic Simulation

The Ecosim model conducts a temporal dynamic analysis with key original parameters from the Ecopath model, which is used as a reference to estimate changes in the biomass of function groups driven by time series data (Christensen et al., 2005). In the modeling framework, a series of differential equations that consider predator–prey interactions and foraging behaviors inherent to Ecopath can be expressed as follows (Christensen et al., 2005):

$$dB_i/dt = (P/Q)_i \sum_j Q_{ji} - \sum_j Q_{ij} + I_i - (M_i + F_i + e_i)B_i,$$

where $dB_i/dt$ is the change in the biomass of group $i$ over time, $(P/Q)_i$ is the net growth efficiency, $M_i$ is the non-predation mortality rate, $F_i$ is the fishing mortality rate, $e_i$ is the emigration rate, $I_i$ is the immigration rate, $B_i$ is the biomass of group $i$, $\Sigma_j Q_{ji}$ is the total consumption rate by group $i$, and $\Sigma_j Q_{ij}$ is the predation by all predators on the same group $i$.

The Ecosim incorporated historical data, including biomass, catches, and fishing mortalities for different function groups to facilitate accurate model predictions. The partial biomass time series calculated for hairtails, small yellow croakers, and piscivores were derived from the SAU database (http://www.seaaroundus.org/). For most nektonic groups, the time series on absolute biomass, catch, and fishing mortalities were obtained from the CFSY and China's offshore marine comprehensive survey and evaluation project. The time series Chl-*a* was from the dataset of Aqua MODIS and SeaWiFS and was used to calibrate primary production anomalies. Once the time series data (**Table S4**) were included in the model, the fit model with the lowest Akaike information criterion value was selected (Burnham and Anderson, 2004). The vulnerabilities ($v$), which represent the impacts of predator biomass for a given prey, are an important parameter in the process of model fitting to time series data (Christensen et al., 2005). To reduce human error and obtain actual $v$ in the calibrating process, the automated "stepwise fitting" procedure was used (Scott et al., 2016).

As mentioned, a series of FMPs have been implemented in the ECS since the 1990s (Cao et al., 2017). However, in this study, we

only evaluated the impacts of the SFM under actual fishing pressure (**Figure S1**) on the recovery of fishery resources. Then, two Ecosim models that did or did not integrate the SFM under the actual fishing pressures were built, which are expressed by $M2018_{SFM}$ and $M2018_{no\text{-}SFM}$. Because the annual landing in Zhoushan (Zhejiang province) can account for 20~40% of the total landing in the ECS (http://zstj.zhoushan.gov.cn/)—there was significant correlation for landing between the ECS and Zhoushan ($r = 0.628$, $p < 0.05$)—the relative fishing effort of every month in the ECS was assumed to be consistent with that in the Zhoushan in $M2018_{SFM}$. In addition, we also employed the fleet data in Global Fishing Watch (https://globalfishingwatch.org/data-download/datasets/public-fishing-effort) to fit the actual fishing effort in the ECS (**Table S5**), whereas the fishing effort of every month in a year was assumed to be the same in the $M2018_{no\text{-}SFM}$ model. Although a minimum mesh size could be beneficial to the juveniles of nektonic groups by selecting suitable lengths for the species (Heikinheimo et al., 2006; Nguyen et al., 2021), the model cannot load this policy due to the lack of body length distribution data for the kinds of function groups. Climate change was considered to affect the physiology, distribution, and biomass of the marine species and alter the community composition of the marine ecosystems (Cheung et al., 2013; Kroeker et al., 2013; Zeng et al., 2019). However, it was negligible from 2000 to 2018 in this study, as shown by Zeng et al. (2019) in the Pearl River estuary, where the non-producer biomass decreased by only 5% from 2000 to 2060. Therefore, the variants for climate change (seawater surface temperature, pH, and dissolved oxygen) were not included in the two Ecosim models.

# 3 RESULTS

## 3.1 Quality of the Ecopath Model and the Sensitivity Analysis

The basic data and output results for M1997 and M2018 are shown in **Table 1**. Except for the plankton and high-trophic groups, the EE of most function groups was close to 1, suggesting that there was a high utilization rate of most groups in the ECS. The gross efficiency was almost in the 0.1–0.3 range. Finally, the pedigrees of the two Ecopath models were both 0.497, which is a reasonable interval; 0.16–0.68 is the range of pedigrees for most EwE models (Morissette, 2007), indicating that the quality of our Ecopath models was acceptable.

A sensitivity analysis was used to evaluate the influence of the variation in input data on the output results. A similar pattern was observed in the two models (**Figure 2**). The biomass of the function groups appeared to be the most influential parameter, with a range of ±30%. The diet appeared to be the least influential parameter on the two balanced models, which is consistent with observations by Han et al. (2017). This further indicated that adjusting the food matrix had the lowest impact on the overall model output.

## 3.2 The 20-Year Change in the East China Sea Ecosystem

The flow diagram for the ECS showed similar trophic levels (TLs) during the two periods, from 1.00–4.05 and 1.00–4.24 in M1997 and M2018, respectively (**Table 1** and **Figure S2**). The mean TLs of caught fishes showed a slight increase, from 3.11 in M1997 to 3.33 in M2018. Transfer efficiency was 10.56% in the M2018

**TABLE 1** | Input and output (bold) parameters for the East China Sea ecosystem mass balance models M1997 (1997–2000) and M2018 (2018–2019).

| Groups | TL | | B (t/km$^2$/year) | | P/B (/year) | | Q/B (/year) | | EE | |
|---|---|---|---|---|---|---|---|---|---|---|
| | M1997 | M2018 | M1997 | M2018 | M1997 | M2018 | M1997 | M2018 | M1997 | M2018 |
| 1. Phytoplankton | **1.000** | **1.000** | 16.52 | 43.20 | 170.7 | 82.75 | – | – | **0.205** | **0.411** |
| 2. Zooplankton | **2.000** | **2.000** | 4.703 | 12.82 | 40.00 | 40.00 | 160.0 | 160.0 | **0.308** | **0.274** |
| 3. Polychaetes | **2.000** | **2.000** | 3.130 | 1.841 | 6.700 | 6.700 | 24.20 | 24.20 | **0.541** | **0.462** |
| 4. Mollusks | **2.169** | **2.169** | 9.510 | 0.343 | 3.000 | 3.000 | 7.000 | 7.000 | **0.300** | **0.957** |
| 5. Benthic Crustaceans | **2.161** | **2.151** | 1.600 | 1.530 | 6.560 | 6.560 | 26.90 | 26.90 | **0.748** | **0.955** |
| 6. Echinoderms | **2.220** | **2.212** | 3.460 | 6.427 | 1.200 | 1.200 | 3.700 | 3.700 | **0.182** | **0.232** |
| 7. Other invertebrates | **2.000** | **2.000** | 3.160 | 1.359 | 1.000 | 2.000 | 9.000 | 9.000 | **0.616** | **0.795** |
| 8. Crabs | **2.322** | **2.334** | 0.143 | 0.0534 | 4.500 | 4.500 | 12.00 | 12.00 | **0.916** | **0.996** |
| 9. Shrimps | **2.314** | **2.314** | 0.161 | 0.288 | 5.100 | 5.100 | 19.20 | 19.20 | **0.999** | **0.998** |
| 10. Cephalopods | **2.818** | **2.955** | 0.549 | 0.894 | 3.000 | 3.000 | 10.00 | 10.00 | **0.984** | **0.946** |
| 11. Planktivores | **2.953** | **2.919** | 0.710 | 4.701 | 3.588 | 4.762 | 14.74 | 22.30 | **0.998** | **0.979** |
| 12. Benthivores | **2.848** | **2.876** | 0.0397 | 0.278 | 2.116 | 2.156 | 7.176 | 8.497 | **0.995** | **0.965** |
| 13. Piscivores | **3.571** | **3.940** | 0.348 | 0.275 | 2.130 | 1.643 | 6.868 | 6.160 | **0.804** | **0.324** |
| 14. Hairtails | **3.169** | **3.369** | 1.336 | 3.369 | 1.104 | 2.900 | 6.467 | 5.600 | **0.998** | **0.338** |
| 15. Bombay duck | **2.905** | **3.420** | 0.110 | 1.497 | 2.120 | 2.120 | 8.964 | 6.190 | **0.956** | **0.953** |
| 16. Planktivores/Benthivores | **2.958** | **2.964** | 0.609 | 2.103 | 1.176 | 1.048 | 10.68 | 11.40 | **0.916** | **0.667** |
| 17. Planktivores/piscivores | **3.116** | **3.522** | 2.588 | 1.294 | 0.885 | 1.287 | 11.72 | 12.23 | **0.353** | **0.695** |
| 18. Benthivores/piscivores | **3.139** | **3.459** | 0.534 | 0.349 | 3.910 | 1.451 | 9.327 | 9.921 | **0.985** | **0.952** |
| 19. Omnivores | **3.136** | **3.433** | 0.136 | 0.439 | 3.279 | 3.279 | 7.992 | 7.992 | **0.999** | **0.826** |
| 20. Large yellow croakers | **3.379** | **3.498** | 0.00107 | 0.0339 | 2.130 | 1.441 | 4.913 | 3.767 | **0.997** | **0.307** |
| 21. Small yellow croakers | **3.085** | **3.206** | 0.356 | 0.0832 | 4.300 | 2.410 | 8.997 | 6.074 | **0.226** | **0.990** |
| 22. Sharks | **4.035** | **4.236** | 0.00889 | 0.00935 | 0.500 | 0.500 | 3.200 | 3.200 | **0.000** | **0.000** |
| 23. Marine mammals | **3.809** | **3.939** | 0.00404 | 0.00404 | 0.050 | 0.050 | 30.00 | 30.00 | **0.000** | **0.000** |
| 24. Detritus | **1.000** | **1.000** | 100 | 100 | — | — | — | — | **0.147** | **0.241** |

*TL, trophic level; B, biomass; P/B, production/biomass; Q/B, consumption/biomass; EE, ecotrophic efficiency.*

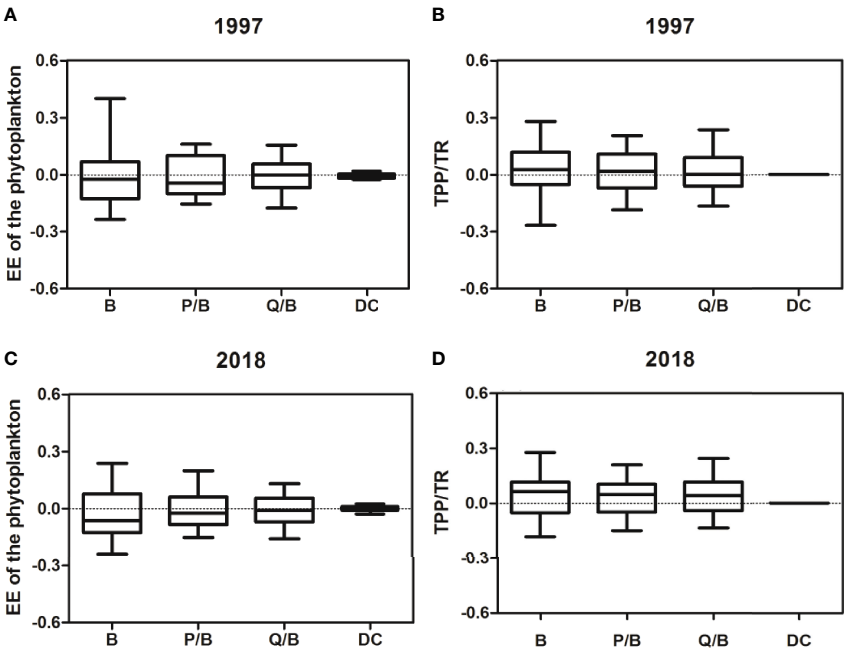


**FIGURE 2** | The sensitivity analysis results for the 20% uncertainty of the Ecopath input parameters. TPP, total primary production; TR, total respiration; EE, ecotrophic efficiency; B, biomass; P/B, production/biomass; Q/B, consumption/biomass; DC, diet composition. The sensitivity analysis results for the 20% uncertainty of the Ecopath input parameters. TPP, total primary production; TR, total respiration; EE, ecotrophic efficiency; B, biomass; P/B, production/biomass; Q/B, consumption/biomass; DC, diet composition. **(A)** represents the impact of the input parameters (B, P/B, Q/B, DC) with 20% uncertainty on the EE of the phytoplankton (M1997); **(B)** represents the impact of the input parameters (B, P/B, Q/B, DC) with 20% uncertainty on the TPP/TR (M1997); **(C)** represents the impact of the input parameters (B, P/B, Q/B, DC) with 20% uncertainty on the EE of the phytoplankton (M2018); **(D)** represents the impact of the input parameters (B, P/B, Q/B, DC) with 20% uncertainty on the TPP/TR (M2018).

model, which was less than the M1997 model (12.01%) but close to the theoretical ranges (10%; Christensen and Pauly, 1992). The TST developed further, from 6503.85 t/km$^2$/year to 8925.33 t/km$^2$/year in the two decades, with detritus flow accounting for 33.33% in M2018 and 40.36% in M1997 (**Table 2**). The consumption and respiration in the TST significantly increased by 14.33% and 5.77% in M2018, respectively, compared to M1997 (**Table 2**).

Total biomass increased considerably, from a value of 49.72 t/km$^2$/year in M1997 to 83.19 t/km$^2$/year in M2018 (**Figure 3**). The biomass of the plankton and fish in M2018 was nearly doubled relative to M1997, especially the planktivores, whose biomass in M2018 increased nearly seven times that in M1997. However, obvious and significant downtrends were noted in the benthic organisms, especially mollusks.

There was a major shift in the keystone indexes of the function groups in the two models (**Figure 4**). Several groups increased, including the benthic crustaceans, Bombay duck, large yellow croakers, sharks, and planktivores. The keystone species in the ECS changed from planktivores/piscivores to planktivores. Zooplankton and planktivores/piscivores (e.g., *Decapterus maruadsi* and *Trachurus japonicus*) were the keystone species revealed by the keystone indexes close to zero in M1997 (−0.0355 and −0.0711, respectively), and they had the largest influence on the ecosystem structure. However, piscivores, hairtails, and small yellow croakers decreased in importance during the study period.

The MTI showed the increasingly negative impact of fisheries in the ECS between M1997 and M2008 (**Figure 5**). In M1997, 36% of the function groups such as large yellow croakers, piscivores, and benthivores/piscivores were negatively affected by the fisheries. The positive impacts on the planktivores and benthivores (around 24%) were ascribed to the indirect effect of removing predators. In M2018, the negative impact of the fisheries further extended to small yellow croakers and omnivores. In addition, the MTI of the fisheries on important fish species such as hairtails and large yellow croakers slightly increased in M2018 relative to M1997, from −0.295 to −0.034 for hairtails and from −0.729 to −0.516 for large yellow croakers. Small yellow croakers had opposite values, 0.0635 in 1997 and −0.395 in 2018. However, the impact of the fisheries on Bombay duck appeared neutral over the two periods due to the limited and poor fishery data.

Ecosystem indicators were used to evaluate the status and variation of the structure and function of the ecosystem (**Table 2**). The ECS ecosystem was more mature and stable in M2018, as reflected by the higher total primary production/total respiration (TPP/TR) and SOI as well as by the lower Finn's cycling index and mean path length (**Table 2**). The TPP/TR declined from 4.89 to 2.74 between M1997 and M2018. The Flow to Detritus/TST was 33.33% in M2018 and 40.36% in M1997, indicating that more energy flowed into production rather than

**TABLE 2 |** Comparison of ecosystem indicators for the East China Sea Ecopath mass balance models M1997 (1997–2000) and M2018 (2018–2019) with other available Ecopath models in adjacent waters (Bohai, Northern South China, and Southwestern Yellow Seas) and in other seas at similar latitudes (Northern Oman Sea and Northern Gulf of Mexico).

| Parameters | The Northern Oman Sea | The Northern Gulf of Mexico | The Bohai Sea | The Northern South China Sea | The Southwestern Yellow Sea | This Study | |
|---|---|---|---|---|---|---|---|
| | | | | | | M1997 | M2018 |
| Sum of all consumption (t/km$^2$/year) | 6,591.37 | 1,908 | 1,213.72 | 7,951.491 | 1,031.03 | 1,058.40 | 2,374.89 |
| Sum of all exports (t/km$^2$/year) | 8,736.78 | 7,530 | 3,922.88 | 3,613.73 | 991.67 | 2,243.97 | 2,268.27 |
| Sum of respiration flows (t/km$^2$/year) | 3,398.37 | 1,046 | 894.61 | 4,137.55 | 643.73 | 576.02 | 1,306.51 |
| Sum of all flows into detritus (t/km$^2$/year) | 8,855.18 | 8,078 | 4,467.43 | 3,588.56 | 1,330.83 | 2,624.96 | 2,975.58 |
| Total system throughput (t/km$^2$/year) (TST) | 2,7581.7 | 18,563 | 10,499.00 | 15,698.05 | 2,825.00 | 6,503.35 | 8,929.63 |
| Flows to Detritus/TST (FD/TST) | 32.11% | 43.52% | 42.55% | 22.86% | 47.11% | 40.36% | 33.37%↑ |
| Total primary production/total respiration (TPP/TR) | 3.57 | 8 | 5.38 | 1.005 | 8.68 | 4.89 | 2.74↑ |
| Transfer efficiency (%) (TE) | 10.60 | 16.93 | 11.35 | 21.94 | 13.22 | 12.03 | 11.52 |
| Connectance index (CI) | 0.44 | 0.396 | 0.33 | 0.31 | 0.280 | 0.35 | 0.35 |
| System omnivory index (SOI) | 0.42 | 0.410 | 0.14 | 0.33 | 0.217 | 0.12 | 0.17↑ |
| Finn's cycling index (FCI) | 5.70 | – | – | 13.68 | 3.983 | 2.832 | 5.175↑ |
| Mean path length (MPL) | 2.27 | – | – | 3.78 | 2.444 | 2.306 | 2.497↑ |
| Ascendency (%) (*A*) | 45.50 | – | – | – | – | 40.54 | 35.65↑ |
| Overhead (%) (*O*) | 54.60 | – | – | – | – | 59.46 | 64.35↑ |

*Bold arrows represent the greater maturity and complexity in the M2018 model.*

detritus. Ascendency decreased from 40.54% to 35.65% from 1997 to 2018, and overhead increased from 59.46% to 64.26%, suggesting that the ECS ecosystem was more robust to resist external disturbance. In addition, the Finn's cycling index values approximately doubled from 1997 to 2018, and there was a slight increase in mean path length (from 2.31 in M1997 to 2.50 in M2018). This further implied an increase in the proportion of material recycling. The same performance was also observed in

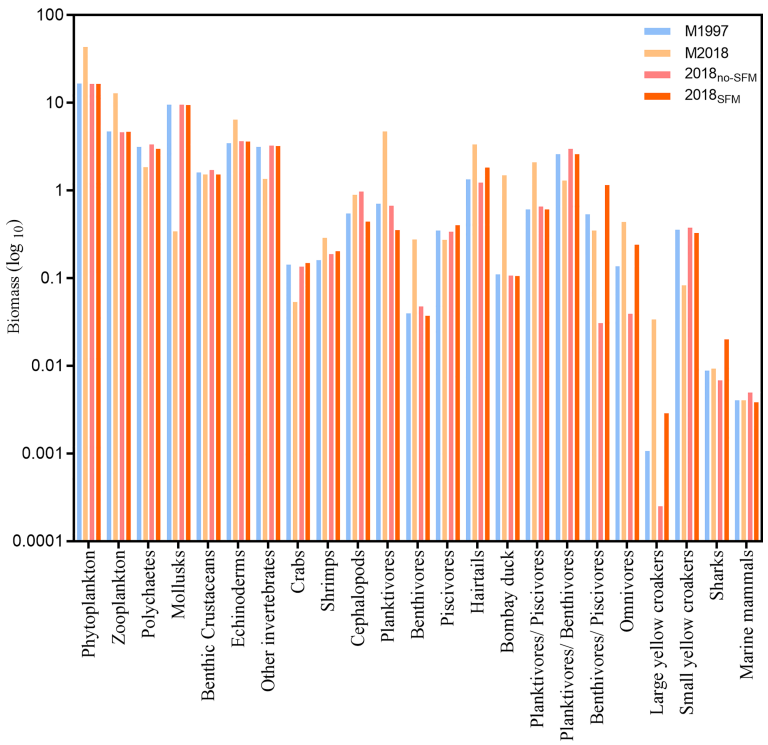


**FIGURE 3 |** Biomass of the function groups in the East China Sea ecosystem in the M1997 (1997–2000) and M2018 (2018–2019) mass balance models and the M2018$_{no\text{-}SFM}$ (no seasonal fishing moratorium) and M2018$_{SFM}$ (with a seasonal fishing moratorium) dynamic simulations (1997–2018).

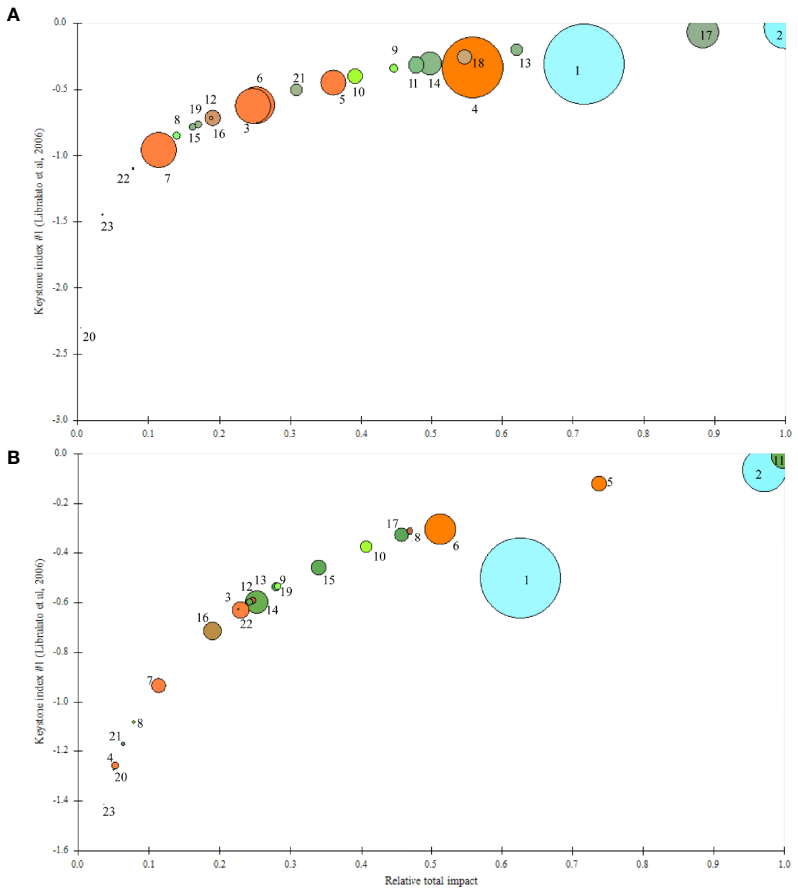


**FIGURE 4** | Keystoneness index and overall effects of each function group from the East China Sea ecosystem in the **(A)** M1997 (1997–2000) and **(B)** M2018 (2018–2019) mass balance models. 1, Phytoplankton; 2, Zooplankton; 3, Polychaetes; 4, Mollusks; 5, Benthic crustaceans; 6, Echinoderms; 7, Other invertebrates; 8, Crabs; 9, Shrimps; 10, Cephalopods; 11, Planktivores; 12, Benthivores; 13, Piscivores; 14, Hairtail; 15, Bombay duck; 16, Planktivores/Benthivores; 17, Planktivores/Piscivores; 18, Benthivores/Piscivores; 19, Omnivores; 20, Large yellow croakers; 21, Small yellow croakers; 22, Sharks; 23, Marine mammals; 24, Detritus.

the SOI. Compared with M1997, the SOI increased from 0.13 to 0.18, whereas the connectivity index remained constant between M1997 and M2018. In summary, a series of ecosystem indicators showed that the maturity and stability of the ECS ecosystem in 2018 had further developed. However, the ECS is still a developing ecosystem with a mass of unused energy.

## 3.3 Effect of the Seasonal Fishing Moratorium

The optimal model for the stepwise fitting process based on time series data was selected by the lowest Akaike information criterion for important economic species, in which the $v$ values were caught (**Table S6** and **Figure S3**). There were significant differences in the biomasses of the kinds of function groups for the four models. There was a higher biomass of low-TL function groups in $M2018_{no\text{-}SFM}$ than in $M2018_{SFM}$ and M2018, i.e., polychaetes, mollusks, and shrimps; conversely, the higher biomass in the high-TL function groups was in $M2018_{SFM}$, i.e., piscivores and benthivores/piscivores. By linearly fitting the actual biomass in M2018 with the one in M1997 and the predicted biomasses in $M2018_{no\text{-}SFM}$ and $M2018_{SFM}$ (**Figure 6**), we found that the slope for $M2018_{SFM}$ was the highest, followed by $M2018_{no\text{-}SFM}$ and M1997. The $M2018_{SFM}$ and $M2018_{no\text{-}SFM}$ models could explain 69.87% and 45.39% of the biomass change, respectively. Note that the linear fit excluded planktivores, planktivores/piscivores, and planktivores/benthivores due to the poor prediction quality for plankton organisms in the two Ecosim models.

Increased biomasses were observed for most function groups during the SFM, but they sharply decreased after the SFM due to the intense fishing intensity (**Figure 7**). The predicted biomass for most function groups was higher compared to M1997, suggesting reduced fishing pressure has a positive influence on resource recovery. However, discrepancies in the biomasses between function groups were found in the two simulated scenarios. Similar patterns emerged in hairtails, benthivores/piscivores, omnivores, and large yellow croakers (**Figures 7G, H, J, L**, respectively). In $M2018_{no\text{-}SFM}$, the biomass of these

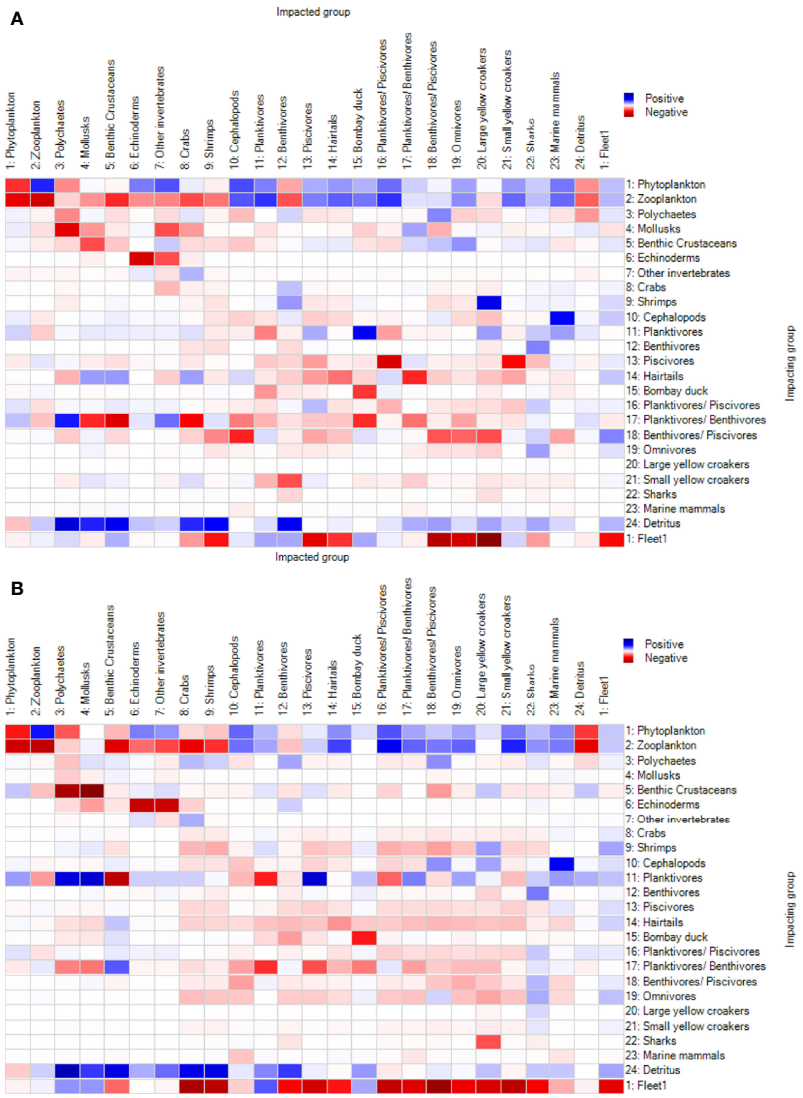


**FIGURE 5** | Mixed trophic impacts of the function groups in the East China Sea ecosystem in the **(A)** M1997 (1997–2000) and **(B)** M2018 (2018–2019) mass balance models.

groups declined substantially from that in M1997 but increased dramatically in $M2018_{SFM}$. This suggests that the SFM facilitates the recovery of these function groups. There were no differences in crabs; shrimps; benthivores, piscivores, and Bombay duck; planktivores/benthivores; and small yellow croakers in the two Ecosim models (**Figures 7A, B, D–F, I, K**, respectively). The landing of benthivores and Bombay duck was not recorded in the CFSY, so the change in fishing effort provided a limited effect on these groups. The excessive exploitation of piscivores after the SFM led to a similar trend in the two Ecosim models. As to crabs and shrimps, the combined effect of fishing and trophic interaction rapidly removed the bioaccumulation from the SFM and brought similar results in the two scenarios. Although the SFM facilitated the recovery of large yellow croakers and benthivores/piscivores, the small yellow croakers and planktivores/benthivores did not increase in the $M2018_{SFM}$ model. The biomass of the cephalopods was lower in $M2018_{SFM}$ than in $M2018_{no\text{-}SFM}$ (**Figure 7C**), which was mainly due to the stronger feeding pressure from higher TL organisms.

# 4 DISCUSSION

## 4.1 Analysis of the Variations in the East China Sea Ecosystem Structure

The widely used EwE software provides for the easy implementation of different network indices that can describe the developing status of an ecosystem structure. Our results indicated a 20-year increase in the ecosystem's maturity and stability after a series of FMPs featuring a higher TST, a lower

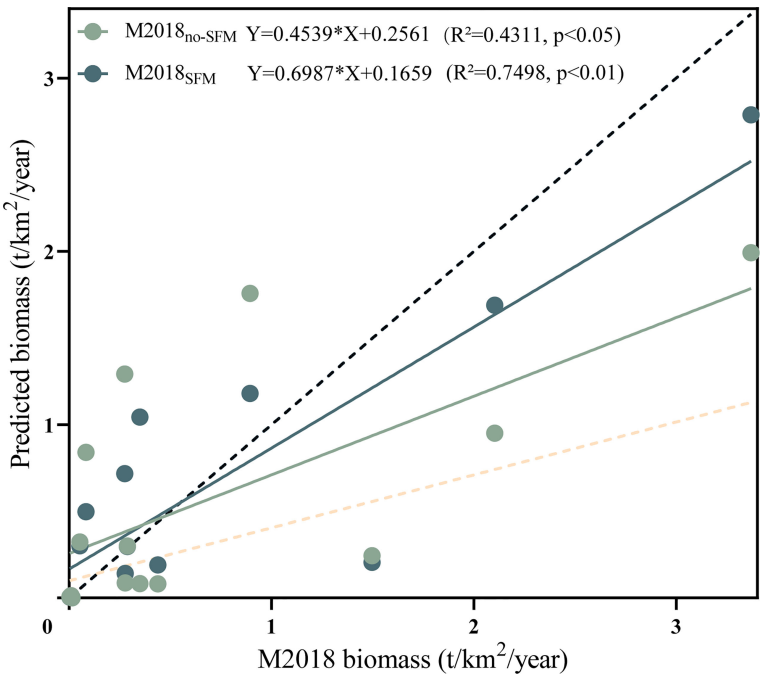


**FIGURE 6** | The linear fit of the actual biomass in M2018 (2018–2019) with the ones predicted by the $M2018_{no\text{-}SFM}$ and $M2018_{SFM}$ dynamic simulations (1997–2018), which represent the predicted model without and with a seasonal fishing moratorium (SFM), respectively. Dotted lines represent the actual biomasses in M1997 (yellow) and M2018 (black).

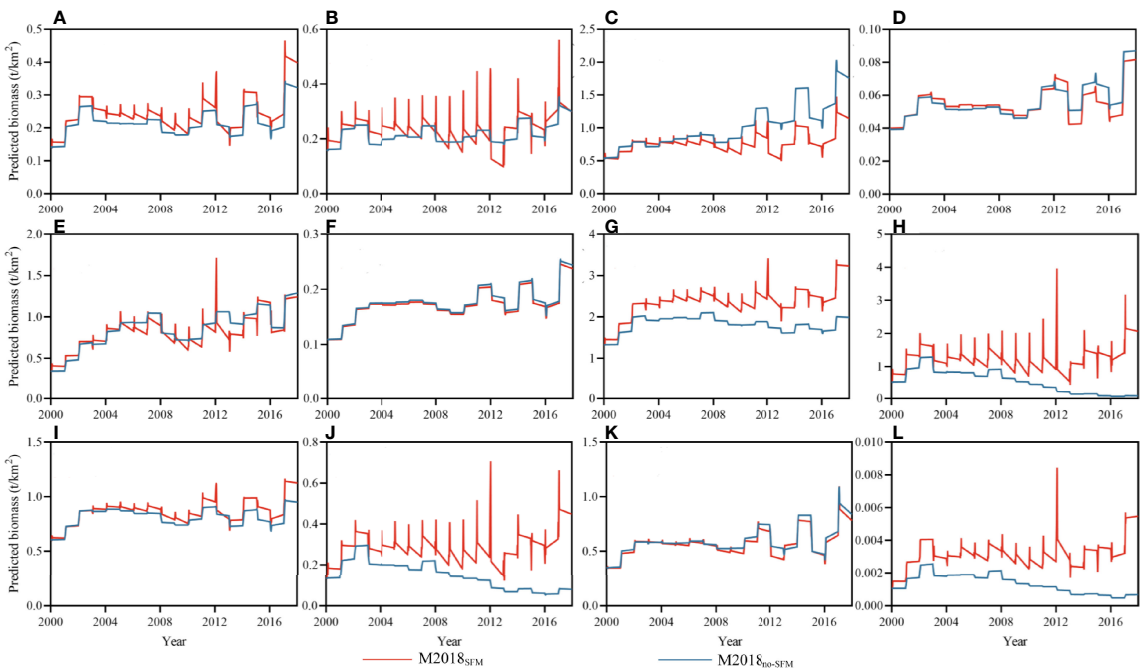


**FIGURE 7** | Biomass of important function groups in the $M2018_{no\text{-}SFM}$ and $M2018_{SFM}$ dynamic simulations (1997–2018), which are the predicted model without and with a seasonal fishing moratorium, respectively; the peak value in $M2018_{SFM}$ represents the seasonal fishing moratorium. **(A)** Crabs, **(B)** Shrimps, **(C)** Cephalopods, **(D)** Benthivores, **(E)** Piscivores, **(F)** Bombay duck, **(G)** Hairtails, **(H)** Benthivores/Piscivores, **(I)** Planktivores/Benthivores, **(J)** Omnivores, **(K)** Small yellow croakers, **(L)** Large yellow croakers.

TPP/TR, longer cycles, faster organic material circulation speed, a higher degree of omnivory in the consumers, and less energy flowing into detritus. Although TST is not necessarily linked with ecosystem status, i.e., degradation or recovery, increased TST means an increase in the "size" of the entire system after a 20-year recovery. The expectation is that there are changes in TST consistent with changes in productivity (Coll et al., 2008b). However, the TPP/TR value indicative of the maturity of the ecosystem in M2018 still reached 2.76. Despite being far less than those of two adjacent seas—the southwest Yellow Sea (Wang et al., 2019) and the Bohai Sea (Lin et al., 2018)—as well as two seas at a comparable latitude, the northern Oman Sea (Tajzadehnamin et al., 2020) and northern Gulf of Mexico (Sagarese et al., 2017), this value was far higher than the 1 that represents a mature status (Christensen et al., 2005) (**Table 2**). This value was also lower than that for the northern South China Sea (Ma et al., 2020). These data suggest that the ECS ecosystem is still immature and unstable, with much energy that still cannot be utilized directly.

The Ecopath results showed a substantial increase in fish biomass, especially for the planktivores in M2018. These findings are consistent with other studies, where an increase in low-TL fish resulted from implementing FMPs after intensive exploitation (Pitcher, 2001; Vijverberg et al., 2012; Gebremedhin et al., 2021). In particular, the biomass of the planktivores increased from 11.06% of the total fish biomass in M1997 to 34.5% in M2018. This has led to an obvious variation in the species composition and a keystone species change from planktivores/piscivores to planktivores (**Figure 4**). This variation in keystone species is consistent with findings in the Bohai Sea and the northern South China Sea, where the dominant species were also low-TL organisms such as cephalopods and mollusks (Chen, 2017; Li, 2020). This might be ascribed to the policy on the minimum mesh size. Since 2004, the minimum mesh size of fishing nets in the China Sea has been 5 cm, but *B. pterotum*, the dominant planktivore species, has only a 3.5-cm maximum body length (Fishbase); thus, this species can benefit from this policy. These low-TL fishes have a short growth period and high reproductive rate that allows them to adapt to intense fishing pressure (Reum et al., 2021). Jiang et al. (2009) also showed that after a fishing moratorium, the community tends to be dominated by fast-growing small groups, which facilitates the expansion of fish in the community. Small fishes also play a considerable role in bridging the low and high TLs (Lira et al., 2021).

The MTI showed the increasingly negative impacts of fishery on the function groups in M2018 versus M1997. The negative effect of fishing activity on large/medium-sized species such as benthivores/piscivores (*Pennahia argentatus* and *Nemipterus virgatus*) and piscivores (*Scomberomorus niphonius*) was obvious in M1997. This negative impact had further developed in M2018. The negative impact of harvesting on piscivores increased due to increased fishing efforts (MTI values declined from −5.30 to −5.81). Moreover, the negative impacts expanded to other groups that had a positive or neutral impact in M1997, including planktivores and small yellow croakers. At this point, the direct harvest effect from fishing exceeds the predator removal effect.

The MTI and keystone index of important commercial fish showed different performances during these two decades. The MTI results showed that the fishery still had a negative impact on hairtails and large yellow croakers over the two periods, but there was a slight increase in the MTI of the fishery. This is also reflected in the keystone index, which had a more important role in the ecosystem. The increase in biomass is responsible for this pattern. Compared with M1997, the biomass of hairtails was tripled and that of large yellow croakers was doubled in M2018. Conversely, the fishing effort for these two commercial fish decreased. Many fish larvae, especially large yellow croakers, have been released into the ECS ecosystem to rebuild the fish stocks (Zhang et al., 2010). However, a significant decrease in the MTI index of small yellow croakers was observed. Fishery landings (according to the SAU database) show that the harvest of small yellow croakers has exceeded the fishing maximum sustainable yield since 2007. Therefore, its keystone index decreased versus that in M1997. In addition, Bombay duck had significant increases in its MTI and keystone index versus other groups, indicating that its ecological roles broadened. Consistent with Liu et al. (2021) and Zhang et al. (2021), Bombay duck has been the dominant species in the ECS, but no catch data were recorded in the CFSY.

## 4.2 Impact of Fisheries Management Policies on Fishery Stocks in the East China Sea

The SFM simulations illustrated that the SFM in the ECS could increase the short-term fish biomass during the period and play a positive role in the long-term bioaccumulation of fish biomass. Compared with $M2018_{no\text{-}SFM}$, the biomass for most function groups increased in $M2018_{SFM}$. Consistent with the observations of Yan et al. (2019a), a significant increase in fish biomass was found in 2017, when there was a longer moratorium and fewer fishery landings (**Figure 7**). However, these efforts were weakened by the intense fishing pressure after the SFM, with the species with high exploitation rates influenced more than others (Chagaris et al., 2020). This result has also been reported in the Western Mediterranean Sea by Samy-Kamal et al. (2015) and in the Visayan Sea (Philippines) by Napata et al. (2020). The fishing effort after the SFM accounted for half of the annual fishing effort, so the effect revealed by the SFM implementation was not significant in the annual biomass survey (Chen et al., 1997; Lu and Zhao, 2015; Yan et al., 2019a).

The SFM led to about a 70% change in biomass, suggesting that there were other factors that promoted the biomass increase in the ECS in M2018. Increased primary production facilitated the biomass of fish communities, which is revealed by a strong linkage between the higher primary production and secondary production of higher-TL organisms or fishery resources (Chassot et al., 2007; Friedland et al., 2012). Compared with M1997, the biomass of the phytoplankton increased approximately three-fold in M2018. Phytoplankton is a basic compartment in an ecosystem to provide food sources for low-TL species and fish larvae (Sun and Liang, 2016). We suspect that the increase in primary production might be due to the high concentrations of dissolved inorganic nitrogen and dissolved inorganic

phosphorus and the high rate of N/P from the nearshore (Ehrnsten et al., 2019; Yang et al., 2020). However, nutrient load was not included in the time series data to verify this pattern, and the predicted plankton biomass in the two simulations was lower than the actual in M2018. In addition, increased biomasses for planktivores and large yellow croakers were also observed by Zhai et al. (2020). However, the change in the fishing net mesh size and the release enhancement were not considered in the Ecosim models, perhaps resulting in the low planktivore and large yellow croaker biomasses in the two dynamic simulations. The seven-fold increase in planktivores (**Figure 3**) also confirmed the role of the policy on minimum mesh size. Release enhancement is also considered a means of restoring recruitment (Moore et al., 2007). For example, from 2001 to 2006, 2~6 million juvenile large yellow croakers were released annually in Zhejiang Province, and tagged adults were recaptured in a fishery survey (Lü et al., 2008). Unfortunately, there was no integrity database to offer reliable and detailed release data, including the release numbers and efforts (Yang et al., 2013). Therefore, it was very difficult to evaluate the effect of the release enhancement in the Ecosim model.

The FMPs in the ECS increased the fish biomass, but the effect was to some extent limited to the recovery of commercial fishes (**Figure 7**). In the 1990s, the total number of landings in the ECS have become quite intense and destructive, e.g., bottom trawling is still widely used (Han et al., 2017), which can destroy benthic communities (Olsgard et al., 2008; Van Denderen et al., 2015; Hiddink et al., 2019). The biomass of the zoobenthos, especially mollusks and polychaetes, sharply declined in M2018 (**Table S1**). This, in turn, influences the transfer of material and energy from primary producers or detritus to higher TLs. Therefore, the government should strengthen the implementation of the FMPs by limiting the depth of trawling and the number of catches as well as by prolonging the duration of the rest period. This would reduce the pressure from overfishing (Dimarchopoulou et al., 2019; Russo et al., 2019) and protect vulnerable benthic habitats (Clark et al., 2019). These measures were simulated in the Gulf of Gabes (Tunisia) by Halouani et al. (2016), who found that limiting the trawling depth and lengthening the rest period duration can both increase the TL of the catch. In addition, lessons can be drawn from successful programs implemented around the world and applied to the FMP system in China. Enhancing the selectivity of species, selecting an optimal body length for species, and evaluating the total allowable catch *via* historical data would also be beneficial to the recovery of fisheries (Coll et al., 2008a; Colloca et al., 2013).

## 5 CONCLUSION

The ECS ecosystem is becoming more mature, although it is still unstable. The high biomass of plankton stimulated an increase in other groups, especially planktivores. FMPs such as the SFM and minimum-mesh size also play positive roles in fish recovery. Despite this, fishing management still requires further development due to the decrease in high-TL groups and the change in keystone species. The commercial fish are still in an unrecovered state. A SFM could promote the fishery recovery, but extending the SFM and reducing fishing pressure after it would play a greater role in rehabilitating the depleted fisheries resources in the ECS.

It must be said that the dynamic simulation in Ecosim in this study only included the SFM and fishing pressure. We cannot evaluate the impacts of the minimum-mesh size and release enhancement due to the difficulty in obtaining precise estimates for fishing effort. The aquatic product and fleet can only represent the tendency of the fishing effort. Therefore, in the future long-term monitoring of keystone species and commercial fish, data on bycatch as well as climate and oceanographic variables are critical to evaluating and predicting future changes in the ECS ecosystem. Reliable and detailed fishery data are also missing, especially the discard data for non-commercial species, which contributes at least 8% to the entire fish yield (Cao et al., 2017). Therefore, it is critical to developing an integrity database for better stock assessment and fishery management.

## DATA AVAILABILITY STATEMENT

The original contributions presented in the study are included in the article/**Supplementary Material**. Further inquiries can be directed to the corresponding authors.

## ETHICS STATEMENT

The animal study was reviewed and approved by the Third Institute of Oceanography, Ministry of Natural Resources, Xiamen 361005, China.

## AUTHOR CONTRIBUTIONS

XZ and LL contributed to the conception and design of the study. LX wrote the first draft of the manuscript. XZ, YW, LX, and PS analyzed the data and reviewed the manuscript. All authors contributed to the article and approved the submitted version.

## FUNDING

This work was funded by the National Key Research and Development Program of China (Grant Numbers: 2018YFC1406301 and 2018YFC1406302) and the Scientific Research Foundation of Third Institute of Oceanography, MNR (Grant Number: 2019017).

## SUPPLEMENTARY MATERIAL

The Supplementary Material for this article can be found online at: https://www.frontiersin.org/articles/10.3389/fmars.2022.865645/full#supplementary-material

## REFERENCES


Bromley, D. W. (2005). Purging the Frontier From Our Mind: Crafting a New Fisheries Policy. *Rev. Fishr. Bio. Fisher.* 15 (3), 217–229. doi: 10.1007/s11160-005-4866-z

Burnham, K. P., and Anderson, D. R. (2004). Multimodel Inference: Understanding AIC and BIC in Model Selection. *Sociol. Method. Res.* 33 (2), 261–304. doi: 10.1177/0049124104268644

Cao, L., Chen, Y., Dong, S., Hanson, A., Huang, B., Leadbitter, D., et al. (2017). Opportunity for Marine Fisheries Reform in China. *Proc. Natl. Acad. Sci.* 114 (3), 435–442. doi: 10.1073/pnas.1616583114

Chagaris, D. D., Patterson, W. F.III, and Allen, M. S. (2020). Relative Effects of Multiple Stressors on Reef Food Webs in the Northern Gulf of Mexico Revealed *Via* Ecosystem Modeling. *Front. Mar. Sci.* 7, 513. doi: 10.3389/fmars.2020.00513

Chassot, E., Mélin, F., Le Pape, O., and Gascuel, D. (2007). Bottom-Up Control Regulates Fisheries Production at the Scale of Eco-Regions in European Seas. *Mar. Ecol. Prog. Ser.* 343, 45–55. doi: 10.3354/meps06919

Chen, Y. (2017). *Analysis of the Present Situation and Prospects of the Fishery Resources Enhancement in Shandong Province* (Shandong, China: Yantai University, Master thesis).

Chen, D., Duan, X., Liu, S., and Shi, W. (2004). Status and Management of Fishery Resources of the Yangtze River. In: *Proc. Second. Int. Symposium. Manage. Large. River. Fish. Vol. IR. Phnom. Penh. Kingdom. Cambodia. Citeseer.* ed, R. L. W. A. T. Petr. 1, 173–182.

Cheng, J., Cheung, W. W. L., and Pitcher, T. J. (2009). Mass-Balance Ecosystem Model of the East China Sea. *Prog. Nat. Sci.* 19 (10), 1271–1280. doi: 10.1016/j.pnsc.2009.03.003

Cheng, J., Lin, L., Ling, J., Li, J., and Ding, F. (2004). Effects of Summer Close Season and Rational Utilization on Redlip Croaker (*Larimichthys Polyactis Bleeker*) Resource in the East China Sea Region. *J. Fish. Sci. China.* 11 (6), 554–560. doi: 10.3321/j.issn:1005-8737.2004.06.012

Chen, W., Li, C., and Hu, F. (1997). A Review of the Fisheries Resource Status in the East China Sea. *J. Fish. Sci. China.* 03), 40–44. doi: CNKI:SUN:ZSCK.0.1997-03-007

Cheung, W. W. L., Watson, R., and Pauly, D. (2013). Signature of Ocean Warming in Global Fisheries Catch. *Nature.* 497(7449), 365–368. doi: 10.1038/nature12156

Christensen, V., and Pauly, D. (1992). Ecopath II—a Software for Balancing Steady-State Ecosystem Models and Calculating Network Characteristics. *Ecol. Model.* 61 (3-4), 169–185. doi: 10.1016/0304-3800(92)90016-8

Christensen, V., Walters, C. J., and Pauly, D. (2005). Ecopath With Ecosim: A User's Guide. *Fish. Centre. Univ. Br. Columbia. Vancouver.* 154, 31.

Clark, M. R., Bowden, D. A., Rowden, A. A., and Stewart, R. (2019). Little Evidence of Benthic Community Resilience to Bottom Trawling on Seamounts After 15 Years. *Front. Mar. Sci.* 6, 63. doi: 10.3389/fmars.2019.00063

Coll, M., Bahamon, N., Sardà, F., Palomera, I., Tudela, S., and Suuronen, P. (2008a). Improved Trawl Selectivity: Effects on the Ecosystem in the South Catalan Sea (Nw Mediterranean). *Mar. Ecol. Prog. Ser.* 355, 131–147. doi: 10.3354/meps07183

Coll, M., Lotze, H. K., and Romanuk, T. N. (2008b). Structural Degradation in Mediterranean Sea Food Webs: Testing Ecological Hypotheses Using Stochastic and Mass-Balance Modeling. *Ecosystems* 11 (6), 939–960. doi: 10.1007/s10021-008-9171-y

Colloca, F., Cardinale, M., Maynou, F., Giannoulaki, M., Scarcella, G., Jenko, K., et al. (2013). Rebuilding Mediterranean Fisheries: A New Paradigm for Ecological Sustainability. *Fish. Res.* 14 (1), 89–109. doi: 10.1111/j.1467-2979.2011.00453.x

Di Franco, A., Bussotti, S., Navone, A., Panzalis, P., and Guidetti, P. (2009). Evaluating Effects of Total and Partial Restrictions to Fishing on Mediterranean Rocky-Reef Fish Assemblages. *Mar. Ecol. Prog. Ser.* 387, 275–285. doi: 10.3354/meps08051

Dimarchopoulou, D., Keramidas, I., Tsagarakis, K., and Tsikliras, A. C. (2019). Ecosystem Models and Effort Simulations of an Untrawled Gulf in the Central Aegean Sea. *Front. Mar. Sci.* 6, 648. doi: 10.3389/fmars.2019.00648

Ehrnsten, E., Bauer, B., and Gustafsson, B. G. (2019). Combined Effects of Environmental Drivers on Marine Trophic Groups–A Systematic Model Comparison. *Front. Mar. Sci.* 492. doi: 10.3389/fmars.2019.00492

Finn, J. T. (1976). Measures of Ecosystem Structure and Function Derived From Analysis of Flows. *J. Theor. Biol.* 56 (2), 363–380. doi: 10.1016/S0022-5193(76)80080-X

Friedland, K. D., Stock, C., Drinkwater, K. F., Link, J. S., Leaf, R. T., Shank, B. V., et al. (2012). Pathways Between Primary Production and Fisheries Yields of Large Marine Ecosystems. *PLos One* 7 (1), e28945. doi: 10.1371/journal.pone.0028945

Fulton, E. A., Smith, A. D., Smith, D. C., and Johnson, P. (2014). An Integrated Approach is Needed for Ecosystem Based Fisheries Management: Insights From Ecosystem-Level Management Strategy Evaluation. *PloS One* 9 (1), e84242. doi: 10.1371/journal.pone.0084242

Funtowicz, S. O., and Ravetz, J. R. (1990). *Uncertainty and Quality in Science for Policy* (Netherlands: Kluwer Academic Publishers).

Gebremedhin, S., Bruneel, S., Getahun, A., Anteneh, W., and Goethals, P. (2021). Scientific Methods to Understand Fish Population Dynamics and Support Sustainable Fisheries Management. *Water* 13 (4), 574. doi: 10.3390/w13040574

Halpern, B. S., Walbridge, S., Selkoe, K. A., Kappel, C. V., Micheli, F., D'Agrosa, C., et al (2008). A Global Map of Human Impact on Marine Ecosystems. *Science.* 319 (5865), 948–952. doi: 10.1126/science.1149345

Halouani, G., Abdou, K., Hattab, T., Romdhane, M. S., Lasram, F. B. R., and Le Loc'h, F. (2016). A Spatio-Temporal Ecosystem Model to Simulate Fishing Management Plans: A Case of Study in the Gulf of Gabes (Tunisia). *Mar. Policy.* 69, 62–72. doi: 10.1016/j.marpol.2016.04.002

Han, Y. (2018). Marine Fishery Resources Management and Policy Adjustment in China Since 1949. *Chin. Rural Economy.* 09, 14–28.

Han, D., Chen, Y., Zhang, C., Ren, Y., Xue, Y., and Wan, R. (2017). Evaluating Impacts of Intensive Shellfish Aquaculture on a Semi-Closed Marine Ecosystem. *Ecol. Model.* 359, 193–200. doi: 10.1016/j.ecolmodel.2017.05.024

Heikinheimo, O., Setälä, J., Saarni, K., and Raitaniemi, J. (2006). Impacts of Mesh-Size Regulation of Gillnets on the Pikeperch Fisheries in the Archipelago Sea, Finland. *Fish. Res.* 77 (2), 192–199. doi: 10.1016/j.fishres.2005.11.005

Hiddink, J. G., Jennings, S., Sciberras, M., Bolam, S. G., Cambiè, G., McConnaughey, R. A., et al. (2019). Assessing Bottom Trawling Impacts Based on the Longevity of Benthic Invertebrates. *J. Appl. Ecol.* 56 (5), 1075–1084. doi: 10.1111/1365-2664.13278

Jiang, Y., Cheng, J., and Li, S. (2009). Temporal Changes in the Fish Community Resulting From a Summer Fishing Moratorium in the Northern East China Sea. *Mar. Ecol. Prog. Ser.* 387, 265–273. doi: 10.3354/meps08078

Kroeker, K. J., Kordas, R. L., Crim, R., Hendriks, I. E., Ramajo, L., Singh, G. S., et al (2013). Impacts of Ocean Acidification on Marine Organisms: Quantifying Sensitivities and Interaction With Warming. *Global Change Biol.* 19 (6), 1884–96. doi: 10.1111/gcb.12179

Lee, S., and Midani, A. R. (2014). National Comprehensive Approaches for Rebuilding Fisheries in South Korea. *Mar. Policy.* 45, 156–162. doi: 10.1016/j.marpol.2013.12.010

Li, Y. (2009). *Ecological Modeling of the East China Sea Shelf Ecosystem* (Shanghai, China: East China Normal University).

Li, C. (2020). Brief Introduction of Fishery Resources Increase in Liaoning Province. *Jiangxi. Agric.* 08, 99–100. doi: 10.1016/j.marpol.2013.12.010

Libralato, S., Christensen, V., and Pauly, D. (2006). A Method for Identifying Keystone Species in Food Web Models. *Ecol. Model.* 195 (3-4), 153–171. doi: 10.1016/j.ecolmodel.2005.11.029

Lin, J., Liu, X., Lai, T., He, B., Du, J., and Zheng, X. (2021). Trophic Importance of the Seagrass Halophila Ovalis in the Food Web of a Hepu Seagrass Bed and Adjacent Waters, Beihai, China. *Ecol. Indic.* 125, 107607. doi: 10.1016/j.ecolind.2021.107607

Lin, Q., Shan, X., Wang, J., and Li, Z. (2018). Changes in Chinese Shrimp (*Fenneropenaeus Chinensis*) Carrying Capacity of the Bohai Sea. *Prog. Fish.Sci.* 39 (04), 19–29. doi: 10.19663/j.issn2095-9869.20170908001

Link, J. S., and Watson, R. A. (2019). Global Ecosystem Overfishing: Clear Delineation Within Real Limits to Production. *Sci. Adv.* 5 (6), eaav0474. doi: 10.1126/sciadv.aav0474

Lira, A. S., Lucena-Fredou, F., and Le Loc'h, F. (2021). How the Fishing Effort Control and Environmental Changes Affect the Sustainability of a Tropical Shrimp Small Scale Fishery. *Fish. Res.* 235, 105824. doi: 10.1016/j.fishres.2020.105824

Liu, J. (2013). Status of Marine Biodiversity of the China Seas. *PLos One* 8 (1), e50719. doi: 10.1371/journal.pone.0050719

Liu, Y., and Cheng, J. (2015). A Preliminary Analysis of Variation Characteristics of Structure and Average Trophic Level of the Main Fishery Species Caught by Paired Bottom Trawl in the East China Sea and the Yellow Sea During the Fall Season. *J. Fish. China.* 39 (05), 691–702. doi: 10.11964/jfc.20141009521

Liu, K., Duan, J., Xu, D., Zhang, M., Fang, D., and Shi, W. (2012). Present Situation of *Coilia Nasus* Population Features and Yield in Yangzte River Estuary Waters in Fishing Season. *Chin. J. Ecol.* 31 (12), 3138–3143. doi: 10.13292/j.1000-4890.2012.0407

Liu, K., Yu, C., Zheng, J., Xu, Y., Jiang, X., Yu, N., et al. (2021). Analysis of Function Groups Characteristics and Niche of Major Fish Species in the Coastal Waters of Zhoushan Islands in Spring and Autumn. *J. Zhejiang. Univ. (Science Edition).* 48 (05), 592–605. doi: 10.3785/j.issn.1008-9497.2021.05.011

Li, Y., and Zhang, Y. (2012). Fisheries Impact on the East China Sea Shelf Ecosystem for 1969-2000. *Helgoland. Mar. Res.* 66 (3), 371–383. doi: 10.1007/s10152-011-0278-8

Lü, H., Xu, J., and Vander Haegen, G. (2008). Supplementing Marine Capture Fisheries in the East China Sea: Sea Ranching of Prawn Penaeus Orientalis, Restocking of Large Yellow Croaker Pseudosciaena Crocea, and Cage Culture. *Rev. Fish. Sci.* 16 (1-3), 366–376. doi: 10.1080/10641260701678207

Lu, C., and Zhao, J. (2015). The Review and Prospect on Fish Moratorium Policy in the East China Sea. *Fish. Info. Stra.* 30 (03), 168–174. doi: 10.1080/10641260701678207

Ma, M., Chen, Z., Xu, S., Zhang, J., and Yu, W. (2020). Trophic Structure and Energy Flow of Continental Slope of the Northern South China Sea Ecosystem. *J. Fish. Sci. China.* 44 (10), 1685–1694. doi: 10.1080/10641260701678207

Majkowski, J. (1982). Usefulness and Applicability of Sensitivity Analysis in a Multispecies Approach to Fisheries Management. *Theory Manage. Trop. fisheries. ICLARM. Conf. Proc.* 9, 149–165.

Mei, J. (2019). Status, Problems and Suggestions of Marine Fishing in the Yellow Sea and the East China Sea Areas. *J. Anhui. Agric. Sci.* 47 (08), 241–243. doi: 10.3969/j.issn.0517-6611.2019.08.063

Moore, M., Early, G., Touhey, K., Barco, S., Gulland, F., and Wells, R. (2007). Rehabilitation and Release of Marine Mammals in the United States: Risks and Benefits. *Mar. Mammal Sci.* 23, 4, 731–750. doi: 10.1111/j.1748-7692.2007.00146.x

Morissette, L. (2007). *Complexity, Cost and Quality of Ecosystem Models and Their Impact on Resilience: A Comparative Analysis, With Emphasis on Marine Mammals and the Gulf of St. Lawrence* (Vancouver, Canada: University of British Columbia).

Napata, R. P., Espectato, L. N., and Serofia, G. D. (2020). Closed Season Policy in Visayan Sea, Philippines: A Second Look. *Ocean. Coast. Manage.* 187, 105–115. doi: 10.1016/j.ocecoaman.2020.105115

Nee, S. (1990). Community Construction. *Trends Ecol. Evol.* 5 (10), 337–340. doi: 10.1016/0169-5347(90)90182-D

Nguyen, K. Q., Do, M. D., Phan, H. T., Nguyen, L. T., Van To, P., Vu, N. K., et al. (2021). Catch Composition and Codend Selectivity of Inshore Trawl Fishery With the Legal Minimum Mesh Size. *Reg. Stud. Mar. Sci.* 47, 101977. doi: 10.1016/j.rsma.2021.101977

Olsgard, F., Schaanning, M. T., Widdicombe, S., Kendall, M. A., and Austen, M. C. (2008). Effects of Bottom Trawling on Ecosystem Functioning. *J. Exp. Mar. Biol. Ecol.* 366 (1-2), 123–133. doi: 10.1016/j.jembe.2008.07.036

OuYang, L., and Guo, X. (2010). Studies on the Q/B Values and Food Consumption of Major Fishes in the East China Sea and the Yellow Sea. *Prog. Fish. Sci.* 31 (02), 23–9. doi: 10.3969/j.issn.1000-7075.2010.02.004

Palomares, M. L., and Pauly, D. (1989). A Multiple Regression Model for Prediction the Food Consumption of Marine Fish Populations. *Mar. Freshwat. Res.* 40 (3), 259–273. doi: 10.1071/MF9890259

Papapanagiotou, G., Tsagarakis, K., Koutsidi, M., and Tzanatos, E. (2020). Using Traits to Build and Explain an Ecosystem Model: Ecopath With Ecosim Modelling of the North Aegean Sea (Eastern Mediterranean). *Estuar. Coast. Shelf.* S. 236, 106614. doi: 10.1016/j.ecss.2020.106614

Paradell, O. G., Methion, S., Rogan, E., and López, B. D. (2021). Modelling Ecosystem Dynamics to Assess the Effect of Coastal Fisheries on Cetacean Species. *J. Environ. Manage.* 285, 112175. doi: 10.1016/j.jenvman.2021.112175

Pauly, D., and Christensen, V. (1993). "Stratified Models of Large Marine Ecosystems: A General Approach and an Application to the South China Sea," in *Large Marine Ecosystems: Stress, Mitigation and Sustainability* (Washington, DC: AAAS Press), 148–174.

Pauly, D., Christensen, V., and Sambilay, V.Jr. (1990). *Some Features of Fish Food Consumption Estimates Used by Ecosystem Modelers* (Metro manlia, Philippines: International Council for the Exploration of the Sea (ICES).

Pikitch, E. K., Santora, C., Babcock, E. A., Bakun, A., Bonfil, R., Conover, D. O., et al (2004). Ecosystem-Based Fishery Management. *Science* 305 (5682), 346–347. doi: 10.1890/1051-0761(2001)011[0601:FMTRER]2.0.CO;2

Pitcher, T. J. (2001). Fisheries Managed to Rebuild Ecosystems? Reconstructing the Past to Salvage the Future. *Ecol. Appl.* 11 (2), 601–617. doi: 10.1890/1051-0761(2001)011[0601:FMTRER]2.0.CO;2

Polovina, J. (1984). An Overview of the ECOPATH Model. *Fishbyte* 2 (2), 5–7.

Reum, J. C. P., Townsend, H., Gaichas, S., Sagarese, S., Kaplan, I. C., and Grüss, A. (2021). It's Not the Destination, It's the Journey: Multispecies Model Ensembles for Ecosystem Approaches to Fisheries Management. *Front. Mar. Sci.* 8, 75. doi: 10.3389/fmars.2021.631839

Russo, T., Bitetto, I., Carbonara, P., Carlucci, R., D'Andrea, L., Facchini, M. T., et al. (2017). A Holistic Approach to Fishery Management: Evidence and Insights From a Central Mediterranean Case Study (Western Ionian Sea). *Front. Mar. Sci.* 4, 193. doi: 10.3389/fmars.2017.00193

Russo, T., D'Andrea, L., Franceschini, S., Accadia, P., Cucco, A., Garofalo, G., et al. (2019). Simulating the Effects of Alternative Management Measures of Trawl Fisheries in the Central Mediterranean Sea: Application of a Multi-Species Bio-Economic Modeling Approach. *Front. Mar. Sci.* 542. doi: 10.3389/fmars.2019.00542

Sagarese, S. R., Lauretta, M. V., and Walter, J. F. (2017). Progress Towards a Next-Generation Fisheries Ecosystem Model for the Northern Gulf of Mexico. *Ecol. Model.* 345, 75–98. doi: 10.1016/j.ecolmodel.2016.11.001

Samy-Kamal, M., Forcada, A., and Lizaso, J. L. S. (2015). Effects of Seasonal Closures in a Multi-Specific Fishery. *Fish. Res.* 172, 303–317. doi: 10.1016/j.fishres.2015.07.027

Scott, E., Serpetti, N., Steenbeek, J., and Heymans, J. J. (2016). A Stepwise Fitting Procedure for Automated Fitting of Ecopath With Ecosim Models. *Software. X.* 5, 25–30. doi: 10.1016/j.softx.2016.02.002

Shen, G., and Heino, M. (2014). An Overview of Marine Fisheries Management in China. *Mar. Pol.* 44, 265–272. doi: 10.1016/j.marpol.2013.09.012

Shi, X. (1995). Fishery Environment and Utilization Status of Important Fishing Resources in the East China Sea. *Mar. Inf.* 09, 16.

Shih, N., Cai, Y., and Ni, I. (2009). A Concept to Protect Fisheries Recruits by Seasonal Closure During Spawning Periods for Commercial Fishes Off Taiwan and the East China Sea. *J. Appl. Ichthyology.* 25 (6), 676–685. doi: 10.1111/j.1439-0426.2009.01328.x

Su, Y., Chen, G., Zhou, Y., Ma, S., and Wu, Q. (2019). Assessment of Impact of Summer Fishing Moratorium in South China Sea During 2015–2017. *South China Fish. Sci.* 15 (2), 20–28. doi: 10.12131/20180149

Sun, C., and Liang, G. (2016). Common Fishery Policy and Fishery Subsidies in the EU. *World Agri.* 06, 78–85. doi: 10.13856/j.cn11-1097/s.2016.06.014

Surma, S., Christensen, V., Kumar, R., Ainsworth, C. H., and Pitcher, T. J. (2019). High-Resolution Trophic Models Reveal Structure and Function of a Northeast Pacific Ecosystem. *Front. Mar. Sci.* 625. doi: 10.3389/fmars.2019.00625

Tajzadehnamin, M., Valinassab, T., Ramezani-Fard, E., and Ehteshami, F. (2020). Trophic Dynamics Analysis and Ecosystem Structure for Some Fish Species of Northern Oman Sea. *Iran. J. Fish. Sci.* 19 (6), 2804–2823.

Tokai, T., Shiode, D., Sakai, T., and Yoda, M. (2019). Codend Selectivity in the East China Sea of a Trawl Net With the Legal Minimum Mesh Size. *Fish. Sci.* 85 (1), 19–32. doi: 10.1007/s12562-018-1270-x

Ulanowicz, R. E. (2012). *Growth and Development: Ecosystems Phenomenology* (New York, the US: Springer Science & Business Media).

Ulanowicz, R. E. (1986). Growth and Development: Ecosystems Phenomenology. *Estuaries* 11(1), 73–74. doi: 10.2307/1351721

Ulanowicz, R. E., and Puccia, C. J. (1990). Mixed Trophic Impacts in Ecosystems. *Coenoses* 5, 7–16. doi: 10.2307/43461017

Van Denderen, P. D., Bolam, S. G., Hiddink, J. G., Jennings, S., Kenny, A., Rijnsdorp, A. D., et al. (2015). Similar Effects of Bottom Trawling and Natural Disturbance on Composition and Function of Benthic Communities Across Habitats. *Mar. Ecol. Prog. Ser.* 541, 31–43. doi: 10.3354/meps11550

Vijverberg, J., Dejen, E., Getahun, A., and Nagelkerke, L. A. (2012). The Composition of Fish Communities of Nine Ethiopian Lakes Along a North-South Gradient: Threats and Possible Solutions. *Anim. Biol.* 62 (3), 315–535. doi: 10.1163/157075611X618246

Wang, Y., Hu, J., Pan, H., and Failler, P. (2020). Ecosystem-Based Fisheries Management in the Pearl River Delta: Applying a Computable General Equilibrium Model. *Mar. Policy*. 112, 103784. doi: 10.1016/j.marpol.2019.103784

Wang, W., Wang, J., Zuo, P., Li, Y., and Zou, X. (2019). Analysis of Structure and Energy Flow in Southwestern Yellow Sea Ecosystem Based on Ecopath Model. *J. Appl. Oceanog.* 38 (04), 528–539. doi: 10.3969/J.ISSN.2095-4972.2019.04.008

Wu, L., Zhang, N., Sun, S., Yuan, J., Chen, J., Li, M., et al. (2021). Application of Microsatellite Markers for Evaluating the Effect of Restocking Enhancement in Larimichthys Crocea. *J. Fish. Sci. China.* 28, 09, 1100–1108. doi: 10.12264/JFSC2020-0542

Xin, Y., Yu, C., Jian, K., Liu, H., Zhang, P., and Liu, K. (2020). The Effectiveness of China's Fishing Policy of Marine Fishing Industry in Zhejiang Province. *Ocean. Dev. Manage.* 37 (05), 25–31. doi: 10.3969/j.issn.1005-9857.2020.05.005

Xu, P., Ke, Q., Su, Y., Liu, J., and Zheng, W. (2021). Protection and Utilization and Prospect of Large Yellow Croaker (*Larimichthys Crocea*) Germplasm Resources. *J. Fish. China* 46 (4), 1–9. doi: 10.11964/jfc.20210312688

Xu, K., and Liu, Z. (2007). The Current Stock of Large Yellow Croaker *Pseudosciaena Crocea* in the East China Sea With Respects of its Stock Decline. *J. Dalian. Ocean. University.* 05, 392–396. doi: 10.16535/j.cnki.dlhyxb.2007.05.015

Yang, Y., Liu, P., Zhou, H., and Xia, L. (2020). Evaluation of the Biodiversity Variation and Ecosystem Health Assessment in Changjiang Estuary During the Past 15 Years. *Acta Ecol. Sin.* 40 (24), 8892–8904. doi: 10.5846/stxb201912272811

Yang, J., Pan, X., Chen, X., Wang, X., Zhao, Y., Li, J., et al. (2013). Overview of the Artificial Enhancement and Release of Endemic Freshwater Fish in China. *Zoo. Res.* 34 (04), 267–280. doi: CNKI:SUN:DWXY.0.2013-04-007

Yan, L., Liu, Z., Jin, Y., and Cheng, J. (2019a). Effects of Prolonging Summer Fishing Moratorium in the East China Sea on the Increment of Fishery Resources. *Mar. Fish.* 41 (05), 513–519. doi: 10.13233/j.cnki.mar.fish.2019.05.001

Yan, L., Liu, Z., Jin, Y., and Cheng, J. (2019b). Effects of Prolonging the Trawl Net Summer Fishing Moratorium in the East China Sea on the Conservation of Fishery Resources. *J. Fish. China*. 26 (01), 118–123. doi: 10.3724/SP.J.1118.2019.18243

Ye, Y., and Rosenberg, A. A. (1991). A Study of the Dynamics and Management of the Hairtail Fishery, Trichiurus Haumela, in the East China Sea. *Aquat. Living. Res.* 4 (2), 65–75. doi: 10.1051/alr:1991007

Yue, D., Wang, L., Zhang, X., Zheng, H., and Zhang, H. (2015). Status and Reflections of the Summer Closed Fishing in the East China Sea. *J. Agric. Sci. Technol.* 17 (04), 122–128. doi: 10.13304/j.nykjdb.2015.113

Zeng, Z., Cheung, W. W. L., Li, S., Hu, J., and Wang, Y. (2019). Effects of Climate Change and Fishing on the Pearl River Estuary Ecosystem and Fisheries. *Rev. Fish. Biol. Fisher.* 29, (4). doi: 10.1007/s11160-019-09574-y

Zhai, L., Liang, C., and Pauly, D. (2020). Assessments of 16 Exploited Fish Stocks in Chinese Waters Using the CMSY and BSM Methods. *Front. Mar. Sci.* 7, 1002. doi: 10.3389/fmars.2020.483993

Zhang, H., Song, P., Li, Y., Liu, S., Wang, X., Zheng, J., et al. (2021). Diversity and Community Structure of Nekton in the Central and Southern East China Sea in Autumn. *J. Appl. Oce.* 40 (04), 575–586. doi: 10.3969/J.ISSN.2095-4972.2021.04.003

Zhang, Q., Hong, W., Yang, S., and Liu, M.. (2010). Survey on Status of Fishery Resources Along the Coastal Waters of the Liuheng Town in Zhoushan City. *Fish. Inf. Stra.* 25 (12), 10–12. doi: 10.3969/j.issn.1004-8340.2010.12.003

Zhang, Y., Xu, K., Li, D., Zhang, H., Dai, G., Li, Z., et al. (2018). The Distribution and Biological Characteristics of *Chelidonichthy Kumu* in the North East China Sea. *J. Zhejiang. Ocean. Univ. (Nat. Sci).* 37 (05), 418–423. doi: 10.3969/j.issn.1008-830X.2018.05.007

Zheng, X., Como, S., Huang, L., and Magni, P. (2020). Temporal Changes of a Food Web Structure Driven by Different Primary Producers in a Subtropical Eutrophic Lagoon. *Mar. Environ. Res.* 161, 105128. doi: 10.1016/j.marenvres.2020.105128

Zhou, S., Smith, A. D., and Knudsen, E. E. (2015). Ending Overfishing While Catching More Fish. *Fish. Res.* 16 (4), 716–722. doi: 10.1111/faf.12077

Zhou, X., Zhao, X., Zhang, S., and Lin, J. (2019). Marine Ranching Construction and Management in East China Sea: Programs for Sustainable Fishery and Aquaculture. *Water* 11 (6), 1237. doi: 10.3390/w11061237

**Conflict of Interest:** The authors declare that the research was conducted in the absence of any commercial or financial relationships that could be construed as a potential conflict of interest.

**Publisher's Note:** All claims expressed in this article are solely those of the authors and do not necessarily represent those of their affiliated organizations, or those of the publisher, the editors and the reviewers. Any product that may be evaluated in this article, or claim that may be made by its manufacturer, is not guaranteed or endorsed by the publisher.

frontiers | Frontiers in Marine Science

ORIGINAL RESEARCH
published: 17 June 2022
doi: 10.3389/fmars.2022.880123

# Trophic Niche Partitioning of Five Sciaenidae Species Sampled in Zhoushan Archipelago Waters *via* Stable Isotope Analysis

*Jing Wang*[1,2], *Ri-Jin Jiang*[1,2,3,4*], *Yi Xiao*[1,2], *Rui Yin*[1], *Feng Chen*[1], *Yong-dong Zhou*[1] *and Han-Xiang Xu*[1,2]

[1] Zhejiang Marine Fisheries Research Institute, Zhoushan, China, [2] Marine and Fisheries Institute of Zhejiang Ocean University, Zhoushan, China, [3] Scientific Observation and Experimental Station of Fishery Resources of Key Fishing Grounds, Ministry of Agriculture and Rural Affairs of the People's Republic of China, Zhoushan, China, [4] Key Laboratory of Sustainable Utilization of Technology Research for Fishery Resources of Zhejiang Province, Zhoushan, China

Sciaenid fishes are usually associated with large freshwater inputs and are the most important economic fish on the coastal shelf off mainland China. To compare the differences in ecological niche and resource sharing among different populations of Sciaenidae species, we collected samples of *Larimichthys polyactis*, *Collichthys lucidus*, *Johnius belangerii*, *Nibea albiflora*, and *Miichthys miiuy* from Zhoushan Archipelago waters from 2019 to 2021 and investigated the carbon and nitrogen isotopic values in muscle tissues, the contribution of each food resource, and trophic niche widths and overlaps. Significant differences were observed in both isotopes in the muscles of the five Sciaenid species. Zooplankton was a key food resource for all Sciaenid species. In addition to zooplankton, *J. belangerii*, *N. albiflora*, and *M. miiuy* also fed on benthos organisms. *C. lucidus* presented a wide trophic niche width and had extensive habitat use. The trophic niche occupied by *N. albiflora* and *M. miiuy* was narrow; they presented a high trophic level, with a high degree of trophic niche overlap. This study showed that sciaenid fishes have overlapping trophic niches due to their common feeding on zooplankton, and differences in body size, migration, habitat, and feeding choices led to the reasonable sharing of resources among the five sciaenid fishes, allowing the coexistence of these species.

**Keywords: sciaenid fish, isotope analysis, trophic niche, niche overlap, food source**

OPEN ACCESS

***Edited by:***
*Jun Xu,*
*Institute of Hydrobiology (CAS), China*

***Reviewed by:***
*Alberto Sánchez-González,*
*Instituto Politécnico Nacional (IPN), Mexico*
*Xuefeng Wang,*
*Guangdong Ocean University, China*

***Correspondence:**
*Ri-Jin Jiang*
*jiangridge@163.com*

***Specialty section:***
*This article was submitted to Marine Ecosystem Ecology, a section of the journal Frontiers in Marine Science*

***Received:*** *21 February 2022*
***Accepted:*** *16 May 2022*
***Published:*** *17 June 2022*

***Citation:***
*Wang J, Jiang R-J, Xiao Y, Yin R, Chen F, Zhou Y-d and Xu H-X (2022) Trophic Niche Partitioning of Five Sciaenidae Species Sampled in Zhoushan Archipelago Waters via Stable Isotope Analysis. Front. Mar. Sci. 9:880123. doi: 10.3389/fmars.2022.880123*

## INTRODUCTION

Marine sciaenid fishes are cosmopolitan, and they are important for fisheries worldwide. These fishes are usually associated with large freshwater inputs, and are mainly distributed in the Atlantic, Indian, and Pacific oceans (Longhurst and Pauly, 1987; McConnell and Lowemcconnell, 1987). In Asia, sciaenid fishes are mainly distributed in the northeast, including the west coast of South Korea, the Bohai Sea, and the East China Sea. *Larimichthys polyactis* (Sciaenidae: Perciformes), is one of the most commercially important fish in South Korea and China, where it has long been used as a source of food and medicine (Choi and Kim, 2020). In China, *L. polyactis* and other sciaenid fishes

are prized because of their delicious meat and high trophic value. Thus, this is an economically important fish species on the coastal shelf of mainland China (Chen et al., 1997).

As one of the four major marine products in China, 400,000 tonnes of *L. polyactis* were harvested in 2010 (Ministry of Agriculture and Rural Affairs of the People's Republic of China, 2009-2018). In recent years, due to overexploitation and overfishing of marine resources, the *L. polyactis* population has severely declined (Lin, 2004). Since the 1990s, China has implemented fishery revitalisation policies, such as fishing bans in summer as well as the proliferation and release of commercial fishes; despite these efforts, the yield of *L. polyactis* continues to decline every year, and individual size miniaturisation is prevalent among the populations in Zhoushan fishing farm (Wang et al., 2021). Furthermore, populations of a comparable species *Larimichthys crocea*, have not rebounded after overfishing, and wild *L.crocea* has almost disappeared (Zhao et al., 2002).

Fishing pressure can lead to different indirect impacts, depending on the species. One of these processes is the competition release process (Walker and Hislop, 1998; Dulvy et al., 2000). For example, large species become locally extinct due to overfishing, whereas the populations of small species increase abundantly (Jin, 2000). According to the China Fishery Statistics Yearbook, during a 10-year survey from 2008 to 2017, the number of *Nibea albiflora* caught in China's offshore fisheries decreased by 22.81% while that of *C. lucidus* increased by 21.9% (Ministry of Agriculture and Rural Affairs of the People's Republic of China, 2009-2018). Moreover, overfishing causes changes in the trophic structure of food webs and trophic niches of species; for example, the food source of the hairtail can change, diversity of nutrient sources can decrease, and trophic niches can become smaller (He et al., 2021).

Niche overlap among species defines species exclusion or coexistence when competition takes place (De Roos et al., 2008). Thus, niche overlap can cause adjustments in habitat use and diet (Oelze et al., 2014; Lush et al., 2017; Merkle et al., 2017) as well as species marginalisation and disappearance (Simon and Townsend, 2003; Beaudrot et al., 2013). In contrast, niche diversification, in which competing species focus on different resources or exploit the same resource with spatial or temporal variation (i.e., spatial or temporal niche partitioning), favours species coexistence (Tilman, 1982; Chesson, 2000).

*L. polyactis*, *Collichthys lucidus*, *Johnius belangerii*, *N. albiflora*, and *Miichthys miiuy* are sciaenid fishes with similar body sizes and ecological habits. Most are medium-sized, and can prey on small fishes (Deng and Yang, 1997). However, these fishes can also serve as potential prey for bigger predators. Among these five species of Sciaenidae, *C. lucidus* is a euryhaline fish that is distributed in estuaries and near islands (Zhuang et al., 2006); the other four species winter in the open sea, and approach the Zhoushan offshore in spring and summer to feed and spawn (Lin et al., 2013; Wang et al., 2012a; Xu and Chen, 2009; Zhong et al., 2010). The morphological similarity of these fishes and interactions resulting from the presence of such similar species in the same community can lead to competition for limited resources (Pianka, 1981). In general, the more ecologically similar two species are, the more likely intense competition is. Intense interspecific competition may lead to exclusion of one species (Wisheu, 1998). However, it is common to find ecologically similar species living together in the same community, indicating that different strategies allow coexistence. Resource partitioning, such as foraging on different food items or at diverse locations or times, minimises interspecific competition and facilitates sympatric coexistence (Schoener, 1974).

Stable isotope analysis, which was first used in diet studies over 40 years ago (DeNiro and Epstein, 1987; Matthews and Bier, 1983), has become a frequently used tool in ecology. Through stable isotopes of carbon ($\delta^{13}C$) and nitrogen ($\delta^{15}N$), we can determine food resources and trophic positions (Crawford et al., 2008). This approach is powerful in its application to communities; for example, for the analysis of resource partitioning and trophic niche dimensions (Polis, 1984; Sheppard et al., 2018; Balčiauskas et al., 2019; Costa et al., 2020; Manlick and Pauli, 2020; De Camargo et al., 2021). Stable isotope ratios facilitate the identification of dietary changes (Koike et al., 2016) and the influence of habitat conditions (Hopkins III and Kurle, 2016). Though isotopic niche is not completely analogous to trophic niche (Hette-Tronquart, 2019), stable isotopes can provide a quantitative indicator of trophic niches as long as all the contributing factors are fully considered in the interpretation of isotope values (Marshall et al., 2019).

In this study we used stable isotope analysis to determine the status of five sciaenid fishes, *L. polyactis*, *C. lucidus*, *J. belangerii*, *N. albiflora*, and *M. miiuy* in the Zhoushan Archipelago. The archipelago is located southeast of the mouth of the Yangtze River and east of Hangzhou Bay. The waters which connect the Yangtze River and the ocean are scattered with thousands of islands, with strong habitat heterogeneity. The river's diluting water brings rich nutrients, and the island can block the ocean current, forming turbulence and whirlpools. In addition, the coastal cold current from the north and the Taiwan warm current from the south are in confluence near the islands (Hou et al., 2013). This accelerates the circulation of nutrients, thus, the waters of the Zhoushan Archipelago have high primary productivity, abundant bait organisms, and are feeding and spawning grounds for many offshore fish (Yu et al., 2010). In this study, based on stable isotopes analysis, we investigated the trophic niche width of five types of sciaenid fishes in the Zhoushan Archipelago waters, the differences in resource sharing, and interspecific competition to determine the status of those species in the area. Our results provide some basic parameters for the study of the structure, function, and stability of the Zhoushan fishing ground fish community.

# MATERIALS AND METHODS

## Research Area

The study was conducted in the east of Hangzhou Bay, southeast of the Yangtze River Estuary, and northeast of Zhejiang Province (29° 00' – 31° 00' N and 121° 30' – 124° 00' E; **Figure 1**). Due to the convergence of Taiwan warm and coastal cold currents,

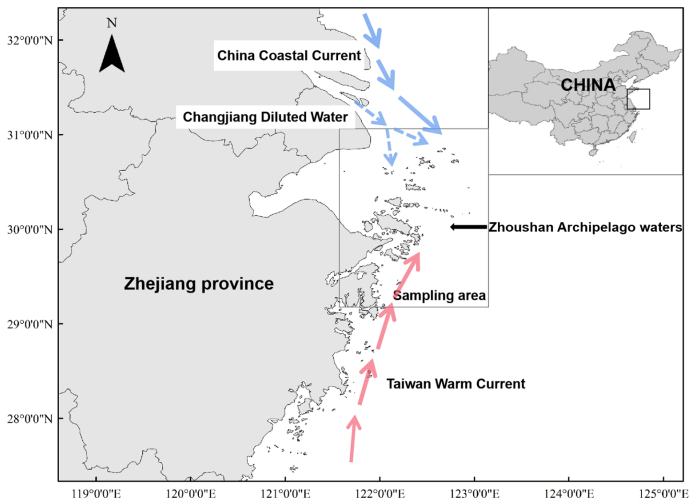


**FIGURE 1** | Area of Zhoushan Archipelago where sciaenid fish species were collected between 2019 and 2021 for assessment of $\delta^{13}C$ and $\delta^{15}N$ values.

Zhoushan Archipelago waters is rich in prey, and it provides a suitable environment for local aquatic animals.

## Sampling

Samples of sciaenid species and their potential prey species were collected from a trawl survey of fishery resources in Zhoushan Archipelago during spring and autumn of 2019–2021. A total of 199 sciaenid fish, including 59 *L. polyactis*, 51 C. *lucidus*, 40 *J. belangerii*, 31 N. *albiflora*, and 18 *M. miiuy*, were collected. A total of 89 prey samples of 13 species were collected. Referring to the results of the stomach content analysis (Wang et al., 2012b; Lin et al., 2013; Wang, 2015; Wang et al., 2020; Zhang et al., 2020), we classified the potential prey of five sciaenid fishes into three main ecological groups: nekton, zoobenthos and zooplankton. Nekton include small fishes such as *Amblychaeturichthys hexanema* and *Benthosema pterotum*; zoobenthos mainly include small shrimps and crabs such as *Palaemon gravieri* and *Charybdis bimaculata*; zooplankton include copepods and krill. All of these prey organisms are widely distributed in Zhoushan Archipelago waters and are easily ingested by other predators. Nekton and zoobenthos were collected by trawl surveys, and the zooplankton such as copepods and krill were collected using a shallow water I-type plankton net (505 μm). The collected samples were refrigerated on a fishing boat and transported to the laboratory *via* cold chain logistics after the fishing boat landed. The samples were then thawed in the laboratory, and biological parameters such as body length (mm), total length (mm), body weight (g), pure weight (g), and stomach fullness were measured (General Administration of Quality Supervision, Inspection and Quarantine of the People's Republic of China, Standardization Administration, 2008).

We collected muscles of fishes, abdominal muscles of shrimps, and the whole body of small planktonic crustaceans, such as copepods. To prevent the C isotopes in crustacean shells from affecting experimental results, small planktonic crustaceans were acidified with 1 $mol{\cdot}L^{-1}$ HCl until no bubbles were generated. The muscle samples were wrapped in tin foil, dried in an Alpha 1-2LDPLUS freeze dryer (Beijing BMH Instruments Co. Ltd., Shanghai, China) for 24 h, and fully ground into powder. The powder was placed in a 2 mL centrifuge tube and stored under dry conditions until further analysis.

## Stable Isotope Analysis

All samples were analysed for stable carbon and nitrogen isotope ratios using an EA-HT Elemental Analyser (Thermo Fisher Scientific, Inc., Bremen, Germany) and DELTA V Advantage Isotope Ratio Mass Spectrometer (Thermo Fisher Scientific). The samples were combusted in an elemental analyser to generate $CO_2$ and $N_2$. The mass spectrometer detected the ratio of $^{13}C$ to $^{12}C$ of $CO_2$ and compared it with an international standard (Pee Dee Belemnite or PDB) to calculate the $\delta^{13}C$ value of each sample. The ratio of $^{15}N$ to $^{14}N$ was compared with the international standard (atmospheric $N_2$) to calculate the $\delta^{15}N$ value of a sample.

Calculation method of isotope abundance:

$$\delta X = [(R_{sa}/R_{st}) - 1] \times 1000,$$

where X is $^{13}C$ or $^{15}N$ and $R_{sa}$ and $R_{st}$ are $^{13}C/^{12}C$ or $^{15}N/^{14}N$ of the unknown and standard samples, respectively. To ensure the precision and accuracy of the test results, 3 international standard samples were put in after every ten samples to calibrate the carbon and nitrogen stable isotopes. 10 replicate tests were performed on the same sample, the accuracy of $\delta^{13}C$ and $\delta^{15}N$ values was less than ±0.1‰ and less than ±0.2‰, respectively.

## Data Processing

One-way analysis of variance (ANOVA) was used to test significant differences in the stable carbon and nitrogen isotope values among the five sciaenid fishes ($\alpha = 0.05$). First, the data were tested for normality and homogeneity of variance. If any of

the above requirements were not met, a non-parametric test (Kruskal-Wallis H test) was performed. Pearson correlation analysis was used to test the correlation between $\delta^{13}C$ and $\delta^{15}N$ values of individuals of the five sciaenid fishes and their body length. Statistical analysis was performed using SPSS version 10.0 (SPSS Inc., Chicago, IL, USA).

Trophic level was calculated according to the following formula (Jake Vander Zanden and Fetzer, 2007):

$$TL = \left[\left(\delta^{15}N_c - \delta^{15}N_b\right)/TEF + \lambda\right],$$

where $TL$ represents the trophic level estimated using stable isotope; $\delta^{15}N_c$ is the $\delta^{15}N$ ratio of consumers, and $\delta^{15}N_b$ is the $\delta^{15}N$ ratio of the baseline organism. The baseline organism selected in this study was *Calanus sinicus*, which is present year-round in the Zhoushan Archipelago waters and has a monotonous diet ($\delta^{15}N$ value is 5.65‰) (Yang, 1997; Xu et al., 2005); TEF is the nitrogen enrichment at a trophic level; we used TEF = 3.4‰ based on Minagawa and Wada (Minagawa and Wada, 1984); and $\lambda$ represents the trophic level of the selected baseline organism, which is 2.

To assess the contribution of different food sources to the isotopic signature of each target fish, separate Bayesian stable isotope mixing models (Moore and Semmens, 2008) with a specified number of putative sources were run for the sections of sea area using the R software package SIAR (R CoreTeam, 2015; Stock and Semmens, 2016). SIAR model fitting was *via* Markov chain Monte Carlo (MCMC) to estimate parameters from observed data and user-specified prior distributions (Parnell et al., 2010). We ran the model for 200,000 iterations, and checked whether the estimated 95% credibility intervals for each proportion contained the original generated proportions (Parnell et al., 2010).

To quantify differences in isotopic niche use among the five species, the probability of a group appearing within the niche region (space) of another group was estimated by using the R package nicheROVER with 95% credible intervals based on 10,000 iterations (Swanson et al., 2015).

To describe the trophic niche ellipses and estimate the trophic niche widths and overlaps of different species, we calculated the standard ellipse area (Yeakel et al.) and corrected for small sample size (SEAc) with the Stable Isotope Bayesian Ellipses (SIBER) package in R (Jackson et al., 2011). The SEAc was set to contain 40% of isotopic observations of each group. The overlap between SEAc was used to quantify the overlapping area of stable isotope niches between fish species (Jackson et al., 2011). An overlap ratio greater than 1 indicates high overlap, and below 0.30 indicates low overlap (Yeakel et al., 2015).

# RESULTS

## Stable Isotopes in Sciaenidae

The highest average value of both $\delta^{13}C$ and $\delta^{15}N$ were found in *M. miiuy*, and the lowest average value of both $\delta^{13}C$ and $\delta^{15}N$ were found in *C. lucidus*. *N. albiflora* had a broader range of $\delta^{13}C$ and $\delta^{15}N$ than other fishes, while *M. miiuy* had the narrowest range of $\delta^{13}C$ and $\delta^{15}N$ compared with other fishes (**Table 1**). Stable isotopes of the five sciaenid species communities were significantly different (Kruskal-Wallis H, $P = 0.000 < 0.050$), which may be due to differences in low trophic-level species (*L. polyactis* and *C. lucidus*) and high trophic-level species (*J. belangerii*, *N. albiflora*, and *M. miiuy*) (**Table 2**).

## Stable Isotopes in Other Groups

One-way ANOVA showed that there were significant differences in the stable isotopes of the three prey groups ($P < 0.01$). Among them, zoobenthos had the highest $\delta^{13}C$ value, nekton had the highest $\delta^{15}N$ value, and zooplankton had the lowest $\delta^{13}C$ and $\delta^{15}N$ values (**Table 3**).

## Stable Isotopes vs. Length

Pearson correlation analysis showed a significant positive correlation between the body length and $\delta^{13}C$ values of *N. albiflora* ($R^2 = 0.500$, $P < 0.01$), and a positive correlation between the body length and $\delta^{15}N$ values of *J. belangerii* ($R^2 = 0.436$, $P < 0.01$). No significant correlations were observed between the body length and $\delta^{13}C$ and $\delta^{15}N$ values of the other three fishes (**Figure 2**).

## SIAR Model

The SIAR model showed that the five sciaenid fishes relied on zooplankton and zoobenthos as their food source, with fishes as the least preferred option. *L. polyactis* and *C. lucidus* were at a lower trophic level, zooplankton contributed more than 80% as their food source, and *C. lucidus* relied more on zooplankton than *L. polyactis*. In addition to zooplankton, *J. belangerii*, *N. albiflora* and *M. miiuy* also fed on zoobenthos. Among these three species, *M. miiuy* fed the most on zoobenthos, followed by *J. belangerii*, and *N. albiflora* the least (**Figure 3**).

**TABLE 1** | $\delta^{13}C$ and $\delta^{15}N$ values observed for five sciaenid fish species in Zhoushan Archipelago waters collected between 2019 and 2021.

| species | Samples (n) | Body length (mm) | δ13C (‰) | | δ15N (‰) | |
|---|---|---|---|---|---|---|
| | | Mean ± SD | Range | Mean ± SD | Range | Mean ± SD |
| *Larimichthys polyactis* | 59 | 143.47 ± 22.13 | -19.49~-15.58 | -17.86 ± 0.82 | 9.03~12.02 | 10.57 ± 0.53 |
| *Collichthys lucidus* | 51 | 103.76 ± 16.55 | -22.85~-16.20 | -18.34 ± 1.56 | 7.22~12.28 | 9.46 ± 1.21 |
| *Johnius belangerii* | 40 | 99.38 ± 31.99 | -19.10~-15.30 | -16.80 ± 0.82 | 8.47~12.95 | 11.37 ± 0.89 |
| *Nibea albiflora* | 31 | 252.29 ± 45.66 | -22.71~-15.00 | -17.18 ± 1.62 | 8.01~14.09 | 11.51 ± 0.95 |
| *Miichthys miiuy* | 18 | 241.83 ± 43.71 | -18.30~-15.19 | -16.30 ± 0.92 | 10.54~12.57 | 11.67 ± 0.53 |

**TABLE 2 |** Comparison of $\delta^{13}C$ and $\delta^{15}N$ values of five sciaenid fish species collected from the Zhoushan Archipelago between 2019 and 2021 based on the Kruskal-Wallis H test.

| | | *Larimichthys polyactis* | *Collichthys lucidus* | *Johnius belangerii* | *Nibea albiflora* |
|---|---|---|---|---|---|
| $\delta^{13}C$ | *Collichthys lucidus* | 1 | | | |
| | *Johnius belangerii* | 0.000** | 0.000** | | |
| | *Nibea albiflora* | 0.005** | 0.001** | 1 | |
| | *Miichthys miiuy* | 0.000** | 0.000** | 1 | 0.376 |
| $\delta^{15}N$ | *Collichthys lucidus* | 0.024* | | | |
| | *Johnius belangerii* | 0.000** | 0.000** | | |
| | *Nibea albiflora* | 0.000** | 0.000** | 1 | |
| | *Miichthys miiuy* | 0.000** | 0.000** | 1 | 1 |

*$P < 0.05$; **$P < 0.01$.

## Trophic Niches

For each species of fish and every pair of isotopes, 10 random elliptical projections of the trophic niche regions were created (**Figure 4**). Smoothed histograms (density plots) and scatterplots indicate no violation of the assumption of normality. Ratios of $\delta^{13}C$ and $\delta^{15}N$ varied more widely in *C. lucidus* and *N. albiflora* than in the other three species, which would obviously contribute to a larger overall (**Figure 4**).

The posterior distributions of the overlap metric were also assessed (**Figure 5**). The nicheROVER analysis revealed the probability of sciaenid individuals to be found in the same niche region of different sciaenid species. The isotope niche of *L. polyactis* showed a high probability to be found in the niche regions of *C. lucidus*, *J. belangerii* and *N. albiflora*. The isotope niche of *C. lucidus* was low in the niche regions of the other four species. The isotope niche of *J. belangerii* was high in the niche regions of the other four species and showed an extremely high probability to be found in the niche regions of *N. albiflora*. the isotope niche of *M. miiuy* was low in the niche regions of *L. polyactis* and *C. lucidus*, but high in *J. belangerii* and *N. albiflora*.

The isotopic niche width of five sciaenid indicated that *C. lucidus* had the largest isotopic niche area, followed by *N. albiflora*, *J. belangerii*, *M. miiuy*, and *L. polyactis* had the smallest isotopic niche area (**Figure 6**). Though *J. belangerii* showed some isotope niche overlap with *N. albiflora* and *M. miiuy*, overall, we found little isotope niche overlap between the five sciaenid fishes.

# DISCUSSION

In this study, the analysis of stable C and N isotopes provided insights into the trophic ecology of five co-occurring and highly abundant sciaenid species in the Zhoushan Archipelago waters. Our results suggest that the coexistence of five sciaenid species in the Zhoushan Archipelago waters may be enabled by spatial and food diversification, as indicated by the diversification of isotopic niches between the sciaenid species.

Generally, during the growth of organisms, carbon and nitrogen stable isotopes are continuously enriched in the body. According to the "optimal feeding theory", as individuals grow, the food organisms ingested by consumers gradually become larger (Xue et al., 2004). A large number of studies have shown

**TABLE 3 |** $\delta^{13}C$ and $\delta^{15}N$ values of the major prey groups of five sciaenid fish species collected from the Zhoushan Archipelago between 2019 and 2021.

| Category | Samples (n) | $\delta^{13}C$ (‰) | | $\delta^{15}N$ (‰) | |
|---|---|---|---|---|---|
| | | Range | Mean ± SD | Range | Mean ± SD |
| Nekton | 25 | -19.90~-15.93 | -17.81 ± 1.51 | 8.62~14.01 | 10.99 ± 1.32 |
| Zoobenthos | 47 | -20.01~-13.32 | -16.91 ± 1.48 | 6.79~11.92 | 9.90 ± 1.18 |
| Zooplankton | 10 | -20.14~-19.16 | –19.61 ± 0.41 | 5.51~9.33 | 7.80 ± 1.33 |

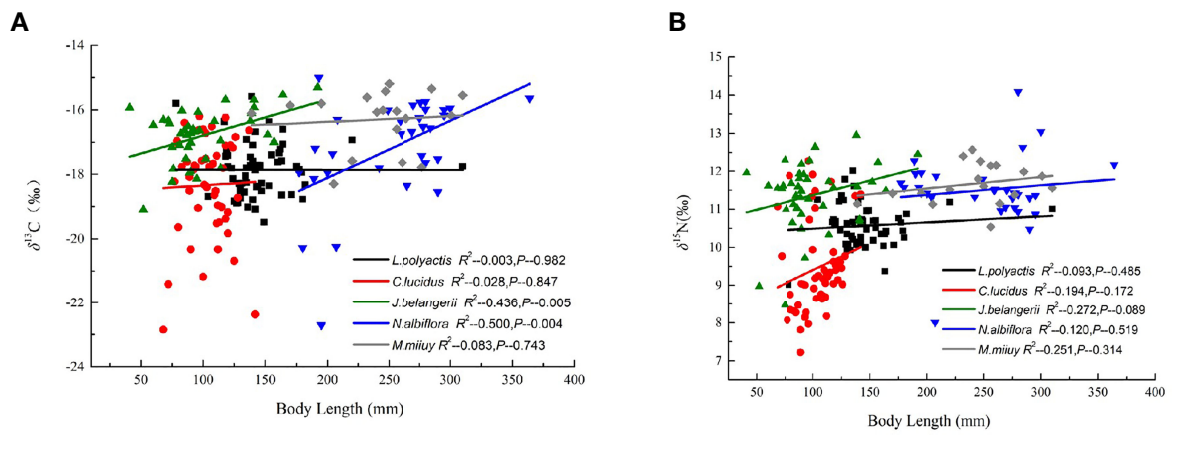


**FIGURE 2 |** Correlation of body length with $\delta^{13}C$ and $\delta^{15}N$ values of five sciaenid fish species collected form the Zhoushan Archipelago between 2019 and 2021.

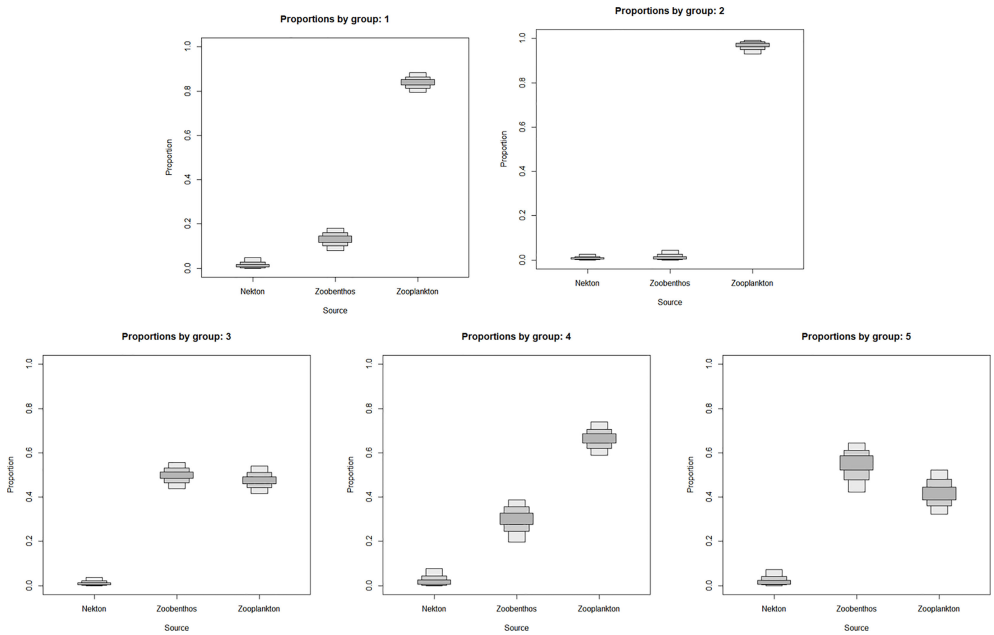


**FIGURE 3** | Contributions of different food sources to five sciaenid fishes collected from the Zhoushan Archipelago between 2019 and 2021. Group 1 is *Larimichthys polyactis*; Group 2 is *Collichthys lucidus*; Group 3 is *Johnius belangerii*; Group 4 is *Nibea albiflora*; Group 5 is *Miichthys miiuy*.

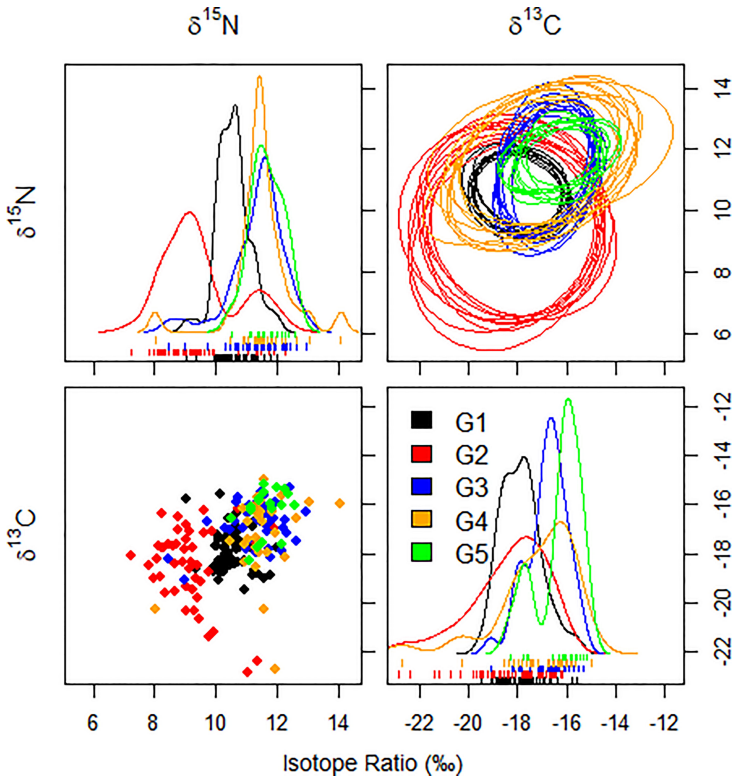


**FIGURE 4** | Ten random elliptical projections of the trophic niche region (NR) for each species of sciaenid fish collected from the Zhoushan Archipelago between 2019 and 2020, as well as a pair of isotopes (elliptical plots). Also displayed are one-dimensional density plots (lines) and two-dimensional scatterplots.

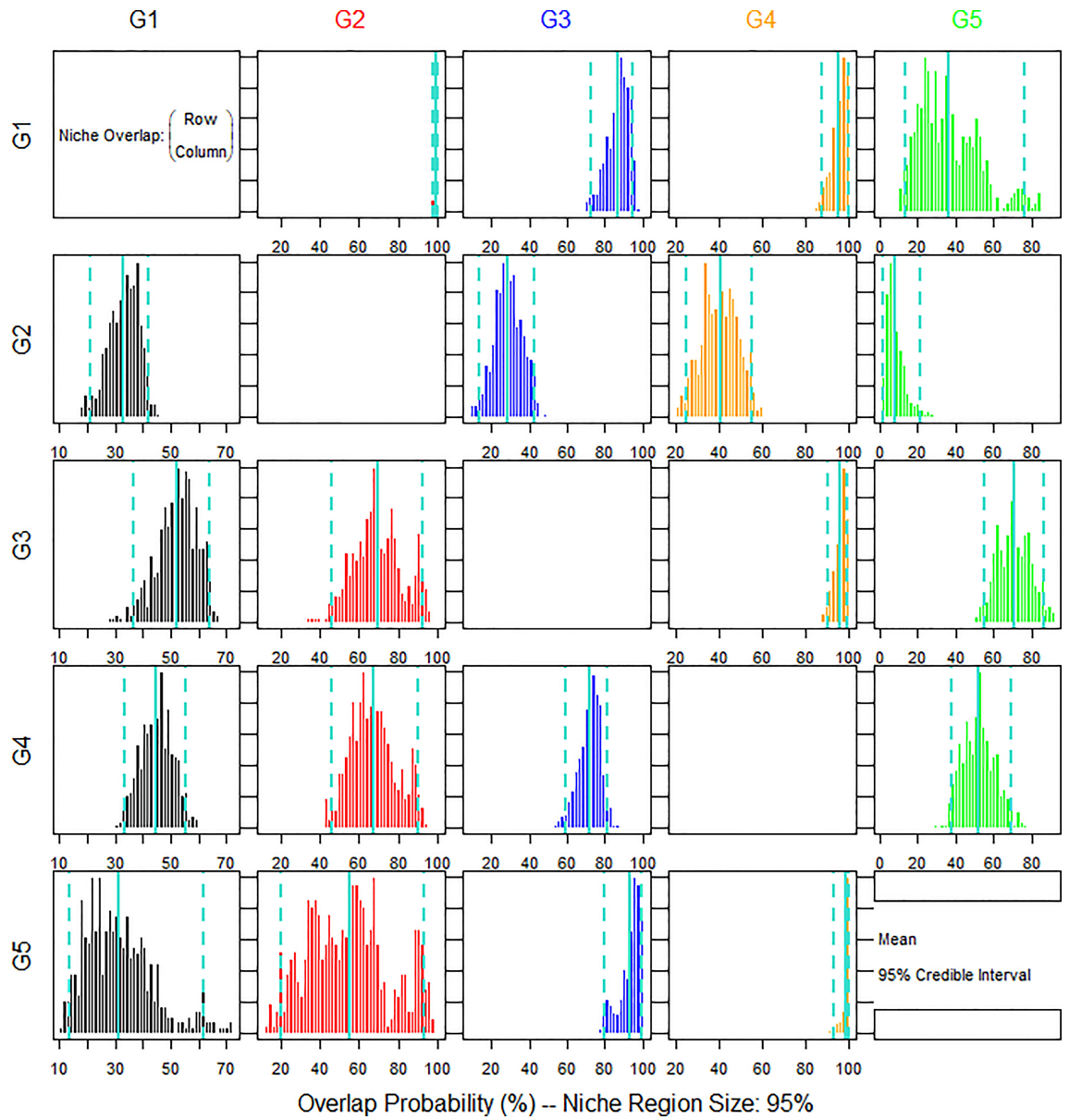


**FIGURE 5** | Bayesian plot of the posterior probability distribution of niche region metric (%) for five species of sciaenid fish collected from the Zhoushan Archipelago between 2019 and 2021 estimated by nicheROVER analysis. The posterior means and 95% credible intervals are displayed in turquoise colour.

that there is a correlation between the stable isotope composition of marine organisms and their own growth stages (Wilson et al., 2009). In our study, we found significant positive relationships between $\delta^{13}$C and $\delta^{15}$N with body length in two of five sciaenid species. The $\delta^{13}$C value of *N. albiflora* varies with the developmental stage. The larger the body length, the larger the $\delta^{13}$C value of the *N. albiflora*. The $\delta^{13}$C value in the organism came from the food it ingested, indicating that the food source of the *N. albiflora* changed greatly during the growth process. The $\delta^{15}$N value of *J. belangerii* increases with the increase of body length. The $\delta^{15}$N value in the organism indicates the trophic level, indicating that the trophic position of *J. belangerii* changed substantially during the growth. Ontogenetic shifts in diet are frequently observed in sciaenid species, with the consumption of prey that is larger and at a higher trophic-level attributable to metabolic requirements of larger individuals and changes in foraging ability due to an increase in gape and swimming speed (He et al., 2012; Wei et al., 2018). Wangkai et al. found that *J. belangerii* juveniles mainly feed on amphipods, while adults mainly feed on fish and shrimp (Wang et al., 2012b). Lin et al. (2013) found that the food intake of *N. albiflora* also changed to a certain extent during the growth process. The *N.*

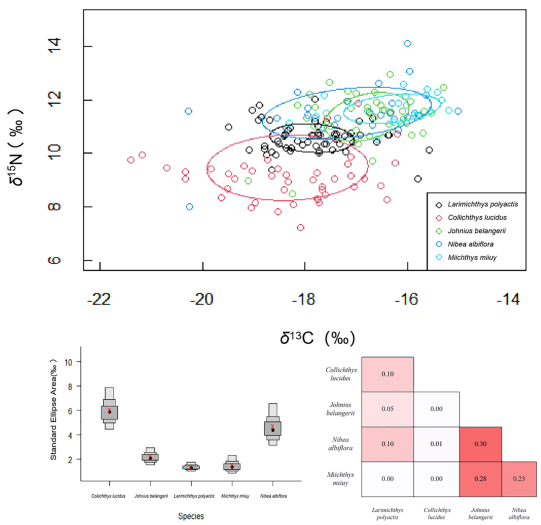


**FIGURE 6** | Corrected standard ellipse area (SEAc) representing the trophic niche width of five sciaenid fish species collected from the Zhoushan Archipelago between 2019 and 2021. SEAc represents the trophic niche width of five sciaenid fishes. Overlap (numbers inside boxes) of corrected standard ellipse areas (SEAcs) of sciaenid fishes estimated using Stable Isotope Bayesian Ellipses (SIBER) in R. Colour intensity increases with SEAc overlap.

*albiflora* with a body length of 80–220 mm mainly fed on small shrimps, while those with a body length of more than 220 mm mainly fed on fish and mantis shrimp (Lin et al., 2013). However, in this study, the isotope ratios in three of the five sciaenid fishes, *L. polyactis, C. lucidus, and M. miiuy*, did not change significantly with the increase of body length, which agrees with the findings of Wilson et al. (2009). Changes in stable isotope composition are related to the organisms ingested, and for species with complex feeding habits, stable isotope ratios may not be identified.

Our results suggest that different species feed at different trophic levels. *L. polyactis* and *C. lucidus* are small, and they mainly feed on zooplankton. *N. albiflora* and *M. miiuy* are larger in size, and they feed more on zoobenthos. This conclusion can also be verified *via* existing reports on stomach content analysis (He et al., 2012; Wang et al., 2012c; Wei et al., 2018; Wang et al., 2020; Zhang et al., 2020). *J. belangerii* is a unique species; although it is small, it has a high trophic level, which may be due to its upper jaw being longer than the lower jaw and the low mouth position, it has a specific selectivity towards prey organisms, preying more on benthic organisms (Zhang et al., 2020).

Furthermore, our results suggest that the widest trophic niche was characteristic of the dominant species *C. lucidus* and *N. albiflora*. Moreover, their ranges of $\delta^{13}$C and $\delta^{15}$N values exceeded that of other species by approximately two times, and the total area of isotopic niche exceeded that of other fishes by 2–6 times. *C. lucidus* showed a broad range of $\delta^{13}$C values as compared to other organisms with similar size ranges, such as *L. polyactis*. This finding suggests that *C. lucidus* has a wider habitat use or greater range of movement and more feeding resources than *L. polyactis*. This may be due to the fact that *C. lucidus* is distributed in estuaries and oceans, with strong habitat heterogeneity, and the stable isotope ratio of its living environment varies greatly. (Tilley et al., 2013; Yeakel et al., 2015). Within a species, differences in diet, trophic position, and habitat use can be related to age (size), sex-specific energy requirements, vulnerability to predators, and reproduction. Such differences affect the structure and dynamics of populations, communities, and ecosystems (Hammerschlag-Peyer et al., 2011; Hussey et al., 2011; Kiszka et al., 2014).

We observed a degree of isotopic niche overlap between *J. belangerii*, *N. albiflora*, and *M. miiuy*, which suggests that these species co-occur in the same space and share feeding resources. These three sciaenid species showed a decreased overlap with *L. polyactis* and *C. lucidus*, suggesting some degree of resource segregation. *J. belangerii* and *N. albiflora* spend their lives near the reef, according to stomach content studies (Wang et al., 2012b; Zhang et al., 2020), and share their main choice of prey (Amphipoda and Decapoda) although in different proportions, while other prey appear less frequently in their diet. In contrast, *L. polyactis* and *C. lucidus* feed on relatively lower trophic-level prey (He et al., 2012; Wei et al., 2018), such as zooplankton and other low trophic level prey. This explains their lower $\delta^{15}$N as compared to the other three species. These factors could clarify the reasons for the relatively low isotopic niche overlap of *L. polyactis* and *C. lucidus* with the other three species. The main prey for each species was different, suggesting some degree of resource partitioning between these species as a possible strategy to reduce interspecific competition.

Our study found that an abundance of prey groups supported the large fishery resources in Zhoushan Archipelago waters, and the coexistence of five species of Sciaenidae in Zhoushan fisheries resulted from the separation of feeding selection and the partitioning of trophic ecological niches. The limitation of this study is that the analysis of differences in feeding choice should be combined with stomach content analysis to improve the reliability of the results.

## DATA AVAILABILITY STATEMENT

The raw data supporting the conclusions of this article will be made available by the authors, without undue reservation.

## ETHICS STATEMENT

The samples used in this study are from ocean trawl surveys approved by the Marine Fisheries Service, so ethical review and approval was not required for this study.

## AUTHOR CONTRIBUTIONS

Conceptualization, JW; methodology, JW; software, JW; validation, YX; formal analysis, JW; investigation, FC; resources,

RY; data curation, R-JJ; writing—original draft preparation, JW; writing—review and editing, JW; visualization, JW; supervision, Y-dZ; project administration, R-JJ. and HX X.; funding acquisition, R-JJ, Y-dZ, and H-XX; All authors have read and agreed to the published version of the manuscript.

## FUNDING

This research was funded by the National Key R&D Program of China (grant numbers 2018YFD0900904 and 2019YFD0901204); and the Public Welfare Technology Application Research Project of Zhejiang Province (grant number: LGN20C190012).

## ACKNOWLEDGMENTS

We would like to express our gratitude to the staff of the Resource Research Office of Zhejiang Marine Fisheries Research Institute for their great help during the data collection process. We also thank the reviewers for their valuable comments and suggestions.

## REFERENCES

Balčiauskas, L., Skipitytė, R., Balčiauskienė, L., and Jasiulionis, M. (2019). Resource Partitioning Confirmed by Isotopic Signatures Allows Small Mammals to Share Seasonally Flooded Meadows. *Ecol. Evol.* 9, 5479–5489. doi: 10.1002/ece3.5144

Beaudrot, L., Struebig, M. J., Meijaard, E., van Balen, S., Husson, S., and Marshall, A. J. (2013). Co-Occurrence Patterns of Bornean Vertebrates Suggest Competitive Exclusion Is Strongest Among Distantly Related Species. *Oecologia* 173, 1053–1062. doi: 10.1007/s00442-013-2679-7

Chen, W. Z., Li, C. S., and Hu, F. (1997). A Review of the Fisheries Resource Status in East China Sea. *J. Fish. Sci. China.* 4, 39–43. doi: 10.3321/j.issn:1005-8737.1997.03.008

Chesson, P. (2000). Mechanisms of Maintenance of Species Diversity. *Annu. Rev. Ecol. Syst.* 31, 343–366. doi: 10.1146/annurev.ecolsys.31.1.343

Choi, M. J., and Kim, D. H. (2020). Assessment and Management of Small Yellow Croaker (*Larimichthys Polyactis*) Stocks in South Korea. *Sustainability* 12, 8257. doi: 10.3390/su12198257

Costa, A. F., Botta, S., Siciliano, S., and Giarrizzo, T. (2020). Resource Partitioning Among Stranded Aquatic Mammals From Amazon and Northeastern Coast of Brazil Revealed Through Carbon and Nitrogen Stable Isotopes. *Sci. Rep.* 10, 1–13. doi: 10.1038/s41598-020-69516-8

Crawford, K., Mcdonald, R. A., and Bearhop, S. (2008). Applications of Stable Isotope Techniques to the Ecology of Mammals. *Mamm. Rev.* 38, 87–107. doi: 10.1111/j.1365-2907.2008.00120.x

De Camargo, N. F., Reis, G. G., Camargo, A. C. L., Nardoto, G. B., Kneitel, J. M., and Vieira, E. M. (2021). Seasonal Isotopic Niche of a Rodent: High Between-Individual Variation But No Changes in Individual Niche Width During the Rich-Resource Period. *Biotropica* 53, 966–975. doi: 10.1111/btp.12921

Deng, J. Y., and Yang, J. M. (1997). Species Interaction and Food Web of Major Predatory Species in the Bohai Sea. *J. Fish. Sci. China* 4, 2–8. doi: 10.3321/j.issn:1005-8737.1997.04.001

DeNiro, M. J., and Epstein, S. (1978). Influence of Diet on the Distribution of Carbon Isotopes in Animals. *Geochimi. Cosmochim. Acta* 42, 495–506. doi: 10.1016/0016-7037(78)90199-0

De Roos, A. M., Schellekens, T., Kooten, T. V., and Persson, L. (2008). Stage-Specific Predator Species Help Each Other to Persist While Competing for a Single Prey. *Proc. Natl. Acad. Sci. U. S. A.* 105, 13930–13935. doi: 10.1073/pnas.0803834105

Dulvy, N. K., Metcalfe, J. D., Glanville, J., Pawson, M. G., and Reynolds, J. D. (2000). Fishery Stability, Local Extinctions, and Shifts in Community Structure in Skates. *Conserv. Biol.* 14, 283–293. doi: 10.1046/j.1523-1739.2000.98540.x

General Administration of Quality Supervision, Inspection and Quarantine of the People's Republic of China and Standardization Administration (2008). "Gb/T 12763.6-2007 Specifications for Oceanographic-Part 6," in *Marine Biological Survey* (Beijing: Standards Press of China).

Hammerschlag-Peyer, C. M., Yeager, L. A., Araújo, M. S., and Layman, C. A. (2011). A Hypothesis-Testing Framework for Studies Investigating Ontogenetic Niche Shifts Using Stable Isotope Ratios. *PLoS One* 6, e27104. doi: 10.1371/journal.pone.0027104

He, X. B., Li, B., Wang, J. X., Yi, M. R., Kang, B., and Yan, Y. R. (2021). Changes in the Trophic Niche of *Trichiurus Japonicus* in the Beibu Gulf in Different Periods. *Chin. J. Appl. Ecol.* 32, 683–690. doi: 10.13287/j.1001-9332.202102.036

He, Z. T., Zhang, Y. Z., Xue, L. J., Jin, H. W., and Zhou, Y. D. (2012). Seasonal and Ontogenetic Diet Composition Variation of *Collichthys Lucidus* in Inshore Waters in the North of East China Sea. *Mar. Fish.* 34, 270–276. doi: 10.13233/j.cnki.mar.fish.2012.03.010

Hette-Tronquart, N. (2019). Isotopic Niche Is Not Equal to Trophic Niche. *Ecol. Let.* 22 (11), 1987–1989. doi: 10.1111/ele.13218

Hopkins, J. B.III, and Kurle, C. M. (2016). Measuring the Realized Niches of Animals Using Stable Isotopes: From Rats to Bears. *Methods Ecol. Evol.* 7, 210–221. doi: 10.1111/2041-210X.12446

Hou, W. F., Yu, C. G., and Chen, X. Q. (2013). Temperature Distribution in Zhoushan Fishing Ground. *J. Ningbo. Univ. (NSEE).* 26, 31–34. doi: CNKI:SUN:NBDZ.0.2013-03-008

Hussey, N. E., Dudley, S. F. J., Mccarthy, I. D., Cliff, G., and Fisk, A. (2011). Stable Isotope Profiles of Large Marine Predators: Viable Indicators of Trophic Position, Diet, and Movement in Sharks? *Can. J. Fish. Aquat. Sci.* 68, 2029–2045. doi: 10.1139/f2011-115

Jackson, A. L., Inger, R., Parnell, A. C., and Bearhop, S. (2011). Comparing Isotopic Niche Widths Among and Within Communities: SIBER — Stable Isotope Bayesian Ellipses in R. *J. Anim. Ecol.* 80, 595–602. doi: 10.1111/j.1365-2656.2011.01806.x

Jake Vander Zanden, M., and Fetzer, W. W. (2007). Global Patterns of Aquatic Food Chain Length. *Oikos* 116, 1378–1388. doi: 10.1111/j.0030-1299.2007.16036.x

Jin, X. S. (2000). The Dynamics of Major Fishery Resources in the Bohai Sea. *J. Fish. Sci. China.* 7, 22–26. doi: 10.3321/j.issn:1005-8737.2000.04.006

Kiszka, J. J., Charlot, K., Hussey, N. E., Heithaus, M. R., Simon-Bouhet, B., Humber, F., et al. (2014). Trophic Ecology of Common Elasmobranchs Exploited by Artisanal Shark Fisheries Off South-Western Madagascar. *Aquat. Biol.* 23, 29–38. doi: 10.3354/ab00602

Koike, S., Nakashita, R., Kozakai, C., Nakajima, A., Nemoto, Y., and Yamazaki, K. (2016). Baseline Characterization of the Diet and Stable Isotope Signatures of Bears That Consume Natural Foods in Central Japan. *Eur. J. Wildl. Res.* 62, 23–31. doi: 10.1007/s10344-015-0969-6

Lin, L. S. (2004). Analysis on Extant Abundance of Small Yellow Croaker Pseudosciaena Polyactis in the East China Sea. *Mar. Fish.* 26, 18–23. doi: 10.3969/j.issn.1004-2490.2004.01.004

Lin, N., Jiang, Y. Z., Yuan, X. W., Ling, J. Z., Yang, L. L., and Li, S. F. (2013). Reproductive Biology of *Nibea Albiflora* in Xiangshan Bay. *J. Fish. Sci. China* 35 (04), 389–395. doi: 10.13233/j.cnki.mar.fish.2013.04.003

Longhurst, A. R., and Pauly, D. (1987). *Ecology of Tropical Oceans* (Orlando, FL: Academic Press).

Lush, L., Ward, A. I., and Wheeler, P. (2017). Dietary Niche Partitioning Between Sympatric Brown Hares and Rabbits. *J. Zool.* 303, 36–45. doi: 10.1111/jzo.12461

Manlick, P. J., and Pauli, J. N. (2020). Human Disturbance Increases Trophic Niche Overlap in Terrestrial Carnivore Communities. *Proc. Natl. Acad. Sci. U. S. A.* 117, 26842–26848. doi: 10.1073/pnas.2012774117

Marshall, H. H., Inger, R., Jackson, A. L., McDonald, R. A., Thompson, F. J., and Cant, M. A. (2019). Stable Isotopes Are Quantitative Indicators of Trophic Niche. *Ecol. Lett.* 22, 1990–1992. doi: 10.1111/ele.13374

Matthews, D. E., and Bier, D. M. (1983). Stable Isotope Methods for Nutritional Investigation. *Annu. Rev. Nutr.* 3, 309–339. doi: 10.1146/annurev.nu.03.070183.001521

McConnell, R., and Lowemcconnell, R. H. (1987). *Ecological Studies in Tropical Fish Communities* Vol. 1987 (England: Cambridge University Press).

Merkle, J. A., Polfus, J. L., Derbridge, J. J., and Heinemeyer, K. S. (2017). Dietary Niche Partitioning Among Black Bears, Grizzly Bears, and Wolves in a Multiprey Ecosystem. *Can. J. Zool.* 95, 663–671. doi: 10.1139/cjz-2016-0258

Minagawa, M., and Wada, E. (1984). Stepwise Enrichment of 15N Along Food Chains: Further Evidence and the Relation Between δ15n and Animal Age. *Geochimi. Cosmochim. Acta* 48, 1135–1140. doi: 10.1016/0016-7037(84)90204-7

Ministry of Agriculture and Rural Affairs of the People's Republic of China. (2009-2018). *China Fishery Statistical Yearbook 2009–2018* (Beijing, China: China Agriculture Press).

Moore, J. W., and Semmens, B. X. (2008). Incorporating Uncertainty and Prior Information Into Stable Isotope Mixing Models. *Ecol. Lett.* 11, 470–480. doi: 10.1111/j.1461-0248.2008.01163.x

Oelze, V. M., Head, J. S., Robbins, M. M., Richards, M., and Boesch, C. (2014). Niche Differentiation and Dietary Seasonality Among Sympatric Gorillas and Chimpanzees in Loango National Park (Gabon) Revealed by Stable Isotope Analysis. *J. Hum. Evol.* 66, 95–106. doi: 10.1016/j.jhevol.2013.10.003

Parnell, A. C., Inger, R., Bearhop, S., and Jackson, A. L. (2010). Source Partitioning Using Stable Isotopes: Coping With Too Much Variation. *PLoS One* 5 (3), e9672. doi: 10.1371/journal.pone.0009672

Pianka, E. R. (1981). "Competition and Niche Theory," in *Theoretical Ecology*, *2nd ed*. Ed. R. M. May (Oxford OX2 0EL, UK: Blackwell Science), 167–196.

Polis, G. A. (1984). Age Structure Component of Niche Width and Intraspecific Resource Partitioning: Can Age Groups Function as Ecological Species? *Am. Nat.* 123, 541–564. doi: 10.1086/284221

R Core Team. (2015). *R: A Language and Environment for Statistical Computing*. (Vienna, Austria: University of Auckland).

Schoener, T. W. (1974). Resource Partitioning in Ecological Communities. *Science* 185, 27–39. doi: 10.1126/science.185.4145.27

Sheppard, C. E., Inger, R., McDonald, R. A., Barker, S., Jackson, A. L., Thompson, F. J., et al. (2018). Intragroup Competition Predicts Individual Foraging Specialisation in a Group-Living Mammal. *Ecol. Lett.* 21, 665–637. doi: 10.1111/ele.12933

Simon, K. S., and Townsend, C. R. (2003). Impacts of Freshwater Invaders at Different Levels of Ecological Organisation, With Emphasis on Salmonids and Ecosystem Consequences. *Freshw. Biol.* 48, 982–994. doi: 10.1046/j.1365-2427.2003.01069.x

Stock, B. C., and Semmens, B. X. (2016). Unifying Error Structures in Commonly Used Biotracer Mixing Models. *Ecology* 97, 2562–2569. doi: 10.1002/ecy.1517

Swanson, H. K., Lysy, M., Power, M., Stasko, A. D., Johnson, J. D., and Reist, J. D. (2015). A New Probabilistic Method for Quantifying N-Dimensional Ecological Niches and Niche Overlap. *Ecology* 96, 318–324. doi: 10.1890/14-0235.1

Tilley, A., López-Angarita, J., and Turner, J. R. (2013). Diet Reconstruction and Resource Partitioning of a Caribbean Marine Mesopredator Using Stable Isotope Bayesian Modelling. *PloS One* 8, e79560. doi: 10.1371/journal.pone.0079560

Tilman, D. (1982). "Resource Competition and Community Structure," in *Monographs in Population Biology Series* (Princeton: Princeton University Press).

Walker, P. A., and Hislop, R. G. (1998). Sensitive Skates or Resilient Rays? Spatial and Temporal Shifts in Ray Species Composition in the Central and North-Western North Sea Between 1930 and the Present Day. *I.C.E.S. J. Mar. Sci.* 55, 392–402. doi: 10.1006/jmsc.1997.0325

Wang, J. F. (2015). *The Preliminary Study of Food Composition and Feeding Habits of Collichthy lucidus in the Yangtze Estuary* (Nanjing, China:Nanjing Agricultural University).

Wang, Y. L., Hu, C. L., Li, Z. H., Jiang, R. J., Zhou, Y. D., Zhang, L. L., et al. (2021). Population Structure and Resource Change of Larimichthys Polyactis in Spring in Zhoushan Fishery Spawning Ground Protection Area, China. *Yingyong. Shengtai. Xuebao.* 09, 3349–3356. doi: 10.13287/j.1001-9332.202109.036

Wang, C. Q., Tang, J. H., Xiong, Y., Wang, Y. P., Shi, J. J., Yan, X., et al. (2020). Feeding Habits of *Miichthys Miiuy* in Jiangsu Coastal Waters. *J. Zhejiang. Ocean. Univ. (Nat. Sci. A)* 39, 372–378. doi: 10.3969/j.issn.1008-830X.2020.04.014

Wang, K., Zhang, S. Y., Wang, Z. H., Xu, M., and Zhao, J. (2012b). Feeding Habits of Small Yellow Croaker Off Ma'an Archipelago. *Acta Hydrobiol. Sin.* 36, 1188–1192. doi: 10.3724/SP.J.1035.2012.01188

Wang, K., Zhang, S. Y., Wang, Z. H., Zhao, J., and Xu, M. (2012a). A Preliminary Study on Fishery Biology of *Johnius Belangerii* Off Ma'an Archipelago. *J. Fish. China* 36, 228–237. doi: 10.3724/SP.J.1231.2012.27691

Wang, K., Zhang, S. Y., Wang, Z. H., Zhao, J., Xu, M., and Lin, J. (2012c). Dietary Composition and Food Competition of Six Main Fish Species in Rocky Reef Habitat Off Gouqi Island. *Yingyong. Shengtai. Xuebao.* 23, 536–544.

Wei, X. J., Zhang, B., Shan, X. J., Jin, X. S., and Ren, Y. P. (2018). Feeding Habits of Small Yellow Croaker *Larimichthys Polyactis* in the Bohai Sea. *J. Fish. Sci. China* 25, 142–151. doi: 10.3724/SP.J.1118.2018.18163

Wilson, R. M., Chanton, J., Lewis, G., and Nowacek, D. (2009). Isotopic Variation (δ15n, δ13c, and δ34s) With Body Size in Post-Larval Estuarine Consumers. *Estuar. Coast. Shelf. Sci.* 83, 307–312. doi: 10.1016/j.ecss.2009.04.006

Wisheu, I. C. (1998). How Organisms Partition Habitats: Different Types of Community Organization can Produce Identical Patterns. *Oikos* 83, 246–258. doi: 10.2307/3546836

Xu, Z. L., and Chen, J. J. (2009). Analysis on Migratory Routine of *Larimichthy Polyactis*. *J. Fish. Sci. China*. 16, 931–940. doi: 10.3321/j.issn:1005-8737.2009.06.014

Xue, Y., Jin, X. S., Zhang, B., and Zhang, C. L. (2004). Diet Composition and Seasonal Variation in Feeding Habits of Small Yellow Croaker *Pseudosciaena Polyactis* Bleeker in the Central Yellow Sea. *J. Fish. Sci. China.* 11, 237–243. doi: 10.3321/j.issn:1005-8737.2004.03.011

Xu, Z. L., Shen, X. Q., and Ma, S. W. (2005). Ecological Characteristics of Dominant Zooplankton Species in Spring and Summer Near Yangtze River Estuary. *Mar. Sci.* 29, 13–19. doi: CNKI:SUN:HYKX.0.2005-12-003

Yang, J. M. (1997). Preliminary Study on the Feeding of Calanus Sinicus of the Bohai Sea. *Oceanol. Limnol. Sin.* 4, 376–382. doi: 10.3321/j.issn:0029-814X.1997.04.007

Yeakel, J. D., Bhat, U., Elliott Smith, E. A., and Newsome, S. D. (2015). Exploring the Isotopic Niche: Isotopic Variance, Physiological Incorporation, and the Temporal Dynamics of Foraging. *Front. Ecol. Evol.* 4, 1. doi: 10.3389/fevo.2016.00001

Yu, C. G., Chen, Q. Z., Chen, X. N., Ning, P., and Zheng, J. (2010). Species Composition and Quantity Distribution of Fishes in the Zhoushan Fishing Ground and Its Adjacent Waters. *Oceanol. Limnol. Sin.* 41, 410–417. doi: 10.11693/hyhz201003018018

Zhang, Y. L., Xu, B. D., Zhang, C. L., Ji, Y. P., Ren, Y. P., Cheng, Y., et al. (2020). Spatial Heterogeneity in the Feeding Habits and Feeding Ground Distribution of *Johnius Belangerii* in Haizhou Bay During Spring. *J. Fish. Sci. China* 27, 315–326. doi: CNKI:SUN:ZSCK.0.2020-03-006

Zhao, S. L., Wang, R. X., and Liu, X. S. (2002). Reasons of Exhaustion of Resources of *Pseudosciaena Crocea* in Zhoushan Fishing Ground and the Measures of Protection and Proliferation. *J. Zhejiang. Ocean. Univ. (Nat. Sci. A)* 21, 160–165. doi: 10.3969/j.issn.1008-830X.2002.02.018

Zhong, X. M., Tang, J. H., Zhang, H., Zhong, F., Zhong, J. S., Wu, L., et al. (2010). Spatial and Temporal Distribution Characteristics of *Miichthys Miiuy* in Jiangsu Coastal Area. *Haiyang. Xuebao.* 32 (03), 95–106. doi: CNKI:SUN:SEAC.0.2010-03-012

Zhuang, P., Wang, Y. H., Li, S. F., Deng, S. M., Li, C. S., Ni, Y., et al. (2006). *Fishes of the Yangtze Estuary* (Shanghai: Shanghai Scientific and Technology Press).

**Conflict of Interest:** The authors declare that the research was conducted in the absence of any commercial or financial relationships that could be construed as a potential conflict of interest.

frontiers | Frontiers in Marine Science

ORIGINAL RESEARCH
published: 22 June 2022
doi: 10.3389/fmars.2022.900372

# Spatial and Seasonal Variations in the Stable Isotope Values and Trophic Positions of Dominant Zooplankton Groups in Jiaozhou Bay, China

*Zhixin Ke*[1,2,3], *Ruofei Li*[1,3], *Danting Chen*[1], *Chunyu Zhao*[1] *and Yehui Tan*[1,2,3]*

[1] Key Laboratory of Tropical Marine Bio-resources and Ecology, South China Sea Institute of Oceanology, Chinese Academy of Sciences, Guangzhou, China, [2] Southern Marine Science and Engineering Guangdong Laboratory (Guangzhou), Guangzhou, China, [3] University of Chinese Academy of Sciences, Beijing, China

The spatial and seasonal distributions of stable carbon and nitrogen isotopes ($\delta^{13}C$ and $\delta^{15}N$) in dominant zooplankton groups were investigated in Jiaozhou Bay. Zooplankton $\delta^{13}C$ values ranged from –22.89‰ to –15.86‰, and $\delta^{15}N$ values ranged from 3.18‰ to 13.57‰, respectively. The $\delta^{13}C$ and $\delta^{15}N$ values generally followed the order of small zooplankton < large calanoids < small *Sagitta* < large *Sagitta*. Spatial distribution patterns of zooplankton $\delta^{13}C$ and $\delta^{15}N$ values varied in different seasons. Our results suggested that the spatial variation of $\delta^{13}C$ was mainly controlled by terrigenous organic matter (OM) input and phytoplankton biomass, but water temperature may have played a key role in the seasonal variation of $\delta^{13}C$. In spring, the high phytoplankton biomass might increase the $\delta^{13}C$ value of small zooplankton in the inner bay. During other seasons, the $\delta^{13}C$ values of zooplankton generally increased from the inner bay to the outer bay, which might be associated with the influence of $^{13}C$-depleted terrigenous OM carried by the river discharge. Small zooplankton stable isotope values were significantly correlated with that of particulate organic matter (POM). The influence of anthropogenic nutrient input on isotopic baseline can be cascaded to the zooplankton, and the effect might be weak at higher trophic levels. The Bayesian standard ellipse areas of dominant zooplankton groups were generally smallest in the winter, suggesting a narrow niche width during that time. The niche partition between small zooplankton, large calanoids, and *Sagitta* was most distinct in winter, and followed by summer. The relative trophic level of *Sagitta* ranged from 2.23 to 4.01, which generally declined from the inner bay to the outer bay during the spring, autumn, and winter seasons. High anthropogenic nutrient loading might reduce the difference in trophic niches among zooplankton groups. This study provided detailed information on the distribution of zooplankton $\delta^{13}C$ and $\delta^{15}N$ in a coastal bay, which will be useful for understanding the anthropogenic influence on the ecosystem structure and function.

**Keywords: zooplankton, trophic structure, food web, stable isotope, anthropogenic influence**

OPEN ACCESS

***Edited by:***
*Jun Xu,*
*Institute of Hydrobiology (CAS), China*

***Reviewed by:***
*Bin Yang,*
*Beibu Gulf University, China*
*Anupam Priyadarshi,*
*Banaras Hindu University, India*

***Correspondence:**
*Yehui Tan*
*tanyh@scsio.ac.cn*

***Specialty section:***
*This article was submitted to Marine Ecosystem Ecology, a section of the journal Frontiers in Marine Science*

***Received:*** *20 March 2022*
***Accepted:*** *17 May 2022*
***Published:*** *22 June 2022*

***Citation:***
*Ke Z, Li R, Chen D, Zhao C and Tan Y (2022) Spatial and Seasonal Variations in the Stable Isotope Values and Trophic Positions of Dominant Zooplankton Groups in Jiaozhou Bay, China. Front. Mar. Sci. 9:900372. doi: 10.3389/fmars.2022.900372*

## INTRODUCTION

Zooplankton play a key role in aquatic ecosystems: they transfer energy and materials from primary producers to higher trophic levels (Hannides et al., 2009). The species composition and abundance of zooplankton can be quickly changed by the variation of environmental factors, and potentially affect ecosystem function and biogeochemical cycling (Dickman et al., 2008). Knowledge of zooplankton trophic structure is necessary to understand food-web function and response to climate change or human activities (Kozak et al., 2020; Nagelkerken et al., 2020).

Carbon and nitrogen stable isotopes ($\delta^{13}C$ and $\delta^{15}N$) are widely used to trace the material source and trophic structure in aquatic ecosystems (Post, 2002; Fry, 2006). Generally, the $\delta^{13}C$ value increases by approximately 1.5‰, and the $\delta^{15}N$ value increases by 2–4‰ per trophic level (Fry, 2006). Due to the fast growth rate and short turnover time, the stable isotope values of zooplankton can quickly change with environmental variation (Rolff, 2000; O'Reilly et al., 2002). Describing the distribution patterns of stable isotopes in pelagic ecosystems is important when assessing the anthropogenic influence on coastal ecosystems. Stable isotopes have the potential to integrate variability in environmental conditions, and help us understand the relationship between eutrophication and the trophic structure of pelagic food web (Fry, 2006; El-Sabaawi et al., 2013). In general, the $\delta^{15}N$ values are more sensitive to environmental change. Nitrogen concentration needs to be considered when using $\delta^{15}N$ values in biota as indicators of anthropogenic nitrogen inputs (Pruell et al., 2020). The $\delta^{15}N$ of zooplankton can also vary over inter-annual scales of climate variability. Décima et al. (2013) reported a significant $^{15}N$ enrichment of approximately 2‰ for zooplankton during the 1998 El Niño in the southern California Current Ecosystem. The zooplankton isotopic niche suggested that the planktonic food web spans >3 trophic levels, ranging from herbivores to higher predators (El-Sabaawi et al., 2009; Chi et al., 2021). Trophic niche and niche overlap among zooplankton species can well reflect the influence of environmental change on ecosystem function and biogeochemical cycling. Generally, short food webs are expected in eutrophic ecosystems compared to oligotrophic ecosystems (Armengol et al., 2019). However, Kozak et al. (2020) reported that increased primary and secondary productivity results in an increase of food web complexity, and produces longer food chains. The response of zooplankton trophic structure to eutrophication might be different in various marine ecosystems. To date, high-resolution studies of trophic dynamics within zooplankton community are still scarce.

Jiaozhou Bay is a semi-enclosed bay in northern China, bordering on the Yellow Sea. Many studies have suggested that the ecosystem of this bay has been strongly disturbed by intensive anthropogenic activities, including aquaculture, wastewater discharge, land reclamation, and harbor construction (Liu et al., 2005; Yuan et al., 2016; Ke et al., 2020). Jiaozhou Bay has been regarded as an ideal region for studying the influence of human activities on coastal ecosystems and there are abundant reports on the structure and function of ecosystem corresponding to anthropogenic influences (Sun et al., 2012; Yuan et al., 2016; Wang et al., 2021). The size structure of zooplankton was significantly associated with environmental factors in this bay, and the total zooplankton abundance and small size ranks presented a decreasing gradient from the inner bay to the outer part (Wang et al., 2020a). Recently, Wang et al. (2020b) indicated that the population explosion of the jellyfish *Aurelia coerulea* in Jiaozhou Bay increased the predation pressure on zooplankton and changed the trophic structure of pelagic ecosystem. Most studies only focused on the species composition and abundance of zooplankton. Few studies have estimated the source of particulate organic matter (POM) or sediment organic matter using carbon and nitrogen stable isotopes. Both the $\delta^{13}C$ value and C/N ratio suggested a higher contribution of marine organic carbon than terrestrial organic carbon in this bay (Yang et al., 2011). Using carbon stable isotopes, Kang et al. (2017) estimated that marine-sourced OM contributed to 45%–79% of total organic carbon in the sediment of Jiaozhou Bay. Ke et al. (2020) indicated that the $^{15}N$ of POM was significantly depleted in the northeastern region due to the strong influence of urban sewage from Qingdao City. In comparison, there are still relatively limited data available on $\delta^{13}C$ and $\delta^{15}N$ of zooplankton in Jiaozhou Bay. The zooplankton trophic position and response to environmental change remain poorly understood.

In this study, we investigated the spatial and seasonal distribution of zooplankton stable isotope values in Jiaozhou Bay. Seasonal variations of stable isotopic signatures in zooplankton remain mostly undescribed in coastal bay, which is important as a baseline reference for trophic structure analyses in marine ecosystem (Kozak et al., 2020). We compared the relative trophic positions of the dominant zooplankton groups in different seasons. The objective of this study was to examine the variations in stable isotope signatures and trophic niches of zooplankton in a coastal bay under anthropogenic influences. The relationships between the zooplankton stable isotopic signatures and environmental variables were also analyzed. The results of this study may assist with assessing the anthropogenic influence on the trophic structure of coastal ecosystems.

## MATERIALS AND METHODS

### Study Area

The Jiaozhou Bay is located in northern China. Its area is about 390 $km^2$, and the average water depth is about 7 m. The bay mouth is narrow with about 2.5 km. The tide is a typical semi-diurnal tide with a mean range of 7 m. This bay is under a temperate oceanic monsoon climate. The average annual temperature is 12°C, and the average annual precipitation is 900 mm in this region. The Jiaozhou Bay is surrounded by Qingdao City, and its ecosystem has been strongly impacted by human activities (Liu et al., 2005). Since the 1980s, the species composition of zooplankton in this bay has changed significantly. Both the abundance and species diversity of small jellyfish have increased in Jiaozhou Bay during the past two decades (Sun et al., 2012; Wang et al., 2020b). The long-term investigation suggested that the ecological environment of Jiaozhou Bay has changed under the influence of

anthropogenic activities, including algal blooms, biodiversity decline, and ecosystem degradation (Yuan et al., 2016; Zhang et al., 2021).

## Sample Collection and Analysis

Seasonal surveys were carried out at 12 stations (S1–S12) in Jiaozhou Bay in spring (April 6–8, 2016), summer (August 17–19, 2017), autumn (November 18–20, 2016), and winter (January 5–8, 2016) (**Figure 1**). Water samples were collected using a 10-L Niskin bottle at a depth of 0.5 m below the surface. Water temperature, salinity, nutrients, and chlorophyll a (Chl *a*) concentrations were measured. The sampling and analysis methods of environment variables were introduced in detail in Ke et al. (2020). POM samples were obtained by filtering 0.5–1 L of surface water through pre-combusted Whatman GF/F filters. Zooplankton samples were collected by vertical tows from the bottom to the surface using a conical plankton net (0.5 m diameter, length 2 m, and mesh size 169 μm). The net was hauled 2–4 times at each station with the speed of about 0.5 m $s^{-1}$. Collected zooplankton specimens were placed in pre-filtrated sea water for about 0.5 h to exclude the gut content. Then, these samples were aggregated using a piece of 180-μm nylon sieve and frozen in liquid nitrogen. When returned to the lab, these zooplankton samples were stored at −20°C until further species identification and separation.

Each zooplankton sample was first sieved using a 500-μm mesh sieve to separate the <500-μm size class that was processed as small zooplankton. Three dominant groups were picked up from the individuals larger than 500 μm, including large calanoids (large CA), small *Sagitta* and large *Sagitta*. These groups contributed to most of the zooplankton biomass in the coastal bays of China (Ma et al., 2014; Wang et al., 2020a). The body length of small *Sagitta* was generally less than 1.2 cm and large *Sagitta* was larger than 1.5 cm. These dominant groups were collected at most stations during the investigation. Because the collected zooplankton contained less carbonate and acid treatment can significantly affect the $\delta^{15}N$ value, these samples were not treated with HCl (Troina et al., 2020). To obtain sufficient samples for stable isotope analysis, several individuals (2-8) of similar size belonging to the same taxonomic group were pooled together. Zooplankton samples were rinsed with distilled water, placed in pre-weighed tin capsules with a 5-mm diameter, and dried at 60°C for 24 h.

## Stable Isotopes Analysis and Statistical Analysis

A total of 0.5–2 mg of zooplankton samples was wrapped into tin capsules and sent for the analysis of stable isotope composition. Stable isotope values of POM and zooplankton were determined with a continuous-flow isotope-ratio mass spectrometer (Delta V Advantage, Thermo Fisher Scientific, Waltham, MA, USA) coupled to an elemental analyzer (Flash EA 1112, Thermo Fisher Scientific, Milan, Italy). Isotopic ratios were expressed in δ notation as the deviation in parts per mil (‰) from a standard reference material: $\delta^{13}C$ or $\delta^{15}N$ (‰) = $(R_{sample}/R_{standard} - 1) \times 1{,}000$, where R is either $^{13}C/^{12}C$ or $^{15}N/^{14}N$. The reference standards of carbon and nitrogen are the PeeDee Belemnite and atmospheric $N_2$, respectively. The analytical precision for both isotopes is ± 0.2‰. Casein protein was used as a working standard, whose certified values for carbon and nitrogen were determined by EA-IRMS calibrated to IAEA-CH-6 and IAEA-N-1 (IAEA, Vienna).

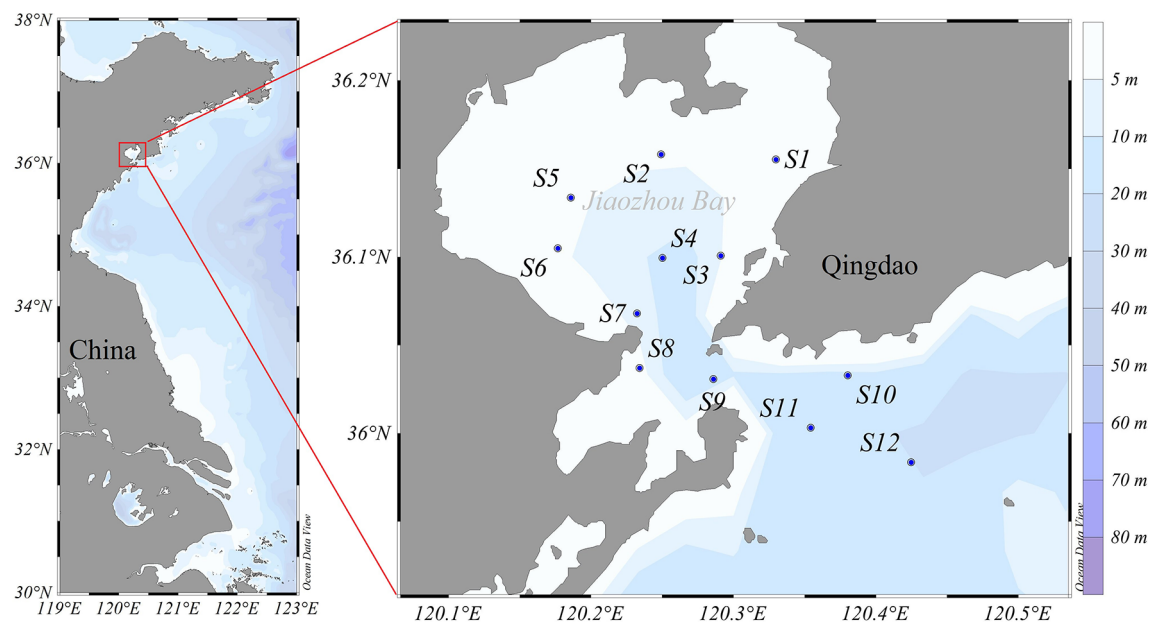


**FIGURE 1** | Map of Jiaozhou Bay and the location of the sampling stations.

Prior to the data analysis, a lipid correction of $\delta^{13}C$ values was carried out for specimens with high C:N ratios (>3.5) according to Post et al. (2007). The correction formula was as follows: $\delta^{13}C_{normalized} = \delta^{13}C_{untreated}$ - 3.32+0.99× C:N, where $\delta^{13}C_{normalized}$ was used for further analysis in this study, $\delta^{13}C_{untreated}$ denotes the raw data, and C:N ratio is the bulk carbon-to-nitrogen ratio. The $\delta^{15}N$ values of POM showed a significant spatial variation in Jiaozhou Bay (Ke et al., 2020). In this study, the trophic level of small zooplankton (<500 μm) was assigned a value of 2 to eliminate the influence of fluctuations in the $\delta^{15}N$ baseline. Relative trophic level calculation: RTL = $\frac{\delta^{15}N_{Zoo}-\delta^{15}N_{Small\ ZP}}{3.4\ ‰} + 2$, where RTL is the relative trophic level, and $\delta^{15}N_{Zoo}$ and $\delta^{15}N_{Small\ ZP}$ are the values of $\delta^{15}N$ in dominant zooplankton groups and small zooplankton, respectively. The trophic enrichment factor of $\delta^{15}N$ is assigned as 3.4‰ for each trophic level (Post, 2002).

The isotopic niches of zooplankton community were estimated by bivariate trophic space, in which the $\delta^{13}C$ and $\delta^{15}N$ values represented the carbon source and trophic level of zooplankton, respectively. The Stable Isotope Bayesian Ellipses in R (SIBER) package in the R-routine was used to estimate the potential isotope niche width and overlap for dominant zooplankton groups during different seasons (Jackson et al., 2011; R Core Team, 2020). The areas of Bayesian standard ellipse were calculated using a bivariate approach of the niche width, as defined by the isotopic space of $\delta^{13}C$ vs. $\delta^{15}N$ plots. Because small and large *Sagitta* were usually not collected at one station simultaneously, the average $\delta^{13}C$ and $\delta^{15}N$ values of small and large *Sagitta* at each station were used to make the comparison between different zooplankton groups. One-way analysis of variance (ANOVA) was used to check the seasonal and spatial differences in stable isotope values or nutrient concentrations. All statistical analyses were performed with SPSS software package, version 19.0 for Windows (SPSS Inc., Chicago, IL, USA). The map and the contour figures were made by the software Ocean Data View 5.2 (Schlitzer, R., http://odv.awi.de).

# RESULTS

## Environmental Conditions

The average values of main environmental variables in four seasons are shown in **Figure 2**. Annual average values of water temperature and salinity were 14.8°C and 30.8, respectively. The variation in water temperature was large in a year. The average sea surface sea temperature (SST) was 6.3°C in winter and 27.4°C in summer. In contrast, sea surface salinity (SSS) was relatively stable in different seasons, but was slightly lower in summer (average 30.1). The seasonal variation of nutrient concentration was great, which was highest in summer and lowest in winter (**Figure 2**). Annual average DIN, $PO_4^{3-}$, and $SiO_3^{2-}$ concentrations were 13.6 μM, 0.3 μM, and 7.2 μM, respectively. Detailed spatial distributions of environmental variables were previously described in Ke et al. (2020). In brief, the concentrations of nutrients and Chl *a* generally decreased from the inner to the outer bay, and were very high at station S1 in the northeastern bay (Ke et al., 2020).

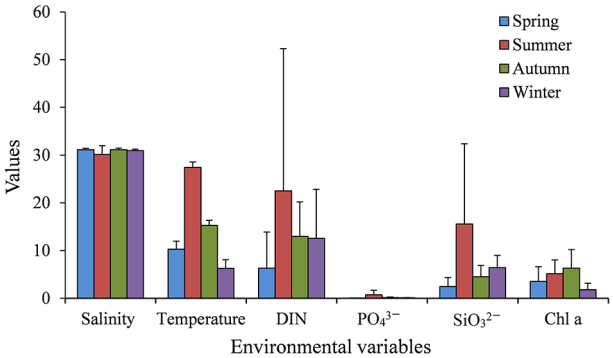


**FIGURE 2** | Seasonal average values of key environmental variables, including salinity, temperature, DIN (μM), $PO_4^{3-}$ (μM), $SiO_3^{2-}$ (μM), and Chl a (μg $L^{-1}$) in Jiaozhou Bay.

## Spatial and Seasonal Variations of Stable Isotopes in Dominant Zooplankton Groups

In this study, the large calanoids were mainly represented by adult *Calanus sinicus*, the large *Sagitta* were mainly represented by adult *Sagitta crassa*, and the small *Sagitta* were mainly represented by junior *Sagitta crassa and Sagitta bedoti*. The spatial distributions of $\delta^{13}C$ and $\delta^{15}N$ values were similar in these dominant zooplankton groups (**Figures 3**, **4**). The seasonal distribution patterns of zooplankton $\delta^{13}C$ values were complicated in Jiaozhou Bay. Lower $\delta^{13}C$ values generally occurred in the inner bay during summer, autumn, and winter. However, in spring, the $\delta^{13}C$ values of zooplankton were higher in the inner bay especially for the small zooplankton (**Figure 3**). In autumn, obviously lower $^{13}C$ values of zooplankton were found at station S6 in the western inner bay. The seasonal average values of $\delta^{13}C$ and $\delta^{15}N$ of these dominant zooplankton groups are shown in **Table 1**. The $\delta^{13}C$ values of zooplankton ranged from −22.89‰ to −15.86‰. Annual average $\delta^{13}C$ value was −19.09‰ for small zooplankton, −18.94‰ for large calanoids, −18.68‰ for small *Sagitta*, and −17.18‰ for large *Sagitta*. In winter, small zooplankton displayed the lowest $\delta^{13}C$ values, which gradually increased from the inner bay to the outer bay.

Generally, a weak increasing trend in the $\delta^{15}N$ values of zooplankton and POM was observed from the inner bay to the outer bay (**Figure 4**). In most cases, zooplankton showed higher $\delta^{15}N$ values in the western inner bay. Only the small zooplankton showed obviously lower $\delta^{15}N$ values in the northeastern bay (**Figure 4**) during summer. The $\delta^{15}N$ values of zooplankton ranged from 3.18‰ to 13.57‰. The annual average $\delta^{15}N$ values were 6.39‰ for small zooplankton, 7.39‰ for large calanoids, 9.38‰ for small *Sagitta*, and 10.14‰ for large *Sagitta*, respectively. In spring, the body size of *Sagitta* showed large variation ranging from 0.5 to 2.1 cm. The large *Sagitta* showed significantly higher $\delta^{15}N$ values (average 9.79‰) than the small *Sagitta* (average 7.68‰) in spring (ANOVA, $F = 22.51$, $p < 0.001$). However, in other seasons, the difference in $\delta^{15}N$ value was very small between them (**Table 1**).

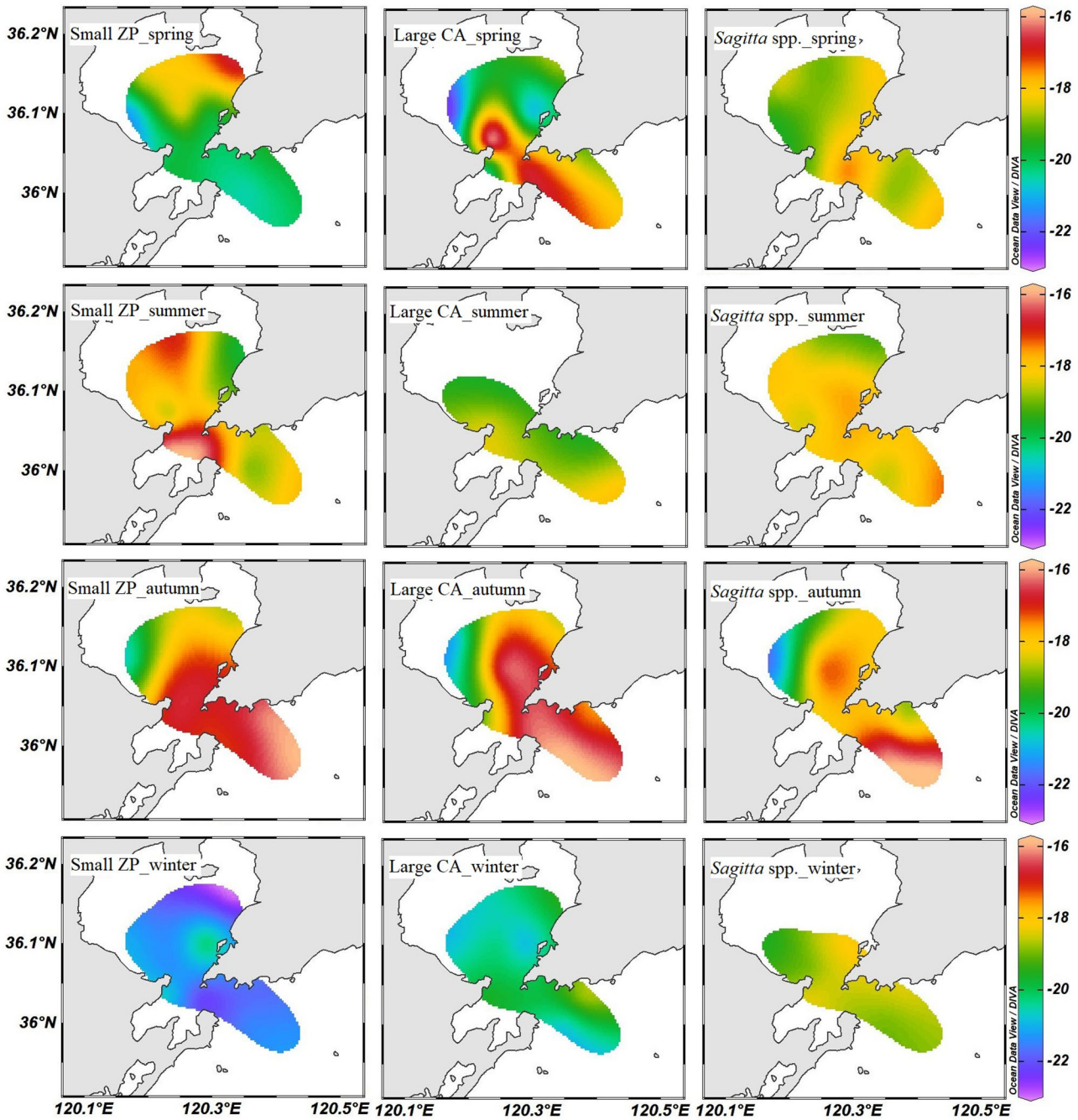


**FIGURE 3** | Horizontal distribution of $\delta^{13}C$ in small zooplankton (small ZP), large calanoids (large CA), and *Sagitta* spp. in Jiaozhou Bay.

## Seasonal Variations in the Trophic Structure of Zooplankton Community

The bivariate approach of the ecological niche defined by $\delta^{13}C$ and $\delta^{15}N$ showed the seasonal variation in the trophic niche of zooplankton community (**Figure 5**). In spring, an intensive overlap occurred among these three zooplankton groups. The niche partition between small zooplankton, large calanoids, and *Sagitta* was most distinct in winter, and followed by summer. The largest standard ellipse areas were observed during autumn and the smallest ones were observed in winter. The range of zooplankton $\delta^{13}C$ values was narrowest in winter, suggesting a simple food source during that period.

The average RTL of large calanoids was 2.24, which was slightly higher than that of small zooplankton. *Sagitta* occupied the

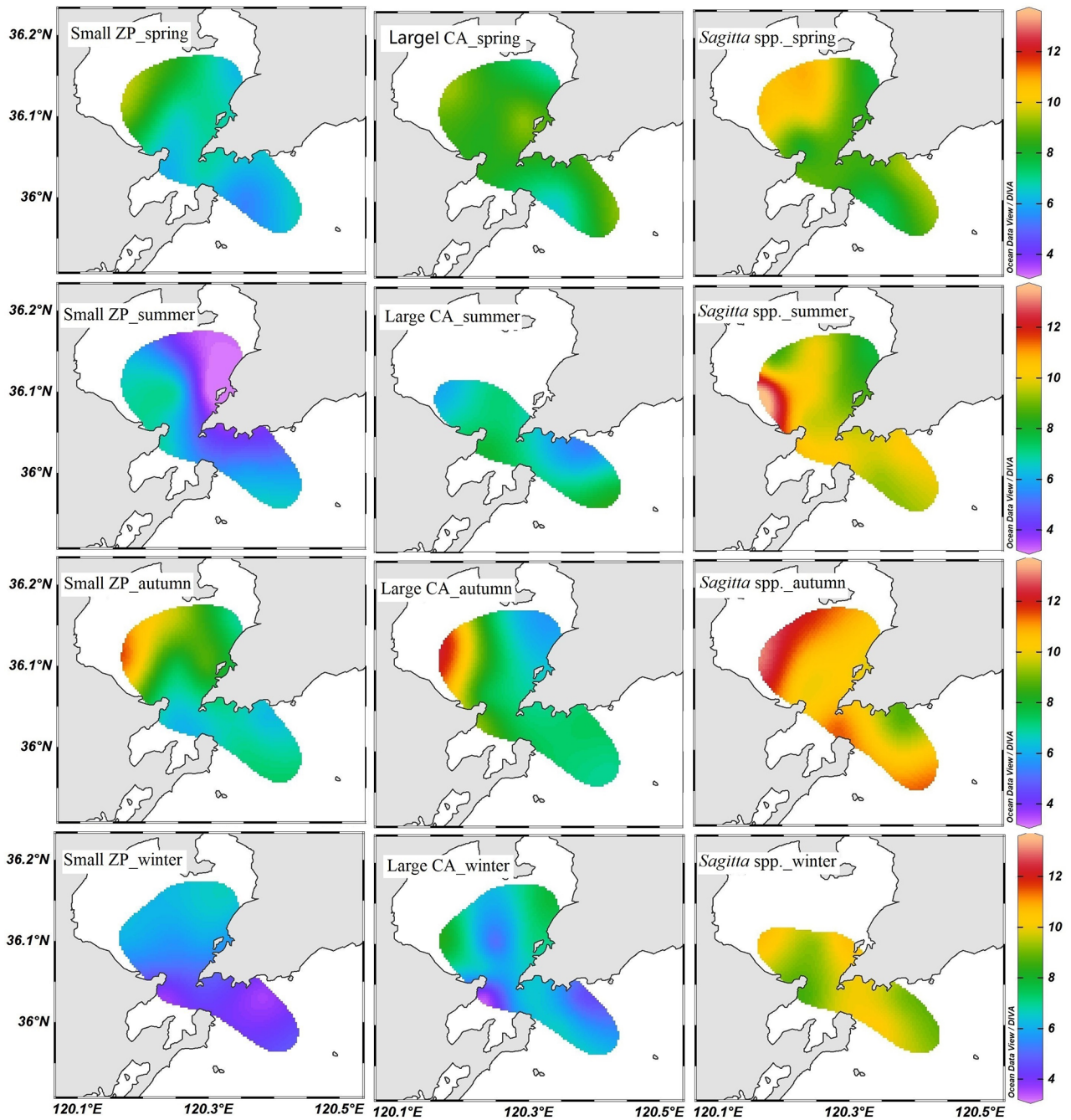


**FIGURE 4** | Horizontal distribution of $\delta^{15}N$ in small zooplankton (small ZP), large calanoids (large CA), and *Sagitta* spp. in Jiaozhou Bay.

highest trophic level in the pelagic food web with an annual average RTL of 3.1. The RTL of *Sagitta* ranged from 2.23 to 4.01, which was closely correlated with body size. Especially in spring, the body size of *Sagitta* varied greatly, and large *Sagitta* have significantly higher RTL than small *Sagitta* (ANOVA, $F = 10.16$, $p < 0.01$). The annual average RTLs of small and large *Sagitta* were 2.97 and 3.14, respectively. According to the spatial distribution patterns, *Sagitta* generally showed a lower RTL in the inner bay during spring, autumn, and winter seasons (**Figure 6**). No regular distribution pattern of RTL was found in the summer.

## Correlation Between Stable Isotopes and Environmental Variables

The correlation coefficients between the stable isotope values of dominant zooplankton groups and key environmental variables are shown in **Figure 7**. The $\delta^{13}C$ values of POM, small zooplankton,

**TABLE 1** | Seasonal average values (‰) of $\delta^{13}C$ and $\delta^{15}N$ in dominant zooplankton groups and suspended particulate organic matter (POM) in Jiaozhou Bay.

| | | Spring | Summer | Autumn | Winter | Average |
|---|---|---|---|---|---|---|
| $\delta^{13}C$ | Large *Sagitta* | −18.07 | −17.86 | −14.29 | −18.48 | −17.18 |
| | Small *Sagitta* | −19.18 | −18.16 | −18.58 | −18.79 | −18.68 |
| | Large calanoids | −18.88 | −18.89 | −17.90 | −20.09 | −18.94 |
| | Small zooplankton | −19.42 | −17.88 | −17.55 | −21.48 | −19.08 |
| | POM | −22.75 | −21.82 | −22.47 | −25.22 | −23.07 |
| $\delta^{15}N$ | Large *Sagitta* | 9.79 | 9.97 | 10.80 | 10.00 | 10.14 |
| | Small *Sagitta* | 7.68 | 10.01 | 10.70 | 9.15 | 9.38 |
| | Large calanoids | 8.27 | 6.96 | 8.22 | 6.10 | 7.39 |
| | Small zooplankton | 7.03 | 5.45 | 7.95 | 5.13 | 6.39 |
| | POM | 4.23 | 3.88 | 5.20 | 4.21 | 4.38 |

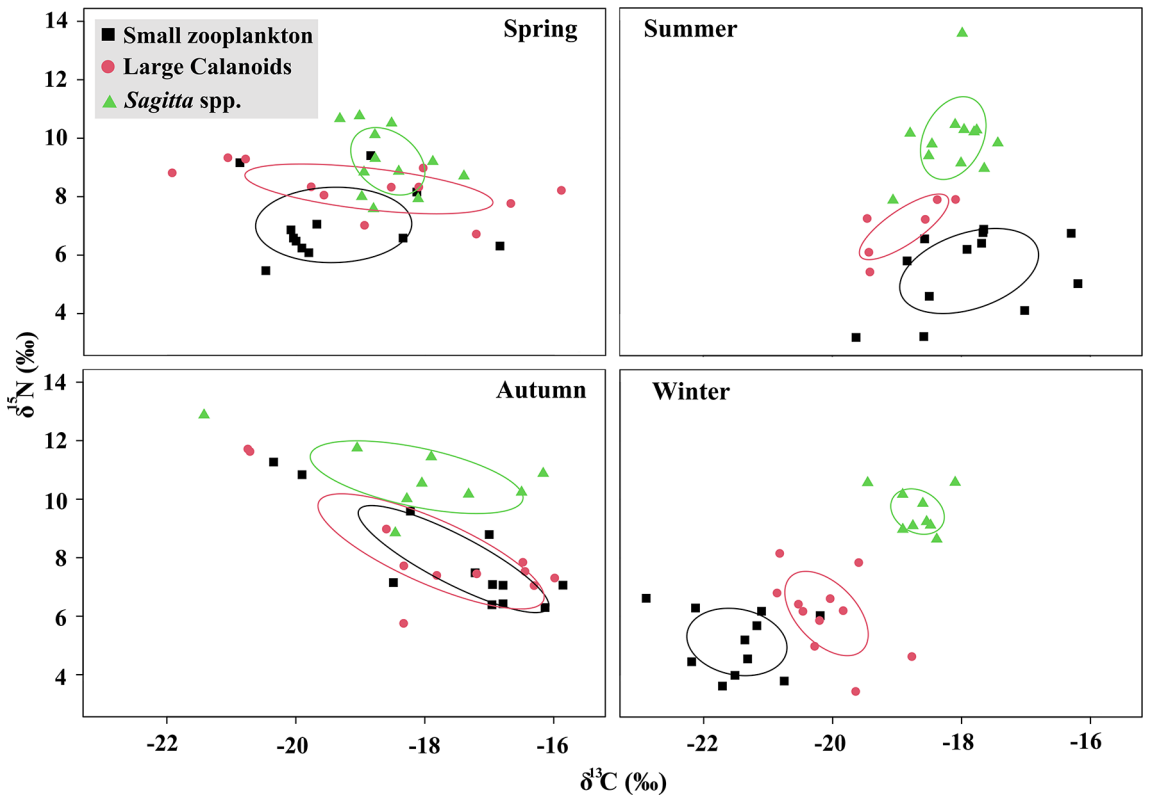


**FIGURE 5** | Seasonal variations in the bivariate trophic niche of dominant zooplankton groups represented by Bayesian ellipses in Jiaozhou Bay.

and large calanoids were significantly positively correlated with SST. The $\delta^{15}N$ value of small zooplankton was positively correlated with SSS. The $\delta^{13}C$ values of large calanoids were significantly positively correlated with $SiO_3^{2-}$ concentrations. The $\delta^{15}N$ values were generally negatively correlated with nutrients. However, the $\delta^{15}N$ of *Sagitta* showed a weak correlation with environmental variables. In addition, the $\delta^{13}C$ and $\delta^{15}N$ values of POM and zooplankton generally showed a positive correlation with Chl *a*.

Compared with the $\delta^{13}C$, the $\delta^{15}N$ values showed a stronger correlation between POM and each dominant zooplankton group (**Figure 8**). The $\delta^{13}C$ values of POM were significantly correlated with that of small zooplankton ($p < 0.01$). The $\delta^{15}N$ values of POM were significantly correlated with that of small zooplankton, large calanoids, and *Sagitta* ($p < 0.01$).

## DISCUSSION

### Spatial and Seasonal Variability in $\delta^{13}C$ and $\delta^{15}N$ of Zooplankton

The stable isotope signatures of zooplankton can well reflect environmental change due to their short life span and relatively fast turnover time (Rolff, 2000; O'Reilly et al., 2002). Variation in the stable isotopes of food items (such as phytoplankton or

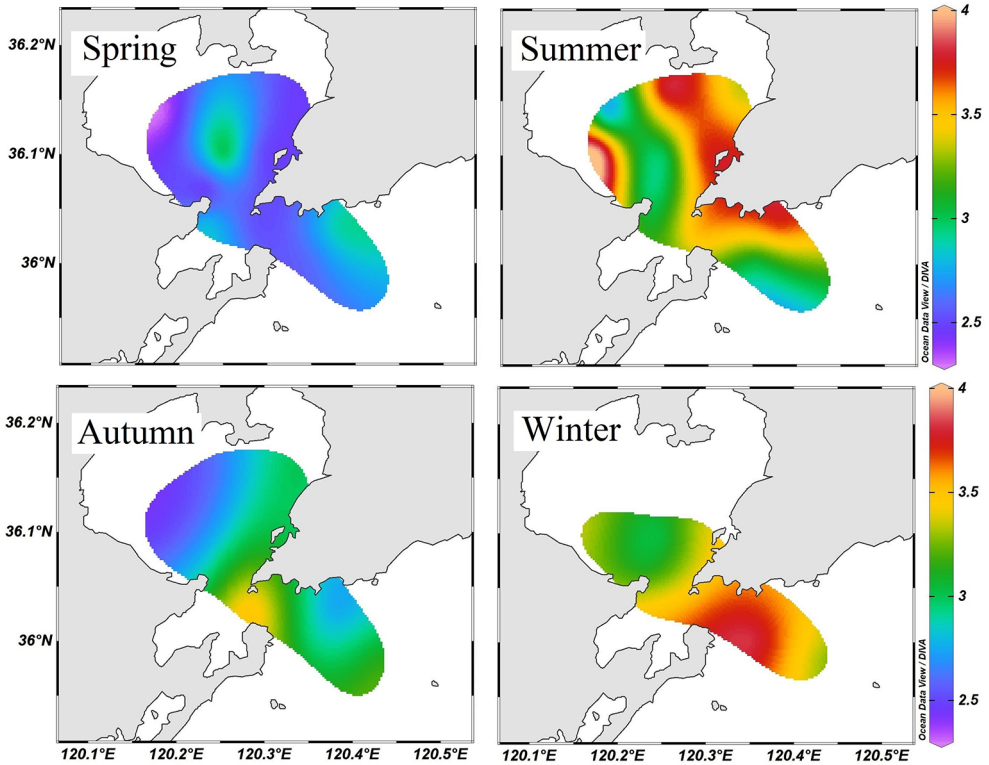


**FIGURE 6** | Relative trophic level of *Sagitta* spp. calculated using small zooplankton (<500 μm) as the baseline (trophic level = 2).

POM) has been recognized as a mechanism inducing the variability in bulk tissue $\delta^{13}C$ and $\delta^{15}N$ values of zooplankton in different environments (Montoya et al., 1990; Edje and Chigbu, 2021). Strong correlations of stable isotope values between POM and zooplankton have been well known (Bănaru et al., 2014). In this study, zooplankton generally showed similar spatial distribution patterns of stable isotopes with POM in Jiaozhou Bay. In the inner bay, more terrigenous OM contributed to the POM. As we know, the terrigenous OM is more depleted in $^{13}C$ (generally < −28‰) than marine organic matter (about -22‰) (Cifuentes and Eldridge, 1998). The general pattern is that the $\delta^{13}C$ values of plankton are more negative in estuarine or inshore regions under the influence of riverine/terrestrial waters (Troina et al., 2020). This mechanism can be used to interpret the spatial distribution pattern of $\delta^{13}C$ during summer, autumn, and winter in Jiaozhou Bay. However, our results suggested that the $\delta^{13}C$ value of small zooplankton was significantly higher in the inner bay in spring. In coastal bays, higher $\delta^{13}C$ values of POM are usually associated with higher Chl-*a* concentrations (Ke et al., 2017). Many studies have indicated that the fast growth rate and high biomass of phytoplankton can increase the $\delta^{13}C$ values of POM (Rau et al., 1996; Perry et al., 1999; Bardhan et al., 2015). In Jiaozhou Bay, Ke et al. (2020) suggested that the higher $\delta^{13}C$ value of POM in the inner bay during spring was mainly due to the significantly higher phytoplankton biomass under the influence of intensive anthropogenic nutrient input. This result suggested that the $\delta^{13}C$ value of zooplankton can be influenced by the food source in Jiaozhou Bay. However, our results showed that only the $\delta^{13}C$ values of small zooplankton were significantly correlated with that of POM, suggesting that the cascade effect of $\delta^{13}C$ might be weak along the food chain.

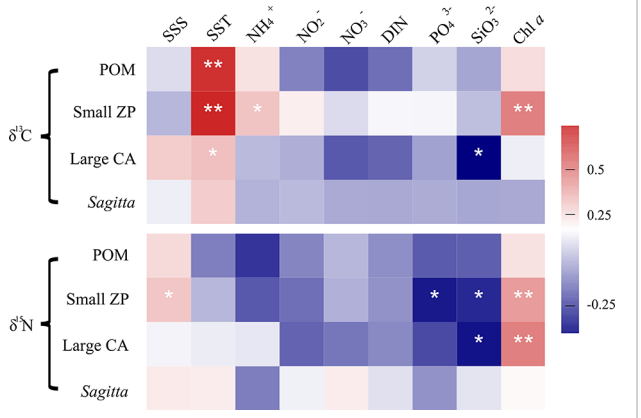


**FIGURE 7** | Correlation coefficients between stable isotopes ($\delta^{13}C$ and $\delta^{15}N$) and key environmental parameters in Jiaozhou Bay. *$p < 0.05$, **$p < 0.01$.

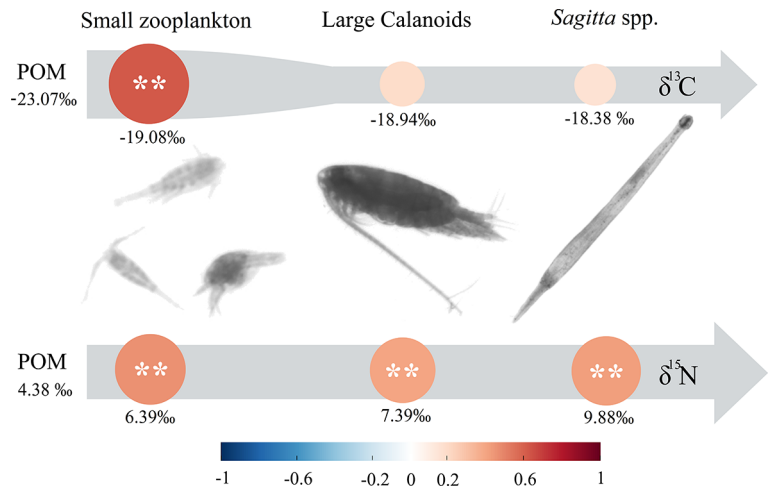


**FIGURE 8** | Annual average $\delta^{13}C$ and $\delta^{15}N$ values and correlation coefficients between POM and dominant zooplankton groups. $^{**}p < 0.01$.

Previous studies have indicated that the regional variation of zooplankton stable isotopes was stronger in $\delta^{15}N$ than in $\delta^{13}C$ (El-Sabaawi et al., 2013). In this study, all the $\delta^{15}N$ values of the three dominant zooplankton groups were significantly correlated with that of POM (**Figure 8**), which suggested that the baseline influence was more significant on the $\delta^{15}N$ of consumers. Spatial heterogeneity or seasonal variation in nitrogen nutrients can drive significant and rapid fluctuations in the $\delta^{15}N$ values of zooplankton (Syväranta et al., 2006). Many studies suggested that the $\delta^{15}N$ value of POM was largely depleted under higher nutrient concentration (Ke et al., 2019; Pruell et al., 2020). Incubation experiments have demonstrated that the $\delta^{15}N$ values of primary producers can be changed significantly with the variation of DIN concentration, and these changes can be quickly transferred into aquatic food webs (Pruell et al., 2020). It has been reported that the $\delta^{15}N$ value of POM showed significantly lower values in the northeaster Jiaozhou Bay where it is intensively influenced by sewage discharge from Qingdao City (Ke et al., 2020). In this study, the distribution pattern of zooplankton $\delta^{15}N$ was generally in accordance with that of POM. This result suggested that the influence of anthropogenic nutrient input on the $\delta^{15}N$ value can be effectively transferred to the higher trophic level in the pelagic ecosystem.

Seasonal variation in zooplankton $\delta^{13}C$ and $\delta^{15}N$ may be due to variations in the composition of diet items and baseline of stable isotopes (Edje and Chigbu, 2021). In general, more $^{13}C$-depleted terrigenous OM was transported into the bay during the wet season. Therefore, it was expected that zooplankton should show lower $\delta^{13}C$ values in Jiaozhou Bay during summer. However, in this study, the dominant zooplankton groups generally showed the highest $\delta^{13}C$ values in the wet summer and the lowest $\delta^{13}C$ values in the dry winter. It seemed that the input of terrigenous OM was not the determining factor for the seasonal variation of $\delta^{13}C$ in the pelagic ecosystem. El-Sabaawi et al. (2013) indicated that it was possible that any influence of $^{13}C$-depleted terrestrial OM on zooplankton $\delta^{13}C$ can be obscured by local or regional variability in primary production. The fast growth of phytoplankton might elevate the background $\delta^{13}C$ value in the summer. On the other hand, temperature is a significant factor causing the change of $\delta^{13}C$ value in phytoplankton, and higher temperature results in higher $\delta^{13}C$ value (Goericke and Fry, 1994). In this study, our results showed that the $\delta^{13}C$ values of POM, small zooplankton, and large calanoids were significantly positively correlated with water temperature. It suggested that temperature might be the most important driving factor for the seasonal variation of $\delta^{13}C$ value in POM and zooplankton.

## Seasonal and Regional Variability in Trophic Niche of Zooplankton

The baseline stable isotope values are very important in trophic ecological studies (Magozzi et al., 2017). The fluctuation in zooplankton $\delta^{15}N$ values might be attributed to either a variation of $\delta^{15}N$ values at the base of the food web or a changed trophic level in different environments (Romero-Romero et al., 2019). The $\delta^{15}N$ values of net zooplankton are usually used as the baseline in the study of aquatic food webs. Our results suggested that the $\delta^{15}N$ values varied greatly among the different zooplankton groups. Niche partitioning was evident among small zooplankton, large calanoids, and *Sagitta*. The *Sagitta* generally occupies the highest trophic level in zooplankton community, feeding preferentially on copepods, and on other small invertebrates and fish larvae (Kimmerer, 1984). In this study, the RTL of *Sagitta* seemed to increase from the inner bay to the outer bay during the spring, autumn, and winter seasons. Due to the strong anthropogenic influence, the nutrient concentration and phytoplankton biomass were generally higher in the inner Jiaozhou Bay (Liu et al., 2005; Ke et al., 2020). High primary productivity and eutrophication can shorten the food chain length (Armengol et al., 2019). Nevertheless, in summer, the RTL of *Sagitta* did not show a

clear difference between the inner and outer bay. The significant spatial variation of baseline $\delta^{15}N$ values in summer might disturb the accurate estimation of zooplankton trophic position.

Seasonal changes in the low levels of pelagic food web can be due to changes in food quality and the active choice of prey type (Kozak et al., 2020). Most copepods are omnivores feeding on a wide range of food items, including phytoplankton, debris, and ciliates (López-Ibarra et al., 2018; Schoo et al., 2018). The composition of food items can change according to the quality and availability of food source. For example, the feeding habit of *Calanus pacificus* can switch between predatory and suspension feeding modes when the relative abundances of phytoplankton and naupliar prey are varied (Landry, 1981). In this study, the Bayesian standard ellipse areas of large calanoids showed great variation in different seasons. It suggested that large calanoids have sufficient dietary flexibility to alter their trophic position in response to environmental change. The trophic flexibility of calanoid copepods acts as a stabilizing force on the basic levels of marine food webs (Sprules and Bowerman, 1988). This ability of trophic flexibility contributes to the resilience in planktonic systems under spatial and temporal environmental variations.

Scatters of $\delta^{13}C$ and $\delta^{15}N$ values suggested that the seasonal variation of zooplankton trophic structure was significant in Jiaozhou Bay. In a pelagic ecosystem, the main perturbation effect on trophic structure may be the absolute decline in food biomass, rather than altered proportions of prey (Décima et al., 2013). There is generally a shorter food web in productive regions and a more complex food web in oligotrophic regions (Armengol et al., 2019). Greater resource opportunity can promote the coexistence of species with similar resource use and enhance the functional redundancy of the community (Ying et al., 2020). Our results suggested that the niche overlap of different zooplankton groups was greater in spring. In Jiaozhou Bay, zooplankton generally reached their peak abundance during spring, and both the small and large *Sagitta* abundances were high in the water. The isotopic niche suggested that the RTL of *Sagitta* was low in spring, which was close to that of large calanoids (**Figure 5**). A large number of small *Sagitta* narrowed the niche partition between *Sagitta* and large calanoids in spring. Many studies have suggested that non-consistent patterns are assumed in the base of pelagic food for the response to the changes of primary productivity and planktonic biomass (Giering et al., 2019; Kozak et al., 2020). Our results showed that the niche partition among different zooplankton groups was most distinct in the winter, and followed by the summer. This might be caused by the distribution pattern of different groups and food availability in different seasons. In summer, the large calanoids were generally collected in the outer bay (**Figure 3**). Large calanoids were mainly composed of *C. sinicus* in Jiaozhou Bay, whose abundance was lower in summer due to the high temperature. The significantly different trophic positions between small zooplankton and large calanoids in summer should be attributed to the difference in distribution region. In winter, the *Sagitta* spp. cannot be collected at several stations in the inner bay (**Figure 3**). It suggested that the *Sagitta* spp. might tend to live in the outer bay during winter and occasionally enter the inner bay with water exchange. The migration of zooplankton between the outer bay and inner bay might greatly affect the trophic structure of zooplankton during summer and winter. On the other hand, the abundance of phytoplankton was low during winter. The shortage of food resource promoted the trophic separation of different zooplankton groups during winter. In summary, seasonal variation of zooplankton trophic structure was controlled by food competition and zooplankton immigration in Jiaozhou Bay. Further study is needed to understand the mechanism of seasonal variation in trophic partitioning.

## CONCLUSION

Our results suggested that the $\delta^{13}C$ and $\delta^{15}N$ values generally followed the order of small zooplankton < large calanoids < small *Sagitta* < large *Sagitta* in Jiaozhou Bay. Spatial variation of zooplankton $\delta^{13}C$ was mainly controlled by terrigenous OM input and phytoplankton biomass. Water temperature might play a key role in seasonal variation of $\delta^{13}C$ value. Our results showed that only the $\delta^{13}C$ values of small zooplankton were significantly correlated with that of POM, suggesting that the cascade effect of $\delta^{13}C$ might be weak along the food chain. However, all the $\delta^{15}N$ values of dominant zooplankton groups showed a significant correlation with POM. This result suggested that the influence of anthropogenic nutrient input on the $\delta^{15}N$ value can be effectively transferred to the higher trophic level in planktonic ecosystem. The Bayesian standard ellipse suggested that the niche partition between small zooplankton, large calanoids, and *Sagitta* was most distinct in the winter, and followed by the summer. The seasonal variation of zooplankton trophic structure might be controlled by food competition and zooplankton immigration in Jiaozhou Bay. The RTL of *Sagitta* generally declined from the inner bay to the outer bay except during summer. High phytoplankton biomass and eutrophication might shorten the food chain length in the inner bay. This study provided detailed information on the seasonal patterns in zooplankton $\delta^{13}C$ and $\delta^{15}N$ that will help to track the change of pelagic trophic structure under anthropogenic influences.

## DATA AVAILABILITY STATEMENT

The raw data supporting the conclusions of this article will be made available by the authors, without undue reservation.

## AUTHOR CONTRIBUTIONS

ZK: methodology, investigation, and original draft writing. ZK and RL: data analysis and writing—review and editing. DC and CZ: investigation. YT: supervision and writing—review and

editing. All authors contributed to the article and approved the submitted version.

## FUNDING

This work was supported by the National Natural Science Foundation of China (32171548), the Key Special Project for Introduced Talents Team of Southern Marine Science and Engineering Guangdong Laboratory (Guangzhou) (GML2019ZD0401, GML2019ZD0405), the National Basic Research Program of China (973 Program, 2015CB452904), and the Science and Technology planning Project of Guangdong Province of China (2021B1212050023).

## ACKNOWLEDGMENTS

The authors would like to thank Dr. Shouhui Dai for his assistance in the stable isotope analysis.

## REFERENCES

Armengol, L., Calbet, A., Franchy, G., Rodríguez-Santos, A., and Hernández-León, S. (2019). Planktonic Food Web Structure and Trophic Transfer Efficiency Along a Productivity Gradient in the Tropical and Subtropical Atlantic Ocean. *Sci. Rep.* 9, 2044. doi: 10.1038/s41598-019-38507-9

Bănaru, D., Carlotti, F., Barani, A., Grégori, G., Neffati, N., and Harmelin-Vivien, M. (2014). Seasonal Variation of Stable Isotope Ratios of Size-Fractionated Zooplankton in the Bay of Marseille (NW Mediterranean Sea). *J. Plankt. Res.* 36 (1), 145–156. doi: 10.1093/plankt/fbt083

Bardhan, P., Karapurkar, S. G., Shenoy, D. M., Kurian, S., Sarkar, A., Maya, M. V., et al. (2015). Carbon and Nitrogen Isotopic Composition of Suspended Particulate Organic Matter in Zuari Estuary, West Coast of India. *J. Mar. Syst.* 141, 90–97. doi: 10.1016/j.jmarsys.2014.7.009

Chi, X. P., Dierking, J., Hoving, H. J., Lüskow, F., Denda, A., Christiansen, B., et al. (2021). Tackling the Jelly Web: Trophic Ecology of Gelatinous Zooplankton in Oceanic Food Webs of the Eastern Tropical Atlantic Assessed by Stable Isotope Analysis. *Limnol. Oceanogr.* 66, 289–305. doi: 10.1002/lno.11605

Cifuentes, L. A., and Eldridge, P. M. (1998). A Mass- and Isotope- Balance Model of DOC Mixing in Estuaries. *Limnol. Oceanogr.* 43, 1872–1882. doi: 10.2307/3037942

Décima, M., Landry, M. R., and Popp, B. N. (2013). Environmental Perturbation Effects on Baseline Values and Zooplankton Trophic Flexibility in the Southern California Current Ecosystem. *Limnol. Oceanogr.* 58 (2), 624–634. doi: 10.4319/lo.2013.58.2.0624

Dickman, E. M., Newell, J. M., Gonzalez, M. N., and Vanni, M. J. (2008). Light, Nutrients and Food-Chain Length Constrain Planktonic Energy Transfer Efficiency Across Multiple Trophic Levels. *Proc. Natl. Acad. Sci. U S A* 105, 18408–18412. doi: 10.1073/pnas.0805566105

Edje, B. O., and Chigbu, P. (2021). Carbon and Nitrogen Stable Isotopes of Copepods in a Tidal Estuarine System in Maryland, USA. *Reg. Stud. Mar. Sci.* 42, 101620. doi: 10.1016/j.rsma.2021.101620

El-Sabaawi, R., Dower, J. F., Kainz, M., and Mazumder, A. (2009). Characterizing Dietary Variability and Trophic Positions of Coastal Calanoid Copepods: Insight From Stable Isotopes and Fatty Acids. *Mar. Biol.* 156, 225–237. doi: 10.1007/s00227-008-1073-1

El-Sabaawi, R., Trudel, M., and Mazumder, A. (2013). Zooplankton Stable Isotopes as Integrators of Bottom-Up Variability in Coastal Margins: A Case Study From the Strait of Georgia and Adjacent Coastal Regions. *Prog. Oceanogr.* 115, 76–89. doi: 10.1016/j.pocean.2013.05.010

Fry, B. (2006). *Stable Isotope Ecology* (New York, 308pp: Springer).

Giering, S. L. C., Wells, S. R., Mayers, K. M. J., Schuster, H., Cornwell, L., Fileman, E. S., et al. (2019). Seasonal Variation of Zooplankton Community Structure and Trophic Position in the Celtic Sea: A Stable Isotope and Biovolume Spectrum Approach. *J. Prog. Oceanogr.* 177, 101943. doi: 10.1016/j.pocean.2018.03.012

Goericke, R., and Fry, B. (1994). Variations of Marine Plankton $\delta^{13}$c With Latitude, Temperature, and Dissolved $CO_2$ in the World Ocean. *Global Biogeochem. Cy.* 8 (1), 85–90. doi: 10.1029/93GB03272

Hannides, C. C. S., Popp, B. N., Landry, M. R., and Graham, B. S. (2009). Quantification of Zooplankton Trophic Position in the North Pacific Subtropical Gyre Using Stable Nitrogen Isotopes. *Limnol. Oceanogr.* 54, 50–61. doi: 10.4319/lo.2009.54.1.0050

Jackson, A. L., Inger, R., Parnell, A. C., and Bearhop, S. (2011). Comparing Isotopic Niche Widths Among and Within Communities: SIBER-Stable Isotope Bayesian Ellipses in R. *J. Anim. Ecol.* 80, 595–602. doi: 10.1111/j.1365-2656.2011.01806.x

Kang, X. M., Song, J. M., Yuan, H. M., Li, X. G., Li, N., and Duan, L. Q. (2017). The Sources and Composition of Organic Matter in Sediments of the Jiaozhou Bay: Implications for Environmental Changes on a Centennial Time Scale. *Acta Oceanol. Sin.* 36 (11), 68–78. doi: 10.1007/s13131-017-1076-1

Ke, Z. X., Chen, D. T., Liu, J. X., and Tan, Y. H. (2020). The Effects of Anthropogenic Nutrient Inputs on Stable Carbon and Nitrogen Isotopes in Suspended Particulate Organic Matter in Jiaozhou Bay, China. *Cont. Shelf Res.* 208, 104244. doi: 10.1016/j.csr.2020.104244

Ke, Z. X., Tan, Y. H., Huang, L. M., Liu, J.X., Xiang, C.H., Zhao, C.Y., et al. (2019). Significantly Depleted 15N in Suspended Particulate Organic Matter Indicating a Strong Influence of Sewage Loading in Daya Bay, China. *Sci. Total Environ.* 650, 759–768. doi: 10.1016/j.scitotenv.2018.09.076

Ke, Z. X., Tan, Y. H., Huang, L. M., Zhao, C. Y., and Jiang, X. (2017). Spatial Distributions of $\delta^{13}$c, $\delta^{15}$n and C/N Ratios in Suspended Particulate Organic Matter of a Bay Under Serious Anthropogenic Influences: Daya Bay, China. *Mar. pollut. Bull.* 114, 183–191. doi: 10.1016/j.marpolbul.2016.08.078

Kimmerer, W. J. (1984). Selective Predation and its Impact on Prey of Sagitta Enflata (Chaetognatha). *Mar. Ecol. Prog. Ser.* 15, 55–62. doi: 10.3354/meps015055

Kozak, E. R., Franco-Gordo, C., Godínez-Domínguez, E., Suárez-Morales, E., and Ambriz-Arreola, I. (2020). Seasonal Variability of Stable Isotope Values and Niche Size in Tropical Calanoid Copepods and Zooplankton Size Fractions. *Mar. Biol.* 167, 37. doi: 10.1007/s00227-020-3653-7

Landry, M. R. (1981). Switching Between Herbivory and Carnivory by the Planktonic Marine Copepod *Calanus Pacificus*. *Mar. Biol.* 65, 77–82. doi: 10.1007/BF00397070

Liu, S. M., Zhang, J., Chen, H. T., and Zhang, G. S. (2005). Factors Influencing Nutrient Dynamics in the Eutrophic Jiaozhou Bay, North China. *Pro. Oceanogr.* 66, 66–85. doi: 10.1016/j.pocean.2005.03.009

López-Ibarra, G. A., Bode, A., Hernández-Trujillo, S., Zetina-Rejón, M. J., and Arreguín-Sánchez, F. (2018). Trophic Position of Twelve Dominant Pelagic Copepods in the Eastern Tropical Pacific Ocean. *J. Mar. Syst.* 187, 13–22. doi: 10.1016/j.jmarsys.2018.06.009

Magozzi, S., Yool, A., Vander Zanden, H. B., Wunder, M. B. , and Trueman, C. (2017). Using Ocean Models to Predict Spatial and Temporal Variation in Marine Carbon Isotopes. *N. Ecosphere* 8 (5), e01763. doi: 10.1002/ecs2.1763

Ma, Y. E., Ke, Z. X., Huang, L. M., and Tan, Y. H. (2014). Identification of Human-Induced Perturbations in Daya Bay, China: Evidence From Plankton Size Structure. *Cont. Shelf Res.* 72, 10–20. doi: 10.1016/j.csr.2013.10.012

Montoya, J. P., Horrigan, S. G., and McCarthy, J. J. (1990). Natural Abundance of $^{15}$N in Particulate Nitrogen and Zooplankton in the Chesapeake Bay. *Mar. Ecol. Prog. Ser.* 65, 35–61. doi: 10.3354/meps065035

Nagelkerken, I., Goldenberg, S. U., Ferreira, C. M., Ullah, H., and Connell, S. D. (2020). Trophic Pyramids Reorganize When Food Web Architecture Fails to Adjust to Ocean Change. *Science* 369, 829–832. doi: 10.1126/science.aax0621

O'Reilly, C. M., Hecky, R. E., Cohen, A. S., and Plisnier, P. D. (2002). Interpreting Stable Isotopes in Food Webs: Recognizing the Role of Time Averaging at Different Trophic Levels. *Limnol. Oceanogr.* 47 (1), 306–309. doi: 10.4319/lo.2002.47.1.0306

Perry, R. I., Thompson, P. A., Mackas, D. L., Harrison, P. J., and Yelland, D. R. (1999). Stable Carbon Isotopes as Pelagic Food Web Tracers in Adjacent Shelf and Slope Regions Off British Columbia, Canada. *Can. J. Fish. Aquat. Sci.* 56, 2477–2486. doi: 10.1139/cjfas-56-12-2477

Post, D. M. (2002). Using Stable Isotopes to Estimate Trophic Position: Model, Methods, and Assumptions. *Ecology* 83, 703–718. doi: 10.1890/0012-9658 (2002)083[0703:USITET]2.0.CO;2

Post, D. M., Layman, C. A., Arrington, D. A., Takimoto, G., Quattrochi, J., and Montana, C. G. (2007). Getting to the Fat of the Matter: Models, Methods and Assumptions for Dealing With Lipids in Stable Isotope Analyses. *Oecologia* 152, 179–189. doi: 10.1007/s00442-006-0630-x

Pruell, R. J., Taplin, B. K., Oczkowski, A. J., Grear, J. S., Mendoza, W. G., Pimenta, A. R., et al. (2020). Nitrogen Isotope Fractionation in a Continuous Culture System Containing Phytoplankton and Blue Mussels. *Mar. pollut. Bull.* 150, 110745. doi: 10.1016/j.marpolbul.2019.110745

Rau, G. H., Riebesell, U., and Wolf-Gladrow, D. (1996). A Model of Photosynthetic $^{13}C$ Fractionation by Marine Phytoplankton Based on Diffusive Molecular $CO_2$ Uptake. *Mar. Ecol. Prog. Ser.* 133, 275–285. doi: 10.3354/meps133275

R Core Team (2020). "R: A Language and Environment for Statistical Computing," in *R Foundation for Statistical Computing*(Vienna, Austria) https://www.R-project.org/.

Rolff, C. (2000). Seasonal Variation in $\delta^{13}c$ and $\delta^{15}n$ of Size Fractionated Plankton at a Coastal Station in the Northern Baltic Proper. *Mar. Ecol. Prog. Ser.* 203, 47–65. doi: 10.3354/meps203047

Romero-Romero, S., Choy, C. A., Hannides, C. C. S., Popp, B. N., and Drazen, J. C. (2019). Differences in the Trophic Ecology of Micronekton Driven by Diel Vertical Migration. *Limnol. Oceanogr.* 64, 1473–1483. doi: 10.1002/lno.11128

Schoo, K. L., Boersma, M., Malzahn, A. M., Löder, M. G. J., Wiltshire, K. H., and Aberle, N. (2018). Dietary and Seasonal Variability in Trophic Relations at the Base of the North Sea Pelagic Food Web Revealed by Stable Isotope and Fatty Acid Analysis. *J. Sea. Res.* 141, 61–70. doi: 10.1016/j.seares.2018.08.004

Sprules, W. G., and Bowerman, J. E. (1988). Omnivory and Food Chain Length in Zooplankton Food Webs. *Ecology* 69 (2), 418–426. doi: 10.2307/1940440

Sun, S., Li, Y. H., and Sun, X. X. (2012). Changes in the Small-Jellyfish Community in Recent Decades in Jiaozhou Bay, China. Chin. *J. Oceanol. Limn.* 30 (4), 507–518. doi: 10.1007/s00343-012-1179-7

Syväranta, J., Hämäläinen, H., and Jones, R. I. (2006). Within-Lake Variability in Carbon and Nitrogen Stable Isotope Signatures. *Freshw. Biol.* 51, 1090–1102. doi: 10.1111/j.1365-2427.2006.01557.x

Troina, G. C., Dehairs, F., Botta, S., and Di Tullio, J. C. (2020). Zooplankton-Based $\delta^{13}c$ and $\delta^{15}n$ Isocapes From the Outer Continental Shelf and Slope in the Subtropical Western South Atlantic. *Deep-Sea Res. Part I.* 159, 103235. doi: 10.1016/j.dsr.2020.103235

Wang, W. C., Sun, S., Sun, X. X., Zhang, G. T., and Zhang, F. (2020a). Spatial Patterns of Zooplankton Size Structure in Relation to Environmental Factors in Jiaozhou Bay, South Yellow Sea. *Mar. pollut. Bull.* 150, 110698. doi: 10.1016/j.marpolbul.2019.110698

Wang, Z. X., Wang, H. P., Fan, S. L., Xin, M., and Sun, X. (2021). Community Structure and Diversity of Macrobenthos in Jiaozhou Bay. *Mar. pollut. Bull.* 171, 112781. doi: 10.1016/j.marpolbul.2021.112781

Wang, P. P., Zhang, F., Sun, S., Wang, W. C., Wan, A. Y., and Li, C. L. (2020b). Experimental Clearance Rates of Aurelia Coerulea Ephyrae and Medusa, and the Predation Impact on Zooplankton in Jiaozhou Bay. *J. Oceanol. Limnol.* 38 (4), 1256–1269. doi: 10.1007/s00343-020-0024-7

Yang, L. Y., Wu, Y., Zhang, J., Liu, S. M., and Deng, B. (2011). Burial of Terrestrial and Marine Organic Carbon in Jiaozhou Bay: Different Response to Urbanization. *Reg. Environ. Change* 11, 707–714. doi: 10.1007/s10113-010-0202-9

Ying, R., Cao, Y. T., Yin, F. M., Guo, J. L., Huang, J. R., Wang, Y. Y., et al. (2020). Trophic Structure and Functional Diversity Reveal Pelagic-Benthic Coupling Dynamic in the Coastal Ecosystem of Daya Bay, China. *Ecol. Indic.* 113, 106241. doi: 10.1016/j.ecolind.2020.106241

Yuan, Y., Song, D., Wu, W., Liang, S., Wang, Y., and Ren, Z. (2016). The Impact of Anthropogenic Activities on Marine Environment in Jiaozhou Bay, Qingdao, China: A Review and a Case Study. *Reg. Stud. Mar. Sci.* 8, 287–296. doi: 10.1016/j.rsma.2016.01.004

Zhang, L., Xiong, L. L., Li, J. L., and Huang, X. P. (2021). Long-Term Changes of Nutrients and Biocenoses Indicating the Anthropogenic Influences on Ecosystem in Jiaozhou Bay and Daya Bay, China. *Mar. pollut. Bull.* 168, 112406. doi: 10.1016/j.marpolbul.2021.112406

**Conflict of Interest:** The authors declare that the research was conducted in the absence of any commercial or financial relationships that could be construed as a potential conflict of interest.

**Publisher's Note:** All claims expressed in this article are solely those of the authors and do not necessarily represent those of their affiliated organizations, or those of the publisher, the editors and the reviewers. Any product that may be evaluated in this article, or claim that may be made by its manufacturer, is not guaranteed or endorsed by the publisher.

frontiers | Frontiers in Marine Science

ORIGINAL RESEARCH
published: 23 June 2022
doi: 10.3389/fmars.2022.941045

# Changes in Distribution Patterns for *Larimichthys polyactis* in Response to Multiple Pressures in the Bohai Sea Over the Past Four Decades

*Qingpeng Han*[1,2], *Xiujuan Shan*[2,3,4*], *Xianshi Jin*[2,3,4], *Harry Gorfine*[5], *Yunlong Chen*[2] *and Chengcheng Su*[2]

[1] College of Fisheries, Ocean University of China, Qingdao, China, [2] Key Laboratory of Sustainable Development of Marine Fisheries, Ministry of Agriculture and Rural Affairs, Shandong Provincial Key Laboratory of Fishery Resources and Ecological Environment, Yellow Sea Fisheries Research Institute, Chinese Academy of Fishery Sciences, Qingdao, China, [3] Function Laboratory for Marine Fisheries Science and Food Production Processes, Qingdao National Laboratory for Marine Science and Technology, Qingdao, China, [4] National Field Observation and Research Center for Fisheries in Changdao Coastal Waters, Yantai, China, [5] School of Biosciences, The University of Melbourne, Parkville, VIC, Australia

OPEN ACCESS

**Edited by:**
Ying Xue,
Ocean University of China, China

**Reviewed by:**
Siquan Tian,
Shanghai Ocean University, China
Yunrong Yan,
Guangdong Ocean University, China

***Correspondence:**
Xiujuan Shan
shanxj@ysfri.ac.cn

**Specialty section:**
This article was submitted to Marine Ecosystem Ecology, a section of the journal Frontiers in Marine Science

**Received:** 11 May 2022
**Accepted:** 24 May 2022
**Published:** 23 June 2022

**Citation:**
Han Q, Shan X, Jin X, Gorfine H, Chen Y and Su C (2022) Changes in Distribution Patterns for Larimichthys polyactis in Response to Multiple Pressures in the Bohai Sea Over the Past Four Decades. Front. Mar. Sci. 9:941045. doi: 10.3389/fmars.2022.941045

Understanding patterns of change in the distribution of species among their critical habitats is important for analyzing population dynamics and adaptive responses to environmental shifts. We investigated spatio-temporal changes in small yellow croaker (*Larimichthys polyactis*) using eight alternative models fitted to data from bottom trawl surveys conducted in the Bohai Sea each spring (spawning period) and summer during 1982–2018. These models included different combinations of local sea temperature, fishing pressure, and individual climate index (i.e., North Pacific index, NPI, and West Pacific index, WPI) as explanatory variables. Selection of the most parsimonious model for each season was based on Akaike's Information Criterion (AIC). The model with NPI as its only explanatory variable was used as a base case for pre-analysis. In spring, a spatio-temporal model with sea temperature as a quadratic effect, plus the spatially varying effects of a climate index and fishing pressure was selected, as the AIC value of this model was reduced by 41.491 compared to the base case model without these effects. In the summer after spawning, the spatio-temporal model with WPI as a climate index covariate lagged by 1-year best explained the spatio-temporal distribution patterns of the stock. The results suggested that small yellow croaker populations significantly decreased in biomass in the Bohai Sea over the study period. A statistically significant northeastward shift in the center of gravity (COG) and a contraction in the distribution range occurred in summer throughout the study period ($p<0.05$). During the spring sequence (1993–2018), a statistically significant northeastward shift in the COG was also found ($p<0.05$). Our results showed that biomass-density hotspots of small yellow croaker in both seasons have shrunk or disappeared in recent years. Overall, these findings suggest that the spatio-temporal patterns of the populations in their spawning, feeding and nursery grounds have been influenced over the past 40 years by multiple pressures, and population density in the southwestern areas of the Bohai Sea declined faster and

more drastically than in the northeastern areas. This study has important implications for developing targeted spatial conservation measures for small yellow croaker at various stages of its life history under different levels of stress.

**Keywords: distribution shifts, spawning and feeding grounds, effective area occupied, spatio-temporal model, spatially-varying coefficient model, climate index, Bohai Sea, small yellow croaker**

## INTRODUCTION

Key ontogenetic habitats for fish populations (spawning grounds, nursery grounds, etc.) support their reproduction and continual replenishment, and are often areas subject to intensive human activities and high levels of exploitation. In the context of global environment change (increasingly intensified impacts of human activities exacerbating adverse climatic conditions), understanding the response mechanisms to environmental change among fish habitats is prerequisite for sustainable development of marine fisheries and protection of their supporting ecosystems (Lotze et al., 2006; Browman and Skiftesvik, 2014; Jin et al., 2015). Studies of sustainable fish production as marine ecosystems evolve under environmental stressors is at the forefront of contemporary fisheries research (Jin et al., 2015).

Tracking and understanding distribution shifts of fish stocks and patterns of expansion or contraction in their spawning, nursery, and feeding grounds is fundamental to effective fisheries management. This understanding can help fisheries scientists and managers to clarify the response mechanisms of stocks to environmental changes (Astarloa et al., 2021) and the downstream effects of these changes on the delivery of fisheries ecosystem services such as food production (Myers and Worm, 2003; Lotze et al., 2006; Cheung et al., 2013). In so doing, it facilitates the establishment of a scientific theoretical framework for ecosystem-based adaptive, and in some instances restorative, management of fisheries (Botsford et al., 1997; Pikitch et al., 2004; Beddington et al., 2007; Jin et al., 2015; Thorson, 2019a).

There is increasing evidence that anthropogenic pressures (e.g., fishing) have led to dramatic distribution changes in the critical habitats of many marine species populations (e.g., Liu et al., 1990; Engelhard et al., 2014; Han et al., 2021; Grüss and Thorson, 2019). Fishing can greatly reduce stock biomass and alter population structure (Li et al., 2012; Bell et al., 2015). It can also give rise to changes in life history characteristics and phenotypic evolution (Sun et al., 2022), typically leading to shrinkage or displacement of the area occupied by exploited fish populations (Engelhard et al., 2014; Bell et al., 2015). Seawater pollution caused by human activities can also seriously damage the functions of key habitats. Species diversity and abundance of fish eggs in polluted waters can become significantly reduced, leading to a narrowing and spatial shift in spawning grounds (Cui et al., 2003).

Environmental stressors (e.g., temperature changes, climate changes) can also lead to spatial shifts among fish stocks (e.g., Blanchard et al., 2005; Pinsky et al., 2013). Many studies have already shown that temperature change is the key factor that initiates migration between key habitats (Feng and Yang, 1955; Liu et al., 1990; Jin et al., 2005), and is also an important environmental determinant of stock distribution. Disruption of migration and restriction of habitable environments may make it difficult to obtain adequate catches from existing fishing grounds in the future (e.g., Overholtz et al., 2011; Cheung et al., 2013; Bell et al., 2015; Su et al., 2015). Water temperature also affects the survival, development and hatching of fish eggs (Bian et al., 2014), thereby causing fluctuations in population replenishment and changes in fish distribution. In some cases, species distributional shifts are related to the nature of climate change rather than increasing temperature *per se* (Pinsky et al., 2013). A study in the Bay of Biscay showed that the regional climate index provided a better explanation than local environmental variables (SST and chlorophyll) in the spatio-temporal distribution patterns of dolphins (Astarloa et al., 2021), although local effects may be more influential on the trophodynamics of teleosts than mammals.

Environmental stressors can also have profound indirect effects on the early life stages of marine fish in both nursery and feeding grounds. It has been found that long-term changes in the water temperature of the North Sea cod (*Gadus morhua*) habitat caused by global climate change has altered species composition, population structure and abundance of copepods that the cod larvae rely upon for food. High larval mortalities from their inadequate food supply, have consequently impaired stock recruitment giving rise to dramatic fluctuations and an overall decline in North Sea cod stocks over the last few decades (Beaugrand et al., 2003; Richardson et al., 2004). In many instances, depending on their specific life history stages, carnivorous fish populations are far less directly sensitive to temperature and other stressors than their planktivorous prey. Ignoring indirect effects from declines in prey may render exploited fish species without adequate protection and preclude their optimal utilization.

Critical habitats are increasingly recognized by researchers as being affected by combinations of multiple stressors. For example, climate warming and fishing pressure have combined to influence a century of distributional shifts of *Gadus morhua* in the North Sea (Engelhard et al., 2014). In China, multiple stressors have caused shifts in ecosystem structure and function during the spawning season in Laizhou Bay (Jin et al., 2013). Jin et al. (2013) showed that top-down effects have been the dominant influence on species composition over the last half century due to increased fishing pressure, whilst bottom-up effects have increased over the last thirty years due to strong changes in environmental stressors (other stressors such as temperature, nutrients, and salinity). These findings imply that

fisheries scientists and managers need to identify and monitor the multiple stressors affecting fish populations to effectively manage exploited fish stocks.

The Bohai Sea is a semi-enclosed shallow sea in China's warm temperate zone and is connected with the Yellow Sea to its east (**Figure 1**), which is a key habitat integrating spawning, nursery and fishing grounds (Liu et al., 1990). Many highly migratory fishes of the Yellow and Bohai Seas with high socio-economic importance spawn and forage in the Bohai Sea, with the latter playing a crucial role in replenishing most fish populations in the Yellow Sea Large Marine ecosystem (Jin et al., 2005; Jin et al., 2015; Bian et al., 2018). Small yellow croaker (*Larimichthys polyactis*, northern Yellow Sea-Bohai Sea stock) is the most iconic and important among exploited species in this region, relying on habitats in the Bohai Sea for its spawning and nursery phases of life before overwintering in the fishing grounds of the Yellow Sea (Liu et al., 1990). Despite the important implications of the relationship between small yellow croaker and multiple stressors during its spawning and nursery periods for stock conservation, scant research has been conducted on this topic. Therefore, there is an urgent need to better elucidate the patterns of variation in the spatial distribution of the stock in its spawning, nursery and feeding grounds of the Bohai Sea, how these patterns change over time, and how these patterns respond to variations in anthropogenic and environmental stressors. This will help with developing strategies for sustainably managing the stock. In the present study we formulated a spatio-temporal variable coefficient model and applied it to the Bohai Sea for the first time to identify the combination of stressors affecting long-term distributional changes in small yellow croaker.

## MATERIAL AND METHODS

In this study, fishery independent catch rates (kg.km$^{-2}$) of small yellow croaker from the Bohai Sea (northern Yellow Sea-Bohai Sea stock) during spring and summer from 1982–2018 were fitted using a spatio-temporal delta-Gamma model. The main objective was to identify shifts in distribution patterns indicative of range expansion or contraction of the stock in its spawning, nursery, and feeding grounds under multiple environmental stressors. Initially, we developed eight alternative spatio-temporal models of the stock for each season, constructed from combinations of explanatory variables that included the effects of sea temperature, climate index, and fishing pressure. The Akaike Information Criterion (AIC; Akaike, 1974) was used to select the most parsimonious from among the eight alternative models in each instance. We included a set of regional climate indices, representing the main modalities of changing conditions in the North Pacific Ocean shown to have important effects on fish populations in the Bohai and Yellow Seas (e. g. Liu et al., 2017). Using a pre-analysis of each season, the best climate index was selected as a model covariate, described below in more detail. Next, we used estimates from the eight models to identify the relative importance of local temperature, climate index, and fishing pressure for each season. Finally, changes in centers of gravity (COGs) i.e., centroid of stock abundance or biomass, and effective area occupied by the stock were analyzed using the model with the smallest AIC in each season, to capture the distributional shifts in geographic range of small yellow croaker in its spawning, nursery and feeding grounds and its relationship with multiple stressors. In this study, the spatially varying coefficient model (SVC, Thorson, 2019b) was used to represent the effects of annual indices (i.e., climate index and fishing pressure index) in our spatio-temporal model.

### Data Used in This Study

The data for small yellow croaker in the Bohai Sea analyzed in the present study were all from scientific i.e. fishery independent, surveys using bottom trawl at fixed stations (**Figure 1**), conducted by the Yellow Sea Fisheries Research Institute (YSFRI). The spring (May) survey years for which records were available included 1982, 1993, 1998, 2004, 2011, 2014, and 2016–2018; Summer (August) survey years included 1982, 1992–1998, 2009–2010, 2012–2013, 2015–2018. Local commercial fishing vessels were hired as the research vessels

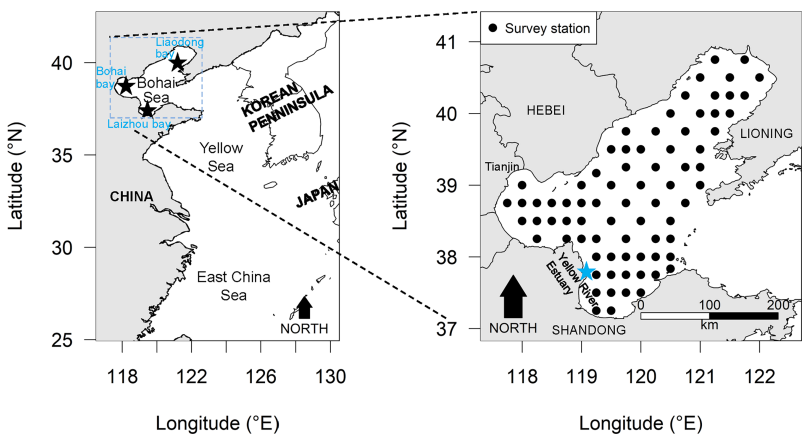


**FIGURE 1** | The locations of the Bohai Sea sampling stations where the small yellow croaker (*Larimichthys polyactis*) data utilized in the present study were gathered.

for trawling (1-hour tows at a speed of 3 knots). Except for 2011 (mono trawl), the surveys were conducted using tandem commercial fishing vessels (pair-trawling). The power of the survey vessels before 2011, 2011 and after 2011 was 200 horsepower, 350 horsepower and 490 horsepower, respectively. Detailed information about these fishing vessels can be found in some published literature (Zhang et al., 2015; Shan and Jin, 2016; Li et al., 2018). The net mouth had a width of 22.6m, height of 6m, circumference of 109.62m, and cod-end mesh size of 20mm. Samples from all stations were identified to the level of species or lowest taxon as far as possible. Biomass was estimated as weight, abundance as number of individuals from each shot.

The environmental stressor data in this study included local sea temperature, climate index, and fishing pressure index for the period 1981–2018. Remotely-sensed sea temperature data were used because temperature data were not collected for the complete survey time series and the entire Bohai Sea area. Daily sea surface temperature (SST) data for the study area from May 1981–2018 were downloaded from the Optimum Sea Surface Temperature (OISST) Database (https://www.ncei.noaa.gov/products/optimum-interpolation-sst) of the National Centers for Environmental Information, NATIONAL OCEANIC AND ATMOSPHERIC ADMINISTRATION (NOAA). The spatial accuracy of the data is 0.25° × 0.25°, which matches the precision of our research grid. We converted the Daily SST into an estimate of mean SST (May) for each survey. Considering that the water depth of the Bohai Sea is relatively shallow, with an average of only 18.7m, and the seawater temperature is low with vertical mixing during spring producing a relatively uniform temperature throughout the water column, SST was used as a proxy for the temperature of each layer of the water column, including the bottom temperature (Jin et al., 2005; Radlinski et al., 2013). The station-measured bottom and surface temperature data obtained during the spring survey in 2017 showed a strong correlation ($r$ = 0.98). Therefore, it is reasonable to assume that SST in spring may have a potential relationship with population dynamics of small yellow croaker in the relatively shallow waters of the Bohai Sea even though it is a benthopelagic species. In summer, SST cannot be used as a substitute for bottom temperature because the upper and lower layers of the water column are not sufficiently mixed, and the 2017 survey data only showed a weak correlation between SST and bottom temperature in August ($r$ = 0.6). Therefore, we downloaded the bottom temperature data with coarse spatial accuracy (0.5° × 0.5°) for the study area from August 1981–2018 and interpolated them. This bottom temperature data information was available at the National Marine Data Center of China (http://mds.nmdis.org.cn/pages/dataViewDetail.html?dataSetId=81).

Pacific Decadal Oscillation (PDO, Mantua et al., 1997), North Pacific index (NPI, Trenberth and Hurrell,1994), West Pacific index (WPI, Barnston and Livezey, 1987), North Atlantic Oscillation (NAO, Hurrell, 1995; Hurrell and Deser, 2010; Hurrell et al., 2003), Northern Oscillation Index (NOI, Schwing et al., 2002), Niño 3.4 index (Trenberth, 1997), Southern Oscillation Index (SOI, Trenberth, 1984) and Arctic Oscillation index (AOI, Thompson and Wallace, 1998; Thompson and Wallace, 2001) data (downloaded from https://psl.noaa.gov/data/climateindices/list/) and their 1-year advance time series that considered the delayed/lag effect (represented by -_lag1, such as PDO_lag1.) were utilized as climatic pressure indices in the present study. These indices were downloaded for spring months (March-May), summer months (June-August), and the annual individual climatic index values for each study season (spring and summer) used in the present study were the average values of the individual indices for the seasonal month groups for each year. Oceanographic indices summarize the physical status of marine ecosystems (Grimmer, 1963; Kidson, 1975), established by many studies to have direct or indirect effects on marine fishery populations (Mantua and Hare, 2002; O'Leary et al., 2018). These climate indicators are briefly described and summarized in the appendix (**Supplementary Table 1**). In this study, time series of these regional indices and their respective advance time series that incorporated a 1-year lag effect were chosen as climate pressure indices because they are well recorded and updated in the Bohai Sea, and many studies have shown them to be largely associated with changes in the North Pacific marine ecosystem (Nakata and Hidaka, 2003; Overland et al., 2008; Tian et al., 2008; Shen, 2012; Tian et al., 2014; Liu et al., 2017; Yuan et al., 2017; He, 2002; Liu et al., 2021). Some of these indices have been shown to be strongly correlated with yield changes in small yellow croaker (Liu et al., 2017).

Finally, fishing mortality has been recognized as a main driver behind variation in distribution in the Bohai and Yellow Seas (Xu et al., 2003; Lin et al., 2016). No accurate commercial catch and effort data were available for the small yellow croaker stock in the Bohai Sea. Fishing power estimates were derived from records provided by the Bureau of Fisheries and Fishery Administration of Ministry of Agriculture and Rural Affairs (Ministry of Agriculture), China. The fishing power for a given year during the period 1982–2018 was obtained as the logarithm of the total engine power of the commercil fishing vessels from the Shandong, Liaoning, and Hebei provinces of China and one Chinese city (Tianjin). In this study, the total vessel power (excluding the vessels operating in the Yellow Sea) was calibrated using internal information obtained by the YSFRI from the fisheries management departments of these provinces. However, with the development of technology and the improving social economy, the number and proportion of high-powered vessels operating in the fishery are increasing, which means that the growth rate in fishing pressure is faster than that of the total fishing vessel's power. Fishing vessel power records had been divided into three categories for the period 2003–2018 (total power above 441kW, between 45 and 440kW, and below 44kW); and into five ranges prior to 2003, but the thresholds of five ranges before 1993 differed from those during 1993–2002. Therefore, we converted the proportion of high-powered fishing vessels into a calibration coefficient for fishing capacity enhancement. The implementation of a summer fishing moratorium reduces the time available for fishing, which affects changes in fishing pressure, so we also needed to account for variations in the proportion of fishing time expended from year

to year. Therefore, we used the product of fishing power × calibration coefficient for fishing capacity enhancement × proportion of fishing months for the period 1982–2018 as the fishing pressure index (*FI*):

$$FI_y = Power_{All,\ y} \times \left(\frac{Power_{MG,\ y}}{Power_{All,\ y}} \times \frac{Maxrange_{LL,\ y}}{Maxrange_{LL,\ y=1}}\right) \times \left(\frac{Months_{a,\ y}}{12}\right), \quad (1)$$

Where $Power_{All,\ y}$ is the total power of fishing vessels in year *y*; $Power_{MG,\ y}$ is the total fishing vessel power in the maximum fishing vessel power group in *y*; $Maxrange_{LL,y}$ is the lower limit of the maximum fishing vessel power grouping threshold for year *y*; $Months_{a,\ y}$ is the number of months available for fishing in *y*. We also compared the performance of the two fishing pressure indicators namely the logarithm of the index *FI* and the logarithm of the total power of fishing vessels $Power_{All,\ y}$ in the model (see the model description below) developed in this study. Our analysis showed that the logarithm of the index *FI* was better than the logarithm of the $Power_{All,\ y}$, so we used the former as a proxy of fishing pressure (**Supplementary Table 2**).

## Spatio-Temporal Modeling

We developed eight alternative spatio-temporal models for the small yellow croaker stock of the Bohai Sea for the spring and summer seasons. These models variously included or excluded the effects of local temperature, fishing pressure and climate pressure indices (e.g., NPI), with the most parsimonious model chosen as the optimal one for each season based on the lowest AIC (Akaike, 1974). These models were a set of vector autoregressive spatio-temporal models, more precisely, delta-Gamma generalized linear mixed models (delta-Gamma GLMMs) with or without the option of adding a spatially varying coefficient (SVC) model, to account for spatiotemporal structures (unmeasured changes that vary over time) and spatial structure (unmeasured changes in long-term patterns, i.e., stable over time) at a fine scale (Thorson et al., 2015; Thorson, 2019a; Thorson, 2019b). The models also accounted for differences in relative fishing efficiency introduced by the different survey vessels (Thorson et al., 2015). We fitted these spatio-temporal models to the catch rate data of small yellow croaker collected during the survey in each season (spring and summer). Specifically, the following eight models comprising up to 3 covariates were fitted, M1: a model with no covariates; M2: a model with the quadratic effect of local temperature, representing a dome-shaped response to local temperatures; M3: a model with the spatially-varying effects of the individual climate indices (e.g., NPI) represented using an SVC model option (Thorson, 2019b), and which was used for pre-analysis, with the climate index in the model with the lowest AIC being selected for each season; M4: a model with the spatially-varying effect of fishing pressure; M5: a model with the quadratic effect of local temperature and the spatially-varying effect of fishing pressure; M6: a model with the quadratic effect of local temperature and the spatially-varying effect of climate index (this climate index was selected from the M3 pre-analysis); M7: a model with the spatially-varying effect of fishing pressure and the spatially-varying effect of climate index (r this climate index is selected by M3 pre-analysis); and M8: a model with the quadratic effect of local temperature, the spatially-varying effect of fishing pressure, and the spatially-varying effect of climate index (this climate index was selected from the M3 pre-analysis).

Because some of the survey catch rate data was zero-inflated, we chose the spatio-temporal delta-Gamma GLMM (Thorson et al., 2015) which comprised a binomial-GLMM and a Gamma-GLMM. This GLMM combination fitted the 0/1 (encounter/non-encounter) data and the data of the stations where small yellow croaker were caught (non-zero catch data), respectively, and multiplied the predicted values of the two parts to obtain the final biomass-density estimates (Lo et al., 1992; Grüss et al., 2019b; Han et al., 2021). In this study, the spatio-temporal delta-GLMM was employed not only to analyse spatio-temporal distribution patterns of small yellow croaker density in spring and summer, but also to identify the extent to which COGs and the effective area occupied by the stock may have shifted during 1982–2018, as described below.

Since model M8 contains the largest number of covariables (including SST, climate index and fishing pressure), its structure is described here; the structures of the M1-M7 models are similar. The binomial-GLMM with a logit link function and linear predictors was used to estimate the probability of small yellow croaker being caught (encounter) $p_i$ at sampling station s (i).The binomial-GLMM included two Gaussian Markov random fields which represent respectively the spatial variation and the spatio-temporal variation in encounter probability:

$$p_i = logit^{-1}\left(\beta^{(p)}_{t(i)} + r^{(p)}_{V(i),t(i)} + \omega^{(p)}_{s(i)} + \epsilon^{(p)}_{s(i),t(i)} + \gamma^{(p)}_{t(i),1} T^{(p)}_{s(i),t(i)} + \gamma^{(p)}_{t(i),2} T^{2(p)}_{s(i),t(i)} + \xi^{(p)}_{s(i),t(i),1} + \xi^{(p)}_{s(i),t(i),\ 2}\right) \quad (2)$$

where $\beta^{(p)}_{t(i)}$ is the intercept for year t(i) in which sample *i*; $r^{(p)}_{(V(i),t(i))}$ is the relative fishing efficiency for the $v^{\text{th}}$ survey vessel at site $s(i)$ in year t(i); $\omega^{(p)}_{s(i)}$ is the spatially correlated variability in encounter probability at the station $s(i)$ where sample *i*; $\epsilon^{(p)}_{s(i)t(i)}$ is the spatially correlated variability in encounter probability at station $s(i)$ in year $t(i)$; $\gamma^{(p)}_{t(i),1} T^{(p)}_{s(i),t(i)}$ is the linear effect of local temperature on encounter probability at station $s(i)$ in year $t(i)$; $\gamma^{(p)}_{t(i),2} T^{2(p)}_{s(i),t(i)}$ is the quadratic effect of local temperature on encounter probability at station $s(i)$ in year $t(i)$; $\xi^{(p)}_{s(i),t(i),1}$ is the spatially-varying effect of the climate indices (e.g., NPI) on encounter probability at $s(i)$ in $t(i)$; and $\xi^{(p)}_{s(i),t(i),\ 2}$ is the spatially-varying effect of fishing pressure on encounter probability at station $s(i)$ in year $t(i)$. Prior to being used in the models, both the $T$ and $T^2$ covariates were standardized to have a mean of zero and a variance of one; this transformation implied that $\gamma^{(p)}_1 T^{(p)}$ and $\gamma^{(p)}_2 T^{2(p)}$ had a standard deviation equal to $\gamma^{(p)}_1$ and $\gamma^{(p)}_2$, respectively (Thorson, 2015; Grüss et al., 2020a; Han et al., 2021).

The $\beta^{(p)}_t$, $\gamma^{(p)}_{t,1} T^{(p)}_{(t)}$ and $\gamma^{(p)}_{t,2} T^{2(p)}_{t(i)}$ are fixed effects. The $r^{(p)}_{V,t}$ $\omega^{(p)}$ $\epsilon^{(p)}_t$, $\xi^{(p)}_{t,1}$ and $\xi^{(p)}_{t,2}$, are random effects and were assumed to follow

a multivariate normal distribution and, in the case of the $\epsilon_t^{(p)}$, temporal variation was expected to conform to a random-walk process (Thorson et al., 2016a) in time to ensure that year intervals or/and stations that have not been sampled do not present mean-reversion:

$$\begin{aligned} r_v^{(p)} &\sim N\left(0, \sigma_{pr}^2\right) \\ \omega^{(p)} &\sim MVN\left(0, \sigma_{p\omega}^2 \mathrm{R}(\kappa)\right) \\ \epsilon_t^{(p)} &\sim MVN\left(\epsilon_{t-1}^{(p)}, \sigma_{p\epsilon}^2 \mathrm{R}(\kappa)\right) \\ \xi_{t,1}^{(p)} &\sim MVN\left(0, \sigma_{p\xi,1}^2 \theta_{s,1} P_{t,1}\right) \\ \xi_{t,2}^{(p)} &\sim MVN\left(0, \sigma_{p\xi,2}^2 \theta_{s,2} P_{t,2}\right), \end{aligned} \tag{3}$$

Where $\sigma_{pr}^2$ is the variance of vessel effects (encounters);$\mathbf{R}(k)$ is the correlation among stations as a function of decorrelation distance $\boldsymbol{k}$;$\sigma_{p\omega}^2$ and $\sigma_{p\epsilon}^2$ are the pointwise variance of $\omega^{(p)}$ theand $\epsilon_t^{(p)}$, respectively; $P_{t,1}$ is the climate indices (e.g., NPI) and $\theta_{s,1}P_{t,1}$ is the climate indices (e.g., NPI) effect; and $\sigma_{p\xi,1}^2$ is the pointwise variance of the climate indices (e.g., NPI) effect.$P_{t,2}$ is the fishing pressure; and $\theta_{s,2}P_{t,2}$ is the effect of fishing pressure and $\sigma_{p\xi,2}^2$ is its pointwise variance. The calculation method of the **R** terms can be found in Thorson et al. (2015).

Similarly, the non-zero catch rate of small yellow croaker $r_i$ at station $s_i$ was estimated by the Gamma components (has a log link function) and linear predictors, including two Gaussian Markov random fields accounting for spatial variation and spatio-temporal variation in non-zero catch rate, respectively:

$$r_i = exp\left(\beta_{t(i)}^{(r)} + r_{V(i),t(i)}^{(r)} + \omega_{s(i)}^{(r)} + \epsilon_{s(i),t(i)}^{(r)} + \gamma_{t(i),1}^{(r)} T_{s(i),t(i)}^{(r)} + \gamma_{t(i),2}^{(r)} T_{s(i),t(i)}^{2(r)} + \xi_{s(i),t(i),1}^{(r)} + \xi_{s(i),t(i),2}^{(r)}\right), \tag{4}$$

where most of the parameters of Eq. (4) have the same meaning as the parameters of Eq. (2), except that they apply to log-catch rate.

To improve computational efficiency, following Han et al. (2021), 100 "knots" $n_j = 100$ were specified to approximate all the $\omega^{(p)}$, $\omega^{(r)}$, $\epsilon_t^{(p)}$,and $\epsilon_t^{(r)}$, over a fixed spatial domain $\Omega$, so that the value of each variation term is tracked at each knot (Shelton et al., 2014; Thorson et al., 2015). These knots were distributed over a grid (**Figure 2**) developed for this study. All $\omega^{(p)}$, $\omega^{(r)}$, $\epsilon_t^{(p)}$, $\epsilon_t^{(r)}$ were tracked at each knot by the model, and the value of each term at a prediction grid cell is interpolated from the value of three knots surrounding that grid cell (see Grüss et al., 2020a; Grüss et al., 2020b; Grüss et al., 2020c). The 100 knots provided a compromise between the estimation accuracy and run time of the GLMM model. As the number of knots increased, the parameter estimates and predictions became similar.

According to the results obtained by multiplying the predicted values of the binomial-GLMM and the predicted values of the Gamma-GLMM, we mapped the biomass-density of small yellow croaker in spring and summer separately on the Bohai Sea prediction grid. Next, the biomass of the small yellow croaker stock in year $t$, $\hat{B}_t$ was estimated, as:

$$\begin{aligned} \hat{B}_t &= \sum_{j=1}^{n_j} A_j \hat{p}_{j,t} \hat{r}_{j,t} \\ &= \sum_{j=1}^{n_j} {}^{A_j} log it^{-1}\left(\hat{B}_t^{(p)} + \hat{r}_{V,t}^{(p)} + \hat{\omega}_j^{(p)} + \hat{\epsilon}_{j,t}^{(p)} + \hat{\gamma}_{t,2}^{(p)} T_{j,t}^{2(p)} + \hat{\xi}_{j,t,1}^{(p)} + \hat{\xi}_{j,t,2}^{(p)}\right) \\ &\quad \exp\left(\hat{\beta}_t^{(r)} + \hat{r}_{V,t}^{(r)} + \hat{\omega}_j^{(r)} + \hat{\epsilon}_{j,t}^{(r)} + \hat{\gamma}_{t,1}^{(r)} T_{j,t}^{(r)} + \hat{\gamma}_{t,2}^{(r)} T_{j,t}^{2(r)} + \hat{\xi}_{j,t,1}^{(r)} + \hat{\xi}_{j,t,2}^{(r)}\right) \end{aligned} \tag{5}$$

where $A_j$ is the surface area of knot $j$ (in km²); $\hat{\beta}_t^{(p)}$, $\hat{\gamma}'^{(p)}_{t,1}$, $\hat{\gamma}_{t,2}^{(p)}$, $\hat{\beta}_t^{(r)}$ and $\hat{\gamma}_{t,1}^{(r)}$ are fixed effects estimated *via* maximum likelihood; and $\hat{r}_{V,t}^{(p)}$,$\hat{\epsilon}_{j,t}^{(p)}$, $\hat{\omega}_j^{(p)}$, $\hat{\xi}_{j,t}^{(p)}$, $\hat{r}_{V,t}^{(r)}$, $\hat{\epsilon}_{j,t}^{(r)}$, $\hat{\omega}_j^{(r)}$, $\hat{\xi}_{j,t,1}^{(r)}$ and $\hat{\xi}_{j,t,2}^{(r)}$ are random effects (Thorson et al., 2015).

To measure the shifts in spatial distribution of the stock over time, we calculated its annual COGs in spring and summer during 1982–2018. The eastward COG, $X_t$, was calculated by (Thorson et al., 2016a; Thorson et al., 2016b; Thorson and Barnett, 2017):

$$X_t = \sum_{j=1}^{nj} x_j \frac{A_j \hat{p}_{j,t} \hat{r}_{j,t}}{\hat{B}_t} \tag{6}$$

where $x_j$ is the easting value (in km) in knot $j$. The northward COG, $Y_t$, can be shown in a similar way, except that $x_j$ is replaced with $y_j$ ,the northing value (in km) in knot $j$, in Eq. (6).

To determine the annual range expansion/contraction of the stock in spring and summer, we estimated the annual effective area occupied by the stock during 1982–2018. Effective area occupied is shown by the ratio of predicted biomass (Eq. (5)) over average density, $D_t$, which is calculated by (Thorson et al., 2016a; Thorson et al., 2016b):

$$D_t = \sum_{j=1}^{n_j} \hat{p}_{j,t} \hat{r}_{j,t} \frac{A_j \hat{p}_{j,t} \hat{r}_{j,t}}{\hat{B}_t}. \tag{7}$$

The models were implemented using the "VAST" package (https://github.com/James-Thorson-NOAA/VAST Thorson, 2019a) within the R statistical software environment on Windows (R Core Team, 2021). The estimation of fixed effects, random effects and their standard deviations, as well as the standard deviations of derived quantities were mainly calculated by the Laplace approximation, the stochastic partial differential equation method (Lindgren et al., 2011), and the generalized delta method (Kass and Steffey, 1989) implemented using the R package "TMB" (Kristensen et al., 2016), and the bias-correction estimator developed in Thorson and Kristensen (2016). Their detailed computational descriptions are documented in Thorson et al. (2015) and Thorson (2019a). The convergence test of the spatio-temporal model comprised two parts: (1) the gradient of marginal logarithmic likelihood of all fixed effects should be less than 0.0001; and (2) the Hessian matrix of the second derivative of negative logarithmic likelihood must be positive definite. In addition, the "VAST" package also has a set of diagnostics, which can further confirm whether the spatio-temporal models were reasonable, i.e., that (1) the observed encounter frequencies were

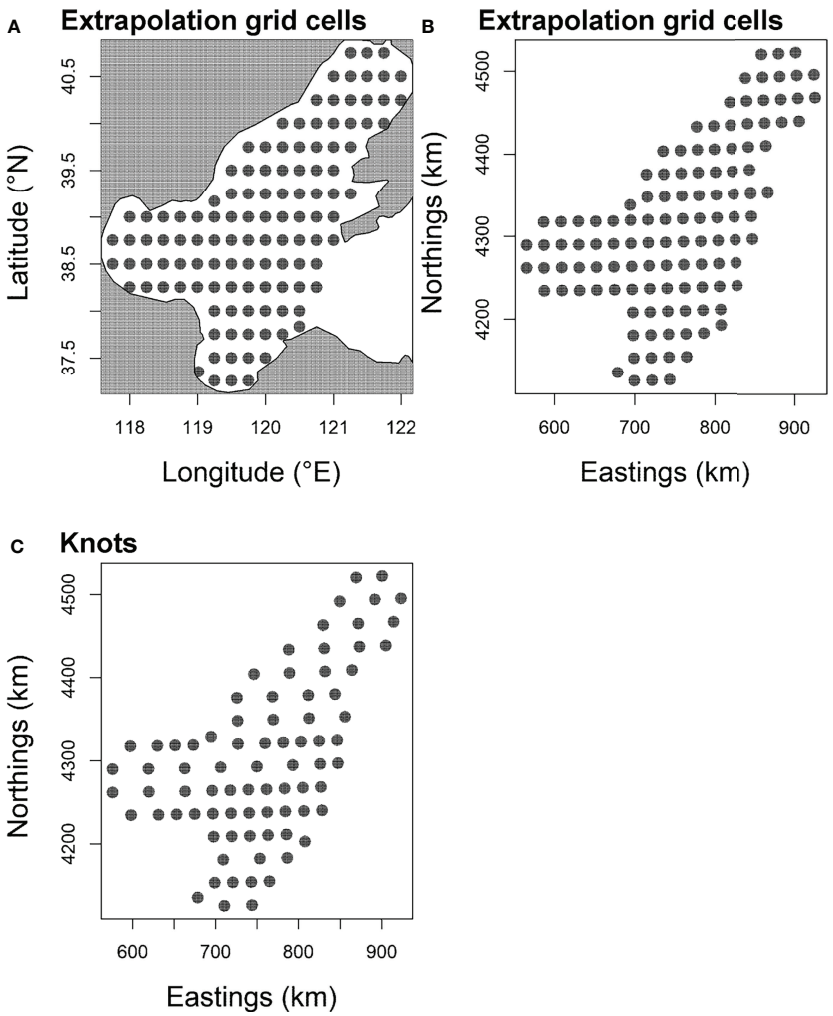


**FIGURE 2** | The barycenter of 116 extrapolation grid cells (15× 15 arc-minutes) and of "knots" of the Bohai Sea in the present study. This barycenters of grid are depicted in **(A, B)**. To improve computational efficiency, 100 "knots" **(C)** were assigned to approximate the spatial and spatio-temporal variation components of the model developed for the present work.

within the 95% prediction interval of the predicted encounter probability; (2) the diagnostics for the positive-catch-rate component using a q-q plot showed the residuals lay along the one-to-one line; and (3) mapping Pearson residuals for encounter-probability and positive catch rates of the small yellow croaker stock showed that there were no visible patterns in the Bohai Sea.

## Understanding the Relative Importance of Three Stressor Covariables in Explaining Distribution Patterns of Small Yellow Croaker

We employed the eight models (with various combinations of the effects of local temperature, climate indices, and fishing pressure) for each season, and applied the method used in Thorson (2015) to analyze the relative importance of multiple stressors explaining the probability patterns of encounter and non-zero density (estimated by the delta-Gamma GLMM) of small yellow croaker in the Bohai Sea in spring and summer, respectively. Based on the method used in Thorson (2015), we compared the variances of the spatio-temporal variations (the sum of the spatial variation term and of the spatio-temporal variation terms) in the probability of encounters and non-zero density for the eight alternative delta-Gamma GLMMs for each season in this study to determine whether some reduction of the variances caused by local temperature and/or climate index and/or fishing pressure covariable(s) was/were included in a model. The desired goal of the inclusion of covariables in the models was to minimize the spatio-temporal variability, which represents the latent (unmeasured) variation in the encounter probability or non-zero density probability of the stock (Thorson et al., 2015; Han et al., 2021).

## Trend Analysis of Local Temperature, Climate Index and Fishing Pressure Index Time Series

We also performed trend analyses of the local temperature, climate index and fishing pressure index time series in spring and summer as an aid for interpreting the estimates of the most parsimonious (i.e., the smallest AIC value) spatiotemporal model. These trend analyses were performed by the regime shift detection method based on a sequential t-test to detect possible regime shifts, which requires the data to be processed with "pre-whitening" prior to use (Rodionov, 2004; Rodionov and Overland, 2005; Rodionov, 2006).

# RESULTS

## The Relative Importance of the Fishing Pressure, SST and the Climate Index in Explaining Distribution Patterns

In this study, eight models (delta-Gamma GLMMs) for the small yellow croaker stock in the Bohai Sea during spring and summer, were developed (M1-M8) by incorporating different combinations of the effects of fishing pressure, local temperature, and climate indices (e.g., NPI). All the models satisfied tests of convergence and diagnostic requirements (The diagnostic results of the AIC-selected models are shown in **Supplementary Figure 1, 2**). Comparisons among the M1-M8 models for each season allowed us to identify the relative importance of fishing pressure, local temperature and the climate indices (e.g., NPI) in explaining the probability patterns of encounter and density of the stock during each specific season. The results from the pre-analysis of M3 in spring indicated that M3 with the NPI covariable had a smaller AIC value than M3 with the other climate index covariables. In spring, we found that when interpreting the probability pattern of encounter, the variances of M1-M8 were all equal to or extremely close to 0, and NPI and fishing pressure were relatively more important than local temperature (**Table 1**). Including NPI or fishing pressure in the model, the variance of spatio-temporal variation of encounter probability remained unchanged relative to M1, while including local temperature in the model caused a negligible increase of the variance. Conversely, we found that SST was more important than NPI and fishing pressure in interpreting the non-zero density pattern during spring (**Table 1**). The inclusion of local temperature in the model caused a large decrease in the spatio-temporal variance in density, whereas the inclusion of NPI or fishing pressure caused a moderate increase in the variance.

The results of pre-analysis of M3 in summer indicated that M3 with the WPI_lag1 (WPI lagged by 1-year) covariable had a smaller AIC value than M3 with other climate index covariables. We found that WPI_lag1 was more important than local

**TABLE 1** | The variances of the spatio-temporal variations of encounter probability and non-zero density probability calculated by the eight models developed in spring and summer in the present study (M1-M8).

| Season | Model (covariates included) | Variance for the binomial component of the model | Percent change in variance for the binomial component | Variance for the Gamma component of the model | Percent change in variance for the Gamma component |
|---|---|---|---|---|---|
| Spring | M1 (None) | 0.0000 | – | 0.0110 | – |
| | M2 (SST) | $1.37\times10^{-33}$ | +100% | 0.0000 | -100% |
| | M3 (NPI) | 0.0000 | 0% | 0.0127 | +15.78% |
| | M4 (Fishing pressure) | 0.0000 | 0% | 0.0139 | +26.11% |
| | M5 (SST+Fishing pressure) | $4.7\times10^{-38}$ | +100% | 0.0000 | -100% |
| | M6 (SST+NPI) | $2.33\times10^{-41}$ | +100% | $1.4767\times10^{-78}$ | -100% |
| | M7 (NPI+Fishing pressure) | 0.0000 | 0% | 0.0132 | +20.54% |
| | M8(SST+NPI +Fishing pressure) | $1.11\times10^{-35}$ | +100% | $2.1839\times10^{-57}$ | -100% |
| Summer | M1 (None) | 0.29330 | – | 0.0023 | – |
| | M2 (BT) | 0.29304 | -0.09% | 0.0005 | -78.33% |
| | M3 (WPI_lag1) | 0.10834 | -63.06% | 0.0000 | -100% |
| | M4 (Fishing pressure) | 0.29224 | -0.36% | 0.0131 | +475.38% |
| | M5 (BT+Fishing pressure) | 0.29467 | +0.47% | 0.0041 | +79.24% |
| | M6 (BT+WPI_lag1) | 0.09190 | -68.67% | 0.0000 | -100% |
| | M7 (WPI_lag1 +Fishing pressure) | 0.01998 | -93.19% | 0.0000 | -100% |
| | M8(BT+WPI_lag1 +Fishing pressure) | 0.01379 | -95.30% | 0.0000 | -100% |

*The variation of encounter probability means the sum of the spatial variation terms and spatio-temporal variation terms calculated by the binomial component of the spatio-temporal delta-Gamma generalized linear mixed model (GLMM). The variation in non-zero density probability means the sum of the spatial variation terms and spatio-temporal variation terms calculated by the Gamma component of the model. Percent change in variance, Percent change in variance compared to M1 (no covariates included); SST, sea surface temperature; BT, sea bottom temperature; NPI, North Pacific index; WPI, West Pacific index; WPI_lag1, West Pacific Index time series with 1-year advance (Consider the 1-year delay/lag effect); AOI, Arctic Oscillation index; Fishing pressure, fishing pressure index.*

temperature and fishing pressure when interpreting the probability pattern of encounter in summer (**Table 1**). Including WPI_lag1 in the model, the spatio-temporal variation in encounter probability showed a large decrease relative to M1, while including local temperature or fishing pressure in the model caused a negligible or small decrease in the variance. Moreover, the WPI_lag1was more important than local temperature and fishing pressure in explaining the probability patterns of density; and local temperature was more important than fishing pressure (**Table 1**). Including the WPI_lag1 or local temperature in the model caused a large decrease in spatio-temporal variation in density probability, whereas including fishing pressure in the model caused a large increase in the variance.

## Change Patterns of Spatiotemporal Distribution and Range of Small Yellow Croaker in the Bohai Sea

In spring, the AIC value of the spatial-temporal model with the quadratic effect of local temperature, the spatially-varying effect of NPI and the spatially-varying effect of fishing pressure was the lowest (**Table 2**). Model M8, selected by AIC, predicted that the biomass-densities of small yellow croaker in the middle and southern area of Liaodong Bay (39°00′-40° 20′N, 120°00′-121° 37.5′E) was the highest in the Bohai Sea during 1982–2018 (**Figure 3**). Other hotspots (i.e. locations with the highest densities) for the stock were in the central Bohai Sea (38°15′-39° 00′N, 119°00′-121°00 ′E). The M8 also predicted the biomass of small yellow croaker in spring would have dropped sharply in general over the period of 1982–2018 (decreasing significantly from 1982 to 1998; mostly increasing from 1998 to 2011; declining sharply from 2011 to 2014; and increasing moderately between 2014 and 2018), leading to large distribution changes of the stock in their spawning ground during the whole study period (**Figure 3** and **Supplementary Figure 3**). The annual intercept of the gamma component (i.e., the $\beta_t^{(r)}$ term in equation (4)) reflected the biomass change, which also declined markedly in 1982–1998; increased largely in 1998–2011; decreased sharply in 2011–2014; and increased modestly in 2014–2018. Since 2011, biomass density in spring decreased significantly, accompanied by the disappearance of the hotspot area (**Figure 3** and **Supplementary Figure 3**). This disappearance/contraction was more pronounced in the western (Bohai Bay) and southern (Laizhou Bay) areas of the Bohai Sea than in the mid-eastern regions. After 2011, the density of the stock in the Yellow River Estuary and the southwest areas of Laizhou Bay was close to zero and showed a slow recovery; especially in the southwest areas of Laizhou Bay, which had a negligible recovery in 2017–2018. In 2018, the central area of Liaodong Bay close to the Liaodong Peninsula remained the only density hotspot in the Bohai Sea (**Supplementary Figure 3**).

In summer, the spatio-temporal model (M3) with the spatially-varying effect of WPI_lag1 had the lowest AIC (**Table 2**). This AIC-selected model M3 predicted that the hotspots of small yellow croaker in the Bohai Sea would be found in the area near the line connecting the junction of Bohai Bay and Laizhou Bay to the northern area of Liaodong Bay in the summer of 1982–2018 (**Figure 4**). We also found that the predicted hotspots moved left (west) or right (east) along the diagonal between years. M3 also predicted that the biomass decreased markedly in general in the summer between 1982 and 2018, leading to substantial distribution changes of the stock in their nursery and feeding grounds over the entire study period (**Figure 4** and **Supplementary Figure 4**). The $\beta_t^{(r)}$ terms also showed a significant overall decline during 1982–2018. Since 2009, the density of the stock in the Bohai Sea in summer decreased significantly, accompanied by shrinkage of the high-density areas (**Figure 4** and **Supplementary Figure 4**). The shrinkage was more obvious in Bohai Bay, the eastern area of Laizhou Bay and the central area of the Bohai Sea than in Liaodong Bay. In 2012 and 2016, the density in the Yellow River estuary remained relatively high in the area south of 39°N. By the second

**TABLE 2 |** Model selection based on Akaike's information criterion (AIC) for the eight alternative spatio-temporal delta-Gamma models in spring and summer, respectively fitted in the present study.

| Season | Model | Covariates | ΔAIC |
|---|---|---|---|
| Spring | M1 | None | 41.491 |
| | M2 | SST | 13.799 |
| | M3 | NPI | 34.495 |
| | M4 | Fishing pressure | 34.100 |
| | M5 | SST+Fishing pressure | 8.955 |
| | M6 | SST+NPI | 5.623 |
| | M7 | NPI+Fishing pressure | 27.597 |
| | M8 | SST+NPI+Fishing pressure | 0.000 |
| Summer | M1 | None | 21.315 |
| | M2 | BT | 14.205 |
| | M3 | WPI_lag1 | 0.000 |
| | M4 | Fishing pressure | 16.939 |
| | M5 | BT+Fishing pressure | 10.220 |
| | M6 | BT+WPI_lag1 | 5.690 |
| | M7 | WPI_lag1+Fishing pressure | 0.708 |
| | M8 | BT+WPI_lag1+Fishing pressure | 0.263 |

*SST, sea surface temperature; BT, sea bottom temperature; NPI, North Pacific index; WPI, West Pacific index; WPI_lag1, West Pacific Index time series with the 1-year delay effect; AOI, Arctic Oscillation index; Fishing pressure, fishing pressure index. * indicated that the gradient of marginal logarithmic likelihood of all fixed effects did not pass the convergence test. NA indicated that the model was not fitted successfully.*

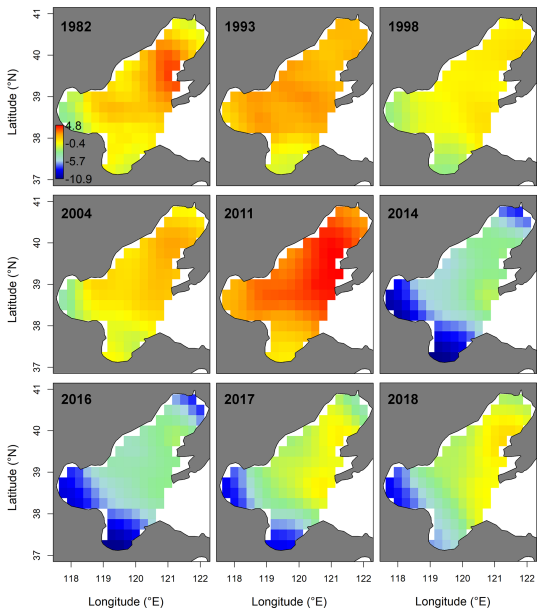


**FIGURE 3** | Spatio-temporal distribution of log-density for the small yellow croaker stock of the Bohai Sea in spring of 1982–2018, predicted by the Akaike's information criterion (AIC)-selected model developed for the stock. The color legend with units ln(kg.km$^{-2}$) is provided in the first panel and has. Only projections for years where sampling for the stock were available (i.e., 1982, 1993, 1998, 2004. 2011, 2014 and 2016–2018) are presented.

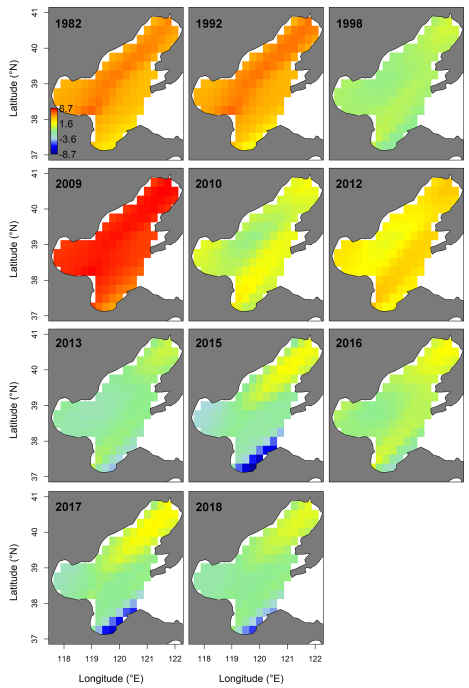


**FIGURE 4** | Spatio-temporal distribution of log-density for the stock of the Bohai Sea in summer of 1982–2018, predicted by the AIC-selected model. The color legend with units ln(kg.km$^{-2}$) is provided in the first panel. Only projections for the years where sampling for the stock were available (i.e., 1982, 1992, 1998, 2009-2010, 2012-2013 and 2015–2018) are presented.

half of the 2010s, except for 2016, only the Liaodong Bay area retained a biomass hotspot for the stock (**Supplementary Figure 4**). Combining the trends of the stock biomass density in the Bohai Sea in the two seasons, we found that the biomass: (1) increased extremely slowly in the early 1980s to early 1990s; (2) subsequently decreased significantly during the early 1990s to late 1990s; (3) increased again largely in the early 2000s to late 2000s; (4) then decreased sharply in the early 2010s to mid-2010s; and finally (5) exhibited an extremely slow recovery trend after 2017.

In spring, the COGs predicted by the AIC-selected M8 suggested that the COG of the stock had moved southward and westward in spring of 1982–1993, and then northward and eastward in spring between 1993 and 2018 (**Figure 5**). Over the period 1982–2018, changes in both the COGs in spring were non-significant (both $p > 0.05$, a two-sided Wald test was used for all significance tests). However, the spring variations in eastward and northward COGs during 1993–2018 were significant ($p$=0.015 and 0.034, respectively). In summer, the COGs estimated by the AIC-selected M3 showed that the COG variation trend was relatively stable in the summer of 1982–2009; and then the COG moved largely to the north and east over the period 2009–2018 (**Figure 5**). Between 1982 and 2018, eastward changes in the COG in summer (i.e., the large move of the COG of the stock towards the east of Bohai Sea) were statistically significant ($p = 0.0004$, a two-sided Wald test was used for all significance tests). In addition, the northward COG changes of small yellow croaker in summer (i.e., the large move of the COG of the stock towards the north of Bohai Sea) were also significant ($p = 0.0024$) from 1982 to 2018.

In spring, the effective area occupied of the stock predicted by the M8 indicated that range contraction had occurred during the study period from 1993 to 2018 (**Figure 5**). However, from 1982 to 2018, the effective area occupied by the stock in spring did not change significantly ($p$ >0.05). In summer, the effective area occupied in the Bohai Sea predicted by the M3 showed that the range of the stock was reduced (**Figure 5**). Statistically, the change in effective area occupied by the stock in summer from 1982 to 2018 was also significant ($p = 0.046$).

## Trend Analysis of Local Temperature, Climate Index and Fishing Pressure Index Time Series

From 1982 to 2018, the local temperature anomalies in May showed an oscillatory rising trend, and the mean SST difference between the former and the latter five years was 1.96℃. The SST time series showed that regime shifts in temperature occurred in 1995/1996 and 2013/2014 respectively (**Figure 6A**), mirroring the switch from a southward to a northward shift of the small yellow croaker COG in spring in 1993 and in 2014 respectively. The time series indicated (**Figure 6B**) that there were no regime shifts in the spring NPI during the period 1981–2018. The change in trend of the cumulative sum of NPI anomalies in

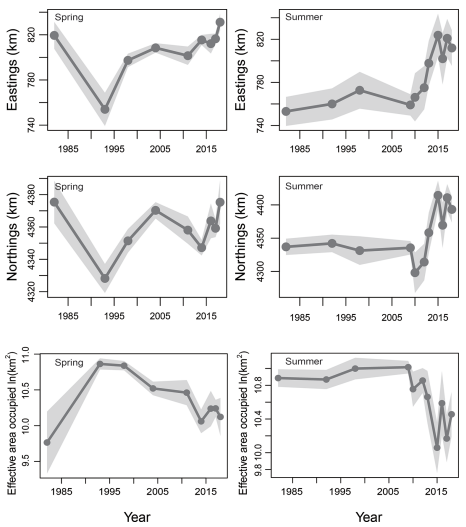


**FIGURE 5** | Eastward center of and northward center of gravity (COG; in km) and effective area occupied for the stock in spring and summer of 1982–2018, predicted by the AIC-selected model. The 95% confidence intervals are represented as shaded areas. Only projections for the years where sampling for the stock were available (i.e., 1982, 1993, 1998, 2004. 2011, 2014 and 2016–2018 for spring; 1982, 1992, 1998, 2009-2010, 2012-2013 and 2015–2018 for summer) are given.

spring was, to a certain extent, similar to the trend in the COG in spring.

In summer, there was a large seasonal oscillation in local temperature anomalies during August of each year (**Figure 7A**). The overall trend of local temperature was stable from 1982 to 2008, whereas it increased greatly from 2008 to 2018. This obviously reflected the trend of the COG and effective area occupied of the stock in summer. Local temperature time series showed that a regime shift of the SST occurred in 2008/2009 (**Figure 7A**). This corresponded to the large increase in density and change in distribution in 2009. The WPI time series indicated that WPI underwent regime shifts in 2001/2002 and 2017/2018 (**Figure 7B**). The change in pattern of positive/negative WPI anomalies in summer between 1981 and 2018 correlated with the change in the summer pattern of biomass density.

The fishing pressure proxy rose sharply from 1982 to 1994; moderately increased during 1994–2002; fell sharply from 2002 to 2009; and increased rapidly and substantially again from 2009 to 2015; then subsequently declined somewhat to remain at relatively stable but high level thereafter (**Figure 8**).

## DISCUSSION

To understand its ecological response to multiple stressors during the spawning and nursery phases of its life history, we developed a spatio-temporal model for the small yellow croaker's populations in the Bohai Sea in spring and summer during 1982–2018. Ours is the first spatio-temporal implementation of the SVC model to determine the effects of annual indices (climate index and fishing pressure index) in the Bohai Sea. Many studies have established that spatio-temporal models which account for both spatial and spatio-temporal variation can produce more accurate estimates, thereby providing increased reliability in the scientific basis for decision-making about how best to manage marine ecosystems, their dependent fish populations, and the fisheries those populations sustain (Rassweiler et al., 2014; Thorson et al., 2015; Grüss et al., 2019b; Han et al., 2019; Thorson, 2019a; Thorson, 2019b; Han et al., 2021).

In the spatio-temporal model we developed, spatial variation refers to variation in biomass density that for the small yellow croaker in the Bohai Sea is assumed to remain constant over time. Spatio-temporal variation refers to the interannual variation in biomass density of the stock. Spatial variation and spatio-temporal variation represent, respectively, the fundamental ecological niche of the stock in the Bohai Sea and the response of the stock to the unmeasured environment stress (Grüss et al., 2017; Thorson, 2019a). Spatio-temporal models can also be used to obtain information on the stressors that cause ecological responses in fish populations and to analyze the relative magnitude of the effects of these stressors (i.e., analyzing the relative importance of the covariates) by including covariates to improve the proportion of response variation explained by a model (Thorson, 2015; Grüss et al., 2020a; Han et al., 2021). Based on these characteristics of the spatio-temporal model, this study identified multiple pressure factors influencing the population dynamics of small yellow croaker during spawning, nursery and feeding phases of their life history in the Bohai Sea.

The model results in spring and summer were expected to accord with those from a study in the East Bering Sea (Thorson, 2019b), which showed that the use of SVC models, including temperature or/and annual index (cold pool), produced more parsimonious models that better described the stock being modeled. The relationship between fishing pressure and local sea temperature with the distribution of small yellow croaker in summer was not as great as that in spring. We suspect that implementation of the summer fishing moratorium system meant that the stock dynamics during summer was not directly affected by fishing. Han et al. (2021) argued that the inclusion of local covariables and/or annual index in a similar model would not be appropriate to describe the stock being modeled in many regions; and the study of Ducharme-Barth et al. (2022) also adds a supporting case for this view. The present study supports and further develops the idea that such regions are not static, and that the inclusion of local or/and distant regional covariates in spatio-temporal models varies greatly in its suitability for describing the modeled stock in different seasons.

Insights about the spawning grounds and reproductive environment of the Bohai Sea stock of small yellow croaker in this study were predominantly consistent with those from previous studies conducted during the 1950s–1980s (Feng and Yang, 1955; Liu et al., 1990), with some additional points. Previous studies indicated that small yellow croaker entered the Bohai Sea from the Yellow Sea and divided into two routes

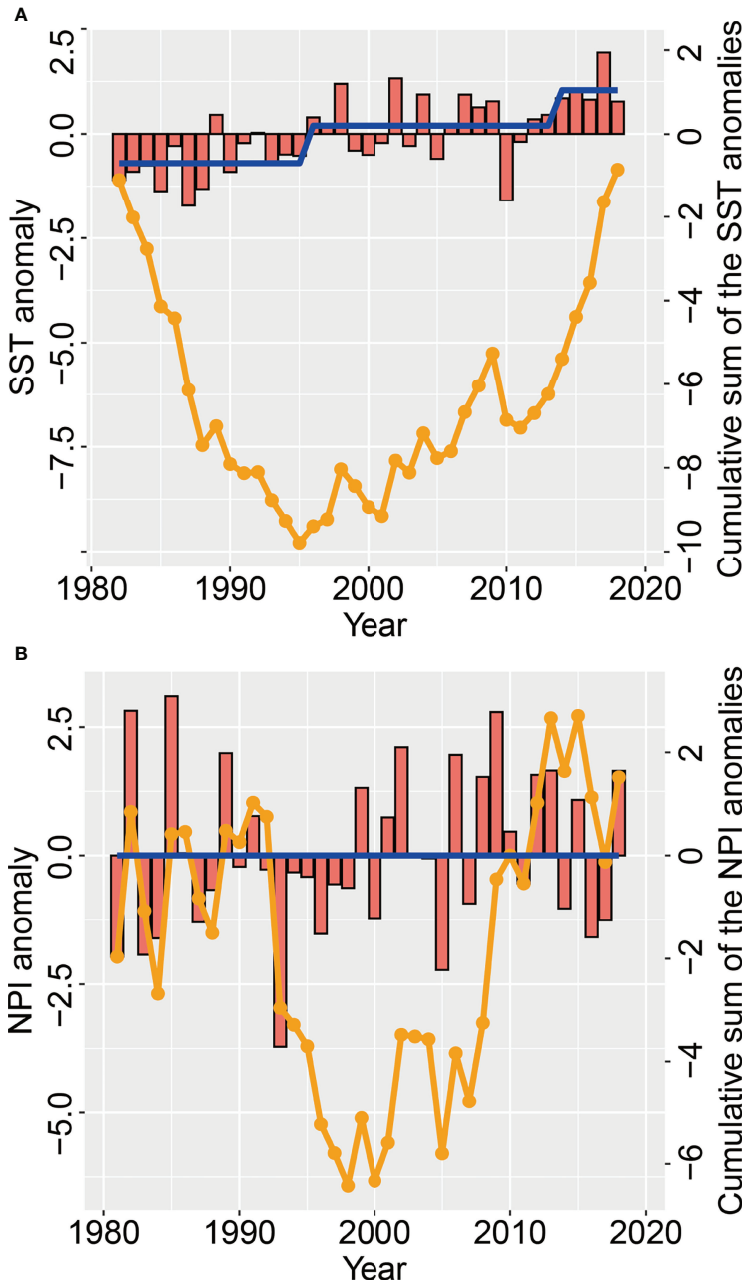


**FIGURE 6** | Changes in **(A)** May sea surface temperature (red bars) anomalies (SSTA) and **(B)** spring North Pacific index (NPI) anomalies (red bars), as well as the cumulative sum of the NPI and SST anomalies (orange line), in the Bohai Sea over the period 1981–2018 The regime shift (blue line) in the NPI and SST is also given.

in late April: the north route entered Liaodong Bay in mid-May; the south route continued to branch, one branch reached the spawning grounds of the Yellow Estuary of Laizhou Bay in early May, and the other branch reached the northern area of Bohai Bay (38°30'N-39°00'N, 118°00'E-118°30'E) in mid-May. Our results showed that even in mid to late May, a significant percentage of the stock remained distributed in the central Bohai Sea. Our model results also indicated that the range of spawning grounds in Bohai Bay was larger than determined in previous studies, and mainly concentrated in the northwestern area of Bohai Bay; and that in Laizhou Bay, in addition to the area around the Yellow River estuary, the stock was also distributed in the southern area of Laizhou Bay during the spawning period. The spawning grounds are crucial for replenishing the populations in the entire Yellow Sea Large Marine Ecosystem, because they attract many spawning adults (Jin et al., 2005). Our model results imply that there is a need to take more measures to focus on protecting the spawning grounds

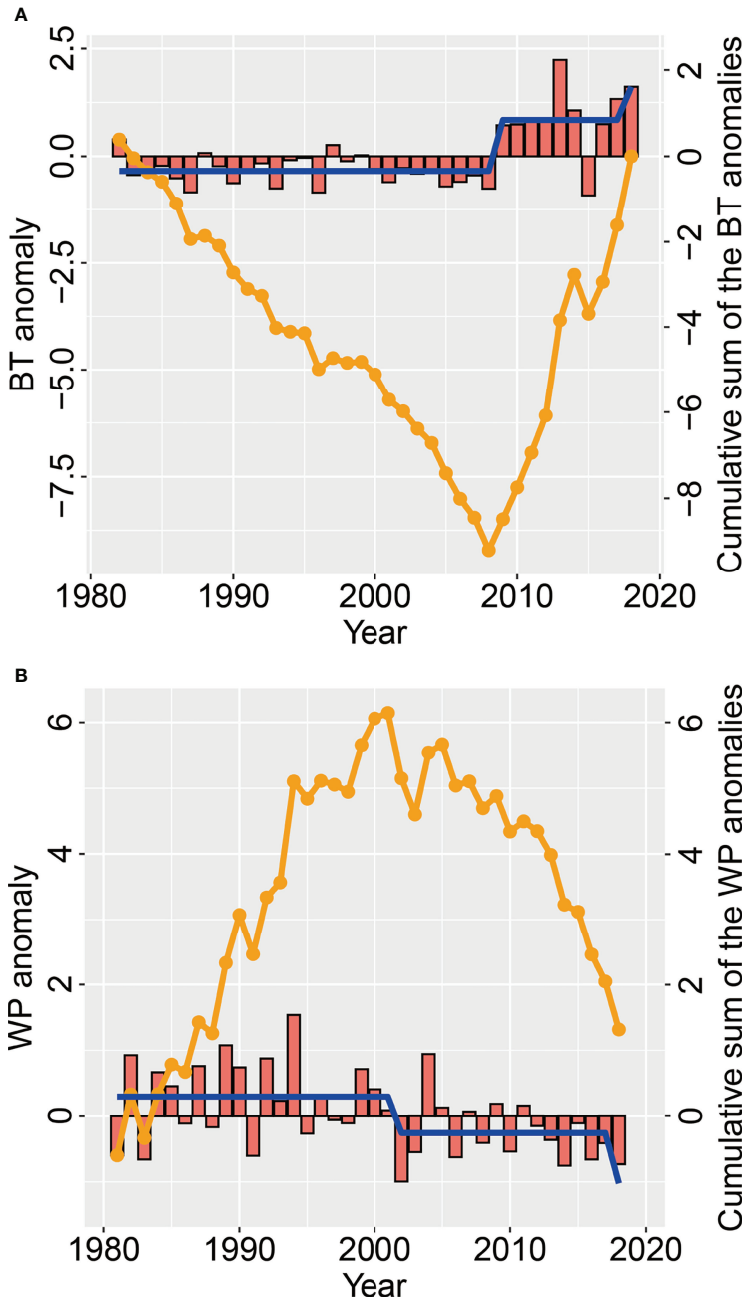


**FIGURE 7** | Changes in **(A)** August bottom temperature (red bars) anomalies (BTA) and **(B)** summer West Pacific index (WPI) anomalies (red bars), as well as the cumulative sum of the BT and WPI anomalies (orange line), in the Bohai Sea over the period 1981–2018. The regime shift (blue line) in the WPI and BT is also given.

in Bohai and Laizhou Bays. Therefore, this study provides fundamental support for marine spatial planning to ensure spawning grounds are sufficiently protected to maintain sustainable fisheries.

Our model indicated that the main feeding grounds (predicted hotspots) were in the area near the line connecting the junction of Bohai Bay and Laizhou Bay to the northern area of Liaodong Bay in summer (August). This location was consistent with the main distribution area of the August fishery yield of the stock in the Bohai Sea observed during 1971–1972 (Xu and Chen, 2009, **Figure 2** of the paper). However, the common feeding ground in Laizhou and Bohai Bays differed from what was identified in a previous study by Lin (1991), which determined that the common feeding ground of the stocks in Laizhou and Bohai Bays was located in the nearshore waters of Bohai Bay in northwestern Shandong Province.

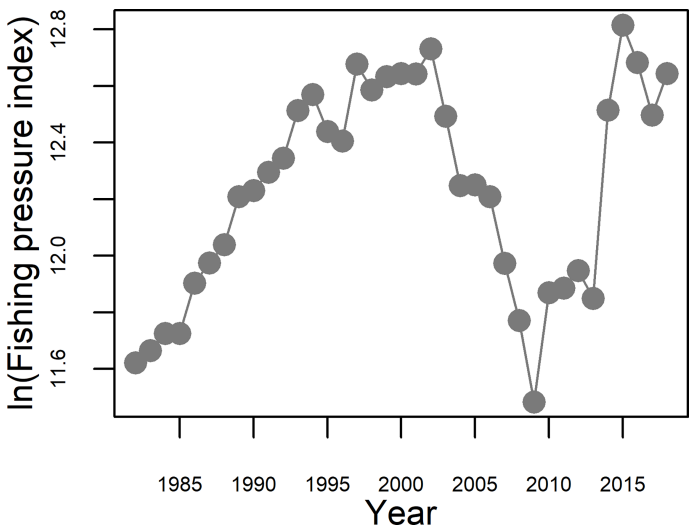


**FIGURE 8** | Changes in the proxy of fishing pressure (in ln(Fishing pressure index)) in the Bohai Sea during the period 1982–2018.

In summer, M3 indicated a statistically significant shift to the northeast and range contraction of the stock in their feeding and nursery grounds over the period 2009–2018. This finding mirrored a decrease in the recruitment capacity of small yellow croaker in the Bohai Sea after 2009, with its northeastern area declining relatively slower than the other regions of the Bohai Sea. As per the spring results, this finding also implied a decline in ecological function (cradle) in Bohai and Laizhou Bays in recent years and the need to focus on restoring their functionality.

Next, we discuss the role of local temperature, climate index and fishing pressure in driving the decadal spatio-temporal patterns of the stock in its spawning, nursery and feeding grounds in the Bohai Sea.

Previous studies have established that fishing pressure is an important driving force for the distribution patterns of marine fish stocks (Jørgensen et al., 2008; Bell et al., 2015). In the Yellow and Bohai Seas, fishing pressure and its heterogeneous distribution have also been identified as important factors leading to changes in fish distribution (Xu et al., 2003; Li, 2011; Wang et al., 2012; Lin et al., 2016). In a spatio-temporal model, the total power of fishing vessels is far from the best method to represent fishing pressure (Han et al., 2021), because it ignores the exponential increase in fishing efficiency of individual vessels and the changes in available fishing periods caused by management regulations. In this study, we recognized this issue, and in the fishing pressure index we constructed, we accounted for the reduction in fishing periods caused by the summer fishing moratorium and for the rapid increase in fishing efficiency arising from the increase in the proportion of high-powered fishing vessels (which tend to have more sophisticated technical equipment). Although there are many other factors affecting fishing pressure, we can only narrow the distance between this index and the actual fishing pressure based on the limited information available, but we believe that the index we used is more effective and realistic than the total power of fishing vessels, and is the most effective proxy of fishing pressure in this area at present. We therefore fitted a spatio-temporal model that included this fishing pressure index effect, modeling it as an annual index. In spring, based on the AIC comparison of the eight alternative spatio-temporal delta-Gamma models, we found that the effect of fishing pressure was second only to the effect of SST. Fishing pressure effect was also included in the final chosen model, M8. We believe that it is possible that heterogeneity in the distribution of fishing pressure has caused a more pronounced decrease in the density of small yellow croaker in the western (Bohai Bay) and southern (Laizhou Bay) areas of the Bohai Sea than elsewhere. This is evident as a decrease in the effective area occupied and a northeasterly shift in the COG of the stock as predicted by the spatio-temporal model. In summer, fishing pressure did not have a direct impact on the small yellow croaker in August for most of the inter-annual time series due to the closure to commercial fishing during summer since 1995 (after several adjustments later, i.e., the duration of the moratorium was increased). The spatio-temporal distribution of the stock in August was indirectly affected by fishing pressure *via* its influence on the spawning parental stock in spring. This explains why in this study, we found that the model including the fishing pressure effect reduced AIC compared with the model without this covariate, but that its AIC was not the smallest.

Previous studies have shown that fishing pressure has a substantial effect on the biomass of small yellow croaker (Liu et al., 1990; Lin et al., 2016). This is confirmed by the results from applying the spatio-temporal models in spring and summer in our study. In terms of trends in the status of the fish stocks in the Bohai and Yellow Seas, Liu et al. (1990) showed that serious overfishing occurred from the early 1970s to the late 1980s. Our results indicate that a substantial part of the large increase in the biomass from the early 2000s to the end of the 2000s was

associated with a steep decrease in fishing pressure during that period (**Figure 8**). Fishing pressure dropped to its lowest in 2009, providing an important respite for the replenishment of stocks, and was directly reflected in the high biomass observed in the following summer of 2009 (no data were available in the spring of 2009, but survey data for the autumn of 2009 also showed that the density of the stock was much higher than in previous years), and indirectly led to the high biomass density of adult small yellow croaker observed during the spring of 2011. This was partly supported by the changes in the density of small yellow croaker in the overwintering grounds of the Yellow Sea (Han et al., 2021), where the density in the northern area (considered to be the overwintering grounds of the Bohai-Northern Yellow Sea stock) and the central overwintering grounds (considered to be the overwintering grounds of the Bohai-Northern Yellow Sea and the central Yellow Sea stocks) increased in 2008 relative to previous years, and relative to the southeastern overwintering grounds of the Yellow Sea. Unfortunately, although the total power of fishing vessels remained stable after 2009, the proportion of high-powered vessels sharply increased (implying faster speed; increased of fish holding capacity; increased periods of continuous operation at sea; advanced fish finding sonar technology, etc.), leading to a sharp increase of fishing pressure, which in turn led to a deterioration in the status of the small yellow croaker resource. Although the summer season closure was extended for another month from 2017, the resource did not recover significantly. The need to constrain fishing pressure has gained more and more attention from fisheries managers, with the Ministry of Agriculture and Rural Affairs of the People's Republic of China (2017) issuing the "Notice on Further Strengthening the Control of Domestic Fishing Vessels and Implementing the Management of Total Marine Catch", which specified clear control targets and an implementation schedule for vessel and catch limitation. In combination these imposed a strong fishing pressure control measure. Our study also shows that reduced fishing pressure can indeed promote the recovery of small yellow croaker stocks. In addition, our results also highlight the destructive effect of high-powered fishing vessels on stocks. At the same time, measures need to be taken to ensure that there are enough spawning adults of small yellow croaker during May and enough numbers of juveniles leaving the Bohai Sea in October to begin their overwintering migrations.

Model selection indicated the importance of incorporating local temperature into the models of the stock during the spawning season (**Table 2**). SST may explain a large proportion of the spatio-temporal variation of non-zero density probability (**Table 1**). This finding is consistent with previous results that changes in ocean temperature affect the onset of spawning migrations and the distribution of spawning grounds (bottom temperature 10–13°C) for the stock (Liu et al., 1990).

During the summer feeding and nursery periods, we found that local temperature also explained a large proportion of the spatio-temporal variation of non-zero density probability and a smaller proportion of the spatio-temporal variation of encounter probability in August, but the proportion explained was less than the climate index WPI_lag1. Model selection also indicated that the spatio-temporal model with a local temperature effect was less suitable for the modeled systems than the spatio-temporal model with WPI_lag1 effects. This is strongly related to the wide temperature range (generally 14–26°C) to which small yellow croaker are subjected during their feeding period (Zhao et al., 1987). WPI_lag1, on the other hand, contains other information in addition to temperature, which will be discussed later. As found in Astarloa et al. (2021), the summer local environmental variable SST in our study was unable or rarely able to capture the association between the environmental and ecological processes because of the time lag of species' response and the inherent non-linear nature of stock dynamics (Hallett et al., 2004). We hypothesized that the distribution of the stock during the summer feeding period may be strongly correlated with the distribution of its primary prey, and the time-lagged driving factors for the primary prey distribution over a period of time in advance can be used as time-lagged covariates among the explanatory effects in the summer spatio-temporal models.

Many species require non-local and regional mechanisms to explain their spatio-temporal distribution shifts and density changes (HilleRisLambers et al., 2013; Heino et al., 2017). Even highly compressed annual indices (climate/oceanographic indices) that lose spatial differences in distribution sometimes contain additional information about species distributions compared to local temperatures (Thorson, 2019b). Thorson (2019b) concluded that the SVC (spatially varying coefficient) for an annual oceanographic/climate index represents a flexible way to proxy the habitat selection as fish respond differently among years in accordance with their changing physical environments. This is the case for the summer model results in this study, where additional information on the distribution of small yellow croaker during the summer feeding period, compared to local temperature, was included in the regional covariate, namely annual climate index WPI_lag1. WPI_lag1 represented the combined effect of lagged and geographically distant habitat conditions, which influence the choice of feeding grounds. WPI_lag1 was the best predictor (lowest AIC) for explaining the biomass density of small yellow croaker in summer. The results showed that biomass density and encounter of small yellow croaker in summer were negatively correlated with WP_lag1 (and, positively correlated with WPI). The east-west and south-north movement of the East Asian jet stream leads to positive and negative WPI patterns, so WPI is related to various aspects of the East Asian climate. WPI mainly affects precipitation, temperature and occurrence of tropical cyclones in East Asia (Wallace and Gutzler, 1981; Barnston and Livezey, 1987; Choi and Moon, 2012). We also found a symmetric relationship between WPI and local temperature during 1982–2018, with positive WPI anomalies often corresponding to negative SST anomalies (**Figure 7**). Astarloa et al. (2021) suggested that climate indices often affect the abundance of high trophic level predators by regulating their food resources rather than directly affecting them. Therefore, we

could assume a potential bottom-up process, in which WPI_lag1 influences the small yellow croaker by regulating the effects of precipitation and other environmental effects on prey.

The results of the spring model showed that the climate index NPI also contains a small part of this combined effect, but does not explain the distribution of small yellow croaker to the extent that the climate index WPI_lag1 does in summer. The model results showed that NPI in spring was negatively correlated with the encounter and density of the stock. Spring NPI is thought to affect the temperature of the Yellow and Bohai Seas to promote gonad development of small yellow croaker (Liu et al., 2017), which could promote the spawning migration of the stock from the overwintering grounds to the spawning grounds of the Bohai and Yellow Seas. In addition, the spawning grounds are also affected by runoff into the sea, and spring NPI may affect the runoff from the River (Jiang et al., 2008; Zhi et al., 2015).

In conclusion, local sea temperature, climate index and fishing pressure exerted measurable effects on the spatial distribution pattern (fundamental ecological niche), shifts in that pattern, and range expansion/reduction of small yellow croaker populations during spawning and feeding seasons. There are still many aspects of these patterns that cannot be explained by these three indices (**Table 1**, **Figures 5**). The fractions of these patterns that were unexplained by the three indices, were to a large extent driven by the decreases in small yellow croaker biomass in 1982–2018 (**Figures 3**, **4**), and partially by other unconsidered factors (shoreline reclamation, seawater pollution) or unknown sources. Jin et al. (2015) summarized the impediments to the sustainable output of Chinese inshore fishery resources, especially in the Yellow and Bohai Seas, and concluded that ecological disasters such as red tides and the fragmentation or functional loss of spawning and nursery grounds caused by high-intensity human activities such as large-scale reclamation projects for coastal development, land-based pollution and mariculture have seriously impaired the replenishment and sustainability of fish stocks. Therefore, it is necessary to develop meaningful proxy indices that can appropriately represent the impacts of these high-intensity human activities for future research and fisheries assessments.

This study has contributed to our further understanding of the spatial distribution pattern of small yellow croaker and its relationship with multiple pressures in spawning, post-spawning feeding and nursery grounds in the Bohai Sea during summer. Other studies of the spatial distribution pattern of small yellow croaker habitat in the Bohai Sea were based on data from the 1950s to 1980s (Feng and Yang, 1955; Liu et al., 1990; Lin, 1991), and therefore do not provide the necessary insight into the present distribution pattern to enable responses to the critical needs of spatial management and protection in the Bohai Sea, as the cradle for the fishery in the Yellow Sea Large Marine Ecosystem. The results of this study are generally compatible with those of previous studies, but our research has highlighted that the patterns of spatial distribution of the small yellow croaker stock in their spawning and feeding grounds in the Bohai Sea have changed significantly over the past 40 years. In addition to the changes in spatial pattern identified in this paper, adaptive responses among the reproductive characteristics of the stock to environmental changes have also been identified by Zeng et al. (2005) who showed that individual fertility of small yellow croaker with the same body length had increased significantly in 2004 compared with 1964. Since the 1980s, the age of sexual maturity of small yellow croaker has significantly advanced, and the reproductive stock is mainly composed of recently matured fish (Li, 2011). We therefore suggest that spatio-temporal models should be further developed to accommodate the effects of these changes in reproductive characteristics and explore their relative importance in explaining patterns in spatial distribution shifts and range expansion/contraction. In this way, future resource management of the Bohai Sea and even the whole Yellow Sea Large Marine Ecosystem can include development of special conservation plans for the restoration of fish stocks based on previous and anticipated environmental and fishing patterns (Grüss et al., 2018; Grüss et al., 2019a; Grüss et al., 2014).

This study has provided important information for the management of small yellow croaker resources in spawning, nursery and feeding grounds in Bohai Sea. It has also provided a spatio-temporal model framework for the study of other highly migratory species in the Bohai Sea, thereby supporting spatial conservation plans and ecosystem-based fisheries management measures. Importantly, this study has demonstrated that SVCs are suitable as an annual index which serves as an important planning tool by including not only climatological information (Thorson, 2019b) but also fishing pressure into species distribution models (SDMs). It also illustrates that other high-intensity human activity pressures (such as pollution and reclamation) could be incorporated into SDMs in the future. This will promote the application of indices of fishing pressure and other highly impactful human activities for predicting changes in the spatio-temporal distributions of fish stocks *via* SDMs, and ultimately promote the implementation of ecosystem-based fishery management.

## DATA AVAILABILITY STATEMENT

The raw data supporting the conclusions of this article will be made available by the authors, without undue reservation.

## ETHICS STATEMENT

The animal study was reviewed and approved by Animal Ethics Committee, Yellow Sea Fisheries Research Institute.

## AUTHOR CONTRIBUTIONS

QH and XS conceived this study. QH conducted to methodology, analysis, writing – original draft, visualization. XJ made substantial contribution to data curation, writing – review &

editing. HG made substantial contribution to conceptualization, writing – review & editing. CS made contribution to writing – review & editing. All authors contributed to the article and approved the submitted version.

## FUNDING

This work was supported in part by the National Natural Science Foundation of China [42176151]; the Special Fund of Taishan Scholar Project, and the David and Lucile Packard Foundation; Innovation team of fishery resources and ecology in Yellow and Bohai Seas [2021TD01].

## ACKNOWLEDGMENTS

We thank the members of the Division of Fishery Resources and Ecosystem of Yellow Sea Fisheries Research Institute, Chinese Academy of Fishery Sciences. Many thanks as well to Arnaud Grüss for providing the basic code.

## SUPPLEMENTARY MATERIAL

The Supplementary Material for this article can be found online at: https://www.frontiersin.org/articles/10.3389/fmars.2022.941045/full#supplementary-material

## REFERENCES

Akaike, H. (1974). A New Look at Statistical-Model Identification. *IEEE Trans. Auto. Cont.* 19, 716–723. doi: 10.1007/978-1-4612-1694-016

Astarloa, A., Louzao, M., Andrade, J., Babey, L., Berrow, S., Boisseau, O., et al. (2021). The Role of Climate, Oceanography, and Prey in Driving Decadal Spatio-Temporal Patterns of a Highly Mobile Top Predator. *Front. Mar. Sci.* 8. doi: 10.3389/fmars.2021.665474

Barnston, A. G., and Livezey, R. E. (1987). Classification, Seasonality and Persistence of Low-Frequency Atmospheric Circulation Patterns. *Month. Weather. Rev.* 115, 1083–1126. doi: 10.1175/1520-0493(1987)1152.0.CO;2

Beaugrand, G., Brander, K. M., Alistair Lindley, J., Souissi, S., and Reid, P. C. (2003). Plankton effect on cod recruitment in the North Sea. *Nature*, 426 (6967), 661-664. doi: 10.1038/nature02164

Beddington, J. R., Agnew, D. J., and Clark, C. W. (2007). Current Problems in the Management of Marine Fisheries. *Science* 316, 1713–1716. doi: 10.1126/science.1137362

Bell, R. J., Richardson, D. E., Hare, J. A., Lynch, P. D., and Fratantoni, P. S. (2015). Disentangling the Effects of Climate, Abundance, and Size on the Distribution of Marine Fish: An Example Based on Four Stocks From the Northeast US Shelf. *ICES. J. Mar. Sci.* 72, 1311–1322. doi: 10.1093/icesjms/fsu217

Bian, X. D., Wan, R. J., Jin, X. S., Shan, X. J., and Guan, L. S. (2018). Ichthyoplankton Succession and Assemblage Structure in the Bohai Sea During the Past 30 Years Since the 1980s. *Prog. Fishery. Sci.* 39, 1–15. doi: 10.19663/j.issn2095-986.20170911001

Bian, X., Zhang, X., Sakrai, Y., Jin, X., Yamamoto, J., Gao, T., et al. (2014). Temperature-Mediated Survival, Development and Hatching Variation of Pacific Cod Gadus Macrocephalus Eggs. *J. Fish. Biol.* 84, 85–105. doi: 10.1111/jfb.12257

Blanchard, J. L., Mills, C., Jennings, S., Fox, C. J., Rackham, B. D., Eastwood, P. D., et al. (2005). Distribution Abundance Relationships for North Sea Atlantic Cod (*Gadus Morhua*): Observation Versus Theory. *Can. J. Fish. Aquat. Sci.* 62, 2001–2009. doi: 10.1139/f05-109

Botsford, L. W., Castilla, J. C., and Peterson, C. H. (1997). The Management of Fisheries and Marine Ecosystems. *Science* 277, 509–515. doi: 10.1126/science.277.5325.509

Browman, H. I., and Skiftesvik, A. B. (2014). The Early Life History of Fish—There is Still a Lot of Work to do! *ICES. J. Mar. Sci.* 71, 907–908. doi: 10.1093/icesjms/fst219

Cheung, W. W. L., Watson, R., and Pauly, D. (2013). Signature of Ocean Warming in Global Fisheries Catch. *Nature* 497, 365–368. doi: 10.1038/nature12156

Choi, K. S., and Moon, I. J. (2012). Influence of the Western Pacific Teleconnection Pattern on Western North Pacific Tropical Cyclone Activity. *Dynam. Atmos. Ocean.* 57, 1–16. doi: 10.1016/j.dynatmoce.2012.04.002

Core Team, R. (2021). *R: A Language and Environment for Statistical Computing* (Vienna, Austria: R Foundation for Statistical Computing). Available at: https://www.R-project.org/.

Cui, Y., Ma, S. S., Li, Y. P., Xing, H. Y., Wang, S. M., Xin, F. Y., et al. (2003). Pollution Situation in the Laizhou Bay and its Effects on Fishery Resources. *Prog. Fishery. Sci.* 24, 35–41. doi: CNKI:SUN:HYSC.0.2003-01-006

Ducharme-Barth, N. D., Grüss, A., Vincent, M. T., Kiyofuji, H., Aoki, Y., Pilling, G., et al. (2022). Impacts of Fisheries-Dependent Spatial Sampling Patterns on Catch-Per-Unit-Effort Standardization: A Simulation Study and Fishery Application. *Fish. Res.* 246, 106169. doi: 10.1016/j.fishres.2021.106169

Engelhard, G. H., Righton, D. A., and Pinnegar, J. K. (2014). Climate Change and Fishing: A Century of Shifting Distribution in North Sea Cod. *Global Change Biol.* 20, 2473–2483. doi: 10.1111/gcb.12513

Feng, L. M., and Yang, Y. A. (1955). Migration of Small Yellow Croaker and Hairtail. *Bull. Biol.* 8, 21–25.

Grimmer, M. (1963). The Space-Filtering of Monthly Surface Temperature Anomaly Data in Terms of Pattern, Using Empirical Orthogonal Functions. *Q. J. R. Meteorol. Soc.* 89, 395–408. doi: 10.1002/qj.49708938111

Grüss, A., Biggs, C. R., Heyman, W. D., and Erisman, B. (2018). Prioritizing Monitoring and Conservation Efforts for Fish Spawning Aggregations in the U.S. Gulf of Mexico. *Sci. Rep.* 8, 8473. doi: 10.1038/s41598-018-28120-7

Grüss, A., Biggs, C. R., Heyman, W. D., and Erisman, B. (2019a). Protecting Juveniles, Spawners or Both: A Practical Statistical Modelling Approach for the Design of Marine Protected Areas. *J. Appl. Ecol.* 56, 2328–2339. doi: 10.1111/1365-2664.13468

Grüss, A., Drexler, M., and Ainsworth, C. H. (2014). Using Delta Generalized Additive Models to Produce Distribution Maps for Spatially Explicit Ecosystem Models. *Fish. Res.* 159, 11–24. doi: 10.1016/j.fishres.2014.05.005

Grüss, A., Gao, J., Thorson, J. T., Rooper, C. N., Thompson, G., Boldt, J. L., et al. (2020a). Estimating Synchronous Changes in Condition and Density in Eastern Bering Sea Fishes. *Mar. Ecol. Prog. Ser.* 635, 169–185. doi: 10.3354/meps13213

Grüss, A., Rose, K. A., Justić, D., and Wang, L. (2020b). Making the Most of Available Monitoring Data: A Grid-Summarization Method to Allow for the Combined Use of Monitoring Data Collected at Random and Fixed Sampling Stations. *Fish. Res.* 229, 105623. doi: 10.1016/j.fishres.2020.105623

Grüss, A., and Thorson, J. T. (2019). Developing Spatio-Temporal Models Using Multiple Data Types for Evaluating Population Trends and Habitat Usage. *ICES. J. Mar. Sci.* 76, 1748–1761. doi: 10.1093/icesjms/fsz075

Grüss, A., Thorson, J. T., Carroll, G., Ng, E. L., Holsman, K. K., Aydin, K., et al. (2020c). Spatio-Temporal Analyses of Marine Predator Diets From Data-Rich and Data-Limited Systems. *Fish. Fish.* 21, 718–739. doi: 10.1111/faf.12457

Grüss, A., Thorson, J. T., Sagarese, S. R., Babcock, E. A., Karnauskas, M., Walter, J. F., et al. (2017). Ontogenetic Spatial Distributions of Red Grouper (*Epinephelus Morio*) and Gag Grouper (*Mycteroperca Microlepis*) in the US Gulf of Mexico. *Fish. Res.* 193, 129–142. doi: 10.1016/j.fishres.2017.04.006

Grüss, A., Walter, III J. F., Babcock, E. A., Forrestal, F. C., Thorson, J. T., Lauretta, M. V., et al. (2019b). Evaluation of the Impacts of Different Treatments of Spatio-Temporal Variation in Catch-Per-Unit-Effort Standardization Models. *Fish. Res.* 213, 75–93. doi: 10.1016/j.fishres.2019.01.008

Hallett, T., Coulson, T., Pilkington, J., Clutton-Brock, T., Pemberton, J., and Grenfell, B. (2004). Why Large-Scale Climate Indices Seem to Predict Ecological Processes Better Than Local Weather. *Nature* 430, 71–75. doi: 10.1038/nature02708

Han, Q. P., Grüss, A., Shan, X. J., Jin, X. S., and Thorson, J. T. (2021). Understanding Patterns of Distribution Shifts and Range Expansion/

Contraction for Small Yellow Croaker (*Larimichthys Polyactis*) in the Yellow Sea. *Fish. Oceanog.* 30, 69–84. doi: 10.1111/fog.12503

Han, Q. P., Shan, X. J., Wan, R., Guan, L. S., Jin, X. S., Chen, Y. L., et al. (2019). Spatiotemporal Distribution and the Estimated Abundance Indices of *Larimichthys Polyactis* in Winter in the Yellow Sea Based on Geostatistical Delta-Generalized Linear Mixed Models. *J. Fish. China.* 43, 1603–1614. doi: 10.11964/jfc.20180911448

He, C. (2002). *Preliminary Study on the Relationship Between the Arctic Oscillation and Temperature and Precipitation Changes in China and its Relationship With the Southern Oscillation* (Nanjing, China: Nanjing Institute of Meteorology).

Heino, J., Soininen, J., Alahuhta, J., Lappalainen, J., and Virtanen, R. (2017). Metacommunity Ecology Meets Biogeography: Effects of Geographical Region, Spatial Dynamics and Environmental Filtering on Community Structure in Aquatic Organisms. *Oecologia* 183, 121–137. doi: 10.1007/s00442-016-3750-y

HilleRisLambers, J., Harsch, M. A., Ettinger, A. K., Ford, K. R., and Theobald, E. J. (2013). How Will Biotic Interactions Influence Climate Change–Induced Range Shifts? *Ann. New York. Acad. Sci.* 1297, 112–125. doi: 10.1111/nyas.12182

Hurrell, J. W. (1995). Decadal Trends in the North Atlantic Oscillation: Regional Temperatures and Precipitation. *Science* 269, 676–679. doi: 10.1126/science.269.5224.676

Hurrell, J. W., and Deser, C. (2010). North Atlantic Climate Variability: The Role of the North Atlantic Oscillation. *J. Mar. Sys.* 78, 28–41. doi: 10.1016/j.jmarsys.2009.11.002

Hurrell, J. W., Kushnir, Y., Ottersen, G., and Visbeck, M. (2003). The North Atlantic Oscillation: Climate Significance and Environmental Impact. American: American Geophysical Union.

Jørgensen, C., Dunlop, E. S., Opdal, A. F., and Fiksen, Ø. (2008). The Evolution of Spawning Migrations: State Dependence and Fishing-Induced Changes. *Ecology* 89, 3436–3448. doi: 10.1890/07-1469.1

Jiang, Z., Yang, S., He, J., and Liang, J. (2008). Interdecadal Variations of East Asian Summer Monsoon Northward Propagation and Influences on Summer Precipitation Over East China. *Meteorol. Atmos. Phys.* 100, 101–119. doi: 10.1007/s00703-008-0298-3

Jin, X. S., Dou, S. Z., Shan, X. J., Wang, Z. Y., Wan, R. J., and Bian, X. D. (2015). Hot Spots of Frontiers in the Research of Sustainable Yield of Chinese Inshore Fishery. *Prog. Fishery. Sci.* 36, 124–131. doi: 10.11758/yykxjz.20150119

Jin, X. S., Shan, X. J., Li, X. S., Cui, Y., and Zuo, T. (2013). Long-Term Changes in the Fishery Ecosystem Structure of Laizhou Bay, China. *Sci. China Earth Sci.* 56, 366–374. doi: 10.1007/s11430-012-4528-7

Jin, X. S., Zhao, X. Y., Meng, T. X., and Cui, Y. (2005). *Biological Resource and Habitation Environment of the Bohai and Yellow Sea* (Beijing, China: Science Press).

Kass, R. E., and Steffey, D. (1989). Approximate Bayesian Inference in Conditionally Independent Hierarchical Models (Parametric Empirical Bayes Models). *J. Am. Stat. Assoc.* 84, 717–726. doi: 10.2307/2289653

Kidson, J. W. (1975). Tropical Eigenvector Analysis and the Southern Oscillation. *Month. Weather. Rev.* 103, 187–196. doi: 10.1175/1520-0493(1975)103.0.CO;2

Kristensen, K., Nielsen, A., Berg, C. W., Skaug, H., and Bell, B. (2016). TMB: Automatic Differentiation and Laplace Approximation. *J. Stat. Software* 70, 1–21. doi: 10.18637/jss.v070.i05

Li, Z. L. (2011). *Interannual Changes in Biological Characteristics of Small Yellow Croaker Larimichthys Polyactis, Pacific Cod Gadus Macrocephalus and Anglerfish Lophius Litulon in the Bohai Sea and Yellow Sea* (Qingdao, China: The Institute of Oceanology, Chinese Academy of Sciences).

Li, Z. L., Jin, X. S., Zhang, B., Zhou, Z. P., Shan, X. J., and Dai, F. Q. (2012). Interannual Variations in the Population Characteristics of the Pacific Cod *Gadus Macrocephalus* in the Yellow Sea. *Oceanol Limnol. Sinica.* 43, 924–931. doi: CNKI:SUN:HYFZ.0.2012-05-009

Lin, J. Q. (1991). Marine Fishery Resources of China (III). *Mar. Sci.* 3, 22–25. doi: CNKI:SUN:HYKX.0.1991-03-011

Lindgren, F., Rue, H., and Lindström, J. (2011). An Explicit Link Between Gaussian Fields and Gaussian Markov Random Fields: The Stochastic Partial Differential Equation Approach. *J. R. Stat. Soc.* 73, 423–498. doi: 10.1111/j.1467-9868.2011.00777.x

Lin, Q., Wang, J., Yuan, W., Fan, Z. H., and Jin, X. S. (2016). Effects of Fishing and Environmental Change on the Ecosystem of the Bohai Sea. *J. Fishery. Sci. China.* 23, 619–629. doi: 10.3724/SP.J.1118.2016.15317

Liu, Y., Tian, Y. J., Yu, J., Wang, X., Zhou, S. D., Shan, G., et al. (2021). Research Cooperation and Prospects in the Field of Marine Environment Between China and Japan. *Acta Oceanol. Sinica.* 43, 160–162. doi: 10.12284/hyxb2021178

Liu, X. X., Wang, J., Xu, B. D., Xue, Y., and Ren, Y. P. (2017). *Impacts of Fishing Pressure and Climate Change on Catches of Small Yellow Croaker in the Yellow Sea and Bohai Sea* Vol. 47 (Qingdao, China: Periodical of Ocean University of China), 58–64. doi: 10.16441/j.cnki.hdxb.20160263

Liu, X. S., Wu, J. N., Han, G. Z., Lin, J. Q., Lin, F. S., and Yao, Y. M. (1990). *Fishery Resources Investigation and Regionalization District in the Bohai Sea and the Yellow Sea* (Beijing, China: China Ocean Press).

Li, Z. Y., Wu, Q., Shan, X. J., Yang, T., Dai, F. Q., and Jin, X. S. (2018). Keystone Species of Fish Community Structure in the Bohai Sea. *J. Fishery. Sci. China.* 25, 229–236. doi: 10.3724/SP.J.1118.2018.17374

Lo, N. C., Jacobson, L. D., and Squire, J. L. (1992). Indices of relative abundance from fish spotter data based on delta-lognornial models Canadian Journal of Fisheries and Aquatic Sciences 49, 2515–2526.https://doi.org/10.1139/f92-278

Lotze, H. K., Lenihan, H. S., Bourque, B. J., Bradbury, R. H., Cooke, R. J., Matthew, C., et al. (2006). Depletion, Degradation, and Recovery Potential of Estuaries and Coastal Seas. *Science* 312, 1806–1809. doi: 10.1126/science.1128035

Mantua, N. J., and Hare, S. R. (2002). The Pacific Decadal Oscillation. *J. Oceanog.* 58, 35–44. doi: 10.1023/A:1015820616384

Mantua, N. J., Hare, S. R., Zhang, Y., Wallace, J. M., and Francis, R. C. (1997). A pacific interdecadal climate oscillation with impacts on salmon production. *Bulletin of the American Meteorological Society*. 78, 1069–1079.. doi: 10.1175/1520-0477(1997)078<1069:APICOW>2.0.CO;2

Ministry of Agriculture and Rural Affairs of the People's Republic of China (2017) *Notice on Further Strengthening the Control of Domestic Fishing Vessels and Implementing the Management of Total Marine Catch*. Available at: http://www.moa.gov.cn/nybgb/2017/derq/201712/t20171227_6130861.htm.

Myers, R., and Worm, B. (2003). Rapid Worldwide Depletion of Predatory Fish Communities. *Nature* 423, 280–283. doi: 10.1038/nature01610

Nakata, K., and Hidaka, K. (2003). Decadal-Scale Variability in the Kuroshio Marine Ecosystem in Winter. *Fish. Oceanog.* 12, 234–244. doi: 10.1046/j.1365-2419.2003.00249.x

O'Leary, C. A., Miller, T. J., Thorson, J. T., and Nye, J. A. (2018). Understanding Historical Summer Flounder (*Paralichthys Dentatus*) Abundance Patterns Through the Incorporation of Oceanography-Dependent Vital Rates in Bayesian Hierarchical Models. *Can. J. Fish. Aquat. Sci.* 76, 1275–1294. doi: 10.1139/cjfas-2018-0092

Overholtz, W. J., Hare, J. A., and Keith, C. M. (2011). Impacts of Interannual Environmental Forcing and Climate Change on the Distribution of Atlantic Mackerel on the U.S. Northeast Continental Shelf. *Mar. Coast. Fish.* 3, 219–232. doi: 10.1080/19425120.2011.578485

Overland, J., Rodionov, S., Minobe, S., and Bond, N. (2008). North Pacific Regime Shift: Definitions, Issues and Recent Transitions. *Prog. Oceanog.* 77, 92–102. doi: 10.1016/j.pocean.2008.03.016

Pikitch, E. K., Santora, C., Babcock, E. A., Bakun, A., Bonfil, R., Conover, D. O., et al. (2004). Ecosystem-Based Fishery Management. *Science* 305, 346–347. doi: 10.1126/science.1098222

Pinsky, M. L., Worm, B., Fogarty, M. J., Sarmiento, J. L., and Levin, S. A. (2013). Marine Taxa Track Local Climate Velocities. *Science* 341, 1239–1242. doi: 10.1126/science.1239352

Radlinski, M. K., Sundermeyer, M. A., Bisagni, J. J., and Cadrin, S. X. (2013). Spatial and Temporal Distribution of Atlantic Mackerel (*Scomber Scombrus*) Along the Northeast Coast of the United State–1999. *ICES. J. Mar. Sci.* 70, 1151–1161. doi: 10.1093/icesjms/fst029

Rassweiler, A., Costello, C., Hilborn, R., and Siegel, D. A. (2014). Integrating Scientific Guidance Into Marine Spatial Planning. *Proc. R. Soc. B.* 281, 20132252. doi: 10.1098/rspb.2013.2252

Richardson, D. E., Palmer, M. C., and Smith, B. E. (2014). The influence of forage fish abundance on the aggregation of Gulf of Maine Atlantic cod (Gadus morhua) and their catchability in the fishery. *Canadian Journal of Fisheries and Aquatic Sciences* 71(9), 1349–1362. doi: 10.1139/cjfas-2013-0489

Rodionov, S. N. (2004). A Sequential Algorithm for Testing Climate Regime Shifts. *Geophys Res. Lett.* 31, L09204. doi: 10.1029/2004gl019448

Rodionov, S. N. (2006). The Use of Prewhitening in Climate Regime Shift Detection, Geophys. *Geophys Res. Lett.* 33, L12707. doi: 10.1029/2006gl025904

Rodionov, S. N., and Overland, J. E. (2005). Application of a Sequential Regime Shift Detection Method to the Bering Sea Ecosystem. *ICES. J. Mar. Sci.* 62, 328–332. doi: 10.1016/j.icesjms.2005.01.013

Schwing, F. B., Murphree, T., and Green, P. M. (2002). The Northern Oscillation Index (NOI): A New Climate Index for the Northeast Pacific. *Prog. Oceanog.* 53, 115–139. doi: 10.1016/S0079-6611(02)00027-7

Shan, X. J., and Jin, X. S. (2016). Population Dynamics of Fish Species in a Marine Ecosystem: A Case Study in the Bohai Sea, China. *Mar. Coast. Fish.: Dynam. Manag. Ecosys. Sci.* 8, 100–117. doi: 10.1080/19425120.2015.1114543

Shelton, A. O., Thorson, J. T., Ward, E. J., and Feist, B. E. (2014). Spatial Semiparametric Models Improve Estimates of Species Abundance and Distribution. *Can. J. Fish. Aquat. Sci.* 71, 1655–1666. doi: 10.1139/cjfas-2013-0508

Shen, X. L. (2012). *Effects of Arctic Oscillation and ENSO on Extreme Climate Events in North China* (Beijing, China: Chinese Academy of Meteorological Sciences).

Su, H., Chen, X. J., and Wang, J. T. (2015). Influence of Sea Surface Temperature Changes on *Scomber Japonicus* Habitat in the Yellow Sea and East China Sea. *Acta Oceanol. Sinica.* 37, 88–96. doi: 10.3969/j.issn.0253-4193.2015.06.009

Sun, P., Shang, Y., Sun, R., Tian, Y., and Heino, M. (2022). The Effects of Selective Harvest on Japanese Spanish Mackerel (*Scomberomorus Niphonius*) Phenotypic Evolution. *Front. Ecol. Evol.* 10. doi: 10.3389/fevo.2022.844693

Thompson, D. W. J., and Wallace, J. M. (1998). The Arctic Oscillation Signature in Wintertime Geopotential Height and Temperature Fields. *Geophys Res. Let.* 25, 1297–1300. doi: 10.1029/98GL00950

Thompson, D. W. J., and Wallace, J. M. (2001). Regional Xlimate Impacts of the Northern Hemisphere Annular Mode. *Science* 293, 85–89. doi: 10.1126/science.1058958

Thorson, J. T. (2015). Spatio-Temporal Variation in Fish Condition is Not Consistently Explained by Density, Temperature, or Season for California Current Groundfishes. *Mar. Ecol. Prog. Ser.* 526, 101–112. doi: 10.3354/meps11204

Thorson, J. T. (2019a). Guidance for Decisions Using the Vector Autoregressive Spatio-Temporal (VAST) Package in Stock, Ecosystem, Habitat and Climate Assessments. *Fish. Res.* 210, 143–161. doi: 10.1016/j.fishres.2018.10.013

Thorson, J. T. (2019b). Measuring the Impact of Oceanographic Indices on Species Distribution Shifts: The Spatially Varying Effect of Cold-Pool Extent in the Eastern Bering Sea. *Limnol. Oceanog.* 9999, 1–14. doi: 10.1002/lno.11238

Thorson, J. T., and Barnett, L. A. K. (2017). Comparing Estimates of Abundance Trends and Distribution Shifts Using Single- and Multispecies Models of Fishes and Biogenic Habitat. *ICES. J. Mar. Sci.* 74, 1311–1321. doi: 10.1093/icesjms/fsw193

Thorson, J. T., and Kristensen, K. (2016). Implementing a Generic Method for Bias Correction in Statistical Models Using Random Effects, With Spatial and Population Dynamics Examples. *Fish. Res.* 175, 66–74. doi: 10.1016/j.fishres.2015.11.016

Thorson, J. T., Pinsky, M. L., and Ward, E. J. (2016a). Model-Based Inference for Estimating Shifts in Species Distribution, Area Occupied, and Center of Gravity. *Methods Ecol. Evol.* 7, 990–1002. doi: 10.1111/2041-210X.12567

Thorson, J. T., Rindorf, A., Gao, J., and Hanselman, D. H. (2016b). Density-Dependent Changes in Effective Area Occupied for Sea-Bottom-Associated Marine Fishes. *Proc. R. Soc. B.* 283, 20161853. doi: 10.1098/rspb.2016.1853

Thorson, J. T., Shelton, A. O., Ward, E. J., and Skaug, H. J. (2015). Geostatistical Delta-Generalized Linear Mixed Models Improve Precision for Estimated Abundance Indices for West Coast Groundfishes. *ICES. J. Mar. Sci.* 72, 1297–1310. doi: 10.1093/icesjms/fsu243

Tian, Y., Kidokoro, H., Watanabe, T., and Iguchi, N. (2008). The Late 1980s Regime Shift in the Ecosystem of Tsushima Warm Current in the Japan/East Sea: Evidence From Historical Data and Possible Mechanisms. *Prog. Oceanog.* 77, 127–145. doi: 10.1016/j.pocean.2008.03.007

Tian, Y., Uchikawa, K., Ueda, Y., and Cheng, J. (2014). Comparison of Fluctuations in Fish Communities and Trophic Structures of Ecosystems From Three Currents Around Japan: Synchronies and Differences. *ICES. J. Mar. Sci.* 71, 19–34. doi: 10.1093/icesjms/fst169

Trenberth, K. E. (1984). Signal Versus Noise in the Southern Oscillation. *Month. Weather. Rev.* 112, 326–332. doi: 10.1175/1520-0493(1984)1122.0.CO;2

Trenberth, K. E. (1997). The Definition of El Niño. *Bulletin of the American Meteorological Society*. 78, 2771–2777. doi: 10.1175/1520-0477(1997)0782.0.CO;2

Trenberth, K. E., and Hurrell, J. W. (1994). Decadal Atmosphere-Ocean Variations in the Pacific. *Climate Dynam.* 9, 303–319. doi: 10.1007/BF00204745

Wallace, J. M., and Gutzler, D. S. (1981). Teleconnections in the Geopotential Height Field During the Northern Hemisphere Winter. *Month. Weather. Rev.* 109, 784–812. doi: 10.1175/1520-0493(1981)109<0784:titghf>2.0.co;2

Wang, Y. Z., Sun, D. R., Lin, Z. J., Wang, X. H., and Jia, X. P. (2012). Analysis on Responses of Hairtail Catches to Fishing and Climate Factors in the Yellow Sea and Bohai Sea, China. *J. Fishery. Sci. China.* 19, 1043–1050. doi: 10.3724/SP.J.1118.2012.01043

Xu, Z. L., and Chen, J. J. (2009). Analysis on Migratory Routine of *Larimichthy Polyactis*. *J. Fishery. Sci. China.* 16, 931–940. doi: 10.3321/j.issn:1005-8737.2009.06.014

Xu, B. D., Jin, X. S., and Liang, Z. L. (2003). Changes of Demersal Fish Community Structure in the Yellow Sea During the Autumn. *J. Fishery. Sci. China.* 10, 148–154. doi: 10.3321/j.issn:1005-8737.2003.02.013

Yuan, X. W., Liu, Z. L., Cheng, J. H., and Tian, Y. J. (2017). Impact of Climate Change on Nekton Community Structure and Some Commercial Species in the Offshore Area of the Northern East China Sea in Winter. *Acta Ecol. Sinica.* 37, 2796–2808. doi: 10.5846/stxb201512222549

Zhang, B., Wu, Q., and Jin, X. S. (2015). Interannual Variation in the Food Web of Commercially Harvested Species in Laizhou Bay From 1959 to 2011. *J. Fishery. Sci. China.* 22, 278–287. doi: 10.3724/SP.J.1118.2015.14299

Zhao, C. Y., Chen, Y. F., Hong, G. C., Gu, X. G., Kong, X. Y., and Mao, X. L. (1987). *Fishery Resources Investigation and Regionalization District in the Donghai Sea* (Shanghai, China: East China Normal University Press).

Zhi, R., Wang, Q. G., Feng, G. L., and Feng, A. X. (2015). Using Moving North Pacific Index to Improve Rainy Season Rainfall Forecast Over the Yangtze River Basin by Analog Error Correction. *J. Meteorol. Res.* 29, 627–638. doi: 10.1007/s13351-015-4019-9

**Conflict of Interest:** The authors declare that the research was conducted in the absence of any commercial or financial relationships that could be construed as a potential conflict of interest.

**Publisher's Note:** All claims expressed in this article are solely those of the authors and do not necessarily represent those of their affiliated organizations, or those of the publisher, the editors and the reviewers. Any product that may be evaluated in this article, or claim that may be made by its manufacturer, is not guaranteed or endorsed by the publisher.

frontiers | Frontiers in Marine Science

ORIGINAL RESEARCH
published: 24 June 2022
doi: 10.3389/fmars.2022.933291

# Setting Conservation Priorities for Marine Sharks in China and the Association of Southeast Asian Nations (ASEAN) Seas: What Are the Benefits of a 30% Conservation Target?

*Jianguo Du[1,2,3], Like Ding[1,4], Shangke Su[1], Wenjia Hu[1,2,3]*, Yuyu Wang[5], Kar-Hoe Loh[6], Shengyun Yang[7], Mingru Chen[7], Kakaskasen Andreas Roeroe[8], Se Songploy[9], Zhenghua Liu[1,2,3] and Bin Chen[1,2,3]**

[1] Third Institute of Oceanography, Ministry of Natural Resources, Xiamen, China, [2] Key Laboratory of Marine Ecological Conservation and Restoration, Ministry of Natural Resources, Xiamen, China, [3] Fujian Provincial Key Laboratory of Marine Ecological Conservation and Restoration, Xiamen, China, [4] College of Marine Science, Shanghai Ocean University, Shanghai, China, [5] School of Ecology and Nature Conservation, Beijing Forestry University, Beijing, China, [6] Institute of Ocean and Earth Sciences, Universiti Malaya, Kuala Lumpur, Malaysia, [7] College of Ocean and Earth Sciences, Xiamen University, Xiame, China, [8] Faculty of Fisheries and Marine Science, Sam Ratulangi University, Manado, Indonesia, [9] Aquatic Resources Research Institute, Chulalongkorn University, Bangkok, Thailand

Sharks play an important role in marine ecosystems as top predators and have been increasingly accepted in recent years as a group for priority conservation worldwide. However, as one of the regions with the highest marine shark species richness, there is still a limited understanding of shark diversity patterns and conservation needs in China and the Association of Southeast Asian Nations (ASEAN) seas. In this study, we applied an ensemble species distribution model of five algorithms to investigate the diversity distribution patterns of 149 shark species in China and the ASEAN seas for the first time. A systematic conservation planning approach involving diversity, scarcity, and biogeographical distinctiveness was used to identify and compare conservation priority settings. Our results showed that bathymetry and dissolved oxygen were the most important variables contributing to shark distribution. The distribution pattern of shark species richness peaked on the continental shelves at 22–26°N, and a hotspot of shark diversity was identified around the Taiwan Strait. The spatial distribution of shark species in the nine orders and the 72 threatened shark species varied considerably. The existing marine protected area network only protects 2.1% of the ocean, 32.9% of the shark species, and 43.1% of the threatened species, highlighting a substantial conservation gap. Among the conservation priorities identified, the high conservation target scenario (30%) protects only 10%–15% more species than the low conservation target scenario (10%). However, under the high conservation target scenario, the conservation range of species tripled. Our results show that low conservation targets were only suitable for

OPEN ACCESS

**Edited by:**
Jun Xu,
Institute of Hydrobiology, Chinese Academy of Sciences (CAS), China

**Reviewed by:**
Xuehui Wang,
South China Sea Fisheries Research Institute, Chinese Academy of Fishery Sciences (CAFS), China
Cui Liang,
Institute of Oceanology, Chinese Academy of Sciences (CAS), China

***Correspondence:**
Wenjia Hu
huwenjia@tio.org.cn
Bin Chen
chenbin@tio.org.cn

**Specialty section:**
This article was submitted to Marine Ecosystem Ecology, a section of the journal Frontiers in Marine Science

**Received:** 30 April 2022
**Accepted:** 30 May 2022
**Published:** 24 June 2022

**Citation:**
Du J, Ding L, Su S, Hu W, Wang Y, Loh K-H, Yang S, Chen M, Roeroe KA, Songploy S, Liu Z and Chen B (2022) Setting Conservation Priorities for Marine Sharks in China and the Association of Southeast Asian Nations (ASEAN) Seas: What Are the Benefits of a 30% Conservation Target? Front. Mar. Sci. 9:933291. doi: 10.3389/fmars.2022.933291

addressing the number of protected species, and that high targets would bring about improved outcomes for the number of protected species and the protected range of threatened species. Furthermore, planned priorities with a large clump pattern had slightly higher conservation achievements than those with small clumps. The results of this study will contribute to the development of a priority area network for sharks and provide a scientific basis for shark conservation and management in the China and ASEAN seas.

**Keywords: conservation gap, elasmobranch, marine sharks, species distribution model, systematic conservation planning, MPA network**

## INTRODUCTION

Sharks are important top predators in marine ecosystems and have played an essential role at the highest trophic levels and in the food web for 400 million years (Compagno et al., 2005; Arai and Azri, 2019). However, sharks are more susceptible to potential extinction risks due to high exploitation rates and fishing pressure coupled with low resilience, such as slow growth, low fecundity, and later maturity ages (Ferretti et al., 2008; Lucifora et al., 2011; Jorgensen et al., 2022). The abundance of oceanic sharks has declined globally by 71.1% over the last half-century, with an average rate of 18.2% per decade (Pacoureau et al., 2021). Overfishing has resulted in almost 20% of the surveyed reefs being without sharks (MacNeil et al., 2020). A total of 37% of sharks and rays were classified as threatened species according to the latest International Union for the Conservation of Nature (IUCN) Red List (IUCN, 2022), with 45 elasmobranchs being listed in the Convention on International Trade in Endangered Species of Wild Fauna and Flora (CITES) Appendix II. The decline of shark resources will have a negative impact on the integrity and service functions of marine ecosystems (Yagnesh et al., 2020; Pimiento et al., 2020). Shark conservation has attracted worldwide attention, and there is an urgent need to develop conservation and management plans to protect them.

The peak diversity area of global shark species is located on continental shelves and at mid-latitudes. Hotspots of species richness have been found in Japan, Taiwan, eastern Australia, southeast Africa, and South America (Lucifora et al., 2011; Dulvy et al., 2014). The China and Association of Southeast Asian Nations (ASEAN) seas are among the regions with the highest marine shark species richness, with 146 species from 21 families, and 196 species from 30 families recorded in Chinese waters and Southeast Asia, respectively (Zhang and Yang, 2005; Ali et al., 2018; Wu and Zhong, 2021). Southeast Asia is one of the areas with the highest number of endangered and data deficient shark species (Dulvy et al., 2017). However, research on sharks in this area has predominantly focused on taxonomy (Zhu, 1960; Ali et al., 2018), fisheries (Lam and Sadovy de Mitcheson, 2011; Friedman et al., 2018) and trade (Van Houtan et al., 2020; Prasetyo et al., 2021). The distribution pattern of shark biodiversity is still poorly understood. Despite the importance of sharks and rays as being recognized as umbrella species, only a few marine protected areas (MPAs) have been designed to protect them (Giménez et al., 2020). Furthermore, many MPAs are ineffective in protecting vulnerable elasmobranchs (Dureuil et al., 2018). The majority of shark sanctuaries are in Oceania, the Caribbean, and the Indian Ocean (Ward-Paige and Worm, 2017). How many shark species have been protected in Chinese and ASEAN seas and which areas should be protected remain unknown. Owing to the unknown, unmonitored, and unmanaged shark populations in Southeast Asia, only 18 of the 109 shark species that have historically been present in the area were found during a market survey, and 65% of these were below their maturity length (Lam and Sadovy de Mitcheson, 2011). Current fishery practices will likely lead to the extinction of some shark species in the future (Arai and Azri, 2019). With these extensive research gaps, our current knowledge is inadequate to meet the challenges of shark protection and management (Prasetyo et al., 2021). There is an urgent need to study the diversity distribution patterns and the current conservation status of the sharks in China and the ASEAN seas.

According to Aichi Target 11 of the Convention on Biological Diversity (CBD), 10% of marine areas were to be conserved by 2020 (https://www.cbd.int/aichi-targets). Based on the World Parks Congress and the Kunming declaration of the CBD, many countries have called to protect 30% of terrestrial and marine areas by 2030 (World Parks Congress, 2014; CBD/COP/15/5/Add.1, 2021). However, at present only 7.93% of the ocean is protected worldwide (UNEP-WCMC and IUCN, 2022). It remains a challenge to assess and identify conservation priority areas for global marine conservation and management, encompassing those that best represent the world's marine biodiversity (Venter et al., 2014; Zhao et al., 2020). Over the last decade, one-third of the increase in the MPA range has been undertaken with the aim of shark conservation. However, 97.4% of the marine species have less than 10% of their geographic range within MPAs (Davidson & Dulvy, 2017). Fifteen countries in the Atlantic, Indian, and Pacific Oceans have declared their entire economic exclusive zones as "shark sanctuaries," which were delimited by administrative boundaries rather than ecological characteristics (Ward-Paige and Worm, 2017). Systematic conservation planning (SCP) can be used to identify conservation priority areas and design protected area networks, providing a new decision-making method for managers (Margules and Pressey, 2000). In recent years, SCP has been widely used in terrestrial (Cuesta et al., 2017; Jellinek, 2017) and oceanic conservation priority area planning (Zhao et al., 2020; Jefferson et al., 2021). Marine spatially explicit annealing (Marxan) is the most widely used software worldwide for SCP analysis (Christodoulou et al., 2021). The marine conservation areas for five demersal sharks and rays were identified using Marxan

decision support tools in the western Mediterranean Sea (Giménez et al., 2020). Marine protected area design was also informed by Marxan combined with movement models for eight elasmobranchs in the Bahamas (Van Zinnicq Bergmann et al., 2022). However, there has been a tendency for shark conservation to address only some species (Dulvy et al., 2017). The representativeness of diversity and specific ecoregions needs to be improved. There is also a lack of research on sharks using the SCP approach in China and the ASEAN seas, where information regarding the spatial distribution of most sharks is still scarce.

Although methods such as long-line, electronic tags, eDNA, and baited remote underwater video stations can provide occurrence records for sharks, distribution data are still scarce for these widely distributed marine megafauna (White et al., 2019; Espinoza et al., 2020; Jorgensen et al., 2022). In recent years, species distribution models (SDMs) have often been used to explore the distribution and assess the habitat suitability for marine species for which records are difficult to obtain (Melo-Merino et al., 2020). A single SDM has been used to explore the distribution of sharks, such as the generalized linear model (GLM) (Kai et al., 2017; Giménez et al., 2020), and maximum entropy (Maxent) (Chan et al., 2021; Noviello et al., 2021; Pottie et al., 2021). However, using a single model is likely to cause high uncertainty, but ensemble SDM, used in many studies, increases the confidence level (Segurado and Araujo, 2004; Thuiller et al., 2019). The distribution of elasmobranchs has been projected using ensemble SDMs, while far fewer studies have been undertaken in the China and ASEAN seas than in the UK, North America, and the Western Central Atlantic (Austin et al., 2019; Garzon et al., 2021).

In the present study, we applied the ensemble SDM and SCP approach to investigate diversity distribution patterns and conservation priority areas for 149 shark species in the China and ASEAN seas. The main objectives were to (i) identify the spatial distribution pattern of shark diversity and its main environmental drivers, (ii) reveal current conservation gaps, and (iii) identify and compare conservation priorities for different conservation targets and explore the best solutions. This study is the first attempt to reveal the diversity distribution characteristics of sharks in the China and ASEAN seas. Through this research, we aimed to identify the conservation effectiveness of different target scenarios, which will contribute to the development of a priority area network for sharks in this region, providing a scientific basis for shark conservation and management.

# MATERIALS AND METHODS

## Study Area

The seas surrounding China and ASEAN form part of the western Pacific, covering a wide range across 52 latitudes in warm-temperate, subtropical, and tropical climate zones. The longitude and latitude of the study region were approximately 41° N–10.5° S and 99° E–135° E, respectively, with an area of approximately $837\times10^4$ km$^2$ (**Figure 1**). Fifteen marine ecoregions were included in the study according to the Marine Ecoregions of the World (MEOW) proposed by Spalding et al. (2007). The study region is affected by the Pacific-to-Indian Ocean throughflow, the Indonesian throughflow, the Kuroshio warm current, and the equatorial current (Liu, 2011). Most parts of the coral triangle are included in this region, which represents a global epicenter of marine life abundance and diversity. The study area included the center of marine shore fish biodiversity (Carpenter and Springer, 2005). It is also among the regions with the highest marine shark diversity, with more than 150 species of sharks and rays in a half-degree cell (Lucifora et al., 2011; Kaschner et al., 2019).

In the present study, 149 shark species from nine orders and 32 families were selected (Supplementary Material) according to data availability. These species account for more than 76% of all the sharks in this region (Zhang and Yang, 2005; Ali et al., 2018; Wu and Zhong, 2021). This encompasses almost all the shark orders and families in China and the ASEAN seas, from the Carcharhiniformes which is the largest group with 78 species, to the Pristiophoriformes which has one species. According to the IUCN Red List, there are 10 critically endangered (CR) species, 28 endangered (EN) species, and 34 vulnerable (VU) species (IUCN, 2022), totaling 72 ETP (endangered, threatened, and protected) species. The selected species come from a range of trophic levels (TLs) and habitats. Most sharks are carnivorous, such as the great white shark (*Carcharodon carcharias*) which has a TL value of 4.5, while some are filter-feeding species such as the basking shark (*Cetorhinus maximus*) which has a TL value of 3.2 (Froese and Pauly, 2022). They also include the largest whale shark (*Rhincodon typus*) and the small Japanese angelshark (*Squatina japonica*). Endemic species were also included in the selected species; for example, the clouded angelshark (*Squatina nebulosa*), which occurs from Japan to Taiwan (Rigby et al., 2021).

## Data Sources and Preparation

Occurrence data for the 149 shark species were collected from the global biogeographic database, field investigation, and the related literature. The occurrence records from the Global Biodiversity Information Faculty (GBIF, www.gbif.org) and the Ocean Biodiversity Information System (OBIS, www.iobis.org) were extracted using the *spocc* R package (Chamberlain et al., 2014), and the data from FishBase (www.fishbase.org) were collected manually. Data from the Chinese Offshore Investigation and Assessment project conducted in 2004–2009 were also collected, which is the most recent and largest marine survey in China (State Oceanic Administration, 2016). Data were also collected from relevant papers and reports in China (Li et al., 2007; Zhang et al., 2018), and Malaysia (Yano et al., 2005; Last et al., 2010). The data were merged to retain the longitude and latitude information. Duplicated, impossible, and incomplete coordinates were removed during the data-cleaning process, retaining 60,426 occurrence records for the 149 shark species. The data-cleaning process was conducted in an R environment using the *scrubr* package (Thuiller et al., 2021; Chamberlain, 2022). Spatial rarefying was then conducted to resample the

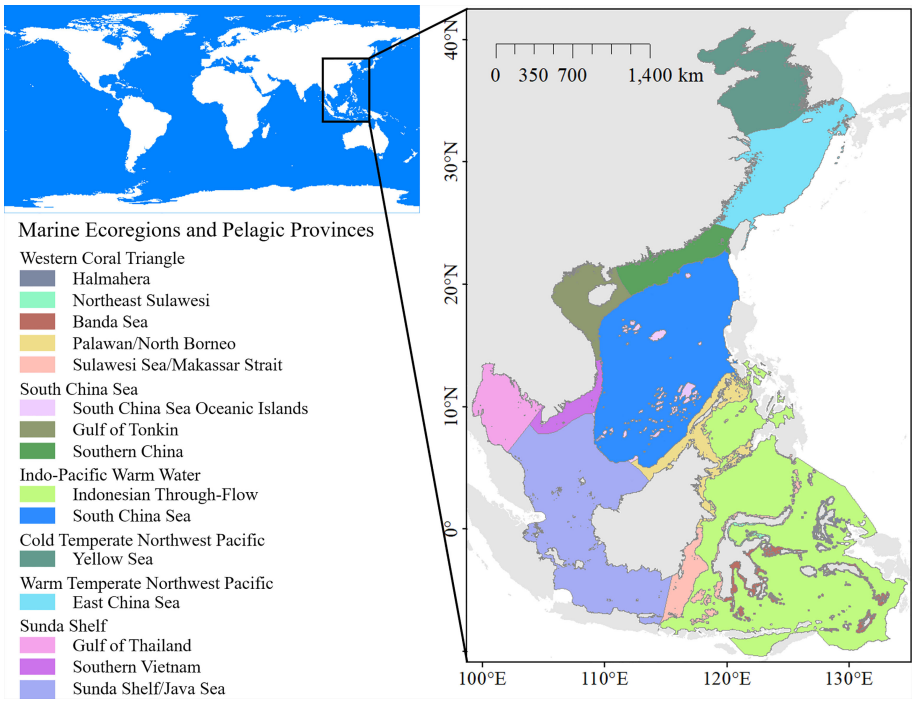


**FIGURE 1** | The study region, marine ecoregions, and the pelagic provinces.

shark occurrence records to the same density as the environmental dataset for SDM modeling.

Sharks are heterothermic animals and temperature has a considerable impact on their distribution (Birkmanis et al., 2020; Diaz-Carballido et al., 2022). Primary productivity is also an important factor that affects shark distribution and abundance (MacKenzie et al., 2019). Many studies have widely demonstrated the relationship between the primary productivity and fisheries catch (Pauly and Christensen, 1995; Watson et al., 2014), and primary productivity variability is significantly and positively correlated to the mean trophic level of catches (Conti and Scardi, 2010); therefore, the primary productivity is used in most SDMs (Gonzalez-Pestana et al., 2020; Chan et al., 2021). Other environmental variables like depth, dissolved oxygen, salinity, and offshore distance are often used in the study of marine shark distribution (Sequeira et al., 2014; Meyers et al., 2017; Chan et al., 2021; Pottie et al., 2021; González-Andrés et al., 2021). In the present study, eight environmental variables including SST, salinity, depth, distance from land, current velocity, primary productivity, dissolved oxygen concentration, and pH were selected as the model predictors. These factors were extracted from public datasets and products of Bio-Oracle and NOAA (**Table 1**). All the environmental variables were processed using ArcGIS 10.5 software, extracted from the boundary of the study area, and resampled to a grid cell size of 5 arcmin. To analyze the conservation gaps, a dataset of MPAs in the study region was extracted from the latest World Database on Protected Areas (UNEP-WCMC and IUCN, 2022).

## SDM Modeling

An ensemble model combining several SDM algorithms was used in this study to produce a distribution map for each shark species. The relationships between shark occurrence data and the eight environmental variables were estimated using five algorithms, namely GLM, generalized boosting model (GBM), random forest (RF), artificial neural network (ANN), and

**TABLE 1** | Environmental predictors used in the ensemble SDM.

| Variable | Units | Source |
|---|---|---|
| Mean temperature | °C | Bio-ORACLE data (Tyberghein et al., 2012; Assis et al., 2018) |
| Mean salinity | ‰ | |
| Bathymetry | m | ETOPO1 data from NOAA |
| Distance from land | m | Data from globalfishingwatch.org |
| Currents velocity | $m^{-1}$ | Bio-ORACLE data (Tyberghein et al., 2012; Assis et al., 2018) |
| Primary productivity | $g/m^3/day$ | |
| Dissolved oxygen | $mol/m^3$ | |
| pH | / | |

Maxent. These five models were fitted by their default parameters in the R environment using the *biomod2* package (Version 3.5.1, Thuiller et al., 2021). Each algorithm was run with 10 replicates, i.e., the predictions for each species were derived from 50 simulations. The predictive abilities of the models were evaluated using true skill statistics (TSS, Allouche et al., 2006), KAPPA, and the area under the receiver operating curve (AUC, Fourcade et al., 2018). Model outputs with a TSS value of ≥ 0.7 were used to ensure a good performance for the predicted results. An ensemble result was then generated for each species using the mean consensus method (Marmion et al., 2009; Crimmins et al., 2013).

## SCP Model Settings

As the most extensively used SCP software (Watts et al., 2009; Giménez et al., 2020), Marxan was used to set the priority areas for the study. A simulating annealing algorithm was used as an optimization method in Marxan to find a reserve network to reach the conservation target. One of the outputs of the Marxan analysis was identified as the best solution file, which was then run with the best objective value from all the good solutions produced by the model (Christodoulou et al., 2021). The study region was divided into planning units (PUs), which were used as candidate conservation units. We divided our study area into 0.25° fishnet units according to the scale of the study region, obtaining a total of 11,652 PUs.

Four conservation targets were set for the SCP model in this study (**Table 2**). The two scenarios were based on the CBD's Aichi Target 11, which states that at least 10% of coastal and marine areas were to be conserved through MPAs by 2020 (https://www. cbd. int/aichi-targets). Two additional scenarios were based on the 30% conservation target proposed by the World Parks Congress and the Kunming declaration (World Parks Congress, 2014; CBD/COP/15/5/Add.1, 2021). Diversity, scarcity (ETP species), and biogeographical distinctiveness (considering the representative across ecoregions) were also selected as targets to stratify the results by study region, so that they can act as coarse filters (Ardron et al., 2008; Levy and Ban, 2013). The boundary length modifier (BLM) was tested through a sensitivity analysis to control the compactness of the reserve solutions, using values of 0.002 and 0.1, representing dispersion and aggregation, respectively. The dispersion option allowed Marxan to select small clumps of PU across the study area; meanwhile, the aggregation option forced Marxan to select large clumps of PU. Each Marxan analysis was performed for 100 replicates, with a penalty factor of 100. All the operating procedures were performed in accordance with the Marxan user manual (Serra et al., 2020). The achievement of each conservation target was spatially calculated using the zonal statistics tool in ArcGIS 10.5.

# RESULTS

## Shark Diversity Distribution and Environmental Drivers

The accuracy test showed that all the models had excellent performance, with TSS, ROC, and KAPPA values between 0.79 and 0.99 (**Table 3**). The environmental variable importance showed that the distribution of 83.2% of species was predominantly influenced by bathymetry and 74.5% was influenced by dissolved oxygen (Supplementary Material). This suggests that bathymetry and dissolved oxygen are crucial variables contributing to the distribution of most sharks. A clear distribution pattern was observed by plotting the relationship between shark species richness and these two variables. The areas with a shark species richness greater than 50 were within the bathymetry at 0–200 m (**Figure 2A**), concentrated between the shoreline and continental shelf. A distinct unimodal pattern was observed in the relationship between the species richness and the dissolved oxygen. Dissolved oxygen concentration with a species richness greater than 25 was recorded between 200–250 mol/$m^3$, and the peak occurred at approximately 215 mol/$m^3$, with species richness exceeding 125 (**Figure 2B**).

The latitudinal distribution pattern of shark species richness showed a peak at 22–26°N (**Figure 3A**). This matched the hotspot of shark diversity in the Taiwan Strait, where shark species richness was as high as 90 to 130. In contrast, shark species richness decreased sharply from 35°N northward. Species richness varied considerably among the different marine ecoregions and the pelagic provinces (**Figure 3B**). The highest and lowest species richness was found in the Province of Temperate Northwest Pacific, where there were 144 species in the East China Sea and 68 species in the Yellow Sea. Shark species richness in tropical and subtropical ecoregions was similar, exceeding 110, except for the Northeast Sulawesi ecoregion.

**TABLE 2** | Four scenario settings used in the Marxan analysis.

| Scenarios | Ocean protected | Diversity protected | Scarcity protected | Regional representativeness | BLM value |
|---|---|---|---|---|---|
| Low target-small clump | 10% | 10% of the area with the highest 15% of species richness | 10% of the ETP species | 10% of each ecoregion | 0.002 |
| Low target-large clump | 10% | 10% of the area with the highest 15% of species richness | 10% of the ETP species | 10% of each ecoregion | 0.1 |
| High target-small clump | 30% | 10% of the area with the highest 45% of species richness | 30% of the ETP species | 30% of each ecoregion | 0.002 |
| High target-large clump | 30% | 10% of the area with the highest 45% of species richness | 30% of the ETP species | 30% of each ecoregion | 0.1 |

**TABLE 3** | TSS, ROC, and KAPPA values for the ensemble model.

| Statistical validation | Maximum | Minimum | Average | Standard deviation |
|---|---|---|---|---|
| TSS | 0.98 | 0.84 | 0.97 | 0.030 |
| ROC | 0.99 | 0.98 | 0.99 | 0.003 |
| KAPPA | 0.98 | 0.79 | 0.95 | 0.038 |

## Distribution Patterns of Different Orders and ETP Groups

The distribution of the different taxa varied substantially (**Figure 4**). The Carcharhiniformes had the highest species richness (79 species) and were the most widespread taxon with a distribution encompassing almost the entire coastline of the study area. The species richness of the Squaliformes was also high with 38 species, but the distribution range was concentrated in the East China Sea. The Pristiophoriformes had the lowest species richness and narrowest distribution range. The Orectolobiformes preferred lower latitudes than the other orders and were distributed within the latitudinal range of 0 ± 10°.

The distribution of ETP species was mapped according to their endangered status, and the results showed that the CR species were predominantly distributed to the south of 30°N, while EN and VU species have pronounced diversity hotspots in the Taiwan Strait (**Figure 5**). The distribution ranges of the different ETP species substantially varied (**Figure 6**). Among the 72 ETP species, the whale shark (*R. typus*) was the most widely distributed, with a predicted distribution range of 87,465 grid cells, followed by the bigeye thresher (*Alopias superciliosus*) with 68,315 grid cells, and the scalloped hammerhead (*Sphyrna lewini*) with 57,884 grid cells. The distribution of the blackspotted smooth-hound (*Mustelus punctulatus*) was the narrowest, with a predicted distribution range of 32 grid cells.

## Setting Conservation Priorities

The existing MPA network currently covers 2.1% of the ocean, with MPAs scattered along the coast and on islands. The patch size and dispersion of conservation priorities substantially differed among scenarios (**Figure 7**). Regarding the achievement of conservation goals, it was found that the existing MPAs (baseline scenario) protected only 32.9% of all species and 43.1% of the ETP species. The average protection range of ETP species was less than 5%, suggesting that there were large conservation gaps within the region (**Table 4**). The number of protected species and the distribution range substantially improved under the four scenarios. The number of protected species increased by 55 to 61, and the number of protected ETP species increased by 25 under low target scenarios. Under the high target scenarios, the number of protected species increased by 79, and the number of protected ETP species increased by 34 to 35. The conservation range of the ETP species was two to three times higher for the low target scenarios than for the baseline scenario. In contrast, it was five to eight times higher with the high target scenarios.

It is likely that low target scenarios are highly beneficial if only the number of protected species is considered. Approximately 10% of the prioritized areas could protect 69.8%–73.8% of all species and 77.8% of the ETP species. However, in the low target scenarios, 11–12% of the habitat range was protected, which is insufficient. In the high target scenarios, 30% of the prioritized areas could protect 85% of all species and more than 90% of the ETP species, and the average protected range of ETP species exceeded 30%. Therefore, 30% of the priority areas would considerably enhance conservation effectiveness. The large clump pattern had a slightly higher conservation achievement than the small clump pattern for similarly high conservation targets. However, we also observed that the priorities under large clump scenarios have various transboundary situations. This may not be conducive to the planning and coordination of conservation actions, resulting in further resistance and challenges in achieving conservation targets.

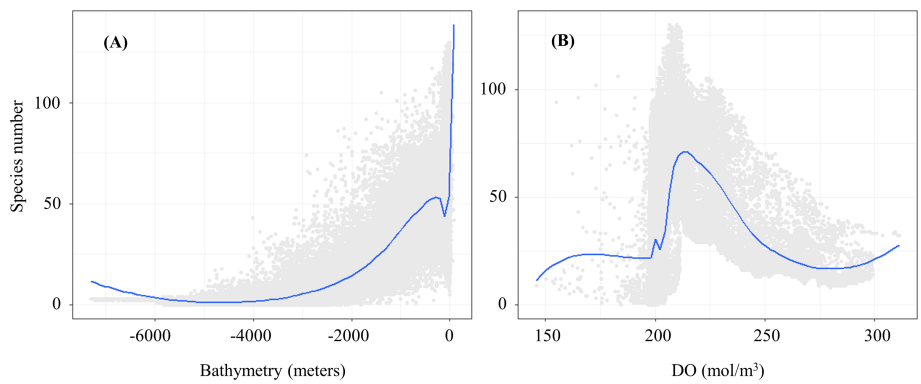


**FIGURE 2** | Response curves among species number and the key environmental drivers (A. Bathymetry; B. DO).

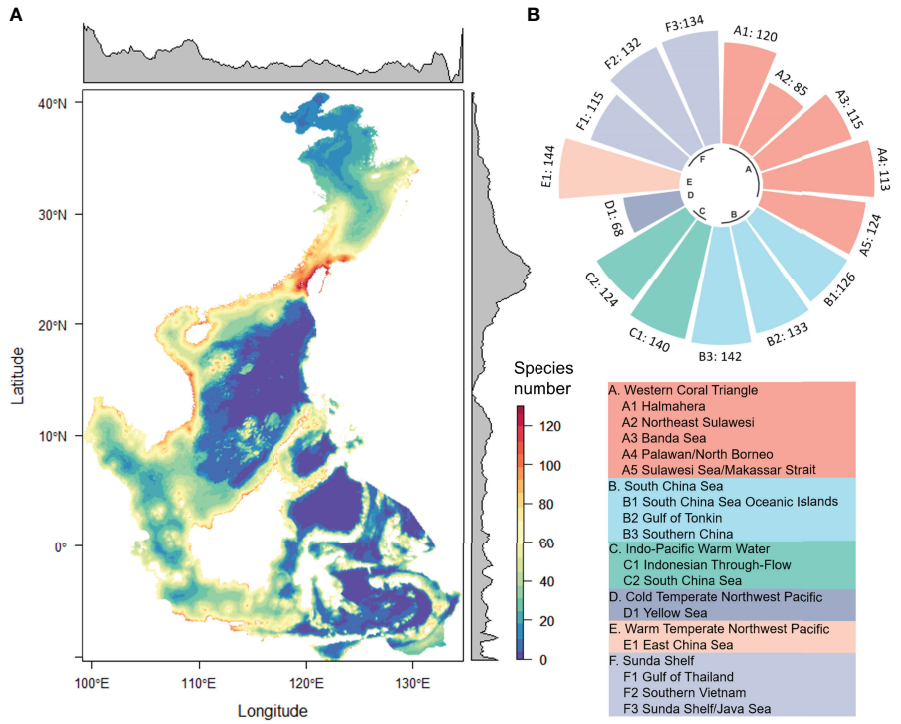


**FIGURE 3** | Species abundance distribution **(A)** and species number in each marine ecoregion and pelagic province **(B)**.

# DISCUSSION

## Environment Factors Affecting Shark Distribution

Shark distribution is affected by several key environmental variables. In the present study, bathymetry and dissolved oxygen were the most important factors contributing to the distribution of most sharks, which is consistent with the conclusions of other studies. Bathymetry is well known to strongly influence the distribution of sharks. Depth limits have been identified for many shark species. Shark species that are widely distributed also show regional variation in their depth limits (Lucifora et al., 2011). Depth was identified as the most important environmental variable for the distribution of whale sharks (*R. typus*), and shallower coastal waters with higher chlorophyll-a values off the coast of northern Peru were predicted to be suitable habitats (Gonzalez-Pestana et al., 2020). Bathymetry was also considered the main environmental variable for the distribution of the angelshark (*Squatina squatina*), which may be because of the importance of depth for diel vertical migration and reproductive activity (Noviello et al., 2021). We found that higher shark species richness was within 200 m (**Figure 2**), which has also been confirmed by other studies. Most of the 33 sharks and rays were caught at a depth of 40–120 m in the waters adjacent to the main islands and reefs of the South China Sea (Chen et al., 2006). There was an occurrence rate of 73.91% at a depth of 120–200 m in the southwestern sea of the Nansha Islands (Zhang et al., 2018), and there was a high probability of occurrence for hammerhead sharks at depths less than 50 m in the southern Gulf of Mexico (Chan et al., 2021).

Dissolved oxygen is a limiting factor for water-breathing animals (Pauly, 2021), and also has an impact on the distribution of sharks and their survival and growth during the early stages of ontogeny (Sims, 2019; Crear et al., 2020; Musa et al., 2020). Maximum dissolved oxygen is the second most important environmental factor for hammerhead sharks (Chan et al., 2021). Dissolved oxygen concentrations can limit the distribution of sharks, such as the shortfin mako (*Isurus oxyrinchus*) (Abascal et al., 2011), the great white shark (*C. carcharias*) (Nasby-Lucas et al., 2009), and bull sharks (*C. leucas*) (Heithaus et al., 2009). Other factors can also contribute to the distribution of sharks, such as the distance from land, current velocity, and primary productivity. Along the edge of the continental shelf, ocean currents can bring nutrient-rich seawater to the surface, and sharks, as the top predators, are attracted to these highly productive areas (Zhu, 1960; Baumgartner, 1998).

## Distribution Patterns and Diversity Hotspots for Sharks

Latitudinal patterns showed a distribution of high species richness between 30°N and 10°S in China and the ASEAN seas (**Figure 3**). This is in line with results from the previous global

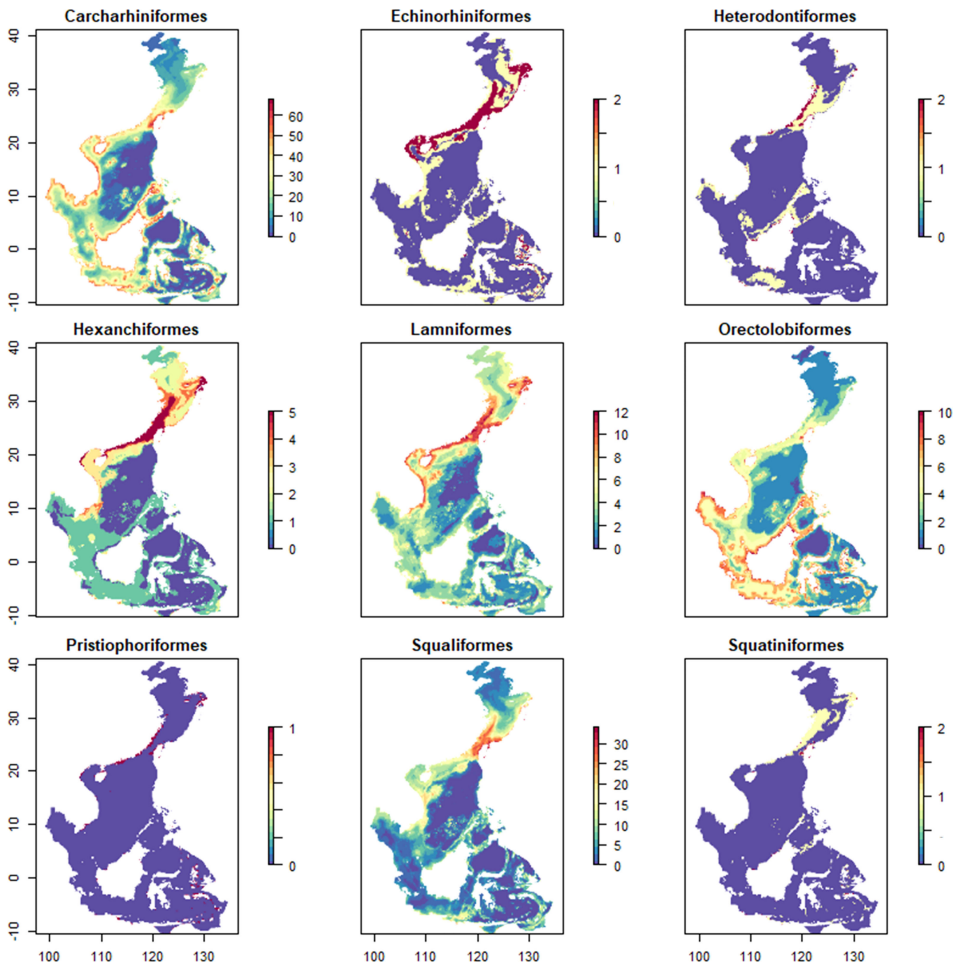


**FIGURE 4** | Species distribution of different orders.

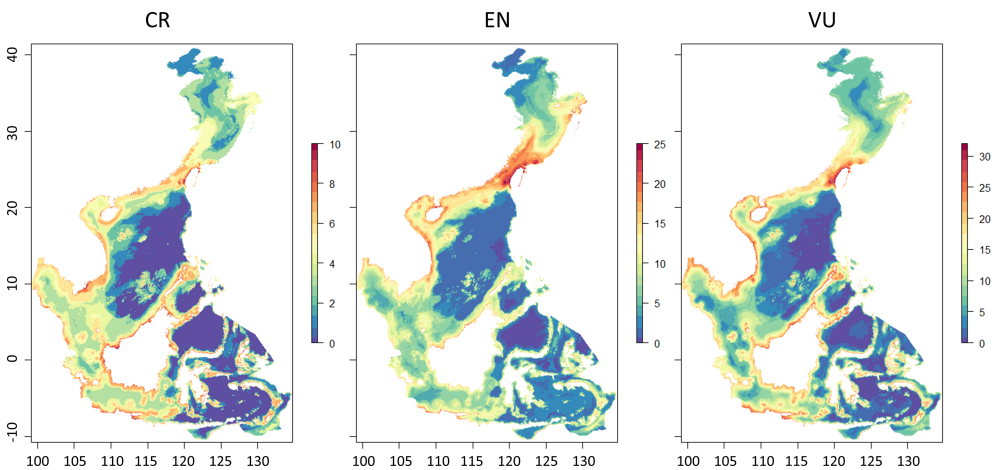


**FIGURE 5** | Species distribution of the different ETP groups.

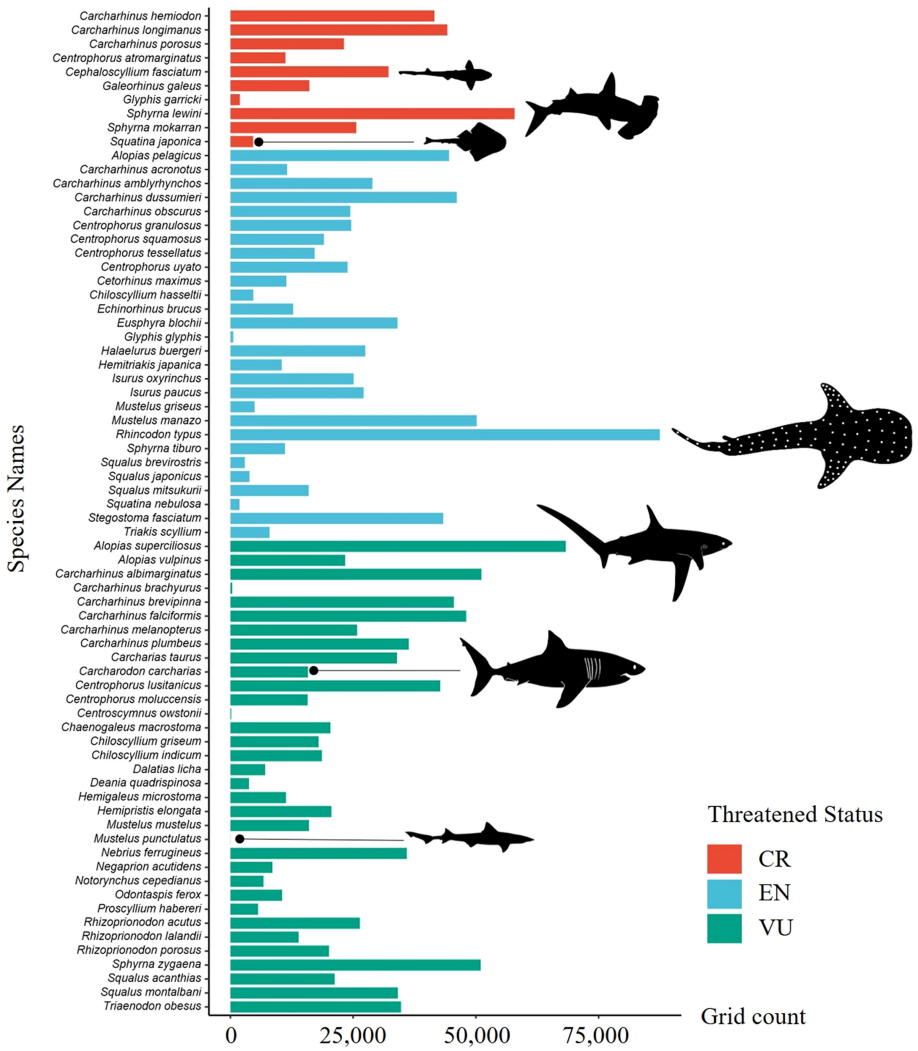


**FIGURE 6** | Potential distribution range of ETP species.

study undertaken between 30 and 40 degrees in both hemispheres (Lucifora et al., 2011; Kaschner et al., 2019). Shark species richness was found to be higher in continental ecoregions such as the East China Sea (144), Southern Vietnam (132), and the Sunda Shelf (134), and lower in deeper waters such as Northeast Sulawesi (85). This is consistent with prior results showing higher species richness on the continental shelves and slopes, and lower species richness in the open sea (Carpenter and Springer, 2005; Lucifora et al., 2011). In this study, the potential number of shark species in the Yellow Sea, East China Sea, and South China Sea were 68, 144, and 124, respectively (**Figure 3**), in line with historical records for these areas. In China, most shark species are found in tropical and subtropical areas (Zhu, 1958). There were 103 shark species recorded in the East China Sea, accounting for 77.4% of the shark species in China. The shark caught in the southern East China Sea was also the highest, accounting for approximately 44% of China's total shark catch (Zhang, 2005). There were 25 and 98 species recorded in the Bohai-Yellow Sea and the South China Sea, respectively (Zhang, 2003; Zhang and Yang, 2005).

The diversity hotspot was identified at 22–26°N around the Taiwan Strait. The shark species richness in this region was approximately 90–130. Globally, several studies have also highlighted that the hotspots for shark species richness were off the coastlines of Taiwan and Japan with up to 85 species. This was attributed to the mixing of temperate and tropical fauna (Carpenter and Springer, 2005; Lucifora et al., 2011). The spatial congruency of shark and ray species richness hotspots was low for all species, endemic species and evolutionarily distinct species. However, the congruency region includes Taiwan and parts of southern China (Derrick et al., 2020). The Taiwan Strait is at the transitional area between the East China Sea and the South China Sea, close to the Tropic of Cancer. It is strongly affected by currents including the Kuroshio tributaries, the

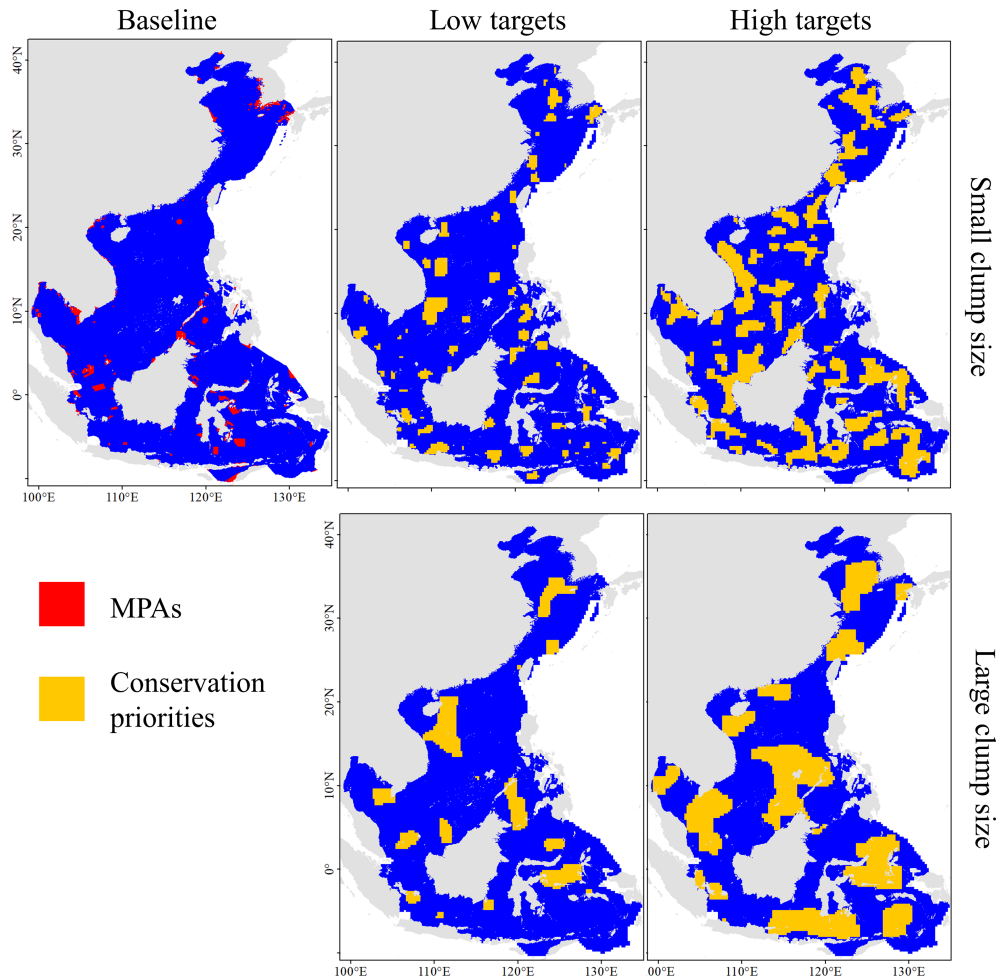


**FIGURE 7** | Best solutions for conservation priorities under different scenarios.

Taiwan Warm Current, the Zhejiang-Fujian Coastal Current, and the South China Sea Warm Current (Liu, 2008). Fish diversity in this area is high, with a total of 1,697 fish and 98 sharks recorded in and around the Taiwan Strait (Zhang and Yang, 2005; Chen et al., 2014). Fujian province is in the western Taiwan Strait and has a long history of using shark resources. Fishermen in coastal counties often catch sharks, and 21 shark species were recorded there approximately 100 years ago (Wu, 1929; Tang, 1936; Qiu, 1954). As early as the 1950s, Fujian had more than 100 longline shark fishing boats (Lin, 1995; Zhang, 2005). Therefore, historical records are in line with the results of the present study in identifying the hotspots of the Taiwan Strait. Shark species richness is lower in the Northeast Sulawesi ecoregion than in tropical areas such as the Banda Sea. These differences may be because of the different habitat requirements of sharks and the unique ecological environmental conditions of each ecoregion (Lucifora et al., 2011).

Most of the shark orders and ETP species were distributed along the coast of the study area. The hotspot was located off the Taiwan Strait, similar to the distribution pattern of all the shark species. The Carcharhiniformes were the largest shark group in this study and were predominantly distributed on the tropical continental shelf (**Figure 4**). The Carcharhinidae have been identified as the most diverse group in the southern South China Sea based on landing data (Arai and Azri, 2019). The Carcharhinidae and Sphyrnidae represented 77.1% and 21.7% of the fins identified in the Hong Kong markets, respectively (Cardeñosa et al., 2020). Carcharhinidae also has been shown to have the highest shark diversity in Thailand (30 species; 34.9%), followed by Scyliorhinidae (8 species; 9.3%) (Krajangdara, 2019). Globally, the main hotspots for threatened and endemic sharks and rays are in the South and East China Sea, coastal southeast South America, and off the coast of eastern Australia (Davidson and Dulvy, 2017; Stein et al., 2018). Sharks in developing countries are at a high risk of overfishing, and there is a disproportionate level of threat for more than three-fourths of coastal species in the tropics and subtropics (Dulvy et al., 2021). There is a large overlap between

**TABLE 4** | Conservation target achievements for different scenarios.

| Scenarios | OceanProtected (%) | Diversity | | Scarcity | | | Regional representativeness |
|---|---|---|---|---|---|---|---|
| | | Number of species | Number of ETP species | Average protection range of CR species (%) | Average protection range of EN species (%) | Average protection range of VU species (%) | Ecoregion Protected-average (%) |
| Baseline | 2.1% | 49 | 31 | 4.9% | 4.0% | 5.0% | 5.5% |
| Low target-small clump | 10.1% | 110 | 56 | 11.7% | 12.4% | 12.0% | 10.3% |
| Low target-large clump | 10.9% | 104 | 56 | 11.5% | 12.3% | 11.9% | 13.0% |
| High target-small clump | 30.3% | 128 | 65 | 32.5% | 33.2% | 33.1% | 31.0% |
| High target-large clump | 32.0% | 128 | 66 | 32.8% | 33.7% | 33.8% | 36.7% |

the shark hotspots and global fishing efforts (Queiroz et al., 2019). The spawning, nursery, and feeding grounds of most sharks often overlap with the fishing grounds in the southern South China Sea (Arai and Azri, 2019). Shark fishing efforts have also been concentrated within exclusive economic zones, mostly in coastal areas in Indonesia and Japan (Van Houtan et al., 2020). The shark fin trade is a considerable source of mortality for many threatened species. Therefore, enhanced international trade regulations for these threatened species are still a conservation priority (Cardeñosa et al., 2020).

The distribution range of each species was found to vary substantially (**Figure 6**). The potential distribution of the whale shark (*R. typus*) was the most extensive in the present study area. The whale shark is a filter-feeding shark with global distribution in tropical and warm temperate regions that fed on zooplankton (Pierce and Norman, 2016; Gonzalez-Pestana et al., 2020). The scalloped hammerhead (*S. lewini*) is also distributed in warm temperate and tropical seas and frequently occurs in the southern South China Sea and the southern Gulf of Mexico. It is the most dominant species in the Sarawak state in East Malaysia (Arai and Azri, 2019; Chan et al., 2021). In contrast, the distribution of the Japanese angelshark (*S. japonica*) was found to be narrow in the present study. This is consistent with the description that it is endemic to the Northwest Pacific Ocean, occurring from southern Russia to southern Taiwan (Walls et al., 2021).

## Conservation Priorities and Uncertainty

Determining where conservation efforts should focus on providing adequate protection is highly important to reduce the risk of extinction for threatened species. At present, 7.93% of the ocean is protected globally (UNEP-WCMC and IUCN, 2022), whereas the existing MPA network in China and the ASEAN protects 2.1% of the ocean (**Table 4**), with less than half of the species being protected in the MPAs. Although awareness of the ecological role and vulnerability of sharks has led to increased conservation attention, only a small number of MPAs have been designated to protect them (Giménez et al., 2020). The majority of these shark sanctuaries are in Palau, the Maldives, the Caribbean, and the Netherlands (Ward-Paige and Worm, 2017), while there are almost no shark MPAs around diversity hotspots in the China and ASEAN seas. Therefore, there is a substantial conservation gap for sharks in the study area.

To sustainably manage and protect coastal and marine biodiversity, international organizations have proposed global marine conservation targets ranging from 10% to 50% (CBD/COP/DEC/X/2, 2010; CBD/COP/15/5/Add.1; World Parks Congress, 2014; Sala et al., 2021). One study suggested that the top 30% of MPAs should be prioritized for marine biodiversity conservation (Zhao et al., 2020), while another found that at least 40% of the seas are required to protect threatened marine species and biodiversity (Jefferson et al., 2021). However, there are complex conservation efficiency and trade-offs in the siting of conservation priority areas. There is a nonlinear relationship between the conservation target distribution and conservation costs. In the present study, the number of protected species increased by only approximately 15% (from 73.8 to 85%) when the global protected area coverage increased by 200% (from 10% to 30%), whereas the protected range of ETP species increased by 170% (from 11% to 30%). This indicates that low conservation targets only improved the number of protected species, and high targets were both better for the number of protected species and the protected range of the ETP species (**Table 4**). Some studies also highlighted a marginal decrease in conservation efficiency. Under the cheapest cost scenario, the number of protected species increased by 6% when global terrestrial protected area coverage increased by 30%. The number of protected species can be substantially increased if costs are appropriately increased (Venter et al., 2014). Furthermore, tight clumping results in fewer but larger selected areas, resulting in a reduced boundary effect, leading to a slightly higher conservation achievement than a small clump (Serra et al., 2020; Christodoulou et al., 2021). Therefore, the high target scenario with large clumps was the most desirable among several protection scenarios. However, conservation within EEZs and transboundaries should be considered when identifying conservation priority areas. Zoning strategies are the most cost-effective conservation approaches that can enhance the protection of marine biodiversity and are more likely to gain stakeholder support (Giménez et al., 2020). Conservation priority areas located within

EEZs can be protected by the countries involved, whereas transboundary conservation requires more effort for communication and collaboration among stakeholders (Friedman et al., 2018; Mason et al., 2020). Many shark species are migratory and each shark species is found in the waters of eight countries on average. The blue shark was found to span the waters of 145 countries (Dulvy et al., 2017). From a global perspective, the management of shark conservation priority areas requires joint participation from relevant countries (Jorgensen et al., 2022).

The present study investigated diversity distribution patterns and conservation priorities for sharks in the China and the ASEAN seas based on 149 species owing to data availability. However, according to historical records, there are approximately 196 shark species in this area. Habitat descriptions of the missing 47 species can only be found in the literature and through expert knowledge without enough occurrence records (Lucifora et al., 2011). The lack of reliable distribution information hinders the comprehensive mapping work. Furthermore, anthropogenic activities and climate change factors, which have been added to the SCP as cost layers in recent studies, were not included in this study (Stein et al., 2018; Arafeh-Dalmau et al., 2021). This study was a preliminary attempt to understand the diversity hotspots and conservation priority areas for sharks in the China and ASEAN seas. Future studies should further evaluate spatial and temporal distribution patterns under anthropogenic drivers and climate change.

## CONCLUSIONS

This study revealed spatial diversity patterns and conservation priority areas for 149 shark species in the China and ASEAN seas. While the results showed that the distribution pattern of shark species richness peaked on the continental shelves and a hotspot for shark diversity was found around the Taiwan Strait, there was a substantial conservation gap identified in the study region. Identifying conservation priority areas under different target scenarios would provide a scientific basis for shark conservation and management.

## DATA AVAILABILITY STATEMENT

The original contributions presented in the study are included in the article/**Supplementary Material**. Further inquiries can be directed to the corresponding authors.

## AUTHOR CONTRIBUTIONS

JD: Conceptualization, Funding acquisition, methodology, software, writing. WH: Conceptualization, funding acquisition, methodology, writing, supervision. LD: Formal analysis, data curation, writing. ShS: Formal analysis, data curation, software. YW: Data curation, software. K-HL: Data curation, software. SY: Data curation. MC: Data curation. KR: Data curation. SeS: Data curation. ZL: Data curation, Funding acquisition. BC: Resources, funding acquisition, supervision. All authors contributed to the article and approved the submitted version.

## FUNDING

This work was financially supported by the National Natural Science Foundation of China (grant numbers 42176153, 41906127), the China-ASEAN Maritime Cooperation Fund "Marine Protected Areas Network in China-ASEAN Countries", the China-Indonesia Maritime Cooperation Fund "Development of Indonesia-China Center for Ocean & Climate", the National Program on Global Change and Air-Sea Interaction (grant number HR01-200701), and partly provided by TIO-UM Cooperation Fund "Diversity and Community Structure of Fishes in Malaysian Water" (grant number IF004-2022).

## SUPPLEMENTARY MATERIAL

The Supplementary Material for this article can be found online at: https://www.frontiersin.org/articles/10.3389/fmars.2022.933291/full#supplementary-material

## REFERENCES

Abascal, F. J., Quintans, M., Ramos-Cartelle, A., and Mejuto, J. (2011). Movements and Environmental Preferences of the Shortfin Mako, *Isurus Oxyrinchus*, in the Southeastern Pacific Ocean. *Mar. Biol.* 158, 1175–1184. doi: 10.1007/s00227-011-1639-1

Ali, A. B., Fahmi, F., Dharmadi, D., Krajangdara, T., and Khiok, A. L. P. (2018). Biodiversity and Habitat Preferences of Living Sharks in the Southeast Asian Region. *Indones. Fish. Res. J.* 24, 133–140. doi: 10.15578/ifrj.24.2.2018.133-140

Allouche, O., Tsoar, A., and Kadmon, R. (2006). Assessing the Accuracy of Species Distribution Models: Prevalence, Kappa and the True Skill Statistic (TSS). *J. Appl. Ecol.* 43, 1223–1232. doi: 10.2307/4123815

Arafeh-Dalmau, N., Brito-Morales, I., Schoeman, D. S., Possingham, H. P., Klein, C. J., and Richardson, A. J. (2021). Incorporating Climate Velocity Into the Design of Climate-Smart Networks of Marine Protected Areas. *Methods Ecol. Evol.* 12, 1969–1983. doi: 10.1111/2041-210X.13675

Arai, T., and Azri, A. (2019). Diversity, Occurrence and Conservation of Sharks in the Southern South China Sea. *PloS One* 14, e0213864. doi: 10.1371/journal.pone.0213864

Ardron, J. A., Possingham, H. P., and Klein, C. J. (2008). *Marxan Good Practices Handbook. Pacific Marine Analysis and Research Association* (Vancouver: Pacific Marine Analysis and Research Association), 149.

Assis, J., Tyberghein, L., Bosh, S., Verbruggen, H., Serrao, E. A., and De Clerck, O. (2018). Bio-ORACLE V2.0: Extending Marine Data Layers for Bioclimatic Modelling. *Glob. Ecol. Biogeogr.* 27, 277–284. doi: 10.1111/geb.12693

Austin, R. A., Hawkes, L. A., Doherty, P. D., Henderson, S. M., Inger, R., Johnson, L., et al (2019). Predicting Habitat Suitability for Basking Sharks (*Cetorhinus Maximus*) in UK Waters Using Ensemble Ecological Niche Modelling. *J. Sea Res.* 153, 101767. doi: 10.1016/j.seares.2019.101767

Baumgartner, M. F. (1998). The Distribution of Risso's Dolphin (*Grampus Griseus*) With Respect to the Physiography of the Northern Gulf of Mexico. *Oceanogr. Lit. Rev.* 1, 124. doi: 10.1111/j.1748-7692.1997.tb00087.x

Birkmanis, C. A., Freer, J. J., Simmons, L. W., Partridge, J. C., and Sequeira, A. M. (2020). Future Distribution of Suitable Habitat for Pelagic Sharks in Australia Under Climate Change Models. *Front. Mar. Sci.* 570. doi: 10.3389/fmars.2020.00570

Cardeñosa, D., Shea, K. H., Zhang, H., Feldheim, K., Fischer, G. A., and Chapman, D. D. (2020). Small Fins, Large Trade: A Snapshot of the Species Composition of Low-Value Shark Fins in the Hong Kong Markets. *Anim. Conserv.* 23, 203–211. doi: 10.1111/acv.12529

Carpenter, K. E., and Springer, V. G. (2005). The Center of the Center of Marine Shore Fish Biodiversity: The Philippine Islands. *Environ. Biol. Fishes* 72, 467–480. doi: 10.1007/s10641-004-3154-4

CBD/COP/15/5/Add.1 (2021). Available at: https://www.cbd.int/doc/c/c2db/972a/fb32e0a277bf1ccfff742be5/cop-15-05-add1-en.pdf.

Chamberlain, S. (2022) *Scrubr: Clean Biological Occurrence Records*. Available at: https://github.com/ropensci/scrubrhttps://docs.ropensci.org/scrubr/(docs).

Chamberlain, S., Ram, K., and Hart, T. (2014) *Spocc: R Interface to Many Species Occurrence Data Sources. R Package Version 0.1.0*. Available at: https://github.com/ropensci/spocc.

Chan, M. Y. C., Sosa-Nishizaki, O., and Pérez-Jiménez, J. C. (2021). Potential Distribution of Critically Endangered Hammerhead Sharks and Overlap With the Small-Scale Fishing Fleet in the Southern Gulf of Mexico. *Reg. Stud. Mar. Sci.* 46, 101900. doi: 10.1016/j.rsma.2021.101900

Chen, G., Li, Y., Chen, X., and Shu, L. (2006). Composition and Distribution of Cartilaginous Fishes in the Adjacent Waters Area of Main Islands and Reefs of South China Sea. *J. Shanghai Ocean Univ.* 15, 461–467. doi: 10.3969/j.issn.1004-7271.2006.04.014

Chen, Y., Zhang, J., Song, P., Zhang, R., Li, Y., Zhong, Z., et al (2014). Composition of the Taiwan Strait Fish Fauna. *Biodivers. Sci.* 22, 525. doi: 10.3724/SP.J.1003.2014.14001

Christodoulou, C. S., Griffiths, G. H., and Vogiatzakis, I. N. (2021). Systematic Conservation Planning in a Mediterranean Island Context: The Example of Cyprus. *Glob. Ecol. Conserv.* 32, e01907. doi: 10.1016/j.gecco.2021.e01907

Compagno, L. J., Dando, M., and Fowler, S. (2005). *Sharks of the World* (New Jersy: Princeton University Press), 496 pp.

Conti, L., and Scardi, M. (2010). Fisheries Yield and Primary Productivity in Large Marine Ecosystems. *Mar. Ecol. Prog. Ser.* 410, 233–244. doi: 10.3354/meps08630

Crear, D. P., Latour, R. J., Friedrichs, M. A., St-Laurent, P., and Weng, K. C. (2020). Sensitivity of a Shark Nursery Habitat to a Changing Climate. *Mar. Ecol. Prog. Ser.* 652, 123–136. doi: 10.3354/meps13483

Crimmins, S. M., Dobrowski, S. Z., and Mynsberge, A. R. (2013). Evaluating Ensemble Forecasts of Plant Species Distributions Under Climate Change. *Ecol. Modell.* 266, 126–130. doi: 10.1016/j.ecolmodel.2013.07.006

Cuesta, F., Peralvo, M., Merino-Viteri, A., Bustamante, M., Baquero, F., Freile, J. F., et al (2017). Priority Areas for Biodiversity Conservation in Mainland Ecuador. *Neotrop. Biodivers.* 3, 93–106. doi: 10.1080/23766808.2017.1295705

Davidson, L. N., and Dulvy, N. K. (2017). Global Marine Protected Areas to Prevent Extinctions. *Nat. Ecol. Evol.* 1, 1–6. doi: 10.1038/s41559-016-0040

Derrick, D. H., Cheok, J., and Dulvy, N. K. (2020). Spatially Congruent Sites of Importance for Global Shark and Ray Biodiversity. *PloS One* 15, e0235559. doi: 10.1371/journal.pone.0235559

Diaz-Carballido, P. L., Mendoza-González, G., Alberto Yáñez-Arenas, C., and Chiappa-Carrara, X. (2022). Evaluation of Shifts in the Potential Future Distributions of Carcharhinid Sharks Under Different Climate Change Scenarios. *Front. Mar. Sci.* 2039. doi: 10.3389/fmars.2021.745501

Dulvy, N. K., Fowler, S. L., Musick, J. A., Cavanagh, R. D., Kyne, P. M., Harrison, L. R, et al (2014). Extinction Risk and Conservation of the World's Sharks and Rays. *eLife* 3, e00590. doi: 10.7554/eLife.00590

Dulvy, N. K., Pacoureau, N., Rigby, C. L., Pollom, R. A., Jabado, R. W., Ebert, D. A., et al (2021). Overfishing Drives Over One-Third of All Sharks and Rays Toward a Global Extinction Crisis. *Curr. Biol.* 31, 4773–4787.e8. doi: 10.1016/j.cub.2021.08.062

Dulvy, N. K., Simpfendorfer, C. A., Davidson, L. N. K., Fordham, S. V., Bräutigam, A., Sant, G, et al (2017). Challenges and Priorities in Shark and Ray Conservation. *Curr. Biol.* 27, 565–572. doi: 10.1016/j.cub.2017.04.038

Dureuil, M., Boerder, K., Burnett, K. A., Froese, R., and Worm, B. (2018). Elevated Trawling Inside Protected Areas Undermines Conservation Outcomes in a Global Fishing Hot Spot. *Science* 362, 1403–1407. doi: 10.1126/science.aau0561

Espinoza, M., Araya-Arce, T., Chaves-Zamora, I., Chinchilla, I., and Cambra, M. (2020). Monitoring Elasmobranch Assemblages in a Data-Poor Country From the Eastern Tropical Pacific Using Baited Remote Underwater Video Stations. *Sci. Rep.* 10, 1–18. doi: 10.1038/s41598-020-74282-8

Ferretti, F., Myers, R. A., Serena, F., and Lotze, H. K. (2008). Loss of Large Predatory Sharks From the Mediterranean Sea. *Conserv. Biol.* 22, 952–964. doi: 10.1111/j.1523-1739.2008.00938.x

Fourcade, Y., Besnard, A. G., and Secondi, J. (2018). Paintings Predict the Distribution of Species, or the Challenge of Selecting Environmental Predictors and Evaluation Statistics. *Glob. Ecol. Biogeogr.* 27, 245–256. doi: 10.1111/geb.12684

Friedman, K., Gabriel, S., Abe, O., Adnan Nuruddin, A., Ali, A., Bidin Raja Hassan, R., et al (2018). Examining the Impact of CITES Listing of Sharks and Rays in Southeast Asian Fisheries. *Fish Fish.* 19, 662–676. doi: 10.1111/faf.12281

Froese, R., and Pauly, D. (2022). *FishBase* (World Wide Web electronic publication). Available at: www.fishbase.org.

Garzon, F., Graham, R. T., Witt, M. J., and Hawkes, L. A. (2021). Ecological Niche Modeling Reveals Manta Ray Distribution and Conservation Priority Areas in the Western Central Atlantic. *Anim. Conserv.* 24, 322–334. doi: 10.1111/acv.12663

Giménez, J., Cardador, L., Mazor, T., Kark, S., Bellido, J. M., Coll, M., et al (2020). Marine Protected Areas for Demersal Elasmobranchs in Highly Exploited Mediterranean Ecosystems. *Mar. Environ. Res.* 160, 105033. doi: 10.1016/j.marenvres.2020.105033

González-Andrés, C., Sánchez-Lizaso, J. L., Cortés, J., and Pennino, M. G. (2021). Predictive Habitat Suitability Models to Aid the Conservation of Elasmobranchs in Isla Del Coco National Park (Costa Rica). *J. Mar. Syst.* 224, 103643. doi: 10.1016/j.jmarsys.2021.103643

Gonzalez-Pestana, A., Maguiño, R., Mendoza, A., Kelez, S., and Ramírez-Macías, D. (2020). Distribution of Whale Shark (*Rhincodon Typus*) Off Northern Peru Based on Habitat Suitability. *Aquat. Conserv.: Mar. Freshw. Ecosyst.* 30, 1325–1336. doi: 10.1002/aqc.3330

Heithaus, M. R., Delius, B. K., Wirsing, A. J., and Dunphy-Daly, M. M. (2009). Physical Factors Influencing the Distribution of a Top Predator in a Subtropical Oligotrophic Estuary. *Limnol. Oceanogr.* 54, 472–482. doi: 10.4319/lo.2009.54.2.0472

IUCN (2022) *The IUCN Red List of Threatened Species*. Available at: https://www.iucnredlist.org.

Jefferson, T., Costello, M. J., Zhao, Q., and Lundquist, C. J. (2021). Conserving Threatened Marine Species and Biodiversity Requires 40% Ocean Protection. *Biol. Conserv.* 264, 109368. doi: 10.1016/j.biocon.2021.109368

Jellinek, S. (2017). Using Prioritisation Tools to Strategically Restore Vegetation Communities in Fragmented Agricultural Landscapes. *Ecol. Manage. Restor.* 18, 45–53. doi: 10.1111/emr.12224

Jorgensen, S. J., Micheli, F., White, T. D., Van Houtan, K. S., Alfaro-Shigueto, J., Andrzejaczek, S., et al (2022). Emergent Research and Priorities for Shark and Ray Conservation. *Endanger. Species Res.* 47, 171–203. doi: 10.3354/esr01169

Kai, M., Thorson, J. T., Piner, K. R., and Maunder, M. N. (2017). Predicting the Spatio-Temporal Distributions of Pelagic Sharks in the Western and Central North Pacific. *Fish. Oceanogr.* 26, 569–582. doi: 10.1111/fog.12217

Kaschner, K., Kesner-Reyes, K., Garilao, C., Segschneider, J., Rius-Barile, J., Rees, T., et al (2019) *AquaMaps: Predicted Range Maps for Aquatic Species*. Available at: https://www.aquamaps.org.

Krajangdara, T. (2019). *Sharks and Rays of Thailand* (Thailand: Department of Fisheries).

Lam, V. Y., and Sadovy de Mitcheson, Y. (2011). The Sharks of South East Asia–unknown, Unmonitored and Unmanaged. *Fish Fish.* 12, 51–74. doi: 10.1111/j.1467-2979.2010.00383.x

Last, P. R., White, W. T., Caira, J. N., Jensen, K., Lim, A. P., Manjaji-Matsumoto, B. M., et al (2010). *Sharks and Rays of Borneo*. (Collingwood, Australia: Csiro publishing)

Levy, J. S., and Ban, N. C. (2013). A Method for Incorporating Climate Change Modelling Into Marine Conservation Planning: An Indo-West Pacific Example. *Mar. Policy* 38, 16–24. doi: 10.1016/j.marpol.2012.05.015

Li, Y., Jia, X., and Chen, G. (2007). *Coral Reef Fish Resources in the South China Sea* (Beijing: Ocean Press).

Lin, C. (1995). Shark Resources and Their Exploitation in Fujian. *Fujian Fish.* 2, 38–41. doi: 10.14012/j.cnki.fjsc.1995.02.022

Liu, R. (2008). *List of Marine Organisms in China* (Beijing: Science Press).

Liu, R. (2011). Progress of Marine Biodiversity Studies in China Seas. *Biodivers. Sci.* 19, 614. doi: 10.3724/SP.J.1003.2011.13185

Lucifora, L. O., García, V. B., and Worm, B. (2011). Global Diversity Hotspots and Conservation Priorities for Sharks. *PloS One* 6, e19356. doi: 10.1371/journal.pone.0019356

MacKenzie, K. M., Robertson, D. R., Adams, J. N., Altieri, A. H., and Turner, B. L. (2019). Structure and Nutrient Transfer in a Tropical Pelagic Upwelling Food Web: From Isoscapes to the Whole Ecosystem. *Prog. Oceanogr.* 178, 102145. doi: 10.1016/j.pocean.2019.102145

MacNeil, M. A., Chapman, D. D., Heupel, M., Simpfendorfer, C. A., Heithaus, M., Meekan, M., et al (2020). Global Status and Conservation Potential of Reef Sharks. *Nature* 583, 801–806. doi: 10.1038/s41586-020-2519-y

Margules, C. R., and Pressey, R. L. (2000). Systematic Conservation Planning. *Nature* 405, 243–253. doi: 10.1038/35012251

Marmion, M., Parviainen, M., Luoto, M., Heikkinen, R. K., and Thuiller, W. (2009). Evaluation of Consensus Methods in Predictive Species Distribution Modelling. *Diversity Distrib.* 15, 59–69. doi: 10.1111/j.1472-4642.2008.00491.x

Mason, N., Ward, M., Watson, J. E., Venter, O., and Runting, R. K. (2020). Global Opportunities and Challenges for Transboundary Conservation. *Nat. Ecol. Evol.* 4, 694–701. doi: 10.1038/s41559-020-1160-3

Melo-Merino, S. M., Reyes-Bonilla, H., and Lira-Noriega, A. (2020). Ecological Niche Models and Species Distribution Models in Marine Environments: A Literature Review and Spatial Analysis of Evidence. *Ecol. Modell.* 415, 108837. doi: 10.1016/j.ecolmodel.2019.108837

Meyers, E. K., Tuya, F., Barker, J., Jiménez Alvarado, D., Castro-Hernández, J. J., Haroun, R., et al (2017). Population Structure, Distribution and Habitat Use of the Critically Endangered Angelshark, *Squatina Squatina*, in the Canary Islands. *Aquat. Conserv.: Mar. Freshw. Ecosyst.* 27, 1133–1144. doi: 10.1002/aqc.2769

Musa, S. M., Ripley, D. M., Moritz, T., and Shiels, H. A. (2020). Ocean Warming and Hypoxia Affect Embryonic Growth, Fitness and Survival of Small-Spotted Catsharks, *Scyliorhinus Canicula*. *J. Fish Biol.* 97, 257–264. doi: 10.1111/jfb.14370

Nasby-Lucas, N., Dewar, H., Lam, C. H., Goldman, K. J., and Domeier, M. L. (2009). White Shark Offshore Habitat: A Behavioral and Environmental Characterization of the Eastern Pacific Shared Offshore Foraging Area. *PloS One* 4, e8163. doi: 10.1371/journal.pone.0008163

Noviello, N., McGonigle, C., Jacoby, D. M., Meyers, E. K., Jiménez-Alvarado, D., and Barker, J. (2021). Modelling Critically Endangered Marine Species: Bias-Corrected Citizen Science Data Inform Habitat Suitability for the Angelshark (*Squatina Squatina*). *Aquat. Conserv.: Mar. Freshw. Ecosyst.* 31, 3451–3465. doi: 10.1002/aqc.3711

Pacoureau, N., Rigby, C. L., Kyne, P. M., Sherley, R. B., Winker, H., Carlson, J. K., et al (2021). Half a Century of Global Decline in Oceanic Sharks and Rays. *Nature* 589, 567–571. doi: 10.1038/s41586-020-03173-9

Pauly, D. (2021). The Gill-Oxygen Limitation Theory (GOLT) and its Critics. *Sci. Adv.* 7, eabc6050. doi: 10.1126/sciadv.abc6050

Pauly, D., and Christensen, V. (1995). Primary Production Required to Sustain Global Fisheries. *Nature* 376, 279. doi: 10.1038/376279b0

Pierce, S. J., and Norman, B. (2016). *Rhincodon Typus* Vol. 2016 (The IUCN Red List of Threatened Species), e.T19488A2365291.

Pimiento, C., Leprieur, F., Silvestro, D., Lefcheck, J. S., Albouy, C., Rasher, D. B., et al (2020). Functional Diversity of Marine Megafauna in the Anthropocene. *Sci. Adv.* 6, eaay7650. doi: 10.1126/sciadv.aay7650

Pottie, S., Flam, A. L., Keeping, J. A., Chivindze, C., and Bull, J. C. (2021). Quantifying the Distribution and Site Fidelity of a Rare, non-Commercial Elasmobranch Using Local Ecological Knowledge. *Ocean Coast. Manag.* 212, 105796. doi: 10.1016/j.ocecoaman.2021.105796

Prasetyo, A. P., McDevitt, A. D., Murray, J. M., Barry, J., Agung, F., Muttaqin, E., et al (2021). Shark and Ray Trade in and Out of Indonesia: Addressing Knowledge Gaps on the Path to Sustainability. *Mar. Policy* 133, 104714. doi: 10.1016/j.marpol.2021.104714

Qiu, S. (1954). Studies on the Sharks of Xiamen (II) Classification. *J. Xiamen Univ. (Nat. Sci. Edition)* 3, 30–49.

Queiroz, N., Humphries, N. E., Couto, A., Vedor, M., da Costa, I., Sequeira, A. M.M., et al. (2019). Global spatial Risk Assessment of Sharks Under the Footprint of Fisheries. *Nature* 572 (7770), 461–466. doi: 10.1038/s41586-019-1444-4

Rigby, C. L., Walls, R., Derrick, D., Dyldin, Y. V., and Yamaguchi, A. (2021). *Squatina Nebulosa* (The IUCN Red List of Threatened Species).

Sala, E., Mayorga, J., Bradley, D., Cabral, R. B., Atwood, T. B., Auber, A., et al (2021). Protecting the Global Ocean for Biodiversity, Food and Climate. *Nature* 592, 397–402. doi: 10.1038/s41586-021-03371-z

Segurado, P., and Araujo, M. B. (2004). An Evaluation of Methods for Modelling Species Distributions. *J. Biogeogr.* 31, 1555–1568. doi: 10.1111/j.1365-2699.2004.01076.x

Sequeira, A. M., Mellin, C., Fordham, D. A., Meekan, M. G., and Bradshaw, C. J. (2014). Predicting Current and Future Global Distributions of Whale Sharks. *Glob. Change Biol.* 20, 778–789. doi: 10.1111/gcb.12343

Serra, N., Kockel, A., Game, E. T., Grantham, H., Possingham, H. P., and McGowan, J. (2020). *Marxan User Manual: For Marxan Version 2.43 and Above* (Victoria, British Columbia, Canada: The Nature Conservancy (TNC), Arlington, Virginia, United States and Pacific Marine Analysis and Research Association (PacMARA).

Sims, D. W. (2019). "The Significance of Ocean Deoxygenation for Elasmobranchs," in *Ocean Deoxygenation: Everyone's Problem-Causes, Impacts, Consequences and Solutions*. Eds. D. Laffoley and J. M. Baxter (Gland: IUCN), p 431–p 448.

Spalding, M. D., Fox, H. E., Allen, G. R., Davidson, N., Ferdaña, Z. A., Finlayson, M. A. X., et al (2007). Marine Ecoregions of the World: A Bioregionalization of Coastal and Shelf Areas. *BioScience* 57, 573–583. doi: 10.1641/B570707

State Oceanic Administration (2016). *Ocean Atlas of China's coastal waters - Marine Biology and Ecology* (Beijing (in Chinese):China Ocean Press).

Stein, R. W., Mull, C. G., Kuhn, T. S., Aschliman, N. C., Davidson, L. N., Joy, J. B., et al (2018). Global Priorities for Conserving the Evolutionary History of Sharks, Rays and Chimaeras. *Nat. Ecol. Evol.* 2, 288–298. doi: 10.1038/s41559-017-0448-4

Tang, D. (1936). The Elasmobranchiate Fishes of Amoy. *Coll. Pap. Dept. Biol. Mar. Biol. Lab. Univ. Amoy* 3, 1–25.

Thuiller, W., Georges, D., Gueguen, M., Engler, R., and Breiner, F. (2021) *Biomod2: Ensemble Platform for Species Distribution Modeling. R Package Version 3.5.1*. Available at: https://CRAN.R-project.org/package=biomod2.

Thuiller, W., Guéguen, M., Renaud, J., Karger, D. N., and Zimmermann, N. E. (2019). Uncertainty in Ensembles of Global Biodiversity Scenarios. *Nat. Commun.* 10, 1–9. doi: 10.1038/s41467-019-09519-w

Tyberghein, L., Verbruggen, H., Pauly, K., Troupin, C., Mineur, F., and De Clerck, O. (2012). Bio-ORACLE: A Global Environmental Dataset for Marine Species Distribution Modelling. *Glob. Ecol. Biogeogr.* 21, 272–281. doi: 10.1111/j.1466-8238.2011.00656.x

CBD/COP/DEC/X/2 (2010). Available at: https://www.cbd.int/doc/decisions/cop-10/cop-10-dec-02-en.pdf.

UNEP-WCMC and IUCN (2022) *Marine Protected Planet*. Available at: www.protectedplanet.net.

Van Houtan, K. S., Gagné, T. O., Reygondeau, G., Tanaka, K. R., Palumbi, S. R., and Jorgensen, S. J. (2020). Coastal Sharks Supply the Global Shark Fin Trade. *Biol. Lett.* 16, 20200609. doi: 10.1098/rsbl.2020.0609

Van Zinnicq Bergmann, M. P., Guttridge, T. L., Smukall, M. J., Adams, V. M., Bond, M. E., Burke, P. J., et al (2022). Using Movement Models and Systematic Conservation Planning to Inform Marine Protected Area Design for a Multi-Species Predator Community. *Biol. Conserv.* 266, 109469. doi: 10.1016/j.biocon.2022.109469

Venter, O., Fuller, R. A., Segan, D. B., Carwardine, J., Brooks, T., Butchart, S. H., et al (2014). Targeting Global Protected Area Expansion for Imperiled Biodiversity. *PloS Biol.* 12, e1001891. doi: 10.1371/journal.pbio.1001891

Walls, R., Rigby, C. L., Derrick, D., Dyldin, Y. V., and Yamaguchi, A. (2021). *Squatina Japonica* (The IUCN Red List of Threatened Species).

Ward-Paige, C. A., and Worm, B. (2017). Global Evaluation of Shark Sanctuaries. *Global Environ. Change* 47, 174–189. doi: 10.1016/j.gloenvcha.2017.09.005

Watson, R., Zeller, D., and Pauly, D. (2014). Primary Productivity Demands of Global Fishing Fleets. *Fish Fish.* 15 (2), 231–241. doi: 10.1111/faf.12013

Watts, M. E., Ball, I. R., Stewart, R. S., Klein, C. J., Wilson, K., Steinback, C., et al (2009). Marxan With Zones: Software for Optimal Conservation Based Land- and Sea-Use Zoning. *Environ. Model. Softw.* 24, 1513–1521. doi: 10.1016/j.envsoft.2009.06.005

White, T. D., Ferretti, F., Kroodsma, D. A., Hazen, E. L., Carlisle, A. B., Scales, K. L., et al (2019). Predicted Hotspots of Overlap Between Highly Migratory Fishes and Industrial Fishing Fleets in the Northeast Pacific. *Sci. Adv.* 5, eaau3761. doi: 10.1126/sciadv.aau3761

World Parks Congress (2014). *A Strategy of Innovative Approaches and Recommendations to Enhance Implementation of Marine Conservation in the Next Decade* (Sydney, Australia: IUCN World Parks Congress).

Wu, X. (1929). Study of the Fishes of Amoy. *Zoo Ser.* 5 (4), 1–89.

Wu, H., and Zhong, J. (2021). *Key to Marine and Estuarial Fishes of China* (Beijing: China Agricultural Press).

Yagnesh, M., Durga, F., Rehanavaz, M., Poojaben, T., and Raj, D. (2020). Importance of Sharks in Ocean Ecosystem. *J. Entomol. Zool. Stud.* 8, 611–613.

Yano, K., Ahmad, A., Gambang, A. C., Idris, A. H., Solahuddin, A. R., and Aznan, Z. (2005). *Sharks and Rays of Malaysia and Brunei Darussalam*. (Kuala Terengganu, Malaysia: Seafdec-Mfrdmd/sp/I2)

Zhang, F. (2003). The Varieties and Use Value of the Chondrichthves in the Huang Sea and the Bo Sea. *Spec. Wild Econ. Anim. Plant Res.* 3, 53–56. doi: 10.3969/j.issn.1001-4721.2003.03.018

Zhang, Z. (2005). The Fishery Resources Statuts of Sharks in Eastern China Sea. *J. Fujian Fish.* 3, 10–13. doi: 10.14012/j.cnki.fjsc.2005.03.02

Zhang, R., Lin, L., Li, Y., Song, P., Chen, Y., and Zhang, J. (2018). Species Composition and Quantity Distribution of Sharks in the Southwestern Sea of the Nansha Islands and Mouth of the Beibu Bay. *Mar. Fish.* 1, 27–37. doi: 10.13233/j.cnki.mar.fish.2018.01.004

Zhang, Q., and Yang, S. (2005). Species, Geography Distribution and Resource of Chondrichthian Fishes of China. *J. Xiamen Univ. (Nat. Sci.)* 44, 207–211. doi: 10.3321/j.issn:0438-0479.2005.z1.048

Zhao, Q., Stephenson, F., Lundquist, C., Kaschner, K., Jayathilake, D., and Costello, M. J. (2020). Where Marine Protected Areas Would Best Represent 30% of Ocean Biodiversity. *Biol. Conserv.* 244, 108536. doi: 10.1016/j.biocon.2020.108536

Zhu, Y. (1958). A Review of the Elasmobranchiate Fishes of China, With Discussion on the Problems of Their Utilization. *Oceanol. Limnol. Sin.* 1, 325–333.

Zhu, Y. (1960). *Chondrichthyes of China* (Beijing: Science Press).

**Conflict of Interest:** The authors declare that the research was conducted in the absence of any commercial or financial relationships that could be construed as a potential conflict of interest.

**Publisher's Note:** All claims expressed in this article are solely those of the authors and do not necessarily represent those of their affiliated organizations, or those of the publisher, the editors and the reviewers. Any product that may be evaluated in this article, or claim that may be made by its manufacturer, is not guaranteed or endorsed by the publisher.

frontiers | Frontiers in Marine Science

ORIGINAL RESEARCH
published: 28 June 2022
doi: 10.3389/fmars.2022.863611

# Carbon Transfer Efficiency and Risk of Fisheries Collapse in Three Large Marine Ecosystems Around China

*Dongxing Chen*[1†], *Xutao Wang*[1,2,3†], *Minchi Hou*[1], *Qiabin Wang*[1], *Qianqian Liu*[4], *He Huang*[1] *and Yafeng Zhang*[1,3*]

[1] Eco-Environmental Monitoring and Research Center, Pearl River Valley and South China Sea Ecology and Environment Administration, Ministry of Ecology and Environment of the People's Republic of China, Guangzhou, China, [2] School of Marine Sciences, Sun Yat-Sen University, Zhuhai, China, [3] Southern Marine Science and Engineering Guangdong Laboratory (Zhuhai), Zhuhai, China, [4] Department of Physics and Physical Oceanography, University of North Carolina Wilmington, Wilmington, NC, United States

Fisheries catch is determined by a complex combination of biological and industrial factors. In this study, using data from the online database Sea Around Us from 1950 to 2018, the risk of fisheries collapse was assessed for the three large marine ecosystems (LMEs) around China by analyzing the carbon transfer efficiency, mean trophic level, and mean maximum length of fisheries catch and expansion factor. In addition, these were compared with the corresponding values for other LMEs, especially the Humboldt Current and the North Sea LMEs, which experienced fisheries collapse.

Our results revealed high carbon transfer efficiencies in LMEs around China, suggesting large fishing efforts compared with LMEs with similar primary production. Although marine fish landings did not decline significantly, they were maintained by potential resources associated with offshore and deep expansion and fishing of lower–trophic-level species and juvenile fish. However, the potential resources have been largely consumed in the East China Sea and South China Sea LMEs, where the ratio of the primary production required to sustain catches to the total primary production (%PPR) was greater than 50%. In contrast, this ratio in the Yellow Sea LME was lower; however, this value was still higher than the sustainable ratio in the Humboldt Current LME. Without proper fisheries management, the three fisheries around China are likely to collapse, as observed in case of the North Sea LME in the 1970s.

**Keywords: large marine ecosystem, primary production, carbon transfer efficiency, fishery collapse, fisheries catch**

OPEN ACCESS

***Edited by:***
*Jun Xu,*
*Institute of Hydrobiology (CAS), China*

***Reviewed by:***
*Jayasankar Jayaraman,*
*Central Marine Fisheries Research Institute (ICAR), India*
*P. U. Zacharia,*
*Central Marine Fisheries Research Institute (ICAR), India*

***Correspondence:**
*Yafeng Zhang*
*zhangyaf@zjnhjg.mee.gov.cn*

*[†]These authors have contributed equally to this work and share first authorship*

***Specialty section:***
*This article was submitted to Marine Ecosystem Ecology, a section of the journal Frontiers in Marine Science*

***Received:*** *27 January 2022*
***Accepted:*** *30 May 2022*
***Published:*** *28 June 2022*

***Citation:***
*Chen D, Wang X, Hou M, Wang Q, Liu Q, Huang H and Zhang Y (2022) Carbon Transfer Efficiency and Risk of Fisheries Collapse in Three Large Marine Ecosystems Around China. Front. Mar. Sci. 9:863611. doi: 10.3389/fmars.2022.863611*

## INTRODUCTION

Fisheries are supported by embedded ecosystems (Unsworth et al., 2019). Therefore, primary production is a fundamental factor influencing fish production and fisheries catch (Pauly and Christensen, 1995; Watson et al., 2014; Anderson et al., 2019). The relationship between primary production and fisheries catch has been extensively investigated since Oglesby (1977) first reported the empirical relationship between the annual catch of fish and primary production in large fresh water systems (Ware and Thomson, 2005; Capuzzo et al., 2018). However, in marine and estuarine

systems, (Nixon, 1982; Nixon, 1992) found that the relationship did not hold, which suggested that primary production was not the only driving factor for fisheries catch.

Although primary production sets the potential for fish production, fisheries catch is determined by a complex combination of biological and industrial factors, such as fishing effort and management policies. For the biological factors, it remains controversial whether long-term sustainable fisheries catches from the global oceans are largely controlled by primary production (bottom-up controls) or by predatory–prey interactions at higher trophic levels (top-down controls) (Ware and Thomson, 2005; Mcowen et al., 2015). This is based on the fact that the reported annual global landings of fish have stagnated around 80 million tons (Mt) with inter-annual fluctuations for many years since 1995 (Watson and Pauly, 2001; Pauly and Froese, 2012). However, fishing capacity, measured by the cumulative power of fishing vessels, has continued to increase, indicating that catches taken per unit of fishing effort have actually declined (Watson et al., 2013; Bell et al., 2017). This suggests that global sustainable harvest limits could be approached (Watson et al., 2014). Considering that the global landings did not show signs of overexploitation or stock collapse (Pauly, 2018), available studies have presented three potential but still debatable reasons contributing to the stable landings: offshore extension of pelagic and demersal fisheries (Watson and Morato, 2013), downtrend of trophic level (Bhathal and Pauly, 2008; Liang and Pauly, 2020), and juvenile fishing (Krumme et al., 2013; Yang et al., 2021).

As one of the most productive fishing zones in the world, coastal oceans around China significantly contribute to seafood production and support food for the high population. Although its fishery-associated resources are crucial for food security and export trade in its bordering countries, studies by Sumaila and Cheung (2015) revealed that some key species sourced from the East and South China Seas are under serious threat due to long-term overfishing, climate change, and other stressors. In this study, fisheries data in the broad coastal oceans around China were comprehensively investigated by considering both biological and industrial controls to assess the vulnerability to collapse of large marine ecosystems (LMEs) in China.

To effectively assess and manage transnational coastal fisheries and environments in the global ocean, scientists divided the ecosystem into LMEs, which are defined as marine ecosystems around the world with unique sets of ecological, oceanographic, and biogeochemical characteristics (Watson et al., 2014; Selig et al., 2019). Coastal LMEs account for 95% of the total annual fisheries catch, although they cover only 20% of the global ocean area (Garibaldi and Limongelli, 2003; Stock et al., 2017). There are three LMEs along China's coasts: Yellow Sea LME, East China Sea LME, and South China Sea LME. Over 60% of the Yellow Sea and East China Sea are on the continental shelf and are among the most productive parts of the world's oceans (Chen, 1996). In contrast, the South China Sea LME, located on the tropical–subtropical rim of the western North Pacific Ocean at an average depth of approximately 1212 m (Sumaila, 2019), has low nutrient concentrations throughout the year (Lu et al., 2020). Owing to the distinct geographical and nutrient conditions in the three LMEs, primary production and fisheries catches are distinct; however, only a few studies comparing their fisheries have been performed (Jin and Tang, 1996; Zhang et al., 2018; Pauly and Liang, 2020). The main objectives of this study were to assess the fisheries in the three LMEs around China and to compare them with other LMEs, especially the Humboldt Current and North Sea LMEs, which experienced fisheries collapse.

Carbon transfer efficiency (CTE) and the ratio of primary production required for fisheries catch to total primary production (%PPR) were two important factors for the assessment of fisheries in this research. The CTE is an indicator for estimating fish production and is widely applied in the study of carbon cycling, marine ecosystems, and food web interactions to determine energy transfer efficiency (Degerman et al., 2018; Fakhraee et al., 2020; Eddy et al., 2021). The %PPR is often used to analyze the ecological pressure of different species or systems (Morissette et al., 2012; Ding et al., 2020). A rough measure of CTE from primary production to fisheries is based on the analysis of 63 LMEs (66 LMEs in total; however, the data for the three of them were missing data, and therefore, these were eliminated from the statistics) around the world (**Figure 1**) was used to evaluate fisheries in the three LMEs around China. To compare the bottom-up and top-down controls, %PPR was assessed under the assumption that the reported marine fish landings effectively reflected total fish production. In addition, the mean maximum length of fish catches, trends in trophic levels, and expansion factors (EFs) were also analyzed to verify whether offshore and deep extension, downtrend of trophic level, and juvenile overfishing occurred in the LMEs around China. Most of the data were obtained from Sea Around Us (https://www.seaaroundus.org, SAU), which is one of the very few databases with near-uniform data regarding major fisheries around the world.

## MATERIALS AND METHODS

### Primary Production

Primary production data for 63 LMEs (1950–2018) were obtained from the online database of the SAU. It was estimated on the basis of the chlorophyll pigment concentration derived from SeaWiFS data (http://seawifs.gsfc.nasa.gov) with a spatial resolution of 9 km (Siswanto et al., 2016; Sharma et al., 2019). Primary production for the northern South China Sea before 1990s may be overestimated as the estimation was based on current nutrients loads, which have been increasing since the 1990s (Liu et al., 2002). However, considering that the northern South China Sea covers only approximately 6% of the entire South China Sea LME (Yu and Zhang, 2005), this overestimation was negligible in the entire LME area.

### Fisheries Catch and Mean Trophic Level

Annual fisheries catch and mean trophic levels of fisheries catch data from the SAU database was derived mainly from the corrected

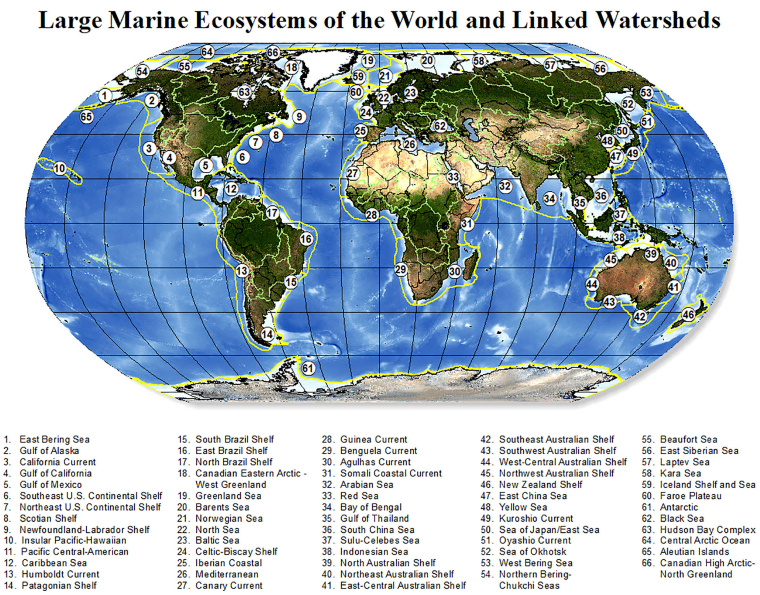


**FIGURE 1** | Global map of Large Marine Ecosystems. The global ocean is divided into 66 LMEs by Oceanographers [Image credit,Sherman and Hamukuaya (2016)].

Food and Agriculture Organization (FAO) of the United Nation's global fisheries landings statistics, complemented by statistics from various international and national agencies and some reconstructed data sets (Watson et al., 2014). It should be noticed that fisheries catch data from the SAU were reanalyzed with catches and discards. For most countries, the baseline data were statistics reported by member countries or international bodies to the FAO. It was also necessary to source available alternative information sources for missing data in other countries. A six-step approach for data processing was developed and reported by Zeller and Pauly (2016) in detail. Chinese catches from China's exclusive economic zone were over-reported since the mid-1980s (Watson and Pauly, 2001). However, this was resolved after China corrected the data submitted to FAO; the FAO subsequently revised the related historical statistics for the period of 1997–2005 (Pauly and Froese, 2012). In addition, this over-reporting was diluted owing to the fact that China's exclusive economic zone being part of the LMEs around China (Pauly et al., 2014). Therefore, the fisheries catch data for LMEs around China were valid for analysis.

## Mean Maximum Length and Expansion Factor

The mean maximum length estimates were mainly obtained from the "ISSCAAP Table" of FishBase 2000 (Rosenberg et al., 2014), which consisted of standard lengths for all species of bony fish. In addition, data from the FAO Species Catalogues and Identification Guides were included to complement the ISSCAAP table for several invertebrate taxa. The mean maximum lengths were averaged by genera, families, and higher groups. To account for the expansion and contraction of fishing fleets over time, reflected by the trophic level of catches, the Fishing-in-Balance (FiB) index was introduced, with an increasing trend representing a geostrophic expansion of fisheries to new grounds (Bhathal and Pauly, 2008). On the basis of this, the spatial EF was introduced to make the implied expansion of fisheries explicit by re-interpretating the FiB index in the form of $EF = 10^{FiB}$ (Bhathal and Pauly, 2008). The EF was used as an indicator of the expansion of fisheries, which is widely used in research regarding changes in fisheries or the health of the ecosystem (Liang and Pauly, 2017; Mashjoor et al., 2018). In the present study, 1950 was used as the reference year (Pauly and Christensen, 1995).

## Primary Production Required

The primary production required (PPR) for the fisheries catch (Pauly and Christensen, 1995) was computed as follows:

$$PPR = \sum_{i=1}^{n} \frac{c_i}{CR} \times \left(\frac{1}{TE}\right)^{(TL_i-1)}$$

Here, $C_i$ is the catch of species i, CR is the conversion rate of wet weight to carbon, TE is the transfer efficiency between trophic levels, $TL_i$ is the trophic level of species i, and n is the total number of species caught in a given area. A CR of 9:1 and TE of 10% were used for this study (Pauly and Christensen, 1995). The TE is a re-estimated value based on annual world fisheries catches (94.3 million tons) from 1988 to 1991, which has been widely used in previous research (Mehner et al., 2018; Barneche et al., 2021). The analysis for the period from 1950 to 2018 was based on the data from the SAU. Using %PPR as the fishing pressutrre index, the relationship between fisheries catch and intrinsic energetic limits for each LME was assessed (Knight and Jiang, 2009; Conti and Scardi, 2010).

# RESULTS

## Primary Production and Fisheries Catch

The relationship between fisheries catches and primary production provided a rough measure of the efficiency in carbon transfer from primary production to fisheries in different LMEs (CTE) (**Figure 2**). Affected by a variety of environmental factors, a positive correlation ($r^2 = 0.21$, $p < 0.05$) was found between the fisheries catch and primary production, with the CTE varying from 0.01% to 0.1% for the 63 LMEs. Our results indicate that LMEs with high primary production usually showed a higher CTE. Yet, fisheries catch could be markedly different for ecosystems with similar primary production levels. In the three LMEs around China, the fisheries were higher than most of the other LMEs with the similar levels of primary production, producing high CTEs of approximately 0.1%. Therefore, the high CTEs in the three LMEs around China were more likely to result from the fishing efforts, rather than primary production.

## Fisheries Catch and Mean Trophic Level

The global and regional fisheries experienced different stages from 1950 to 2018 (**Figure 3**). The global fisheries catch increased from 24.1 Mt in 1950 to a peak of 107.8 Mt in 1996 and then declined and stabilized at about 90 Mt, with inter-annual fluctuations. In contrast to the global trend, the fisheries catch in the Humboldt Current and North Sea peaked around 1970 and then declined, whereas in the Humboldt Current, the fisheries catch recovered in the mid-1980s. The fisheries catch in the three LMEs around China experienced the same pattern as the global trend, with a peak in the 2000s, and then stabilized or slightly declined. Therefore, the global annual fisheries catch was relatively stable since it reached the maximum, and the regional fisheries catch can vary significantly, regardless of trends, peak periods, or their magnitudes.

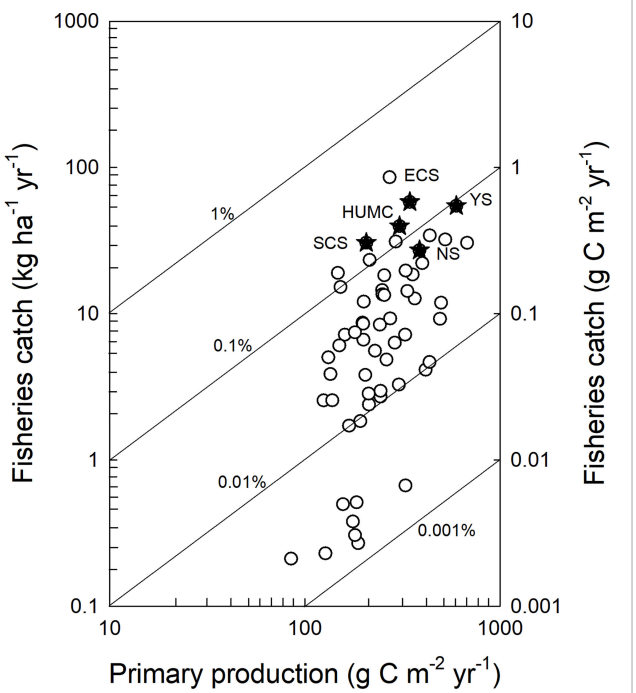


**FIGURE 2** | Relationships between primary production and fisheries catch in the 63 large marine ecosystems (LMEs) in 2018 based on the data from SAU. The asterisks indicate the South China Sea (SCS), Humboldt Current (HUMC), East China Sea (ECS), North Sea (NS), and Yellow Sea (YS). The diagonal lines and associated % values show different levels of efficiency in carbon transfer from primary production to fisheries catch [carbon transfer efficiency (CTE)].

By examining the mean trophic level of global and regional fisheries over 68 years starting in 1950 (**Figure 4**), we found that, although the downtrend of the mean trophic level for global fisheries was found to be modest, the mean trophic level in some regional fisheries decreased remarkably. The trophic level varied less than 0.3 in the global ocean and South China Sea in the past decades. In contrast, a remarkable downward trend occurred in the Humboldt Current during the 1950s, with a trophic level decrease of 1, from 3.9 in 1950 to 2.7 in 1960, and then, the trophic level stabilized at a low level of 3.0. For the Yellow Sea and East China Sea, the mean trophic level change from 1950 to 2018 was small but showed a trough during the 1980s and the 1990s.

## Mean Maximum Length and Expansion Factor

The mean maximum length of fisheries catch was an important indicator for evaluating the impact of fishing on marine ecosystems (**Figure 5**). The mean maximum length in the global ocean and Humboldt Current stabilized following the sharp drop in the 1950s; however, in the Humboldt Current, the value decreased by 80%, which was much larger than that in the global ocean (25%). There was a recovery when the mean maximum length in the Humboldt Current during the 2010s was 64.8 cm, which was close to that in the global ocean (64.9 cm). Similar to the North Sea, the mean maximum length in the South China Sea continually decreased from 1950 to 2018; however, the total decline was only ~15 cm. The mean maximum length in the Yellow Sea and East China Sea varied in the same pattern, with the largest fall in the 1980s and then slightly rebounded; however, the overall decrease was smaller than that in the South China Sea. In general, the mean maximum length of the fisheries catch decreased in the past 56 years, although different variation patterns were observed for different LMEs.

To assess fishing efforts around China, the spatial expansion in the three LMEs around China were analyzed and compared them with the North Sea LME, Humboldt Current LME, and the global ocean (**Figure 6**). The EF for the Humboldt Current LME showed an increasing trend prior to the mid-1990s and a decreasing trend thereafter, with strong interannual variabilities. The EFs in the global ocean and most of the regional fisheries in LMEs around China increased from 1950 to 2018, except in the North Sea, where the EF remained lower than 1.5, except in the years around 1970, when a peak occurred. Among the regions with increasing fishing efforts, the South China Sea was especially prominent as the EF increased from approximately 1 in 1950 to ~15 in 2018. In 2018, its EF was approximately 3.5 times the EF of the global ocean, without signs of decrease. In contrast, the increasing speed for the

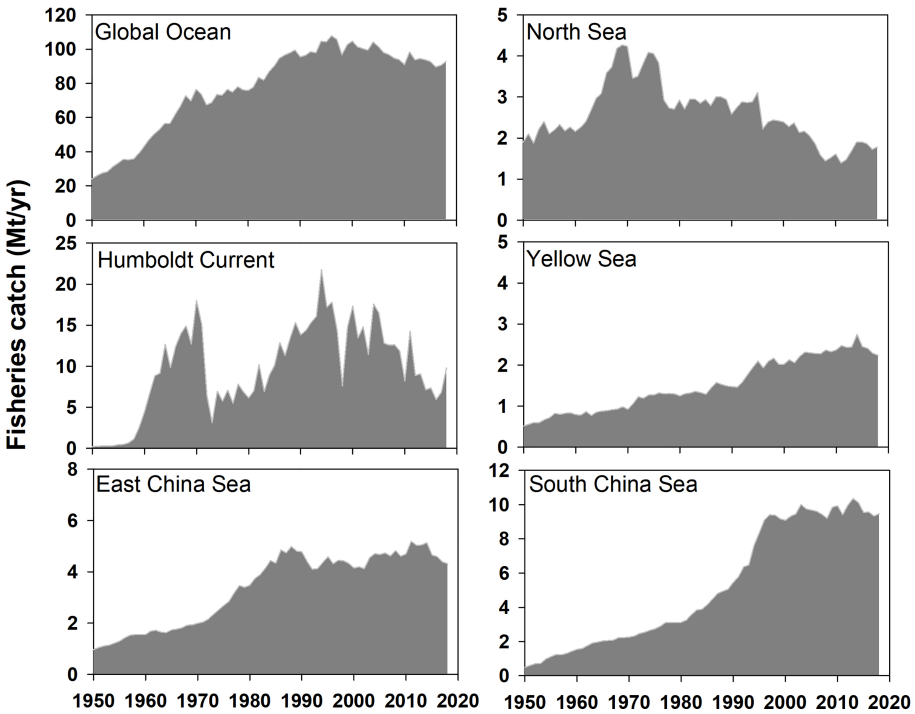


**FIGURE 3** | Fisheries catch (Mt/yr) in the global ocean and five LMEs from 1950 to 2018.

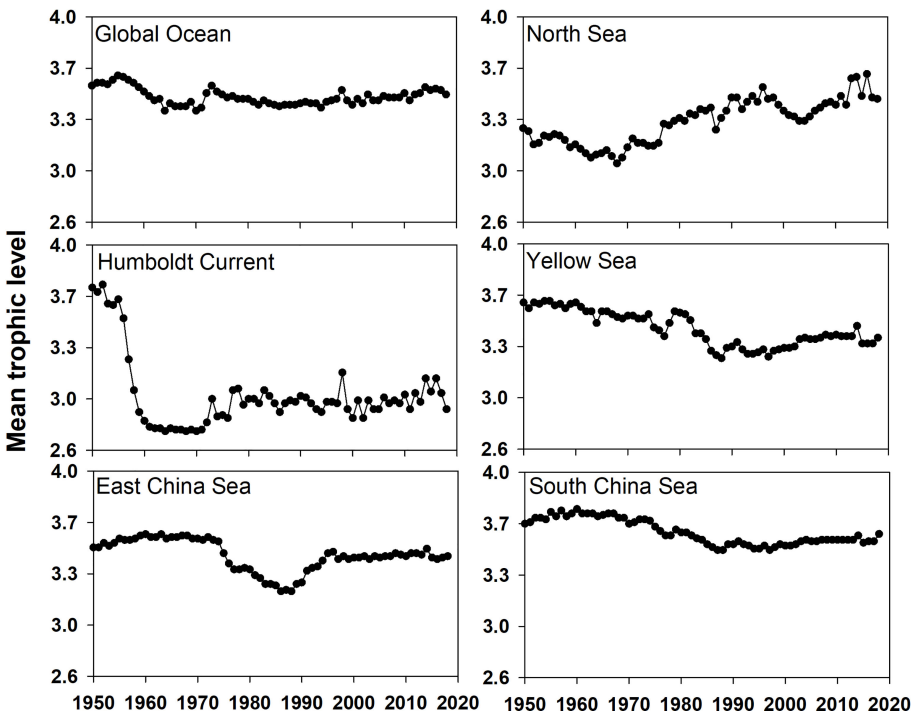


**FIGURE 4** | Mean trophic level of fisheries catch in the global ocean and five LMEs from 1950 to 2018.

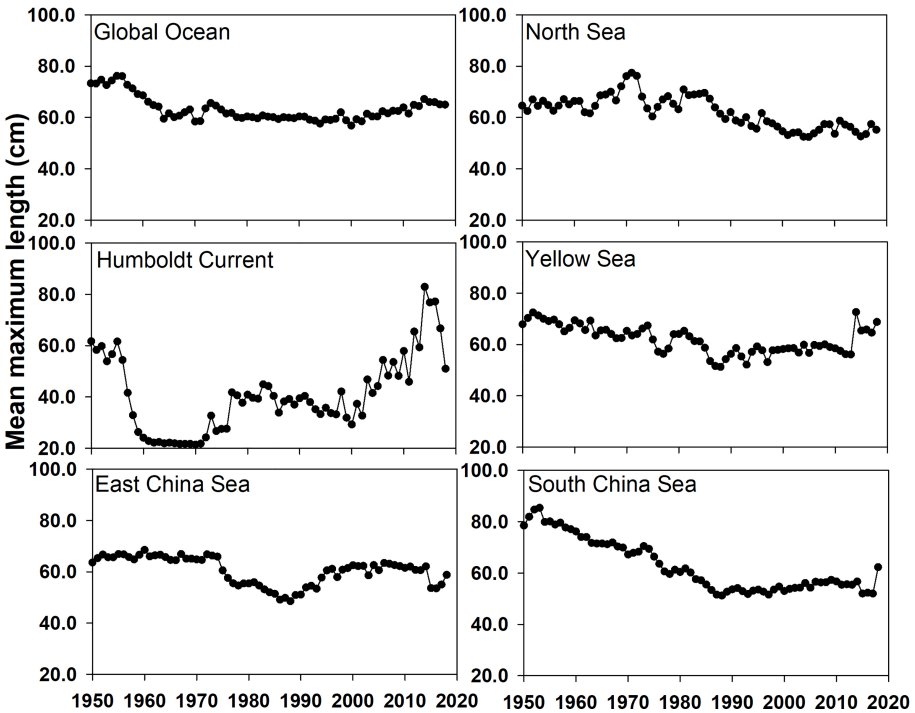


**FIGURE 5** | Mean maximum length of fisheries catch in the global ocean and five LMEs from 1950 to 2018.

Yellow Sea and East China Sea was comparable to that of the global ocean, with an increase of less than 3 from 1950 to 2018.

## Primary Production Required to Sustain The Fisheries Catch

The ratio of the primary production required for fisheries to the total primary production (%PPR) in global and regional fisheries from 1950 to 2018 (**Figure 7**) was examined; it was found that, since the late 1990s, accompanied by a rising demand for fishery-associated resources, global fishing fleets removed approximately 5%–6% of the total primary production by fishing. The ratios were larger than 30% in the 1990s for the North Sea, East China Sea and South China Sea; this was caused by the ever-increasing marine fish landings in the three LMEs around China since the 1990s. The ratio in the East China Sea and South China Sea was approximately 50% in 2018, which was almost two and five times higher than the values for the North Sea Humboldt Current, respectively. The analysis demonstrated that although the global %PPR had stabilized at a low level, the regional ratios could be quite high and unstable.

# DISCUSSION

## Comparisons of CTE Between LMEs

The positive correlation between primary production and fisheries catch in the 63 LMEs further proved that bottom-up processes set the potential for fisheries catch (Pauly and Christensen, 1995). Meanwhile, the CTE variations among different LMEs with similar levels of primary production indicated that top-down controls, including fishing effort and differences in ecosystem structure, also contributed to fisheries catch (Stock et al., 2017; Henson et al., 2019; Ding et al., 2020). Therefore, although primary production in the three LMEs around China (except the Yellow Sea) were moderate or even low among the 63 LMEs, their CTEs were all near the highest due to the high fishing effort, as indicated by their high EFs. This was consistent with the findings of the study by Watson and Pauly (2014) found for the South China Sea LME and other LMEs, revealing the general intensification and extension of fishing offshore and into depths over the decades.

The PPR estimated the amount of primary production needed to support the biomass of fish removed from marine ecosystems. For comparison, the sustainable %PPR for the Humboldt Current LME, a highly productive ecosystem with rich nutrient supply by ocean currents (Gutiérrez et al., 2016), was about 10%–15% in recent years. Although the ratios in the three LMEs around China were much higher, the values for the East China Sea and South China Sea LMEs were larger than 50% after the 2000s, indicating that the carbon fixed by phytoplankton in these regions could not support such high demands. This high %PPR due to high fishing intensity will threatens the diversity of the ecosystem (Watson et al., 2014). Therefore, both fishing effort and environmental drivers shape the fisheries catch in the three LMEs around China, with high fishing effort being the main reason for the high CTE and %PPR.

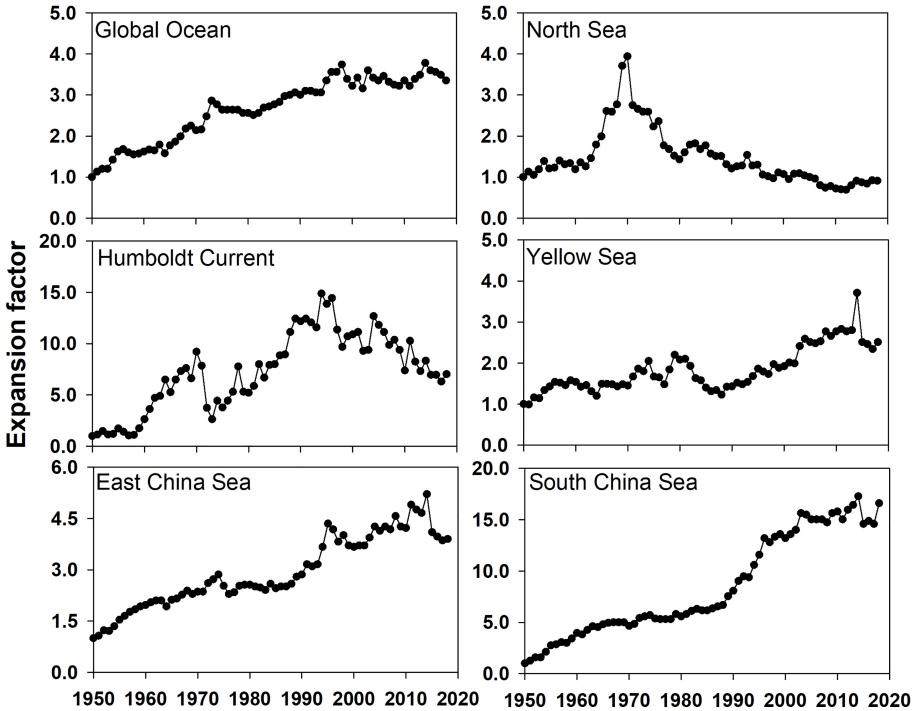


**FIGURE 6** | The expansion factors in the global ocean and five LMEs from 1950 to 2018.

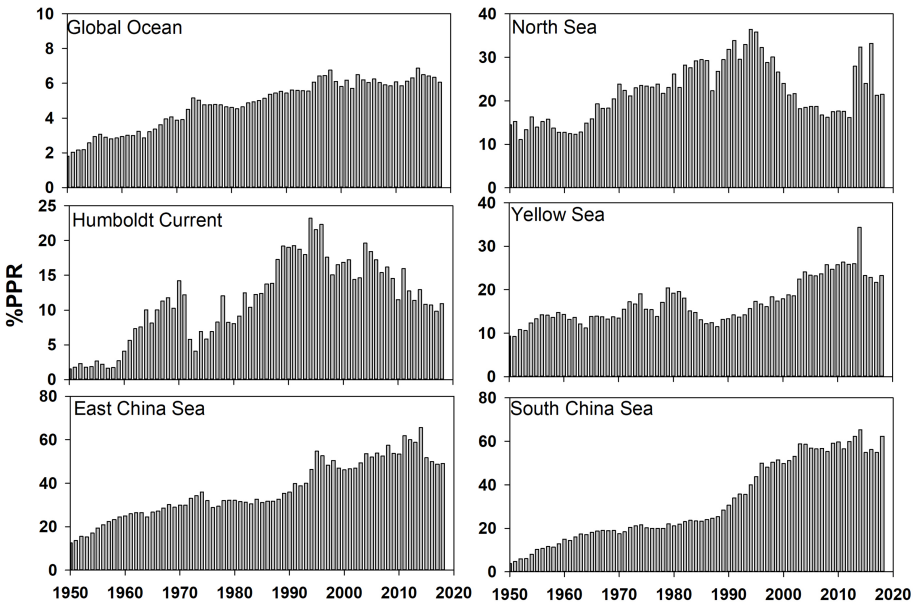


**FIGURE 7** | The ratios of primary production required for fisheries catch to the total primary production (%PPR) in the global ocean and five LMEs from 1950 to 2018.

## Obscuration of Overexploitation in Fisheries Catch

Global annual marine fish landings have stagnated around 80 Mt since the1990s, with an additional 20 Mt of additional illegal/unreported catches (Agnew et al., 2009), reaching the upper limits for sustainable marine fish landings, which was between 100 and 140 Mt per year (Grainger and Garcia, 1996; Chassot et al., 2010; Watson et al., 2014). Considering that fishing effort is

still increasing, high marine fish landings are maintained by unsustainable factors, including spatial expansion, fishing of lower trophic level species, and juvenile fish.

Watson and Pauly (2014) reported that fishing gear improvements has increased the mean depth of fishing to 600 m in the late 1960s. EFs in the global ocean and LMEs confirmed this offshore and deep extension trend; however, the extension intensity among the different LMEs was quite different. Owing to shallow water depths, the potential for deep extension in the Yellow Sea and East China Sea LMEs was limited. In contrast, the extension of the South China Sea LME was still increasing, although the present EF is already very high. This could result from fishermen struggling to find new grounds in tropical fisheries because of reduced catches within the inshore area (Watson and Pauly, 2014). Pauly and Liang (2020) reported that fisheries in the South China Sea LME further intensified and gradually extended to encompass the entire LME. Although the mean trophic level for the entire global ocean had not significantly decreased in the past 60 years, Branch et al. (2010) argued that in some LMEs, such as the Humboldt Current, Yellow Sea, and East China Sea, remarkable downtrends had appeared. A low mean trophic level could result in more biological production to being captured by fishing in an ecosystem (Chassot et al., 2010). A decline in the mean maximum length for global LMEs confirmed the overfishing of juveniles, as the commercial fisheries with long-lived and slow-growing species were almost depleted (Pauly et al., 1998; He and Field, 2019). Furthermore, the increasing demand for trash fish as feed for mariculture led to the increased overfishing of juvenile fish stocks in the Asia-Pacific region (Krumme et al., 2013; Mahesh et al., 2019; Zhang et al., 2020). In addition, the impact of climatic events on decadal variation at the trophic level was one of the factors that could not be ignored, for example, the abnormal change in the Humboldt LME due to the El Niño-Southern Oscillation in the 1960s and 1970s (Alheit and Niquen, 2004).

In general, although global sustainable harvest limits have been exceeded, overexploitation in fisheries for individual LMEs was obscured by the sustainable marine fish landings. This was supported by the offshore, deep expansion, and overfishing of lower–trophic-level species and juvenile fish, which could directly influence exploited populations and alter their structure, function, and dynamics of fisheries.

## Lessons From the North Sea and Risks to Fisheries Around China

Marine fisheries in the Asia-Pacific region play an important role in global and national economies. Many fisheries in this region are overexploited, both biologically and economically (Pang et al., 2018; Lam and Pauly, 2019). Historical data show that, once a fishery has collapsed, it is difficult for the ecosystem to reconstruct its productive potentials and diversity, and one typical example was the sudden fisheries collapse in the North Sea in 1970s (Fromentin, 2009; Dadswell et al., 2022). Since the early 21st century, various management intervention schemes were implemented to recover fisheries in the North Sea (Steadman et al., 2014; Hutchings and Kuparinen, 2020). Although the %PPR had sharply decreased and fishing mortality had decreased below the sustainable level, various studies suggested that the reduction in fishing mortality was too late to prevent irrevocable, long-term genetic, and population disturbance (Steadman et al., 2014). Olsen et al. (2009) found that variability in body size for the Skagerrak juvenile population was reduced in the 21st century, compared with the data from the 20th century, which suggested that the North Sea sub-population had already suffered functional extinction. The opportunity to rebuild the stocks may have passed (Winter et al., 2020). Recent studies indicated that the changes in oceanic climate conditions induced a certain degree of limitation to fisheries catch recovery in the North Sea as well (Sguotti et al., 2019; Bluemel et al., 2022).

The three fisheries around China are likely to experience the same collapse as the North Sea LME. Given the similarity between the fishery-associated indicators for the three LMEs around China (particularly the trend in %PPR) and the North Sea before the fisheries collapse period, this lesson should be taken into account. Chinese fishery managers instituted a 2- to 3-month fishing-off season every year to reduce fishing effort and to sustain yields since mid-1990. However, marine fish landings in the East China Sea and South China Sea LMEs continue to grow, with a corresponding %PPR of > 50% at its peak. Potential fishery-associated resources, based on offshore and deep extension, and fisheries catch of lower–trophic-level species and juvenile fish could have been depleted during the 1980s to 2000s, according to the sharp increase in fisheries catch and EFs and decrease in trophic level and mean maximum length. Although the mean trophic level recovered to some extent after the 1990s, owing to the regulation of the fishing-off season in China, the overall situation is still hardly optimistic. The decline in fisheries catch since the early 2010s was a sign of fish resource depletion. This was supported by the results of a study by Wan and Bian (2012), who found that anchovy egg size had notably decreased and mortality rates had notably increased from the 1980s to the 2000s; these authors compared the size and natural mortality rates of anchovy eggs from the spawning grounds in the Yellow Sea and East China Sea LMEs. Although the marine fish landings in the South China Sea LME did not significantly decrease, supported by the assessment of the potential fishery-associated resources in offshore and deep-water and juvenile fishing (Butchart et al., 2010), they were already at the highest level and %PPR was already as high as 60%, which was much higher than the sustainable ratio of 40% (Pauly and Christensen, 1995). Therefore, well-organized and strict fishing policies should be implemented in the future for a long time to reduce fishing pressure and ensure the sustainable development of the LMEs in China.

# CONCLUSION

The SAU data from 1950 to 2018 were analyzed and compared with the data for the LMEs of the global ocean, Humboldt Current, and the North Sea, to assess the situations of the fisheries in the three LMEs around China. Fisheries catch was controlled by both primary production (bottom-up controls) and fishing effort (top-down controls); however, fishing effort mainly accounted for the high efficiency of carbon lost to fishing in the

Yellow Sea, East China Sea, and South China Sea, which showed a high CTE. The high fisheries landings were maintained by exhausting the potential fish resources provided by the offshore and deep expansion, the lower trophic level, juvenile fishing, and mariculture, which could result in the irrevocable destruction of fishery-associated ecosystems.

## DATA AVAILABILITY STATEMENT

The original contributions presented in the study are included in the article/**Supplementary Material**. Further inquiries can be directed to the corresponding authors.

## AUTHOR CONTRIBUTIONS

DC and XW developed the conceptualization and methodology. DC, XW, and HH wrote the original manuscript. XW, YZ, and QL revised the manuscript. MH and QW are responsible for conducting the research and collecting data. All authors contributed to the article and approved the submitted version.

## ACKNOWLEDGMENTS

We thank David Kirchman, School of Marine Science and Policy, University of Delaware, for his valuable comments. We also thank to Yongsong Qiu, the Chief of the Fishery Resources Division at South China Sea Fisheries Research Institute, Chinese Academy of Fishery Sciences, who provided some valuable insights. We acknowledge the support from the Sea Around Us, funded by a number of philanthropic foundations.

## SUPPLEMENTARY MATERIAL

The Supplementary Material for this article can be found online at: https://www.frontiersin.org/articles/10.3389/fmars.2022.863611/full#supplementary-material

## REFERENCES

Agnew, D. J., Pearce, J., Pramod, G., Peatman, T., Watson, R., Beddington, J. R., et al. (2009). Estimating the Worldwide Extent of Illegal Fishing. *PLoS One* 4 (2), e4570. doi: 10.1371/journal.pone.0004570

Alheit, J., and Niquen, M. (2004). Regime Shifts in the Humboldt Current Ecosystem. *Prog. Oceanog.* 60 (2-4), 201–222. doi: 10.1016/j.pocean.2004.02.006

Anderson, T. R., Martin, A. P., Lampitt, R. S., Trueman, C. N., Henson, S. A., and Mayor, D. J. (2019). Quantifying Carbon Fluxes From Primary Production to Mesopelagic Fish Using a Simple Food Web Model. *Ices. J. Mar. Sci.* 76 (3), 690–701. doi: 10.1093/icesjms/fsx234

Barneche, D. R., Hulatt, C. J., Dossena, M., Padfield, D., Woodward, G., Trimmer, M., et al. (2021). Warming Impairs Trophic Transfer Efficiency in a Long-Term Field Experiment. *Nature* 592 (7852), 76–79. doi: 10.1038/s41586-021-03352-2

Bell, J. D., Watson, R. A., and Ye, Y. (2017). Global Fishing Capacity and Fishing Effort From 1950 to 2012. *Fish. Fisheries.* 18 (3), 489–505. doi: 10.1111/faf.12187

Bhathal, B., and Pauly, D. (2008). 'Fishing Down Marine Food Webs' and Spatial Expansion of Coastal Fisheries in India 1950–2000. *Fish. Res.* 91 (1), 26–34. doi: 10.1016/j.fishres.2007.10.022

Bluemel, J. K., Fischer, S. H., Kulka, D. W., Lynam, C. P., and Ellis, J. R. (2022). Decline in Atlantic Wolffish Anarhichas Lupus in the North Sea: Impacts of Fishing Pressure and Climate Change. *J. Fish. Biol.* 100 (1), 253–267. doi: 10.1111/jfb.14942

Branch, T. A., Watson, R., Fulton, E. A., Jennings, S., McGilliard, C. R., Pablico, G. T., et al. (2010). The Trophic Fingerprint of Marine Fisheries. *Nature* 468 (7322), 431–435. doi: 10.1038/nature09528

Butchart, S. H., Walpole, M., Collen, B., Van Strien, A., Scharlemann, J. P., Almond, R. E., et al. (2010). Global Biodiversity: Indicators of Recent Declines. *Science* 328 (5982), 1164–1168. doi: 10.1126/science.1187512

Capuzzo, E., Lynam, C. P., Barry, J., Stephens, D., Forster, R. M., Greenwood, N., et al. (2018). A Decline in Primary Production in the North Sea Over 25 Years, Associated With Reductions in Zooplankton Abundance and Fish Stock Recruitment. *Global. Change. Biol.* 24 (1), e352–e364. doi: 10.1111/gcb.13916

Chassot, E., Bonhommeau, S., Dulvy, N. K., Mélin, F., Watson, R., Gascuel, D., et al. (2010). Global Marine Primary Production Constrains Fisheries Catches. *Ecol. Lett.* 13 (4), 495–505. doi: 10.1111/j.1461-0248.2010.01443.x

Chen, C. (1996). The Kuroshio Intermediate Water is the Major Source of Nutrients on the East China Sea Continental Shelf. *Oceanol. Acta* 19 (5), 523–527.

Conti, L., and Scardi, M. (2010). Fisheries Yield and Primary Productivity in Large Marine Ecosystems. *Mar. Ecol. Prog. Ser.* 410, 233–244. doi: 10.3354/meps08630

Dadswell, M., Spares, A., Reader, J., McLean, M., McDermott, T., Samways, K., et al. (2022). The Decline and Impending Collapse of the Atlantic Salmon (Salmo Salar) Population in the North Atlantic Ocean: A Review of Possible Causes. *Rev. Fish. Sci. Aquac.* 30 (2), 1–44. doi: 10.1080/23308249.2021.1937044

Degerman, R., Lefébure, R., Byström, P., Båmstedt, U., Larsson, S., and Andersson, A. (2018). Food Web Interactions Determine Energy Transfer Efficiency and Top Consumer Responses to Inputs of Dissolved Organic Carbon. *Hydrobiologia* 805 (1), 131–146. doi: 10.1007/s10750-017-3298-9

Ding, Q., Shan, X., and Jin, X. (2020). Ecological Footprint and Vulnerability of Marine Capture Fisheries in China. *Acta Oceanol. Sin.* 39 (4), 100–109. doi: 10.1007/s13131-019-1468-y

Eddy, T. D., Bernhardt, J. R., Blanchard, J. L., Cheung, W. W., Colléter, M., Du Pontavice, H., et al. (2021). Energy Flow Through Marine Ecosystems: Confronting Transfer Efficiency. *Trends Ecol. Evol.* 36 (1), 76–86. doi: 10.1016/j.tree.2020.09.006

Fakhraee, M., Planavsky, N. J., and Reinhard, C. T. (2020). The Role of Environmental Factors in the Long-Term Evolution of the Marine Biological Pump. *Nat. Geosci.* 13 (12), 812–816. doi: 10.1038/s41561-020-00660-6

Fromentin, J. M. (2009). Lessons From the Past: Investigating Historical Data From Bluefin Tuna Fisheries. *Fish. Fisheries.* 10 (2), 197–216. doi: 10.1111/j.1467-2979.2008.00311.x

Garibaldi, L., and Limongelli, L. (2003). Trends in Oceanic Captures and Clustering of Large Marine Ecosystems. *Two Stud. based. FAO capture. database* 639 (2), 435.

Grainger, R. J., and Garcia, S. M. (1996). "Trend Analysis and Fisheries Potential," in *Chronicles of Marine Fishery Landings, (1950-1994)* (Rome: FAO).

Gutiérrez, D., Akester, M., and Naranjo, L. (2016). Productivity and Sustainable Management of the Humboldt Current Large Marine Ecosystem Under Climate Change. *Environ. Dev.* 17, 126–144. doi: 10.1016/j.envdev.2015.11.004

He, X., and Field, J. C. (2019). Effects of Recruitment Variability and Fishing History on Estimation of Stock-Recruitment Relationships: Two Case Studies From US West Coast Fisheries. *Fish. Res.* 217, 21–34. doi: 10.1016/j.fishres.2018.06.001

Henson, S., Le Moigne, F., and Giering, S. (2019). Drivers of Carbon Export Efficiency in the Global Ocean. *Global. Biogeochem. Cy* 33 (7), 891–903. doi: 10.1029/2018GB006158

Hutchings, J. A., and Kuparinen, A. (2020). Implications of Fisheries-Induced Evolution for Population Recovery: Refocusing the Science and Refining its Communication. *Fish. Fisheries.* 21 (2), 453–464. doi: 10.1111/faf.12424

Jin, X., and Tang, Q. (1996). Changes in Fish Species Diversity and Dominant Species Composition in the Yellow Sea. *Fish. Res.* 26 (3-4), 337–352. doi: 10.1016/0165-7836(95)00422-X

Knight, B. R., and Jiang, W. (2009). Assessing Primary Production Constraints in New Zealand Fisheries. *Fish. Res.* 100 (1), 15–25. doi: 10.1016/j.fishres.2009.06.001

Krumme, U., Wang, T. C., and Wang, D. R. (2013). From Food to Feed: Assessment of the Stationary Lift Net Fishery of East Hainan, Northern South China Sea. *Cont. Shelf. Res.* 57, 105–116. doi: 10.1016/j.csr.2012.04.011

Lam, V. W., and Pauly, D. (2019). Status of Fisheries in 13 Asian Large Marine Ecosystems. *Deep. Sea. Res. Part II* 163, 57–64. doi: 10.1016/j.dsr2.2018.09.002

Liang, C., and Pauly, D. (2017). Fisheries Impacts on China's Coastal Ecosystems: Unmasking a Pervasive 'Fishing Down'effect. *PLoS One* 12 (3), e0173296. doi: 10.1371/journal.pone.0173296

Liang, C., and Pauly, D. (2020). Masking and Unmasking Fishing Down Effects: The Bohai Sea (China) as a Case Study. *Ocean. Coast. Manage.* 184, 105033. doi: 10.1016/j.ocecoaman.2019.105033

Liu, K.-K., Chao, S.-Y., Shaw, P.-T., Gong, G.-C., Chen, C.-C., and Tang, T. (2002). Monsoon-Forced Chlorophyll Distribution and Primary Production in the South China Sea: Observations and a Numerical Study. *Deep. Sea. Res. Part I* 49 (8), 1387–1412. doi: 10.1016/S0967-0637(02)00035-3

Lu, Z., Gan, J., Dai, M., Zhao, X., and Hui, C. R. (2020). Nutrient Transport and Dynamics in the South China Sea: A Modeling Study. *Prog. Oceanogr.* 183, 102308. doi: 10.1016/j.pocean.2020.102308

Mahesh, V., Dineshbabu, A. P., Naik, A., Anjanayappa, H. N., and Khavi, M. (2019). Characterization of Low Value Bycatch in Trawl Fisheries Off Karnataka Coast, India and its Impact on Juveniles of Commercially Important Fish Species. *Indian J. Mar. Sci.* 48 (11), 1733–1742.

Mashjoor, S., Jamebozorgi, F. H., and Kamrani, E. (2018). Fishery-Induced Inter-Annual Changes in the Mean Trophic Level, the Northern Sea of Oman Off the Iranian Coast 2002–2011. *Ocean. Sci. J.* 53 (4), 655–665. doi: 10.1007/s12601-018-0046-7

Mcowen, C. J., Cheung, W. W., Rykaczewski, R. R., Watson, R. A., and Wood, L. J. (2015). Is Fisheries Production Within L Arge M Arine E Cosystems Determined by Bottom-Up or Top-Down Forcing? *Fish. Fisheries.* 16 (4), 623–632. doi: 10.1111/faf.12082

Mehner, T., Lischke, B., Scharnweber, K., Attermeyer, K., Brothers, S., Gaedke, U., et al. (2018). Empirical Correspondence Between Trophic Transfer Efficiency in Freshwater Food Webs and the Slope of Their Size Spectra. *Ecology* 99 (6), 1463–1472. doi: 10.1002/ecy.2347

Morissette, L., Christensen, V., and Pauly, D. (2012). Marine Mammal Impacts in Exploited Ecosystems: Would Large Scale Culling Benefit Fisheries? *PLoS One* 7 (9), e43966. doi: 10.1371/journal.pone.0043966

Nixon, S. W. (1982). Nutrient Dynamics, Primary Production and Fisheries Yields of Lagoons. *Oceanol. Acta. Special. Issue* 4, 357–71.

Nixon, S. W. (1992). Quantifying the Relationship Between Nitrogen Input and the Productivity of Marine Ecosystem. *Pro. Adv. Mar. Tech. Conf. Tokyo* 5, 57–83.

Oglesby, R. T. (1977). Relationships of Fish Yield to Lake Phytoplankton Standing Crop, Production, and Morphoedaphic Factors. *J. Fisheries. Board. Canada.* 34 (12), 2271–2279. doi: 10.1139/f77-305

Olsen, E. M., Carlson, S. M., Gjøsæter, J., and Stenseth, N. C. (2009). Nine Decades of Decreasing Phenotypic Variability in Atlantic Cod. *Ecol. Lett.* 12 (7), 622–631. doi: 10.1111/j.1461-0248.2009.01311.x

Pang, Y., Tian, Y., Fu, C., Wang, B., Li, J., Ren, Y., et al. (2018). Variability of Coastal Cephalopods in Overexploited China Seas Under Climate Change With Implications on Fisheries Management. *Fish. Res.* 208, 22–33. doi: 10.1016/j.fishres.2018.07.004

Pauly, D. (2018). A Vision for Marine Fisheries in a Global Blue Economy. *Mar. Policy* 87, 371–374. doi: 10.1016/j.marpol.2017.11.010

Pauly, D., Belhabib, D., Blomeyer, R., Cheung, W. W., Cisneros-Montemayor, A. M., Copeland, D., et al. (2014). China's Distant-Water Fisheries in the 21st Century. *Fish. Fisheries.* 15 (3), 474–488. doi: 10.1111/faf.12032

Pauly, D., and Christensen, V. (1995). Primary Production Required to Sustain Global Fisheries. *Nature* 374 (6519), 255–257. doi: 10.1038/374255a0

Pauly, D., Christensen, V., Dalsgaard, J., Froese, R., and Torres, F. (1998). Fishing Down Marine Food Webs. *Science* 279 (5352), 860–863. doi: 10.1126/science.279.5352.860

Pauly, D., and Froese, R. (2012). Comments on FAO's State of Fisheries and Aquaculture, or 'SOFIA 2010'. *Mar. Policy* 36 (3), 746–752. doi: 10.1016/j.marpol.2011.10.021

Pauly, D., and Liang, C. (2020). The Fisheries of the South China Sea: Major Trends Since 1950. *Mar. Policy* 121, 103584. doi: 10.1016/j.marpol.2019.103584

Rosenberg, A. A., Fogarty, M. J., Cooper, A. B., Dickey-Collas, M., Fulton, E. A., Gutiérrez, N. L., et al. (2014). Developing New Approaches to Global Stock Status Assessment and Fishery Production Potential of the Seas. *FAO Fisheries. Aquaculture. Circular.* Rome: FAO 1086, 175.

Selig, E. R., Hole, D. G., Allison, E. H., Arkema, K. K., McKinnon, M. C., Chu, J., et al. (2019). Mapping Global Human Dependence on Marine Ecosystems. *Conserv. Lett.* 12 (2), e12617. doi: 10.1111/conl.12617

Sguotti, C., Otto, S. A., Frelat, R., Langbehn, T. J., Ryberg, M. P., Lindegren, M., et al. (2019). Catastrophic Dynamics Limit Atlantic Cod Recovery. *P. Roy.l Soc B* 286 (1898), 20182877. doi: 10.1098/rspb.2018.2877

Sharma, P., Marinov, I., Cabre, A., Kostadinov, T., and Singh, A. (2019). Increasing Biomass in the Warm Oceans: Unexpected New Insights From SeaWiFS. *Geophys. Res. Lett* 46 (7), 3900–10. doi: 10.1029/2018GL079684

Sherman, K., and Hamukuaya, H. (2016). Sustainable Development of the World's Large Marine Ecosystems. *Environ. Dev.* 17, 1–6. doi: 10.1016/j.envdev.2015.12.002

Siswanto, E., Honda, M. C., Matsumoto, K., Sasai, Y., Fujiki, T., Sasaoka, K., et al. (2016). Sixteen-Year Phytoplankton Biomass Trends in the Northwestern Pacific Ocean Observed by the SeaWiFS and MODIS Ocean Color Sensors. *J. Oceanogr.* 72 (3), 479–489. doi: 10.1007/s10872-016-0357-1

Steadman, D., Appleby, T., and Hawkins, J. (2014). Minimising Unsustainable Yield: Ten Failing European Fisheries. *Mar. Policy* 48, 192–201. doi: 10.1016/j.marpol.2014.03.030

Stock, C. A., John, J. G., Rykaczewski, R. R., Asch, R. G., Cheung, W. W., Dunne, J. P., et al. (2017). Reconciling Fisheries Catch and Ocean Productivity. *Proc. Natl. Acad. Sci.* 114 (8), E1441–E1449. doi: 10.1073/pnas.1610238114

Sumaila, U. R. (2019). Comparative Valuation of Fisheries in Asian Large Marine Ecosystems With Emphasis on the East China Sea and South China Sea LMEs. *Deep. Sea. Res. Part II* 163, 96–101. doi: 10.1016/j.dsr2.2018.12.008

Sumaila, U. R., and Cheung, W. W. (2015). *Boom or Bust: The Future of Fish in the South China Sea* (Vancouver, BC: University of British Columbia).

Unsworth, R. K., Nordlund, L. M., and Cullen-Unsworth, L. C. (2019). Seagrass Meadows Support Global Fisheries Production. *Conserv. Lett.* 12 (1), e12566. doi: 10.1111/conl.12566

Wan, R., and Bian, X. (2012). Size Variability and Natural Mortality Dynamics of Anchovy Engraulis Japonicus Eggs Under High Fishing Pressure. *Mar. Ecol. Prog. Ser.* 465, 243–251. doi: 10.3354/meps09795

Ware, D. M., and Thomson, R. E. (2005). Bottom-Up Ecosystem Trophic Dynamics Determine Fish Production in the Northeast Pacific. *Science* 308 (5726), 1280–1284. doi: 10.1126/science.1109049

Watson, R. A., Cheung, W. W., Anticamara, J. A., Sumaila, R. U., Zeller, D., and Pauly, D. (2013). Global Marine Yield Halved as Fishing Intensity Redoubles. *Fish. Fisheries.* 14 (4), 493–503. doi: 10.1111/j.1467-2979.2012.00483.x

Watson, R. A., and Morato, T. (2013). Fishing Down the Deep: Accounting for Within-Species Changes in Depth of Fishing. *Fish. Res.* 140, 63–65. doi: 10.1016/j.fishres.2012.12.004

Watson, R., and Pauly, D. (2001). Systematic Distortions in World Fisheries Catch Trends. *Nature* 414 (6863), 534–536. doi: 10.1038/35107050

Watson, R., and Pauly, D. (2014). Coastal Catch Transects as a Tool for Studying Global Fisheries. *Fish. Fisheries.* 15 (3), 445–455. doi: 10.1111/faf.12025

Watson, R., Zeller, D., and Pauly, D. (2014). Primary Productivity Demands of Global Fishing Fleets. *Fish. Fisheries.* 15 (2), 231–241. doi: 10.1111/faf.12013

Winter, A. M., Richter, A., and Eikeset, A. M. (2020). Implications of Allee Effects for Fisheries Management in a Changing Climate: Evidence From Atlantic Cod. *Ecol. Appl.* 30 (1), e01994. doi: 10.1002/eap.1994

Yang, B., Herrmann, B., Yan, L., Li, J., and Wang, T. (2021). Effects of Six Codend Meshes on the Size Selection of Juvenile White Croaker (Pennahia Argentata) in Demersal Trawl Fishery of the South China Sea. *PLoS One* 16 (7), e0253723. doi: 10.1371/journal.pone.0253723

Yu, X., and Zhang, Z. (2005). Characteristics of Neogene Depositional Systems on the Northern Continental Slope of the South China Sea and Their Relationships With Gas Hydrate. *Geology. China* 32 (3), 470–476.

Zeller, D., and Pauly, D. (2016). Catch Reconstruction: Concepts, Methods, and Data Sources. *Global Atlas. Mar. Fisheries.: A. Crit. Appraisal. Catches. Ecosystem. Impacts.* 59 (5), 12–33.

Zhang, W., Liu, M., Sadovy de Mitcheson, Y., Cao, L., Leadbitter, D., Newton, R., et al. (2020). Fishing for Feed in China: Facts, Impacts and Implications. *Fish. Fisheries.* 21 (1), 47–62. doi: 10.1111/faf.12414

Zhang, K., Zhang, J., Xu, Y., Sun, M., Chen, Z., and Yuan, M. (2018). Application of a Catch-Based Method for Stock Assessment of Three Important Fisheries in the East China Sea. *Acta Oceanol. Sin.* 37 (2), 102–109. doi: 10.1007/s13131-018-1173-9

**Conflict of Interest:** The authors declare that the research was conducted in the absence of any commercial or financial relationships that could be construed as a potential conflict of interest.

**Publisher's Note:** All claims expressed in this article are solely those of the authors and do not necessarily represent those of their affiliated organizations, or those of the publisher, the editors and the reviewers. Any product that may be evaluated in this article, or claim that may be made by its manufacturer, is not guaranteed or endorsed by the publisher.

frontiers | Frontiers in Marine Science

ORIGINAL RESEARCH
published: 13 July 2022
doi: 10.3389/fmars.2022.921595

# Species and Functional Dynamics of the Demersal Fish Community and Responses to Disturbances in the Pearl River Estuary

*Zeyu Zeng[1], William W. L. Cheung[2], Han Lai[1], Huadong Yi[1], Sheng Bi[1], Haiyang Li[1], Xiaoli Chen[1], Yuqin Su[1], Xuange Liu[1], Qiuxian Chen[1], Zhilun Zhang[1], Xuchong Wei[1], Jiahui Chen[1] and Guifeng Li[1]**

[1] State Key Laboratory of Biocontrol, Southern Marine Science and Engineering Guangdong Laboratory (Zhuhai), School of Life Sciences, Sun Yat-Sen University, Guangzhou, China, [2] Institute for the Oceans and Fisheries, The University of British Columbia, Vancouver, BC, Canada

OPEN ACCESS

**Edited by:**
Jun Xu,
Institute of Hydrobiology (CAS), China

**Reviewed by:**
Meilin Wu,
South China Sea Institute of Oceanology (CAS), China
Li Liu,
South China Agricultural University, China

***Correspondence:**
Guifeng Li
liguif@mail.sysu.edu.cn

**Specialty section:**
This article was submitted to Marine Ecosystem Ecology, a section of the journal Frontiers in Marine Science

**Received:** 16 April 2022
**Accepted:** 31 May 2022
**Published:** 13 July 2022

**Citation:**
Zeng Z, Cheung WWL, Lai H, Yi H, Bi S, Li H, Chen X, Su Y, Liu X, Chen Q, Zhang Z, Wei X, Chen J and Li G (2022) Species and Functional Dynamics of the Demersal Fish Community and Responses to Disturbances in the Pearl River Estuary. Front. Mar. Sci. 9:921595. doi: 10.3389/fmars.2022.921595

Fishery resources are threatened by environmental changes and anthropogenic pressures, particularly in coastal ecosystems. It is crucial to understand the changes of fish communities and their responses to environmental changes and human disturbances to formulate rational fisheries and ecosystem-based management. The Pearl River Estuary (PRE) is a typical sub-tropic coastal ecosystem located in the center of the Guangdong-Hong Kong-Macao Greater Bay Area in the northern South China Sea. The demersal fish in the PRE is traditionally targeted as commercial fishing and severely impacted by overexploitation and hypoxia in the last few decades. In this study, we analyze the fish survey data during the period of 2020~2021 using multivariate statistics to investigate the impacts of human disturbances on the species and functional dynamics of the demersal fish community in the PRE. The results reveal that dissolved oxygen and temperature have significant correlations with the functional traits of the demersal fish community. The impacts of hypoxia on the demersal fish vary with species and locations. We found that the mean functional redundancy of the demersal fish community in the PRE was high across three surveys, but the functional diversity was low in this region. The abundance and richness of the demersal fish community increased during the summer fishing moratorium in the South China Sea in 2021, but the functional diversity did not increase significantly. We conclude that the high functional redundancy in the PRE might not be sufficient to buffer against environmental disturbances because of its low functional diversity. Our study highlights the complicated interactions between the demersal fish community and disturbances in the PRE. Understanding the traits structure and functional diversity of the fish community can help elucidate the factors determining the dynamic responses of the fish community to disturbances.

**Keywords: demersal fish community, functional diversity, functional redundancy, hypoxia, Pearl River Estuary (PRE)**

## INTRODUCTION

Over-exploitation, climate changes, pollution and other anthropogenic pressures are threatening the sustainability of global marine ecosystems and fishery resources (Rouyer et al., 2008; Cheung et al., 2013; Frelat et al., 2018). These human pressures play important roles in shaping the spatial distribution of marine species (Perry et al., 2005; Poloczanska et al., 2016; Frelat et al., 2018), impacting the temporal dynamics of communities and ecosystem functions (Rouyer et al., 2008; Mollmann et al., 2009; Brind'Amour et al., 2011; Asefa et al., 2017).

The resilience of communities to environmental changes and disturbances depends on the biological traits, species and functional diversity of communities (Cadotte, 2017; Craven et al., 2018; McLean et al., 2019). Species' persistence is dependent on environmental conditions and the adaptability of their biological traits. Functional diversity of the community, which is dependent on the functional traits of species, decreases in more extreme environmental conditions where a subset of traits can adapt (Mouillot et al., 2014; McLean et al., 2019). When several species perform similar functions, functional redundancy of communities occurs. It can prevent the loss of communities' functions caused by the declines in the species and functional diversity (Yachi and Loreau, 1999; Fonseca and Ganade, 2001). Thus, community studies should focus on not only the change of species but also the change in community function and even the interrelation between functional diversity and distributions.

In the marine realm, estuaries are important transitional regions for the material exchanges between land and ocean ecosystems, and generally host remarkable diversity of fishes. Fish communities sustain key ecosystem processes and provide fishery resources in estuary ecosystems. However, the fish communities in estuaries face high pressure due to overfishing and changes in environmental conditions (Duan et al., 2009; Cornwall and Eddy, 2015; Gobler and Baumann, 2016). Acidification and hypoxia in bottom water in temperate and tropical estuaries were frequently reported (Gobler and Baumann, 2016; Marshall et al., 2017).

The Pearl River Estuary (PRE) is a typical subtropical estuary ecosystem, a traditional fishing ground and an important nursery ground for many species (Jia et al., 2005). In the last decades, human pressures have deteriorated the water conditions and fish community in the PRE (Jia et al., 2005; Ke et al., 2007). For instance, the hypoxia in the bottom water expanded the intensity and influence range since being discovered in 1985, which directly impacts the demersal fish community in the PRE (Yin et al., 2004; Wang et al., 2018; Cui et al., 2019). Demersal fishes are the traditional commercial fishes in the PRE, and have experienced over-exploitation since 1978 because of the high increase in the number of fishing boats and the advance in the fishing technology (Jia et al., 2005). The PRE can be a typical overexploited estuary ecosystem to analyze the dynamics of the demersal fish community and the response to distributions.

In the last two decades, multivariate statistical analysis have been developed and provide ecologists with tools to investigate the relationships between species, functional traits and environmental conditions (Dray et al., 2003; Villeger et al., 2008; Laliberte and Legendre, 2010; Dray et al., 2014; Frelat et al., 2018). In this study, we used multivariate statistical analysis to analyze the temporal and spatial variations of species, the dynamics of trait structure, the functional diversity and the functional redundancy of the demersal fish community, and further explore the impacts of environmental variation on the demersal fish community in the PRE.

## MATERIALS AND METHODS

### Fish Abundance Data

We focus on the demersal fish community in the PRE. Since 2020, we conducted three surveys, two in summer (August 2020 and July 2021) and another in winter (December 2020). The summer survey in 2021 was carried out during the fishing moratorium in the South China Sea, including the PRE. The bottom trawl boat used in our surveys is about 120 tons with an engine power of 138 kW. The surveys were conducted at 4 knots for about 30 minutes on average. The surveys covered most of the shallow areas of the PRE (**Figure 1**). Three surveys include 66 hauls, around 20-24 hauls per survey in the same spatial coverage of the PRE. Fish catches were stored frozen by sites and taken to the laboratory for species identification. We removed the rare and pelagic fish species, which are less than 0.01% of the total abundance of the recorded species in our surveys. Finally, we got 80 fish species from 66 hauls in the PRE.

### Fish Traits Dataset and Environmental Variables in the PRE

Ecological traits, which are associated to the energy transfer, the environmental filtering and biological interactions, are usually taken into consideration in community studies because they can be used to describe the ecosystem processes and species' responses to environmental changes (McLean et al., 2018; McLean et al., 2019). we integrated six ecological traits to examine the dynamic processes of communities, including

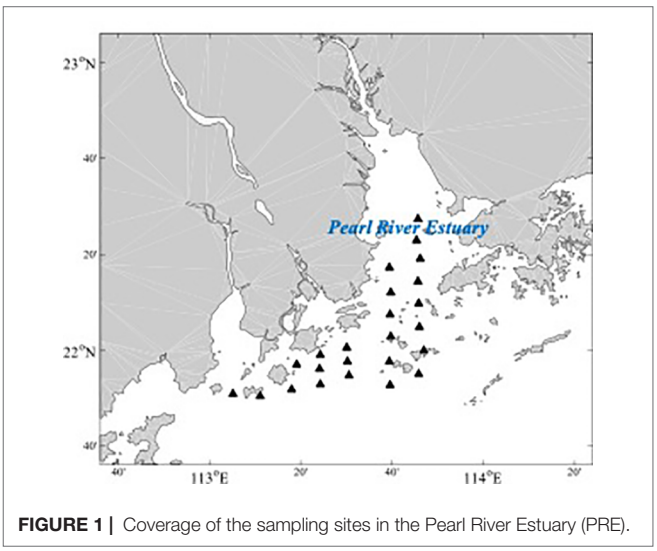


**FIGURE 1 |** Coverage of the sampling sites in the Pearl River Estuary (PRE).

body size, trophic level, the resilience ability of species, salinity preference and habitat preference in the water column position (**Table S6**). The functional traits we used in this study represent the trophic ecology, morphologic characteristics, life history and habitat preference of fish species, referring to Mouillot et al. (2014). The salinity preference and water column position of the species are adopted to describe the ecological traits of fish species in estuary ecosystems. The detailed information on species traits was obtained from the Fishbase (https://www.fishbase.se/search.php). Environmental variables can shape the structure of fish communities since species tend to live in their preferred environment (Frelat et al., 2018). Temperature, dissolved oxygen (DO) and pH of the bottom water and the average depth of each site are taken into account in this study.

## RLQ Analysis and Fourth-Corner Method

The multivariate statistic methodologies allow ecologists to investigate the impacts of environmental variables on the temporal, spatial and functional dynamics of communities simultaneously (Frelat et al., 2018). We applied the RLQ analysis and fourth-corner method to clarify the relationships among the fish distribution, the community composition, the species traits and environmental variables in the PRE. The RLQ analysis and the fourth-corner approach are the most integrated methods for analyzing trait–environment relationships (Kleyer et al., 2012). The RLQ analysis is an extension method of co-inertia analysis to simultaneously perform the ordinations of three matrices, the abundance data (called A or L), the matrix of species by biological or behavioral traits (called B or Q) and the matrix of sites by habitat characteristics (called C or R) (**Figure 2**). The fourth-corner method uses the formula, $D=Q'L'R$ *or* $D=R'LQ$, to calculate the matrix $D$ and test the significance of the species traits and environmental characteristics (Legendre and Legendre, 2012; Borcard et al., 2018).

## Diversity Indices

### Beta Diversity

Beta diversity can reflect the spatial variance of the community composition in a region by measuring variations in species composition and abundance among all sites (Anderson et al., 2006). We use a method independent from alpha and gamma diversity to estimate the beta diversity, which is the total variance

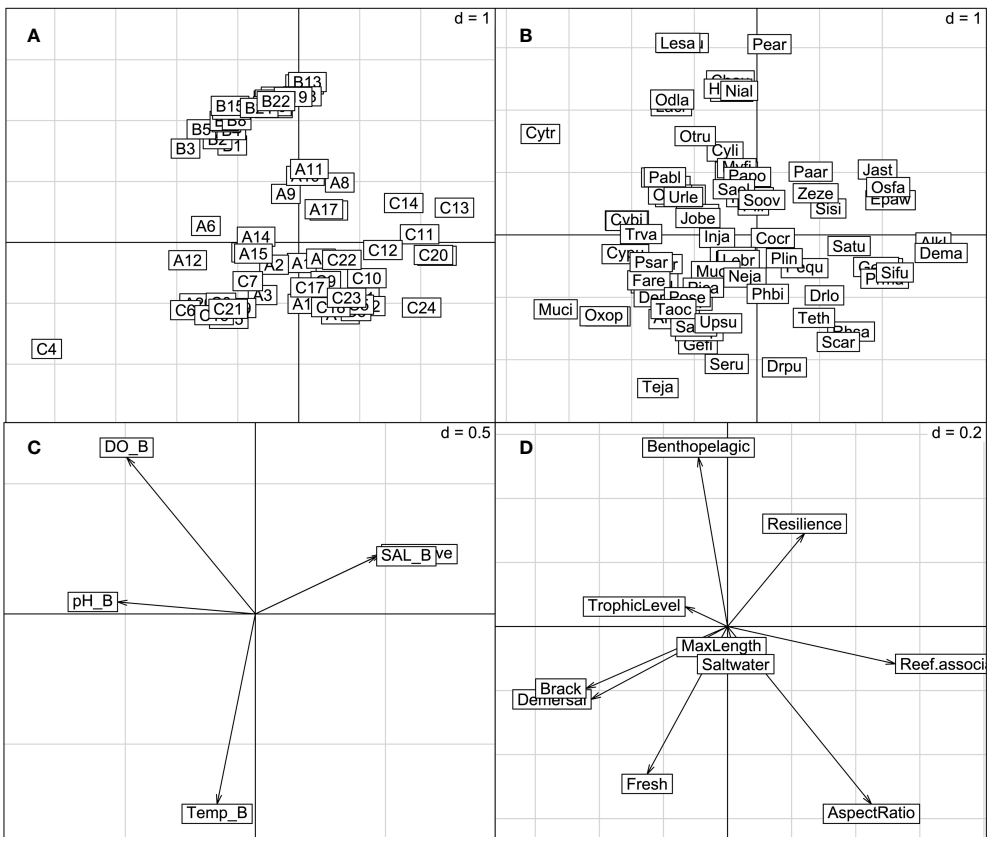


**FIGURE 2 |** Results of the RLQ analysis on the demersal fish community in the PRE: **(A)** the site (L) scores, **(B)** the species (Q) scores, **(C)** the environmental variables and **(D)** the species traits. Ai, Bi and Ci in **(A)** are the sampling sites in August 2020, December 2020 and July 2021, respectively (**Table S1, S2 and S3**). The acronyms with four letters in **(B)** are the species in the PRE (**Table S4**). The variates in **(C)** are the environmental variables, where DO_B is the DO in the bottom water, pH_D is the pH in the bottom water, Temp_D is the temperature in the bottom water and Depth_Ave is the average depth of the sampling site. The acronyms in **(D)** are the functional traits of species (**Table S6**).

of the site-by-species table Y, Var(Y), called $BD_{Total}$ (Borcard et al., 2018). The $BD_{Total}$ is written as

$$BD_{Total} = Var(Y) = SS_{Total} / (n-1)$$

where the $SS_{Total}$ is the total sum-of-squares of Y (Legendre and De Caceres, 2013; Borcard et al., 2018).

Beta diversity results from the processes of species replacement and richness difference (species gain and loss) (Williams, 1996; Lennon et al., 2001; Borcard et al., 2018). In this study, Podani's Jaccard-based indices were adopted to describe the richness difference and replacement values of the sampling sites. We used the triangle plots to show the richness difference, replacement and the corresponding similarity of all pairs of the sites. The points in triangle plots represent the triplet of values of a pair of sites, which correspond to the similarity (1-D), replacement (Repl) and richness difference (RichDiff) (Legendre, 2014).

### Functional Diversity and Functional Redundancy Indices

Four distance-based multi-trait diversity indices, including functional richness (FRic), functional evenness (Feve), functional divergence (Fdiv) and functional dispersion (Fdis), were proposed by Villeger et al. (2008) and Laliberte and Legendre. (2010). They were independent components in the functional diversity of the demersal fish community in the PRE and are related to or can be used to measure the functional space of a given community, the regularity of the abundance distribution in the multidimensional function space and species abundances distributing within the functional trait space (Villeger et al., 2008; Laliberte and Legendre, 2010).

The inverse Simpson diversity (TD) can represent the potential maximum value of the functional diversity in a community (de Bello et al., 2010; Borcard et al., 2018). The difference between the inverse Simpson diversity and the functional diversity (FD) can be used to measure functional redundancy (FR) (de Bello et al., 2007). Functional diversity is described by using the Rao coefficient, which is calculated as the sum of trait dissimilarities between pairs of species, multiplied by species abundance (Leps et al., 2007). The difference between species *i* and species *j* ($d_{ij}$) is conducted by the dissimilarities in functional traits.

$$FD = Q = \sum_{i=1}^{q}\sum_{j=1}^{q} d_{ij} p_{ic} p_{jc}$$

Because the number of traits may influence the results of the functional indices (Guillemot et al., 2011), we also performed sensitivity analyses to test the robustness of the functional indices by rerunning all analyses with all combinations of five traits out of six. We did not reduce the number of traits to less than five to process the sensitivity analyses to keep the important dimensions of the functional space of fish assemblage (McLean et al., 2019).

## RESULTS

### Traits and Distributions of the Demersal Fish Community Linked With Environmental Variables in the PRE

A total of 6930 individuals representing 80 species were sampled in our study (**Table S1–S3**). There are 36 common species found in the three surveys (**Figure S1**), but the dominant species are different in each survey. The most abundant species were *Ambassis gymnocephalus*, *Johnius belangerii* and *Decapterus maruadsi* for the three surveys, respectively (**Table S5**). The sampling sites were divided into summer and winter sub-assemblages, based on the Ward hierarchical clustering. The environmental variables in the summer are characterized by higher water temperature and lower oxygen concentrations, compared to those in winter (**Figure 2**). DO of bottom water reduced sharply during the summer investigation in 2021. Most of the sites underwent hypoxia processes (**Table S3**), and the DO of sites C9, C11, C12, C18, C19, C20, C23 and C24 were even less than 2.0 mg/l (**Table S3**).

The main relationships between fish traits and environmental variables can be explained by the first two RLQ axes. The right (positive) part of the first RLQ axis identifies species of reef-associated habitat preference, such as *Decapterus maruadsi*, *Priacanthus macracanthus*, *Siganus fuscescens* and *Saurida tumbil* (**Figures 2A, C**), which are mainly located at the hypoxia areas in the summer of 2021 (**Figure 2B**). The left part of the first RLQ axis distinguished the species of high trophic levels and habitat preference of the brackish and demersal. The second RLQ axis profiles the assemblages of the winter and summer sampling sites. The positive part associated the winter sampling sites with high salinity and low temperature. The related species, *Cynoglossus lineolatus*, *Lepturacanthus savala* and *Odontamblyopus lacepedii*, were mainly caught in these sites (**Figures 2A, C**). The negative part of the axis was associated with the summer sampling sites, and the species *Drepane punctate, Photopectoralis bindus, Secutor ruconius* and *Upeneus sulphureus* distributed throughout these sites.

The D matrix shows detailed interpretations of the traits of the demersal fish and environment variables in the PRE. According to the results, the temperature and DO of the bottom water were strongly linked with the traits of benthopelagic, the preference for saltwater habitat and the aspect ratio of the caudal fin of the demersal fish in the PRE (**Figure 3**). For instance, the trait of preference for saltwater habitat is positively associated with the temperature in the bottom water but negatively related with the DO in the bottom water. The aspect ratio of the caudal fin of fishes, as the only morphological trait taken into consideration, is negatively associated with the DO of the bottom water. It indicates that the species with a small aspect ratio tend to distribute in non-hypoxic areas. Based on the analysis results of RLQ, the species with a small aspect ratio, such as the *Cynoglossus lineolatus and Cynoglossus puncticeps*, were mainly caught in the winter of 2020, and these species were also found in the sites with high DO in summer (**Figure 2**).

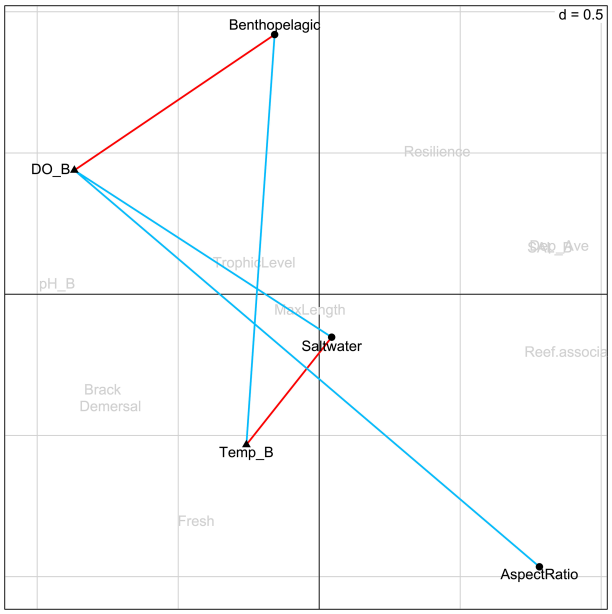


**FIGURE 3 |** Biplot of the fish traits and environmental variables from the RLQ analysis. The significant positive correlations between fish traits and environmental variables are represented by red cells and negative ones by blue cells, which are obtained from the multiple testing using the FDR (false discovery rate) procedure with the $\alpha = 0.05$ level. DO_B is the DO in the bottom water; Temp_D is the temperature in the bottom water; Benthopelagic is the trait of species for water column position; Saltwater is the trait of species of salinity preference; AspectRatio is the trait of species of the aspect ratio of the caudal fin. See **Table S6** for acronyms of traits.

## Community Structure and Functional Diversity of the Demersal Fish in the PRE

The beta diversity indices, representing the spatial variations of the demersal fish structure, are 0.71, 0.63, and 0.79 for the summer and winter in 2020 and the summer in 2021, respectively (**Table 1**). According to the indices of pairwise sites in the similarity, replacement and richness difference, the among-site variations of the demersal fish community were dominated by replacement with the means of 0.5 in **Figure 4A** and 0.479 in **Figure 4B** for the winter and summer in 2020, respectively. The mean value of richness differences in the summer of 2021 was 0.471, higher than the mean value of replacement 0.396 (**Figure 4C**). Even though there was a relatively higher abundance of fish in the summer, we did not catch any fish in site C19 where the DO reduced to 0.08 mg/L. The environmental factor of the most significant variation is the reduction of DO in the summer of 2021. The results indicate that the hypoxia and anoxia do impact the richness of the fish assemblage in the sampling sites. The impacts of hypoxia depend on the species' tolerance to hypoxia (Wu, 2002).

The alpha functional diversity indices (functional richness, functional evenness, functional divergence and functional dispersion) fluctuated with wide ranges in the PRE (**Table 1**). The mean values of the alpha functional diversity indices of the demersal fish community in summer were generally higher than those in winter (**Table 1**). Functional richness indices were significantly low in winter, which indicated that the functional trait space of the demersal fish community was small in winter. The functional richness increased in summer with the increase of abundance and richness of species. According to the sensitivity analyses (**Figure S2**), our findings on the trends of the functional diversity are robust in the PRE.

The mean functional diversity of the demersal fish community was low across all the surveys in the PRE (**Figure 5**). The mean functional redundancy of the demersal fish community was high in the PRE (**Figure 5**), indicating that many species in this region showed similar functional traits. The functional diversity and the functional redundancyof the demersal fish community in the PRE were characterized by a typical seasonal pattern. The abundance and richness of species increased during the summer fishing moratorium in the South China Sea in 2021. However, there was no significant difference in the functional diversity of the demersal fish community in the PRE during the summer fishing moratorium of 2021 and out of the fishing moratorium in the summer of 2020. On the contrary, the mean functional redundancy decreased in the summer of 2021 during the summer fishing moratorium, showing a mismatch with the increase of the abundance and richness of species. The trends of abundance and richness of species in and out of the fishing moratorium indicate that the summer fishing moratorium in the South China Sea does benefit some demersal fish species. Nevertheless, for the functional diversity of the demersal fish community, there is no significant benefits from the fishing moratorium.

## DISCUSSION

Based on the multivariate analyses and the statistical tests, the sampling sites were separated into the summer cluster and the winter cluster in the PRE. The abundance, richness of fish species

**TABLE 1 |** The species diversity and the functional diversity indices of the demersal fish community in the PRE.

| Index | 2020.08 Mean (Min-Max) | 2020.12 Mean (Min-Max) | 2021.07 Mean (Min-Max) |
|---|---|---|---|
| **$BD_{total}$** | 0.71 | 0.63 | 0.79 |
| **Abundance** | 76 (2-488) | 71 (1-194) | 167.30 (2-1108) |
| **Species richness** | 9.3 (2-16) | 10.72 (1-17) | 12.04 (1-28) |
| **Functional richness** | 0.38 (0.06-0.78) | 0.03 (0.0004-0.31) | 0.53 (0.04-0.87) |
| **Functional evenness** | 0.66 (0.40-0.83) | 0.56 (0.26-0.80) | 0.60 (0.20-0.98) |
| **Functional divergence** | 0.78 (0.35-0.99) | 0.67 (0.48-0.88) | 0.79 (0.52-0.99) |
| **Functional dispersion** | 2.32 (0.25-3.35) | 1.97 (0-2.60) | 2.18 (0-3.21) |

**$BD_{total}$** *is the beta diversity, which is value of the total variance of the site-by-species table Y.*

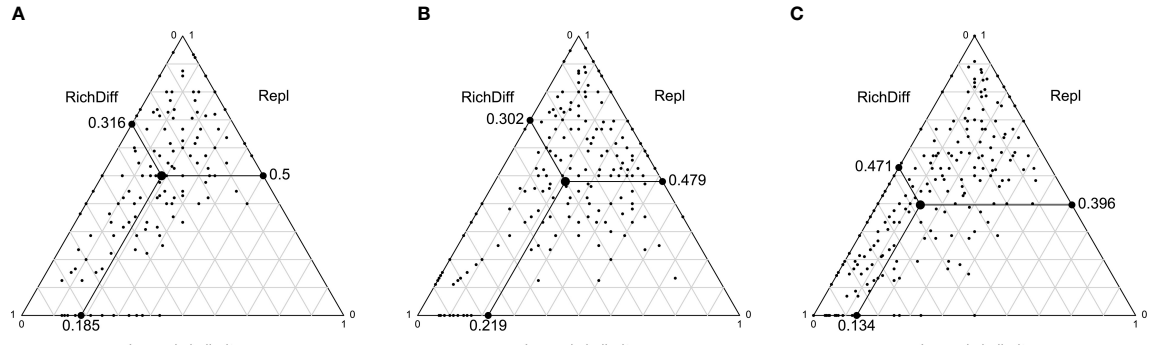


**FIGURE 4 |** Triangle plots of all pairs of sites in the PRE demersal fish data set for the three surveys, based on the Podani indices of richness, abundance difference, replacement and corresponding similarities. The larger black dots in each plot is the mean values of the indices, as well as the position of a "mean pair of sites". RichDiff is the richness difference. Repl is the replacement.

and the composition of the demersal fish community in the PRE change dynamically in summer and winter. The temperature of the bottom water is significantly associated with the functional traits of the demersal fish community. Since our surveys are limited to 2020-2021, the change in water temperature mainly represents the seasonal changes in these two years. However, our findings suggest that temperature is an important factor shaping demersal fish communities in the PRE. Thus, the past and future ocean warming in the South China Sea region are likely to impact the PRE fish community (Cheung et al., 2013; Cheung et al., 2016). The PRE is an important fish breeding ground in the Chinese coastal areas. The seasonal fluctuation of the water temperature could affect the species' reproduction processes that impact fish communities beyond the PRE (Jia et al., 2005). Previous studies also demonstrated that ocean warming would be the main threat to the fish communities and fishery resources in the PRE in the next decades (Zeng et al., 2019). Continuous surveys in the future can provide time-series data that help understand the influences of inter-annual changes of water temperature on the fish communities in the PRE.

Hypoxia in coastal waters impacts the fish community compositions by changing their distributions and abundances all around the world (Breitburg et al., 2018). During our survey period in the summer of 2021, there were serious hypoxia processes in the PRE. In some hypoxia sites, the abundance and richness of the demersal fish did not reduce, while the abundance and richness of the demersal fish reduced sharply in other hypoxia sites such as in the C19, no fish being found. Hypoxia affects the physiological and ecological processes of species, then reduces species distribution in ecosystems (Wu, 2002; Vaquer-Sunyer and

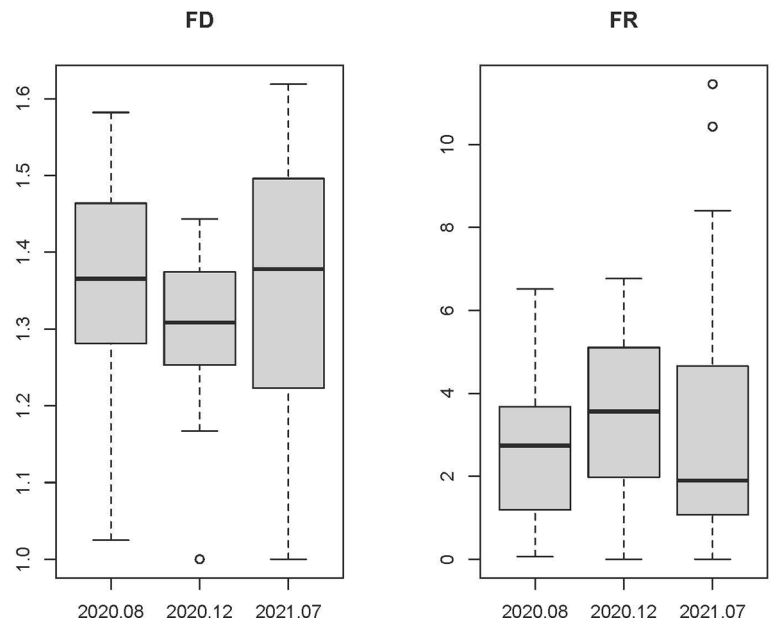


**FIGURE 5 |** Variations in the functional diversity (FD) and functional redundancy (FR) indices of the demersal fish communities in the PRE.

Duarte, 2008; Seibel, 2011; Hughes et al., 2015). Fish species of high tolerance to hypoxia can expand their distributions in the hypoxic areas. Furthermore, hypoxia can alter the predator-prey relationship and foraging dynamics of fish communities, so some species can benefit from decreasing the predation risks of hypoxia progress (Chan et al., 2008; A. A. Keller et al., 2010; A. A. Keller et al., 2015). Zeng et al. (2019) pointed out that the DO decrease was an important potential factor to the ecosystem and fishery resources in the PRE. The fish species and functional groups in the PRE have different sensitivity to the DO change. The impacts of the hypoxia on the demersal fish in the PRE are complicated and vary among species and locations.

According to the insurance hypothesis, the functional redundancy of communities provides communities with a buffer against the impacts of environmental variables, for many species perform similar functions in communities (Sanders et al., 2018). There would be potential declines in the functional diversity, following the loss of species in ecosystems with little functional redundancy among species (Guillemot et al., 2011; Mouillot et al., 2014). In the PRE, the average functional redundancy of the sampling sites was high, while the average functional diversity was low across the three surveys. The abundance and richness of the demersal fish increased during the summer fishing moratorium in 2021, but the functional diversity of the demersal fish community did not significantly change in this period. In the PRE, the high functional redundancy of the demersal fish community may not be able to endure the impacts of environmental changes and anthropogenic pressure with a low functional diversity.

Functional diversity and functional redundancy represent the difference and similarity of interspecific functional traits, and affect the ecosystem function through the ecological complementarity and insurance effect, respectively (Yao et al., 2016). However, there is no necessary connection between the higher trait diversity and higher functional redundancy (Mouillot et al., 2013; McLean et al., 2019). Given the low functional diversity and high functional redundancy in the PRE, there would be alternative explanations for the functional redundancy of such highly exploited coastal ecosystems. In the PRE, the high functional redundancy of the demersal fish community might be attributed to the heavy fishing intensity. Anthropogenic stresses on communities may lead to the homogenization of the trait structure of communities to adapt to environmental changes and perturbations (Diaz and Cabido, 2001; Sasaki et al., 2009; Yao et al., 2016). There has been overexploitation of the fish resources for decades in the PRE (Jia et al., 2005; Duan et al., 2009). With the impact of high fishing intensity, the small fish species with short generation and high resilience, which share similar traits, would become the dominant species (Pauly et al., 1998; Ling et al., 2009; Fisher et al., 2010). The compositions of the organismal traits in ecosystems also impact the resistivity of communities to the disturbances (McLean et al., 2019). McLean et al. (2019) found that the increase of the sensitivity of the climatically vulnerable traits (e.g., small, fast-growing species) caused fish communities in the English Channel and Seychelles Islands ecosystem sensitive to climate change (McLean et al., 2019). In the PRE, this kind of apparent insurance provided by the high redundancy with smaller fish species may hide a high vulnerability to the disturbances of environmental variables and fish pressure.

Our study is limited by the data collected over two years. It is hard to extend the survey data to long-time series data, since such fish community data in the PRE is scarce and not publicly available. Our study focuses on the seasonal and spatial changes of the taxa, traits and functional diversity of the demersal fish community in the PRE. Although the survey data does not allow us to examine the long-term trends in functional diversity and vulnerability, the observed patterns are valuable to understand the response of the demersal fish community to environmental stresses such as hypoxia in the PRE. Our findings can also contribute to the development of ecosystem models to understand the trophodynamics of the PRE ecosystems and their responses to environmental change (Duan et al., 2009; Zeng et al., 2019). Furthermore, because fishing is the main factor shaping the structure of demersal fish in the PRE, further analysis is needed to find out the effects of the functional redundancy on the stability of the demersal fish community and address the relationship between the functional redundancy and the stability of communities.

## SUPPLEMENTARY DATA

We provide the details of the species richness, abundance and dissolved oxygen of the bottom water of sampling sites, the ecological traits used in this study, and the sensitivity analyses of the average functional diversity of sampling sites in the **supplementary material**.

## DATA AVAILABILITY STATEMENT

The original contributions presented in the study are included in the article/**Supplementary Material**. Further inquiries can be directed to the corresponding author.

## AUTHOR CONTRIBUTIONS

ZYZ: building the research framework of this study and administering the sampling survey; analyzing the survey data; concluding the results and findings of this study; writing and revising the manuscript; WC: Highlighting and sublimating the findings of this study; HL: Participating in making the survey plan and data analysis; HY: assisting in collecting field fishery data; SB: assisting in collecting field fishery data; HYL: assisting in collecting field fishery data; XLC: assisting in collecting field fishery data Su: assisting in collecting field fishery data; XL: assisting in collecting field fishery data; QXC: assisting in collecting environmental parameters; ZLZ: assisting in collecting environmental parameters; XW: assisting in collecting environmental parameters; JHC: Collecting environmental

parameters; GFL: in charge of the sampling survey and supervising this study, is the corresponding author of this work. All authors contributed to the article and approved the submitted version.

## FUNDING

This study is supported by the Fundamental Research Funds for the Central Universities, Sun Yat-sen University (No. 22qntd2618), the Innovation Group Project of Southern Marine Science and Engineering Guangdong Laboratory (Zhuhai) (No.311021004), the Guangdong Basic and Applied Basic Research Foundation (No.2019B1515120065), the National Key R&D Program of China (2019YFD0901205) and the NSFC-Guangdong Joint Fund (No. U1901209).

## ACKNOWLEDGMENTS

We are grateful to Shiyu Li, Shaotian Li and Jiatang Hu, who provided very useful suggestion.

## SUPPLEMENTARY MATERIAL

The Supplementary Material for this article can be found online at: https://www.frontiersin.org/articles/10.3389/fmars.2022.921595/full#supplementary-material

## REFERENCES

Anderson, M. J., Ellingsen, K. E., and McArdle, B. H. (2006). Multivariate Dispersion as a Measure of Beta Diversity. *Ecol. Lett.* 9 (6), 683–693. doi: 10.1111/j.1461-0248.2006.00926.x

Asefa, M., Cao, M., Zhang, G. C., Ci, X. Q., Li, J., and Yang, J. (2017). Environmental Filtering Structures Tree Functional Traits Combination and Lineages Across Space in Tropical Tree Assemblages. *Sci. Rep.* 7, 132. doi: 10.1038/s41598-017-00166-z

Borcard, D., Gillet, F., and Legendre, P. (2018). Numerical Ecology with R: Springer Cham.

Breitburg, D., Levin Lisa, A., Oschlies, A., Grégoire, M., Chavez Francisco, P., Conley Daniel, J., and Zhang, J. (2018). Declining Oxygen in the Global Ocean and Coastal Waters. *Science*, 359(6371), eaam7240. doi: 10.1126/science.aam7240

Brind'Amour, A., Boisclair, D., Dray, S., and Legendre, P. (2011). Relationships Between Species Feeding Traits and Environmental Conditions in Fish Communities: A Three-Matrix Approach. *Ecol. Appl.* 21 (2), 363–377. doi: 10.1890/09-2178.1

Cadotte, M. W. (2017). Functional Traits Explain Ecosystem Function Through Opposing Mechanisms. *Ecol. Lett.* 20 (8), 989–996. doi: 10.1111/ele.12796

Chan, F., Barth, J. A., Lubchenco, J., Kirincich, A., Weeks, H., Peterson, W. T., et al. (2008). Emergence of Anoxia in the California Current Large Marine Ecosystem. *Science* 319 (5865), 920–920. doi: 10.1126/science.1149016

Chen, C., Zhu, Z., Li, Y., Yao, T., Pan, S., Wei, X., et al. (2016). Effects of Interspecific Trait Dissimilarity and Species Evenness on the Relationship Between Species Diversity and Functional Diversity in an Alpine Meadow. *Acta Ecol. Sinca.* 36 (3), 661–674. doi: 10.5846/stxb201405070903

Cheung, W. W. L., Reygondeau, G., and Frölicher, T. L. (2016). Large Benefits to Marine Fisheries of Meeting the 1.5 C Global Warming Target. *Science* 354 (6319), 1591–1594. doi: 10.1126/science.aag2331

Cheung, W. W., Watson, R., and Pauly, D. (2013). Signature of Ocean Warming in Global Fisheries Catch. *Nature* 497 (7449), 365–368. doi: 10.1038/nature12156

Cornwall, C. E. and Eddy, T. D. (2015). Effects of Near-Future Ocean Acidification, Fishing, and Marine Protection on a Temperate Coastal Ecosystem. *Conserv. Biol.* 29 (1), 207–215. doi: 10.1111/cobi.12394

Craven, D., Eisenhauer, N., Pearse, W. D., Hautier, Y., Isbell, F., Roscher, C., et al. (2018). Multiple Facets of Biodiversity Drive the Diversity-Stability Relationship. *Nat. Ecol. Evol.* 2 (10), 1579–1587. doi: 10.1038/s41559-018-0647-7

Cui, Y. S., Wu, J. X., Ren, J., and Xu, J. (2019). Physical Dynamics Structures and Oxygen Budget of Summer Hypoxia in the Pearl River Estuary. *Limnol. Oceanog.* 64 (1), 131–148. doi: 10.1002/lno.11025

de Bello, F., Lavergne, S., Meynard, C. N., Leps, J., and Thuiller, W. (2010). The Partitioning of Diversity: Showing Theseus a Way Out of the Labyrinth. *J. Vegetat. Sci.* 21 (5), 992–1000. doi: 10.1111/j.1654-1103.2010.01195.x

de Bello, F., Leps, J., Lavorel, S., and Moretti, M. (2007). Importance of Species Abundance for Assessment of Trait Composition: An Example Based on Pollinator Communities. *Community, Ecol.* 8 (2), 163–170.

Diaz, S. and Cabido, M. (2001). Vive La Difference: Plant Functional Diversity Matters to Ecosystem Processes. *Trends Ecol. Evol.* 16 (11), 646–655. doi: 10.1016/s0169-5347(01)02283-2

Dray, S., Chessel, D., and Thioulouse, J. (2003). Co-Inertia Analysis and the Linking of Ecological Data Tables. *Ecology* 84 (11), 3078–3089. doi: 10.1890/03-0178

Dray, S., Choler, P., Doledec, S., Peres-Neto, P. R., Thuiller, W., Pavoine, S., et al. (2014). Combining the Fourth-Corner and the RLQ Methods for Assessing Trait Responses to Environmental Variation. *Ecology* 95 (1), 14–21. doi: 10.1890/13-0196.1

Duan, L. J., Li, S. Y., Liu, Y., Moreau, J., and Christensen, V. (2009). Modeling Changes in the Coastal Ecosystem of the Pearl River Estuary From 1981 to 1998. *Ecol. Model.* 220 (20), 2802–2818.

Fisher, J. A. D., Frank, K. T., and Leggett, W. C. (2010). Global Variation in Marine Fish Body Size and its Role in Biodiversity-Ecosystem Functioning. *Mar. Ecol. Prog. Ser.* 405, 1–13. doi: 10.3354/meps08601

Fonseca, C. R., and Ganade, G. (2001). Species Functional Redundancy, Random Extinctions and the Stability of Ecosystems., *Eco*. 89 (1), 118–125. doi: 10.1046/j.1365-2745.2001.00528.x

Frelat, R., Orio, A., Casini, M., Lehmann, A., Merigot, B., Otto, S. A., et al. (2018). A Three-Dimensional View on Biodiversity Changes: Spatial, Temporal, and Functional Perspectives on Fish Communities in the Baltic Sea. *ICES. J. Mar. Sci.* 75 (7), 2463–2475. doi: 10.1093/icesjms/fsy027

Gobler, C. J., and Baumann, H. (2016). Hypoxia and Acidification in Ocean Ecosystems: Coupled Dynamics and Effects on Marine Life. *Biology Lett.* 12 (5), 20150976. doi: 10.1098/rsbl.2015.0976

Guillemot N., Kulbicki M., Chabanet P., and Vigliola, L. (2011). Functional Redundancy Patterns Reveal Non-Random Assembly Rules in a Species-Rich Marine Assemblage. *PLoS ONE* 6 (10), e26735. doi: 10.1371/journal.pone.0026735

Hughes, B. B., Levey, M. D., Fountain, M. C., Carlisle, A. B., Chavez, F. P. and Gleason, M. G. (2015). Climate Mediates Hypoxic Stress on Fish Diversity and Nursery Function at the Land-Sea Interface. *Proc. Natl. Acad. Sci. U.S.A.* 112 (26), 8025–8030. doi: 10.1073/pnas.1505815112

Jia, X. P., Li, C. H., and Qiu, Y. S. (2005). Survey and Evaluation of Guangdong Marine Fishery Resources and the Measures for Sustainable Utilization. Chinese marine publication.

Ke, D. S., Guan, Z. B., and Yu, H. S. (2007). Environmental Pollution and Study Trend in Pearl River Estuary. *Mar. Environ Res*. (05), 488–491. (In Chinese)

Keller, A. A., Ciannelli, L., Wakefield, W. W., Simon, V., Barth, J. A. and Pierce, S. D. (2015). Occurrence of Demersal Fishes in Relation to Near-Bottom Oxygen Levels Within the California Current Large Marine Ecosystem. *Fish. Oceanog.* 24 (2), 162–176. doi: 10.1111/fog.12100

Keller, A. A., Simon, V., Chan, F., Wakefield, W. W., Clarke, M. E., Barth, J. A., et al. (2010). Demersal Fish and Invertebrate Biomass in Relation to an Offshore Hypoxic Zone Along the US West Coast. *Fish. Oceanog.* 19 (1), 76–87. doi: 10.1111/j.1365-2419.2009.00529.x

Kleyer, M., Dray, S., Bello, F., Lepš, J., Pakeman, R. J., Strauss, B., Thuiller, W. and Lavorel, S. (2012). Assessing Species and Community Functional Responses to Environmental Gradients: Which Multivariate Methods? *J. Veg. Sci.* 23, 805–821. doi: 10.1111/j.1654-1103.2012.01402.x

Laliberte, E. and Legendre, P. (2010). A Distance-Based Framework for Measuring Functional Diversity From Multiple Traits. *Ecology* 91 (1), 299–305. doi: 10.1890/08-2244.1

Legendre, P. (2014). Interpreting the Replacement and Richness Difference Components of Beta Diversity. *Global Ecol. Biogeog.* 23 (11), 1324–1334. doi: 10.1111/geb.12207

Legendre, P. and De Caceres, M. (2013). Beta Diversity as the Variance of Community Data: Dissimilarity Coefficients and Partitioning. *Ecol. Lett.* 16 (8), 951–963. doi: 10.1111/ele.12141

Legendre, P. and Legendre, L. (2012). *Numerical Ecology*. 3rd English edn (Amsterdam: Elsevier Science).

Lennon, J. J., Koleff, P., Greenwood, J. J. D. and Gaston, K. J. (2001). The Geographical Structure of British Bird Distributions: Diversity, Spatial Turnover and Scale. *J. Anim. Ecol.* 70 (6), 966–979. doi: 10.1046/j.0021-8790.2001.00563.x

Leps, J., de Bello, F., Lavorel, S. and Berman, S. (2007). Quantifying and Interpreting Functional Diversity of Natural Communities: Practical Considerations Matter. *Preslia* 79 (1), 100–100.

Ling, S. D., Johnson, C. R., Frusher, S. D. and Ridgway, K. R. (2009). Overfishing Reduces Resilience of Kelp Beds to Climate-Driven Catastrophic Phase Shift. *Proc. Natl. Acad. Sci. U.S.A.* 106 (52), 22341–22345. doi: 10.1073/pnas.0907529106

Marshall, K. N., Kaplan, I. C., Hodgson, E. E., Hermann, A., Busch, D. S., McElhany, P., et al. (2017). Risks of Ocean Acidification in the California Current Food Web and Fisheries: Ecosystem Model Projections. *Glob. Chang. Biol.* 23 (4), 1525–1539. doi: 10.1111/gcb.13594

McLean, M., Auber, A., Graham, N. A. J., Houk, P., Villeger, S., Violle, C., et al. (2019). Trait Structure and Redundancy Determine Sensitivity to Disturbance in Marine Fish Communities. *Glob. Chang. Biol.* 25 (10), 3424–3437. doi: 10.1111/gcb.14662

McLean, M., Mouillot, D., Lindegren, M., Engelhard, G., Villeger, S., Marchal, P., et al. (2018). A Climate-Driven Functional Inversion of Connected Marine Ecosystems. *Curr. Biol.* 28 (22), 3654–3660. doi: 10.1016/j.cub.2018.09.050

Mollmann, C., Diekmann, R., Muller-Karulis, B., Kornilovs, G., Plikshs, M. and Axe, P. (2009). Reorganization of a Large Marine Ecosystem Due to Atmospheric and Anthropogenic Pressure: A Discontinuous Regime Shift in the Central Baltic Sea. *Glob. Chang. Biol.* 15 (6), 1377–1393. doi: 10.1111/j.1365-2486.2008.01814.x

Mouillot, D., Graham, N. A. J., Villeger, S., Mason, N. W. H. and Bellwood, D. R. (2013). A Functional Approach Reveals Community Responses to Disturbances. *Trends Ecol. Evol.* 28 (3), 167–177. doi: 10.1016/j.tree.2012.10.004

Mouillot, D., Villeger, S., Parravicini, V., Kulbicki, M., Arias-Gonzalez, J. E., Bender, M., et al. (2014). Functional Over-Redundancy and High Functional Vulnerability in Global Fish Faunas on Tropical Reefs. *Proc. Natl. Acad. Sci. U.S.A.* 111 (38), 13757–13762. doi: 10.1073/pnas.1317625111

Pauly, D., Christensen, V. V., Dalsgaard, J., Froese, R. and Torres, F., Jr. (1998). Fishing Down Marine Food Webs. *Science* 279 (5352), 860–863. doi: 10.1126/science.279.5352.860

Perry, A. L., Low, P. J., Ellis, J. R. and Reynolds, J. D. (2005). Climate Change and Distribution Shifts in Marine Fishes. *Science* 308 (5730), 1912–1915. doi: 10.1126/science.1111322

Poloczanska, E. S., Burrows, M. T., Brown, C. J., Molinos, J. G., Halpern, B. S., Hoegh-Guldberg, O., et al. (2016). Responses of Marine Organisms to Climate Change Across Oceans. *Front. Mar. Sci.* 362., doi:10.3389/fmars.2016.00062

Rouyer, T., Fromentin, J. M., Menard, F., Calzelles, B., Briand, K., Pianet, R., et al. (2008). Complex Interplays Among Population Dynamics, Environmental Forcing, and Exploitation in Fisheries. *Proc. Natl. Acad. Sci. U.S.A.* 105 (14), 5420–5425. doi: 10.1073/pnas.0709034105

Sanders, D., Thebault, E., Kehoe, R. and van Veen, F. J. F. (2018). Trophic Redundancy Reduces Vulnerability to Extinction Cascades. *Proc. Natl. Acad. Sci. U.S.A.* 115 (10), 2419–2424. doi: 10.1073/pnas.1716825115

Sasaki, T., Okubo, S., Okayasu, T., Jamsran, U., Ohkuro, T. and Takeuchi, K. (2009). Two-Phase Functional Redundancy in Plant Communities Along a Grazing Gradient in Mongolian Rangelands. *Ecology* 90 (9), 2598–2608. doi: 10.1890/08-1850.1

Seibel, B. A. (2011). Critical Oxygen Levels and Metabolic Suppression in Oceanic Oxygen Minimum Zones. *J. Exp. Biol.* 214 (2), 326–336. doi: 10.1242/jeb.049171

Vaquer-Sunyer, R. and Duarte, C. M. (2008). Thresholds of Hypoxia for Marine Biodiversity. *Proc. Natl. Acad. Sci. U.S.A.* 105 (40), 15452–15457. doi: 10.1073/pnas.0803833105

Villeger, S., Mason, N. W. H. and Mouillot, D. (2008). New Multidimensional Functional Diversity Indices for a Multifaceted Framework in Functional Ecology. *Ecology* 89 (8), 2290–2301. doi: 10.1890/07-1206.1

Wang, B., Hu, J., Li, S., Yu, L. and Huang, J. (2018). Impacts of Anthropogenic Inputs on Hypoxia and Oxygen Dynamics in the Pearl River Estuary. *Biogeosciences* 15 (20), 6105–6125. doi: 10.5194/bg-15-6105-2018

Williams, P. H. (1996). Mapping Variations in the Strength and Breadth of Biogeographic Transition Zones Using Species Turnover. *Proc. R. Soc. London. Ser. B. Biol. Sci.* 263 (1370), 579–588. doi:10.1098/rspb.1996.0087

Wu, R. S. S. (2002). Hypoxia: From Molecular Responses to Ecosystem Responses. *Mar. pollut. Bull.* 45 (1), 35–45. doi: 10.1016/s0025-326x(02)00061-9

Yachi, S. and Loreau, M. (1999). Biodiversity and Ecosystem Productivity in a Fluctuating Environment: The Insurance Hypothesis. *Proc. Natl. Acad. Sci. U.S.A.* 96 (4), 1463–1468. doi: 10.1073/pnas.96.4.1463

Yao, T., Zhu, Z., Li, Y., Pan, S., Kong, B., Wei, X., et al. (2016). Effects Offunctional Diversity and Functional Redundancy on the Community Stability of an Alpine Meadow. *Acta Ecol. Sinca.* 36 (6), 1547–1558.

Yin, K., Lin, Z. and Ke, Z. (2004). Temporal and Spatial Distribution of Dissolved Oxygen in the Pearl River Estuary and Adjacent Coastal Waters. *Continent. Shelf. Res.* 24 (16), 1935–1948. doi: 10.1016/j.csr.2004.06.017

Zeng, Z., Cheung, W. W. L., Li, S., Hu, J. and Wang, Y. (2019). Effects of Climate Change and Fishing on the Pearl River Estuary Ecosystem and Fisheries. *Rev. Fish. Biol. Fish.* 29 (4), 861–875. doi: 10.1007/s11160-019-09574-y

**Conflict of Interest:** The authors declare that the research was conducted in the absence of any commercial or financial relationships that could be construed as a potential conflict of interest.

frontiers | Frontiers in Marine Science

ORIGINAL RESEARCH
published: 18 July 2022
doi: 10.3389/fmars.2022.932678

# The Application of DNA Barcoding in Crustacean Larvae Identification from the Zhongsha Islands, South China Sea

*Lei Xu*[1,2], *Xuehui Wang*[1,2], *Delian Huang*[1,2], *Lianggen Wang*[1,2], *Jiajia Ning*[1,2], *Yafang Li*[1,2], *Shuangshuang Liu*[1,2] *and Feiyan Du*[1,2]*

[1] South China Sea Fisheries Research Institute, Chinese Academy of Fishery Sciences, Guangzhou, China, [2] Guangdong Provincial Key Laboratory of Fishery Ecology and Environment, Guangzhou, China

Marine crustaceans are known as a group with high morphological diversity and great economic value. Most species have planktonic larval stages that are difficult to identify to species level using traditional approaches because of insufficient morphological diagnostic characters or taxonomic descriptions. We used DNA barcoding and molecular species identification to investigate the species diversity and distribution of crustacean larvae in the Zhongsha Islands waters, South China Sea. In total, 108 sequences were obtained from crustacean larvae collected in the Zhongsha Islands waters in 2019 using vertical hauls between the depths of 5 and 200 m. The molecular classification approach confirmed that 108 sequences represented crustaceans typical to the South China Sea, with 70 species identified, representing 43 genera, 23 families, and 4 orders. However, the cytochrome c oxidase subunit I gene sequences of only 27 species identified from the larval samples matched with available sequences taken from adults in GenBank. The comparison of K2P distances yielded a notable gap of 3.5–10.7% between intraspecific and interspecific distances across the sequence dataset. More than 80% of the crustacean larvae species belonged to the order Decapoda, and they displayed marked differences in their distributionsin the Zhongshan Islands waters. The orders Calanoida and Amphipoda were represented by the fewest species, which were recorded only at the edge of the Zhongsha Atoll.

**Keywords: DNA identification, COI gene, crustacean larvae, coral reef, Zhongsha Islands**

OPEN ACCESS

***Edited by:***
*Jun Xu,*
*Institute of Hydrobiology (CAS), China*

***Reviewed by:***
*Weichun Li,*
*Jiangxi Agricultural University, China*
*Qiuqi Lin,*
*Jinan University, China*

***Correspondence:**
*Feiyan Du*
*feyanegg@163.com*

***Specialty section:***
*This article was submitted to Marine Ecosystem Ecology, a section of the journal Frontiers in Marine Science*

***Received:*** *30 April 2022*
***Accepted:*** *10 June 2022*
***Published:*** *18 July 2022*

***Citation:***
*Xu L, Wang X, Huang D, Wang L, Ning J, Li Y, Liu S and Du F (2022) The Application of DNA Barcoding in Crustacean Larvae Identification from the Zhongsha Islands, South China Sea. Front. Mar. Sci. 9:932678. doi: 10.3389/fmars.2022.932678*

## INTRODUCTION

The majority of extant species of crustaceans live in oceans and estuarine regions and adjacent coastal waters. Crustaceans are one of the largest and most morphologically diverse and economically important marine invertebrate groups, and play important roles in marine food webs. Most marine crustacean species have a complex life history including planktonic (larval) and benthic (juvenile to adult) phases (Radulovici et al., 2010). Traditional taxonomic identification of marine crustaceans is largely based on visible morphological characteristics, such as shape of the carapace and features of the thoracic somites, antennae, and mandibles (Anger, 2001). However, these characters are insufficient to identify every species, especially at larval stages. The larvae show a wide array of

adaptations to the ocean environment, including characteristics of their morphology, developmental stage, behavior, and ecology (Forward, 1990; Bertram and Strathmann, 1998). In addition, different larval stages within species can exhibit different morphological features, and most crustacean larvae bear little resemblance to their adult forms (Alford and Jackson, 1993). Thus, the same crustacean species at different larval stages may be erroneously identified as a different species when depending on morphological characteristics; conversely, different species at the same larval stage can have similar morphological features (Ko et al., 2013). Furthermore, identifications and classifications based on morphological characteristics can be difficult and time-consuming; though species identifications generally require considerable taxonomic knowledge, even the same specimen can be identified inconsistently among taxonomists (Bilgin et al., 2014). Therefore, diagnoses of crustacean larvae are problematic and challenging given the generally small amount of morphological characteristics available, especially in the context of a species' rapid development from larval to juvenile stages.

DNA-based methods provide a quick, reliable, and cost-effective identification system that applies specific DNA sequences as "DNA barcodes" to identify species. Hebert et al. (2003) was the first to propose the use of a short and standardize fragment of the mitochondrial cytochrome c oxidase subunit I (COI) gene for identifications throughout the entire animal kingdom based on the sequence diversity among different taxa (Ratnasingham and Hebert, 2007; Ratnasingham and Hebert, 2013). The COI gene has several characteristics that make it highly efficient and reliable for species identification in most animals. For instance, it has an almost exclusively haploid mode of inheritance from the mother, high substitution rates, large copy numbers in mitochondria, and an absence of recombination and introns (Ballard and Whitlock, 2004; Bernt et al., 2013). In the decades since a DNA barcoding system for specimen identifications was established, numerous studies have proven that this technique is effective for identifying species (Hajibabaei et al., 2006; Ward et al., 2009; Radulovici et al., 2010). DNA barcoding has now been successfully applied in insects (Janzen et al., 2005; Smith et al., 2005), crustaceans (Costa et al., 2007; Bilgin et al., 2014; Bucklin et al., 2022), fish (Ward et al., 2005; Hubert et al., 2008; Ghouri et al., 2020; Guimarães-Costa et al., 2020; Xu et al., 2021), birds (Hebert et al., 2004), and mammals (Lorenz et al., 2005; Clare et al., 2007). These achievements have benefited from the establishment of the Barcode of Life Data Systems (BOLDSystems), which is a global public standard dataset platform with general technical rules and identification systems for animal taxonomy. Data deposited in BOLD include not only DNA barcode sequences but also the geographical coordinates of collection sites, primer sequences, taxonomic information, photographs of vouchers, and even electropherogram files (Ratnasingham and Hebert, 2007). The database implies standardization, which allows comparisons of specimens identified by morphological and molecular characters among the datasets of different researchers, sometimes revealing potential cryptic species or cosmopolitan species consisting of species complexes (Ratnasingham and Hebert, 2013). Given that marine crustacean larvae pose considerable problems in terms of identification, owing to limited morphological characteristics in the complex life cycle of marine crustaceans, DNA barcoding has been applied by matching the COI sequences of unknown larval morphotypes with the sequences of previously described adults deposited in the database. Through DNA barcoding, Tang et al. (2010) found 14 larval morphotypes of stomatopods from Hong Kong waters belonged to seven species; Kusbiyanto et al. (2020) identified the larvae of eight species of crustaceans from the eastern part of Segara Anakan Lagoon, Indonesia; and Barber and Boyce (2006) explored the biodiversity of stomatopods in the Coral Triangle (western Pacific) and the Red Sea.

The South China Sea is the largest semi-enclosed sea located in the western Pacific region, hosting rich coral reef ecosystem, and diverse fish and crustacean taxa. It extends across the subtropical and tropical zones, with an area of ~3,400,000 km$^2$ and average depth of 1,200 m (Morton and Blackmore, 2001; Liu, 2013). The Zhongsha Islands are located approximately at the center of the South China Sea; they consist of Huangyan Island (or Scarborough Shoal), Zhongsha Atoll (or Macclesfield Bank), and four other main reefs. Zhongsha Atoll is situated approximately 510–670 km from the Philippine Islands, Indo-China Peninsula, and China mainland. It is a ring-shaped reef complex, arranged along the outer edge of a submerged atoll structure; its maximum length exceeds 150 km (southwest–northeast) and the width is ~75 km, and it covers an area of ~23,500 km$^2$. The discontinuous marginal reefs of Zhongsha Atoll surround a lagoon with depths of 50–70 m (Huang et al., 2020). Zhongsha Atoll is one of the most important coral reef ecosystems in the South China Sea owing to high biodiversity and abundant fishery resources (Tittensor et al., 2010; Li et al., 2020; Zhao and Jia, 2020; Lu et al., 2021; Huang et al., 2022).

Here, we obtained specimens of crustacean larvae from waters around the Zhongsha Islands to investigate the species diversity and distribution of marine crustaceans at the islands by using DNA barcodes to identify unknown larval morphotypes. This study will provide useful additional information for understanding the diversity crustaceans in the Zhongsha Islands waters and will improve the accuracy of marine crustacean larvae identification. Moreover, our reference DNA barcoding information on larval crustaceans should benefit estimations of the recruitment and productivity potential of the Zhongsha Islands waters as a nursery ground. Overall, such data are vital as a scientific basis for biodiversity and ecosystem conservation of the South China Sea.

# MATERIALS AND METHODS

## Sample Collection

Sampling around the Zhongsha Islands (including at Zhongsha Atoll and Huangyan Island) was carried out by the scientific expedition vessel *Yueyuzhanke10* during an investigation by the South China Sea Institute of Oceanology, conducted 9–29 August in 2019. Twenty-two sampling sites were visited within a total investigation area covering 8,000 km$^2$ (**Figure 1**). Crustacean larvae were collected using a bongo net, with a 330-μm mesh size and 80-cm mouth diameter, equipped with a flow meter in the net opening. The net was hauled vertically from 300-m

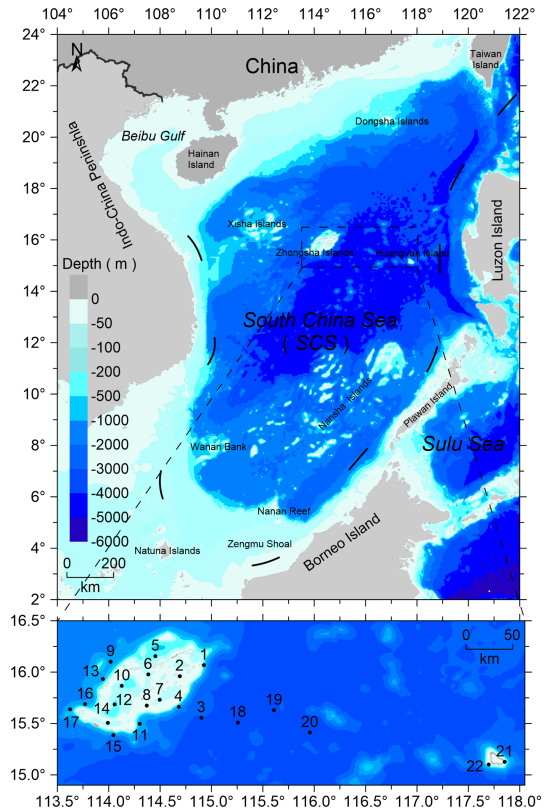


**FIGURE 1 |** Map showing the 22 sampling sites around the Zhongsha Islands, South China Sea.

deep (or 10 m above the bottom at sampling sites in depths of <300 m) to the surface at a speed of 2 m $s^{-1}$. After the net was retrieved, the samples were fixed in 70% ethanol solution. Upon returning to the laboratory, all fixed samples were transferred to a new bottle and preserved in 95% ethanol solution at −20°C for subsequent analysis. Before DNA extraction, the samples were placed in distilled water for 10 min at room temperature. Next, an entire sample was emptied into a counting tray and scanned for crustacean larvae under a stereo-dissecting microscope at 20–50× magnification (Olympus SZX71; Japan), until exhaustion of the sample. Each crustacean larva was identified to the lowest taxonomic level based on general morphological characteristics, following the guilds described by Anger (2001).

## DNA Extraction

Total genomic DNA was extracted from crustacean larvae individuals using the Wizard Genomic DNA Purification Kit (Promega, USA). Here, we modified the standard DNA extraction protocol as follows (Xu et al., 2011): each specimen was picked out of the 95% ethanol solution, rinsed with distilled water, transferred to a reaction tube. Next, we added 200 µL of preheating cell-lysis solution (65°C) and 3 µL of proteinase K (20 mg $mL^{-1}$) then incubated the mixture for 2 h at 65°C after vortexed, and then for 24 h at 55°C with addition of 2 µL of fresh Proteinase K. After that, we added 200 µL of precipitation solution, vortexed at a middle speed for 20 s, and then centrifuged at RCF 19,000×*g* for 15 min at 4°C. Then, we removed the supernatant and transferred it to a new 500-µL microcentrifuge tube with 200 µL of isopropanol, centrifuged at RCF 19,000×*g* for 1 min at 4°C, decanted the supernatant. Finally, the pellet was washed with 70% ethanol and dissolved in 50 µL of DNA hydration solution then stored at −20°C. All the collected specimens and the extracted DNA were stored at the Guangdong Provincial Key Laboratory of Fishery Ecology and Environment. The concentration of each DNA extraction was measured using a NanoDrop ND-1000 spectrophotometer (NanoDrop Technologies, USA). Only the DNA samples with an A260/A280 ratio of 1.8–2.1 were used as template for subsequent PCR amplification.

## PCR Amplification and Sequencing

The barcoding fragment of the mitochondrial cytochrome c oxidase subunit I gene was amplified from genomic DNA using PCR with the universal primers LCO1490 and HCO2198 (Folmer et al., 1994). Each 30-µL PCR reaction consisted of 3 µL of PCR buffer, 18.75 µL of dd $H_2O$, 2.4 µL of 25 M $MgCl_2$, 3 µL of Coral Load Concentrate, 0.3 µL of 25 M solution of each primer, 0.6 µL of 10 M dNTPs, 0.15 µL of TopTaq DNA Polymerase (QIAGEN, Germany) and 1.5 µL of DNA template. The PCR conditions for amplification were: 35 cycles of 30 s at 96°C, 30 s at 51°C and 60 s at 72°C, followed by 7 min at 72°C on a 2720 Thermal Cycler (Applied Biosystems, USA). For some individuals for which we were unsuccessful with the Folmer primers, we also used a specific set of primers for decapods (Costa et al., 2007), following the protocols specified by the authors. The PCR products were sequenced bi-directionally on an ABI PRISM 3130XLDNA Analyzer.

## DNA Identification

The authenticity of all COI sequences wasfirst verified in GenBank by BLAST search, which compares sequences for the highest match (98–100%). Sequences corresponding to maximum species identity were downloaded for the subsequent analysis. All sequences were then assembled and examined with BioEdit (Hall, 1999), aligned using the ClustalW progressive algorithm under default options, as no indels were found. To evaluate taxonomic units from DNA identification, we applied two different methods: Automatic Barcode Gap Discovery analysis (ABGD; Puillandre et al., 2012) and the Generalized Mixed Yule Coalescent model (GMYC; Pons et al., 2006; Fujisawa and Barraclough, 2013), to infer putative species boundaries based on the COI sequence dataset. The ABGD approach tests for the existence of the barcode gap in the distribution of the pairwise genetic distances and identifies groups of individuals united by genetic distances shorter than the gap. This was performed on the COI alignment through an online tool (https://bioinfo.mnhn.fr/abi/public/abgd) with default settings: prior limit to intraspecific diversity (P), ranging between 0.001 and 0.1; gap widths (X) = 1, using the available models JC86 (Jukes–Cantor) and K80 (Kimura).

The other method, the GMYC approach, uses the maximum-likelihood method to optimize the shift in the branching patterns of the phylogenetic tree from interspecific branches (Yule model) to intraspecific branches (neutral coalescent), and it thereby identifies clusters of sequences corresponding to independently evolving entities. This approach requires a dichotomous and rooted ultrametric tree without duplicated sequences. Therefore, we reconstructed the ultrametric tree without duplicated sequences using BEAST1.8.0 (Drummond and Rambaut, 2007). Parameters for BEAST were set in BEAUti 1.8.0 (Drummond et al., 2012), assuming a coalescent model with constant population size, uncorrelated relaxed clock model, general time-reversible substitution model, and gamma shape site model, with a chain length of 100,000,000 iterations for Markov chain Monte Carlo simulations, and sampled every 10,000 generations. We obtained a maximum clade credibility consensus tree in TreeAnnotator v1.8.2, with the first 1,000,000 generations discarded as burn-in. The GMYC model was performed in R 3.0.1 (R Development Core Team, 2017), with "splits" package (Ezard et al., 2009).

## Genetic Divergence and Phylogenetic Relationships

COI sequence divergences were calculated with the K2P (Kimura two-parameter) nucleotide substitution model in MEGA version 6.0 (Tamura et al., 2013). We used uniform rates, and standard error estimates were obtained by a NJ (neighbor-joining) bootstrap procedure with 10,000 replicates. K2P genetic distances were calculated, categorized as: intraspecific distances, interspecies distances within the congener, intergeneric distances within intrafamily, distances between different families within the same order, and distances between different orders within same class. We performed the phylogenetic analysis with all COI sequences to visually reflect the relationships of marine crustacean species and the distribution patterns of crustacean larvae at the Zhongsha Islands. Before phylogenetic analysis, we first used MrModeltest v.2.3 (Nylander, 2004) to select the best-fit models of nucleotide substitution under the AIC (Akaike information criterion). Bayesian inference analysis was performed using MrBayes v.3.1.2 (Huelsenbeck et al., 2001). MCMC simulationswere run in four parallel chains for 2,000,000 generations, sampling every 1,000 generations. Majority rule consensus trees were reconstructed after discarding the burn-in of 500 and displayed using TreeView v.1.6.6 (Page, 1996).

# RESULTS

## DNA Identification and Phylogenetic Analysis

In total, we analyzed 135 sequences in our COI dataset, namely the 108 partial sequences of COI obtained from crustacean larvae collected from the Zhongsha Islands waters, and the 27 crustacean COI sequences available from public databases (maximum species identity corresponding sequences), to ensure that the nomenclature in our study would be solid for each species (**Supplementary Table S1**). The length of partial sequences of the COI fragments after alignment was 539 bp (a small portion of both ends could not be used). The average base composition of the COI gene was 26.3% A, 17.7% G, 19.7% C, and 36.3% T, and the ratio of transition to transversion (Ti/Tv) was 1.11. This value is similar to that of other crustaceans (Richter et al., 2007).

DNA-based classification with ABGD method could detect a barcode gap from the COI sequence dataset and suggested that the 135 sequences represented 68 taxonomic units (confidence interval: 65–72). Two species of snapping shrimp (*Alpheus dolerus* and *Alpheus* sp.) and two species of *Lucifer* prawns (*Lucifer typus* and *Lucifer* sp.) were suggested as the same taxonomic units by the ABGD method (**Figure 2**). Nevertheless, the GMYC method supported the scenario that all analyzed sequences presented 70 taxonomic units (confidence interval: 67–74); hence, the likelihood of the null model with one taxonomic unit was significantly worse (likelihood = 588.89, likelihood ratio test = 196.56, $p = 3.22 \times 10^{-8}$) than the likelihood of the solution with more than one taxonomic unit (likelihood = 687.17; **Figure 2**). Therefore, the DNA-based classification confirmed that all 108 sequences represented typical crustaceansfound in the South China Sea, and belonged to 70 species, of 43 genera, 23 families, and 4 orders (**Table 1**). Comparing each of the COI sequences amplified from our samples with the sequences deposited in GenBank, 55 sequences (51%) from 27 species were recovered as species of crustaceans (sequence similarity >98%). A total of 53 sequences from 43 species showed low or no similarity matches at the species level with sequences deposited in the database, indicating that these species have not been barcoded ever. Consequently, the sequences identified to species level were uploaded to GenBank (accession numbers

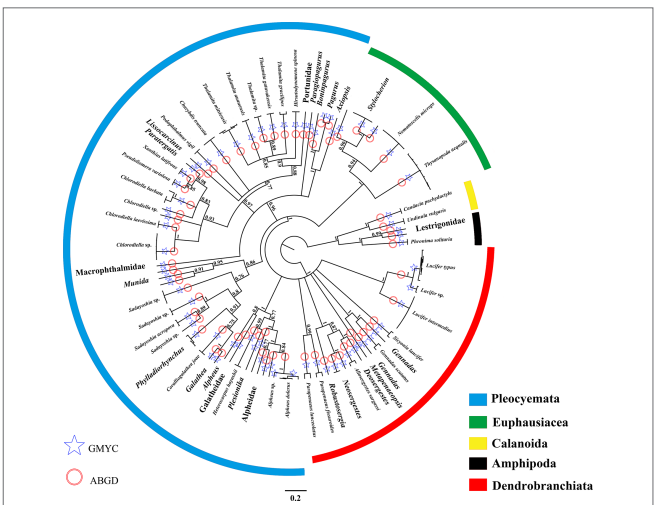


**FIGURE 2 |** Phylogenetic tree obtained through Bayesian inference of the COI dataset for marine crustacean larvae present at the Zhongsha Islands, using MrBayes, with the scale bars proportional to substitution rates. Bayesian posterior probabilities are shown on the branches (values below 0.7 are not shown). DNA identifications through the molecular approaches (Generalized Mixed Yule Coalescent model [GMYC] and Automatic Barcode Gap Discovery analysis [ABGD]) are shown on the branches. The major clades are depicted by different colors to reflect groups of species in the same order.

**TABLE 1 |** Summary of identification based on species barcode using BLAST search from GenBank.

| Sequence ID | Order | Family | Genus | Species (identification based on barcode) | Similarity (%) |
|---|---|---|---|---|---|
| 6.S18TYC4 | Decapoda | Alpheidae | *Alpheus* | *Alpheus dolerus* | 99 |
| D4.S10TYC5 | Decapoda | Alpheidae | *Alpheus* | *Alpheus dolerus* | 100 |
| 26.S19TYC5 | Decapoda | Alpheidae | *Alpheus* | *Alpheus dolerus* | 100 |
| 11.S12TYC13 | Calanoida | Candaciidae | *Candacia* | *Candaciapachydactyla* | 100 |
| 1.S11TYC1 | Decapoda | Portunidae | *Charybdis* | *Charybdis truncata* | 100 |
| 36.S6TYC4 | Decapoda | Portunidae | *Charybdis* | *Charybdis truncata* | 100 |
| 33.S2TYC7 | Decapoda | Xanthidae | *Chlorodiella* | *Chlorodiellabarbata* | 94 |
| 16.S4TYC9 | Decapoda | Xanthidae | *Chlorodiella* | *Chlorodiellabarbata* | 100 |
| 43.S13TYC6 | Decapoda | Xanthidae | *Chlorodiella* | *Chlorodiellalaevissima* | 99 |
| 37.S6TYC5 | Decapoda | Xanthidae | *Chlorodiella* | | 90 |
| 41.S6TYC7 | Decapoda | Xanthidae | *Chlorodiella* | | 90 |
| 42.S5TYC2 | Decapoda | Xanthidae | *Chlorodiella* | | 90 |
| 28.S2TYC2 | Decapoda | Xanthidae | *Chlorodiella* | | 90 |
| 6.S16TYC8 | Decapoda | Xanthidae | *Chlorodiella* | | 90 |
| F10.S13TYC3 | Decapoda | Galatheidae | *Coralliogalathea* | *Coralliogalatheajoae* | 99 |
| 31.S3TYC10 | Decapoda | Pandalidae | *Heterocarpus* | *Heterocarpushayashii* | 99 |
| 31.S6TYC1 | Decapoda | Dynomenidae | *Hirsutodynomene* | *Hirsutodynomene spinosa* | 99 |
| 35.S13TYC6 | Decapoda | Luciferidae | *Lucifer* | *Lucifer intermedius* | 99 |
| 6.S12TYC6 | Decapoda | Luciferidae | *Lucifer* | *Lucifer intermedius* | 99 |
| E11.S8TYC7 | Decapoda | Luciferidae | *Lucifer* | *Lucifer intermedius* | 99 |
| 33.S17TYC6 | Decapoda | Luciferidae | *Lucifer* | *Lucifer intermedius* | 99 |
| 38.S17TYC12 | Decapoda | Luciferidae | *Lucifer* | *Lucifer intermedius* | 99 |
| C10.S10TYC1 | Decapoda | Luciferidae | *Lucifer* | *Lucifer intermedius* | 99 |
| A3.S9TYC3 | Decapoda | Luciferidae | *Lucifer* | *Lucifer typus* | 99 |
| 3.S21TYC3 | Decapoda | Luciferidae | *Lucifer* | *Lucifer typus* | 99 |
| 7.S6TYC9 | Decapoda | Luciferidae | *Lucifer* | *Lucifer typus* | 99 |
| 7.S12TYC7 | Decapoda | Luciferidae | *Lucifer* | *Lucifer typus* | 99 |
| C4.S9TYC18 | Decapoda | Luciferidae | *Lucifer* | *Lucifer typus* | 99 |
| 27.S3TYC6 | Euphausiacea | Euphausiidae | *Nematoscelis* | *Nematoscelismicrops* | 99 |
| 30.S14TYC6 | Euphausiacea | Euphausiidae | *Nematoscelis* | *Nematoscelismicrops* | 99 |
| 15.S7TYC8 | Euphausiacea | Euphausiidae | *Nematoscelis* | *Nematoscelismicrops* | 99 |
| 13.S15TYC9 | Euphausiacea | Euphausiidae | *Nematoscelis* | *Nematoscelismicrops* | 99 |
| 28.S17TYC1 | Decapoda | Penaeidae | *Parapenaeus* | *Parapenaeusfissuroides* | 99 |
| 36.S14TYC12 | Decapoda | Penaeidae | *Parapenaeus* | *Parapenaeuslanceolatus* | 99 |
| 22.S1TYC4 | Amphipoda | Phronimidae | *Phronima* | *Phronima solitaria* | 99 |
| 11.S15TYC3 | Decapoda | Portunidae | *Podophthalmus* | *Podophthalmus vigil* | 99 |
| 29.S22TYC1 | Decapoda | Xanthidae | *Pseudoliomera* | *Pseudoliomeravariolosa* | 99 |
| 11.S4TYC4 | Decapoda | Munididae | *Sadayoshia* | *Sadayoshiaacropora* | 99 |
| 30.S17TYC3 | Decapoda | Sicyoniidae | *Sicyonia* | *Sicyonialancifer* | 99 |
| B1.S9TYC2 | Decapoda | Portunidae | *Thalamita* | *Thalamitaauauensis* | 99 |
| 25.S3TYC4 | Decapoda | Portunidae | *Thalamita* | *Thalamitagatavakensis* | 99 |
| 24.S3TYC3 | Decapoda | Portunidae | *Thalamita* | *Thalamitagracilipes* | 97 |
| 47.S16TYC1 | Decapoda | Portunidae | *Thalamita* | *Thalamitamitsiensis* | 98 |
| 5.S16TYC7 | Decapoda | Portunidae | *Thalamita* | *Thalamitamitsiensis* | 100 |
| 13.S4TYC6 | Decapoda | Portunidae | *Thalamita* | *Thalamitamitsiensis* | 99 |
| 17.S3TYC1 | Euphausiacea | Euphausiidae | *Thysanopoda* | *Thysanopodaaequalis* | 99 |
| 27.S14TYC8 | Euphausiacea | Euphausiidae | *Thysanopoda* | *Thysanopodaaequalis* | 99 |
| 15.S15TYC11 | Euphausiacea | Euphausiidae | *Thysanopoda* | *Thysanopodaaequalis* | 99 |
| 3.S15TYC2 | Euphausiacea | Euphausiidae | *Thysanopoda* | *Thysanopodaaequalis* | 99 |
| 15.S20TYC3 | Euphausiacea | Euphausiidae | *Thysanopoda* | *Thysanopodaaequalis* | 99 |
| 23.S3TYC4 | Euphausiacea | Euphausiidae | *Thysanopoda* | *Thysanopodaaequalis* | 99 |
| B6.S9TYC5 | Calanoida | Candaciidae | *Undinula* | *Undinula vulgaris* | 99 |
| B11.S9TYC9 | Decapoda | Xanthidae | *Xanthias* | *Xanthiaslatifrons* | 99 |
| 37.S5TYC1 | Amphipoda | Hyperiidae | *Hyperietta* | | 88 |
| 21.S17TYC5 | Amphipoda | Lestrigonidae | *Phronimopsis* | | 90 |
| 1.S12TYC1 | Decapoda | Galatheidae | *Galathea* | | 93 |
| 17.S22TYC2 | Decapoda | Galatheidae | *Galathea* | | 95 |
| 9.S4TYC2 | Decapoda | Munididae | *Sadayoshia* | | 93 |
| 19.S17TYC3 | Decapoda | Munididae | *Sadayoshia* | | 93 |
| 6.S4TYC10 | Decapoda | Munididae | *Sadayoshia* | | 93 |
| 26.S22TYC11 | Decapoda | Munididae | *Munida* | | 90 |
| 21.S22TYC6 | Decapoda | Munididae | *Munida* | | 92 |
| 31.S22TYC3 | Decapoda | Munididae | *Munida* | | 90 |
| 7.S18TYC3 | Decapoda | Munididae | *Sadayoshia* | | 91 |
| 44.S13TYC7 | Decapoda | Munididae | *Sadayoshia* | | 90 |
| 12.S16TYC14 | Decapoda | Munididae | *Sadayoshia* | | 90 |
| 23.S14TYC2 | Decapoda | Galatheidae | *Phylladiorhynchus* | | 90 |
| A4.S9TYC1 | Decapoda | Galatheidae | *Phylladiorhynchus* | | 90 |

*(Continued)*

**TABLE 1** | Continued

| Sequence ID | Order | Family | Genus | Species (identification based on barcode) | Similarity (%) |
|---|---|---|---|---|---|
| 35.S4TYC3 | Decapoda | Galatheidae | *Phylladiorhynchus* | | 90 |
| 2.S4TYC6 | Euphausiacea | Euphausiidae | *Stylocherion* | | 90 |
| 8.S6TYC10 | Euphausiacea | Euphausiidae | *Stylocherion* | | 96 |
| 25.S19TYC4 | Euphausiacea | Euphausiidae | *Stylocherion* | | 96 |
| 2.S21TYC2 | Euphausiacea | Euphausiidae | *Stylocherion* | | 96 |
| 25.S22TYC10 | Euphausiacea | Euphausiidae | *Stylocherion* | | 96 |
| 22.S19TYC1 | Euphausiacea | Euphausiidae | *Stylocherion* | | 93 |
| 20.S20TYC8 | Decapoda | Luciferidae | *Lucifer* | *Lucifer typus* | 97 |
| 4.S4TYC8 | Decapoda | Luciferidae | *Lucifer* | *Lucifer typus* | 97 |
| E5.S8TYC2 | Decapoda | Penaeidae | *Metapenaeopsis* | | 89 |
| A9.S9TYC8 | Decapoda | Benthesicymidae | *Gennadas* | *Gennadasscutatus* | 98 |
| 19.S14TYC3 | Decapoda | Benthesicymidae | *Gennadas* | | 86 |
| 39.S6TYC6 | Decapoda | Benthesicymidae | *Gennadas* | | 85 |
| 14.S20TYC2 | Decapoda | Sergestidae | *Allosergestes* | *Allosergestessargassi* | 97.6 |
| 8.S21TYC3 | Decapoda | Sergestidae | *Deosergestes* | | 90 |
| 9.S12TYC11 | Decapoda | Sergestidae | *Robustosergia* | | 94 |
| 19.S20TYC7 | Decapoda | Sergestidae | *Neosergestes* | | 90 |
| 40.S13TYC9 | Decapoda | Sergestidae | *Neosergestes* | | 90 |
| 15.S4TYC8 | Decapoda | Sergestidae | *Neosergestes* | | 87 |
| 34.S4TYC2 | Decapoda | Alpheidae | *Alpheus* | | 95 |
| 14.S12TYC3 | Decapoda | Palaemonidae | *Macrobrachium* | | 83 |
| 24.S22TYC9 | Decapoda | Alpheidae | *Alpheus* | | 83 |
| 40.S6TYC7 | Decapoda | Alpheidae | *Alpheus* | | 85 |
| 28.S3TYC7 | Decapoda | Alpheidae | *Alpheus* | *Alpheus dolerus* | 98 |
| 14.S16TYC2 | Decapoda | Alpheidae | *Alpheus* | | 90 |
| 9.S15TYC6 | Decapoda | Pandalidae | *Plesionika* | | 92 |
| 32.S14TYC9 | Decapoda | Galatheidae | *Lauriea* | | 84 |
| 2.S16TYC4 | Decapoda | Pilumnidae | *Pilumnus* | | 86.8 |
| 8.S18TYC4 | Decapoda | Macrophthalmidae | *Macrophthalmus* | | 85 |
| 9.S16TYC11 | Decapoda | Xanthidae | *Liomera* | | 87 |
| 42.S13TYC5 | Decapoda | Xanthidae | *Paratergatis* | | 93 |
| 32.S19TYC2 | Decapoda | Portunidae | *Lissocarcinus* | | 90 |
| 20.S3TYC2 | Decapoda | Portunidae | *Thalamita* | | 88 |
| 12.S18TYC8 | Decapoda | Portunidae | *Thalamita* | | 99 |
| 13.S18TYC9 | Decapoda | Portunidae | *Thalamita* | *Thalamitagatavakensis* | 99.3 |
| 48.S16TYC2 | Decapoda | Paguridae | *Pagurus* | | 89 |
| 16.S15TYC12 | Decapoda | Parapaguridae | *Paragiopagurus* | | 91 |
| 3.S16TYC5 | Decapoda | Paguridae | *Boninpagurus* | | 87 |
| 35.S5TYC12 | Decapoda | Axiidae | *Axiopsis* | | 93 |
| C1.S9TYC16 | Decapoda | Axiidae | *Axiopsis* | | 93.5 |

OM679168–OM679215). The best-fitting model fora Bayesian inference tree selected by MrModeltest 2.3 was GTR+I+G, with gamma distribution shape parameter of 0.163 and relative AIC weight of 1.000. The COI phylogenetic tree revealed fourmain well-supported clades: Amphipoda, Calanoida, Euphausiacea, and Decapoda. The clade Decapoda could be further divided into Pleocyemata and Dendrobranchiata (**Figure 2**). Pleocyemata was the most abundant taxon, encompassing 56.5% of the total specimens, assignable to 45 species. Dendrobranchiata and Euphausiacea followed, with 15 species (24.1% of the total specimens) and 4 species (14.8% of the total specimens), respectively. Amphipoda and Calanoida together comprised 4.6% of the total specimens and 5 species.

## Genetic Divergence and Distribution Pattern

The uncorrected K2P pairwise distances within species averaged 0.81% and ranged from 0 to 4.04%. The congeneric divergences averaged 11.99%, and varied from the lowest of 5.18% in *Parapenaeus* to the highest of 17.82% in *Alpheus*. The confamilial divergences averaged 16.01%, varied from 11.14% (Sergestidae) to 19.56% (Candaciidae), and the divergences within orders averaged 23.12%, varied from 19.11% (Calanoida) to 26.79% (Decapoda; **Tables 2**, **S2**). The frequency distribution of pairwise K2P distances is shown in **Figure 3**. It displayed a notable gap of 3.5–10.7% between intraspecific and interspecific distances within theentire sequence dataset.

The spatial distribution of the crustacean larvae in the Zhongsha Islands waters is shown in **Figure 4**. High crustacean species numbers were found in western (sites 9 and 16) and southeastern (site 4) areas, while low species numbers were found in northeastern (site 1) and southern (sites 11 and 7) areas of the Zhongsha Islands. Larvae of Decapoda were recorded from all sampling sites except site 1; larvae of Amphipoda were only found at the edge of the Zhongsha Islands; larvae of Calanoida appeared only in the western area at the islands; and larvae of Euphausiacea were mainly distributed at the outer edge of Zhongsha Atoll and in the area between the atoll and Huangyan Island.

**TABLE 2 |** Summary of pairwise mitochondrial cytochrome c oxidase I (COI) barcode nucleotide divergences within various taxonomic levels, using K2P distances (%).

| Comparisons within | Minimum | Mean distance | Maximum | S.E. |
|---|---|---|---|---|
| Species | 0 | 0.81 | 4.04 | ± 0.28 |
| Genera | 5.18 | 11.99 | 17.82 | ± 1.27 |
| Families | 11.14 | 16.01 | 19.56 | ± 1.47 |
| Orders | 19.11 | 23.12 | 26.79 | ± 1.83 |
| Classes | 24.74 | 33.14 | 36.29 | ± 2.32 |

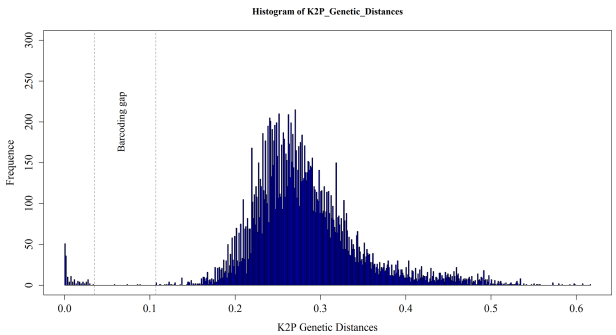


**FIGURE 3 |** Frequency distributions of intraspecific and interspecific pairwise genetic K2P distances based on all marine crustacean larvae sampled at the Zhongshan Islands. The area between dashed lines shows the "barcoding gap" between the intra- and interspecific distances.

## DISCUSSION

The South China Sea is regarded as one of thecenters of world marine biodiversity, which holds particular attraction for biodiversity researchers globally (Barber et al., 2000). The South China Sea biota is rich in warm-water species, comprising subtropical and tropical fauna of the Indo-Pacific biotic region, paralleled with the Philippines–Indonesia–New Guinea Coral Triangle as one of the typical tropical faunal centers. Crustaceans are the second-most-diverse group of marine metazoans in the South China Sea. Previous surveys and studies have together recorded a total of at least 2,150 species of crustaceans in the South China Sea (Liu, 2013). In our study, two DNA identification approaches, ABGD and GMYC, suggested that the 108 sequences obtained from marine crustacean larvae matched 68 and 70 species, respectively. Two species of snapping shrimp (*Alpheus dolerus* and *Alpheus* sp.) and two species of *Lucifer* prawns (*L. typus* and *Lucifer* sp.) were suggested as the same taxonomic units by ABGD. The results of the two molecular approaches were largely consistent. Our previous studies of fishes in the South China Sea similarly indicated that sibling or cryptic species are common among marine organisms (Trevor and Marti, 2003; Radulovici et al., 2009; Xu et al., 2019; Xu et al., 2021).

The efficacy of DNA barcoding is based on the assumption that the same species will have similar DNA barcodes representing their intraspecific variation, while interspecific divergence will far exceed intraspecific divergence. A clear "barcode gap" could be observed between the intraspecific and interspecific divergences (**Figure 3**). Intraspecific divergences are usually less than 1%, and rarely more than 2%, when the COI genes are used as DNA barcoding for animal species (Hebert et al., 2003). In our study, the intraspecific K2P distances for marine crustacean larvae ranged from 0 to 4.04% (average 0.81%). The highest intraspecific divergence (4.04%) was still below the common species identity cutoff value of 5% that has been used for both insects and crustaceans (Čandek and Kuntner, 2015; Karanovic, 2015). Intraspecific divergence values obtained in our study are common for crustaceans that have been precisely identified, though the values can be highly variable from one to another crustaceanspecies. For example, Jeffery et al. (2011) reported that intraspecific divergences in the Branchiopoda ranged from 0 to 3.4%, and Matzen da Silva et al. (2011) reported intraspecific divergences in Decapoda ranging between 0and 4.6%. However, the intraspecific divergence can be even higher in some crustacean groups. Aguilar et al. (2017) found the highest intraspecific divergence in *Branchinectalindahli* (order Anostraca) was 7.4%; Radulovici et al. (2009) reported that the highest intraspecific divergence in *Ampeliscaeschrichtii* (Amphipoda) reached 13.6%. Weiss et al. (2014) reported the highest range of intraspecific divergences in crustaceans, with the intraspecific divergences of *Gammarus fossarum* (Amphipoda) ranging from 0 to 23.3% (average 14.4%); the genetic divergence values among individuals within *Gammarus* were even higher than interspecific divergences among some crustaceans. However, because the genetic divergence values appeared extreme, Weiss et al. (2014) suggested that *G. fossarum* is a species complex of several highly divergent species. The congeneric divergences in our data ranged

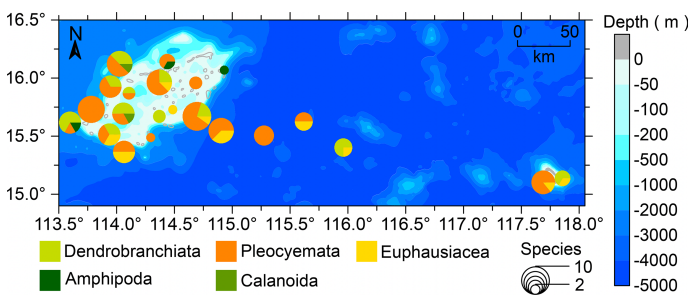


**FIGURE 4 |** The species composition and spatial distributions of marine crustacean larvae collected at the Zhongsha Islands, South China Sea.

from 5.18 to 17.82% and averaged 11.99%. Such a wide range of genetic divergences within congeneric species indicates that some taxa are more divergent from each other. For instance, the average congeneric divergence within genus *Parapenaeus* was 5.18%, considerably lower than 17.82% divergence within the genus *Alpheus*. These different values between genera perhaps reflect the average evolutionary time of congeneric species, as some species within genera will differentiate before others.

Previous studies proved that DNA barcoding is a reliable, rapid, and effective tool for precise species identification of morphologically similar crustacean larvae, such as through matching the COI sequences of unknown larvae with the available sequences of previously described adults in databases (Barber and Boyce, 2006; Webb et al., 2006; Tang et al., 2010; Kusbiyanto et al., 2020). In our study, the DNA identification method using the GMYC model suggested that the 108 sequences obtained from crustacean larvae represented 70 species. However, only 55 specimens (51%) of the larvae of 27 crustacean species matched with the COI sequences taken from adults of previously described species in the database. Altogether, 53 sequences from larvae of 43 species showed no or low similarity matches on the species level with sequences in the database, indicating that these species had never before been barcoded. Thus, our results imply that a minimum of three-fifths of additional marine crustacean species in the Zhongsha Islands waters are not yet described in their adult forms. Similar studies have reported on other sea areas. For example, Webb et al. (2006) reported that the majority of Antarctic marine crustacean larvae (60%) could be identified only to family level by matching the COI sequences with the database, and some were only identifiable to phylum or subphylum because of a lack of comparator sequences in databases. Barber and Boyce (2006) likewise found that only about 20% of the larval stomatopods collected in the Red Sea could be identified, while most of the adult forms represented yet undiscovered or undescribed species. Therefore, identifying novel DNA sequences is problematic in that a species definition cannot be assigned to the sequence without morphological identification. Together, these studies, including our reported cases, imply that the success rate of DNA identification largely depends on broad coverage of DNA barcodes for known species. Once the public databases are sufficiently complete, these query sequences, aided by the query-optimized search library, might be readily matched with reference sequences and assigned to reasonable species.

Our study not only confirms the utility of DNA barcoding for the identification of marine crustacean larvae but also provides insights into the diversity and distribution of crustaceans in the Zhongsha Islands waters. Crustaceans are one of the most speciose groups of coral reef fauna, comprising approximately 20% of all invertebrate species (Kramer et al., 2014). Our finding of numerous species in such restricted habitat types, water depths, and relatively small area, with at least three-fifths of the species seemingly not yet described, suggests that crustacean diversity at the Zhongsha Islands has been seriously underestimated until now.

We found that more than 80% of the crustacean larvae belonged to the order Decapoda, which are mostly larger-bodied species. The orders Calanoida and Amphipoda were represented by the fewest species. Decapods, as reef-associated crustaceans, are dominant benthic invertebrate group on the continental shelf and slope and are especially important contributors to coral reef ecosystems. For example, they can defend living corals from predators and remove parasites from fishes (Pratchett, 2001; Becker and Grutter, 2004). Several surveys of coral reef communities were carried out by international scientists in the South China Sea in the 1960s and 1990s. These surveys recorded as many as 694 species of decapods in the South China Sea and found that several species of coral-dwelling decapods are commonly found in the northern part of the South China Sea, such as *Synalpheusdemani*, *Trapezia* spp., *Coralliocaris* spp., *Tetralia* spp., and *Thalamita* spp. (Liu, 2013). However, except for coral reef crab *Thalamita* spp., we did not find larvae of the above species at the Zhongsha Islands. This difference in survey findings implies that there is potential larval dispersal between the Zhongsha Islands and adjacent areas. In addition, understanding the nature of marine crustacean larval dispersal is key to understanding the evolution and dynamics of marine crustacean populations and for implementing effective stock management and conservation plans (Largier, 2003). Our results revealed notable differences in the distributions of larvae of different crustacean species present in the Zhongsha Islands waters. The species numbers were higher in the northwestern and southeastern areas of the Zhongsha Atoll, and lower in sites at the northeastern edge. Amphipoda larvae were only found at the edge of the Zhongsha Atoll, and Calanoida larvae appeared in the western part of the atoll. The distribution of crustacean larvae in the Zhongsha Islands waters is doubtlessly related to oceanographic features. The surface currents at the Zhongsha Islands are strongly influenced by the East Asian Monsoon cycle; the surface current is northeastward during the summer monsoon, and southwestward during the winter monsoon (Yang et al., 2002). The upwelling water causes by the monsoon would promote larval dispersal and provides sufficient food sources, for example supporting the highly diverse crustacean larvae in the western part of the Zhongsha Atoll. Furthermore, the variety of microhabitats on coral reefs creates shelter for crustacean larvae, helping to maintain higher survival. Since coral reefs worldwide currently face a variety of environmental and anthropogenic pressures, comprehensive understanding of crustacean larvae community structure, and the ecological processeson coral reef would establish a basis for the restoration and protection of coral reef ecosystems.

## CONCLUSION

Our study demonstrates DNA barcoding as a reliable, rapid, and effective tool for precise species identification of morphologically similar marine crustacean larvae, such as those collected from the Zhongsha Islands waters. However, sequences obtained from larvae of only 27 species were matched with the COI sequences taken from previously described adults in the BOLD database. Consequently, less than half of the crustacean larvae collected in the present study at the Zhongsha Islands could be identified to

species. This outcome was not a failure of the DNA barcoding methodology, yet it reflects that the crustacean diversity at the islands has been seriously underestimated until now.

Our study shows that the success rate of DNA identification largely depends on broad coverage of DNA barcodes for known species. However, without adequate taxonomic descriptions for all known species, barcode sequences can lose much of their value. More than 80% of the marine crustacean larvae collected in the Zhongsha Islands waters belonged to the order Decapoda, which are relatively large-bodied species. The orders Calanoida and Amphipoda were represented by the fewest species and these larvae appeared only at the edge of Zhongsha Atoll.

## DATA AVAILABILITY STATEMENT

The datasets presented in this study can be found in online repositories. The names of the repository/repositories and accession number(s) can be found in the article/**Supplementary Material**.

## AUTHOR CONTRIBUTIONS

LX: conceptualization, methodology, formal analysis, data curation, writing—original draft, writing—review and editing. LW, JN, DH, YL, and SL: methodology and formal analysis. XW and FD: funding acquisition, project administration, and resources. All authors contributed to the article and approved the submitted version.

## FUNDING

This study was funded by Science and Technology Basic Resources Investigation Program of China (2018FY100105, 2017FY201405) and Fund of Guangdong Provincial Key Laboratory of Fishery Ecology and Environment (FEEL-2019-9).

## ACKNOWLEDGMENTS

We thank all colleagues and students for their help with sampling. Cynthia Kulongowski with Liwen Bianji (Edanz; https://www.liwenbianji.cn) assisted with editing the language of a draft of this manuscript.

## SUPPLEMENTARY MATERIAL

The Supplementary Material for this article can be found online at: https://www.frontiersin.org/articles/10.3389/fmars.2022.932678/full#supplementary-material

## REFERENCES

Aguilar, A., Maeda-Martínez, A. M., Murugan, G., Obregón-Barboza, H., Christopher Rogers, D., McClintock, K., et al. (2017). High Intraspecific Genetic Divergence in the Versatile Fairy Shrimp Branchinecta Lindahli With a Comment on Cryptic Species in the Genus Branchinecta (Crustacea: Anostraca). *Hydrobiologia* 801 (1), 59–69. doi: 10.1007/s10750-017-3283-3

Alford, R. A. and Jackson, G. D. (1993). Do Cephalopods and Larvae of Other Taxa Grow Asymptotically? *Am. Nat.* 141 (5), 717–728. doi: 10.1086/285501

Anger, K. (2001). *The Biology of Decapod Crustacean Larvae* (Rotterdam: A. A. Balkema Publishes).

Ballard, J. W. O. and Whitlock, M. C. (2004). The Incomplete Natural History of Mitochondria. *Mol. Ecol.* 13 (4), 729–744. doi: 10.1046/j.1365-294X.2003.02063.x

Barber, P. and Boyce, S. L. (2006). Estimating Diversity of Indo-Pacific Coral Reef Stomatopods Through DNA Barcoding of Stomatopod Larvae. *Proc. R. Soc B.* 273 (1597), 2053–2061. doi: 10.1098/rspb.2006.3540

Barber, P. H., Palumbi, S. R., Erdmann, M. V. and Moosa, M. K. (2000). A Marine Wallace's Line? *Nature* 406 (6797), 692–693. doi: 10.1038/35021135

Becker, J. H. and Grutter, A. S. (2004). Cleaner Shrimp do Clean. *Coral Reefs* 23 (4), 515–520. doi: 10.1007/s00338-004-0429-3

Bernt, M., Braband, A., Schierwater, B. and Stadler, P. F. (2013). Genetic Aspects of Mitochondrial Genome Evolution. *Mol. Phylogen. Evol.* 69 (2), 328–338. doi: 10.1016/j.ympev.2012.10.020

Bertram, D. F. and Strathmann, R. R. (1998). Effects of Maternal and Larval Nutrition on Growth and Form of Planktotrophic Larvae. *Ecology* 79 (1), 315–327. doi: 10.2307/176885

Bilgin, R., Utkan, M. A., Kalkan, E., Karhan, S. U. and BekbÖLet, M. (2014). DNA Barcoding of Twelve Shrimp Species (Crustacea: Decapoda) From Turkish Seas Reveals Cryptic Diversity. *Mediterr. Mar. Sci.* 16 (1), 36–45. doi: 10.12681/ mms.548

Bucklin, A., Batta-Lona, P. G., Questel, J. M., Wiebe, P. H., Richardson, D. E., Copley, N. J., et al. (2022). COI Metabarcoding of Zooplankton Species Diversity for Time-Series Monitoring of the NW Atlantic Continental Shelf. *Front. Mar. Sci.* 9. doi: 10.3389/fmars.2022.867893

Čandek, K. and Kuntner, M. (2015). DNA Barcoding Gap: Reliable Species Identification Over Morphological and Geographical Scales. *Mol. Ecol. Resour.* 15 (2), 268–277. doi: 10.1111/1755-0998.12304

Clare, E. L., Lim, B. K., Engstrom, M. D., Eger, J. L. and Hebert, P. D. N. (2007). DNA Barcoding of Neotropical Bats: Species Identification and Discovery Within Guyana. *Mol. Ecol. Notes* 7 (2), 184–190. doi: 10.1111/j.1471-8286.2006.01657.x

Costa, F. O., deWaard, J. R., Boutillier, J., Ratnasingham, S., Dooh, R. T., Hajibabaei, M., et al. (2007). Biological Identifications Through DNA Barcodes: The Case of the Crustacea. *Can. J. Fish. Aquat. Sci.* 64 (2), 272–295. doi: 10.1139/f07-008

Drummond, A. J. and Rambaut, A. (2007). BEAST: Bayesian Evolutionary Analysis by Sampling Trees. *BMC Evol. Biol.* 7 (1), 214. doi: 10.1186/1471-2148-7-214

Drummond, A. J., Suchard, M. A., Xie, D. and Rambaut, A. (2012). Bayesian Phylogenetics With BEAUti and the BEAST 1.7. *Mol. Biol. Evol.* 29 (8), 1969–1973. doi: 10.1093/molbev/mss075

Ezard, T. H. G., Fujisawa, T. and Barraclough, T. G. (2009). *Splits: Species' LImits by Threshold Statistics*.

Folmer, O., Black, M., Hoeh, W., Lutz, R. and Vrijenhoek, R. (1994). DNA Primers for Amplification of Mitochondrial Cytochrome C Oxidase Subunit I From Diverse Metazoan Invertebrates. *Mol. Mar. Biol. Biotechnol.* 3 (5), 294–299.

Forward, R. B. (1990). Behavioral Responses of Crustacean Larvae to Rates of Temperature Change. *Biol. Bull.* 178 (3), 195–204. doi: 10.2307/1541819

Fujisawa, T. and Barraclough, T. G. (2013). Delimiting Species Using Single-Locus Data and the Generalized Mixed Yule Coalescent Approach: A Revised Method and Evaluation on Simulated Data Sets. *Syst. Biol.* 62 (5), 707–724. doi: 10.1093/sysbio/syt033

Ghouri, M. Z., Ismail, M., Javed, M. A., Khan, S. H., Munawar, N., Umar, A. B., et al. (2020). Identification of Edible Fish Species of Pakistan Through DNA Barcoding. *Front. Mar. Sci.* 7. doi: 10.3389/fmars.2020.554183

Guimarães-Costa, A., Machado, F. S., Reis-Filho, J. A., Andrade, M., Araújo, R. G., Corrêa, E. M. R., et al. (2020). DNA Barcoding for the Assessment of the Taxonomy and Conservation Status of the Fish Bycatch of the

Northern Brazilian Shrimp Trawl Fishery. *Front. Mar. Sci.* 7. doi: 10.3389/fmars.2020.566021

Hajibabaei, M., Janzen Daniel, H., Burns John, M., Hallwachs, W. and Hebert Paul, D. N. (2006). DNA Barcodes Distinguish Species of Tropical Lepidoptera. *Proc. Natl. Acad. Sci. U.S.A.* 103 (4), 968–971. doi: 10.1073/pnas.0510466103

Hall, T. A. (1999). BioEdit: A User-Friendly Biological Sequence Algnment Editor and Analysis Program for Windows 95/98/NT. *Nucl. Acids Symp. Ser.* 41, 95–98.

Hebert, P. D., Cywinska, A., Ball, S. L. and deWaard, J. R. (2003). Biological Identifications Through DNA Barcodes. *Proc. R. Soc B.* 270 (1512), 313–321. doi: 10.1098/rspb.2002.2218

Hebert, P. D., Stoeckle, M. Y., Zemlak, T. S. and Francis, C. M. (2004). Identification of Birds Through DNA Barcodes. *PLos Biol.* 2 (10), e312. doi: 10.1371/journal.pbio.0020312

Huang, X., Betzler, C., Wu, S., Bernhardt, A., Eagles, G., Han, X., et al. (2020). First Documentation of Seismic Stratigraphy and Depositional Signatures of Zhongsha Atoll (Macclesfield Bank), South China Sea. *Mar. Pet. Geol.* 117, 104349. doi: 10.1016/j.marpetgeo.2020.104349

Huang, D., Chen, J., Xu, L., Wang, X., Ning, J., Li, Y., et al. (2022). Larval Fish Assemblages and Distribution Patterns in the Zhongsha Atoll (Macclesfield Bank, South China Sea). *Front. Mar. Sci.* 8. doi: 10.3389/fmars.2021.787765

Hubert, N., Hanner, R., Holm, E., Mandrak, N. E., Taylor, E., Burridge, M., et al. (2008). Identifying Canadian Freshwater Fishes Through DNA Barcodes. *PLos One* 3 (6), e2490. doi: 10.1371/journal.pone.0002490

Huelsenbeck, J. P., Ronquist, F., Nielsen, R. and Bollback, J. P. (2001). Bayesian Inference of Phylogeny and Its Impact on Evolutionary Biology. *Sci. (New York N.Y.)* 294 (5550), 2310–2314. doi: 10.1126/science.1065889

Janzen, D. H., Hajibabaei, M., Burns, J. M., Hallwachs, W., Remigio, E. and Hebert, P. D. (2005). Wedding Biodiversity Inventory of a Large and Complex Lepidoptera Fauna With DNA Barcoding. *Philos. Trans. R. Soc Lond. B Biol. Sci.* 360 (1462), 1835–1845. doi: 10.1098/rstb.2005.1715

Jeffery, N. W., Elias-Gutierrez, M. and Adamowicz, S. J. (2011). Species Diversity and Phylogeographical Affinities of the Branchiopoda (Crustacea) of Churchill, Manitoba, Canada. *PLos One* 6 (5), e18364. doi: 10.1371/journal.pone.0018364

Karanovic, I. (2015). Barcoding of Ancient Lake Ostracods (Crustacea) Reveals Cryptic Speciation With Extremely Low Distances. *PLos One* 10 (3), e0121133. doi: 10.1371/journal.pone.0121133

Ko, H. L., Wang, Y. T., Chiu, T. S., Lee, M. A., Leu, M. Y., Chang, K. Z., et al. (2013). Evaluating the Accuracy of Morphological Identification of Larval Fishes by Applying DNA Barcoding. *PLos One* 8 (1), e53451. doi: 10.1371/journal.pone.0053451

Kramer, M. J., Bellwood, D. R. and Bellwood, O. (2014). Benthic Crustacea on Coral Reefs: A Quantitative Survey. *Mar. Ecol. Prog. Ser.* 511, 105–116. doi: 10.3354/meps10953

Kusbiyanto, K., Bhagawati, D. and Nuryanto, A. (2020). DNA Barcoding of Crustacean Larvae in the Eastern Areas of Segara Anakan Cilacap, Central Java Indonesia. *Biodiversitas* 21 (10), 4878–4887. doi: 10.13057/biodiv/d211054

Largier, J. L. (2003). Considerations in Estimating Larval Dispersal Distances From Oceanographic Data. *Ecol. Appl.* 13 (sp1), 71–89. doi: 10.1890/1051-0761(2003)013[0071:CIELDD]2.0.CO;2

Liu, J. Y. (2013). Status of Marine Biodiversity of the China Seas. *PLos One* 8 (1), e50719. doi: 10.1371/journal.pone.0050719

Li, Y., Zhang, J., Chen, Z., Gong, Y., Cai, Y., Yang, Y. et al., (2020). Study on Taxonomic Diversity of Fish in Zhubi Reef of Nansha Islands. *South China Fish. Sci.* 16, 36–41. doi: 10.12131/20190159

Lorenz, J. G., Jackson, W. E., Beck, J. C. and Hanner, R. (2005). The Problems and Promise of DNA Barcodes for Species Diagnosis of Primate Biomaterials. *Phil. Trans. R. Soc B.* 360 (1462), 1869–1877. doi: 10.1098/rstb.2005.1718

Lu, Z., Li, M., Zhang, J., Zhang, S., Li, H., Jiang, P., et al. (2021). Preliminary Study on Species Composition of Fish Eggs of Meiji Reef Lagoon in South China Sea Based on DNA Barcoding. *South China Fish. Sci.* 17, 12–21. doi: 10.12131/20210091

Matzen da Silva, J., Creer, S., dos Santos, A., Costa, A. C., Cunha, M. R., Costa, F. O., et al. (2011). Systematic and Evolutionary Insights Derived From mtDNA COI Barcode Diversity in the Decapoda (Crustacea: Malacostraca). *PLos One* 6 (5), e19449. doi: 10.1371/journal.pone.0019449

Morton, B. and Blackmore, G. (2001). South China Sea. *Mar. Pollut. Bull.* 42 (12), 1236–1263. doi: 10.1016/s0025-326x(01)00240-5

Nylander, J. A. A. (2004). *MrModeltest V2. Program Distributed by the Author* (Sweden: Evolutionary Biology Centre,Uppsala University).

Page, R. D. M. (1996). Tree View: An Application to Display Phylogenetic Trees on Personal Computers. *Bioinformatics* 12 (4), 357–358. doi: 10.1093/bioinformatics/12.4.357

Pons, J., Barraclough, T. G., Gomez-Zurita, J., Cardoso, A., Duran, D. P., Hazell, S., et al. (2006). Sequence-Based Species Delimitation for the DNA Taxonomy of Undescribed Insects. *Syst. Biol.* 55 (4), 595–609. doi: 10.1080/10635150600852011

Pratchett, M. (2001). Influence of Coral Symbionts on Feeding Preferences of Crown-of-Thorns Starfish Acanthaster Planci in the Western Pacific. *Mar. Ecol. Prog. Ser.* 214, 111–119. doi: 10.3354/meps214111

Puillandre, N., Lambert, A., Brouillet, S. and Achaz, G. (2012). ABGD, Automatic Barcode Gap Discovery for Primary Species Delimitation. *Mol. Ecol.* 21 (8), 1864–1877. doi: 10.1111/j.1365-294X.2011.05239.x

Radulovici, A. E., Archambault, P. and Dufresne, F. (2010). DNA Barcodes for Marine Biodiversity: Moving Fast Forward? *Diversity* 2 (4), 450–472. doi: 10.3390/d2040450

Radulovici, A. E., Sainte-Marie, B. and Dufresne, F. (2009). DNA Barcoding of Marine Crustaceans From the Estuary and Gulf of St Lawrence: A Regional-Scale Approach. *Mol. Ecol. Resour.* 9 (s1), 181–187. doi: 10.1111/j.1755-0998.2009.02643.x

Ratnasingham, S. and Hebert, P. D. N. (2007). BOLD: The Barcode of Life Data System. *Mol. Ecol. Notes* 7 (3), 355–364. doi: 10.1111/j.1471-8286.2007.01678.x

Ratnasingham, S. and Hebert, P. D. N. (2013). A DNA-Based Registry for All Animal Species: The Barcode Index Number (BIN) System. *PLos One* 8 (7), e66213. doi: 10.1371/journal.pone.0066213

R Development Core Team (2017). *R: A Language and Environment for Statistical Computing* (Vienna, Austria: R Foundation for Statistical Computing).

Richter, S., Olesen, J. and Wheeler, W. C. (2007). Phylogeny of Branchiopoda (Crustacea) Based on a Combined Analysis of Morphological Data and Six Molecular Loci. *Cladistics* 23 (4), 301–336. doi: 10.1111/j.1096-0031.2007.00148.x

Smith, M. A., Fisher, B. L. and Hebert, P. D. N. (2005). DNA Barcoding for Effective Biodiversity Assessment of a Hyperdiverse Arthropod Group: The Ants of Madagascar. *Phil. Trans. R. Soc B.* 360 (1462), 1825–1834. doi: 10.1098/rstb.2005.1714

Tamura, K., Stecher, G., Peterson, D., Filipski, A. and Kumar, S. (2013). MEGA6: Molecular Evolutionary Genetics Analysis Version 6.0. *Mol. Biol. Evol.* 30 (12), 2725–2729. doi: 10.1093/molbev/mst197

Tang, R. W. K., Yau, C. and Ng, W.-C. (2010). Identification of Stomatopod Larvae (Crustacea: Stomatopoda) From Hong Kong Waters Using DNA Barcodes. *Mol. Ecol. Resour.* 10 (3), 439–448. doi: 10.1111/j.1755-0998.2009.02794.x

Tittensor, D. P., Mora, C., Jetz, W., Lotze, H. K., Ricard, D., Berghe, E. V., et al. (2010). Global Patterns and Predictors of Marine Biodiversity Across Taxa. *Nature* 466 (7310), 1098–1101. doi: 10.1038/nature09329

Trevor, J. W. and Marti, J. A. (2003). Structure of Cryptic Reef Fish Assemblages: Relationships With Habitat Characteristics and Predator Density. *Mar. Ecol. Prog. Ser.* 257, 209–221. doi: 10.3354/meps257209

Ward, R. D., Hanner, R. and Hebert, P. D. (2009). The Campaign to DNA Barcode All Fishes, FISH-BOL. *J. Fish. Biol.* 74 (2), 329–356. doi: 10.1111/j.1095-8649.2008.02080.x

Ward, R. D., Zemlak, T. S., Innes, B. H., Last, P. R. and Hebert, P. D. (2005). DNA Barcoding Australia's Fish Species. *Phil. Trans. R. Soc B.* 360 (1462), 1847–1857. doi: 10.1098/rstb.2005.1716

Webb, K. E., Barnes, D. K. A., Clark, M. S. and Bowden, D. A. (2006). DNA Barcoding: A Molecular Tool to Identify Antarctic Marine Larvae. *Deep. Sea. Res. (II Top. Stud. Oceanogr.)* 53 (8), 1053–1060. doi: 10.1016/j.dsr2.2006.02.013

Weiss, M., Macher, J. N., Seefeldt, M. A. and Leese, F. (2014). Molecular Evidence for Further Overlooked Species Within the Gammarus Fossarum Complex (Crustacea: Amphipoda). *Hydrobiologia* 721 (1), 165–184. doi: 10.1007/s10750-013-1658-7

Xu, L., Han, B.-P., Van Damme, K., Vierstraete, A., Vanfleteren, J. R. and Dumont, H. J. (2011). Biogeography and Evolution of the Holarctic Zooplankton Genus

Leptodora (Crustacea: Branchiopoda: Haplopoda). *J. Biogeogr.* 38 (2), 359–370. doi: 10.1111/j.1365-2699.2010.02409.x

Xu, L., Van Damme, K., Li, H., Ji, Y., Wang, X. and Du, F. (2019). A Molecular Approach to the Identification of Marine Fish of the Dongsha Islands (South China Sea). *Fish. Res.* 213, 105–112. doi: 10.1016/j.fishres.2019.01.011

Xu, L., Wang, X., Van Damme, K., Huang, D., Li, Y., Wang, L., et al. (2021). Assessment of Fish Diversity in the South China Sea Using DNA Taxonomy. *Fish. Res.* 233, 105771. doi: 10.1016/j.fishres.2020.105771

Yang, H., Liu, Q., Liu, Z., Wang, D. and Liu, X. (2002). A General Circulation Model Study of the Dynamics of the Upper Ocean Circulation of the South China Sea. *J. Geophys. Res.* 107 (C7), 22–21-22-14. doi: 10.1029/2001JC001084

Zhao, X. and Jia, P. (2020). Towards Sustainable Small-Scale Fisheries in China: A Case Study of Hainan. *Mar. Policy* 121, 103935. doi: 10.1016/j.marpol.2020.103935

**Conflict of Interest:** The authors declare that the research was conducted in the absence of any commercial or financial relationships that could be construed as a potential conflict of interest.

frontiers | Frontiers in Marine Science

ORIGINAL RESEARCH
published: 18 July 2022
doi: 10.3389/fmars.2022.895219

# The Effects of Trans-Basin Climate Variability on Skipjack Tuna in the Northwest Pacific Ocean: Causal and Nonstationary

*Xiangyun Hou*[1], *Shuyang Ma*[1], *Yongjun Tian*[1,2*] *and Shaoqing Zhang*[3,4]

[1] *Frontiers Science Center for Deep Ocean Multispheres and Earth System and Key Laboratory of Mariculture, Ministry of Education, Ocean University of China, Qingdao, China,* [2] *Laboratory for Marine Fisheries Science and Food Production Processes, Pilot National Laboratory for Marine Science and Technology (Qingdao), Qingdao, China,* [3] *Frontiers Science Center for Deep Ocean Multispheres and Earth System and Key Laboratory of Physical Oceanography, Institute for Advanced Ocean Study, The College of Ocean and Atmosphere, Ocean University of China, Qingdao, China,* [4] *Functional Laboratory for Ocean Dynamical Processes and Climate, Pilot National Laboratory for Marine Science and Technology (Qingdao), Qingdao, China*

Skipjack tuna *(Katsuwonus pelamis*, SKJ), a widely distributed and highly migratory pelagic fish, dominates the global tuna catch, especially in the Pacific Ocean, with nearly 70% of world catch. Studies have reported that SKJ in the tropical Pacific was strongly associated with Niño-Southern Oscillations, while the relationship between SKJ in the Northwest Pacific (NWP, the second-contributed statistical area of SKJ Pacific catch) and climate variability has not yet been well understood. Considering the teleconnection between western Pacific and Atlantic Ocean, this study investigates the potential relationship between the relative abundance CPUE (Catch Per Unit Effort) of SKJ and climate indices including trans-basin and basin signals at different spatial-temporal scales in the NWP during 1972–2019 using Convergent Cross Mapping (CCM) and Threshold Generalized Additive Model (TGAM) techniques. Results show the Atlantic Multidecadal Oscillation (AMO) plays a causal role in the temporal SKJ variations with an optimal lag at 15 months, while further analysis preliminarily reveals sea surface temperature acts as a vital medium in the relationship through teleconnection. The AMO effected SKJ processes are nonstationary over the study time, of which the transition years occurred in the early 1990s (around 1991/92). Providing an unprecedented insight into climate variability effect on SKJ in the NWP, this study has essential implications and reference for predicting and managing SKJ fishery through incorporating the climate index in estimating the SKJ abundance in advance, and for the connection between large-migrating species and tans-basin climatic variation.

**Keywords: Skipjack tuna, climate variability, causality, trans-basin teleconnection, nonstationary relationship**

OPEN ACCESS

***Edited by:***
*Jun Xu,*
*Institute of Hydrobiology (CAS), China*

***Reviewed by:***
*Xinqing Zheng,*
*State Oceanic Administration, China*
*Lilis Sadiyah,*
*Center for Fisheries Research, Indonesia*

***Correspondence:**
*Yongjun Tian*
*yjtian@ouc.edu.cn*

***Specialty section:***
*This article was submitted to Marine Ecosystem Ecology, a section of the journal Frontiers in Marine Science*

***Received:*** *13 March 2022*
***Accepted:*** *01 June 2022*
***Published:*** *18 July 2022*

***Citation:***
*Hou X, Ma S, Tian Y and Zhang S (2022) The Effects of Trans-Basin Climate Variability on Skipjack Tuna in the Northwest Pacific Ocean: Causal and Nonstationary. Front. Mar. Sci. 9:895219. doi: 10.3389/fmars.2022.895219*

## 1 INTRODUCTION

Tunas are important in ecological meaning and are highly commercial for being an upper predator distributed extensively in the ocean. Studies have found that population dynamics of tunas were involved with climate variability, which was shown in aspects of the recruitment variability, fishing ground distribution, and catch fluctuations (Sugimoto et al., 2001; Lima &

Naya, 2011; Carlos Baez et al., 2020; Wu et al., 2020a), and could be well described by large-scale climate patterns, such as the ENSO (El Niño-Southern Oscillation), IOD (Indian Ocean Dipole), and AMO (Atlantic Multi-decadal Oscillation) (Lehodey et al., 1997; Lan et al., 2013; Faillettaz et al., 2019).

Skipjack tuna (*Katsuwonus pelamis*, hereinafter as SKJ), has been the most productive tuna fishery species worldwide. Its catch ranked third among the ten marine capture species for the ninth consecutive year in 2017 (FAO, 2020). SKJ catch in the Pacific (nearly 0.9 million tons per year) has contributed to more than 70% of global SKJ catch since 1950. This can be attributed to its shorter life cycle with the first mature length (about 45 cm) and wider habitats from temperate to equatorial areas than other tunas (Collette & Nauen, 1983). Up to date, the maximum reported SKJ age was 12 years (Collette & Nauen, 1983). Studies involved with stock assessment and tagging surveys typically assume that SKJ forms a single stock in the Pacific Ocean with long-distance movement, which is characterized by migrating from west to east along the equator and migrating across the equator longitudinally (Kiyofuji et al., 2019; Ashida, 2020; Moore et al., 2020). Despite this, Ashida (2020) found that the first mature time, spawning mode, and fecundity of SKJ varied between the tropical Pacific Ocean and the extratropical waters.

The first response of SKJ to climate oscillations was verified in the western tropical Pacific (the highest production area among the Pacific (**Figure S1**, FAO online data), which supported the prediction of SKJ fishery two months in advance through ENSO index (Lehodey et al., 1997). By contrast, whether SKJ in the Northwest Pacific (hereinafter as NWP), the major contributor in the extratropical Pacific and the second contributor in the whole Pacific from 1950 to 2000 (**Figure S1**, FAO online data), is linked with climate variability remains unclear. SKJ in the NWP comprises individuals with various migration patterns evidenced through parasite identification (Takano et al., 2021). Based on the tagging experiments, SKJ in the NWP mainly comprises three groups: the first group that the North Pacific Gyre Oscillation (NPGO) or Pacific Decadal Oscillation (PDO) might influence as it migrated from the northeast Pacific, the second group whose parents linked with ENSO, mainly comprised small-size SKJ individuals traveled from the western tropical Pacific (Lehodey et al., 1997; Arai et al., 2005; Moore et al., 2020), and the third group who spawns at the offshore area of the Nansei Islands, Japan and makes a northward seasonal migration across Kuroshio Current in the NWP (defined as a local group too) (Kiyofuji et al., 2019; Tawa et al., 2020) (**Figure 1**). Previous studies showed that the effects of basin-scale climate variability on fisheries varied largely in the NWP. For example, the suitable habitat of neon flying squid extended southward with increasing abundance during La Niña events, whereas albacore tuna Catch Per Unit Effort (CPUE). is lower (Mukti & Saitoh, 2004; Yu et al., 2019). In contrast, Japanese anchovy was positively related to PDO on a centurial scale through sea surface temperature (SST) (Zhou et al., 2015). Notably, recent research discovered the trans-basin interaction between the Pacific and Atlantic Oceans (Enfield et al., 2001; Zhang & Delworth, 2007), and the AMO plays a vital role in the natural variability of the western Pacific (Sun et al., 2017; Sun et al., 2020; Sun et al., 2021), especially on the NWP through the North Pacific subtropical mode water (Wu et al., 2020b). In this sense, whether one or multiply long-term climate oscillations could be a proxy for

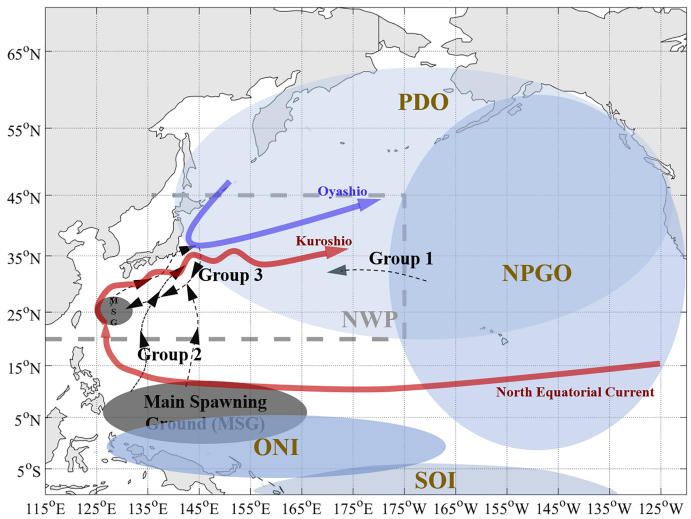


**FIGURE 1 |** Schematic of the study area in the north Pacific with main currents, climate background, and migration routes of skipjack tuna inside. The study area (Northwest Pacific, NWP) is surrounded by the grey-dotted lines and the mainland coast of countries, including China, Korea, South Korea, Japan, and Russia. Blue ellipses show the defined scope of climate indices with different brightness. The main spawning grounds (MSG) of SKJ in the western Pacific and potential migration routes of three groups of skipjack tuna in the NWP are indicated with black arrow lines and grey ellipses, respectively (Arai et al., 2005; Kiyofuji et al., 2019; Tawa et al., 2020; Moore et al., 2020). The paths of Kuroshio Current with its origin (North Equatorial Current) and extension and Oyashio Current are shown by red and dark blue arrow lines, respectively.

controlling the SKJ fluctuation in the NWP is to be concerned and is of great economic importance for adopting pre-emptive management rules to keep the sustainable development of the SKJ fishery.

Many studies found that the tuna response to climatic regime shifts was "seesaw"-like. Such as, yellowfin tuna in the western Indian Ocean was in phase with the Dipole Modular Index during negative IOD phases, and vice versa (Lan et al., 2013).The suitable habitat of Atlantic bluefin tuna in the North Atlantic Ocean was controlled by an opposite pattern in the zonal direction during different AMO phases (Faillettaz et al., 2019). Indeed, the modulation of climate oscillations would be more complex and uncertain with longer time, especially for the upper predator on the ecosystem, such as tunas on a decadal scale. Ménard et al. (2007) reported that yellowfin tuna and bigeye tuna were intermittently linked with the Indian Oscillation Index at decadal scales (from 1955 to 2003). Therefore, the relationship between climate indices and tuna is probably time-dependent or phase-dependent rest on the regime shift point of the climate index. Recent studies supported that Threshold Generalized Additive Model (TGAM) performs well in identifying the change point of a relationship by fitting two functions for different periods (Puerta et al., 2019; Ma et al., 2020; Ma et al., 2021), which can be used to understand whether the SKJ-climate relationship in the NWP is nonstationary and determine the regime-shift point as well.

Correlation analysis is frequently used in the ecological study to couple with environment, while the correlation does not imply causation because of the joint driving factor between two variables. Moreover, a mirage correlation that is characterized by a weak or an intermittent correlation across the long time series could hide the real causation signal (Sugihara et al., 2012; Chang et al., 2017). Sugihara et al. (2012) developed a non-parametric method that could distinguish the real cause-effect relationship from the above situations through transforming the time series into low-dimension and nonlinear dynamic systems in the state space, which is called the cross-convergence mapping (CCM). It has been successfully used in fishery oceanography, Doi et al. (2021) revealed that temperature influenced species richness over thousands-year time scales. Nakayama et al. (2018) showed that the population dynamics of anchovy and sardine in the NWP were controlled by the double effect of climate change and interspecies dynamics.

Combined with the above considerations, this study applies CCM and TGAM methods to SKJ in the NWP, and the prominent climate patterns that overlap migratory SKJ habitat to identify: a) whether there is a causal connection between SKJ in the NWP and climate variability, especially for the AMO), b) whether the interaction process between climate variability and SKJ is nonstationary on the decadal scale.

# 2 MATERIALS AND METHODS

## 2.1 Study Area

NWP area is referred to as FAO Major Fishing Area 61, which is compassed by the north of 20°N and the west of 175°W across the mainland coast of countries, including China, North Korea, South Korea, Japan, and Russia. Note that SKJ catch in the southwestern corner of FAO Area 61, i.e., west of 115°E and south of 20°N, is excluded in the study as it is near zero and the study area is limited to the south of 45°N of NWP area, considering the distribution of SKJ (**Figure 1**).

## 2.2 Fishery Data

Monthly aggregated SKJ catch data using fishery gear types (pole and line, and purse seine) were provided from WCPFC (Western and Central Pacific Fisheries Commission, http://www.wcpfcnt/public-domain, last accessed in November 2020). The primary result of retrieved data for the NWP area showed that pole and line fishery was the main operating gear with its catch nearly six times to the purse seine fishery during 1972–2019. Finally, this study uses the pole and line data with a resolution of 5°, which comprises year, month, catch, effort (operating days), latitude, and longitude. CPUE is assumed to be a common proxy for fish relative abundance. In this study, the CPUE of SKJ is defined as SKJ catch in metric tons per operating day.

**TABLE 1 |** The definition and sources of climatic indices.

| Climatic indices | Definition | Data source | Resolution |
|---|---|---|---|
| ONI3,4 | The ocean part of ENSO event, is defined as a 3-month running mean of SST anomalies in the Niño 3.4 region (5°N–5°S, 120°–170°W). | https://origin.cpc.ncep.noaa.gov/products/analysis_monitoring/ensostuff/ONIv5.php | Monthly |
| SOI | The atmospheric part of the ENSO climate pattern by comparing surface air pressure anomalies at Darwin, Australia, to pressure anomalies at Tahiti. | https://www.ncdc.noaa.gov/teleconnections/enso/soi | Monthly |
| PDO | The leading pattern of SST anomalies in the North Pacific basin north of 20°N. | http://swww.ncdc.noaa.govteleconnectionspdo | Monthly |
| NPGO | A climate pattern that emerges as the 2nd dominant mode of sea surface height variability (2nd EOF SSH) in the Northeast Pacific. | http://www.oces.us/npgo/enso.html | Monthly |
| AMO | The average SST anomalies in the North Atlantic basin, typically over 0–65° N, 80° W–0°. | http://www.psl.noaa.gov/data/timeseries/AMO/ | Monthly |
| SST | Sea surface temperature of the NWP. | https://www.met.office.gov.uk/hadobs/hadsst3 | Monthly & 5°(spatial) |

## 2.3 Climatic Data

Five climate indices associated largely with the NWP and SKJ migration (**Figure 1**), and SST data of the NWP with a resolution of 5°are employed in this study (**Table 1**). All data were monthly time series with a period of 1972–2019.

## 2.4 Convergent Cross Mapping

Convergent cross mapping (CCM) is an approach that can distinguish causality from mirage correlation in time series from dynamical (i.e., nonlinear) systems, which is nonparametric and rooted on state space reconstruction (Sugihara et al., 2012). The fundamental CCM principle is that the cause time series left its footprints on the effect time series at a state space level. Before applying CCM analysis, CPUEda is created to represent the anomaly fluctuations of SKJ relative abundance by detrending CPUE first and subsequently monthly anomaly of the detrended CPUE. The relationship between CPUEda and climate indices were preliminarily analyzed using the Spearman rank correlation, which provides a measure of a monotonic relationship between two continuous random variables and is useful with non-normal data, the 95% significance level is set on the correlation analysis. Results showed no prominent relationship between climate indices and SKJ existed except for a weak and negative correlation between NPGO and SKJ (**Table S1**). Here, time series are transformed into a dynamic system of low-dimension and nonlinear to represent its space state before performing CCM by the following steps:

### 1) Determining the Best Embedding Dimension (*E*)

Based on Takens' Theorem, the dynamics of the system can be gotten from the time lags of a single time series. For one time series X of length $L$, $\{X\}=\{X_1,X_2,...,X_L\}$ the lagged-coordinate vectors series, $\{ x_t \}=< X_t,X_{t-1\tau},X_{t-2\tau}\ldots, X_{t-(E-1)\tau} >$ $(1+(E-1)\tau<t<L)$, are reconstructed as "shadow" attractor manifold $\boldsymbol{M}_X$ to be used in CCM (Sugihara et al., 2012). Here, $\tau$ is the time lag, $E$ is the embedding dimension (i.e., the number of time-delayed coordinates). Following the simplex projection method (Sugihara & May, 1990), the selection of $E$ was based on leave-one out cross-validation. The best E for each time series was determined from 2 to 10 dimensions according to the prediction skill (here Pearson correlation coefficient ($\rho$) was used).

### 2) Identifying Nonlinear Dynamical Systems From Linear Stochastic Systems ($\theta$)

The nonlinearity of time series embedded with the optimal $E$ could be identified using the S-map procedure, which fits local linear maps to describe the dynamics through various weight options (Sugihara, 1994). The nonlinear localization parameter, $\theta$, is defined to determine the degree to which points are weighted when fitting the local linear map. Specifically, when $\theta > 0$, nearby points in the state space receive larger weight, and the local linear map can differ in state-space to accommodate nonlinear behavior, suggestive of nonlinear dynamics. When $\theta = 0$, all points are equally weighted, meaning that the local linear map is identical for various points in the reconstructed state-space. Following (Chang et al., 2017; Tsonis, 2018), if predictability improves with increasing $\theta$ (i.e., the best $\theta > 0$), indicating the evidence for nonlinear dynamics; if not (i.e., the best $\theta = 0$), the time series would be first-differenced to extract the nonlinear characteristic further. Here, the first-differenced derivates of NGPO, PDO, and SOI (NPGOfd, PDOfd, and SOIfd) are created based on the posterior results (**Figures S3**, **S4**). Finally, CPUEda, AMO, ONI, NPGOfd, PDOfd, and SST are qualified indices with nonlinear dynamics to sequent CCM experiments (**Figures S3**–**S5**).

### 3) Causality Test and Lag-Time Analysis by CCM and Extended CCM

CCM determines causality by generating a cross-mapped estimate of $Y(t)$, denoted by $\hat{Y}(t) \mid \boldsymbol{M}_X$ i.e., predicting the current quantity of one variable $M_y$ using the time lags of another variable $M_x$ (Sugihara et al., 2012; Chang et al., 2017). This prediction skill ($\rho$) is quantified by calculating the Pearson correlation coefficient between the predicted and observed values of $Y(t)$ and is be computed over many random subsamples of the time series to quantify convergence. The parameter library size ($L$) depended on the sample length ($L_{max}$), and best E+1 ($L_{min}$) represents the subsample size. The significance of the cross-mapping skill is tested using 1000 surrogate time series to simulate null distributions. If there is a causal relationship between X and Y, the cross-mapping plot would be "convergent," which means that the prediction skill ($\rho$) enhances and approaches a definite limit with increasing $L$. Note that the direction of cross-mapping (xmap) is opposite to the direction of the cause-effect, that is, the prediction skill of X xmap Y reached a convergence indicates Y causes X and vice visa.

Extended CCM (ECCM) was developed to determine the optimal delay-lag and distinguish the real unidirectional causal relationship from bidirectional causation through adjusting the cross-map lag time ($l$) (Ye et al., 2015). The true unidirectional causality means that a negative lag for cross mapping tested in the true causal direction (i.e., the result variable is better at predicting the past values of the causal variable rather than future values) and a positive lag exists tested in the other direction (the causal variable best predicts the future result variable). Based on the posterior results (**Figures 4**, **8A**), a significant and unidirectional causal relationship between CPUEda and AMO and a strong bidirectional relationship between SST and AMO were determined. For CPUEda and AMO, the detailed time lag is further determined using ECCM to understand the potential process better. Considering the maximum SKJ age is 12 years (mentioned earlier), the yearly lag-time was first determined by the time-interval parameter ($l$ = 1 year, $l_{max}$ = 12), and the accurate monthly lag-time ($l$ = 1 month) was determined over 1000 random libraries (with various seed value) of Library size ($L_{max}$=565). For SST and AMO, ECCM would check whether the direction is truly unidirectional further.

The "rEDM" package conducted analyses in this section in R. Details algorithm for this methods can be found in (Sugihara et al., 2012; Ye et al., 2015).

## 2.5 Generalized Additive Model and Threshold Generalized Additive Model

Generalized additive models (GAM) and threshold generalized additive models (TGAM) were used to determine the relationship type (stationary or non-stationary) between SKJ and the causal climate index (AMO, from the above results). Specifically, a "stationary" relationship is better fitted by a single function throughout the period of the time series and is typically formulated using a GAM (Ciannelli et al., 2004):

$$Y = \alpha + s(X_1) + X_2 + \epsilon \quad (1)$$

where Y is the response variable (the square root of CPUE that conforms to normal distribution), $X_1$ is the predictor (AMO), $X_2$ is the month variable (as a categorical variable), and s, α, and ε are smooth function (with k ≤ 3 to avoid overfitting), intercept, and error terms, respectively.

Different functions better fits a "non-stationary" relationship for different periods, and the responses to drivers have an abrupt change over a threshold year (Litzow et al., 2018), which is formulated using a TGAM (with specific to two time periods) (Puerta et al., 2019):

$$Y(t) = \begin{cases} \alpha_1 + s_1(X_1) + X_2 + \epsilon_t, & t \le y \\ \alpha_2 + s_2(X_1) + X_2 + \epsilon_t, & t > y \end{cases} \quad (2)$$

where y is the threshold year that separates two periods with varying responses to drivers, set as between the 0.1 lower and the 0.9 upper quantiles of the time series at a month scale, the designations of $X_1$, $X_2$, and Y are the same as them in the GAM. The nonstationary optimization model is selected by minimizing the model's generalized cross-validation score (GCV) (Casini et al., 2009). The superior model was selected and further conducted based on the minimum Akaike information criterion (AIC). The analyses in this section were conducted using "mgcv" package in R.Analyses flow is shown in **Figure 2**.

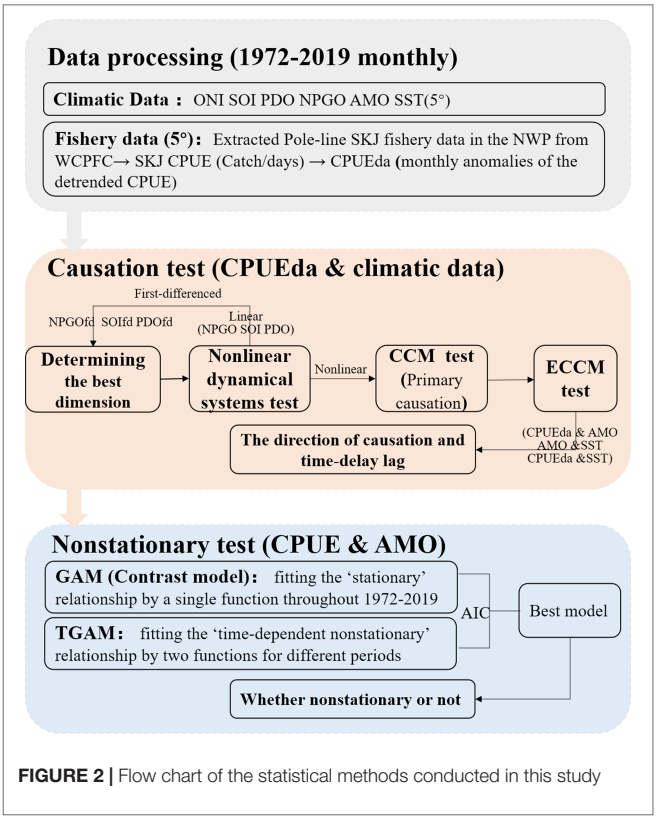


**FIGURE 2 |** Flow chart of the statistical methods conducted in this study

# 3 RESULTS

## 3.1 Temporal and Spatial Variations in CPUE and Catch of SKJ

The fluctuations of SKJ catch present earlier increase and later decrease in trend during 1972–2019: An increasing trend was determined from 1972 to 1984 with the highest catch (151,649-mt) occurring in 1984; a relative stable segment during 1985–2005 is characterized by a slight decline; at last, an obvious declining trajectory appeared since 2006, where the lowest catch (25,267-mt) occurred in 2014. (**Figure 3A**). The CPUE of SKJ fluctuates with a rising trend over the study period at the decadal scale. It remains a line before the 1980s, but increases sharply in the mid-1990s, reaching the first peak (5.61-mt/day) in 1993 and gently fluctuating during 1994–2014, then the maximum peak (5.84-mt/day) occurred in 2015. (**Figure 3A**).

The high-catch areas distribute along the western boundary of the NWP, which overlaps the path of the Kuroshio Current fitly. Among these, the biggest patchy area of high catch is near the mixed area between Kuroshio Current front and Oyashio Current (**Figure 3B**). By contrast, the spatial distribution of SKJ CPUE is characterized by many meridional strips, where two intensified trips of CPUE are located at the most northern area (along 35°–40° N) and the southeast corner (150°E across on the 20°N), respectively (**Figure 3C**).

## 3.2 Causal Relationships Between SKJ CPUEda and Climate Indices

An obvious convergence of the AMO causing on CPUEda and a declined trend of the opposite predicting skill (CPUEda causing on the AMO) are found with the library size larger (**Figure 4**), which shows the interaction between the AMO and SKJ is unidirectional, and indicates that the abnormal fluctuation of SKJ CPUE in the NWP depended on the long-term variation of the AMO, despite the insignificant correlation (r = −0.004, **Table S1**). The ECCM results further

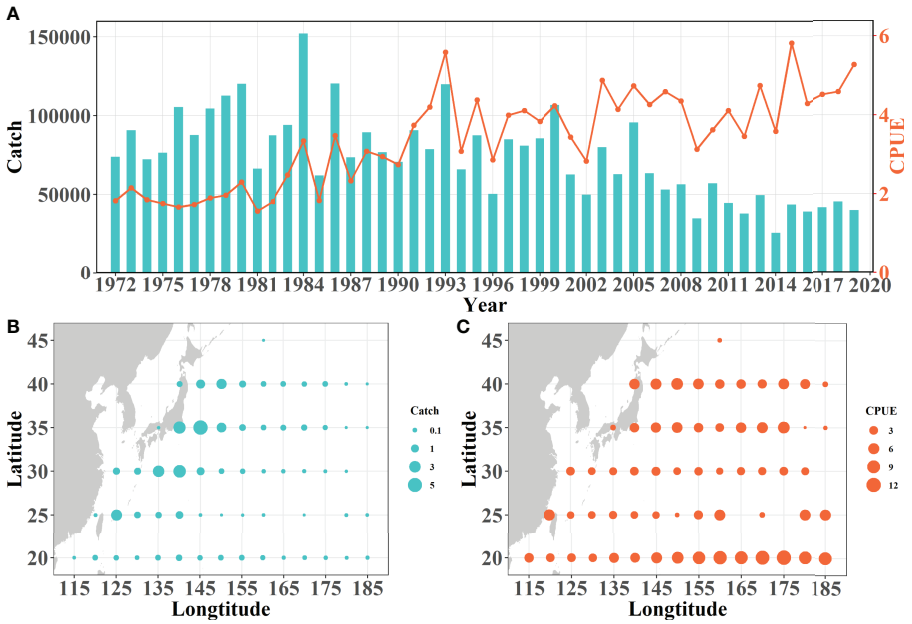


**FIGURE 3 |** Characteristics of temporal variations and spatial distributions of skipjack tuna in the study area during 1972–2019. **(A)** Timeseries variations of skipjack catch (blue lake bar) and CPUE (bright orange line). **(B)** Spatial distribution of skipjack accumulative catches (million metric tons). **(C)** Spatial distribution of skipjack mean CPUE (metric tons per day).

attest that the strongest causation occurs at a lag of 1 year at an annual scale. (**Figure 5A**). More specifically, the maximum lag on the month scale is identified at 15 months (**Figure 5B**).

For other climate indices, the predicting skill of the ONI causing on CPUEda shows a weak convergence at the library size ($L$ = 400) with a declined trend after the library size reached 400 (**Figure S6**). Considering the maximum predicting skill is less than 0.1, the ONI effect on SKJ is almost neglected. The predicting skills between PDOfd and NPGOfd cross-with CPUEda presented with negative values make no sense (**Figure S6**), which shows no causal interaction between SKJ with PDO and NPGO at the statistical level.

## 3.3 Nonstationary Relationship Between SKJ CPUE and the AMO

For the comparison between stationary and nonstationary models, the TGAM model obviously causes lower AIC (**Figure 6**), showing better model performances than the GAM model. Consequently, the relationship between SKJ and the AMO during the whole period is nonstationary. Following the variations in the GCV of TGAM model, the threshold years that distinguished eras for fitting AMO-CPUE relationship separately was around 1991/92 (**Figure 7**). Two eras were found with various relationships between CPUE and the AMO (**Table 2**), where the AMO is significantly related to CPUE in the era1 (1972–1991), while this relationship was insignificant in the era2 (1992–2019, **Figure 8**).

# 4. DISCUSSION

This study presents the continuous pole-line catch data of SKJ in the NWP area over the 1972–2019 period, where the SKJ catch shows a relatively higher level before the 21st century and contributed secondly to the SKJ catch in the Pacific while its role

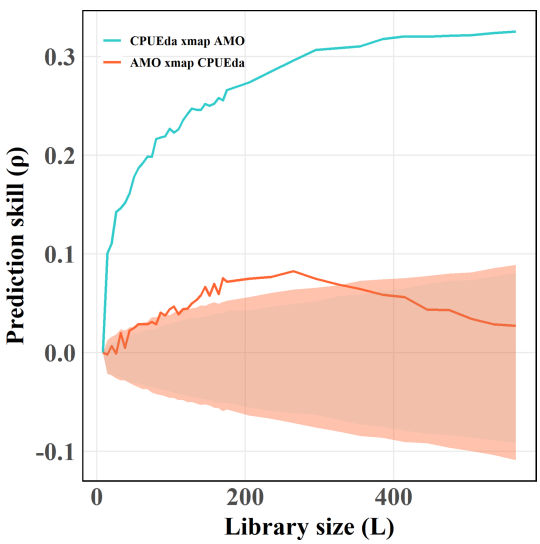


**FIGURE 4 |** Results of the CCM applied to the nonlinear dynamics of CPUEda and AMO. The blue lake and bright orange lines represent the effect of AMO on skipjack and the opposite effective direction, respectively. The different color shadows represent the 95th percentile of the results of CCM for the surrogate data versus the original effect time series.

**TABLE 2 |** Significant covariates degrees of freedom goodness of fit (Akaike Information Criterion, AIC), model performance with deviance explained in percentage and regression coefficient R-sq. adjusted are indicated for identified threshold year GAM models.

| Model | Covariates | Degrees of freedom | significance | AIC | Deviance explained | $R^2$ adjusted | GCV |
|---|---|---|---|---|---|---|---|
| Year <=r | AMO | 1 | <0.01** | 106.952 | 74.1% | 0.727 | 0.092528 |
| Year>r | AMO | 1 | >0.05 | 455.0047 | 37.8% | 0.356 | 0.21798 |

***means coefficients significant at 0.01.*

has been weakening in the recent two decades. (**Figures 3A**; **S1**). As pole-line is the uniform fishing gear and the effort defined as days is homogeneous, the reduction in SKJ catch may result from the decreased effort instead of the fishing method since 1981 (**Figure S2**). By contrast, CPUE indicates an increasing trend during the whole period, which conforms with the stock assessment report in 2019 that SKJ is not over-fished and the population level is healthy (Vincent et al., 2019). Therefore, this study uses CPUE, to obtain the long-term change feature of SKJ relative abundance at the temporal scale, to link with climate indices. The CCM results showed that the AMO was causally related to the variability of SKJ relative abundance in the NWP, while the ONI, NPGO, and PDO have little effect on SKJ in this study.

## 4.1 Relationships Between SKJ Groups in the NWP With Climate Patterns

As mentioned earlier, three groups migrated from distinct areas constitute most SKJ in the NWP (**Figure 1**). Because of the least contribution of the northeast Pacific SKJ catch to its catch in Pacific during 1972–2019 (**Figure S1**), and the scared long-scale SKJ movement between the northeast Pacific and NWP through the conventional tagging (Moore et al., 2020), it is assumed that the SKJ from the northeast Pacific (i.e., group 1) hardly contributes to the SKJ in the NWP. Besides, no causal linkage between NPGO and SKJ in this paper supports the assumption from another perspective (**Figure S6**).

In contrast, the second group from the western tropical Pacific is considered as an important component of the SKJ in the NWP. SKJ catch in the western tropical Pacific has ranked the first since 1950 (**Figure S1**) and was significantly related to ENSO events (Lehodey et al., 1997). During the ENSO episodes, the SKJ purse seine fishery in the western tropical Pacific showed profound displacement between the warm and cold pools with catch fluctuations. Tag-release programs and otolith studies showed that there are one or two various migratory routes between the NWP and western tropical Pacific (Arai et al., 2005; Kiyofuji et al., 2019). However, the ONI makes a weak linkage with SKJ in this study. Accounting for a weaker effect on the high-latitude extratropical area (like the NWP) of ENSO than on low-latitude tropical areas (Alexander et al., 2004), ENSO records may be faded in the NWP, which may have little effect on SKJ. Besides, recent studies found that the fluctuation of SST in the western tropical Pacific is largely in phase with AMO on the decadal scales through atmospheric teleconnection and the interaction of air-ocean dynamics (Sun et al., 2017; Sun et al., 2021). When the Atlantic is in a positive phase with positive SST anomalies, so is the western tropical Pacific, which fitly overlaps and affects the migratory environment of the second group to reach the NWP area (**Figure 11**). Therefore, the production of the second migratory group may largely depends on the spawning parents linked with ENSO in the western tropical

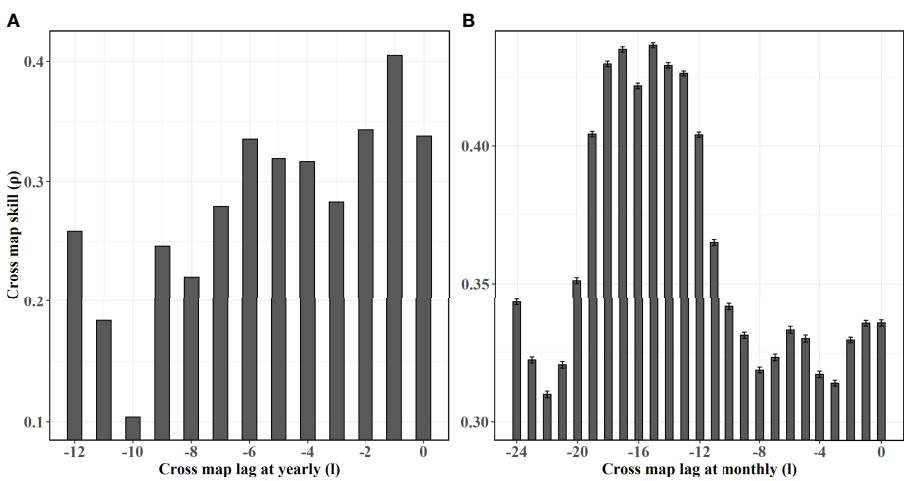


**FIGURE 5 |** Results of the ECCM applied to the nonlinear dynamics of CPUEda and AMO at yearly scales (panel a) and month scales (panel b). The black bar shows the mean cross map skill from AMO to skipjack at various time lags, where the units of **(A, B)** are year and month, respectively. Specifically, the vertical lines in panel B show the standard deviations over 1000 random libraries.

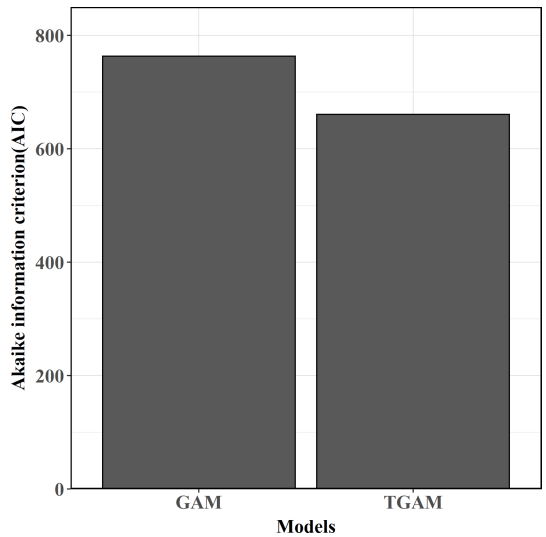


**FIGURE 6 |** Model comparisons between stationary and non-stationary models

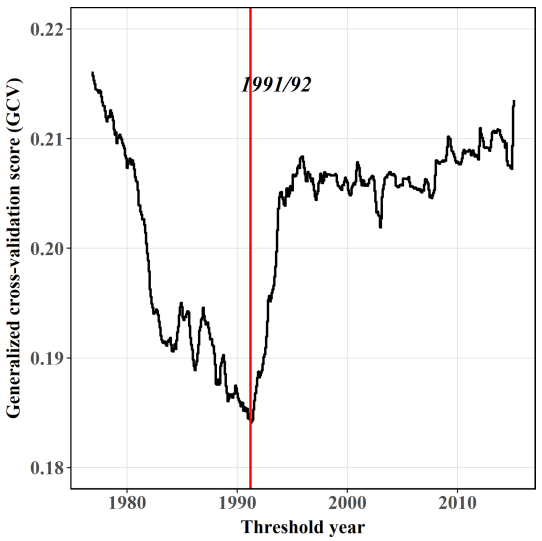


**FIGURE 7 |** Generalized cross-validation score (GCV) paths of the best fitted models by TGAM. The red line represents the threshold year characterized by concave GCV paths

Pacific, while the survival rate of the second group migrated to the NWP is most likely to rest on the AMO.

More notably, the subsurface layer of the NWP was evidenced to correlate with the AMO without lag (Wu et al., 2020b). Since the 21st century, studies have indicated that the AMO dominates the multidecadal variability of the Atlantic Ocean and exhibits significant footprints on transoceanic basins, especially on the Pacific Ocean, which reflects in modulating the variability of Pacific prominent modes (such as ENSO, PDO *et al.*) and inducing the synchronous response of physical environment (such as the anomalous warm of western Pacific SST, the increased upper ocean heat content and the intensified tropical cyclones during positive AMO phases) (Enfield et al., 2001; d'Orgeville & Peltier, 2007; Levine et al., 2017; Sun et al., 2017; Wang et al., 2017; Gong et al., 2020; Sun et al., 2020; Wu et al., 2020b; Zhang & Delworth, 2007). Moreover, a novel discovery is that the AMO played a decisive role in SKJ in the NWP during 1972–2019, which is consistent with the notion that the AMO could explain fish catch variability in the NWP by dominating the subtropical mode water (**Figure 11**) (Wu et al., 2020b).

Indeed, an obvious and significant causal affection of the AMO on SST in the NWP is identified in this paper using CCM and ECCM techniques (**Figures 9A,B**), due to the negative optimal SST lag caused (predicted) by the AMO and the positive optimal AMO lag caused by SST (**Figure 9B**), which indicates that SST should be the essential oceanographic

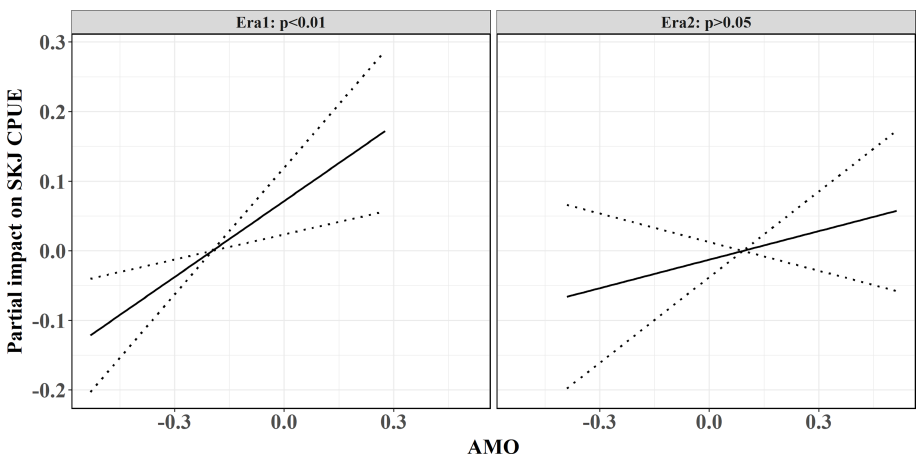


**FIGURE 8 |** Fitting relationships between the AMO and SKJ CPUE in various eras using the best-fitted models. The left and right panels represent the first era before 1991 and the second era posterior 1991, respectively.

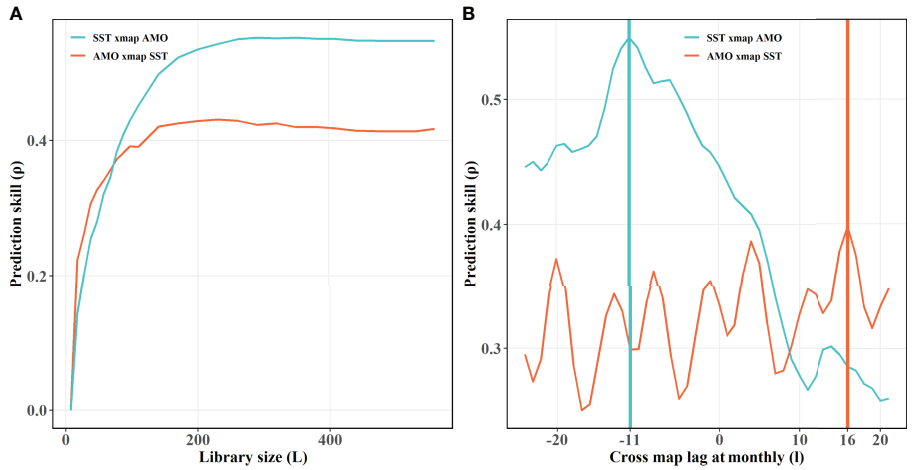


**FIGURE 9 |** Results of the CCM and ECCM applied to the nonlinear dynamics of SST and the AMO. **(A)** Results of the CCM without time lag, **(B)** Results of the ECCM at different lags (l = 1 month). The blue lake lines indicate that the AMO causes SST; the bright orange lines represent the opposite effective directions from SST to AMO. The vertical lines in panel b represent the optimal lag times by the best prediction skills at varying interaction directions, respectively

medium between the AMO and SKJ, and which is further verified using CCM test between SST and CPUEda who showed an obvious convergent trait of the prediction skill from CPUEda to SST (**Figure 10**). Accordingly, the SKJ inhabiting in the NWP, especially for the residents (i.e., the third group) and the immigrants from the second group, are possibly forced by the AMO through SST (**Figure 11**).

Previous studies have shown that environmental changes caused by climate variability could affect tunas in recruitment, spawning, distribution, etc. For instance, SST anomaly concurred

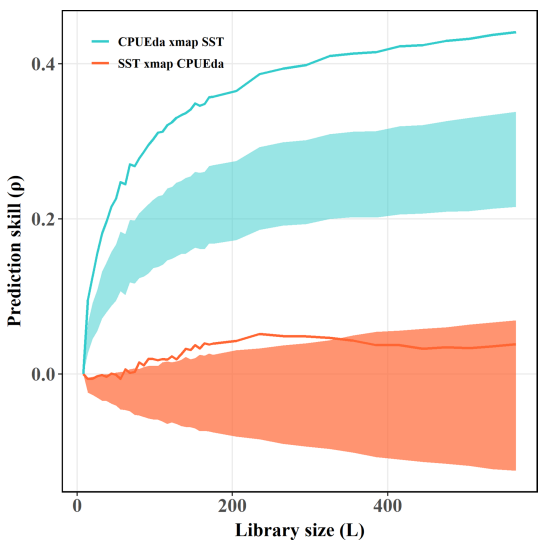


**FIGURE 10 |** Results of the CCM applied to the nonlinear dynamics of CPUEda and SST. The blue lake and bright orange lines indicate the effect of SST on CPUE and the opposite effective direction from CPUE to SST, respectively. The shadows represent the 95th percentile of the results of the CCM for the surrogate data versus the original effect time series.

with ENSO events in the Indian Ocean could reflect in the tuna fishery (e.g., yellowfin tuna and bigeye tuna) in the Indian Ocean (Syamsuddin et al., 2013; Báez et al., 2020). Although PDO is the proxy of SST anomaly signals in the north Pacific, this study shows that PDO makes no causality with SKJ in the NWP, which is consensus with the point that the NWP ecosystem could not be completely explained by PDO, of which many species fluctuations could not be associated with PDO yet on a decadal scale (Tian et al., 2014; Ma et al., 2020; Wu et al., 2020b; Ma et al., 2021). Conversely, in this study, SKJ in the NWP over 1972–2019 is caused by the AMO through SST. The plausible explanation for this is that SST variation first affects the habitat suitability of SKJ and second triggers the SKJ relative abundance anomalies. Similar phenomena was confirmed in Atlantic bluefin tuna in the north Atlantic and SKJ in the tropical Pacific (Lehodey et al., 1997; Faillettaz et al., 2019). However, the fishery ground covered the whole study area without obvious changes all the way in this paper. Therefore, the possible explanation is that the SST variability involves in the growth and development of SKJ during its lifetime. SKJ could adopt various breeding strategies depending on the external SST; it could spawn all over the year in the tropical ocean, but spawn seasonally in the extratropical water (Ashida, 2020). Moreover, the early-life ontogenetic SKJ development (juvenile) is positive and significantly related to SST (Ashida et al., 2018) too. Combined with the maturity age (1.1–1.6 year) of SKJ in the NWP (Ashida, 2020), and the optimal causal relationship between the AMO and SKJ at the lag of 15 months (**Figure 5B**), this paper implies the AMO effects on the recruitment process of one generation of SKJ cohort through SST. Specifically, the second group leading a bold and long-distance migration for feeding ground in the NWP (Moore et al., 2020) would experience SST variability caused by the AMO in their migratory processes, which directly influenced their survival and growth rates. On the

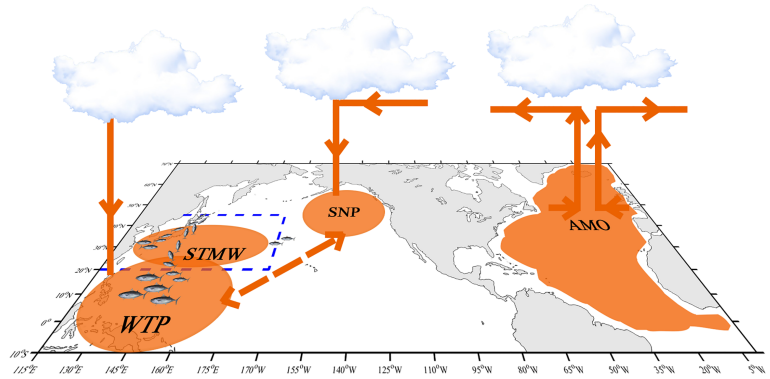


**FIGURE 11 |** Schematic process of SKJ in the Northwest Pacific affected by the AMO. The blue dotted line shows the study area in this paper. The orange patches, lines, and arrows show the possible affection process in the western pacific caused by the AMO in the north Atlantic (Sun et al., 2017; Wu et al., 2020b). SNP means subtropical North Pacific, WTP means western tropical Pacific, STMW means subtropical mode water in the study area.

other hand, the fecundity of the local spawning cohort and the subsequent growth and development rate of SKJ would depend on SST controlled by the AMO. Consequently, the early life of SKJ in the NWP is affected by the AMO through SST.

## 4.2 Possible Explanations for the Nonstationary Relationship Between the AMO and SKJ

TGAM results show that SKJ CPUE correlates linearly with AMO at the former era (1972–1991), while the correlation disappears at the latter era (1992–2019). Although the most famous and climatic regime shift documented in the North Pacific Ocean was in 1976–1977, recent major alterations in some components of the North Pacific ecosystem were identified a further shift in 1989 in the northeast Pacific and a nonlinear and non-stationary with threshold years in the 1990s in the NWP, respectively (Hare & Mantua, 2000; Litzow et al., 2018; Ma et al., 2021). This time-dependent nonstationary responses between AMO and SKJ occurred around the early 1990s as well, which may indicate a complex ecological effect of the ecosystem. As the opportunistic feeder, SKJ could consume various preys, such as squid, crustaceans, and some mackerel or perciform fish during migration (Aoki et al., 2017). Such region-dependent feeding could probably moderate the down-top biotic effect on SKJ through the food chain, while the inverse control from predators (like sharks and billfishes in the eastern tropical Pacific Ocean, (Hunsicker et al., 2012; Chang et al., 2022) is unclear in the NWP.

Studies to date have explored the teleconnection mechanism between the AMO and Pacific ocean through the atmosphere bridge and ocean-atmosphere interaction, of which the direct oceanographic variations in the western pacific surface triggered by the AMO is SST (Sun et al., 2020; Wu et al., 2020b), In this sense, this paper explored the causation between local SST and SKJ, which is consistent with many studies that highlighted the importance of SST on tuna abundance (Zainuddin, 2011; Tangke et al., 2020; Salazar et al., 2021). The distinct relationships between the AMO and SKJ during two eras in this study may respond to the various stages in the thermal niche response curve of SKJ with warmer SST. SST before 1991 may be within the ascending stages of the niche response curve, which is slowly more suitable for the SKJ growth. While SST since 1991 could match the gentle slope stages of the curve (relative decrease but still in positive). Apart from SST, other biotic factors (such as Mixed layer depths and Chlorophyll-a) could also represent the primary habitat environment in defining SKJ suitable habitat (Mugo et al., 2020; Salazar et al., 2021). Although no obvious shift of the SKJ fishery ground is found during different eras in current study, future work is needed to explore the multi-effect from environment factors on the SKJ distribution and abundance. Additionally, the temporal evolution of AMO has shown a trend of increasing volatility in recent decades, indicating that the AMO is non-stationary (Beyraghdar Kashkooli & Modarres, 2020). Chen et al. (2019)reported that modulating effect from the AMO on the relationship between wintertime North Pacific oscillations and ENSO is different during various AMO episodes, which may further show the nonstationary relationship between the AMO and Pacific. Therefore, the nonstationary trait between AMO and SKJ may be attributed to a comprehensive process coupled with the AMO variability, the SKJ population dynamics affected by biotic and abiotic factors.

## 4.3 The Strength and Extension of the CCM Technique

Compare with the spearman correlation results (**Table S1**), CCM method shows a stronger ability for determining a distinct causation between SKJ and climate variability (AMO) in this study, and provides the key evidence of the causation direction from AMO *via* SST effecting on SKJ. This is consistent with the notion that the CCM is superior to traditional correlation techniques on determining the caused signal with big datasets (Chang et al., 2017). With the high development of observed tools and computer science, big ocean data are birthed and how

to mine the potential information under these common datasets becomes a hot issue. The CCM method is of great benefit to prompt this analysis. Moreover, the extension of CCM methods involved with multiple factors, such as Multivariate CCM and Multiview CCM (Ye & Sugihara, 2016; Hu et al., 2021) are also recommended understanding the comprehensive mechanism between organisms with climate variability and local physical factors in the ecosystem.

This study proposes that the trans-basin interaction between the AMO and Pacific Ocean has affected the NWP SKJ fishery at 15 months in advance. Similar phenomena occurred in the Indian ocean as well. Such as, the tuna fishery in the Indian ocean could suffer an obvious decline were out of phase with PDO (Báez et al., 2020; Wu et al., 2020a). Tunas or other large pelagic fish (such as swordfishes, sharks) who migrated at the meso-large spatial scale experiences large environmental variation during its whole life history, large-scale climate indices that combine many physical variables would likely serve as an appropriate proxy for explaining and predicting the long-term abundance variation of the species. With the deeper understanding of the teleconnection pattern among oceans and atmosphere under the global climate change, the trans-basin effect of climate patterns on the prediction of the large-scale migratory species should be highlighted as the same as the basin climatic oscillations in the future.

## DATA AVAILABILITY STATEMENT

The raw data supporting the conclusions of this article will be made available by the authors, without undue reservation.

## ETHICS STATEMENT

Ethical review and approval was not required for the animal study because this study didn't involve with the physiology scope of the skipjack tuna, while it focused on relationship between the stock variation of skipjack tuna with climate based on the data derived from the international fishery manage organization—WCPFC (Western and Central Pacific Fisheries Commission).

## AUTHOR CONTRIBUTIONS

XH, YT, and SM conceived the study. XH and SM provided guidance in the methods. XH conducted the data compilation and analysis. XH, YT, SM, and SZ wrote and revised the manuscript. YT obtained funding for the study. All authors contributed to the article and approved the submitted version.

## FUNDING

This work was supported by the National Natural Science Foundation of China (Grant Nos. 41930534).

## ACKNOWLEDGMENTS

The authors appreciate the online open-access data and scripts providers. And the two reviewers for their invaluable comments on the manuscript.

## SUPPLEMENTARY MATERIAL

The Supplementary Material for this article can be found online at: https://www.frontiersin.org/articles/10.3389/fmars.2022.895219/full#supplementary-material

**Supplementary Figure 1 |** The composition of skipjack tuna catches in the pacific from 1950–2019 (FAO). The different colors represent the catch in six major fishing areas.

**Supplementary Figure 2 |** Timeseries variations of skipjack tuna effort (days) during 1972–2019.

**Supplementary Figure 3 |** The optimal embedding dimensions of the time series.

**Supplementary Figure 4 |** The identification and quantification of nonlinearity of the time series.

**Supplementary Figure 5 |** The nonlinearity tests of the first-differenced indices (NPGOfd, PDOfd, SOIfd). The first row represents the optimal embedding dimensions of climate indices at the state space level; the second row represents the identification and quantification of nonlinearity of climate indices.

**Supplementary Figure 6 |** The CCM results between CPUEda and climate indices (NPGOfd, ONI, PDOfd). Blue lines represent the climate indices effect on CPUE.

**Supplementary Figure 7 |** Graphical residuals exploration results for the model during the first era (1972–1991).

**Supplementary Figure 8 |** Graphical residuals exploration results for the model during the second era (1992–2019).

**Supplementary Table 1 |** Linear Correlations between SKJ CPUEda and climate indices during 1972–2019. *means coefficients significant at 0.05.

## REFERENCES

Alexander, M. A., Lau, N.-C. and Scott, J. D. (2004). "Broadening the Atmospheric Bridge Paradigm: ENSO Teleconnections to the North Pacific in Summer and to the Tropical West Pacific-Indian Oceans Over the Seasonal Cycle," in *Earth Climate: The Ocean-Atmosphere Interaction*, Oxford, England. vol. 147 . Eds. Wang, C., Xie, S.-P. and Carton, J. (AGU Monograph).

Aoki, Y., Kitagawa, T., Kiyofuji, H., Okamoto, S. and Kawamura, T. (2017). Changes in Energy Intake and Cost of Transport by Skipjack Tuna (Katsuwonus Pelamis) During Northward Migration in the Northwestern Pacific Ocean. *Deep. Sea. Res. Part II: Topical. Stud. Oceanography.* 140, 83–93. doi: 10.1016/j.dsr2.2016.05.012

Arai, T., Kotake, A., Kayama, S., Ogura, M. and Watanabe, Y. (2005). Movements and Life History Patterns of the Skipjack Tuna Katsuwonus Pelamis in the Western Paci¢c, as Revealed by Otolith Sr:Ca Ratios. *J. Mar. Biol. Assoc. United Kingdom* 6. 1–9 doi: 10.1017/S0025315405012336

Ashida, H. (2020). Spatial and Temporal Differences in the Reproductive Traits of Skipjack Tuna Katsuwonus Pelamis Between the Subtropical and Temperate Western Pacific Ocean. *Fisheries Res.* 221, 105352. doi: 10.1016/j.fishres.2019.105352

Ashida, H., Watanabe, K. and Tanabe, T. (2018). Growth Variability of Juvenile Skipjack Tuna (Katsuwonus Pelamis) in the Western and Central Pacific Ocean. *Environ. Biol. Fishes* 101 (3), 429–439. doi: 10.1007/s10641-017-0708-9

Báez, J. C., Czerwinski, I. A. and Ramos, M. L. (2020). Climatic Oscillations Effect on the Yellowfin Tuna (*Thunnus Albacares*) Spanish Captures in the Indian Ocean. *Fisheries Oceanography.* 29 (6), 572–583. doi: 10.1111/fog.12496

Beyraghdar Kashkooli, O. and Modarres, R. (2020). Is the Volatility and non-Stationarity of the Atlantic Multidecadal Oscillation (AMO) Changing? *Global Planetary Change* 189, 103160. doi: 10.1016/j.gloplacha.2020.103160

Carlos Baez, J., Czerwinski, I. A. and Lourdes Ramos, M. (2020). Climatic Oscillations Effect on the Yellowfin Tuna (Thunnus Albacares) Spanish Captures in the Indian Ocean. *Fisheries Oceanography.* 29 (6), 572–583. doi: 10.1111/fog.12496

Casini, M., Hjelm, J., Molinero, J.-C., Lovgren, J., Cardinale, M., Bartolino, V., et al. (2009). Trophic Cascades Promote Threshold-Like Shifts in Pelagic Marine Ecosystems. *Proc. Natl. Acad. Sci.* 106 (1), 197–202. doi: 10.1073/pnas.0806649105

Chang, Y.-C., Chiang, W.-C., Madigan, D. J., Tsai, F.-Y., Chiang, C.-L., Hsu, H.-H., et al. (2022). Trophic Dynamics and Feeding Ecology of Skipjack Tuna (Katsuwonus Pelamis) Off Eastern and Western Taiwan. *Molecules* 27 (3), 1073. doi: 10.3390/molecules27031073

Chang, C.-W., Ushio, M. and Hsieh, C. (2017). Empirical Dynamic Modeling for Beginners. *Ecol. Res.* 32 (6), 785–796. doi: 10.1007/s11284-017-1469-9

Chen, S., Song, L. and Chen, W. (2019). Interdecadal Modulation of AMO on the Winter North Pacific Oscillation–Following Winter ENSO Relationship. *Advances in Atmospheric Sciences*. 36, 11. doi: 10.1007/s00376-019-9090-1

Ciannelli, L., Chan, K.-S., Bailey, K. M. and Stenseth, N. (2004). Nonadditive Effects of The Environment on The Survival of a Large Marine Fish Population. *Ecology* 85 (12), 3418–3427. doi: 10.1890/03-0755

Collette, B. B. and Nauen, C. E. (1983). FAO Species Catalogue. Vol. 2. Scombrids of the World. An Annotated and Illustrated Catalogue of Tunas, Mackerels, Bonitos and Related Species Known to Date. *FAO Fish. Synop.* 125 (2), 137.

Doi, H., Yasuhara, M. and Ushio, M. (2021). Causal Analysis of the Temperature Impact on Deep-Sea Biodiversity. *Biol. Lett.* 17 (7), 20200666. doi: 10.1098/rsbl.2020.0666

d'Orgeville, M. and Peltier, W. R. (2007). On the Pacific Decadal Oscillation and the Atlantic Multidecadal Oscillation: Might They be Related: PDO and AMO Related? *Geophysical. Res. Lett.* 34 (23) L23705. doi: 10.1029/2007GL031584

Enfield, D. B., Mestas-Nunez, A. M. and Trimble, P. J. (2001). The Atlantic Multidecadal Oscillation and its Relation to Rainfall and River Flows in the Continental US. *Geophysical. Res. Lett.* 28 (10), 2077–2080. doi: 10.1029/2000GL012745

Faillettaz, R., Beaugrand, G., Goberville, E. and Kirby, R. R. (2019). Atlantic Multidecadal Oscillations Drive the Basin-Scale Distribution of Atlantic Bluefin Tuna. *Sci. Adv.* 5 (1), eaar6993. doi: 10.1126/sciadv.aar6993

Gong, Y., Li, T. and Chen, L. (2020). Interdecadal Modulation of ENSO Amplitude by the Atlantic Multi-Decadal Oscillation (AMO). *Climate Dynamics.* 55 (9–10), 2689–2702. doi: 10.1007/s00382-020-05408-x

Hare, S. R. and Mantua, N. J. (2000). Empirical Evidence for North Pacific Regime Shifts in 1977 and 1989. *Prog. Oceanography.* 47 (2–4), 103–145. doi: 10.1016/S0079-6611(00)00033-1

Hunsicker, M., Olson, R., Essington, T., Maunder, M., Duffy, L. and Kitchell, J. (2012). Potential for Top-Down Control on Tropical Tunas Based on Size Structure of Predator–Prey Interactions. *Mar. Ecol. Prog. Ser.* 445, 263–277. doi: 10.3354/meps09494

Hu, J., Wang, P. and Zhang, H. (2021). The Relationship Between Environmental Factors and Catch Abundance of Hairtail in the East China Sea Using Empirical Dynamic Modeling. *Fishes* 6 (4), 80. doi: 10.3390/fishes6040080

Kiyofuji, H., Aoki, Y., Kinoshita, J., Okamoto, S., Masujima, M., Matsumoto, T., et al. (2019). Northward Migration Dynamics of Skipjack Tuna (Katsuwonus Pelamis) Associated With the Lower Thermal Limit in the Western Pacific Ocean. *Prog. Oceanography.* 175, 55–67. doi: 10.1016/j.pocean.2019.03.006

Lan, K.-W., Evans, K. and Lee, M.-A. (2013). Effects of Climate Variability on the Distribution and Fishing Conditions of Yellowfin Tuna (Thunnus Albacares) in the Western Indian Ocean. *Climatic. Change* 119 (1), 63–77. doi: 10.1007/s10584-012-0637-8

Lehodey, P., Bertignac, M., Hampton, J., Lewis, A. and Picaut, J. (1997). El Niño Southern Oscillation and Tuna in the Western Pacific. *Nature* 389 (6652), 715–718. doi: 10.1038/39575

Levine, A. F. Z., McPhaden, M. J. and Frierson, D. M. W. (2017). The Impact of the AMO on Multidecadal ENSO Variability: AMO IMPACTS ON ENSO. *Geophysical. Res. Lett.* 44 (8), 3877–3886. doi: 10.1002/2017GL072524

Lima, M. and Naya, D. E. (2011). Large-Scale Climatic Variability Affects the Dynamics of Tropical Skipjack Tuna in the Western Pacific Ocean. *Ecography* 34 (4), 597–605. doi: 10.1111/j.1600-0587.2010.06422.x

Litzow, M. A., Ciannelli, L., Puerta, P., Wettstein, J. J., Rykaczewski, R. R. and Opiekun, M. (2018). Non-Stationary Climate–Salmon Relationships in the Gulf of Alaska. *Proc. R. Soc. B: Biol. Sci.* 285 (1890), 20181855. doi: 10.1098/rspb.2018.1855

Ma, S., Tian, Y., Fu, C., Yu, H., Li, J., Liu, Y., et al. (2021). Climate-Induced Nonlinearity in Pelagic Communities and non-Stationary Relationships With Physical Drivers in the Kuroshio Ecosystem. *Fish. Fisheries* 22 (1), 1–17. doi: 10.1111/faf.12502

Ma, S., Tian, Y., Li, J., Yu, H., Cheng, J., Sun, P., et al. (2020). Climate Variability Patterns and Their Ecological Effects on Ecosystems in the Northwestern North Pacific. *Front. Mar. Sci.* 7. doi: 10.3389/fmars.2020.546882

Ménard, F., Marsac, F., Bellier, E. and Cazelles, B. (2007). Climatic Oscillations and Tuna Catch Rates in the Indian Ocean: A Wavelet Approach to Time Series Analysis. *Fisheries Oceanography.* 16 (1), 95–104. doi: 10.1111/j.1365-2419.2006.00415.x

Moore, B. R., Bell, J. D., Evans, K., Farley, J., Grewe, P. M., Hampton, J., et al. (2020). Defining the Stock Structures of Key Commercial Tunas in the Pacific Ocean I: Current Knowledge and Main Uncertainties. *Fisheries Res.* 230, 105525. doi: 10.1016/j.fishres.2020.105525

Mugo, R., Saitoh, S.-I., Igarashi, H., Toyoda, T., Masuda, S., Awaji, T., et al. (2020). Identification of Skipjack Tuna (Katsuwonus Pelamis) Pelagic Hotspots Applying a Satellite Remote Sensing-Driven Analysis of Ecological Niche Factors: A Short-Term Run. *PLoS One* 15 (8), e0237742. doi: 10.1371/journal.pone.0237742

Mukti, Z. and Saitoh, S. (2004). Detection of Potential Fishing Ground for Albacore Tuna Using Synoptic Measurements of Ocean Color and Thermal Remote Sensing in the Northwestern North Pacific. *Geophysical. Res. Lett.* 31 (20), L20311. doi: 10.1029/2004GL021000

Nakayama, S., Takasuka, A., Ichinokawa, M. and Okamura, H. (2018). Climate Change and Interspecific Interactions Drive Species Alternations Between Anchovy and Sardine in the Western North Pacific: Detection of Causality by Convergent Cross Mapping. *Fisheries Oceanography.* 27 (4), 312–322. doi: 10.1111/fog.12254

Puerta, P., Ciannelli, L., Rykaczewski, R. R., Opiekun, M. and Litzow, M. A. (2019). Do Gulf of Alaska Fish and Crustacean Populations Show Synchronous non-Stationary Responses to Climate? *Prog. Oceanography.* 175, 161–170. doi: 10.1016/j.pocean.2019.04.002

Salazar, J. E., Benavides, I. F., Portilla Cabrera, C. V., Guzmán, A. I. and Selvaraj, J. J. (2021). Generalized Additive Models With Delayed Effects and Spatial Autocorrelation Patterns to Improve the Spatiotemporal Prediction of the Skipjack (Katsuwonus Pelamis) Distribution in the Colombian Pacific Ocean. *Regional. Stud. Mar. Sci.* 45, 101829. doi: 10.1016/j.rsma.2021.101829

Sugihara, G. (1994). Nonlinear Forecasting for The Classification of Natural Time-Series. *Philos. Trans. R. Soc. A-Mathematical. Phys. Eng. Sci.* 348 (1688), 477–495. doi: 10.1098/rsta.1994.0106

Sugihara, G. and May, R. (1990). Nonlinear Forecasting as A Way of Distinguishing Chaos From Measurement Error in Time-Series. *Nature* 344 (6268), 734–741. doi: 10.1038/344734a0

Sugihara, G., May, R., Ye, H., Hsieh, C., Deyle, E., Fogarty, M., et al. (2012). Detecting Causality in Complex Ecosystems. *Science* 338 (6106), 496. doi: 10.1126/science.1227079

Sugimoto, T., Kimura, S. and Tadokoro, K. (2001). Impact of El Niño Events and Climate Regime Shift on Living Resources in the Western North Pacific. *Prog. Oceanography.* 49 (1–4), 113–127. doi: 10.1016/S0079-6611(01)00018-0

Sun, C., Kucharski, F., Li, J., Jin, F.-F., Kang, I.-S. and Ding, R. (2017). Western Tropical Pacific Multidecadal Variability Forced by the Atlantic Multidecadal Oscillation. *Nat. Commun.* 8 (1), 15998. doi: 10.1038/ncomms15998

Sun, C., Liu, Y., Gong, Z., Kucharski, F., Li, J., Wang, Q., et al. (2020). The Footprint of Atlantic Multidecadal Oscillation on the Intensity of Tropical Cyclones Over the Western North Pacific. *Front. Earth Sci.* 8. doi: 10.3389/feart.2020.604807

Sun, C., Liu, Y., Xue, J., Kucharski, F., Li, J. and Li, X. (2021). The Importance of Inter-Basin Atmospheric Teleconnection in the SST Footprint of Atlantic Multidecadal Oscillation Over Western Pacific. *Climate Dynamics*. 57 (1-2), 239-252. doi: 10.1007/s00382-021-05705-z

Syamsuddin, M. L., Saitoh, S.-I., Hirawake, T., Bachri, S. and Harto, A. B. (2013). Effects of El Niño–Southern Oscillation Events on Catches of Bigeye Tuna (Thunnus Obesus) in the Eastern Indian Ocean Off Java. *Fishery. Bull.* 111 (2), 175–188. doi: 10.7755/FB.111.2.5

Takano, T., Iwaki, T., Waki, T., Murata, R., Suzuki, J., Kodo, Y., et al. (2021). Species Composition and Infection Levels of Anisakis (Nematoda: Anisakidae) in the Skipjack Tuna Katsuwonus Pelamis (Linnaeus) in the Northwest Pacific. *Parasitol. Res.* 120 (5) , 1605-1615. doi: 10.1007/s00436-021-07144-5

Tangke, U., Silooy, F. D., Rochmady, and Saing, Z. (2020). Sea Surface Temperature and Chlorophyll-a Condition of Skipjack Tuna (*Katsuwonus Pelamis*) Catching Area in Ternate Island Marine Waters. *J. Physics.: Conf. Ser.* 1517, 12039. doi: 10.1088/1742-6596/1517/1/012039

Tawa, A., Kodama, T., Sakuma, K., Ishihara, T. and Ohshimo, S. (2020). Fine-Scale Horizontal Distributions of Multiple Species of Larval Tuna Off the Nansei Islands, Japan. *Mar. Ecol. Prog. Ser.* 636, 123–137. doi: 10.3354/meps13216

Tian, Y., Uchikawa, K., Ueda, Y. and Cheng, J. (2014). Comparison of Fluctuations in Fish Communities and Trophic Structures of Ecosystems From Three Currents Around Japan: Synchronies and Differences. *ICES. J. Mar. Sci.* 71 (1), 19–34. doi: 10.1093/icesjms/fst169

Tsonis, A. A. (Ed.) (2018). *Advances in Nonlinear Geosciences* (Springer International Publishing), Cham, Switzerland. doi: 10.1007/978-3-319-58895-7

Vincent, M. T., Pilling, G. M., and Hampton, J. (2019) Stock assessment of skipjack tuna in the western and central Pacific Ocean. *Scientific Committee Fifteenth Regular Session,* WCPFC-SC15-2019/SA-WP-05-Rev2.

Wang, J., Yang, B., Ljungqvist, F. C., Luterbacher, J., Osborn, T. J., Briffa, K. R., et al. (2017). Internal and External Forcing of Multidecadal Atlantic Climate Variability Over the Past 1,200 Years. *Nat. Geosci.* 10 (7), 512–517. doi: 10.1038/ngeo2962

Wu, Y.-L., Lan, K.-W. and Tian, Y. (2020a). Determining the Effect of Multiscale Climate Indices on the Global Yellowfin Tuna (Thunnus Albacares) Population Using a Time Series Analysis. *Deep. Sea. Res. Part II: Topical. Stud. Oceanography.* 175, 104808. doi: 10.1016/j.dsr2.2020.104808

Wu, B., Lin, X. and Yu, L. (2020b). North Pacific Subtropical Mode Water is Controlled by the Atlantic Multidecadal Variability. *Nat. Climate Change* 10 (3), 238–243. doi: 10.1038/s41558-020-0692-5

Ye, H., Deyle, E. R., Gilarranz, L. J. and Sugihara, G. (2015). Distinguishing Time-Delayed Causal Interactions Using Convergent Cross Mapping. *Sci. Rep.* 5 (1), 14750. doi: 10.1038/srep14750

Ye, H. and Sugihara, G. (2016). Information Leverage in Interconnected Ecosystems: Overcoming the Curse of Dimensionality. *Science* 353 (6302), 922–925. doi: 10.1126/science.aag0863

Yu, W., Chen, X., Zhang, Y. and Yi, Q. (2019). Habitat Suitability Modelling Revealing Environmental-Driven Abundance Variability and Geographical Distribution Shift of Winter-Spring Cohort of Neon Flying Squid Ommastrephes Bartramii in the Northwest Pacific Ocean. *Ices. J. Mar. Sci.* 76 (6), 1722–1735. doi: 10.1093/icesjms/fsz051

Zainuddin, M. (2011). Skipjack Tuna in Relation to Sea Surface Temperature and Chlorophyll-A Concentration of Bone Bay Using Remotely Sensed Satellite Data. *Jurnal. Ilmu. Dan. Teknologi. Kelautan. Tropis.* 3 (1), 9. doi: 10.29244/jitkt.v3i1.7837. doi: 10.29244/jitkt.v3i1.7837

Zhang, R. and Delworth, T. L. (2007). Impact of the Atlantic Multidecadal Oscillation on North Pacific Climate Variability: Impact on North Pacific Variability. *Geophysical. Res. Lett.* 34 (23), 229–241. doi: 10.1029/2007GL031601

Zhou, X., Sun, Y., Huang, W., Smol, J. P., Tang, Q. and Sun, L. (2015). The Pacific Decadal Oscillation and Changes in Anchovy Populations in the Northwest Pacific. *J. Asian Earth Sci.* 114, 504–511. doi: 10.1016/j.jseaes.2015.06.027

**Conflict of Interest:** The authors declare that the research was conducted in the absence of any commercial or financial relationships that could be construed as a potential conflict of interest.

frontiers | Frontiers in Marine Science

TYPE Original Research
PUBLISHED 27 July 2022
DOI 10.3389/fmars.2022.961990



OPEN ACCESS

EDITED BY
Jun Xu,
Institute of Hydrobiology, Chinese Academy of Sciences (CAS), China

REVIEWED BY
Binsong Jin,
Hangzhou Normal University, China
Chuanxin Qin,
South China Sea Fisheries Research Institute, Chinese Academy of Fishery Sciences (CAFS), China

*CORRESPONDENCE
Feng Chen
cf0421223@163.com

†These authors have contributed equally to this work

SPECIALTY SECTION
This article was submitted to Marine Ecosystem Ecology, a section of the journal Frontiers in Marine Science

RECEIVED 05 June 2022
ACCEPTED 28 June 2022
PUBLISHED 27 July 2022

CITATION
Jiang RJ, Yang F, Chen F, Yin R, Liu MZ, Zhu WB, Guo A and Liu LW (2022) Assessing trophic interactions among three tuna species in the Solomon Islands based on stomach contents and stable isotopes. *Front. Mar. Sci.* 9:961990. doi: 10.3389/fmars.2022.961990



# Assessing trophic interactions among three tuna species in the Solomon Islands based on stomach contents and stable isotopes

Ri Jin Jiang[1,2,3†], Fan Yang[1,2,3,4†], Feng Chen[1,2,3*], Rui Yin[1,2,3], Ming Zhi Liu[1,2,3,4], Wen Bin Zhu[1,2,3], Ai Guo[1,2,3] and Lian Wei Liu[1,2,3]

[1]Zhejiang Marine Fisheries Research Institute, Zhoushan, China, [2]Scientific Observation and Experimental Station of Fishery Resources of Key Fishing Grounds, Ministry of Agriculture and Rural Affairs of the People's Republic of China, Zhoushan, China, [3]Key Laboratory of Sustainable Utilization of Technology Research for Fishery Resources of Zhejiang Province, Zhoushan, China, [4]Marine and Fisheries Institute, Zhejiang Ocean University, Zhoushan, China

Trophic research is essential to the conservation and management of fishery resources. This study analyzed the feeding habits and nutritional interactions among three tuna species in the waters of the Solomon Islands (5°12′S–15°20′S, 157°31′E–172°19′E). A total of 103 bigeye tuna (*Thunnus obesus*), 296 yellowfin tuna (*Thunnus albacores*), and 264 albacore tuna (*Thunnus alalunga*) samples were collected from September to December 2019. Samples for stomach content and stable isotope analysis were randomly selected. The stomach content analysis results showed that the stomach contents of the three tuna species were rich in prey, and 48 prey species were identified, including fish, cephalopods, and crustaceans, with high between-phenotype component (BPC). Yellowfin tuna consumed the largest variety of food and bigeye tuna consumed the smallest. The feeding intensity of bigeye tuna were higher than that of yellowfin and albacore tuna. Yellowfin tuna had the highest empty stomach rate (35.69%) and lowest average stomach fullness index (0.064). The degree of stomach fullness in the three tuna species was mainly 1, and the difference in the stomach fullness index among them was significant ($P<0.001$). Food overlap (0.3–0.6) and Levins index (<0.6) among the three species were low, indicating a specialized feeding tendency. Bigeye tuna mainly feed on *Ommastrephes bartrami* and Myctophidae, yellowfin tuna mainly feed on Hyperiidea and *Aluterus monoceros*, and albacore tuna mainly feed on *Gempylus serpens* and *Loligo chinensis*. The stable isotope results showed that the $\delta^{13}C$ and $\delta^{15}N$

values of the three tuna species were significant ($P<0.001$). The standard ellipse area corrected for small sample sizes (SEAc) and total niche area (TA) of bigeye tuna, range of $\delta^{15}N$ (NR) of yellowfin tuna, and range of $\delta^{13}C$ (CR) of albacore tuna were the highest. The results of this study will help improve our understanding of the feeding ecology of these three tuna species and their important roles in the ecosystem and food web structure.

KEYWORDS

Solomon Islands, tuna, food composition, carbon and nitrogen stable isotopes, trophic niche

## Introduction

Trophic research is an important part of ecosystem conservation and comprehensive assessment of marine living resources (Martins et al., 2021). Feeding is an important component of this process. Through feeding research, we can understand the trophic relationships and functional roles of species in ecosystems (Willson et al., 2010). Understanding the feeding habits of large pelagic fish, such as tuna and other top predators, is important for modeling nutrient relationships and understanding the dynamics of marine ecosystems (Albuquerque et al., 2019). As top predators, tuna occupy a high trophic level in oceanic ecosystems (Zhu et al., 2008b). They can control the resource and population changes of prey organisms at all trophic levels through the top-down effect, thereby affecting the entire marine ecosystem and food web.

Stomach content analysis is commonly used to quantify fish food types and the distribution of resources among predators, as it allows visualizing the food composition of a species (Braga et al., 2012). However, the results of stomach contents analysis can represent only the instantaneous feeding situation of predators (Gee, 1989). The stable carbon and nitrogen isotopes of fish muscle can preserve dietary information for a long time, and the similarity between $\delta^{13}C$ from fish muscle and that of prey organisms can provide information about food sources (Peterson and Fry, 1987). The enrichment effect of $\delta^{15}N$ between adjacent trophic levels is approximately 3–4‰ and can be used to estimate the trophic levels of organisms (Caut et al., 2009). In addition, a series of multivariate statistical indicators developed based on the ratio of stable carbon and nitrogen isotopes provide an important means for comparing the breadth overlap of trophic niche between species and identifying trophic relationships (Jackson et al., 2011). Niche Cait measures how well a species uses resources (Crozier, 1985), while niche overlap can reflect species' competition for prey (Zhang et al., 2010). The combination of these two methods facilitates better research on food webs (Peterson and Fry, 1987) and is, therefore, used worldwide (Tripp-Valdez et al., 2015; Wang et al., 2021).

The Solomon Islands (5°–15°S, 154°–174°E), located in the central and western Pacific Ocean, are a large archipelago comprising 992 islands (Denley et al., 2020). The islands have an area of 28,370 $km^2$, a coastline of 4,270 km, and an exclusive economic zone of 1.34 million $km^2$. In addition, the islands are surrounded by 1,325 $km^2$ of marine protected areas, including 113 $km^2$ of coral reefs. Archipelagos are of unique importance to the surrounding marine environment, with an uninterrupted abundance of plankton that attract gatherings of marine life due to the perennial circulation of ocean currents. They are rich in marine resources that provide a variety of food types and habitats for numerous predators and are a part of the migration routes of highly migratory species such as tuna (White et al., 2014).

In the waters surrounding the Solomon Islands, we observed three tuna species: bigeye tuna (*Thunnus obesus*), yellowfin tuna (*Thunnus albacores*), and albacore (*Thunnus alalunga*). These warm-water migratory fishes are widely distributed in the tropical and subtropical waters of the Atlantic, Pacific, and Indian Oceans, of which the Pacific Ocean has most abundant tuna resources (Shi et al., 2022). The Solomon Islands mainly fall under FAO's Region 71. According to data from the FAO website (https://www.fao.org/fishery/en/facp/slb?lang=en), the total annual catch of tuna in the region is over 1.4 million tons, accounting for approximately 38% of the world's major tuna (*Thunnus alalunga*, *Thunnus obesus*, *Katsuwonus pelamis*, and *Thunnus albacores*) production, the highest among the world's fisheries and FAO fisheries regions. Solomon tuna is mainly caught using longlines, purse seines, and bait boats. In recent years, the production has remained between 39,000 and 67,000 tons, with an average output of 55,000 tons. In 2019, the tuna production reached an all-time high of 67,000 tons, of which more than 85% was caught using purse seines.

To understand the food composition of tuna diets, the feeding ecology of these predators has been studied in the Atlantic, Pacific, and Indian Oceans (King and Ikehara, 1956; Moteki et al., 2001; Zhu et al., 2007). Studies have shown that

they are opportunistic, feeding mainly on fish, cephalopods, and crustaceans. However, no studies have been conducted specifically on tuna feeding in the waters of the Solomon Islands. Therefore, to explore the feeding situations and nutritional relationships of tuna species in this area, tuna samples were collected from the waters of the Solomon Islands from September to December 2019. A preliminary study of food diversity was conducted, and the nutrient relationships between them were quantitatively analyzed using stomach content analysis data and carbon and nitrogen stable isotope data. This study fills a gap in nutritional knowledge regarding important fishery resources around the Solomon Islands and can inform further assessment, conservation, and management of fishery resources.

# Materials and methods

## Sample collection

The tuna samples were collected by a Chinese longline tuna fishing boat that operated in the waters of the Exclusive Economic Zone (5°12′S–15°20′S, 157°31′E–172°19′E) of the Solomon Islands from September to December 2019. Sampling sites are shown in Figure 1. Biological data of three tuna species are shown in Table 1. For ease of description, an abbreviation is used for each tuna species, BET (*Thunnus obesus*),YFT (*Thunnus albacores*), and LFT (*Thunnus alalunga*).

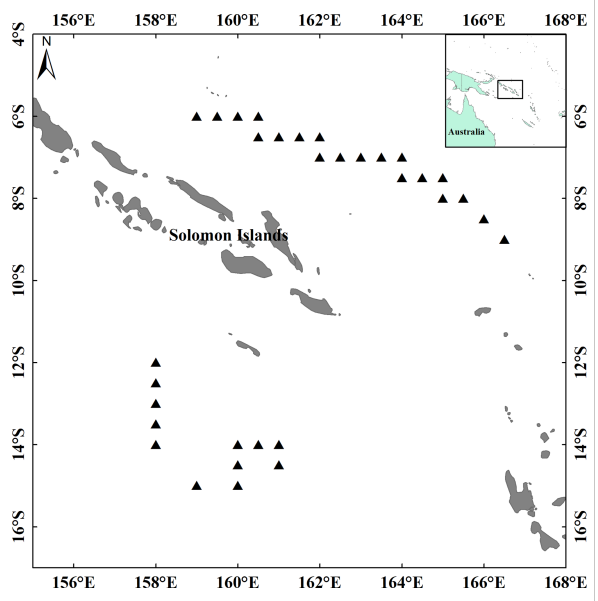


FIGURE 1
Sampling locations.

## Biological assay

Biological data including body length (cm), fork length (cm), and body weight (kg) of the tuna were measured on-site. According to the size, some tuna were randomly selected for stomach content analysis and stable isotope analysis, and the pure body weight (kg) and stomach weight (g) were measured. The degree of stomach filling was divided into five grades, ranging from 0 to 4. The grades 0–4 were: 0 (empty stomach); 1 (there is a small amount of food in the stomach, its volume does not exceed half of the stomach cavity); 2 (more food in the stomach, its volume is more than half of the stomach cavity); 3 (the stomach is full of food, but the stomach wall is not inflated); 4 (the stomach is full of food, and the stomach wall expands and becomes thin). The stomach and back muscles of the tuna were dissected out and packaged separately, then stored frozen at −20° C until subsequent identification of prey species and stable isotope determination. Prey were divided into broad categories (fish, cephalopods, and crustaceans) and the FishBase (Froese and Pauly, 2022) and the book by Kent and Volker (2001) were used to determine species names. Undigested and partially digested prey were counted and weighed. Partially digested prey were grouped into broad categories (e.g., fish) and weighed using a Mettler Toledo PL403 electronic balance with a precision of 0.001 g. Before weighing, the surface of the prey was dried using paper towels to ensure it was free of moisture. Undigested prey were identified and counted using a Nikon SMZ-2000 dissecting microscope. The corrected mass (average mass of intact prey individuals) was calculated for partially or fully digested prey.

## Data analysis

To determine the contribution of each prey organism to the diet composition of tuna, the following metrics were used: weight percentage (*W%*), numerical abundance (*N%*), frequency of occurrence (*FO%*) (Hyslop, 1980), and the index percentage of relative importance (*IRI%*) (Pinkas, 1971), which reduces bias in descriptions of animal dietary data. Because *Sardinella zunas* are used as bait in longline fishing, the data for this genus were excluded when calculating the importance of prey. These metrics were calculated as follows:

$$W\% = \textit{actual mass of a prey} / \textit{total mass of stomach contents} \times 100$$

$$N\% = \textit{the number of prey} / \textit{total number of prey in stomach contents} \times 100$$

$$FO\% = \textit{the actual number of stomachs containing a prey} / \textit{the number of non} - \textit{empty stomachs} \times 100$$

$$IRI = (N\% + W\%) \times F\% \times 10^4$$

TABLE 1 Biological data for three species of tuna.

| | BET | YFT | LFT |
|---|---|---|---|
| Number | 103 | 296 | 264 |
| Fork length range (cm) | 65.40–140.50 | 83.10–150.50 | 80.80–108.40 |
| Average fork length (cm) | 100.85 ± 17.72 | 132.03 ± 7.78 | 96.45 ± 2.98 |
| Weight range (kg) | 5.84–58.87 | 10.21–64.85 | 9.86–23.54 |
| Average weight (kg) | 23.46 ± 12.74 | 39.94 ± 7.81 | 18.20 ± 1.47 |

Thunnus obesus (BET), Thunnus albacores (YFT), Thunnus alalunga (LFT).

$$IRI\,\% = \frac{IRI_{\mathrm{i}} \times 100}{\sum_{i=1}^{n} IRI_i}$$

A strong correlation exists between the stomach content weight and body length of fish, which can be expressed by the fullness index; therefore, the fullness index can be used to determine the feeding status of fish (Wang et al., 2013). The proportion of different feeding grades in the stomach can also reflect the feeding status. The empty stomach rate is the proportion of grade 0. The empty stomach rate index and the fullness index (Figueiredo et al., 2005) can comprehensively reflect the feeding status of fish (Zhu et al., 2008). The formula used is as follows:

$$Fullness\ index\ =\ actual\ weight\ of\ food\ mass\ (kg)\ /\ fork\ length\ (cm)\ \times\ 100$$

$$Empty\ stomach\ rate\ (\%)\ =\ number\ of\ empty\ stomachs\ /\ total\ number\ of\ stomachs\ \times\ 100$$

The trophic niche range of tuna was calculated using the Levins index, whereby a value of<0.6 indicates that the predator selected a small group of prey, and a value closer to 1 (>0.6) indicates that the predator has a wide range of food sources. The Levins index is calculated as follows:

$$B = 1 / \left(n\sum P_{xi}^2\right)$$

where $P_{xi}$is the proportion of predator $x$ ingesting prey organism $i$, expressed as a percentage (N%), and n is the number of species of prey organisms that can be ingested (Feinsinger et al., 1981).

To determine the niche overlap, Pianka's niche overlap index ($Oij$) was calculated as follows:

$$O_{ij} = \frac{\sum_{k=1}^{s} P_{ik} \times P_{jk}}{\sqrt{\sum_{k=1}^{s} P_{ik}^2 \times \sum_{k=1}^{s} P_{jk}^2}}$$

where $P_{ik}$ is the weight percentage of prey $i$ in the food composition of predator $k$, $s$ is all prey types consumed by the three tuna species, and the variation range of $O_{ij}$is 0–1. The larger the value, the higher the degree of overlap. $O_{ij}$ >0.3 indicates a small degree of overlap, and $O_{ij}$ >0.6 indicates significant overlap (Krebs, 1999).

Amundsen et al. (1996) improved the graphic method proposed by Costello (1990) for the ecological study of feeding. The feeding strategy graph was formed by taking the occurrence frequency of prey $F_i$as the abscissa and the abundance of a specific prey $P_i$ as the ordinate. The feeding strategies of the three tuna species are visually displayed according to the scatter positions in Figure 3. Along the vertical axis, the top denotes a narrow eating strategy, and the bottom denotes a broad eating strategy. Along the horizontal axis, the lower left corner represents the non-important or rare prey, and the upper right corner represents the important prey. The upper left corner represents a high between-phenotype component (BPC), and the lower right corner represents a high within-phenotype component (WPC). The formula for calculating the abundance of specific prey is as follows:

$$P_i = \left(\sum S_i / \sum S_{ti}\right) \times 100$$

where $P_i$is the abundance of specific prey, $S_i$ is the weight of prey $i$ in the stomach contents, and $S_{ti}$ is the weight of the stomach contents of individuals with prey $i$ in their stomach.

## Stable isotope analysis

The back muscle tissue extracted from tuna was washed with distilled water, wrapped with tin foil, dried in an Alpha 1-2LDplus freeze dryer (Beijing BMH Instruments Co. Ltd., Shanghai, China) for 24 h, and thoroughly ground. The sample powder was placed in a 2 ml centrifuge tube and stored under dry conditions. Stable carbon and nitrogen isotope ratios were determined for all samples using an EA-HT elemental analyzer (Thermo Fisher Scientific, Inc., Bremen, Germany) and a DELTA V Advantage Isotope Ratio Mass Spectrometer (Thermo Fisher Scientific). After the sample was burned at a high temperature in the elemental analyzer, $CO_2$ and $N_2$ were generated. A mass spectrometer was used to detect the ratio of $^{13}C$ to $^{12}C$ of $CO_2$ and compare it with the international standard Peedee Belemnite to calculate the $\delta^{13}C$ value of the sample, and to detect the ratio of $^{15}N$ to $^{14}N$ of $N_2$ and compare it with the international standard (Atm-$N_2$) to calculate the $\delta^{15}N$ value of the sample. The calculation method of isotope abundance is as follows:

$$\delta X = [(R_{sample}/R_{standard}) - 1] \times 1000$$

where δX = $\delta^{13}C$ or $\delta^{15}N$, and R = $^{13}C/^{12}C$ or $^{15}N/^{14}N$. The $\delta^{13}C$ and $\delta^{15}N$ accuracies were< ± 0.1‰ and< ± 0.2‰, respectively. $R_{sample}$ is the isotope ratio of the measured sample and $R_{standard}$ is the isotope ratio of the standard material. To ensure the precision and accuracy of the detection results, three international standard samples were placed after every 10 samples to calibrate the stable isotopes of carbon and nitrogen. Moreover, each sample was measured 10 times.

## Trophic niche

The $\delta^{15}N$-$\delta^{13}C$ double-bit map drawn from the average isotopic value of an individual can be used to study the isotopic composition of a species (Layman et al., 2007). Using quantitative indicators of the nutritional structure of the food web and analyzing the coordinate point information in the double-bit map can better show the characteristics of a nutritional niche (Li et al., 2021). The main indicators include diversity of food sources (CR; range of $\delta^{13}C$; range of stable carbon isotope values), nutrient length (NR; range of $\delta^{15}N$; range of stable nitrogen isotope values), total niche area (TA; total convex hull area; convex polygon area of coordinate points represented by all individuals), and core niche area (SEA; standard ellipse area). The SEA generally needs to conform to a normal distribution, and the sample size should be greater than 30. For a small sample size, the standard ellipse area corrected for small sample sizes (SEAc) is typically used (Jackson et al., 2011). The relationship between the SEA and SEAc is as follows:

$$SEAc = SEA \times (n-1)/(n-2),$$

where n is the number of samples of a species.

SPSS version 24 and Excel 2019 were used for data analysis. One-way ANOVA was used to test whether there were significant differences between carbon and nitrogen stable isotope values and the average stomach fullness index among the three tuna species ($\alpha = 0.05$). First, data were tested for normality and homogeneity of variance. If any of the above requirements were not met, a non-parametric test (Kruskal-Wallis) was performed. The Pearson correlation coefficient was used to test the relationship between the fork length and stable isotopes of carbon and nitrogen. The trophic structures of $\delta^{13}C$ and $\delta^{15}N$ for the three tuna species were mapped using the Stable Isotope Bayesian Ellipses in R (SIBER) package in the program R Core Team (2021) (version 4.0.2). SIBER model fitting was performed *via* Markov chain Monte Carlo (MCMC) simulation, which calculates a posterior estimate by combining the priors and likelihoods. The model was run for 10,000 iterations (Jackson et al., 2011). The trophic niche indicators and Bayesian standard ellipse areas ($SEA_B$) of various tuna species were calculated, with confidence intervals of 95%, 75%, and 50% presented in the resulting graphs, respectively. To quantify the differences in isotopic niche utilization among the three tuna species, the R package nicheROVER was used to estimate the probability of one population occurring within the niche area (space) of another population with 95% confidence intervals based on 10,000 iterations (Swanson et al., 2015).

# Results

## Food composition of tuna

Analysis of the stomach contents of 42 BET, 84 YFT, and 75 LFT showed that the three tuna species fed on 48 prey species, including fish, cephalopods, and crustaceans (**Table 2**). A total of 31 families (26 fish families and 5 cephalopod families), 12 fish species (including *Sternoptyx diaphana*, *Alepisaurus ferox*, *Gempylus serpens*, and *Ruvettus pretiosus*), and 3 cephalopod species were identified. The BET stomachs contained 23 identified species, including 16 fishes, 4 cephalopods, and 3 crustaceans with *IRI*s of 49.82%, 38.68%, and 11.49%, respectively, and unidentified fishes and cephalopods. The dominant prey were *Ommastrephes bartrami* (*IRI* = 25.01%) and Myctophidae (*IRI* = 12.34%), followed by *Penacus* sp. (*IRI* = 10.24%%) and *G. serpens* (*IRI* = 8.72%). The *IRI*s of *S. diaphana*, *A. ferox*, and *L.*chinensis were 6.76%, 5.65%, and 5.61%, respectively. YFT fed on unidentified fish and cephalopods, and 35 identified species, including 22 fishes, 4 cephalopods, and 9 crustaceans with *IRI*s of 67.84%, 10.32%, and 21.84%, respectively; fish accounted for the largest proportion of prey taxa. The dominant prey were Hyperiidea spp. (*IRI* = 19.57%), *Aluterus monoceros* (*IRI* = 11.74%), *Eumegistus illustris* (*IRI* = 8.13%), and *O. bartrami* (*IRI* = 7.55%). The *IRI* of unrecognizable fish was 38.99%, and the digestion degree was high. LFT ingested unidentifiable fish and cephalopods, and 31 identified species, including 18 fishes, 3 cephalopods, and 8 crustaceans with *IRI*s of 76.43%, 15.45%, and 8.12%, respectively. Fish made up the largest proportion of prey, unidentifiable fish had the highest *IRI* (48.72%), and the degree of digestion was high, which was similar to the results for YFT. The dominant prey was *G. serpens* (*IRI* = 17.16%), and its *IRI* proportion was the largest among the identified prey species. This was followed by *L.*chinensis (*IRI* = 8.58%), and Hyperiidea spp. (*IRI* = 6.45%). In addition, the *IRI* of *Synodus* spp. was also high (6.37%), second only to that of *L. chinensis* and Hyperiidea spp.

## Feeding intensity

Grade 1 was the dominant feeding grade in all three tuna species; that is, most individuals had only a small amount of food in their stomach. The feeding grade of all LFT was less than 4

(Figure 2). There was a significant difference in the stomach fullness index among the three species ($P$<0.001), and the empty stomach rate and the average fullness index showed opposite trends; that is, the higher the empty stomach rate, the smaller the average fullness index. The empty stomach rates of BET, YFT, and LFT were 14.40%, 35.69%, and 31.60%, respectively, and the corresponding average gastric fullness indices were 0.188, 0.064, and 0.065, respectively.

## Feeding strategies and food overlap

Feeding strategies showed that prey concentrations were generally high with low occurrence frequency ($F_i$) and low abundance of specific prey ($P_i$) (Figure 3). Regarding distribution of prey, *O. bartrami* was the most important food for BET, with the highest occurrence frequency and food abundance. There was also a moderate proportion of *A. ferox*, *G. serpens*, and *L. chinensis*. Despite their low frequency, Sphyraenidae and Belonidae had higher prey-specific abundances because of their larger size. Conversely, despite their high frequency, Sternoptychidae, Myctophidae, and *Penacus* sp. are small in size and low in quality, resulting in lower prey-specific abundance. Taxa such as Octopodidae and *Synodus* spp. in the lower left corner of the graph belong to the secondary prey species of BET (Figure 3). *Ommastrephes bartrami*, *A. monoceros*, Hyperiidea, and Bramidae were the most important prey for YFT. The main prey of LFT were Gempylidae, *L. chinensis*, Synodontinae, Cephalopoda, and *Apogon* spp. Non-important prey accounted for the largest proportion of ingested organisms (Figure 3). In general, most of the prey were distributed on the left side of the graph; that is, there were differences in food composition among larger polyphagous individuals. However, the tuna species tended to utilize exclusive resources, as evidenced by the low B values (0.48, 0.19, and 0.32 for BET, YFT, and LFT, respectively) and low dietary overlap between species (Table 3). Fifteen prey species overlapped among the three tuna species, including nine species of fish, three species of cephalopods, and two species of crustaceans. The overlap index ($O_{ij}$) results showed that the food overlap coefficient among the three tuna species was greater than 0.3, and there was a possibility of food competition.

## Ratios of stable isotope

Some tuna with stomach food were selected for isotope analysis. The $\delta^{13}C$ and $\delta^{15}N$ values for the three tuna species are listed in Table 4. The total $\delta^{13}C$ values ranged from −19.96‰ to −13.64‰, with an average of −16.94 ± 1.64‰. The total $\delta^{15}N$ values ranged from 6.6‰ to 21.03‰, with an average of 14.48 ± 3.87‰. LFT had the widest range of $\delta^{13}C$ values, and the mean $\delta^{13}C$ values for YFT and LFT were similar. BET had the highest $\delta^{15}N$ value and YFT had the lowest $\delta^{15}N$ value. The ANOVA showed significant differences in carbon ($P$<0.001) and nitrogen ($P$<0.001) isotope values among the three species. The Pearson correlation results showed that $\delta^{15}N$ and $\delta^{13}C$ had no significant effect on the fork length of the three species ($P$>0.05), whereas $\delta^{15}N$ and $\delta^{13}C$ were positively correlated with the fork length of YFT and LFT (Figure 4).

## Trophic niche

As shown in Table 5 and Figure 5, BET had the largest SEAc and TA, YFT had the largest NR, and LFT had the largest CR. The Bayesian standard ellipse area ($SEA_B$) representations

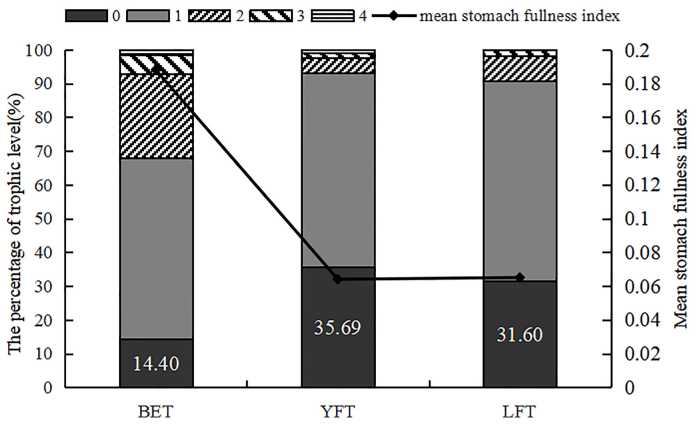


FIGURE 2
The percentage of trophic level and mean stomach fullness index of three species of tuna. BET, big eye tuna, *Thunnus obesus*; YFT, yellow fin tuna, *T. albacares*; LFT, albacore tuna, *T. alalunga*.

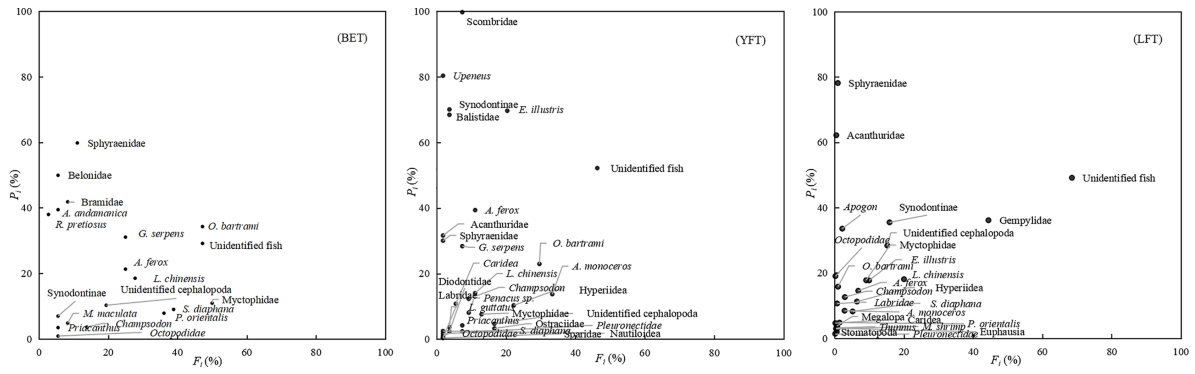


FIGURE 3
Relationship between relative prey-specific abundance (Pi, %) and frequency of occurrence (Fi, %) of prey items in the diet of three species of tuna. BET, big eye tuna, *Thunnus obesus*; YFT, yellow fin tuna, *T. albacares*; LFT, albacore tuna, *T. alalunga*.

(Figure 6) showed that BET had the largest $SEA_B$ mode value (9.53‰$^2$) and a 95% confidence interval of 6.05–15.45‰$^2$, followed by YFT with a $SEA_B$ mode value of 8.61‰$^2$ and 95% confidence interval of 5.27–13.19‰$^2$. LFT had the smallest $SEA_B$ mode value (5.79‰$^2$) and a 95% confidence interval of 3.28–9.01‰$^2$. The results showed that the bigeye tuna had a greater niche width.

The trophic niche area composed of the carbon and carbon stable isotopes of each tuna species, and the 10 randomly generated elliptical projections are shown in Figure 7. Smoothing histograms (density plots) and scatter plots showed no violation of normality. As shown in Figure 5, BET had higher $\delta^{15}N$ ratios, YFT had more extensive NR, and LFT had the largest CR. The three species occupied different trophic niche areas that were overlapping.

Figure 8 shows the posterior distribution of the overlap metric. The nicheROVER analysis revealed the probability of a species being found in the niche area of another species. The isotopic niches of BET were found in 13% and 17% of the niche areas of YFT and LFT, respectively. The isotopic niches of YFT were found in 11% and 42% of the niche areas of BET and LFT, respectively. The isotopic niches of LFT were found in 29% and 75% of the niche areas of BET and YFT, respectively. Therefore, YFT and LFT are more likely to occupy the same niche area.

## Discussion

The results of the food composition analysis indicated that the three species of tuna in the Solomon Islands were polyphagous, mainly eating fish, cephalopods, and crustaceans, which is consistent with the findings of other studies (Xu et al., 2008; Zhu et al., 2015; Tao et al., 2017). Although the composition of food could be identified by observing stomach contents, owing to the influence of fish digestion and artificial errors, many prey, most of which were fish, could not be identified. For example, unidentifiable fish accounted for 38.99% and 48.72% of prey composition in YFT and LFT, respectively. This affects the results to a certain extent; therefore, it is necessary to use the carbon and nitrogen stable isotope values of prey organisms and potential food sources to determine the contribution rates of different food types. Studies have shown that tuna are opportunistic predators (Ménard et al., 2006), with diets that vary according to the abundance of food in a region (Mendoza-Ávila et al., 2017). In different seas, the types of prey that tuna eat are different. BET in the central Pacific Ocean mainly consume Alepisauridae, Gempylidae, and Bramidae (King and Ikehara, 1956), whereas those in the tropical waters of the eastern Pacific Ocean mainly consume Myctophidae, Gempylidae, and Sternoptychidae (Moteki et al., 2001). The main families that BET feed on in the western Atlantic Ocean are Alepisauridae, Ommastrephidae, and Clupeidae (Zhu et al., 2007). YFT mainly consume squid, sardines, and shrimp in the middle of the Atlantic Ocean (Song et al., 2004); *Lestrolepis japonica*, *Benthosema pterotum*, *Mene maculata*, Exocoetidae, and Chaetodontidae in the waters off Taiwan (Weng et al., 2015); and *Oxyporhamphus micropterus*, *Auxis thazard*, *Lampanyctus alatus*, *Onykia carribbaea*, and Gammaridea in the eastern Pacific Ocean (Perrin et al., 1973). LFT mainly feed on Triacanthus, Alepisauridae, and Gempylidae in the western Indian Ocean (Koga, 1958), whereas the main food sources in the southern Pacific Ocean are crustaceans (such as shrimp), squid, and fish (Saito, 1973).

The combined results of the food composition analysis and feeding strategy map showed that all three tuna species had the characteristics of polyphagia, and their food sources were wide and rich. The three tuna types showed high between-phenotype

TABLE 2 Diet composition of three species of tuna.

| prey items | BET | | | | YFT | | | | LFT | | | |
|---|---|---|---|---|---|---|---|---|---|---|---|---|
| | *W%* | *N%* | *FO%* | *IRI%* | *W%* | *N%* | *FO%* | *IRI%* | *W%* | *N%* | *FO%* | *IRI%* |
| **Fish** | **64.07** | **50.73** | **272.22** | **54.03** | **88.39** | **46.22** | **255.56** | **67.84** | **78.69** | **52.31** | **209.80** | **76.43** |
| Sternoptychidae | | | | | | | | | | | | |
| *Sternoptyx diaphana* | 5.47 | 6.78 | 38.89 | 6.76 | 0.23 | 0.49 | 9.26 | 0.14 | 2.38 | 0.77 | 5.88 | 0.27 |
| Synodontinae | | | | | | | | | | | | |
| *Synodus* spp. | 0.52 | 4.21 | 5.56 | 0.41 | 1.65 | 0.98 | 5.56 | 0.31 | 7.29 | 7.41 | 29.41 | 6.37 |
| Alepisauridae | | | | | | | | | | | | |
| *Alepisaurus ferox* | 10.61 | 5.31 | 25.00 | 5.65 | 3.71 | 2.44 | 12.96 | 1.67 | 3.13 | 2.01 | 13.73 | 1.04 |
| Myctophidae | | | | | | | | | | | | |
| Myctophidae spp. | 6.58 | 10.81 | 50.00 | 12.34 | 1.18 | 2.07 | 14.81 | 1.01 | 1.90 | 1.54 | 5.88 | 0.30 |
| *Diaphus* spp. | 0.60 | 0.55 | 2.78 | 0.05 | | | | | 2.28 | 1.08 | 3.92 | 0.19 |
| Priacanthidae | | | | | | | | | | | | |
| *Priacanthus* spp. | 0.28 | 0.37 | 5.56 | 0.05 | 0.14 | 0.49 | 9.26 | 0.12 | 0.13 | 0.15 | 1.96 | 0.01 |
| Bramidae | | | | | | | | | | | | |
| *Taractes rubescens* | 1.18 | 0.18 | 2.78 | 0.05 | | | | | | | | |
| *Eumegistus illustris* | 0.29 | 0.37 | 5.56 | 0.05 | 15.67 | 1.83 | 22.22 | 8.13 | 4.57 | 2.78 | 15.69 | 1.70 |
| Champsodontidae | | | | | | | | | | | | |
| *Champsodon* spp. | 0.96 | 2.56 | 16.67 | 0.83 | 0.71 | 2.07 | 11.11 | 0.65 | 1.35 | 1.23 | 5.88 | 0.22 |
| Sphyraenidae | | | | | | | | | | | | |
| Sphyraenidae spp. | 4.75 | 1.65 | 11.11 | 1.01 | 0.20 | 0.24 | 3.70 | 0.03 | 0.42 | 0.15 | 1.96 | 0.02 |
| Menidae | | | | | | | | | | | | |
| *Mene maculata* | 0.67 | 0.73 | 8.33 | 0.17 | | | | | | | | |
| Carangidae | | | | | | | | | | | | |
| *Alectis ciliaris* | 0.04 | 0.18 | 2.78 | 0.01 | | | | | | | | |
| Gempylidae | | | | | | | | | | | | |
| *Gempylus serpens* | 14.07 | 6.04 | 30.56 | 8.72 | 0.95 | 0.95 | 9.26 | 0.37 | 18.55 | 9.72 | 41.18 | 17.16 |
| *Ruvettus pretiosus* | 0.67 | 0.37 | 2.78 | 0.04 | | | | | 1.89 | 0.31 | 1.96 | 0.06 |
| Leiognathidae | | | | | | | | | | | | |
| Leiognathidae sp. | 0.14 | 0.18 | 2.78 | 0.01 | | | | | | | | |
| Belonidae | | | | | | | | | | | | |
| Belonidae sp. | 3.70 | 1.83 | 5.56 | 0.44 | | | | | | | | |
| Scombridae | | | | | | | | | | | | |
| *Thunnus* sp. | | | | | 9.03 | 0.24 | 5.56 | 1.08 | 0.38 | 0.62 | 5.88 | 0.09 |
| *Katsuwonus pelamis* | | | | | 27.86 | 0.12 | 3.70 | 2.17 | | | | |
| *Acanthocybium solandri* | | | | | 0.04 | 0.12 | 3.70 | 0.01 | | | | |
| Monacanthidae | | | | | | | | | | | | |
| *Aluterus monoceros* | | | | | 3.27 | 12.68 | 35.19 | 11.74 | 1.31 | 2.01 | 3.92 | 0.19 |
| Ostraciidae | | | | | | | | | | | | |
| Ostraciidae sp. | | | | | 0.49 | 1.46 | 18.52 | 0.76 | 0.13 | 0.15 | 1.96 | 0.01 |
| Lampridida | | | | | | | | | | | | |
| *Lampris guttatus* | | | | | 0.09 | 0.37 | 5.56 | 0.05 | 0.09 | | | |
| Mullidae | | | | | | | | | | | | |
| *Upeneus* sp. | | | | | 1.57 | 0.73 | 3.70 | 0.18 | 1.57 | | | |
| Acanthuridae | | | | | | | | | | | | |
| Acanthuridae spp. | | | | | + | 0.73 | 3.70 | 0.06 | 0.21 | 0.15 | 1.96 | 0.01 |
| Pleuronectidae | | | | | | | | | | | | |
| Pleuronectidae spp. | | | | | 0.13 | 0.37 | 3.70 | 0.04 | 0.06 | 0.31 | 1.96 | 0.01 |
| Anguillidae | | | | | | | | | | | | |

*(Continued)*

TABLE 2 Continued

| prey items | BET | | | | YFT | | | | LFT | | | |
|---|---|---|---|---|---|---|---|---|---|---|---|---|
| | *W%* | *N%* | *FO%* | *IRI%* | *W%* | *N%* | *FO%* | *IRI%* | *W%* | *N%* | *FO%* | *IRI%* |
| Anguillidae sp. | | | | | 0.03 | 0.12 | 3.70 | 0.01 | | | | |
| Balistidae | | | | | | | | | | | | |
| Balistidae sp. | | | | | 0.26 | 1.59 | 5.56 | 0.21 | | | | |
| Sparidae | | | | | | | | | | | | |
| Sparidae sp. | | | | | 0.03 | 0.49 | 3.70 | 0.04 | | | | |
| Labridae | | | | | | | | | | | | |
| Labridae spp. | | | | | 0.03 | 0.37 | 3.70 | 0.03 | 0.19 | 0.15 | 1.96 | 0.01 |
| Diodontidae | | | | | | | | | | | | |
| Diodontidae sp. | | | | | 0.04 | 0.37 | 5.56 | 0.05 | | | | |
| Apogonidae | | | | | | | | | | | | |
| *Apogon* spp. | | | | | | | | | 1.01 | 0.62 | 1.96 | 0.05 |
| Unidentified fish | 13.55 | 8.61 | 55.56 | 17.47 | 21.08 | 14.88 | 51.85 | 38.99 | 31.53 | 21.14 | 62.75 | 48.72 |
| **Cephalopoda** | **31.80** | **33.33** | **119.44** | **35.43** | **8.81** | **9.15** | **79.63** | **10.32** | **16.70** | **21.76** | **60.78** | **15.45** |
| Ommastrephidae | | | | | | | | | | | | |
| *Ommastrephes bartrami* | 18.02 | 17.22 | 50.00 | 25.01 | 6.20 | 4.63 | 33.33 | 7.55 | 0.44 | 0.77 | 1.96 | 0.04 |
| Loliginidae | | | | | | | | | | | | |
| *Loligo chinensis* | 7.00 | 6.04 | 27.78 | 5.14 | 1.96 | 1.83 | 16.67 | 1.32 | 9.18 | 10.03 | 31.37 | 8.88 |
| Enoploteuthidae | | | | | | | | | | | | |
| *Abralia andamanica* | 3.59 | 1.47 | 5.56 | 0.40 | | | | | | | | |
| Octopodidae | | | | | | | | | | | | |
| Octopodidae spp. | 0.11 | 0.55 | 5.56 | 0.05 | 0.01 | 0.12 | 3.70 | 0.01 | 0.09 | 0.62 | 1.96 | 0.02 |
| Nautilidae | | | | | | | | | | | | |
| Nautiloidea sp. | | | | | 0.02 | 0.11 | 3.70 | 0.01 | | | | |
| Unidentified cephalopoda | 3.08 | 8.06 | 30.56 | 4.83 | 0.63 | 2.44 | 22.22 | 1.43 | 6.99 | 10.34 | 25.49 | 6.51 |
| **Crustacea** | **4.14** | **15.93** | **55.56** | **10.54** | **2.80** | **44.63** | **75.93** | **21.84** | **4.61** | **25.93** | **78.43** | **8.12** |
| Caridea spp. | 0.30 | 1.28 | 11.11 | 0.25 | 0.21 | 2.56 | 7.41 | 0.43 | 0.09 | 0.77 | 3.92 | 0.05 |
| Isopoda spp. | | | | | 0.23 | 4.88 | 5.56 | 0.59 | 0.26 | 1.23 | 9.80 | 0.22 |
| Oratosquilla sp. | | | | | 0.01 | 0.12 | 3.70 | 0.01 | 0.18 | 0.31 | 3.92 | 0.03 |
| Stomatopoda spp. | | | | | 0.01 | 0.37 | 7.41 | 0.06 | 0.00 | 0.00 | 0.00 | 0.00 |
| Hyperiidea spp. | 0.07 | 1.10 | 2.78 | 0.05 | 1.70 | 29.88 | 29.63 | 19.57 | 2.96 | 14.20 | 25.49 | 6.45 |
| Amphipoda sp. | | | | | 0.09 | 1.71 | 3.70 | 0.14 | | | | |
| Euphausia spp. | | | | | 0.02 | 0.49 | 5.56 | 0.06 | 0.20 | 3.40 | 7.84 | 0.42 |
| *Penacus* sp. | 3.76 | 13.55 | 41.67 | 10.24 | 0.52 | 4.51 | 9.26 | 0.98 | 0.45 | 2.31 | 11.76 | 0.48 |
| Megalopa sp. | | | | | | | | | 0.27 | 1.85 | 7.84 | 0.25 |
| Unidentified shrimp larvae | | | | | 0.03 | 0.12 | 3.70 | 0.01 | 0.19 | 1.85 | 7.84 | 0.24 |

† indicates a value less than 0.01; Thunnus obesus (BET), Thunnus albacores (YFT), Thunnus alalunga (LFT).
The bold values are the sum of broad categories.

component (BPC) and low intraspecific food overlap and consumed a large variety of rare or incidental prey. Archipelagos provide abundant food for marine predators and are important environments for maintaining local biodiversity and non-resident species because surrounding physical processes trigger increases in primary biomass that affect entire adjacent food webs. Although tuna are oceanic migratory fish, species that inhabit coastal areas or islands, such as Hyperiidea and the larvae of shrimp, also appear in their stomach contents, as found in this study. Coral reefs are distributed around the Solomon Islands and studies have shown that they provide abundant food for oceanic predators (Allain et al., 2012). Several coral reef fishes, such as Balistidae, Acanthuridae, Monacanthidae, and Synodontinae, are found in

TABLE 3 Food overlap coefficient of three species of tuna: *Thunnus obesus* (BET), *Thunnus albacores* (YFT), and *Thunnus alalunga* (LFT).

| Fish species | YFT | LFT |
|---|---|---|
| BET | 0.35 | 0.33 |
| YFT | | 0.32 |

TABLE 4 Comparison of stable isotope differences among three species of tuna.

| Items/Fish Species | | Total n=58 | BET n=20 | YFT n=20 | LFT n=18 |
|---|---|---|---|---|---|
| $\delta^{13}C$ (‰) | Mean ± SD | −16.94 ± 1.64 | −18.39 ± 2.94 | −16.31 ± 1.11 | −15.90 ± 1.38 |
| | Range | −19.96–13.64 | −19.96–15.81 | −17.64–13.71 | −18.62–13.64 |
| $\delta^{15}N$ (‰) | Mean ± SD | 14.48 ± 3.87 | 18.39 ± 2.94 | 11.18 ± 2.57 | 13.80 ± 1.43 |
| | Range | 6.60–21.03 | 11.89–21.03 | 6.60–17.15 | 11.02–15.95 |

"n" indicates the sample size; Thunnus obesus (BET), Thunnus albacores (YFT), and Thunnus alalunga (LFT).

the stomachs of tuna. In this study, reef fish constituted a low proportion of the BET diet because it foraged in deeper habitats, whereas YFT mainly foraged in shallower waters.

Generally, the type and size of food consumed by fish varies with body length or fork length (Yan et al., 2012), which is related to factors such as an increase in body length and body mass, and the gradual development of mouthparts (Li et al., 2019). For example, Ménard et al. (2006) studied the relationship between tuna size and prey size and found that tuna prey choice is related to the size of its mouth opening. Tuna usually only consume prey that they can swallow whole; therefore, as they grow, their mouths open wider, and they consume larger prey. To process the data, we briefly analyzed the dietary shifts of the three tuna species. With an increase in fork length, the proportion of fish and cephalopods in the stomach contents of BET and YFT increased, and the proportion of crustaceans decreased. No crustaceans were found in the stomach contents of LFT with a fork length >100 cm.

Studies on isotope differences among species have strengthened dietary analyses of feeding strategies and foods with different nutrient levels (Li et al., 2016). In the marine environment, there are more primary producers and nutrients in the waters around oceanic islands, and the $\delta^{13}C$ ratio of primary producers decreases with decreasing offshore distance (Hobson et al., 1994). This spatial heterogeneity is transmitted to predators along the food chain, which affects the $\delta^{13}C$ ratio of predators. The LFT in this study had higher $\delta^{13}C$ values and the largest CR, whereas BET had lower $\delta^{13}C$ values and YFT had the smallest CR. The CR reflects the diversity of food sources available to predators (Kong et al., 2020). The larger the CR, the more extensive and simpler the food sources of predators. Although they are all migratory species, the different $\delta^{13}C$ values indicate that the three tuna species use different habitats. The $\delta^{15}N$ ratio reflects the nutrient position of the organism, with BET having the highest $\delta^{15}N$ ratio. The $\delta^{15}N$ ratio results combined with the results of the stomach content analysis indicated the BET diet consisted of more high-nutrient prey, whereas YFT and LFT diets contained a small proportion of planktonic crustaceans. NR represents the diversity of nutrient levels and vertical structure of the food web. A larger NR value indicates a longer food chain (Davenport and Bax, 2002). The largest NR in YFT indicates that it was part of a longer food chain and may have fed in different water layers.

There was no significant correlation between fork length and the $\delta^{15}N$ and $\delta^{13}C$ values for the three tuna species. $\delta^{15}N$ was positively correlated with the fork length of YFT, suggesting that nitrogen concentration may increase with individual growth. This positive correlation may be related to the decreased dietary importance of small zooplankton and increased consumption of large prey with high nutritional value. The positive correlation

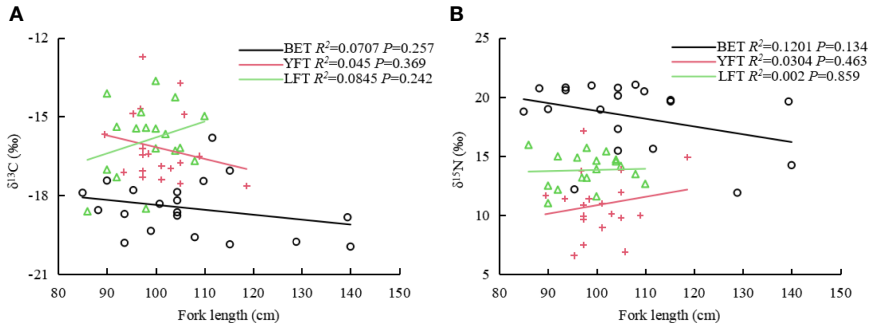


FIGURE 4
Correlation between fork lengths of three tuna species and $\delta^{13}C$ **(A)** and $\delta^{15}N$ **(B)**. BET: big eye tuna, *Thunnus obesus*; YFT, yellow fin tuna, *T. albacares*; LFT, albacore tuna, *T. alalunga*.

TABLE 5 Trophic structure parameters of three species of tuna: *Thunnus obesus* (BET), *Thunnus albacores* (YFT), and *Thunnus alalunga* (LFT).

| Indicator | BET | YFT | LFT |
|---|---|---|---|
| CR | 4.15 | 3.93 | 4.98 |
| NR | 9.14 | 10.55 | 4.93 |
| SEAc | 10.57 | 9.34 | 6.11 |
| TA | 28.00 | 24.66 | 14.96 |

between the fork length and $\delta^{13}C$ values of LFT suggests that individual size influences $\delta^{13}C$ values.

Niche width reflects the adaptability and tolerance of organisms to the environment (Crozier, 1985), whereas niche overlap reflects the similarity of resources used and potential prey competition between species (Zhang et al., 2010). The BET in this study had a larger niche width, which indicates that it had a relatively strong utilization capacity for environmental resources and occupied more ecological resources, thus having a higher dominant position in this area. According to the food overlap coefficient of the three tuna species, there was food competition among them, but the food overlap was not significant. This is similar to the results of Young et al. (2010). As top predators, tuna species differ in hunting type and size, timing, and depth to reduce competition. BET, for example, have similar feeding depths to LFT, but feed during both day and night, whereas LFT forage mainly during the day. Although YFT are thought to feed mainly above the thermocline, they can also dive deeper in search of food. Responding to habitat differences in prey is a strategy to reduce competition between species (Costa et al., 2020). In addition, the similarity between diets usually points to the overlap level, representing the food resources that can be shared between organisms, and does not necessarily indicate the existence of competition (Lucena et al., 2000). Therefore, the possibility of fierce food competition among the three tuna species is low, and food competition among them can be alleviated by the differentiation of prey type, feeding proportion, feeding time, and feeding depth (Song et al., 2020).

## Conclusion

In this study, stomach contents and stable isotope analysis were used to determine the feeding situation and nutritional relationships of three tuna species in the Solomon Islands. The food sources of the tuna species were wide, with high phenotypic composition (BPC) and low intraspecific food overlap. The feeding intensity and nutrient location of BET were higher than those of YFT and LFT. BET had a greater niche breadth based on the ratio of carbon and nitrogen stable isotopes. There was no significant overlap of food among the three species, although there was some competition; however, because of the differences in feeding times and depths, they fed

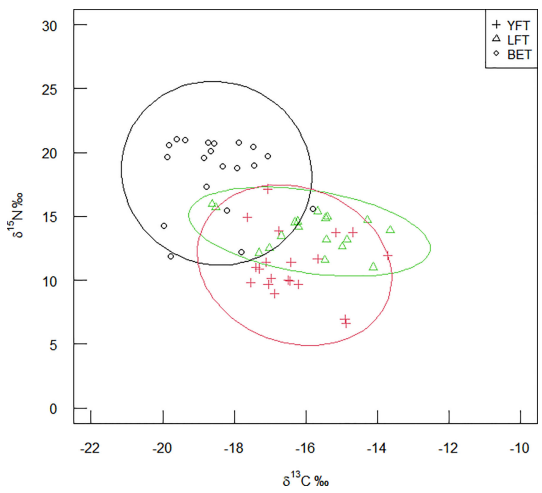


FIGURE 5
Trophic structure of three species of tuna. BET, big eye tuna, *Thunnus obesus*; YFT, yellow fin tuna, *T. albacares*; LFT, albacore tuna, *T. alalunga*.

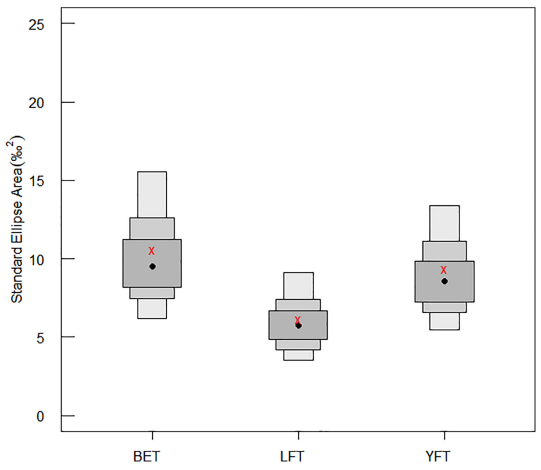


FIGURE 6
Bayesian standard ellipse area ($SEA_B$) for three species of tuna (with credibility intervals of 50%, 75%, and 95%). BET, big eye tuna, *Thunnus obesus*; YFT, yellow fin tuna, *T. albacares*; LFT, albacore tuna, *T. alalunga*.

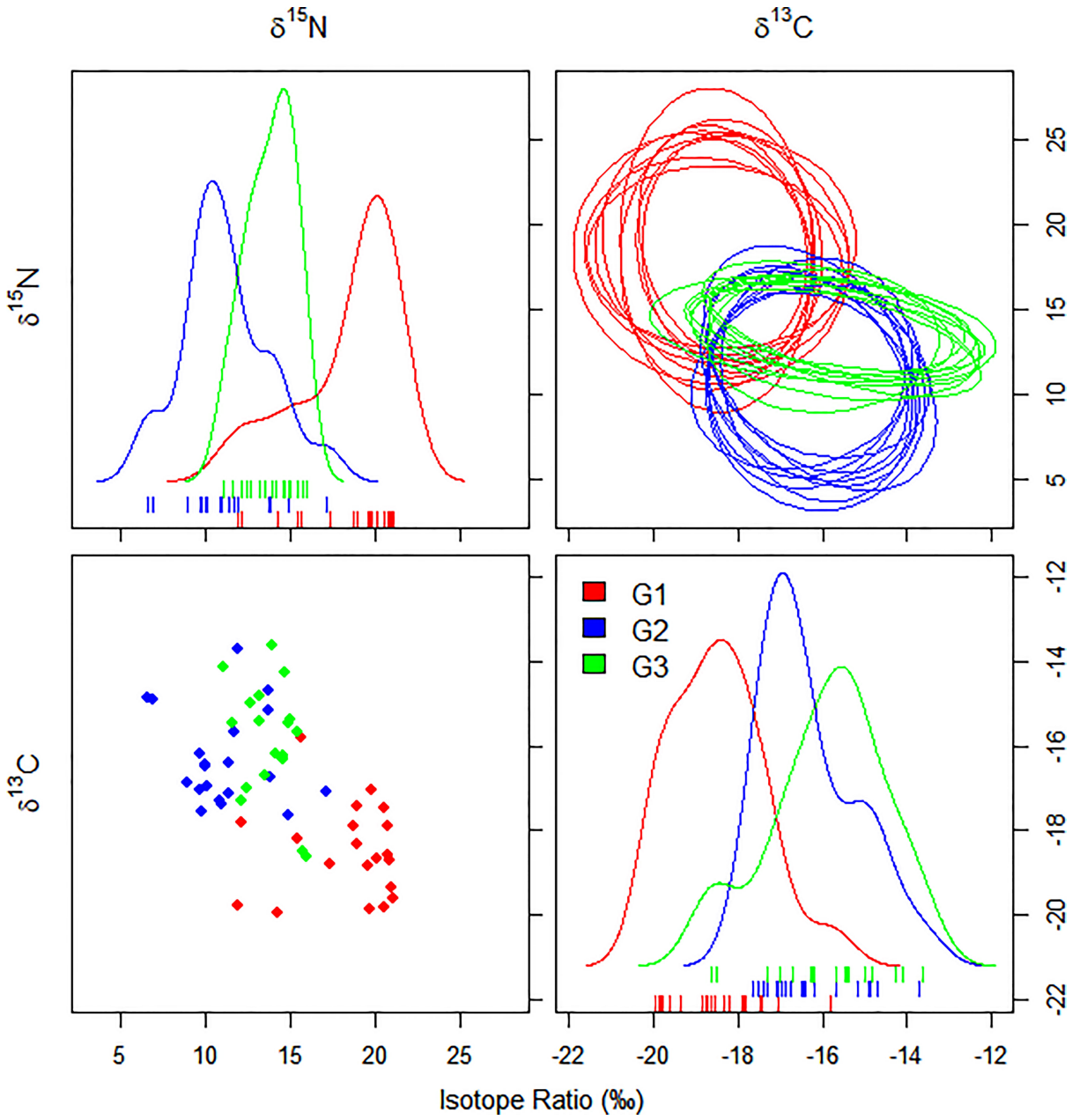


FIGURE 7
Ten random elliptical projections of trophic niche region (NR) for each tuna species and pair of isotopes (elliptical plots). One-dimensional density plots (lines) and two-dimensional scatterplots are also displayed. G1, big eye tuna, *Thunnus obesus*; G2, yellow fin tuna, *T. albacares*; G3, albacore tuna, *T. alalunga*.

on different prey, which can maximize the use of resources and reduce competition. Understanding the trophic interactions within and among fishery resources is useful in assessing the ecological role of the Solomon Islands and supporting the development of management policies based on an ecosystem approach. The combined use of multiple methods, such as gastric content analysis and stable isotope analysis, can also provide the basis for further analysis of food web dynamics to develop ecosystem models of energy flow. Finally, owing to the economic importance of these predators, further consideration of ontogeny patterns, isotopic information on food, and seasonal variation is required to better understand spatiotemporal changes in feeding habits and nutritional dynamics.

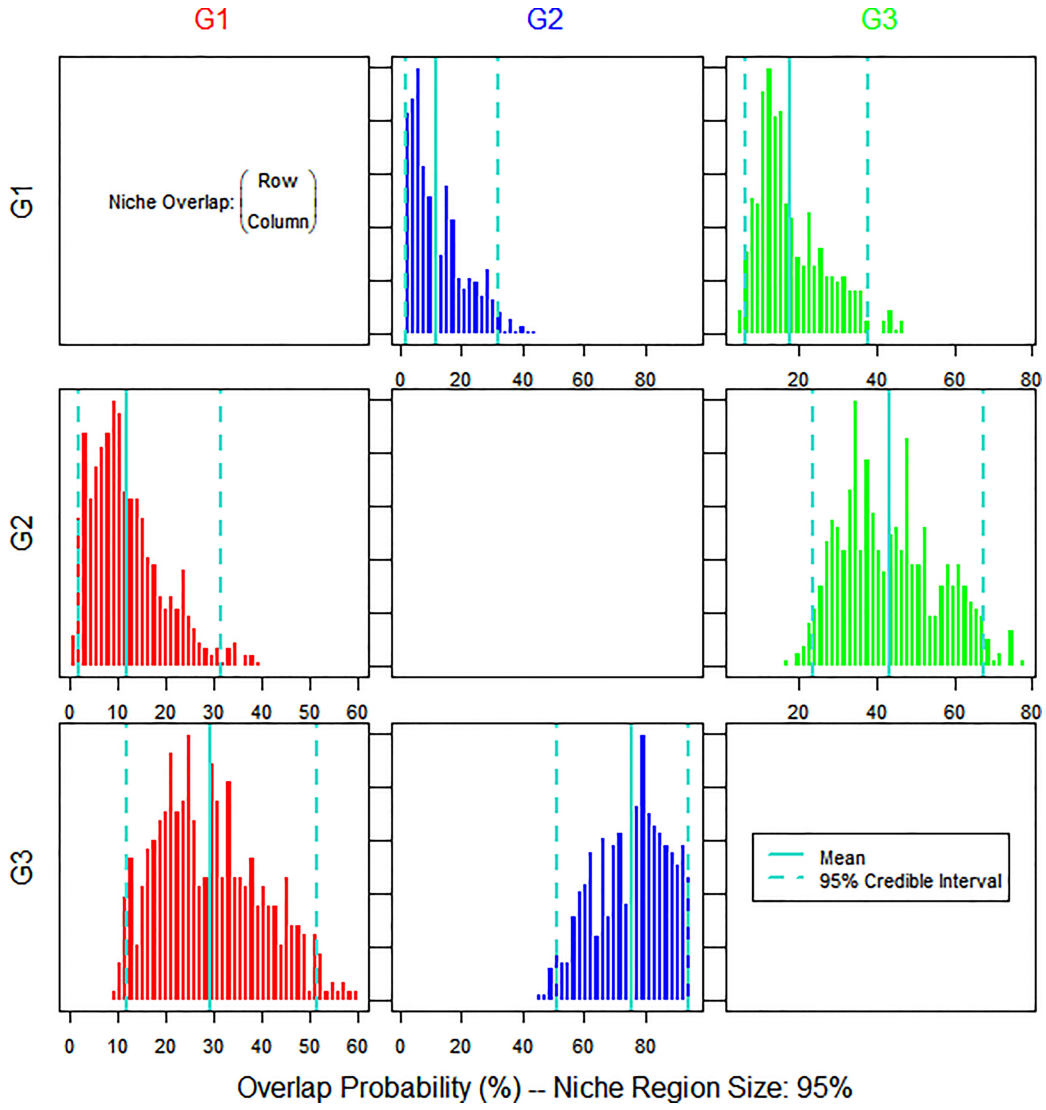


FIGURE 8
Bayesian plot of the posterior probability distribution of niche region metric (%) for the tuna species estimated using nicheROVER analysis. The posterior means and 95% credible intervals are displayed in turquoise. G1, big eye tuna, *Thunnus obesus*; G2, yellow fin tuna, *T. albacares*; G3, albacore tuna, *T. alalunga*.

## Data availability statement

The original contributions presented in the study are included in the article/**Supplementary Material**. Further inquiries can be directed to the corresponding author.

## Ethics statement

The animal study was reviewed and approved by the Zhejiang Marine Fisheries Research Institute.

## Author contributions

RRJ designed the paper and the experiment, and FY wrote the paper, these authors contributed equally to this work. RY adjusted and tested the equipment. MZL helped with the analysis and discussions. WBZ assisted with the experiment. AG coordinated the sampling. LWL offered technical support. FC contributed to the conception of the study. All authors contributed to the article and approved the submitted version.

## Funding

This study was supported by grants from the Chinese Ministry of Science and Technology through the National Key Research and Development Program of China (2019YFD0901405, 2020YFD0901205), Key Research and Development program of Zhejiang Province (2018C02026), and Routine monitoring project of Zhejiang distant-fishery resources.

## Acknowledgements

We thank Feng Cheng and the technical staff from the Zhejiang Marine Fisheries Research Institute for their assistance with sample collection and stomach content analyses.

## Conflict of interest

The authors declare that the research was conducted in the absence of any commercial or financial relationships that could be construed as a potential conflict of interest.

## Publisher's note



## Supplementary material

The Supplementary Material for this article can be found online at: https://www.frontiersin.org/articles/10.3389/fmars.2022.961990/full#supplementary-material

## References

Albuquerque, F. V., Navia, A. F., Vaske, T.Jr., Crespo, O., and Hazin, F. H. V. (2019). Trophic ecology of large pelagic fish in the saint Peter and saint Paul archipelago, Brazil. *Mar. Freshw. Res.* 70, 1402–1418. doi: 10.1071/MF18352

Allain, V., Fernandez, E., Hoyle, S. D., Caillot, S., Jurado-Molina, J., Andréfouët, S., et al. (2012). Interaction between coastal and oceanic ecosystems of the western and central pacific ocean through predator-prey relationship studies. *PLos One* 7, e36701. doi: 10.1371/journal.pone.0036701

Amundsen, P. A., Gabler, H. M., and Staldvik, F. J. (1996). A new approach to graphical analysis of feeding strategy from stomach contents data: modification of the Costello, (1990) method. *J. Fish Biol.* 48, 607–614. doi: 10.1111/j.1095-8649.1996.tb01455.x

Braga, R. R., Bornatowski, H., and Simões Vitule, J. R. (2012). Feeding ecology of fishes: an overview of worldwide publications. *Rev. Fish Biol. Fish.* 22, 915–929. doi: 10.1007/s11160-012-9273-7

Caut, Stéphane., Angulo, E., and Courchamp, F. (2009). Variation in discrimination factors (δ15N and δ13C):the effect of diet isotopic values and applications for diet reconstruction. *J. Appl. Ecol.* 46, 443–453. doi: 10.1111/j.1365-2664.2009.01620.x

Costa, A. F., Botta, S., Siciliano, S., and Giarrizzo, T. (2020). Resource partitioning among stranded aquatic mammals from Amazon and northeastern coast of Brazil revealed through carbon and nitrogen stable isotopes. *Sci. Rep.* 10, 12897. doi: 10.1038/s41598-020-69516-8

Costello, M. J. (1990). Predator feeding strategy and prey importance: A new graphical analysis. *J. Fish Biol.* 36, 261–263. doi: 10.1111/j.1095-8649.1990.tb05601.x

Crozier, W. W. (1985). Observations on the food and feeding of the angler-fish, lophim piscatorius l., in the northern Irish Sea. *J. Fish Biol.* 27, 655–665. doi: 10.1111/j.1095-8649.1985.tb03210.x

Davenport, S. R., and Bax, N. J. (2002). A trophic study of a marine ecosystem off southeastern Australia using stable isotopes of carbon and nitrogen. *Can. J. Fish. Aquat. Sci.* 59, 514–530. doi: 10.1139/f02-031

Denley, D., Metaxas, A., and Scheibling, R. (2020). Subregional variation in cover and diversity of hard coral (Scleractinia) in the Western province, Solomon islands following an unprecedented global bleaching event. *PLos One* 15, e0242153. doi: 10.1371/journal.pone.0242153

Feinsinger, P., Spears, E. E., and Poole, R. W. (1981). A simple measure of niche breadth. *Ecology.* 62, 27–32. doi: 10.2307/1936664

Figueiredo, M., Morato, T., Barreiros, J. P., Afonso, P., and Santos, R. S.. (2005). Feeding ecology of the white seabream, Diplodus sargus, and the ballan wrasse, labrus bergylta, in the Azores. *Fish Res.* 75, 107–119. doi: 10.1016/j.fishres.2005.04.013

Froese, R., and Pauly, D. (2022). *FishBase*. Available at: https://www.fishbase.se/search.php.

Gee, J. M. (1989). An ecological and economic review of meiofauna as food for fish. *Zool. J. Linn. Soc* 96, 243–261. doi: 10.1111/j.1096-3642.1989.tb01830.x

Hobson, K. A., Piatt, J. F., and Pitocchelli, J. (1994). Using stable isotopes to determine seabird trophic relationships. *J. Anim. Ecol.* 63, 786–798. doi: 10.2307/5256

Hyslop, E. J. (1980). Stomach contents analysis-a review of methods and their application. *J. Fish Biol.* 17, 411–429. doi: 10.1111/j.1095-8649.1980.tb02775.x

Jackson, A. L., Inger, R., Parnell, A. C., and Bearhop, S. (2011). Comparing isotopic niche widths among and within communities: SIBER- stable isotope Bayesian ellipses in r. *J. Anim. Ecol.* 80, 595–602. doi: 10.1111/j.1365-2656.2011.01806.x

Kent, E. C., and Volker, H. N. (2001). "FAO species identification guide for fishery purposes," in *The living marine resources of the Western central pacific*, vol. Volume 1-6. Food and Agriculture Organization of the United Nations.

King, J. E., and Ikehara, I. I. (1956). Comparative study of food of bigeye and yellowfin tuna in the central. *Fish. Bull.* 57, 61–85.

Koga, S. (1958). On the stomach contents of tuna in the west Indian ocean. *Bull. Faculty Fish* 6, 85–92.

Kong, Y. F., Wu, Zh.X., and Yan, Y. R. (2020). Trophic structure of pelagic fishery organism assemblage in the central and western south China Sea in spring revealed by carbon and nitrogen stable isotope analysis.Chin. *J. Appl. Ecol.* 31, 3559–3567. doi: 10.13287/j.1001-9332.202010.038

Krebs, C. J. (1999). *Ecological. methodology* (Menlo Park: Benjamin).

Layman, C. A., Arrington, A. A., Montaña, C. G., and Post, D. M. (2007). Can stable isotope ratios. Provide for community-wide measures of trophic structure? *Ecology* 88 (1), 42–48. doi: 10.1890/08-0167.1

Li, Y. K., Cheng, Z. A., Gong, Y., and Chen, X. J. (2021). A review on the methods used in trophic niche studies of marine animals and their applications. *J. Trop. Oceanogr.* 40, 143–156. doi: 10.11978/2020071

Li, B., Yang, X. F., Wang, J. X., Yi, M. R., He, X. B., Tao, J. Y., et al. (2019). Feeding ecology of bigeye tuna (Thunnus obesus) in the south of China Sea. *Oceaanologia Limnologia Sinica.* 50, 336–346. doi: 10.11693/hyhz20180900215

Li, Y., Zhang, Y., and Dai, X. (2016). Trophic interactions among pelagic sharks and Large predatory. teleosts in the northeast central pacific. *J. Exp. Mar. Biol. Ecol.* 483, 97–103. doi: 10.1016/j.jembe.2016.04.013

Lucena, F. M., Vaske, T., Ellis, J. R., and O'Brien, C. M. (2000). Seasonal variation in the diets of bluefish, pomatomus saltatrix (Pomatomidae) and striped weakfish, cynoscion guatucupa (Sciaenidae) in southern Brazil: Implications of food partitioning. *Environ. Biol. Fishes.* 57, 423–434. doi: 10.1023/A:1007604424423

Martins, K., Pelage, L., Justino, A. K. S., Frédou, F. L., Júnior, T. V., Loc'h, F. L., et al. (2021). Assessing trophic interactions between pelagic predatory fish by gut content and stable isotopes analysis around Fernando de noronha archipelago (Brazil), equatorial west Atlantic. *J. Fish Biol.* 99, 1576–1590. doi: 10.1111/jfb.14863

Ménard, F., Labrune, C., Shin, Y. J., Asine, A., and Bard, F. (2006). Opportunistic predation in tuna: a size-based approach. *Mar. Ecol. Prog. Ser.* 323, 223–231. doi: 10.3354/meps323223

Mendoza-Ávila, M., Zavala-Zambrano, G., Galván-Magaña, F., and Loor-Andrade, P. (2017). Feeding habits of wahoo (Acanthocybium solandri) in the eastern pacific ocean. *J. Mar. Biol. Ass. UK.* 97, 1505–1510. doi: 10.1017/S0025315416000850

Moteki, M., Arai, M., Tsuchiya, K., and Okamoto, H. (2001). Composition of piscine prey in the diet of large pelagic fish in the eastern tropical pacific ocean. *Fisheries. Sci.* 67, 1063–1074. doi: 10.1046/j.1444-2906.2001.00362.x

Perrin, W. F., Warner, R. R., Fiscus, C. H., and Holts, D. B. (1973). Stomach contents of porpoise, stenella spp., and yellowfin tuna, thunnus albacares, in mixed-species aggregations. *Fishery Bull.* 71, 1077–1092.

Peterson, B. J., and Fry, B. (1987). Stable isotopes in ecosystem studies. *Annu. Rev. Ecol. Syst.* 18, 293–320. doi: 10.1146/annurev.es.18.110187.001453

Pinkas, L. (1971). Food habits of albacore, bluefin tuna, and bonito in California waters. *Fish. Bull.* 152, 1–105.

R Core Team. (2021). *R: A language and environment for statistical computing*. Vienna, Austria: R Foundation for Statistical Computing. Available at: https://www.R-project.org/.

Saito, S. (1973). "Studies on fishing of albacore, thunnus alalunga(Bon-naterre) by experimental deep sea tuna long – line," in *Memoirs of the Faculty of Fisheries*. (Hokkaido University). 21, 107–184. Available at: http://eprints.lib.hokudai.ac.jp/dspace/bitstream/2115/21856/1/2.

Shi, X. F., Wang, X., Wang, Y. X., Shi, J. G., and Zhang, J. (2022). Feeding biology of yellowfin tuna(Thunnus albacares) in tropical central and western pacific ocean. *S. China Fish. Sci.* 18, 43–51. doi: 10.12131/20210140

Song, L. M., Chen, X. J., and Xu, L. X. (2004). Preliminary analysis of biological characteristics of yellowfin tuna thunnus albacares in the tuna longline fishing ground of the central Atlantic ocean. *Oceanologia Limnologica Sinica.* 35, 538–542. doi: 10.3321/j.issn:0029-814X.2004.06.009

Song, Y. H., Xue, Y., Xu, B. D., Zhang, C., and Ren, Y. P. (2020). Composition of food and niche overlap of three sciaenidae species in haizhou bay. *J. Fish. China.* 44, 2017–2027.

Swanson, H. K., Lysy, M., Power, M., Stasko, , , A. D., Johnson, J. D., Reist, J. D., et al. (2015). A new probabilistic method for quantifying n-dimensional ecological niches and niche overlap. *Ecology.* 96, 318–324. doi: 10.1890/14-0235.1

Tao, Y. J., Mo, M., and He, (2017). Feeding habits and ontogenetic diet shifts of yellowfin tuna (Thunnus albacores) in the south China Sea. *Process Fishery Sci.* 38, 1–10.

Tripp-Valdez, A., Galván-Magaña, F., and Ortega-García, S. (2015). Food sources of common dolphinfish (Coryphaena hippurus) based on stomach content and stable isotopes analyses. *J. Mar. Biol. Assoc. United Kingdom.* 95, 579–591. doi: 10.1017/S0025315414001842

Valerie, A., Emilie, F., Simon, D. H., Sylvain, C., Jurado-Molina, J., Andréfouët, S., et al. (2012). Interaction between coastal and oceanic ecosystems of the Western and central pacific ocean through predator-prey relationship studies. *PLos One* 7 (5), e36701. doi: 10.1371/journal.pone.0036701

Wang, J., Jiang, R. J., Hu, C. L., Li, Z., Xiao, Y., Xu, Y. J., et al. (2021). Feeding ecology of engraulis japonicus based on stomach contents and stable isotope. *Ying Yong Sheng Tai Xue Bao.* 32, 2035–2044. doi: 10.13287/j.1001-9332.202106.029

Wang, X. F., Xu, L. X., Zhou, Ch., Zhu, G. P., and Tang, H. (2013). The relationship between fishing success and feeding status in skipjack tuna katsuwonus pelamis in tuna purse seine. *J. Dalian Ocean Univ.* 28, 622–626. doi: 10.3969/j.issn.2095-1388.2013.06.020

Weng, J., Lee, M., Liu, K., Hsu, M. S., Hung, M. K., Wu, L. J., et al. (2015). Feeding ecology of juvenile yellowfin tuna from waters southwest of Taiwan inferred from stomach contents and stable isotope analysis. *Mar. Coast. Fish.* 7, 537–548. doi: 10.1080/19425120.2015.1094157

White, A. T., Aliño, P. M., Cros, A., Fatan, N. A., Green, A. L., Teoh, S. J., et al. (2014). Marine protected areas in the coral triangle: progress, issues, and options. *Coast. Management.* 42, 87–106. doi: 10.1080/08920753.2014.878177

Willson, J. D., Winne, C. T., Pilgrim, M. A., Romanek, C. S., and Gibbons, J. W. (2010). Seasonal variation in terrestrial resource subsidies influences trophic niche width and overlap in two aquatic snake species: a stable isotope approach. *Oikos.* 119, 1161–1171. doi: 10.1111/j.1600-0706.2009.17939.x

Xu, L. X., Zhu, G. P., and Song, L. M. (2008). Feeding behavior of thunnus obesus in the west-central Indian ocean. *J. Fish. China.* 03, 387–394. doi: 10.3321/j.issn:1000-0615.2008.03.009

Yan, Y. R., Zhang, W. K., Lu, H. S., Wang, X. F., and Lai, J. Y. (2012). Using stable isotopes to analyze feeding habits and trophic position of hairtail (Trichiurus lepturus) from the beibu gulf, south China sea. *Oceaanologia Limnologia Sinica.* 43, 192–200. doi: 10.11693/hyhz201201031031

Young, J. W., Lansdell, M. J., Campbell, R. A., Cooper, S. O., Francis Juanes Guest, M. A., et al. (2010). Feeding ecology and niche segregation in oceanic top predators off eastern Australia. *Mar. Biol.* 157, 2347–2368. doi: 10.1007/s00227-010-1500-y

Zhang, X. J., Cheng, J. H., Shen, W., and Liu, Z. L. (2010). Feeding ecology of lophius litulon in the south of yellow Sea. *Acta Ecol. Sin.* 30, 3117–3125. doi: 10.1016/S1872-5813(11)60001-7

Zhu, W. J., Xu, L. X., Jiang, J. J., and Chen, J. T. (2015). Fishery biology of albacore thunnus alalunga in the north pacific ocean. *J. Dalian Ocean Univ.* 30, 546–552. doi: 10.16535/j.cnki.dlhyxb.2015.05.018

Zhu, G. P., Xu, L. X., Zhou, Y. Q., and Song, L. M. (2008a). Feeding habits and its seasonal variations of thunnus albacares in the west-central Indian ocean. *J. Fish. China.* 32, 725–732. doi: 10.3724/SP.J.00001

Zhu, G. P., Zhou, Y. Q., and Xu, L. X. (2008b). Long-term changes in the mean trophic level of tuna fishery in the Indian ocean. *J. Dalian Ocean Univ.* 23, 484–488. doi: 10.3969/j.issn.1000-9957.2008.06.015

Zhu, G. P., Zhou, Y. Q., Xu, L. X., and Jiang, W. X. (2007). Feeding ecology of thunnus obesus in the western aylantic ocean. *J. Fish. China.* 31, 23–30. doi: 10.3321/j.issn:1000-0615.2007.01.004

frontiers | Frontiers in Marine Science

TYPE Original Research
PUBLISHED 15 August 2022
DOI 10.3389/fmars.2022.961591



OPEN ACCESS

EDITED BY
Jun Xu,
Institute of Hydrobiology, Chinese Academy of Sciences (CAS), China

REVIEWED BY
Kaizhi Li,
South China Sea Institute of Oceanology, Chinese Academy of Sciences, China
Wuchang Zhang,
Institute of Oceanology, Chinese Academy of Sciences (CAS), China

*CORRESPONDENCE
Quan-Zhen Chen
chenquanzhen@sio.org.cn

SPECIALTY SECTION
This article was submitted to Marine Ecosystem Ecology, a section of the journal Frontiers in Marine Science

RECEIVED 04 June 2022
ACCEPTED 28 June 2022
PUBLISHED 15 August 2022

CITATION
Du P, Ye W-J, Deng B-P, Mao M, Zhu Y-L, Cheng F-P, Jiang Z-B, Shou L and Chen Q-Z (2022) Long-term changes in zooplankton in the Changjiang estuary from the 1960s to 2020. *Front. Mar. Sci.* 9:961591. doi: 10.3389/fmars.2022.961591



# Long-term changes in zooplankton in the Changjiang estuary from the 1960s to 2020

Ping Du[1,2,3,4], Wen-Jian Ye[3], Bang-Ping Deng[2], Ming Mao[1], Yuan-Li Zhu[1,4], Fang-Ping Cheng[1,4], Zhi-Bing Jiang[1,3,4], Lu Shou[1,4] and Quan-Zhen Chen[1,3]*

[1]Key Laboratory of Marine Ecosystem Dynamics & Second Institute of Oceanography, Ministry of Natural Resources (MNR), Hangzhou, China, [2]Key Laboratory of Marine Ecological Monitoring and Restoration Technology, Ministry of Natural Resources (MNR), East China Sea Environmental Monitoring Center, State Oceanic Administration, Shanghai, China, [3]Marine Space Resources Management Technology Key Laboratory, Ministry of Natural Resources (MNR), Marine Academy of Zhejiang Province, Hangzhou, China, [4]Observation and Research Station of Yangtze River Delta Marine Ecosystems, Ministry of Natural Resources (MNR), Zhoushan, China

The Changjiang estuary (CJE) is a large estuary that is affected by multiple anthropogenic stressors and climate change. The long-term trend of zooplankton in the CJE is an important indicator of the ecological response to stressors. We applied the Mann–Kendall trend analysis and Pettitt test to detect the trend and breakpoints of the biomass of the large mesozooplankton (LMZ; 505–20 000 μm) in four seasons, abundance of main LMZ taxa in summer from the 1960s to 2020, and abundance of dominant species in summer from 2000 to 2020 in the CJE. Results showed that LMZ biomass increased significantly during spring and summer, and the breakpoints both occurred in the 1980s. After the breakpoint, the mean biomass increased from 142.88 to 429.42 mg/m$^3$ in spring and from 296.28 to 723.92 mg/m$^3$ in summer. After 2000, the abundance of Copepoda in summer increased by more than 10 times compared to the 1960s. Under the conditions of warming and increased dinoflagellate abundance in the CJE, the abundance of the warm-water and omnivorous small calanoid copepod *Paracalanus aculeatus* increased significantly. Meanwhile, the significant decrease in the abundance of the temperate brackish species *Labidocera euchaeta* was probably mainly related to warming. The rapid changes in LMZ biomass during the late 1980s and mid-1990s is probably the result of a combination of enhanced bottom–up support, reduced top–down pressure, and promotion of temperature. This study provides scientific evidence and insights into the adaptive management of the Changjiang Basin.

KEYWORDS

**zooplankton, multidecadal trend, anthropogenic stressors, global warming, Changjiang estuary**

## Introduction

Estuaries are located at the transition zone between a river and shelf, which are characterized by strong coastal nonlinear physical processes (current, wind, and tide), and receive terrestrial materials from mega-river systems, including abundant dissolved or particulate organic and inorganic matter (Ge et al., 2020a). Additionally, estuaries are affected by climate change (Giosan et al., 2014). Anthropogenic activities in river basins, especially agricultural and industrial drainage and damming, have resulted in reduced sediment and increased nutrient transport into estuaries in recent decades, such as in the Mississippi, Indus, Nile, and Changjiang estuaries (Giosan et al., 2014; Chen et al., 2021). Nitrogen (N), phosphorus (P), and silicon (Si) are the three major nutrients. Among these, N and P concentrations have increased in river systems and associated estuaries, mainly because of fertilization. The Si concentration remained relatively stable, but exceptions have been observed following hydrological perturbations in upper river catchments, such as damming and water diversion for irrigation (Ge et al., 2020a). Increasing nutrient inputs, changing relative nutrient ratios, decreasing sediment loads, and global warming affect the biogeochemical dynamics of estuarine ecosystems. Phytoplankton abundance increases, harmful algal blooms, and seasonal hypoxia have been detected in regions with large riverine inputs in summer when vertical stratification is the strongest over a year, for example, the northern Gulf of Mexico, Chesapeake Bay, Baltic Sea, and East China Sea (ECS; Zhang et al., 2021). The responses of zooplankton are inconsistent across estuaries and may be determined by different trophic interactions in the food web. For example, the abundance of the ctenophore *Mnemiopsis leidyi* increased and that of the copepod *Acartia tonsa* decreased in the Chesapeake Bay (Kimmel et al., 2012; Stone et al., 2018), and the zooplankton standing crop reduced in the Nile delta (Chen et al., 2021), while the abundance ratio of copepods to cladocerans changed in the San Francisco estuary (Lehman et al., 2010).

The Changjiang (Yangtze) River is one of the largest rivers in the world, delivering approximately $9.28 \times 10^{11}$ $m^3$/yr of freshwater and $3.51 \times 10^8$ tons/yr of sediments into the estuary (multi-year mean between 1951 and 2020 at the Datong hydrological gauging station) (CWRCMWR, 1951–2020). As the longest river in China, over 30% of its population lives within the Changjiang drainage basin (Zhang et al., 2021). Since the 1960s, population growth and economic development in the basin have resulted in a rapid increase in nutrient fluxes into the Changjiang estuary (CJE), particularly dissolved inorganic N (Chai et al., 2006; Wang et al., 2018). In addition, over the past 60 years, more than 50,000 dams have been built in drainage basins; the sediment load of the Changjiang River has decreased significantly in recent decades, particularly after the construction of the world's largest dam, the Three Gorges Dam (TGD) in 2003 (Zhao et al., 2021). The ECS, where the CJE is located, is one of the most rapidly warming large marine ecosystems (Belkin, 2009). Similar to other typical estuaries that are severely impacted by anthropogenic activities and warming, the CJE and its adjacent waters have been suffering from serious eutrophication, nutrient ratio shifts, phytoplankton and harmful algal blooms, seasonal hypoxia (Li et al., 2018; Li et al., 2019), and deterioration of fishery resources and jellyfish blooms exacerbated by overfishing (Xian et al., 2005).

Mesozooplankton play an important role in linking primary production to fish production and are excellent sentinels for the response of oceanic biota to climate change (Dam, 2013; Rice et al., 2015; Steinberg and Landry, 2017). Warm-water species generally refer to marine organisms whose growth and reproductive temperature range is higher than 20°C, and whose monthly average water temperature in their natural distribution area is higher than 15°C, and includes subtropical and tropical species. Temperate species generally refer to marine species with a wide range of suitable temperatures for growth and reproduction (4–20°C) and a wide range of monthly average water temperatures (0–25 °C) in their natural distribution areas, and includes cold-temperate species and warm-temperate species. Several previous studies comparing historical data from the 1960s, 1980s, and early 2000s in the CJE indicated that under the impact of warming, the abundance of warm-temperate species [*Euphausia pacifica* (Euphausiacea), *Euchaeta plana* (Copepoda)] decreased, whereas that of warm-water species [*Pseudeuphausia sinica* (Euphausiacea), *Lucifer intermedius* (Decapoda), and *Lucifer hanseni* (Decapoda), *Euchaeta concinna* (Copepoda), *Temora turbinata* (Copepoda)] increased (Ma et al., 2009; Zhang et al., 2010; Gao and Xu, 2011; Xu et al., 2013; Xu and Zhang, 2014). In addition, based on data in the CJE from 1996 to 2005, Li et al. (2010) revealed that the dominance of copepods decreased, while that of medusae increased. However, overall changes in the zooplankton community (including community biomass, main taxa, and dominant species) have not been reported in the CJE, especially when combined with data from the last two decades. We speculated that zooplankton biomass may increase under the background of warming, food increase, and overfishing; meanwhile, the abundance of warm-water and hypoxic-tolerant species may increase under warming and hypoxic stress.

Based on the above hypothesis and available data, we examined (1) the trend of zooplankton biomass in the four seasons from the 1960s to 2020, (2) the trend of abundance of zooplankton taxa in summer from the 1960s to 2020, and (3) the trend of abundance of dominant species of zooplankton in summer from 2000 to 2020. These results will provide an understanding of the response of mesozooplankton communities to the combined impacts of global

warming and human perturbations in a large subtropical estuary and identify the factors that influence the changes in zooplankton characteristics.

# Materials and methods

## Study area

The CJE and inner shelf of the ECS are typical estuarine-shelf coastal zones with complicated hydrological systems, which are mainly affected by Changjiang Diluted Water (CDW), coastal currents, and the Taiwan Warm Current. CDW brings a large input of freshwater and sediment from the upstream. The mixing of freshwater with oceanic water forms a low-salinity plume. This plume changes seasonally in terms of its spreading areas and pathways, flowing either into the shelf of ECS during summer or farther away along the ECS coast during winter. A large quantity of suspended sediments from the river experience the dynamics of local vertical resuspension and settle in the estuary to form a sediment front (SF), which is jointly determined by the low-salinity plume and tidal mixing (Ge et al., 2020b; Li et al., 2021). A sediment plume usually co-occurs with a dissolved nutrient plume and a low-salinity plume. Sediment and dissolved nutrient fronts are located near the river mouth, whereas the low-salinity front (LSF) extends offshore over the shelf (Li et al., 2021; Figure 1A).

Estuarine fronts are important mesoscale physical processes that shape spatial patterns of different water masses. The water masses on either side of the front are characterized by different water properties, generating different spatial patterns of primary productivity and habitats for plankton assemblages. In the CJE and its adjacent waters, the shoreward water mass of the SF was characterized by the highest nutrients and total suspended matter (TSM). Consequently, the extensive light limitation led to the lowest chlorophyll-*a* (Chl-*a*). The water mass between the SF and LSF displayed the highest Chl-*a*, which benefited from the increased light availability and higher nutrients contributed by the plume and coastal upwelling. The shelf water mass beyond the LSF showed the lowest TSM and nutrients, and hence, the distinct reduction in nutrient supply resulted in relatively low Chl-*a* (Li et al., 2021).

Zooplankton near the CJE are usually divided into three or four groups, depending on the preference of species for water temperature and salinity. Freshwater species (e.g., *Sinocalanus sinensis*) can only be found inside the river mouth and are usually scarce. Estuarine species (e.g., *Pseudodiaptomus* sp. and *Tortanus* sp.) live near the river mouth, where salinity varies from 6 to 20. Oceanic species from the Yellow and East China Seas (e.g., *Calanus sinicus*, *Euchaeta* spp., *Paracalanus* spp., and *Sagitta enflata*) usually appear offshore. Shelf species (*Acartia pacifica*, *Centropages dorsispinatus*, *Labidocera euchaeta*, *Sagitta nagae*, and *Diphyes chamissonis*) live between estuarine and oceanic species, and those from neritic areas of both the Yellow and East China Seas can be observed in this area (Gao and Zhang, 1992).

On the other hand, the Changjiang River is affected by the East Asian monsoon, which results in higher rainfall in summer and lower rainfall in winter. The maximum runoff occurs from May to October, contributing 71.8% of the annual flow recorded at the Datong station, the last station before the river enters the coast, approximately 600 km upstream of the river mouth. The operation mode of the TGD changed the seasonal discharge at the river mouth, and reduced peak flooding in the summer, while increased the flow in winter.

## Description of datasets

A survey of the zooplankton community in the CJE began in 1959, during the China National Oceanic Census. Since then, surveys, including on zooplankton, have been conducted every decade, except in the 1990s. In addition, zooplankton monitoring observations in the summer have been conducted almost every year since 2000. All zooplankton samples were collected using a plankton net with a mesh size of 505 μm (diameter: 50 cm and length: 145 cm when the water depth was < 30 m; diameter: 80 cm and length: 280 cm when the water depth was > 30 m). Therefore, in this study, we analyzed the long-term changes of the designated "large mesozooplankton" which range in size from 505 to 20,000 μm (generally, mesozooplankton are zooplankton ranging in size from 200 to 20,000 μm).

Zooplankton data were derived from the literatures covering a similar region and our studies (Figure 1B). Historical data included zooplankton biomass from 1959 to 2017 in spring and winter, 1959 to 2020 in summer, and 1959 to 2010 in autumn. Historical data also included the abundance of zooplankton taxa in summer from 1961 to 2020, and the abundance of dominant species in summer from 2000 to 2020, although there were several missing values (Table 1). Eleven zooplankton taxa were collected; unfortunately, with many missing values. Data on Copepoda and Euphausiacea covered the 1960s, 1980s, 2000s, and the 2010s. Data on Mysidacea, Amphipoda, and Decapoda covered the 1960s, 2000s, and 2010s. Data on Chaetognatha, Tunicata, Diplostraca, Medusa (including Hydrozoa and Ctenophora), Polychaeta, and planktonic larvae only covered the 2000s and the 2010s. Zooplankton data representing spring, summer, autumn, and winter were collected in May, August, November, and January, respectively.

Zooplankton samples were collected using plankton nets *via* vertical tows from 2 m above the bottom to the surface. The collected samples were stored in 5% formalin in 1-L plastic bottles. The volume of the filtered water was measured using a digital flow meter. In the laboratory, mesozooplankton samples were filtered through a silk sieve with a mesh size of 160 μm and then weighed with a 0.1-mg electronic balance after

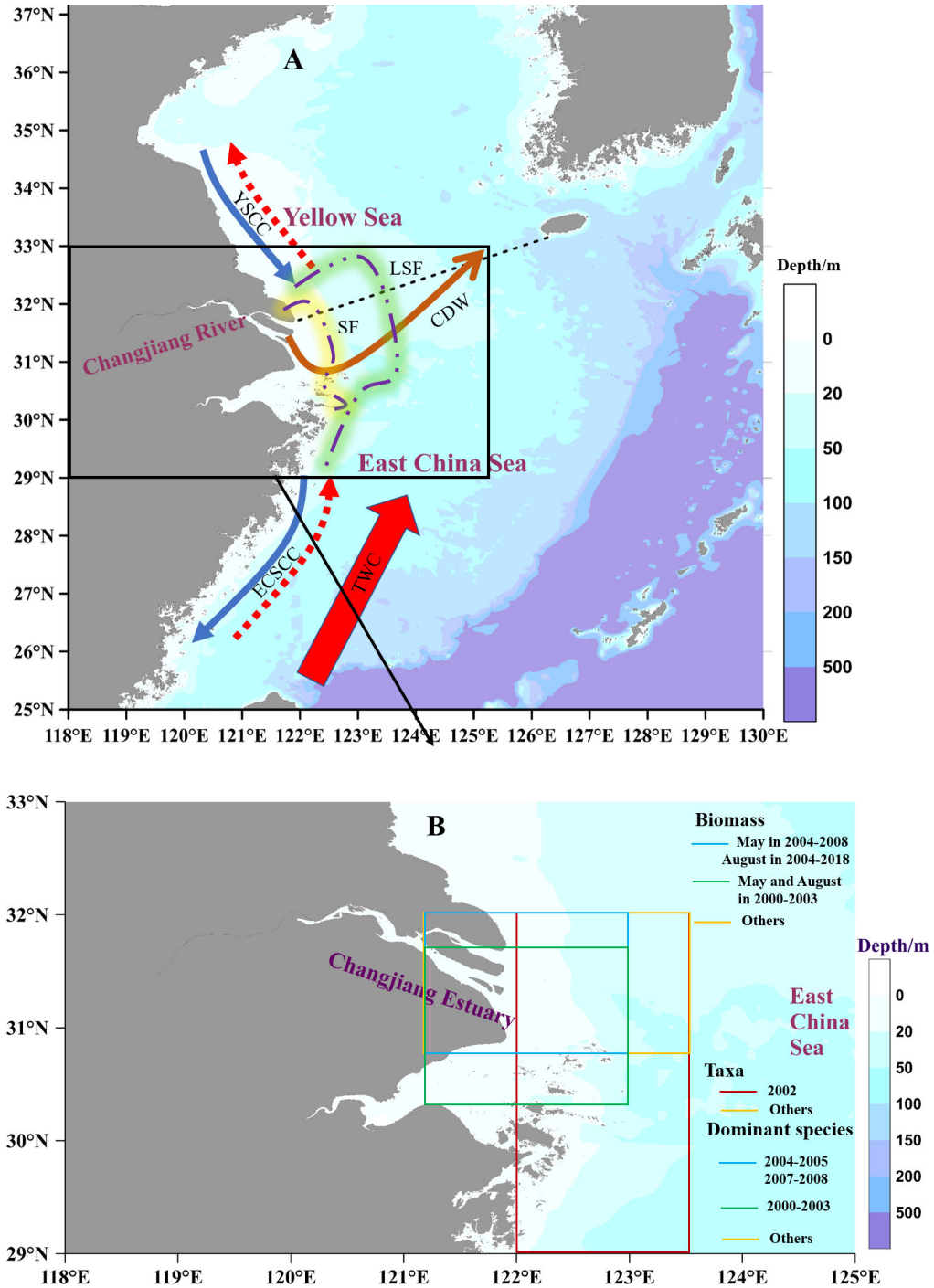


FIGURE 1
Hydrological system around the Changjiang estuary **(A)** and sampling areas of historical zooplankton data in Table 1 **(B)**. CDW: Changjiang Diluted Water; YSCC: Yellow Sea Coastal Currents, ECSCC: East China Sea Coastal Currents, blue solid and red dotted arrows indicate the different seasonal flow directions of Coastal Currents; TWC: Taiwan Warm Current; SF: Sediment Front; LSF: Low-Salinity Front.

picking out sundries. Taxonomic identification and enumeration were performed using a stereoscope and microscope. Zooplankton biomass was determined as the ratio of the zooplankton wet weight to the filtered water volume, and abundance was determined as the ratio of the number of individuals to the filtered water volume. Dominant species were defined as those with a dominance index ($Y$) greater than 0.02. $Y = (n_i/N) \times f_i$ , where $n_i$ represents the

TABLE 1 List of historical data on zooplankton in the Changjiang estuary and source.

| Biomass | | | | | | | | | | Taxa | | Dominant species | |
|---|---|---|---|---|---|---|---|---|---|---|---|---|---|
| Annual mean | | Winter | | Spring | | Summer | | Autumn | | Summer | | Summer | |
| Years | Source | Years | Source | Years | Source | Years | Source | Years | Source | Years | Source | Years | Source |
| 1959 | Luo and Shen, 1994 | 1959-1960 | Luo and Shen, 1994 | 1959-1961 | Xian and Luo, 2015 | 1959-1961 | Luo and Shen, 1994 | 1959-1961 | Xian and Luo, 2015 | 1961 | Chen et al., 1985 | 2000-2003 | Xu et al., 2005 |
| 1960 | | 1983 | Zhu, 1988 | 1972-1973 | | 1973 | | 1972-1973 | | 1984 | EBMA, 1991 | 2004-2005 | Xu et al., 2009 |
| 1961 | | 1986 | Luo and Shen, 1994 | 1983 | | 1982 | Zhu, 1988 | 1982 | | 2002 | Gu and Xu, 2008; Cai et al., 2008; Chen et al., 2008; Hu et al, 2008; Zhou and Xu, 2009; Chen and Xu, 2009 | 2006 | This study |
| 1973 | | 2007 | This study | 1986 | | 1985 | Luo and Shen, 1994 | 1985 | | 2006 | This study | 2007-2008 | Liu et al., 2013 |
| 1982/1983 | Zhu, 1988 | 2017 | | 1999 | | 2000-2003 | Xu and Shen, 2005 | 1998 | | 2017-2018 | | 2010 | Wang et al., 2016 |
| 1985/1986 | Luo and Shen, 1994 | | | 2000-2003 | Xu and Shen, 2005 | 2004-2018 | Yang et al., 2020 | 2000 | | 2020 | | 2017-2018 | This study |
| 2006/2007 | This study | | | 2004, 2006 | Zhang et al., 2008 | 2020 | This study | 2002 | | | | 2020 | |
| | | | | 2007-2008 | Liu et al., 2013 | | | 2007 | This study | | | | |
| | | | | 2011 | Wang et al., 2016 | | | 2010 | Wang et al., 2016 | | | | |
| | | | | 2017 | This study | | | | | | | | |

abundance of the species $i$, $N$ is the total abundance of the community, and $f_i$ is the appearance frequency at all of the stations (Dufrene and Legendre, 1997).

The seasonal mean sea surface temperature (SST) from 1982 to 2020 was derived from level-4 daily products from multiple sensors including Advanced Very High Resolution Radiometers (AVHRRs), the series of Along Track Scanning Radiometers (ATSRs), and the Sea and Land Surface Temperature Radiometer (SLSTR) (2.1 version with 0.05° × 0.05° resolution; https://cds.climate.copernicus.eu/cdsapp#!/dataset/satellite-sea-surface-temperature?tab=form).

## Statistical analyses

Trend analyses of annual zooplankton biomass in four seasons and abundance of taxa and dominant species in summer were performed using the nonparametric Mann–Kendall test (M–K test), which is widely used to detect monotonic increasing or decreasing trends of time series. Test S was exported to indicate a monotonic trend when the number of years n ≤ 10, whereas Test Z was exported to indicate a monotonic trend when n > 10. Sen's nonparametric method was used to estimate the true slope of the existing trend (Salmi et al., 2002). Differences were considered statistically significant at $p<$ 0.05. The Pettitt test was employed to determine whether at least one "breakdown-type" discontinuity existed in the time series. The time series were treated as nonstationary when the Pettitt test detected a change point in Pettitt test at $p<$ 0.05. The nonstationary time series was further divided into subsets using the change points as breakpoints, and the nonparametric Kruskal–Wallis test (K–W test) was performed to confirm a shift in the mean value. K–W tests were also used to detect the differences in abundance of zooplankton taxa among decades. Spearman nonparametric tests were used to analyze the correlation between zooplankton biomass and SST. The M–K test, Sen's slope estimation, and Pettitt test were executed in R using "zyp" and "trend" packages (R Development Core Team,

2014) (http://cran.r-project.org). The K–W test and Spearman test were calculated in SPSS 20.0.

# Results

## Trends of zooplankton biomass in four seasons

The annual mean zooplankton biomass for the years 1959, 1960, 1961, 1973, 1982/1983, 1985/1986, and 2006/2007 showed a gradual upward trend, from 109.59 mg/m$^3$ around 1960 to 150.25 mg/m$^3$ in the early 1970s and from 183.90 mg/m$^3$ in the mid-1980s to 298.04 mg/m$^3$ in the mid-2000s (Figure 2A; Table 2).

Long-term data on zooplankton biomass for the four seasons showed significant increasing trends during spring and summer at rates of 15.55 and 23.32 mg/m$^3$/yr, respectively, according to Sen's slope of the time series ($p_{spring}$< 0.05; $p_{summer}$< 0.01). The biomass in spring increased from 117 mg/m$^3$ around 1960 to 168 mg/m$^3$ from the early 1970s to early 1980s, and from 278 mg/m$^3$ in the late 1980s to 443 mg/m$^3$ from the end of 1990s to the present. The biomass in summer increased from 183 mg/m$^3$ around 1960 to 324 mg/m$^3$ from the early 1970s to early 1980s, and from 439 mg/m$^3$ in the late 1980s to 724 mg/m$^3$ from the end of 1990s to the present. The Pettitt test revealed 1983 and

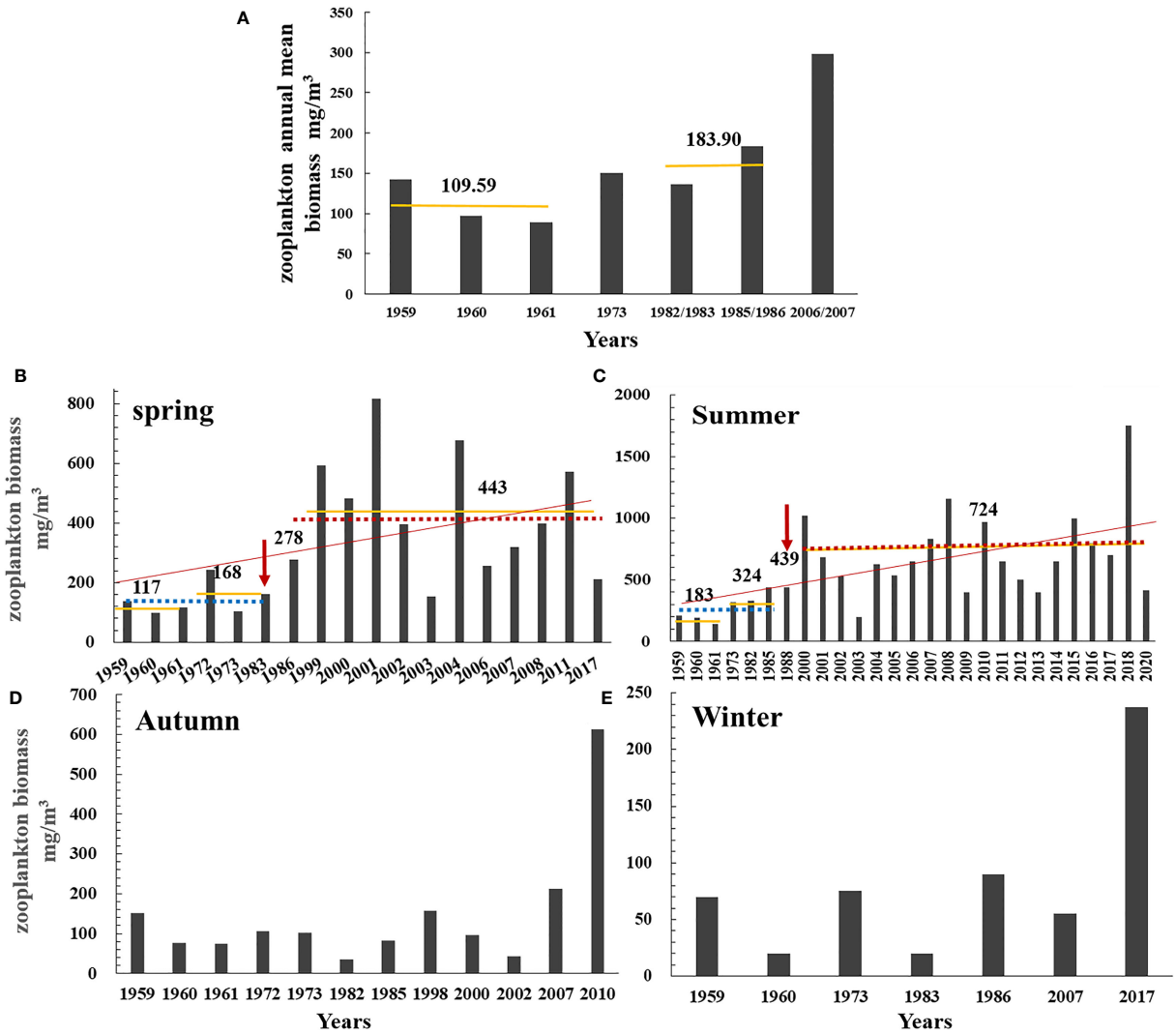


FIGURE 2
The annual mean biomass of zooplankton from 1959 to 2007 **(A)** and zooplankton biomass in spring from 1959 to 2017 **(B)**, in summer from 1959 to 2020 **(C)**, in autumn from 1959 to 2010 **(D)**, and in winter from 1959 to 2017 **(E)** in the Changjiang estuary. Red line: trend line. Yellow line and the value above it: the mean biomass over a period. Red arrow: change point (breakpoint). Blue dotted line: mean biomass before breakpoint; red dotted line: mean biomass after breakpoint.

TABLE 2 Trend and change point test of zooplankton and SST in the Changjiang estuary.

| | | Trend test | | | Change point test | | |
|---|---|---|---|---|---|---|---|
| | | n | Test S/ Test Z | Q | Change year | Mean before the change year | Mean after the change year |
| Zooplankton biomass /mg/m$^3$ | Annual mean | 7 | 11 | 23.49 | — | — | — |
| | Spring | 18 | **2.20*** | 15.55 | 1983 | **142.88±53.69** | **429.42±202.29** |
| | Summer | 27 | **3.13**** | 23.32 | 1988 | **296.28±117.64** | **723.92±341.25** |
| | Autumn | 12 | 0.89 | 6.56 | — | — | — |
| | Winter | 7 | 8 | 8.80 | — | — | — |
| Abundance of taxa in summer /ind/m$^3$ | Copepoda | 6 | **15**** | 71.81 | 1984 | 46.55±19.03 | 493.12±156.03 |
| | Euphausiacea | 7 | **17*** | 2.40 | 1984 | 1.45±0.78 | 14.50±9.38 |
| Abundance of dominant species in summer /ind/m$^3$ | *Acartia pacifica* | 13 | 1.77+ | 13.69 | 2006 | **63.10±77.33** | **177.82±84.08** |
| | *Centropages dorsispinatus* | 13 | -0.18 | -1.22 | — | — | — |
| | *Calanus sinicus* | 13 | 0.61 | 2.09 | — | — | — |
| | *Labidocera euchaeta* | 13 | **-2.99**** | -5.65 | 2005 | **59.72±29.15** | **9.25±10.53** |
| | *Paracalanus aculeatus* | 13 | **2.45*** | 6.06 | 2008 | **9.10±14.27** | **75.07±48.00** |
| | *Euchaeta* spp. | 13 | -0.06 | 0.00 | — | — | — |
| SST /°C | Spring | 39 | **4.26***** | 0.05 | 1996 | **12.90±0.52** | **14.21±0.69** |
| | Summer | 39 | **2.27*** | 0.02 | 1993 | **24.89±0.41** | **25.50±0.47** |
| | Autumn | 39 | **3.58***** | 0.02 | 1995 | **21.92±0.32** | **22.50±0.31** |
| | Winter | 39 | 1.02 | 0.01 | — | — | — |

n is the number of years used for tests. Test S and Test Z were exported to indicate a monotonic trend when n ≤10 and n >10, respectively. Test S/Z>0: monotonic increasing trend; Test S/Z<0: monotonic decreasing trend. Bold values mean the monotonic trends or the differences before and after the breakpoint are significant. ***: p< 0.001, **: p< 0.01 and *: p< 0.05. —: the change year and the values before and after the breakpoint were not shown when the monotonic trends are not significant. *Labidocera* spp. includes *Euchaeta concinna* and large numbers of *Euchaeta* larvae.

1988 as the breakpoints of biomass during spring for the period 1959–2017 ($p$ = 0.013) and during summer for the period 1959–2020 ($p$ = 0.001), respectively (Figures 2B, C). After the breakpoint, the mean biomass increased from 142.88 to 429.42 mg/m$^3$ in spring ($p$ = 0.002 in the K–W test) and from 296.28 to 723.92 mg/m$^3$ in summer ($p$ = 0.001 in the K–W test), or approximately 200% and 144% increased after the breakpoint in spring and summer, respectively (Table 2). However, no obvious monotonic long-term trend in biomass for autumn and winter was detected (Figures 2D, E; Table 2).

## Trends of abundance of zooplankton groups in summer

Long-term changes in the abundance of 11 zooplankton taxa in summer were analyzed. Based on the time span of data, the monotonic trends of abundance were examined for Copepoda and Euphausiacea, while the differences in abundance between decades were examined for the other taxa. Results showed significant increasing trends in the abundances of Copepoda and Euphausiacea, according to Sen's slope of the time series ($p_{Copepoda}$< 0.01; $p_{Euphausiacea}$< 0.05). The Pettitt test revealed 1984 as the breakpoint of the abundance of Copepoda ($p$ = 0.012) and Euphausiacea ($p$ = 0.050) (Figures 3A, B). After the breakpoint, the mean abundance of Copepoda and Euphausiacea increased from 46.55 to 493.12 ind/m$^3$ and from 4.45 to 15.51 ind/m$^3$, respectively. However, the K–W test showed that the differences in the abundance of Copepoda ($p$ = 0.064) and Euphausiacea ($p$ = 0.077) were not significant before and after the breakpoint (Table 2). In addition, there was no obvious interdecadal variation in the abundances of Mysidacea ($p$ = 0.888), Amphipoda ($p$ = 0.117), Decapoda ($p$ = 0.304), Medusa ($p$ = 0.180), Chaetognatha ($p$ = 0.083), Tunicata ($p$ = 0.180), Diplostraca ($p$ = 0.655), Polychaeta ($p$ = 0.180), and planktonic larvae ($p$ = 0.655; Figures 3C–K; Table 3).

## Trends of abundance of dominant species in summer

In the CJE, in summer, the dominant species of Copepoda were *A. pacifica*, *C. dorsispinatus*, *C. sinicus*, *L. euchaeta*, *P. aculeatus*, and *Euchaeta* spp. (*Euchaeta concinna* and large numbers of *Euchaeta* larvae). During 2000–2020, the monotonic trend of the abundance of the dominant species *P. aculeatus* was significantly increasing and it was significantly decreasing for *L. euchaeta* based on the Sen's slope of the time

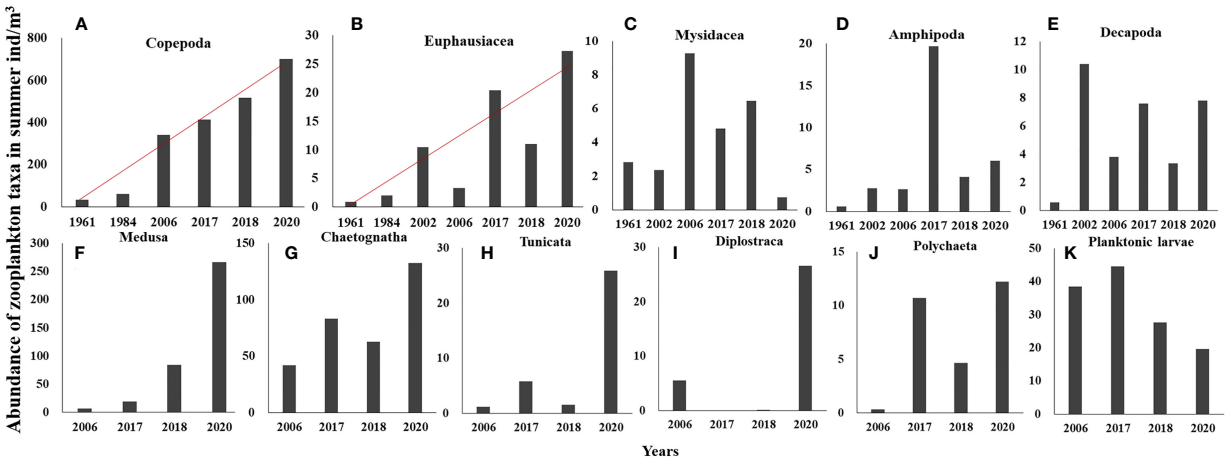


FIGURE 3
Abundance of Copepoda **(A)** and Euphausiacea **(B)** in summer in the 1960s, 1980s, 2000s, and 2010s; abundance of Mysidacea **(C)**, Amphipoda **(D)**, and Decapoda **(E)** in summer in the 1960s, 2000s, and 2010s; abundance of Medusa (including Hydrozoa and Ctenophora) **(F)**, Chaetognatha **(G)**, Tunicata **(H)**, Diplostraca **(I)**, Polychaeta **(J)**, Planktonic larvae **(K)** in summer in the 2000s and 2010s. Red line: trend line. The different scales of the Y-axis are adjusted for different taxa abundances.

series ($p_{P.\ aculeatus} < 0.05$; $p_{L.\ euchaeta} < 0.01$). The Pettitt test revealed 2008 and 2005 as the breakpoints of abundance of *P. aculeatus* ($p = 0.005$) and *L. euchaeta* ($p = 0.006$), respectively (Figures 4D, E). After the breakpoint, the mean abundance of *P. aculeatus* increased from 9.10 to 75.07 ind/m$^3$ ($p = 0.009$ in the K–W test), while the mean abundance of *L. euchaeta* decreased from 59.72 to 9.25 ind/m$^3$ ($p = 0.004$ in the K–W test) (Table 2). In addition, the abundance of *A. pacifica* increased slightly at a non-significant level with 2006 as the breakpoint ($p = 0.038$) (Figure 4A; Table 2). The mean abundance of *A. pacifica* before and after the breakpoint was 63.10 and 177.82 ind/m$^3$ respectively, ($p = 0.032$ in the K–W test). However, there was no obvious long-term trend in the abundance of the other dominant species of Copepoda (Figures 4B, C, F; Table 2).

# Discussion

## Significant increase in biomass

The annual average biomass of zooplankton in the CJE increased by 1.68 times from around 1960 to mid-1980s, and by 2.72 times from around 1960 to the mid-2000s. In terms of seasons, we found that zooplankton biomass from the 1960s to 2020 increased significantly during spring and summer, and breakpoints occurred in the 1980s. Biomass in spring increased by 1.67, 3.87, and 3.33 times from around 1960 to 1970s–1980s, 2000s, and 2010s, respectively. Similarly, biomass in summer increased by 2.08, 3.63, and 4.28 times from around 1960 to 1970s–1980s, 2000s, and 2010s, respectively. Owing to the lack

TABLE 3 Interdecadal differences in average abundance of zooplankton taxa in the Changjiang estuary.

| Zooplankton taxa | Decadal mean of abundance /ind/m$^3$ | | | *p* in Kruskal-Wallis test |
|---|---|---|---|---|
| | 1960s | 2000s | 2010s | |
| Mysidacea | 2.81 | 5.82 | 4.01 | 0.888 |
| Amphipoda | 0.57 | 2.69 | 9.95 | 0.117 |
| Decapoda | 0.57 | 7.11 | 6.24 | 0.304 |
| Medusa | ND | 7.03 | 123.15 | 0.180 |
| Chaetognatha | ND | 42.02 | 92.93 | 0.083 |
| Tunicata | ND | 1.13 | 11.06 | 0.180 |
| Diplostraca | ND | 5.53 | 8.87 | 0.655 |
| Polychaeta | ND | 0.35 | 9.20 | 0.180 |
| Planktonic larvae | ND | 38.51 | 30.56 | 0.655 |

ND, no data.

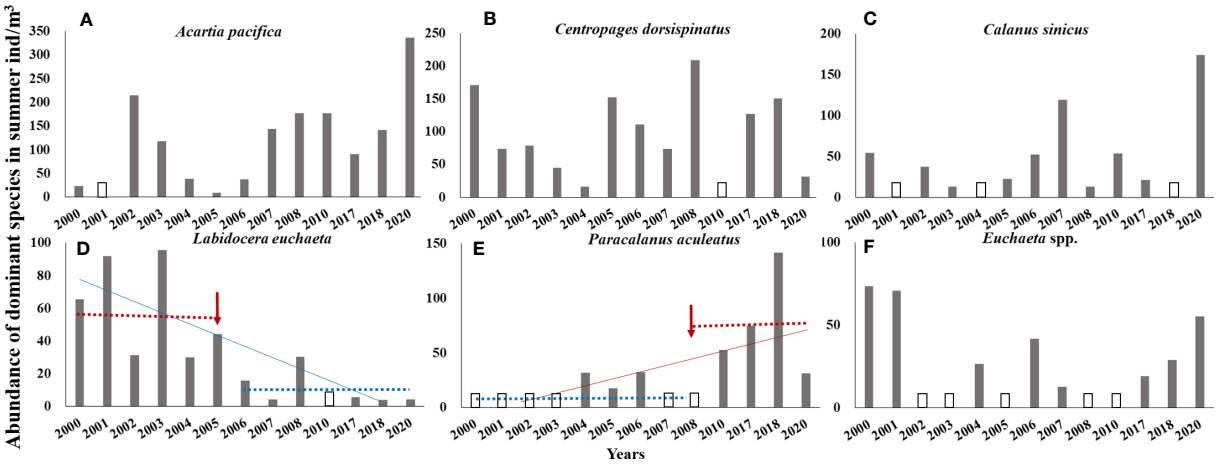


FIGURE 4
Abundance of *Acartia pacifica* **(A)**, *Centropages dorsispinatus* **(B)**, *Calanus sinicus* **(C)**, *Labidocera euchaeta* **(D)**, *Paracalanus aculeatus* **(E)**, and *Euchaeta* spp. **(F)** in summer from 2000 to 2020. Red and blue lines: trend lines. Red arrow: change point (breakpoint). Blue dotted line: mean abundance before/after breakpoint; red dotted line: mean abundance before/after breakpoint. An empty column indicates that the species is not the dominant species in a given year. *Euchaeta* spp. includes *Euchaeta concinna* and large numbers of *Euchaeta* larvae.

of historical data for the early to mid-1990s, we can only identify the shift in zooplankton biomass occurring between the late 1980s and the mid-1990s. This period coincided with the rapid increase in N and P in the Changjiang Basin caused by the extensive application of fertilizers, rapid development of industry and urbanization after 1980, and the rapid rise in water temperature since 1982 in the ECS (Belkin, 2009; Wang et al., 2021).

N- and P-fertilizer application in the Changjiang Basin increased gradually from 1–2 × $10^6$ t/yr and 0.2–0.5 × $10^6$ t/yr during the 1960s–1970s to 7–8 × $10^6$ t/yr and 2.5 × $10^6$ t/yr at the end of the 1990s, respectively, and both were stable after 2000 because of changes in national policies (Wang et al., 2021). The rapid increase in N and P in the Changjiang Basin led directly to an increase in dissolved inorganic nitrogen (DIN) and dissolved inorganic phosphorus (DIP) in the CJE. DIN concentrations in the Datong station increased from 20 μmol/L in the 1960s to 65.1, 89.4, and 150 μmol/L in the 1980s, 2000s, and 2010, respectively, and then decreased slightly in the last decade. DIP concentrations increased from 0.5 μmol/L in the 1960s to 0.6, 1.1, and 1.4 μmol/L in the 1980s, 2000, and 2005, respectively, and then reduced to 1.0 μm/L after 2010 (Jiang et al., 2010; Wang et al., 2021). Instead, the dissolved silicate concentration continued to decline during this period, from 320 μmol/L in the early 1960s to 100 μmol/L after 2000, and it has been almost stable in the last two decades (Wang et al., 2021). Belkin (2009) found that the SST in the ECS was relatively stable during 1957–1981, but accelerated warming was observed from 1982 to 2003 at a rate of up to 1.0°C/decade. A significant warming trend was also detected in our study area during 1982–2020 in spring ($p$< 0.001), summer ($p$< 0.05), and autumn ($p$< 0.001), with warming rates of 0.52, 0.21, and 0.20 °C/decade, and the Pettitt test revealed breakpoints at 1996, 1993, and 1995 during spring ($p$< 0.01), summer (p< 0.05), and autumn (p< 0.01), respectively (Figure 5; Table 2).

Jiang et al. (2010) revealed that the year-round average phytoplankton abundance decreased from 4.7 × $10^4$ cell/L in 1958–1959 to 2.6 × $10^4$ cell/L in 1985–1986, and then increased significantly to 9.9 × $10^4$ cell/L in 2004–2005 in the area that is consistent with this study (approximately twice from the end of the 1950s to the mid-2000s), due to the increase in DIN concentration. This upward trend seems to be consistent with that of the annual average zooplankton biomass from the early 1960s to the mid-2000s. Furthermore, phytoplankton abundance increased in all seasons during this period, with the largest increase in spring (from 3 × $10^2$ cell/L to 2 × $10^5$ cell/L), followed by winter (from 5 × $10^1$ cell/L to 1 × $10^4$ cell/L) and autumn (from 2 × $10^1$ cell/L to 3 × $10^3$ cell/L), while an increase of more than two orders of magnitude in summer occurred beyond the LSF (Jiang et al., 2010). Conversely, fishery resource density decreased significantly between 1960 and the early 2000s. The catch per fishing effort decreased from 636.26, 1130.55, and 659.26 kg/h in 1960 to 16.26, 26.23, and 222.01 kg/h in 2004 during spring, summer, and autumn, respectively (Li et al., 2007), and then to 4.44 kg/h in 2011 during spring (Ding, 2013). In terms of temperature effects, the Spearman nonparametric test showed that zooplankton biomass was positively correlated with SST in spring (R = 0.214, $p$ = 0.482, and n = 13), summer (R = 0.416*, $p$ = 0.049, and n = 23), and autumn (R = 0.607, $p$ = 0.148, n = 7), and the correlation was significant in summer. Therefore, the increase in zooplankton biomass in the CJE is a combined effect of enhanced bottom–up

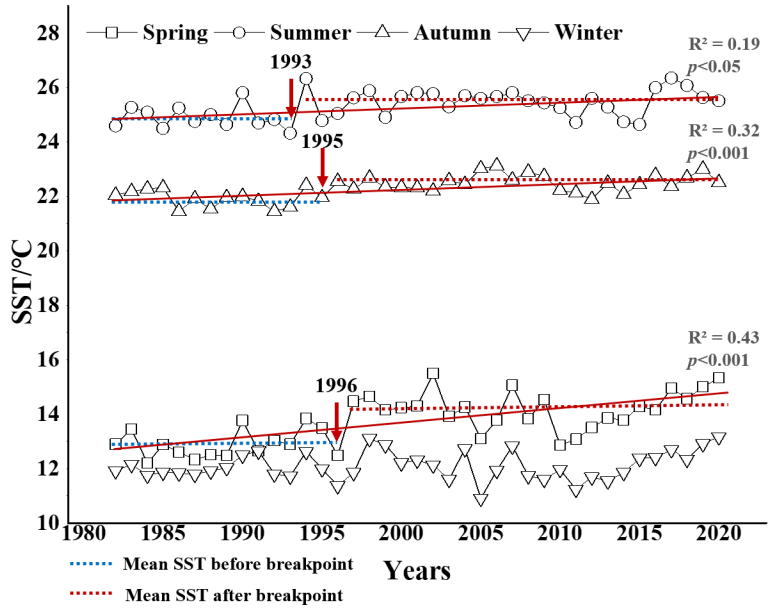


FIGURE 5
Sea surface temperature (SST) in the Changjiang estuary in four seasons from 1982 to 2020. Red line: trend line. Red arrow: change point (breakpoint). Blue dotted line: mean SST before breakpoint; red dotted line: mean SST after breakpoint.

support, reduced top–down pressure, and promotion of temperature. The increase in zooplankton biomass was gradual, but a rapid rise occurred between the late 1980s and the 1990s, when all these three effects changed significantly. Coincidentally, Rebstock and Kang (2003) revealed that the zooplankton biomass in the ECS increased gradually from the 1980s to the early 1990s and sharply in the 1990s as a response to climate change. The significant positive correlation between zooplankton biomass and SST in summer observed in this study combined with Rebstock and Kang (2003) results suggests that climate change probably plays an important role in the rapid change in zooplankton biomass in the CJE.

Additionally, the increases in zooplankton biomass were significant in spring and summer, but not in autumn and winter, which could not be ascertained clearly because of numerous missing data. The concentrations of DIN, DIP, and phytoplankton abundance in the four seasons increased to almost the same extent (Jiang et al., 2010), and the degree of warming in autumn was similar to that in summer (Table 2); however, the decrease in fishery resources in autumn was smaller than that in spring and summer (Li et al., 2007). Therefore, it is difficult to determine whether the non-significant increases in zooplankton biomass in autumn and winter were only due to the small sample size. More data are required for causal analysis.

Specific to the changing taxa in summer, significant increases were detected in the abundances of Copepoda and Euphausiacea, which continued to increase from the 1960s to 2020, but they were considerably higher after 2000 than before 2000. Furthermore, the degree of increase in the abundance of Copepoda was greater than that of Euphausiacea. The former was more than 10 times higher after 2000 than it was in the 1960s. Water temperature and food availability are the most important factors that affect the population dynamics of copepods (Ban, 1994; Devreker et al., 2005). The Chl-*a* concentration increased by only a factor of four (from 2 to 8 μg/L) from the 1980s to the 2000s (Wang, 2006; Jiang et al., 2014). We speculate that ocean warming was also an important cause of the increase in copepod abundance in the summer. Rebstock and Kang (2003) showed that the increase in the abundance of Copepoda, Chaetognatha, and Euphausiacea (both copepod predators) was synchronous with the increase in zooplankton biomass in the ECS due to warming. Based on these facts, we propose that the increase in zooplankton abundance was mainly due to the increase in crustaceans such as copepods in the CJE and ECS, and the effect of temperature cannot be ignored.

The increase in abundance of small copepods had limited contribution to the increase in biomass, due to their small size of individuals. However, small copepods are important food source for gelatinous zooplankton, e.g., small-jellyfish (Medusa in our study) and Chaetognatha (Wang et al., 2020a). The areas with high abundance of small copepods and Medusa overlapped near the CJE in summer (Gao et al., 2015). Therefore, the long-term increases in copepod abundance and SST might provide more abundant food and suitable temperature for gelatinous zooplankton. A study on trends in Large Marine Ecosystems

showed that jellyfish populations increased obviously in the ECS and Yellow Sea ecosystems (Brotz et al., 2012). In addition, the abundance of small-jellyfish in Jiaozhou Bay (located in the Yellow Sea) increased by almost 4 times from the 1990s to 2000s (Sun et al., 2012). Our study also found that the abundance of Medusa and Chaetognatha in summer was higher in the 2010s than in the 2000s (Table 3), although the difference was not significant. Therefore, we speculated that the increase of zooplankton biomass in the CJE in summer might be related to the increase of gelatinous zooplankton.

## Decrease in temperate species and increase in warm-water species

The effects of climate change on zooplankton have been discussed over several years. The trend in zooplankton biomass with warming was not consistent in different trophic ecosystems, but the expansion of warm-water species was almost uniform (Rebstock and Kang, 2003; Batten and Welch, 2004; Beaugrand, 2004; Sheridan and Landry, 2004; Hooff and Peterson, 2006; Wiafe et al., 2008; Piontkovski and Castellani, 2009; Keister et al., 2011; Rice et al., 2015). The impacts of climate change on China's marine ecosystems have also been reviewed (Kang et al., 2021). Changes in zooplankton include a decrease in abundance of large-sized copepods (e.g., *L. euchaeta* and *C. sinicus*), northward expansion in distribution and an increase in abundance of small-sized copepods (e.g., *A. pacifica* and *C. dorsispinatus*) in the eutrophic temperate semi-enclosed Bohai Sea (Yang et al., 2018), northward migration of temperate species (e.g., *C. sinicus*, *E. pacifica*, and *Sagitta crassa*) and ctenophore *Pleurobrachia globosa*, blooms of Jellyfish and Thaliacea in the temperate continental shelf of Yellow Sea and subtropic continental shelf of the ECS (Xu et al., 2013; Shi et al., 2015; Xu and Zhang, 2014; Shi et al., 2016; Wang et al., 2020b), an increase in the abundance of small-sized copepods (e.g., *Oncaea conifer*), and species diversity in the tropic South China Sea (Wang et al., 2014; Gong et al., 2017).

In the present study, we found that the abundance of *L. euchaeta* and *P. aculeatus* during 2000–2020 significantly decreased and increased, respectively. *L. euchaeta* is a temperate brackish species with an optimum distribution temperature of approximately 16 °C and an optimum salinity of 12–20, whose abundance was higher in winter and spring, but lower in summer and autumn in the CJE (Xu and Gao, 2009). It has been reported that the abundance of *L. euchaeta* in spring, summer, and winter decreased significantly in 2002 compared to 1959 and this phenomenon was linked to warming (Xu and Gao, 2009). Our study reconfirmed the negative effects of warming on *L. euchaeta* based on data from the last two decades. This is the first report to show that the abundance of *P. aculeatus* increased significantly in the CJE. *Paracalanus* spp. are neritic, warm-water, small calanoid copepods, and could be found in the CJE in four seasons, with higher abundances in summer and spring (data from 2006 in this study). *P. aculeatus* was not a dominant species before 2004 in this area in summer, but it was the dominant species in 2004 and 2006, indicating that its abundance and relative abundance increased; however, the significance of this increase could not be determined (Zhang et al., 2010; data from 2006 in this study). The significant increase in the abundance of *P. aculeatus* was confirmed by data from the last two decades in this study. We propose that the increase in the abundance of *P. aculeatus* is related to its small size, warm-water preference, and feeding habits. Rice et al. (2015) found that an increase in temperature can benefit smaller-sized copepods in eutrophic systems where food was not limited, probably due to the allometric growth law and food availability. Measurements of the *in situ* egg production rate (EPR) of *Paracalanus parvus* revealed that EPR and weight-specific female growth were both strongly positively related to water temperature (Jang et al., 2013). On the other hand, *Paracalanus* spp. often ingest ciliates, dinoflagellates, and nanoflagellates in large quantities in addition to phytoplankton (Suzuki et al., 1999). This was also confirmed by the weak correlation between EPR and female growth of *Paracalanus* spp. and Chl-*a* concentration (Jang et al., 2013). Wang et al. (2021) showed the change in phytoplankton from siliceous to non-siliceous-dominated communities around 2000 along with the increase in species number and abundance of dinoflagellates due to excessive N and lowering of dissolved silicate. Therefore, the increase in abundance of dinoflagellates in the CJE can also be one of the reasons for the increase in *P. aculeatus* (Wang et al., 2021).

Hypoxia in the CJE started in late spring and early summer, became the most serious in August, decreased in autumn, and finally, disappeared in winter. Hypoxia is primarily associated with marine-sourced organic carbon production, which is stimulated by coastal eutrophication, resulting from excessive terrestrial nutrient runoff. The intensity, duration, and frequency of hypoxia has increased significantly in recent decades (Li et al., 2018). It has been documented that jellyfish can survive in low-oxygen water at the bottom, which allows them to avoid predators (Purcell et al., 2007; Purcell, 2012); and *Acartia tonsa* appears to be quite tolerant to low oxygen relative to the co-occurring copepod species *Labidocera aestiva* and *Centropages hamatus* (Stalder and Marcus, 1997). Our results show a continuous increase in Medusa abundance from 2006 to 2020 (Figure 3F), but without a significant trend owing to the short time span of data. A slight increase in abundance of *A. pacifica* was also detected in this study (Figure 4A). However, jellyfish also benefit from warming (Purcell, 2005; Wang et al., 2012); therefore, it is difficult to determine the effect of hypoxia on zooplankton composition by comparing historical data. A number of studies in the northern Gulf of Mexico and Chesapeake Bay showed that hypoxia can drive the size structure of the zooplankton community and the vertical distribution in the water column, but few studies have describe detailed taxonomic composition in relation to hypoxia (Elliott et al., 2012).

## Conclusions

Long-term changes in large mesozooplankton (505–20,000 μm) in the CJE from the 1960s to 2020 were revealed in this study. Zooplankton biomass increased, and the regime shift occurred between the late 1980s and the mid-1990s, when nutrient concentrations, phytoplankton abundance, and SST increased synchronously, while fishery resource density decreased significantly. The abundance of Copepoda in summer increased significantly from the 1960s to 2020, and it was more than 10 times after 2000 compared to the 1960s. In the context of warming and increase in dinoflagellate abundance, the abundance of the warm-water and omnivorous small calanoid copepod *P. aculeatus* increased significantly, whereas that of the temperate brackish species *L. euchaeta* decreased mainly due to warming. However, it is difficult to determine the effects of hypoxia on long-term zooplankton changes. Moreover, some increasing or decreasing trends were not significant, such as zooplankton biomass in autumn and winter, and abundance of Medusa and Chaetognatha in summer, probably because of the small sample size. Hence, long-term monitoring is necessary for the adaptive management of the Changjiang Basin.

## Data availability statement

The raw data supporting the conclusions of this article will be made available by the authors, without undue reservation.

## Author contributions

PD wrote the draft. W-JY acquired zooplankton data during 2017–2020 and participated in zooplankton data collecting. B-PD collected zooplankton data during 2003–2018 in summer. MM acquired SST data. Y-LZ participated in data analysis in R software package. F-PC participated in zooplankton data collecting. Z-BJ revised the manuscript LS participated in the manuscript discussion. Q-ZC funded the work and composed the idea. All authors contributed to the article and approved the submitted version.

## Funding

This work is supported by the National Key Research and Development Program of China (2018YFD0900901, 2018YFD0900905), the Open Research Fund of Marine Ecological Monitoring and Restoration Technology (MEMRT202106), the Open Research Fund of Key Laboratory of Marine Ecosystem Dynamics (MED202005), the Long-term Observation and Research Plan in the Changjiang Estuary and the Adjacent East China Sea Project (LORCE, No. 14282), Zhejiang Provincial Project (330000210130313013006), Key Research and Development Program of Zhejiang Province (2021C03186). and the Yangtze Delta Estuarine Wetland Ecosystem Observation and Research Station, Ministry of Education & Shanghai Science and Technology Committee (ECNU-YDEWS-2020).

## Acknowledgments

We are grateful to Cheng-Gang Liu from second institute of oceanography, MNR for Figure 1 modification, and Wen-Wen Chen from Shanghai Ocean University for her help in collecting historical data.

## Conflict of interest

The authors declare that the research was conducted in the absence of any commercial or financial relationships that could be construed as a potential conflict of interest.

## Publisher's note



## References

Ban, S. (1994). Effect of temperature and food concentration on post-embryonic development, egg production and adult body size of calanoid copepod *Eurytemora affinis*. *J. Plankton Res.* 16 (6), 721–735. doi: 10.1093/plankt/16.6.721

Batten, S., and Welch, D. (2004). Changes in oceanic zooplankton populations in the north-east pacific associated with the possible climatic regime shift of 1998/1999. *Deep Sea Res. Part II: Topical Stud. Oceanogr.* 51, 863–873. doi: 10.1016/j.dsr2.2004.05.009

Beaugrand, G. (2004). The north Sea regime shift: Evidence, causes, mechanisms and consequences. *Prog. Oceanogr.* 60 (2), 245–262. doi: 10.1016/j.pocean.2004.02.018

Belkin, I. M. (2009). Rapid warming of Large marine ecosystems. *Prog. Oceanogr.* 81 (1), 207–213. doi: 10.1016/j.pocean.2009.04.011

Brotz, L., Cheung, W. W. L., Kleisner, K., Pakhomov, E., and Pauly, D. (2012). Increasing jellyfish populations: trends in Large marine ecosystems. *Hydrobiologia* 690 (1), 3–20. doi: 10.1007/s10750-012-1039-7

Cai, M., Xu, Z. L., and Zhu, D. D. (2008). Distribution characteristics of pelagic amphipoda in the Changjiang estuary and adjacent waters. *Acta Oceanolog. Sin.* 30 (5), 81–87. doi: 10.3321/j.issn:0253-4193.2008.05.011

Chai, C., Yu, Z., Song, X., and Cao, X. (2006). The status and characteristics of eutrophication in the Yangtze river (Changjiang) estuary and the adjacent East China Sea, China. *Hydrobiologia* 563, 313–328. doi: 10.1007/s10750-006-0021-7

Chen, H., and Xu, Z. L. (2009). Seasonal distribution of pelagic ostracoda in the Changjiang estuary and its adjacent waters. *Chin. J. Appl. Environ. Biol.* 15 (1), 072–077. doi: 10.3724/SP.J.1145.2009.00072

Chen, Z., Xu, H., and Wang, Y. (2021). Ecological degradation of the Yangtze and Nile delta-estuaries in response to dam construction with special reference to monsoonal and arid climate settings. *Water* 13 (9): 1145. doi: 10.3390/w13091145

Chen, J. J., Xu, Z. L., and Zhu, D. D. (2008). Seasonal abundance and distribution of pelagic euphausiids in the Changjiang estuary, China. *Acta Ecolog. Sin.* 28 (11), 5279–5285. doi: 10.3321/j.issn:1000-0933.2008.11.009

Chen, Y. Q., Zheng, G. X., and Zhu, Q. Q. (1985). A preliminary study of the zoo plankton in the Changjiang estuary area. *Donghai Mar. Sci.* 3 (3), 53–61. doi: CNKI:SUN:DHHY.0.1985-03-008

CWRCMWR (Changjiang Water Resource Commission of the Minstry of Water Resource) (1951-2020). *Internal report of Changjiang water and sediment bulltion* (Wuhan, China: Yangtze Press).

Dam, H. G. (2013). Evolutionary adaptation of marine zooplankton to global change. (Beijing, China: Science Press), 289.

Devreker, D., Souissi, S., and Seuront, L. (2005). Effects of chlorophyll concentration and temperature variation on the reproduction and survival of *temora longicornis* (Copepoda, calanoida) in the Eastern English channel. *J. Exp. Mar. Biol. Ecol.* 318, 145–162. doi: 10.1016/j.jembe.2004.12.011

Ding, P. X. (2013). *Evolution and cause analysis of typical coastal zones in China during the last 50 years*. (Beijing, China: Science Press) ,289.

Dufrene, M., and Legendre, P. (1997). Species assemblages and indicator species: the need for a flexible asymmetrical approach. *Ecol. Monogr.* 67, 345–366. doi: 10.1890/0012-9615(1997)067

Editorial board for marine atlas (EBMA) (1991). *Marine atlas of Bohai Sea, Yellow Sea, East China Sea: Biology* (Beijing, China: China Ocean Press), 91–187.

Elliott, D., Pierson, J., and Roman, M. (2012). Relationship between environmental conditions and zooplankton community structure during summer hypoxia in the northern gulf of Mexico. *J. Plankton Res.* 34, 602–613. doi: 10.1093/plankt/fbs029

Gao, Q., Chen, J. J., Xu, Z. L., and Zhu, D. D. (2015). Abundance distribution and seasonal variation of medusae, siphonophores, and ctenophores in the Changjiang (Yangtze river) estuary and the adjacent East China Sea. *Acta Ecolog. Sin.* 35 (22), 7328–7337. doi: 10.5846/stxb201403210505

Gao, Q., and Xu, Z. (2011). Effect of regional warming on the abundance of *Pseudeuphausia sinica* Wang et Chen (Euphausiacea) off the Changjiang river (Yangtze river) estuary. *Acta Oceanolog. Sin.* 30, 122–128. doi: 10.1007/s13131-011-0169-5

Gao, S. W., and Zhang, H. Q. (1992). On the ecology of zooplankton in the Changjiang river estuary. *Stud. Mar. Sin.* 33, 201–216.

Ge, J., Shi, S., Jie, L., Xu, Y., Chen, C., Bellerby, R., et al. (2020a). Interannual variabilities of nutrients and phytoplankton off the Changjiang estuary in response to changing river inputs. *J. Geophys. Res.: Oceans* 125 (3), e2019JC015595. doi: 10.1029/2019JC015595

Ge, J., Torres, R., Chen, C., Jie, L., Xu, Y., Bellerby, R., et al. (2020b). Influence of suspended sediment front on nutrients and phytoplankton dynamics off the Changjiang estuary: A FVCOM-ERSEM coupled model experiment. *J. Mar. Syst.* 204, 103292. doi: 10.1016/j.jmarsys.2019.103292

Giosan, L., Syvitski, J., Constantinescu, S., and Day, J. (2014). Climate change: Protect the world's deltas. *Nature* 516, 31–33. doi: 10.1038/516031a

Gong, Y. Y., Yang, Y. T., Fang, J. T., Cai, Y. C., Xu, S. N., and Chen, Z. Z. (2017). Spatial distribution of zooplankton in continental slope of northern South China Sea in summer. *South China Fish. Sci.* 13 (5), 8–15. doi: 10.3969/j.issn.2095-0780.2017.05.002

Gu, X. L., and Xu, Z. L. (2008). Ecological character of pelagic mysids in Yangtze estuary of China. *Chin. J. Appl. Ecol.* 19 (9), 2042–2048. doi: CNKI:SUN:YYSB.0.2008-09-029

Hooff, R. C., and Peterson, W. T. (2006). Copepod biodiversity as an indicator of changes in ocean and climate conditions of the northern California Current ecosystem. *Limnol. Oceanogr.* 51, 2607–2620. doi: 10.4319/lo.2006.51.6.2607

Hu, J., Xu, Z. L., and Zhu, D. D. (2008). Seasonal changes of ecological characteristics of pelagic mollusc in Yangtze river estuary. *J. Fish. Sci. China* 15 (6), 111–123. doi: 10.3321/j.issn:1005-8737.2008.06.011

Jang, M. C., Shin, K., Hyun, B., Lee, T., and Choi, K. H. (2013). Temperature-regulated egg production rate, and seasonal and interannual variations in *Paracalanus parvus*. *J. Plankton Res.* 35 (5), 1035–1045. doi: 10.1093/plankt/fbt050

Jiang, Z., Liu, J., Chen, J., Chen, Q., Xuan, J., and Zeng, J. (2014). Responses of summer phytoplankton community to drastic environmental changes in the Changjiang (Yangtze river) estuary during the past 50 years. *Water Res.* 54, 1–11. doi: 10.1016/j.watres.2014.01.032

Jiang, T., Yu, Z., Song, X., Cao, X., and Yuan, Y. (2010). Long-term ecological interactions between nutrient and phytoplankton community in the Changjiang estuary. *Chin. J. Oceanol. Limnol.* 28, 887–898. doi: 10.1007/s00343-010-9059-5

Kang, B., Pecl, G., Lin, L., Sun, P., Zhang, P., Li, Y., et al. (2021). Climate change impacts on China's marine ecosystems. *Rev. Fish. Biol. Fish.* 31, 599–629. doi: 10.1007/s11160-021-09668-6

Keister, J., Di Lorenzo, E., Morgan, C., Combes, V., and Peterson, W. (2011). Zooplankton species composition is linked to ocean transport in the northern California Current. *Glob. Change Biol.* 17, 2498–2511. doi: 10.1111/j.1365-2486.2010.02383.x

Kimmel, D., Boynton, W., and Roman, M. (2012). Long-term decline in the calanoid copepod *Acartia tonsa* in central Chesapeake bay, USA: An indirect effect of eutrophication? *Estuarine Coast. Shelf Sci.* 101, 76–85. doi: 10.1016/j.ecss.2012.02.019

Lehman, P., Teh, S. J., Boyer, G., Nobriga, M., Bass, E., and Hogle, C. (2010). Initial impacts of *microcystis aeruginosa* blooms on the aquatic food web in the San Francisco estuary. *Hydrobiologia* 637, 229–248. doi: 10.1007/s10750-009-9999-y

Li, L., Cen, J., Cui, L., and Lu, S. (2019). Response of size-fractionated phytoplankton to environmental factors near the Changjiang estuary. *Acta Oceanol. Sin.* 38, 151–159. doi: 10.1007/s13131-018-1259-4

Li, W., Ge, J., Ding, P., Ma, J., Glibert, P., and Liu, D. (2021). Effects of dual fronts on the spatial pattern of chlorophyll-a concentrations in and off the Changjiang river estuary. *Estuaries Coasts* 44 (5), 1408–1418. doi: 10.1007/s12237-020-00893-z

Li, J. S., Li, S. F., and Ding, F. Y. (2007). Analysis on annual change of fish diversity in Yangtze estuary offshore water area. *J. Fish. Sci. China* 14, 637–643.

Li, Y., Li, D., Tang, J., Wang, Y., Liu, Z., and He, S. (2010). Long-term changes in the Changjiang estuary plankton community related to anthropogenic eutrophication. *Aquat. Ecosyst. Health Manage.* 13, 66–72. doi: 10.1080/14634980903579942

Li, Z., Song, S., Li, C., and Yu, Z. (2018). The sinking of the phytoplankton community and its contribution to seasonal hypoxia in the Changjiang (Yangtze river) estuary and its adjacent waters. *Estuarine Coast. Shelf Sci.* 208, 170–179. doi: 10.1016/j.ecss.2018.05.007

Liu, S. H., Xiang, L. Y., Liu, C. C., and Wang, J. H. (2013). Ecological distribution characteristics of zooplankton in Yangtze river estuary in spring and summer during 2007-2008. *Mar. Sci. Bull.* 32 (2), 184–190. doi: 10.11840/j.issn.1001-6392.2013.02.010

Luo, B. Z., and Shen, H. T. (1994). *Three gorges project and estuarine ecological environment* (Beijing, China: Science Press), 212–214.

Ma, Z., Xu, Z., and Zhou, J. (2009). Effect of global warming on the distribution of Lucifer intermedius and *L. hanseni* (Decapoda) in the Changjiang estuary. *Prog. Nat. Sci.* 19, 1389–1395. doi: 10.1016/j.pnsc.2008.12.008

Piontkovski, S., and Castellani, C. (2009). Long-term declining trend of zooplankton biomass in the tropical Atlantic. *Hydrobiologia* 632, 365–370. doi: 10.1007/s10750-009-9854-1

Purcell, J. E. (2005). Climate effects on formation of jellyfish and ctenophore blooms: a review. *J. Mar. Biol. Assoc. U. K.* 85 (3), 461–476. doi: 10.1017/S0025315405011409

Purcell, J. (2007). Environmental effects on asexual reproduction rates of the scyphozoan, *Aurelia labiata*. *Mar. Ecol.: Prog. Ser.* 348, 183–196. doi: 10.3354/meps07056

Purcell, J. E. (2012). Jellyfish and ctenophore blooms coincide with human proliferations and environmental perturbations. *Ann. Rev. Mar. Sci.* 4 (1), 209–235. doi: 10.1146/annurev-marine-120709-142751

Purcell, J. E., Uye, S., and Lo, W. (2007). Anthropogenic causes of jellyfish blooms and their direct consequences for humans: a review. *Mar. Ecol.: Prog. Ser.* 350, 153–174. doi: 10.3354/meps07093

R Development Core Team (2014). *R: A language and environment for statistical computing* (Vienna, Austria: R Foundation for Statistical Computing). Available at: http://www.R-project.org/, ISBN: .

Rebstock, G. A., and Kang, Y. S. (2003). A comparison of three marine ecosystems surrounding the Korean peninsula: Responses to climate change. *Prog. Oceanogr.* 59, 357–379. doi: 10.1016/j.pocean.2003.10.002

Rice, E. (2015). Impact of climate change on estuarine zooplankton: Surface water warming in long island sound is associated with changes in copepod size and community structure. *Estuaries Coasts* 38, 13–23. doi: 10.1007/s12237-014-9770-0

Salmi, T., Määttä, A., Anttila, P., Ruoho-Airola, T., and Amnell, T. (2002). *Detecting trends of annual values of atmospheric pollutants by the Mann-Kendall test and sen's slope estimates-the excel template application MAKESENS* (Helsinki: Finnish Meteorological Institute).

Sheridan, C. C., and Landry, M. R. (2004). A 9-year increasing trend in mesozooplankton biomass at the Hawaii ocean time-series station ALOHA. *J. Mar. Sci.* 61 (4), 457–463. doi: 10.1016/j.icesjms.2004.03.023

Shi, Y., Song, S., Zhang, G. T., Wang, S., and Li, C. (2015). Distribution pattern of zooplankton functional groups in the Yellow Sea in June: A possible cause for geographical separation of giant jellyfish species. *Hydrobiologia* 754, 43–58. doi: 10.1007/s10750-014-2070-7

Shi, Y., Sun, S., Li, C., and Zhang, G. T. (2016). Interannual changes in the abundance of zooplankton functional groups in the southern Yellow Sea in early summer. *Oceanolog. Limnolog. Sin.* 47, 1–8. doi: 10.11693/hyhz20150300095

Stalder, L., and Marcus, N. (1997). Zooplankton responses to hypoxia: Behavioral patterns and survival of three species of calanoid copepods. *Mar. Biol.* 127, 599–607. doi: 10.1007/s002270050050

Steinberg, D., and Landry, M. (2017). Zooplankton and the ocean carbon cycle. *Ann. Rev. Mar. Sci.* 9, 413–444. doi: 10.1146/annurev-marine-010814-015924

Stone, J., Steinberg, D., and Fabrizio, M. (2018). Long-term changes in gelatinous zooplankton in Chesapeake bay, USA: Environmental controls and interspecific interactions. *Estuaries Coasts* 42 (2), 513–527. doi: 10.1007/s12237-018-0459-7

Sun, S., Li, Y., and Sun, X. (2012). Changes in the small-jellyfish community in recent decades in Jiaozhou bay, China. *Chin. J. Oceanol. Limnol.* 30 (4), 507–518. doi: 10.1007/s00343-012-1179-7

Suzuki, K., Nakamura, Y., and Hiromi, J. (1999). Feeding by the small calanoid copepod *Paracalanus* sp. on heterotrophic dinoflagellates and ciliates. *Aquat. Microb. Ecol.* 17 (1), 99–103. doi: 10.3354/ame017099

Wang, B. (2006). Cultural eutrophication in the Changjiang (Yangtze river) plume: History and perspective. *Estuarine Coast. Shelf Sci.* 69, 471–477. doi: 10.1016/j.ecss.2006.05.010

Wang, Y., Chen, X. Q., Lin, M., Xiang, P., Wang, C. G., and Wang, Y. G. (2014). Composition distribution and interannual variation of zooplankton communities in the northern South China Sea. in *The 14th annual proceedings of Fujian Marine Society*, Xiamen, China.

Wang, B., Mming, X., Wei, Q., and Xie, L. (2018). A historical overview of coastal eutrophication in the China seas. *Mar. pollut. Bull.* 136, 394–400. doi: 10.1016/j.marpolbul.2018.09.044

Wang, Y. T., Sun, S., Li, C. L., and Zhang, F. (2012). Effects of temperature and food on asexual reproduction of the scyphozoan, *Aurelia* sp.1. *Oceanolog. Limnolog. Sin.* 43 (5), 900–904. doi: 10.11693/hyhz201205004004

Wang, L., Wang, B. D., Chen, Q. W., Tang, X. W., and Han, R. (2016). Characteristics of the zooplankton community and impact factors in the Yangtze estuary coastal erea after third stage impoundment of the Three Gorges Dam. *Acta Ecolog. Sin.* 36 (9), 2505–2512. doi: 10.5846/stxb201412062423

Wang, Y., Xu, H., and Li, M. (2021). Long-term changes in phytoplankton communities in China's Yangtze estuary driven by altered riverine fluxes and rising sea surface temperature. *Geomorphology* 376, 107566. doi: 10.1016/j.geomorph.2020.107566

Wang, P., Zhang, F., Liu, M., Sun, S., and Xian, H. (2020). Isotopic evidence for size-based dietary shifts in the jellyfish *cyanea nozakii* in the northern East China Sea. *J. Plankton. Res.* 42(6), 689–701. doi: 10.1093/plankt/fbaa042

Wang, S., Zhang, G.T., Zhou, K., and Song, S. (2020b). Long-term population variability and reproductive strategy of a northward expanded ctenophore *pleurobrachia globosa* mose In a temperate bay, China. *J. Exp. Mar. Biol. Ecol.* 533, 151457. doi: 10.1016/j.jembe.2020.151457

Wiafe, G., Yaqub, H., Mensah, M., and Frid, C. (2008). Impact of climate change on long-term zooplankton biomass in the upwelling region of the gulf of Guinea. *J. Mar. Sci.* 65, 318–324. doi: 10.1093/icesjms/fsn042

Xian, W. W., Kang, B., and Liu, R. Y. (2005). Jellyfish blooms in the Yangtze estuary. *Science* 307, 41. doi: 10.1126/science.307.5706.41c

Xian, W. W., and Luo, B. Z. (2015). *Estuarine ecology and environment before impoundment of three gorges project* (Beijing, China: China Ocean Press), 176–177.

Xu, Z. L., and Gao, Q. (2009). *Labidocera euchaeta*: its distribution in Yangtze river estuary and responses to global warming. *Chin. J. Appl. Ecol.* 20 (5), 1196–1201.

Xu, Z. L., Gao, Q., Kang, W., and Zhou, J. (2013). Regional warming and decline in abundance of *Euchaeta plana* (Copepoda, calanoida) in the nearshore waters of the East China Sea. *J. Crustacean Biol.* 33, 323–331. doi: 10.2307/23446134

Xu, R., Li, Y. H., Li, Z. E., and Wang, J. H. (2009). Quantitative comparison of zooplankton in different habitats of the Changjiang estuary. *Acta Ecolog. Sin.* 29 (4), 1688–1696. doi: 10.3321/j.issn

Xu, Z. L., and Shen, X. Q. (2005). Zooplankton biomass and its variation in water near Changjiang estuary. *Resourcis Environ. Yangtze basin* 14 (3), 282–286. doi: 10.3969/j.issn.1004-8227.2005.03.004

Xu, Z. L., Shen, X. Q., and Ma, S. W. (2005). Ecological characters of zooplankton dominant species in the waters near the Changjiang estuary in spring and summer. *Mar. Sci.* 29 (12), 13–19. doi: 10.1360/biodiv.050121

Xu, Z. L., and Zhang, D. (2014). Dramatic declines in *Euphausia pacifica* abundance in the East China Sea: Response to recent regional climate change. *Zool. Sci.* 31, 135–142. doi: 10.2108/zsj.31.135

Yang, L., Liu, J., Wang, X. L., Xu, Y., Li, X., and He, L. (2018). Zooplankton community variation and its relationship with environmental variables in Bohai bay. *J. Mar. Sci.* 36 (1), 93–101.

Yang, Y., Liu, P. X., Zhou, H. H., and Xia, L. H. (2020). Evaluation of the biodiversity variation and ecosystem health assessment in Changjiang estuary during the past 15 years. *Acta Ecolog. Sin.* 40 (24), 8892–8904. doi: 10.5846/stxb201912272811

Zhang, W., Moriarty, J., Wu, H., and Feng, Y. (2021). Response of bottom hypoxia off the Changjiang river estuary to multiple factors: A numerical study. *Ocean. Modelling.* 159, 101751. doi: 10.1016/j.ocemod.2021.101751

Zhang, G. T., Song, S., Xu, Z., and Zhang, Q. (2010). Unexpected dominance of the subtropical copepod *temora turbinata* in the temperate Changjiang river estuary and its possible causes. *Zool. Stud.* 49, 492–503. doi: 10.1111/j.1365-2141.1995.tb05244.x

Zhang, D. J., Yan, Q. L., and Wang, Z. L. (2008). Variation in species number and biomass of zooplankton in typical estuaries of China. *Oceanolog. Et Limnolog. Sin.* 39 (5), 536–540. doi: 10.3321/j.issn:0029-814X.2008.05.017

Zhao, B., Yao, P., Li, D., and Yu, Z. (2021). Effects of river damming and delta erosion on organic carbon burial in the Changjiang estuary and adjacent East China Sea inner shelf. *Sci. Total Environ.* 793, 148610. doi: 10.1016/j.scitotenv.2021.148610

Zhou, X. D., and Xu, Z. L. (2009). Ecological characteristics of the pelagic decapods in the Changjiang estuary. *J. Fish. China* 12 (2), 111–123. doi: 10.3321/j.issn:1000-0615.2009.01.005

Zhu, Q. Q. (1988). An investigation on the ecology of zooplankton in Changjiang estuary and Hangzhou bay. *J. Fish. China* 12 (2), 111–123.

frontiers | Frontiers in Marine Science

TYPE Original Research
PUBLISHED 22 August 2022
DOI 10.3389/fmars.2022.915765



OPEN ACCESS

EDITED BY
Jun Xu,
Institute of Hydrobiology, (CAS), China

REVIEWED BY
Yunrong Yan,
Guangdong Ocean University, China
Yuan Li,
State Oceanic Administration, China

*CORRESPONDENCE
Yang Liu
Yangliu315@ouc.edu.cn

SPECIALTY SECTION
This article was submitted to Marine Ecosystem Ecology, a section of the journal Frontiers in Marine Science

RECEIVED 08 April 2022
ACCEPTED 01 August 2022
PUBLISHED 22 August 2022

CITATION
Zhang R, Liu Y, Tian H, Liu S, Zu K and Xia X (2022) Impact of climate change on long-term variations of small yellow croaker (*Larimichthys polyactis*) winter fishing grounds.
*Front. Mar. Sci.* 9:915765.
doi: 10.3389/fmars.2022.915765



# Impact of climate change on long-term variations of small yellow croaker (*Larimichthys polyactis*) winter fishing grounds

Rui Zhang[1], Yang Liu[1]*, Hao Tian[1], Shuhao Liu[1], Kaiwei Zu[2] and Xinmei Xia[1]

[1]Laboratory of Fisheries Oceanography, Fishery College, Ocean University of China, Qingdao, China, [2]Jiangsu Marine Fisheries Research Institute, Nantong, China

Small yellow croaker (*Larimichthys polyactis*) is one of the key demersal species with high economic values and wide distribution in the China Seas. In this study, a Winter Fishing ground Abundance Index (WFAI) was developed by using fisheries survey data in 1971–1982 and used as the response variable to investigate the impacts of environmental variables, including surface current velocity (SCV), sea surface salinity (SSS), sea surface temperature (SST), and depth (DE). A total of 45 combinatorial generalized additive models (GAMs), generalized linear models (GLMs), and random forest models (RFs) were used to select the optimal WFAI prediction. The final WFAI distribution results showed that the winter fishing ground hotspots of small yellow croaker were mainly distributed between 11°C and 16°C isotherms and between 50-m and 100-m isobaths, and the area of winter fishing ground hotspots (WFHA) significantly decreased and the hotspots tended to move northward over the past 50 years. The shape of hotspots was strongly affected by temperature fronts and salinity fronts. Analysis with the climate indices revealed that the Atlantic Multidecadal Oscillation (AMO) might have a large influence on the distribution of small yellow croaker by affecting SST and SSS in the China Seas more than the Pacific Decadal Oscillation (PDO), North Pacific Gyre Oscillation (NPGO), and Arctic Oscillation Index (AOI). The future prediction based on two extreme scenarios (RCP2.6 and RCP8.5) indicated that the hotspots would obviously move northward. These findings will serve effectively the fishery resources monitoring, management, and evaluation of small yellow croaker in the China Seas.

KEYWORDS

**small yellow croaker, winter fishing ground indices, abundance index distribution models, climate change, regime shifts**

## Introduction

Growing evidence has demonstrated that changing climates have shown a large effect on species distribution worldwide, and many species have performed distribution shifts to higher latitudes (Thomas, 2010; Vanderwal et al., 2013). The future climate is expected to be unprecedentedly warmer due to human influence (Masson-Delmotte et al., 2021), which may threaten species to go extinct because of their limited ability to adapt (Thomas et al., 2004). Many researchers have revealed the impact of climate changes on fishery resources through climate indices in recent years. For instance, the landings of small pelagic fishes in the North Pacific performed as regime shifts strongly associated with PDO in the mid-1970s (Chavez et al., 2003). A negative effect was found between juvenile North Pacific albacore distribution and the Pacific Decadal Oscillation (PDO) (Phillips et al., 2014). The survival rates of both coho and chinook salmon along western North America could be explained by the North Pacific Gyre Oscillation (NPGO) (Kilduff et al., 2015). The long-term catch fluctuations of abalone were closely related to the Arctic Oscillation Index (AOI) in Japan (Van Vuuren et al., 2011). A northward expansion of the species distributions was related to the Atlantic Multidecadal Oscillation (AMO) (Drinkwater et al., 2013). The effect of climate change especially long-term change on species is poorly understood in the China Seas, which is a productive system located in the northwest Pacific and probably affected by climate change (Bao and Ren, 2014; Ma et al., 2018).

Small yellow croaker (*Larimichthys polyactis*) is one of the most commercially important demersal fish species in the China Seas and is mainly exploited by China, South Korea, and Japan (Fishery Bureau of Ministry of Agriculture, 1987). Annual landings of small yellow croaker in Chinese coastal waters, between 1970 and 2019, have ranged from 3,300 tons to 400,000 tons (Bureau of fishery of Ministry of Agriculture of China 1970-2019). The resources of small yellow croaker have suffered three periods, a relatively high yield period before the 1960s (160,000 tons in 1957), a declining period during the 1960s to 1980s (16,000 tons in 1989), and a recovering period after the 1990s (340,000 tons in 2010) (Shui, 2003; Jin et al., 2005; Lin et al., 2008). The recovery could benefit from protective measures such as the summer moratorium (Cheng et al., 2004; Liu et al., 2018b). However, small yellow croaker have shown a younger age structure and a shorter body length in recent years (Lin and Cheng, 2004; Shan et al., 2017). Previous studies of small yellow croaker have focused mostly on resources, growth, diet composition, migration route, and population identification (Xue et al., 2004; Lin et al., 2008; Xu and Chen, 2009; Yan et al., 2014). Few comprehensive studies have explored the distribution variability and environmental conditions within the context of climate change. There is an essential need to understand the changes in the spatial distribution of small yellow croaker resulting from changed population structure and life history characteristics. The species is described as moving to shallow waters to breed and spawn during the warm seasons and moving back to deeper waters in cooler seasons (Xu and Chen, 2009). It is not that easy to track them year-round for migration species while they are relatively concentrated and stable in the overwintering period. The wintering grounds play an important role in the life-history of these long-distance migration species, where they can avoid intolerable conditions and prepare for the following reproduction period (Watanabe, 1970; Grubbs et al., 2007). Understanding the variations in wintering grounds will provide effective information on small yellow croaker stock assessment and management.

Species distribution models (SDMs) have been used to explore the relationship between species distribution and environmental variables (Guisan and Thuiller, 2005; Elith and Leathwick, 2009). Generalized linear models (GLMs) and generalized additive models (GAMs) are traditionally used in earlier SDMs. GLMs are based on a regression approach and can handle presence–absence data and simple additive combinations of linear terms (Guisan et al., 2002). GAMs are similar to GLMs but can handle the nonlinear relationship between distribution and environmental variables by using quadratic, cubic, and other non-linear parametric transforms (Welch et al., 2011). With the advances in technology, machine learning and data mining models have been developed such as artificial neural networks (ANNs) (Katz et al., 1992), random forest models (RFs), support vector machines (SVMs), and multivariate adaptive regression splines (MARSs) (Friedman, 1991). For example, reefs and subtidal rocky habitats were forecasted through ANNs (Watts et al., 2011), and the spatial distribution of the potential yield of Manila clam were predicted in Italy using RFs (Vincenzi et al., 2011). Moreover, new advances in satellite remote sensing and numerical simulation technology provide a wide range and high time-efficiency information for SDMs, which contributes to understanding the relationship between fishery resource variations and marine phenomena (Klemas, 2012; Chiu et al., 2017; Kroodsma et al., 2018). At the same time, Geographic Information Systems (GIS) could provide an excellent convenience in extracting the environmental ranges and mapping the species distribution (Valavanis et al., 2008; Roberts et al., 2010). For instance, the suitable habitat of short-finned squid was modeled including abiotic and biotic parameters based on GIS in the eastern Mediterranean Sea (Valavanis et al., 2004). The temporal and spatial patterns of swordfish catch distribution were analyzed based on GIS and remote sensed data in the central Mediterranean Sea (Perzia et al., 2016). Deriving indices of abundance that reflect the spatial distribution of a species and its dynamics over time is widely used in fisheries stock assessment and management to deal with the high complexity inherent in the survey data in terms of spatial and temporal variation (Kidokoro and Sakurai, 2008; Beale and Lennon, 2012; Smoliński and Radtke, 2016; Potts and Rose, 2018). The habitat suitability index (HSI) was developed to reflect the habitat quality for a particular species or life stage over a range of possible environmental conditions (Brown

et al., 2000). Spawning ground indices were developed using remote sensed data and GIS to analyze the variations in potential spawning grounds of Japanese flying squid (Liu et al., 2021) and Pacific saury (Liu et al., 2018a), and wintering ground indices were developed to explore the impacts of wintering ground conditions on chub mackerel abundance (Wang et al., 2021). Few SDM studies have been conducted to investigate long-term variations of small yellow croaker winter fishing grounds in the China Seas within the context of climate change, which limits exploring the resource variability mechanism.

Climate change may have a profound influence on species distribution range expansion or contraction (Thomas, 2010); therefore, future distribution prediction can be important for fishery resource conservation and sustainable exploitation. It has been reported that among 36 target species in the North Sea, nearly two-thirds of species showed responses to climate warming with distribution shifts in mean latitude or depth or both over 25 years (Perry et al., 2005). Many research studies have forecasted the future distribution of species based on different Representative Concentration Pathway scenarios (RCPs). The RCPs are derived from estimated emissions computed by a set of Integrated Assessment Models to define a range of possible future atmospheric composition over the 21st century (Masui et al., 2011; Riahi et al., 2011; Van Vuuren et al., 2011). The RCPs include a high-emission scenario (RCP8.5), two medium-emission scenarios (RCP4.5 and RCP6.0), and a low-emission scenario (RCP2.6) based on different greenhouse gas emissions (Collins et al., 2013; Nurdin et al., 2017; Silva et al., 2018). It is reported that the habitats of 20 marine fishes will move northward based on different RCPs up to the 2050s (Hu et al., 2022). Common halfbeak and ballyhoo halfbeak were predicted to benefit from climate change with potential increase in their occurrence area in coastal regions of the Americas (Guerra et al., 2021). Therefore, future prediction of small yellow croaker winter fishing grounds distribution will serve effectively in fishery resource management and exploration.

The objectives of this research are (1) to develop the optimal model for predicting the abundance index of small yellow croaker in winter fishing grounds, (2) to elucidate the key factors that influence small yellow croaker distribution variabilities in winter fishing grounds and analyze the mechanism of regime shifts in the last 50 years, (3) to predict future distribution of small yellow croaker in winter under different climate scenarios (RCP2.6 and RCP8.0).

# Materials and methods

## Study area

The present study was conducted in the China Seas (26°N–42°N and 118°E–128°E), which is located at the western edge of the North Pacific Ocean. Small yellow croaker shows large-scale migrations in the China Seas and off the west coast of Korea, which is more concentrated in the northern East China Sea and the southern Yellow Sea during the overwintering period (Figure 1) (Zhu et al., 1963). This region is also considered to be the mainly overwintering site for the South Yellow Sea and the East China Sea stocks (Liu et al., 1990).

## Fishery data

Monthly catch data are collected by trawling fishery statistics for the period 1971–1982, which comprehensively reflect the small yellow croaker resources in the Bohai Sea, Yellow Sea, and East China sea (hereafter referred to as "the China Seas"). The catch data were recorded by fishing areas with catch and numbers of nets covering a total of 266 fishing areas. Each fishing area consists of 0.5°×0.5° (latitude × longitude); the location of the latitude and longitude of each fishing area was described as the central point.

Winter data (January) were used to explore the distribution of small yellow croaker during the overwintering period, including 554 records in 140 fishing areas with distributions ranging from 26°N–38°N to 120°E–128°E. A total of 505 records in 139 fishing areas from 1971 to 1981 were used to construct the model, and data in 1982 (49 records in 49 fishing areas) were used for model validation.

Generally, CPUE is regarded as an indicator of fish abundance due to its positive correlation with the availability of fishery resources in fishing grounds (Sakurai et al., 2000; Yu et al., 2018; Liu et al., 2020), and in this study, the index associated with CPUE was used to represent the abundance of small yellow croaker. CPUE data for each fishing area was calculated by dividing the total catch by the number of nets, in kg/net.

## Environmental data

(1) Environmental variables

Monthly environmental data included surface current velocity (SCV) derived from meridional velocity (V) and zonal velocity (U), sea surface salinity (SSS), and sea surface temperature (SST). SCV is derived from meridional velocity (V) and zonal velocity (U), and the equation of SCV (1) is shown below:

$$SCV_{ij} = \sqrt{V_{ij}^2 + U_{ij}^2} \quad (1)$$

where $SCV_{ij}$ is the surface current velocity of grid $j$ in year $i$; $V_{ij}$ is the meridional velocity of grid $j$ in year $i$; and $U_{ij}$ is the zonal velocity of grid $j$ in year $i$.

The data for 1971–1992 from Simple Ocean Data Assimilation (SODA) v3.3.1 were downloaded from the APDRC data at a spatial resolution of 0.5° ×0.5° (latitude × longitude), and

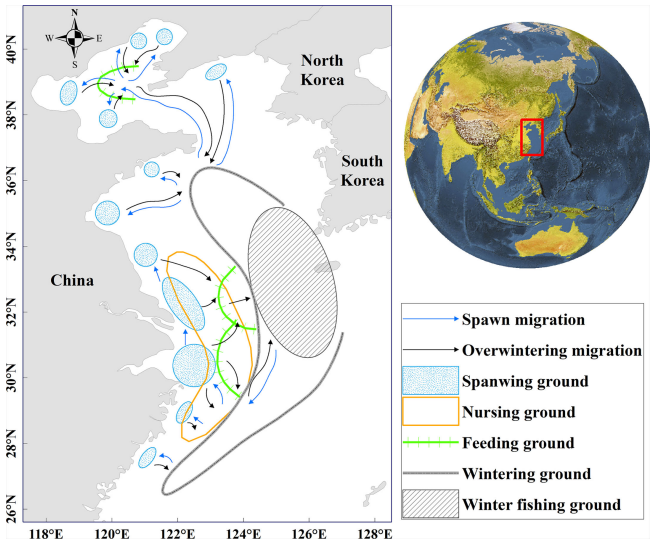


FIGURE 1
Study area of small yellow croaker. The slash-shaded area indicates the location of potential winter fishing grounds for small yellow croaker.

1993–2020 data were obtained from the Copernicus Marine Service at a spatial resolution of 0.25°×0.25° (latitude × longitude). Submarine elevation data were derived from the ETOPO1 Global Relief Model at a resolution of 1/60° (Table 1). All data were resampled into a 0.1° ×0.1° resolution (latitude × longitude) for consistent spatial resolution.

(2) Climate indices

The monthly mean climate indices are from online public datasets and previous literature reports. According to previous literature reports, winter is the most intense period of climate activities, significantly affecting the regional environment. In this study, the PDO, NPGO, AOI, and AMO were used to explore the effects of climate change on fishing ground variations (Table 2).

(3) IPCC-RCP scenarios

The monthly mean environmental conditions in the future (2040–2050 and 2090–2100) were downloaded from a public dataset (https://www.bio-oracle.org). Max depth data from Bio-ORACLE (ocean rasters for analysis of climate and environment), including the temperature, salinity, and surface current velocity of RCP 2.6, RCP4.5, RCP6.0, and RCP8.5, were used to predict the distribution in the future (Lennert et al., 2012; Assis et al., 2018). Rasters were assembled at a resolution of 0.083°×0.083° (latitude × longitude), and were resampled into a 0.1°×0.1° resolution (latitude × longitude) for consistent spatial resolution.

## Winter fishing ground indices

To describe the abundance of small yellow croaker under a uniform standard and to observe the winter variation, a Winter Fishing ground Abundance Index (WFAI) was developed to

TABLE 1 Environmental data used for research and model construction.

| Time | Variable (unit) | Data sources | Spatiotemporal resolution |
|---|---|---|---|
| 1971–1992 | SSS<br>SST (°C)<br>U (m/s)<br>V (m/s) | SODA<br>(http://apdrc.soest.hawaii.edu/) | 0.5°×0.5°<br>monthly |
| 1993–2020 | SSS<br>SST (°C)<br>U (m/s)<br>V (m/s) | Copernicus Marine Service<br>(http://marine.copernicus.eu/) | 0.25°×0.25°<br>monthly |
| 1971–2020 | Depth (m) | ETOPO1 Global Relief Model<br>(https://www.ngdc.noaa.gov/) | 1/60° |

TABLE 2 Climate index used for subsequent analysis.

| Climate index | Data sources | Temporal resolution |
|---|---|---|
| Pacific Decadal Oscillation (PDO) | https://www.ngdc.noaa.gov/ | Monthly |
| North Pacific Gyre Oscillation (NPGO) | http://o3d.org/ | Monthly |
| Arctic Oscillation Index (AOI) | https://www.ncdc.noaa.gov/ | Monthly |
| Atlantic Multidecadal Oscillation (AMO) | https://psl.noaa.gov/ | Monthly |

represent the abundance of small yellow croaker qualitatively. The catch and the number of nets in each fishing area were used to calculate the abundance index, and the equation of WFAI (2) is shown below:

$$g\left(WFAI_{ij}\right) = \ln\left(CPUE_{ij} + 1\right) \quad (2)$$

The region with WFAI higher than 5 is regarded as winter fishing ground hotspots and could be considered to have a higher occurrence probability of small yellow croaker in winter. The area of winter fishing ground hotspots (WFHA) was calculated as an index to measure the variation of annual dynamic fishing ground in winter. The calculation formula of WFHA (3) is as follows:

$$WFHA_i = \sum_{j=1}^{N_i} S_j \quad (3)$$

where $N_i$ is the grid number of WFAI > 5 in the winter fishing ground in year $i$; $S_j$ is the size of grid $j$ at 0.1° × 0.1° (latitude × longitude) resolution.

The location of potential winter fishing ground was delineated based on the predicted WFAI distribution. The annual mean values of SST, SSS, and SCV in potential winter fishing ground were calculated separately to represent the environmental condition fluctuations. WFHA and the mean value of WFAI in potential winter fishing ground are used to describe the annual variation of small yellow croaker.

The hotspots center is the center of gravity of hotspots, which is used to indicate the location of winter fishing ground hotspots. In this study, the center of hotspots is obtained by the Mean Center Tool of ArcGIS 10.7.

## Develop prediction models for WFAI

A total of 45 combinatorial GLMs, GAMs, and RFs were simulated by incrementally adding variables. The model was constructed with the Marine Geospatial Ecology Tool (MGET) of ArcGIS 10.7, an additional program that applies advanced analytical methods (Roberts et al., 2010). Environmental data [SSS, SST, SCV, and depth (DE)] were used as predictive variables to predict the WFAI distribution of small yellow croaker, and environmental variables were gradually added to the models. The variable inflation factors (VIFs) were examined to determine whether these environmental variables have multicollinearity, the results show that no variable has a VIF value greater than 5, and the VIF of SSS, SST, SCV, and DE were 2.40, 2.06, 1.80, and 1.80, respectively.

GAMs and GLMs were constructed using the "mgcv" package and "glm" package, respectively. (Wood, 2006). The equations for GAM(4) and GLM(5) are as follows:

$$g(Y) = \alpha + \sum_{i=1}^{n} F_i(X_i) + \epsilon \quad (4)$$

$$g(Y) = \alpha + \sum_{i=1}^{n} \beta(X_i) + \epsilon \quad (5)$$

where $g$ is the link function that constructs the relationship between the response variable and predictor variables, $Y$ is the response variable (WFAI), $X_i$ is the predictor variable (SSS, SST, SCV, and DE), $n$ is the number of variables, $F_i$ is the smoothing function for predictor $X_i$, $\alpha$ is the intercept, $\beta$ is the model constant, and $\epsilon$ is the random error (Guisan et al., 2002; Wood, 2006).

RF is an ensemble learning method that uses multiple decision trees; usually, a number of trees are trained from the original decision tree (Breiman, 2001). The random forest algorithm is as follows (Liaw and Wiener, 2002): firstly, draw $n_{tree}$ bootstrap samples from the original data; secondly, for each of the bootstrap samples, grow an unpruned classification or regression tree, with the following modification: at each node, rather than choosing the best split among all predictors, randomly sample $m_{try}$ of the predictors and choose the best split from among those variables; thirdly, aggregate these trees' information to predict new data. In this study, $n_{tree}$ was set to 500 and a "random forest" software package was used to build RF models.

The GLM, GAM, and RF models were developed using monthly raster data from 1971 to 1981 and then predicted the WFAI in 1982; the model performance was evaluated by comparing the predicted and actual values. Increasing variables incrementally caused changes in the explanatory rate and the Akaike information criterion (AIC) in the GAMs and GLMs, and deviance was explained in RFs. Therefore, the highest deviance explained and the lowest AIC (Johnson and Omland, 2004) were used to seek out the best GAM and GLM, and choose RF with the highest deviance explained.

## Detection method for regime shift

The Sequential *t*-test Analysis of Regime Shift (STARS) was applied to detect trends and step changes within the time series data, including WFAI, WFHA, SST, SSS, SCV, and climate indices (Rodionov, 2004). STARS results are determined by significance level (P), cutoff length (L), and the Huber's weight parameter (H), which controls the magnitude and scale of the regimes and the weights assigned to the outliers. In this study, the STARS cutoff length was set to 10, the Huber's weight parameter to 2, and the significance level to 0.1, consistently. In addition, the Cumulative sum (CuSum) of the anomalies was used to denote the trend of all exponential time series (Beamish et al., 1999).

# Results

## Optimal prediction model for WFAI

The best-performing GAM, GLM, and RF models are shown in Table 3. In GAM, the best-performing model has three significant predictor variables (SCV and SST with $p < 0.001$ and DE with $p < 0.01$) with the lowest AIC (2010.26) and the highest deviance explained (34.7%). For GLM, the final selected model with three significant predictors (SCV and SST with $p < 0.001$ and DE with $p < 0.01$) had the lowest AIC (2,116.40) and a high explained variance (15.80%). In RF, the predictive model containing four variables was selected, with deviance explained at 37.7%. Compared with the three models, the RF model has the highest explanation.

Figure 2 shows the comparison of actual WFAI and RF, GAM, and GLM model prediction results in 1982. The predicted hotspot distributions of RF, GAM, and GLM are consistent with the actual values, indicating that the prediction performance was reasonable. However, GAM predictions show high values in nearshore waters that are not consistent with reality. Among the validation data, 30.61% were underestimated and 12.24% were overestimated in GLM predictions. Figure 3 shows that RF was the best model by comparing the relationships between the predicted and actual WFAI for each selected model. The RF-based model showed the highest correlation ($R^2 = 0.54$, $p < 0.01$), which was greater than those from GAM ($R^2 = 0.47$, $p < 0.01$) and GLM ($R^2 = 0.29$, $p < 0.01$). Therefore, the RF model was selected as the most suitable model for subsequent prediction.

## Spatial distribution of WFAI

The final predicted WFAI of small yellow croaker from 1971 to 2020 (Figure 4) was produced by using the RF model; spatial variation showed that in the past 50 years, WFHA has gradually decreased, and the WFHA in 2020 is significantly lower than in 1971. It was shown that winter fishing ground hotspots mainly concentrated in 30°N–35°N, 123°E–127°E with annual variations; these regions may become a potential winter fishing ground for small yellow croaker. In the Yellow Sea, the range of hotspots gradually decreased, with the most extensive distribution in the 1970s. The smallest range of hotspots occurred in 1985, followed by 1992. After the 1990s, the northern boundary of the hotspots barely exceeded 35°N. In the East China Sea, the hotspot range was also widely distributed in the 1970s, decreasing from the 1980s to the 1990s and increasing after the 2000s. While the smallest area appeared in 1972, the largest area appeared in 1989. In addition, the hotspots in the Yellow Sea and the East China Sea were contiguous in the 1970s and 1980s, and from the 1990s, the winter fishing ground tended to divide into two parts. There are also only a few years

TABLE 3 GAM, GLM, and RF models included predictor variables, AIC, *p*-value, IncMSE, and deviance explained.

| Model | Predictor variable | AIC | *p*-value | IncMSE | Deviance explained |
|---|---|---|---|---|---|
| GAM | SSS | 2010.26 | 0.1421 | - | 34.70% |
| | SST | | $2 \times 10^{-16}$ *** | - | |
| | SCV | | $2 \times 10^{-16}$ *** | - | |
| | Depth | | 0.00203 ** | - | |
| GLM | SSS | 2116.40 | 0.72393 | - | 15.80% |
| | SST | | $1.24 \times 10^{-5}$ *** | - | |
| | SCV | | $6.21 \times 10^{-12}$ *** | - | |
| | Depth | | 0.00284 ** | - | |
| RF | SSS | - | - | 1.07 | 37.70% |
| | SST | | - | 1.71 | |
| | SCV | | - | 1.06 | |
| | Depth | | - | 0.84 | |

**p ′ 0.01, ***p ′ 0.001.

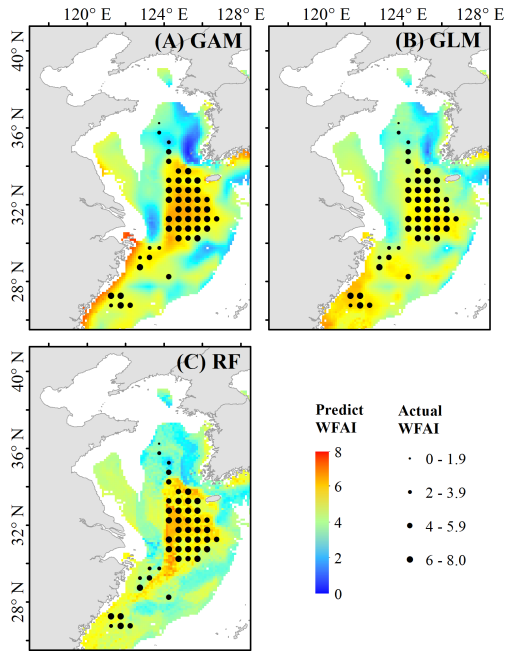


FIGURE 2
Comparison of the predicted distribution and the actual WFAI values in 1982. Distribution map in **(A)** is the prediction result of the generalized additive model (GAM), **(B)** is the prediction result of the generalized linear model (GLM), and **(C)** is the prediction result of the random forest model (RF).

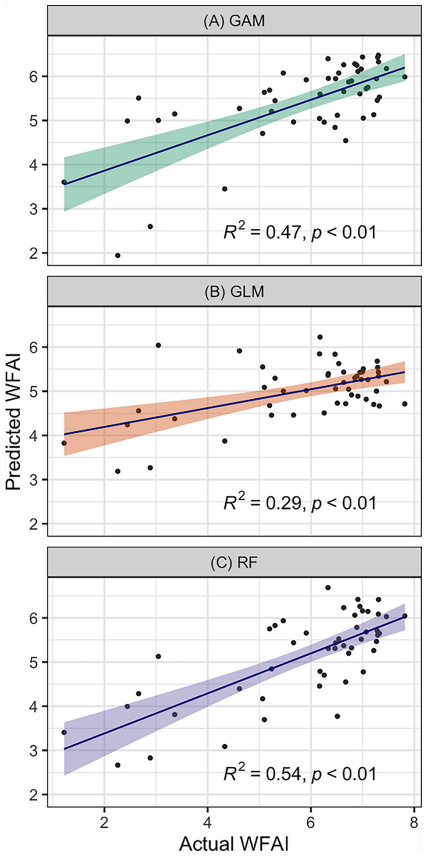


FIGURE 3
Validation of predicted and actual WFAI values of GAM **(A)**, GLM **(B)**, and RF **(C)** in 1982.

with hotspots distributed in the eastern part of Jeju island, which are 1971–1975, 1981, and 1991.

## Temporal variations in winter fishing grounds

Winter fishing grounds of small yellow croaker were defined as shown in Figure 1, which are distributed in the offshore area between 29°N and 35°N according to the average distribution of WFAI from 1971 to 2020.

The mean values of WFAI, WFHA, SSS, SST, and SCV of winter fishing grounds were calculated annually. WFAI and WFHA displayed a decreasing trend in fluctuation, while SSS, SST, and SCV had a dynamic increase (Figures 5, 6). The dynamic trends of WFAI and WFHA are almost identical, with a sudden drop in 1985 and then rise again, followed by another dip in 1992 and then fluctuating changes. Maximum and minimum values occurred in 1973 (5.39 for WFAI; 123,328 km$^2$ for WFHA) and 1985 (4.24 for WFAI; 50,896 km$^2$ for WFHA), respectively (Figures 5A, B).

Surface current velocity shows the opposite trend, which was extremely high in 1985 and 1992 and decreased in the middle years (Figure 6A). A correlation analysis revealed that WFAI ($r$ = 0.61, $p$ < 0.01) and WFHA ($r$ = 0.62, $p$ < 0.01) were negatively correlated with SCV. SST and SSS remained low during this period, with a minimum value in 1985 (Figures 6B, C).

## Climate-induced variations in WFAI

STARS analysis results show that the mean values of WFAI highlighted regime shifts with significant decreasing trends during 1981/1982 and 1991/1992, so was WFHA, which displayed the same regime shift trends in 1981/1982 and 1991/1992 (Figures 7A, B). SSS shows regime shifts with increasing trends in 1992/1993 and SCV in 1984/1985 separately (Figures 7C, E). SST highlighted that regime shifts decreased in 1980/1981 and increased in 1992/1993 (Figure 7D). The climatic indices showed evident decadal variability from 1971 to 2020 with regime shifts in 1976/1977 and 1988/1989 for PDO (Figure 7F), increasing shift in 1997/1998 and decreasing in 2013/2014 for NPGO (Figure 7G), and only one increased

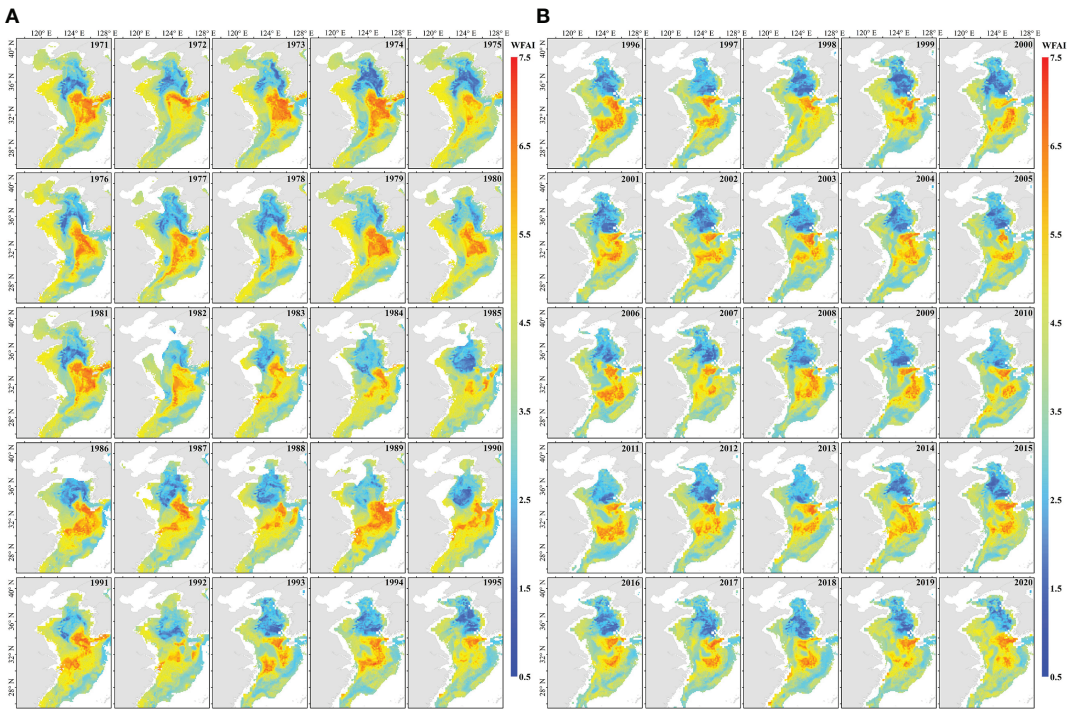


FIGURE 4
The annual WFAI distribution map of small yellow croaker in the China Seas during 1971–1995 **(A)** and 1996–2020 **(B)**.

regime shift in 1988/1989 for AOI, and 1994/1995 for AMO (Figures 7H, I).

## Future prediction of WFAI

Based on different greenhouse gas emissions in 2040–2050 and 2090–2100, WFAI distribution of small yellow croaker in the mid- and late 21st century under the RCP2.6 and RCP8.5 scenarios with the highest and lowest gas emissions is shown in Figure 8.

The RCP2.6 scenario prediction (Figures 8B, C) shows that the hotspot area shifted significantly northward in the mid-to-late 21st century compared to 2020 (Figure 8A), with the southern boundary moving from 30°N to 33°N, the western edge moving from 123°E to 121°E, the hotspot region moving from the East China Sea to the Yellow Sea, and the WFHA increasing significantly from 2020. At the end of the 21st century, the northern boundary of hotspots shifts southward and becomes more concentrated than in the middle of the century.

In the RCP8.5 scenario predictions (Figures 8D, E), the hotspots of winter fishing grounds also shifted northward in the mid-to-late 21st century. The dynamics in the 2050s are similar to RCP2.6, with the hotspots in the East China Sea moving to the Yellow Sea, and with the southern boundary near 35°N. At the end of the 21st century, hotspots became smaller and more concentrated, mainly between 122°E–124°E and 34° N–36°N in the Yellow Sea, with fewer hotspots appearing at 125° E–126°E.

# Discussion

## Model performance

In this research, a series of SDMs (GLMs, GAMs, and RFs) were simulated based on WFAI and environmental variables. The RF model was selected to be the optimal prediction model for small yellow croaker in the overwintering period with the highest deviance explained at 37.70%. GAMs were suboptimal compared with GLMs, which had the lowest deviance explained at 15.80%. We also compared the prediction performance of three model types. The results showed that the RF model had the highest correlation between predicted and actual WFAI, slightly higher than GAM and nearly two times higher than GLM. Moreover, GAM predictions showed unexpectedly high values in nearshore waters where there were overestimated and GLM predictions underestimated approximately 30% of the whole area of hotspots compared with RF. GLMs are based on linear

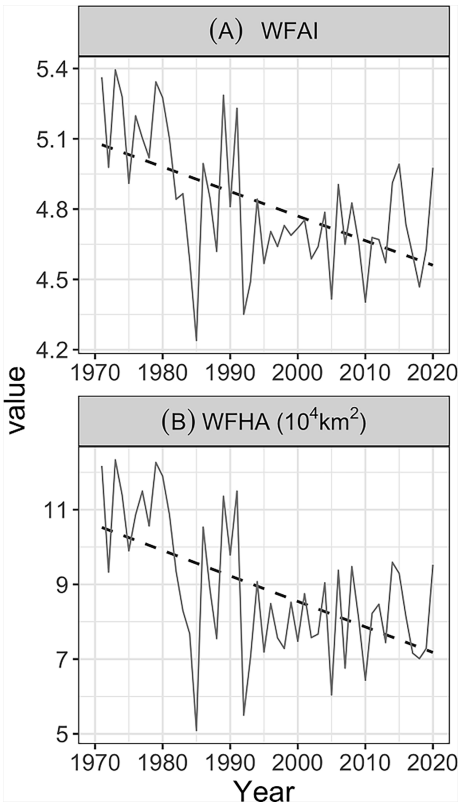


FIGURE 5
Annual variations (solid lines) of WFAI **(A)** and WFHA **(B)** from 1971 to 2020. The black dashed lines represent linear trends.

multiple regression and can deal with presence–absence data. GAMs are similar to GLMs and can handle nonlinear responses using quadratic, cubic, or other smoothers. Generally, the relationship between species distribution and environmental variables could be nonlinear. Our results also indicated that GAMs had better performance than GLMs. Several studies have demonstrated that machine learning approaches (e.g., RFs, SVMs, and ANNs) could outperform traditional regression approaches (e.g., GLMs and GAMs) (De Clercq et al., 2015; Luan et al., 2018; Catucci and Scardi, 2020). Among the six candidate methods (GLMs, GAMs, RTs, RFs, ANNs, and SVMs) applied to Japanese Spanish mackerel, the higher predictive quality of four machine learning models (RTs, ANNs, RFs, and SVMs) has also been expressed over GLMs and GAMs (Li et al., 2015). Machine learning models have advantages in handling non-linear relationships and could avoid overfitting the training data (Luan et al., 2020). Machine learning approaches can provide well-controlled variable selection and coefficient estimation; hence, their prediction performance may exceed conventional regression models. It would see machine learning approaches becoming more and more popular in SDMs because of their advantages in prediction.

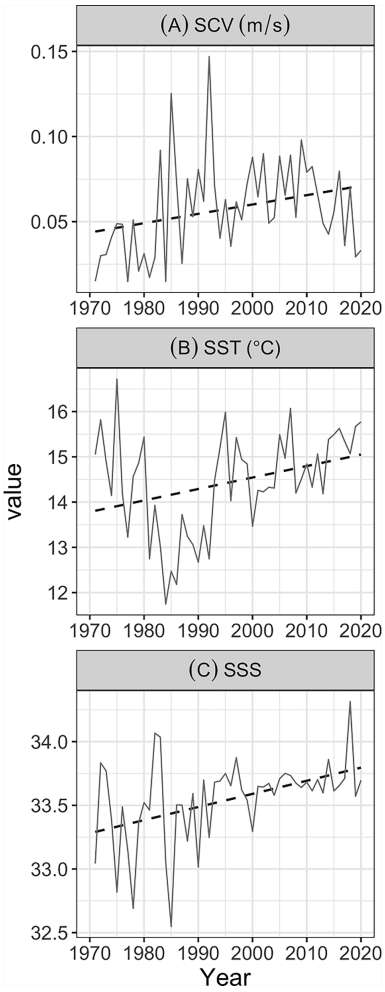


FIGURE 6
Annual variations (solid lines) of SCV **(A)**, SST **(B)**, and SSS **(C)** in winter fishing grounds from 1971 to 2020. The black dashed lines represent linear trends.

## Impact of environmental variables on the WFAI of small yellow croaker

The 50-year average distribution map of small yellow croaker in winter was generated combined with an isoline map of SST and DE (Figure 9). The results showed that the hotspots of small yellow croaker winter fishing grounds were mainly distributed between 11°C and 16°C isotherms and between 50-m and 100-m isobaths, similar to previous studies which described a suitable temperature range between 8°C and 18°C and a depth between 50 m and 80 m (Lin, 1987; Liu et al., 2020b). It has been reported that small yellow croaker had a higher occurrence probability of between 11.5°C and 16.2°C and a higher abundance of between 15.1°C and 16.7°C in winter (Liu and Cheng, 2018). These indicated that small yellow croaker could

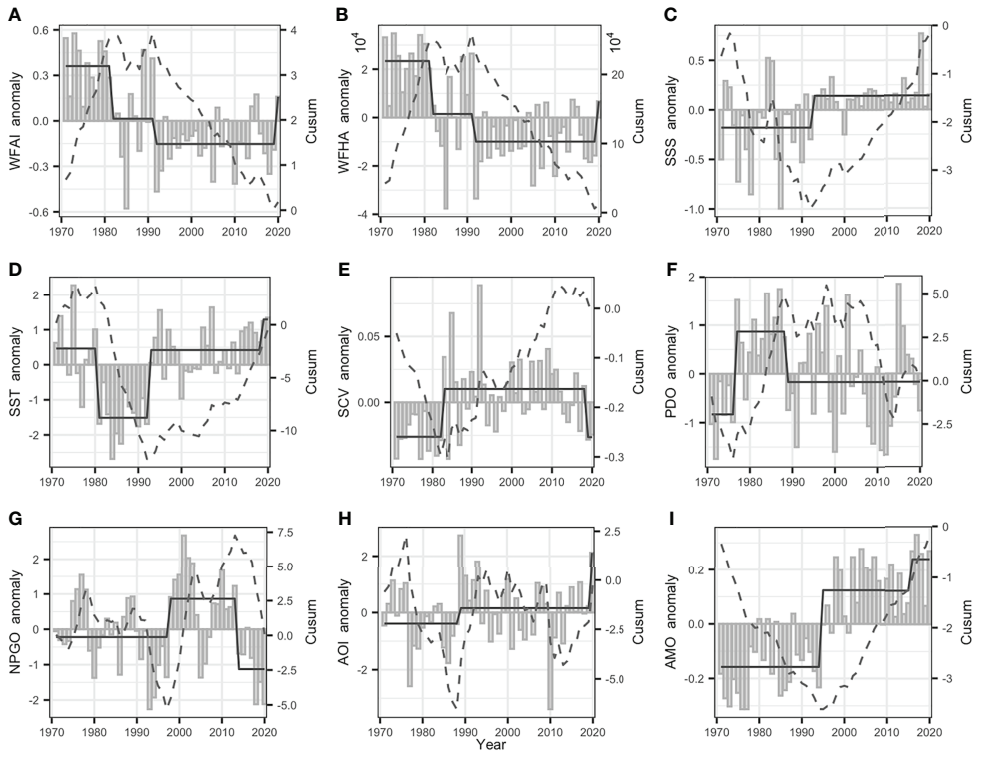


FIGURE 7
The gray bars represent annual anomalies of WHAI **(A)**, WFHA **(B)**, SSS **(C)**, SST **(D)**, SCV **(E)**, PDO **(F)**, NPGO **(G)**, AOI **(H)**, AMO **(I)**, and the solid and dashed lines represent the cumulative sum of SRSD-detected anomalies and regime shifts (CuSum).

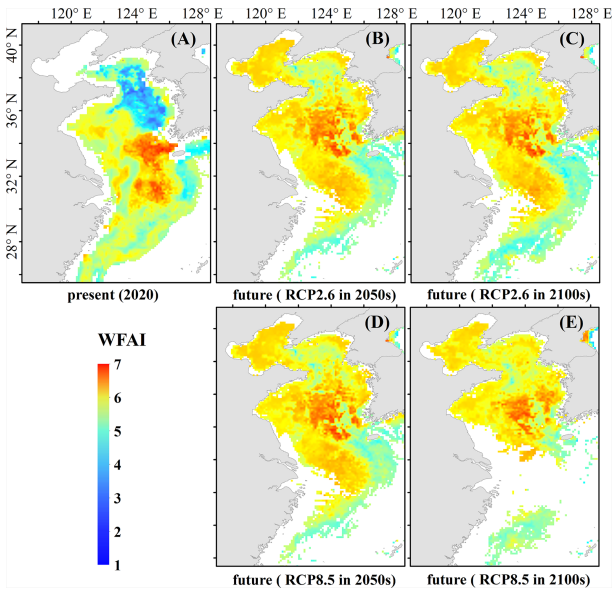


FIGURE 8
Present and two scenarios based on future predicted WFAI of small yellow croaker. **(A)** Present distribution in 2020, **(B)** future distribution in RCP2.6 (2050s), **(C)** future distribution in RCP2.6 (2100s), **(D)** future distribution in RCP8.5 (2050s), and **(E)** future distribution in RCP8.5 (2100s).

tolerate lower temperatures under 11°C, but more concentrated on suitable winter fishing grounds. The suitable depth range in our study was between 50 m and 100 m, a little larger than previous studies. This may be related to the benefit from remote sensed data that provide a broader range of environmental data.

The decadal distribution map emphasized the impact of environmental variables on winter fishing grounds. It has shown that temperature and salinity front jointly determine the boundary of hotspots of WFAI (Figure 10). The potential winter fishing grounds of small yellow croaker are affected by the Yellow Sea Warm Current (YSWC) and the coastal currents. The YSWC is believed to be the only mean flow that brings warm and saline water into the interior of the Yellow Sea and forms warm and saline tongue structures in winter (Ma et al., 2006). Furthermore, freshwater discharge from the Yangtze River also affects the salinity of the East China Sea (Delcroix and Murtugudde, 2002). This complex current system generated temperature and salinity fronts, which limited the boundary of winter fishing ground of small yellow croaker. The distribution of WFAI showed a strong relationship with fronts, with a clear boundary that was hardly north than 35°N. The shape of the small yellow croaker winter fishing ground hotspots is also strongly associated with temperature fronts and salinity fronts.

The long-term change of mean WFAI showed a decreasing trend in the last 50 years, similar to the WFHA (Figure 6). Similar results were described in the work of Han et al. (2020), which found that the biomass of small yellow croaker in the winter period showed a marked decline, but the study was only conducted between 2001 and 2017, while the long-term changes of environmental variables showed an increasing trend (Figure 6), indicating that the environmental changes may have a negative effect on the WFAI and the WFHA of small yellow croaker. The STARS analyses for mean values of WFAI and WFHA in winter fishing grounds suggested that regime shifts took place in 1981/1982 and 1991/1992. SST showed regime shifts in 1980/1981 and 1992/1993, while SSS showed regime shifts in 1992/1993 and SCV in 1984/1985. The almost synchronous regime shifts also indicated that the potential winter fishing grounds of small yellow croaker were directly affected by environmental variables. The decadal average anomaly map manifested that the current velocity in the potential winter fishing ground of small yellow croaker was relatively smaller than in other regions (excluding the Kuroshio region) (Figure 11). This may indicate that small yellow croaker prefers gentle areas during winter, which could be related to a lower feeding rate and energy conserved. The small yellow croaker mainly preys on Japanese anchovy, Kammal thryssa, Kishi velvet shrimp, and Mitre squid (Xiao et al., 2019). Due to the limited data, the influence of prey conditions was not involved in this research.

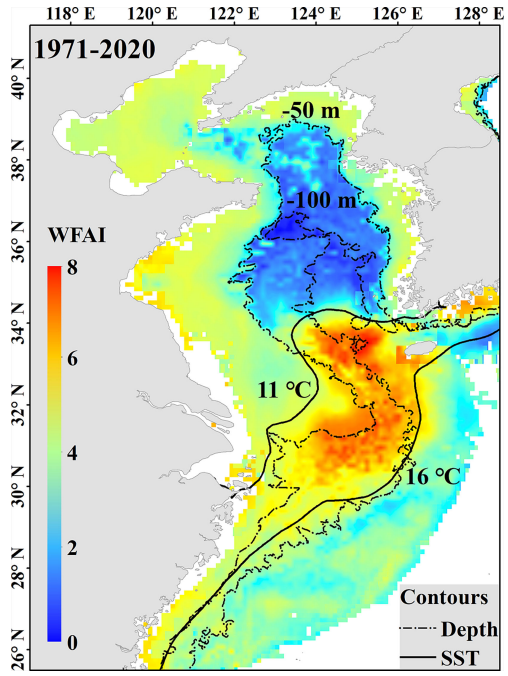


FIGURE 9
The 50-year average WFAI distribution map of small yellow croaker with environmental conditions (the dashed lines represent isobaths, and the solid lines represent isotherms).

## Effect of climate change on small yellow croaker

The correlation analyses between the annual mean WFAI and environmental variables are detected in Figure 12. WFAI showed a weak relationship with SST and SSS, but a strong negative relationship with SCV ($r = -0.61$, $p < 0.001$). The WFAI and WFHA highlighted a significant positive correlation ($r = 0.97$, $p < 0.001$); hence, WFHA also showed a strong negative correlation with SCV ($r = -0.62$, $p < 0.001$). As for climate indices, PDO highlighted regime shifts in 1976/1977 and 1988/1989, NPGO showed regime shifts in 1997/1998 and 2013/2014, AOI showed a regime shift only in 1988/1989, and AMO showed a regime shift only in 1994/1995. The correlation tests indicated that WFAI and WFHA highlighted a strong negative correlation with AMO (WFAI: $r = -0.44$, $p < 0.01$; WFHA: $r = -0.46$, $p < 0.01$) and a relatively weak correlation with AOI, NPGO, and PDO (Figure 12). This may imply that AMO had a closer relationship with WFAI and WFHA than AOI, NPGO, and PDO. Previous studies have attributed the decadal variability in the North Pacific to PDO, but recent studies have illustrated that the AMO instead controlled it using long records of observations (Wu et al., 2020). They found that PDO had little relationship with the North Pacific subtropical mode water when the data were extended back to the 1940s, and only after 1978 did the negative correlation appear, which reflected the fact that the warming trend of the mode water

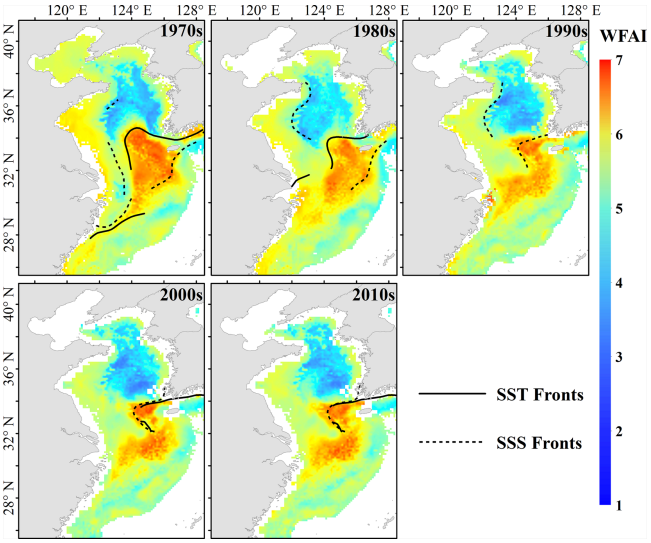


FIGURE 10
The decadal average WFAI distribution map of small yellow croaker with environmental variable in front (the black solid line is the front of decadal average temperature, and the dashed line is the front of decadal average salinity).

coincided with a phase transition of the PDO index from a positive to a negative phase, rather than a robust relationship. Our results also supported this view with a strong correlation between WFAI and AMO and a lower correlation with PDO. Among environmental variables and climate indices, SST and SSS showed relatively strong positive correlations with AMO ($r = 0.33$, $p < 0.05$ for SST; $r = 0.39$, $p < 0.05$ for SSS), and SCV showed a weak correlation with AMO ($r = 0.17$, $p < 0.1$). SST had a positive correlation with SSS ($r = 0.34$, $p < 0.05$). This could be related because the salinity and temperature were related to the ocean current in the China Seas (Chen, 2009). From these observations, we proposed a potential process to explain the variations of small

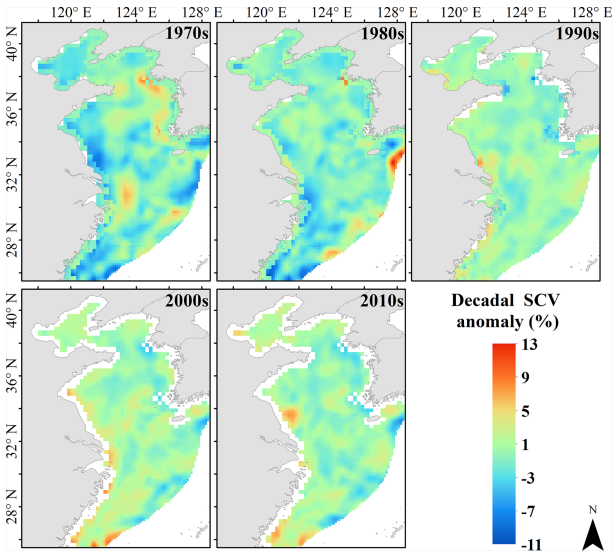


FIGURE 11
Decadal average anomaly map of surface current velocity in 1971–2020.

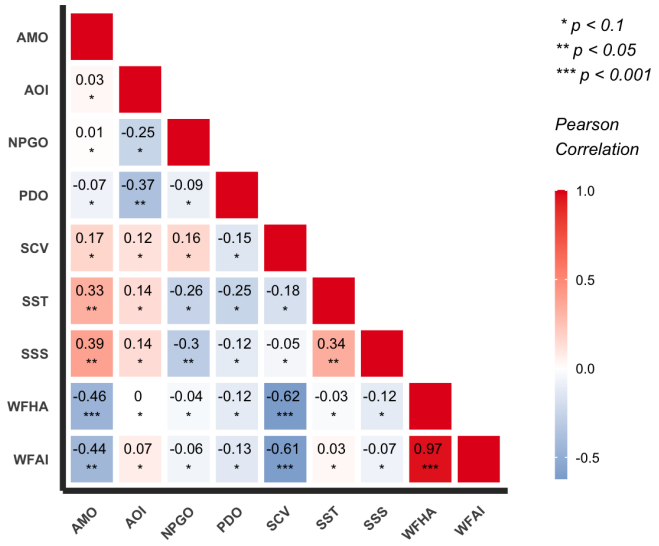


FIGURE 12
The correlation analyses between the annual mean WFAI, WFHA, mean values of environmental variables, and climate indices.

yellow croaker in the overwintering period. AMO-based climate regimes led to changes in the Kuroshio Current region through ocean–atmosphere interactions. The Kuroshio Current entered the China Seas, which were located on the western edge of the North Pacific and were affected by the Kuroshio Current and its branches. The potential winter fishing grounds of small yellow croaker were directly affected by the coastal currents and the Yellow Sea Warm Current (YSWC), which was the branch of the Kuroshio Current (Bian et al., 2013). The YSWC brings warm and saline water into the interior of the Yellow Sea (Ma et al., 2006). The abundance of small yellow croaker was directly influenced by the environmental conditions (SST, SSS, and SCV) in winter fishing grounds. Therefore, the long-term changes of WFAI and WFHA were more likely associated with AMO than other climate indices.

## Future prediction of winter fishing ground change

Based on the optimal prediction model, the decadal distribution maps of hotspots were generated to investigate variations in winter fishing grounds (Figure 10). The decadal distribution maps indicated that the spatial range and area of hotspots tended to be shrinking. Moreover, the winter fishing grounds tended to be divided into two parts, and this trend became more distinct after the 1990s. The boundary of hotspot distribution also changed with time. The north boundary of hotspots moved southward to 34°N after the 1970s, which was also reported by Han et al. (2020). The south boundary of hotspots tended to move northward near 30°N after the 1970s. The east boundary of the north parts of the winter fishing grounds extended eastward to 127°E and the west boundary of the south parts tended to move westward to 123°E. Moreover, the hotspot distribution showed a more concentrated trend though the area became smaller. Our results indicated that the spatial distribution changes in the winter fishing ground of small yellow croaker were likely to be embodied in the boundary.

We conducted future distribution maps based on two extreme scenarios (RCP2.6 and RCP8.0). The results showed that the distribution of small yellow croaker will move obviously northward and the WFHA will become broader (Figure 8), and the southernmost overwintering districts might become less important to the stock under future climate change. The north boundary of WFHA can reach 40°N, and the south boundary can reach 30°N. The west boundary moves to 118°E, and the east boundary moves to 127°E. The center of the winter fishing ground was also generated to investigate the long-term changes with a focus on hotspots (Figure 13). Results showed that the center of winter fishing ground would distinctly move northward in the 2050s and the 2100s than in 1970–2020 related to 16°C isotherms. Distribution movement driven by climate change has been found in a large number of species (Perry et al., 2005; Last et al., 2011). Thirteen fish species have been newly recorded in the Taiwan Strait beyond their historic range in the South China Sea (Du et al., 2013). The hotspot distribution of hairtail in the East China Sea was found to move north eastward from 1991 to 2011 (Yuan et al., 2017). Many species have been simulated to move poleward under different scenario predictions of climate change (Jones and Cheung, 2015; Morley et al., 2018). These shifts were projected to lead to increases in mid- and high-latitude oceans and decreases in

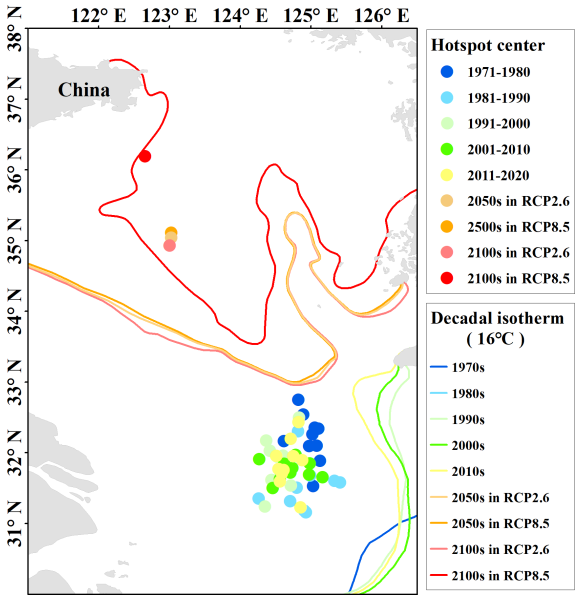


FIGURE 13
The hotspot center and decadal isotherm from 1971 to 2020 and the future prediction in two RCP scenarios.

tropical regions (Cheung et al., 2009). All these changes call for the improvement of resource management and conservation.

## Conclusion

Three types of SDMs (GLMs, GAMs, and RFs) of small yellow croaker were developed using WFAI as the response variable and environmental variables as explanatory variables. A comparison of the models revealed that the RF model was the optimal prediction model. Results showed that the WFAI distribution was related to SST, SSS, SCV, and DE, and the winter fishing ground hotspots were mainly distributed between 11°C and 16°C isotherms and between 50-m and 100-m isobaths. The shape of hotspots was strongly affected by temperature fronts and salinity fronts. A long-time scale analysis revealed a decreasing trend in the winter fishing ground hotspots—the northern boundary shifts southward, the southern border shifts northward, and there was a tendency to divide into two parts, gradually. The WFHA has significantly decreased over the past 50 years. WFAI and WFHA highlighted similar regime shift trends, and the distribution of small yellow croaker might be more closely related to AMO than PDO, AOI, and NPGO in winter fishing grounds. Future predictions based on two extreme climate scenarios (RCP2.6 and RCP8.0) indicated that the winter fishing ground hotspots of small yellow croaker would move obviously northward by the end of this century under climate warming. Climate and environmental changes could have far-reaching effects on changes in small yellow croaker fisheries.

## Data availability statement

The raw data supporting the conclusions of this article will be made available by the authors, without undue reservation.

## Author contributions

RZ performed data analyses, model construct, and wrote the paper. YL conceived the idea for the study, analyses, and edited the manuscript. HT edited part of the figures. SL and XX extracted part of environmental data. KZ edited the manuscript. All authors listed have made a direct and substantial contribution to this work. All authors read and approved the final manuscript.

## Acknowledgments

This study was supported by the National Key R&D Program of China (2018YFD0900902). The study benefited from statistics on fishing vessels from the Yellow Sea Fisheries Research Institute and the East China Sea Fisheries Research Institute for the period 1971–1982. We are particularly grateful to the Yellow Sea Fisheries Research Institute and the East China Sea Fisheries Research Institute of the Chinese Academy of Fishery Sciences for their support.

## Conflict of interest

The authors declare that the research was conducted in the absence of any commercial or financial relationships that could be construed as a potential conflict of interest.

## Publisher's note

# References


Assis, J., Tyberghein, L., Bosch, S., Verbruggen, H., Serrão, E. A., and De Clerck, O. (2018). Bio-ORACLE v2.0: Extending marine data layers for bioclimatic modelling. *Glob. Ecol. Biogeogr.* 27, 277–284. doi: 10.1111/geb.12693

Bao, B., and Ren, G. (2014). Climatological characteristics and long-term change of SST over the marginal seas of China. *Cont. Shelf. Res.* 77, 96–106. doi: 10.1016/j.csr.2014.01.013

Beale, C., and Lennon, J. (2012). Incorporating uncertainty in predictive species distribution modelling. *Philos. Trans. R. Soc Lond. B. Biol. Sci.* 367, 247–258. doi: 10.1098/rstb.2011.0178

Beamish, R. J., Noakes, D. J., McFarlane, G. A., Klyashtorin, L., Ivanov, V. V., and Kurashov, V. (1999). The regime concept and natural trends in the production of pacific salmon. *Can. J. Fish. Aquat. Sci.* 56, 516–526. doi: 10.1139/f98-200

Bian, C., Jiang, W., and Greatbatch, R. J. (2013). An exploratory model study of sediment transport sources and deposits in the bohai Sea, yellow Sea, and East China Sea. *J. Geophys. Res. Ocean.* 118, 5908–5923. doi: 10.1002/2013JC009116

Breiman, L. (2001). Random forests. *Mach. Learn.* 45, 5–32. doi: 10.1023/A:1010933404324

Brown, S. K., Buja, K. R., Jury, S. H., Monaco, M. E., and Banner, A. (2000). Habitat suitability index models for eight fish and invertebrate species in casco and sheepscot bays, Maine. *North Am. J. Fish. Manage.* 20, 408–435. doi: 10.1577/1548-8675(2000)020<0408:HSIMFE>2.3.CO;2

Bureau of fishery of Ministry of Agriculture of China.*China Fishery statistical yearbook*. (1970-2019) (Beijing: China Agriculture Press).

Catucci, E., and Scardi, M. (2020). A machine learning approach to the assessment of the vulnerability of posidonia oceanica meadows. *Ecol. Indic.* 108, 105744. doi: 10.1016/j.ecolind.2019.105744

Chavez, F., Ryan, J., Lluch-Cota, S., and Niquen, M. (2003). From anchovies to sardines and back: multidecadal CHANGE in the pacific ocean. *Science* 299, 217–221. doi: 10.1126/science.1075880

Chen, C. T. A. (2009). Chemical and physical fronts in the bohai, yellow and East China seas. *J. Mar. Syst.* 78, 394–410. doi: 10.1016/j.jmarsys.2008.11.016

Cheng, J., Lin, L., Jiang, Y., Yuan, X., Li, J., and Gao, T. (2004). Effects of summer close season and rational utilization on redlip croaker (*Larimichthys polyactis beeker*)resources in the East China Sea region. *J. Fish. China* 11, 554–560. doi: 10.3321/j.issn:1005-8737.2004.06.012

Cheung, W. W. L., Lam, V. W. Y., Sarmiento, J. L., Kearney, K., Watson, R., and Pauly, D. (2009). Projecting global marine biodiversity impacts under climate change scenarios. *Fish. Fish.* 10, 235–251. doi: 10.1111/j.1467-2979.2008.00315.x

Chiu, T.-Y., Chiu, T.-S., and Chen, C.-S. (2017). Movement patterns determine the availability of Argentine shortfin squid illex argentinus to fisheries. *Fish. Res.* 193, 71–80. doi: 10.1016/j.fishres.2017.03.023

Collins, M., Knutti, R., Arblaster, J., Jean-Louis Dufresne, T. F., Pierre Friedlingstein, X. G., William, J., Gutowski, T. J. Jr, et al (2013). Long-term Climate Change: Projections, Commitments and Irreversibility. In: Climate Change 2013: The Physical Science Basis. Contribution of Working Group I to the Fifth Assessment Report of the Intergovernmental Panel on Climate Change. [Stocker, T.F., D. Cambridge, United Kingdom and New York, NY, USA.: Cambridge University Press.

De Clercq, E. M., Leta, S., Estrada-Peña, A., Madder, M., Adehan, S., and Vanwambeke, S. O. (2015). Species distribution modelling for *Rhipicephalus microplus* (Acari: Ixodidae) in Benin, West Africa: Comparing datasets and modelling algorithms. *Prev. Vet. Med.* 118, 8–21. doi: 10.1016/j.prevetmed.2014.10.015

Delcroix, T., and Murtugudde, R. (2002). Sea Surface salinity changes in the East China Sea during 1997–2001: Influence of the Yangtze river. *J. Geophys. Res. Ocean.* 107, SRF 9–1-SRF 9-11. doi: 10.1029/2001JC000893

Drinkwater, K. F., Miles, M. W., Medhaug, I., Otterå, O. H., Kristiansen, T., Sundby, S., et al. (2013). The Atlantic multidecadal oscillation: Its manifestations and impacts with special emphasis on the Atlantic region north of 60°N. *J. Mar. Syst.* 133. doi: 10.1016/j.jmarsys.2013.11.001

Du, J., William, W. L. C., Chen, B., Qiulin, Z., Shengyun, Y., and Guanqiong, Y. (2013). Progress and prospect of climate change and marine biodiversity. *Biodivers. Sci.* 20, 745–754. doi: 10.3724/SP.J.1003.2012.10051

Elith, J., and Leathwick, J. R. (2009). Species distribution models: Ecological explanation and prediction across space and time. *Annu. Rev. Ecol. Evol. Syst.* 40, 677–697. doi: 10.1146/annurev.ecolsys.110308.120159

Fishery Bureau of Ministry of Agriculture (1987). *The fisheries resources survey and divisions in the East China Sea region* (Shanghai: East China Normal University Press).

Friedman, J. H. (1991). Multivariate adaptive regression splines. *Ann. Stat.* 19, 1–67. doi: 10.1214/aos/1176347963

Grubbs, R. D., Musick, J. A., Conrath, C. L., and Romine, J. G. (2007). Long-term movements, migration, and temporal delineation of a summer nursery for juvenile sandbar sharks in the Chesapeake bay region. *Am. Fish. Soc Symp. Ser.* 50, 87–107.

Guerra, T. P., Santos, J. M. F. F., Pennino, M. G., and Lopes, P. F. M. (2021). Damage or benefit? how future scenarios of climate change may affect the distribution of small pelagic fishes in the coastal seas of the americas. *Fish. Res.* 234. doi: 10.1016/j.fishres.2020.105815

Guisan, A., Edwards, T. C., and Hastie, T. (2002). Generalized linear and generalized additive models in studies of species distributions: setting the scene. *Ecol. Modell.* 157, 89–100. doi: 10.1016/S0304-3800(02)00204-1

Guisan, A., and Thuiller, W. (2005). Predicting species distribution: Offering more than simple habitat models. *Ecol. Lett.* 8, 993–1009. doi: 10.1111/j.1461-0248.2005.00792.x

Han, Q., Grüss, A., Shan, X., Jin, X., and Thorson, J. (2020). Understanding patterns of distribution shifts and range expansion/contraction for small yellow croaker (*Larimichthys polyactis*) in the yellow Sea. *Fish. Oceanogr.* 30. doi: 10.1111/fog.12503

Hu, W., Du, J., Su, S., Tan, H., Yang, W., Ding, L., et al. (2022). Effects of climate change in the seas of China: Predicted changes in the distribution of fish species and diversity. *Ecol. Indic.* 134, 108489. doi: 10.1016/j.ecolind.2021.108489

Jin, X., Zhao, X., and Meng, T. (2005). *Biological resource and habitation environment of the bohai and yellow Sea* (Beijing, China: Science Press).

Johnson, J. B., and Omland, K. S. (2004). Model selection in ecology and evolution. *Trends Ecol. Evol.* 19, 101–108. doi: 10.1016/j.tree.2003.10.013

Jones, M. C., and Cheung, W. W. L. (2015). Multi-model ensemble projections of climate change effects on global marine biodiversity. *ICES. J. Mar. Sci.* 72, 741–752. doi: 10.1093/icesjms/fsu172

Katz, W. T., Snell, J. W., and Merickel, M. B. (1992). Artificial neural networks. *Methods Enzymol.* 210, 610–636. doi: 10.1016/0076-6879(92)10031-8

Kidokoro, H., and Sakurai, Y. (2008). Effect of water temperature on gonadal development and emaciation of Japanese common squid todarodes pacificus (Ommastrephidae). *Fish. Sci.* 74, 553–561. doi: 10.1111/j.1444-2906.2008.01558.x

Kilduff, D. P., DiLorenzo, E., Botsford, L. W., and Teo, S. L. H. (2015). Changing central pacific El niños reduce stability of north American salmon survival rates. *Proc. Natl. Acad. Sci. U. S. A.* 112, 10962–10966. doi: 10.1073/pnas.1503190112

Klemas, V. (2012). Remote sensing of environmental indicators of potential fish aggregation:An overview. *Baltica* 25, 99–112. doi: 10.5200/baltica.2012.25.10

Kroodsma, D. A., Mayorga, J. S., Hochberg, T., Miller, N. A., Boerder, K., F erretti, F., et al. (2018). Tracking the global footprint of fisheries. *Sci. (80-. ).* 359, 904–908. doi: 10.1126/science.aao5646

Last, P. R., White, W. T., Gledhill, D. C., Hobday, A. J., Brown, R., Edgar, G. J., et al. (2011). Long-term shifts in abundance and distribution of a temperate fish fauna: a response to climate change and fishing practices. *Glob. Ecol. Biogeogr.* 20, 58–72. doi: 10.1111/j.1466-8238.2010.00575.x

Liaw, A., and Wiener, M. (2002). Classification and regression by randomForest. *R. News* 2, 18–22.

Lin, X. (1987). Biological characteristics and resources status of three main commercial fishes in offshore waters of China. *J. Fish. China* 11. doi: 10.3321/j.issn:1000-0933.2008.08.001

Lin, L., and Cheng, J. (2004). An analysis of the current situation of fishery biology of small yellow croaker in the East China Sea. *J. Fish. Sci. China* 11. doi: 10.3969/j.issn.1672-5174.2004.04.008

Lin, L., Cheng, J., Jiang, Y., Yuan, X., Li, J., and Gao, T. (2008). Spatial distribution and environmental characteristics of the spawning grounds of small yellow croaker in the southern yellow Sea and the East China Sea. *Acta Ecol. Sin.* 28, 3485–3494. doi: 10.3321/j.issn:1000-0933.2008.08.001

Liu, Y., and Cheng, J. (2018). Bottom-temperature distribution characteristics of small yellow croaker (*Larimichthys polyactis*) in the East China Sea and comparison of analysis methods. *J. Fish. Sci. China* 25, 423–435. doi: 10.3724/SP.J.1118.2018.17216

Liu, S., Liu, Y., Fu, C., Yan, L., Xu, Y., Wan, R., et al. (2018a). Using novel spawning ground indices to analyze the effects of climate change on pacific saury abundance. *J. Mar. Syst.* 191. doi: 10.1016/j.jmarsys.2018.12.007

Liu, Z., Chen, C., Yuan, X., Yang, L., Yan, L., Jin, Y., et al. (2018b). Evaluation of temporal changes of small yellow croaker stock status in East China Sea using trawl survey indices. *J. Fish. Sci. China* 25, 632–641. doi: 10.3724/SP.J.1118.2018.17274

Liu, X., Wu, J., and Han, G. (1990). *Fishery resources investigation and regionalization district in the bohai Sea and the yellow Sea* (Beijing, China: China Ocean Press).

Liu, Y., Xia, X., Tian, Y., Alabia, I., Ma, S., Sun, P., et al. (2021). Influence of spawning ground dynamics on the long-term abundance of Japanese flying squid (Todarodes pacificus) winter cohort. *Front. Mar. Sci.* 8. doi: 10.3389/fmars.2021.659816

Liu, S., Liu, Y., Alabia, I. D., Tian, Y., Ye, Z., Yu, H, et al (2020a). Impact of Climate Change on Wintering Ground of Japanese Anchovy (Engraulis japonicus) Using Marine Geospatial Statistics. *Front. Mar. Sci.* 7, 1–15. doi: 10.3389/fmars.2020.00604

Liu, Z., Yang, L., and Yuan, X. (2020b). Overwintering distribution and its environmental determinants of small yellow croaker based on ensemble habitat suitability modeling. *Chin. J. Appl. Ecol.* 31, 2076–2086.

Li, Z., Ye, Z., Wan, R., and Zhang, C. (2015). Model selection between traditional and popular methods for standardizing catch rates of target species: A case study of Japanese Spanish mackerel in the gillnet fishery. *Fish. Res.* 161, 312–319. doi: 10.1016/j.fishres.2014.08.021

Luan, J., Zhang, C., Xu, B., Xue, Y., and Ren, Y. (2018). Modelling the spatial distribution of three portunidae crabs in haizhou bay, China. *PloS One* 13. doi: 10.1371/journal.pone.0207457

Luan, J., Zhang, C., Xu, B., Xue, Y., and Ren, Y. (2020). The predictive performances of random forest models with limited sample size and different species traits. *Fish. Res.* 227, 105534. doi: 10.1016/j.fishres.2020.105534

Ma, S., Cheng, J., Li, J., Liu, Y., Wan, R., and Tian, Y. (2018). Interannual to decadal variability in the catches of small pelagic fishes from China seas and its responses to climatic regime shifts. *Deep. Sea. Res. Part II. Top. Stud. Oceanogr.* 159, 112–129. doi: 10.1016/j.dsr2.2018.10.005

Ma, J., Qiao, F., Xia, C., and Kim, C. S. (2006). Effects of the yellow Sea warm current on the winter temperature distribution in a numerical model. *J. Geophys. Res. Ocean.* 111, 2–13. doi: 10.1029/2005JC003171

Masson-Delmotte, V., Zhai, P., Pirani, A., Connors, S. L., Péan, C., Berger, S., et al. (2021). "IPCC 2021: Climate change 2021: The physical science basis," in *Contribution of working group I to the sixth assessment report of the intergovernmental panel on climate change*. doi: 10.3724/sp.j.7103161536

Masui, T., Matsumoto, K., Hijioka, Y., Kinoshita, T., Nozawa, T., Ishiwatari, S., et al. (2011). An emission pathway for stabilization at 6 wm–2 radiative forcing. *Clim. Change* 109, 59. doi: 10.1007/s10584-011-0150-5

Morley, J. W., Selden, R. L., Latour, R. J., Frölicher, T. L., Seagraves, R. J., and Pinsky, M. L. (2018). Projecting shifts in thermal habitat for 686 species on the north American continental shelf. *PloS One* 13, 1–28. doi: 10.1371/journal.pone.0196127

Nurdin, S., Mustapha, M. A., Lihan, T., and Zainuddin, M. (2017). Applicability of remote sensing oceanographic data in the detection of potential fishing grounds of rastrelliger kanagurta in the archipelagic waters of spermonde, Indonesia. *Fish. Res.* 196, 1–12. doi: 10.1016/j.fishres.2017.07.029

Perry, A., Low, L., Paula, J., et al. (2005). Climate change and distribution shifts in marine fishes. *Sci. (80-. ).* 308, 1912–1915. doi: 10.1126/science.1111322

Perzia, P., Battaglia, P., Consoli, P., Andaloro, F., and Romeo, T. (2016). Swordfish monitoring by a GIS-based spatial and temporal distribution analysis on harpoon fishery data: A case of study in the central Mediterranean Sea. *Fish. Res.* 183, 424–434. doi: 10.1016/j.fishres.2016.07.006

Phillips, A. J., Ciannelli, L., Brodeur, R. D., Pearcy, W. G., and Childers, J. (2014). Spatio-temporal associations of albacore CPUEs in the northeastern pacific with regional SST and climate environmental variables. *Ices. J. Mar. Sci. J. Du. Cons.* 71, 1717–1727. doi: 10.1093/icesjms/fst238

Potts, S. E., and Rose, K. A. (2018). Evaluation of GLM and GAM for estimating population indices from fishery independent surveys. *Fish. Res.* 208, 167–178. doi: 10.1016/j.fishres.2018.07.016

Riahi, K., Rao, S., Krey, V., Cho, C., Chirkov, V., Fischer, G., et al. (2011). RCP 8.5–a scenario of comparatively high greenhouse gas emissions. *Clim. Change* 109, 33. doi: 10.1007/s10584-011-0149-y

Roberts, J. J., Best, B. D., Dunn, D. C., Treml, E. A., and Halpin, P. N. (2010). Marine geospatial ecology tools: An integrated framework for ecological geoprocessing with ArcGIS, Python, r, MATLAB, and c++. *Environ. Model. Software* 25, 1197–1207. doi: 10.1016/j.envsoft.2010.03.029

Rodionov, S. N. (2004). A sequential algorithm for testing climate regime shifts. *Geophys. Res. Lett.* 31, 2–5. doi: 10.1029/2004GL019448

Sakurai, Y., Kiyofuji, H., Saitoh, S., Goto, T., and Hiyama, Y. (2000). Changes in inferred spawning areas of todarodes pacificus (Cephalopoda : Ommastrephidae) due to changing environmental conditions. *ICES. J. Mar. Sci.* 57, 24–30. doi: 10.1006/jmsc.2000.0667

Shan, X., Li, X., Yang, T., Sharifuzzaman, S. M., Zhang, G., Jin, X., et al. (2017). Biological responses of small yellow croaker (*Larimichthys polyactis*) to multiple stressors: a case study in the yellow Sea, China. *Acta Oceanol. Sin.* 36, 39–47. doi: 10.1007/s13131-017-1091-2

Shui, B. (2003). Study on the age and growth of pseudosciaena polyacti s in the south of the yellow Sea and the north of the East China Sea. *J. Zhejiang. Ocean. Univ.* 29, 80–83. doi: 10.3969/j.issn.1008-830X.2003.01.004

Silva, C., Leiva, F., and Lastra, J. A. (2018). Predicting the current and future suitable habitat distributions of the anchovy (*Engraulis ringens*) using the maxent model in the coastal areas off central-northern Chile. *Fish. Oceanogr.* 28. doi: 10.1111/fog.12400

Smoliński, S., and Radtke, K. (2016). Spatial prediction of demersal fish diversity in the Baltic Sea: Comparison of machine learning and regression-based techniques. *ICES. J. Mar. Sci.* 74. doi: 10.1093/icesjms/fsw136

Thomas, C. D. (2010). Climate, climate change and range boundaries. *Divers. Distrib.* 16, 488–495. doi: 10.1111/j.1472-4642.2010.00642.x

Thomas, C. D., Cameron, A., Green, R. E., Bakkenes, M., Beaumont, L. J., Collingham, Y. C., et al. (2004). Extinction risk from climate change. *Nature* 427, 145–148. doi: 10.1038/nature02121

Valavanis, V. D., Georgakarakos, S., Kapantagakis, A., Palialexis, A., and Katara, I. (2004). A GIS environmental modelling approach to essential fish habitat designation. *Ecol. Modell.* 178, 417–427. doi: 10.1016/j.ecolmodel.2004.02.015

Valavanis, V. D., Pierce, G. J., Zuur, A. F., Palialexis, A., Saveliev, A., Katara, I., et al. (2008). Modelling of essential fish habitat based on remote sensing, spatial analysis and GIS. *Hydrobiologia* 612, 5–20. doi: 10.1007/s10750-008-9493-y

Vanderwal, J., Murphy, H. T., Kutt, A. S., Perkins, G. C., Bateman, B. L., Perry, J. J., et al. (2013). Focus on poleward shifts in species' distribution underestimates the fingerprint of climate change. *Nat. Clim. Change* 3, 239–243. doi: 10.1038/nclimate1688

Van Vuuren, D. P., Edmonds, J., Kainuma, M., Riahi, K., Thomson, A., Hibbard, K., et al. (2011). The representative concentration pathways: an overview. climatic change. this issue. *Clim. Change* 109, 5–31. doi: 10.1007/s10584-011-0148-z

Vincenzi, S., Zucchetta, M., Franzoi, P., Pellizzato, M., Pranovi, F., De Leo, G., et al. (2011). Application of a random forest algorithm to predict spatial distribution of the potential yield of ruditapes philippinarum in the Venice lagoon, Italy. *Ecol. Modell.* 222, 1471–1478. doi: 10.1016/j.ecolmodel.2011.02.007

Wang, L., Ma, S., Liu, Y., Li, J., Liu, S., Lin, L., et al. (2021). Fluctuations in the abundance of chub mackerel in relation to climatic/oceanic regime shifts in the northwest pacific ocean since the 1970s. *J. Mar. Syst.* 218, 103541. doi: 10.1016/j.jmarsys.2021.103541

Watanabe, T. (1970). Morphology and ecology of early stages of life in Japanese common mackerel, scomber japonicus houttuyn, with special reference to fluctuation of population. *Bull.tokai. Reg.fish.res.lab.* 62.

Watts, M. J., Li, Y., Russell, B. D., Mellin, C., Connell, S. D., and Fordham, D. A. (2011). A novel method for mapping reefs and subtidal rocky habitats using artificial neural networks. *Ecol. Modell.* 222, 2606–2614. doi: 10.1016/j.ecolmodel.2011.04.024

Welch, D. W., Chigirinsky, A. I., and Ishida, Y. (2011). Upper thermal limits on the oceanic distribution of pacific salmon (*Oncorhynchus* spp.) in the spring. *Can. J. Fish. Aquat. Sci.* 52, 489–503. doi: 10.1139/f95-050

Wood, S. N. (2006). *Generalized additive models: an introduction with r* (Boca Raton: Chapman and Hall/CRC Press). doi: 10.1201/9781315370279

Wu, B., Lin, X., and Yu, L. (2020). North pacific subtropical mode water is controlled by the Atlantic multidecadal variability. *Nat. Clim. Change* 10, 238–243. doi: 10.1038/s41558-020-0692-5

Xiao, Z., Wu, J., Xu, B., Zhang, C., Ren, Y., and Xue, Y. (2019). Uniqueness measure based on the weighted trophic field overlap of species in the food web. *Ecol. Indic.* 101, 640–646. doi: 10.1016/j.ecolind.2019.01.042

Xu, Z., and Chen, J. (2009). Analysis on migratory routine of larimichthy polyactis. *J. Fish. Sci. China* 16, 931–940. doi: 10.3321/j.issn:1005-8737.2009.06.014

Xue, Y., Jin, X., Zhang, B., and Liang, Z. (2004). Ontogenetic and diel variation in feeding habits of small yellow croaker pseudosci- aena polyactis bleeker in the central part of yellow Sea. *J. Fish. Sci. China* 11. doi: 10.3321/j.issn:1005-8737.2004.05.007

Yan, L., Liu, Z., Zhang, H., Ling, J., Yuan, X., and Li, S. (2014). On the evolution of biological characteristics and resources of small yellow croaker. *Mar. Fish.* 36, 481–488. doi: 10.3969/j.issn.1004-2490.2014.06.001

Yuan, X., Liu, Z., Jin, Y., CUI, X., Zhou, W., and Cheng, J. (2017). Inter-decadal variation of spatial aggregation of trichiurus japonicus in East China Sea based on spatial autocorrelation analysis. *Chin. J. Appl. Ecol.* 28, 3409–3416. doi: 10.13287/j.1001-9332.201710.040

Yu, W., Zhang, Y., Chen, X., Yi, Q., and Qian, W. (2018). Response ofwinter cohort abundance of Japanese common squid todarodes pacificus to the ENSO events. *Acta Oceanol. Sin.* 37, 61–71. doi: 10.1007/s13131-018-1186-4

Zhu, Y., Luo, Y., and Zhu, Y. (1963). *Study on the classification of sciaenid fishes in China and description of new genus and species* (Shanghai: Shanghai Scientific and Technical Publishers).

frontiers | Frontiers in Marine Science

TYPE Original Research
PUBLISHED 25 August 2022
DOI 10.3389/fmars.2022.961735



OPEN ACCESS

EDITED BY
Jun Xu,
Institute of Hydrobiology, (CAS), China

REVIEWED BY
Xiujuan Shan,
Yellow Sea Fisheries Research Institute, (CAFS), China
Xuefeng Wang,
Guangdong Ocean University, China

*CORRESPONDENCE
Yongdong Zhou
zyd511@126.com

†These authors have contributed equally to this work and share first authorship

SPECIALTY SECTION
This article was submitted to Marine Ecosystem Ecology, a section of the journal Frontiers in Marine Science

RECEIVED 05 June 2022
ACCEPTED 08 August 2022
PUBLISHED 25 August 2022

CITATION
Jiang R, Sun H, Li X, Zhou Y, Chen F, Xu K, Li P and Zhang H (2022) Habitat suitability evaluation of *Harpadon nehereus* in nearshore of Zhejiang province, China.
*Front. Mar. Sci.* 9:961735.
doi: 10.3389/fmars.2022.961735



# Habitat suitability evaluation of *Harpadon nehereus* in nearshore of Zhejiang province, China

Rijin Jiang[1†], Haoqi Sun[2†], Xiafang Li[2], Yongdong Zhou[1*], Feng Chen[1], Kaida Xu[1], Pengfei Li[1] and Hongliang Zhang[1]

[1]Zhejiang Marine Fisheries Research Institute, Scientific Observing and Experimental Station of Fishery Resources for Key Fishing Grounds, Ministry of Agriculture, Key Laboratory of Sustainable Utilization of Technology Research for Fishery Resources of Zhejiang Province, Zhoushan, China, [2]Marine and Fishery Institute, Zhejiang Ocean University, Zhoushan, China

Coastal waters provide an important spawning and nursery ground for offshore marine organisms. To understand the suitable habitat and distribution of *Harpadon nehereus*, a key nearshore species, this study assessed the survey data of fishery resources and environment in Zhejiang's nearshore fishery in Spring of 2017 to 2020. We used the generalized additive model (GAM) and random forests model (RF) to analyze the environmental factors affecting the selection of spawning habitats by *H. nehereus* and analyzed the suitable habitat characteristics of *H. nehereus* in nearshore fisheries. Our results indicate that *H. nehereus* is widely distributed in Zhejiang's nearshore and that its density is higher in waters near islands and reefs. Among the relative importance scores of predictors calculated based on RF, seawater salinity is an important environmental factor affecting the distribution of *H. nehereus* in April (surface seawater salinity was 38.67% and bottom seawater salinity was 34.5%), followed by depth (34.19%), whereas the change in water temperature had no obvious effect on *H. nehereus* distribution. The suitable habitat characteristics of *H. nehereus* mainly include high salinity near a water depth of 40 m and a water area with sea bottom dissolved oxygen levels < 6 mg/L. The prediction results of the model indicate that the suitable habitat of *H. nehereus* is mainly located in the region near Zhoushan Islands in the north of the fishing grounds. Overall, these results may serve as a basis for determining the protection strategies of key nearshore species and enhancing fishery management units.

KEYWORDS

***Harpadon nehereus*, species distribution model, suitable habitat characteristics, environmental factors, coastal waters**

# 1 Introduction

Marine fishery resources provide a strong guarantee for human survival (Botsford et al., 1997), and their optimal utilization and a healthy ecosystem are prerequisites for sustainable fisheries production (Rice, 2005). The choice of the location is important for marine fish to increase opportunities for feeding and escaping predation and to fulfill the necessary requirements of fish for survival from the egg to the adult stage and subsequently dispersing across different habitats (Ciannelli et al., 2015). Individuals usually choose their aquatic habitats based on factors such as salinity and temperature within their physiological tolerance range as habitat (Gordó-Vilaseca et al., 2021).

Coastal waters provide important habitats for a wide range of fish species. These waters sustain terrestrial and marine-origin nutrient supplies and spatiotemporal changes in the nearshore physicochemical environment (e.g., water depth, temperature and salinity) due to flood and ebb tides (Kasai et al., 2010; Wang et al., 2019; Kume et al., 2021). Furthermore, they create different types of fluctuating habitats, which provide a highly productive, ever-changing ecosystem for fish communities (Seitz et al., 2014; Potter et al., 2015). Environmental factors (e. g., water temperature, salinity, and their fluctuations) are thought to be some of the main contributors to large-scale patterns of coastal fish communities (Florin et al., 2009; Pasquaud et al., 2015; Kume et al., 2021). For example, adult *Perca fluviatilis* prefer shallow areas with suitable temperature development as their spawning habitat during spring (Snickars et al., 2010). The depth and habitat use affect seasonal up and downslope movements of *Gadus morhua* in the Western Baltic Sea (Funk et al., 2020). Coastal waters are, therefore, recognized to play an important ecosystemic role at the land–sea interface in order to generate and sustain high levels of production in the fisheries. However, these areas are also highly susceptible to human activities, including fishing and urban construction, which can lead to changes in coastal fish habitats (Ciannelli et al., 2015).

*Harpadon nehereus* is a marine species dependent on coastal habitats, especially in early developmental stages. Compared to other economic species (e.g., *Larimichthys crocea*, *Trichiurus haumela*), *H. nehereus* had long been considered as a low-valued species for a long time and was not the main target species for fisheries. However, due to its muti-stage of spawning, high survival rates and fast growth, *H. nehereus* comprised the majority of fishery composition in Zhejiang coastal areas (Chen and Zhang, 2015; Wang et al., 2021, Jiang et al., 2019). The suitability of the habitat, as well as the availability of feed preferred by fish may play important roles in the thriving. Recent surveys of fisheries community resources indicate that *H. nehereus* has become a dominant species in some areas off the coast of China, such as the Yueqing Bay and the Yangtze River Estuary (Sun et al., 2015; Yuan et al., 2017). Among the fish species found in the southern Zhejiang coastal waters (Wang et al., 2022), *H. nehereus* is the second most important species after *Trichiurus lepturus*, which plays a decisive role in the stability of fish community structure and the transmission of interspecies information in coastal waters. Changes in the patterns of activities of different species can change the food web structure at the regional scale, affect the relationship between feeding and competition, and alter ecosystem functions (Long and Seitz, 2008). The habitat preferences of fish determine their food sources in waters of different depths. *H. nehereus* is an omnivorous fish with a wide range of feeding habits, and large individuals demonstrate cannibalistic behavior (Allen et al., 2014); its increasing dominance has widespread implications for existing food webs and community structures. Wang et al. (2021) pointed out that with climate change, *H. nehereus* is moving northward along the coast of China, which may compress the ecological niches of other coastal species and affect marine ecosystems.

The relationship between resources and the marine environment is complex. Generally, the movement, activity, and connectivity patterns of fish are influenced by dynamic environmental conditions (Perry et al., 2018). Ambient salinity determines a fish's capability to adapt to environmental variations. For instance, when fish such as *Trachinotus marginatus* and *Sparus aurata* are exposed to low salinity gradients, fish oxygen consumption increases and fish mortality increases, and as salinity increases, fish become more tolerant of toxic compounds, such as ammonia (Costa et al., 2008; Kir and Sunar, 2018; Kir et al., 2019). Annual mean benthic water temperature is reportedly the most important variable in determining the distribution of *H. nehereus* (Wang et al., 2021). Moreover, water temperature has a strong influence on the distribution patterns of coastal fish such as *Gadus morhua* (Staveley et al., 2019) and *Homarus americanus* (Jury and Watson, 2013), that seek suitable habitats by migrating seasonally in relation to water temperature (Freitas et al., 2021).

Habitat protection of coastal fishery resources is a hotspot of relevant research. At present, research on the characteristics of fish habitats mainly focuses on particular species (e.g., *Conger myriaster*, *Albula vulpes*) with high economic and ecological value (Li et al., 2017; Brownscombe et al., 2019). According to pertinent research in recent years, *H. nehereus* has gradually become an important dominant species in the coastal waters of China, occupying a dominant position in some sea areas, but few studies have assessed its habitat needs. In the present study, we chose *H. nehereus* as an example to evaluate the modelling approach for the key species affecting coastal ecosystems. The objectives of this study were to: (1) assess the driving environmental variables for determining the distribution of *H. nehereus*; and (2) The distribution pattern of suitable habitats of *H. nehereus* in Zhejiang's coastal waters. This study could help strengthen environmental impact assessments and support decision-making in ocean planning.

# 2 Material and methods

## 2.1 Sampling method and stations

The study area is located in the mid-west of the East China Sea (Figure 1) and is affected by different water masses and scouring waters; the salinity gradient changes greatly, and food is plentiful. The coastal waters of Zhejiang are located in the western East China Sea, which is an important site for fish spawning, feeding, breeding, and migration (Wang and Fan, 2004; Su and Yuan, 2005). The area has many islands, and the coastline is tortuous. Water circulation and water mass interactions make this area a suitable hydrological environment rich in basic nutrients that provide a variety of habitats for various fish species (Wang and Fan, 2004; Zhang et al., 2020).

Bottom trawl surveys were carried out in the spring (April) of 2017–2020 off the coast of Zhejiang (27°00′N–31°00′N, 120°30′E –121°30′E). The isobath of the surveyed sea area is parallel to the shoreline. Therefore, we set up a total of 123 stations according to the distance from the shore and adopted the fixed-point survey method for sampling in different years. The type of fishing boat used was a single-bottom trawler, with a main engine power of 220 kw. The surveys were conducted at 3 knots for about 30 minutes on average. The mesh size of the capsule net was 25 mm, and the perimeter of the net port was 50 m. A catch was landed at each survey station, and the weight of the catch was converted into the catch per unit net with a drag speed of 2.0 kn and a trawl time of 1.0 h as the resource abundance index.

## 2.2 Environmental variables

In addition to obtaining the resource data of the dominant fish at various stations, we also used multifunctional water quality meters to synchronously obtain environmental data. Organisms have a tolerance range for environmental variables and environmental conditions suitable for their habitats (Shelford, 1911). The spawning period of *H. nehereus* is mainly from May to September. In April, *H. nehereus* migrates from offshore to coastal waters for spawning. *H. nehereus* is benthopelagic, living in brackish water and seawater, preferring to inhabit shallow depths (0–150 m). *H. nehereus* lays floating eggs, which are greatly affected by the sea surface environment. Considering the biological characteristics, and the availability and reliability of data, the chosen environmental variables mainly included depth, surface, and bottom environment variables (sea temperature, salinity, chlorophyll, and dissolved oxygen). The environmental variables (temperature, salinity, chlorophyll, and dissolved oxygen) were sampled simultaneously. The details are included in Table 1.

## 2.3 Data analysis

This study mainly used models to analyze trends in environmental variables that affect species distribution.

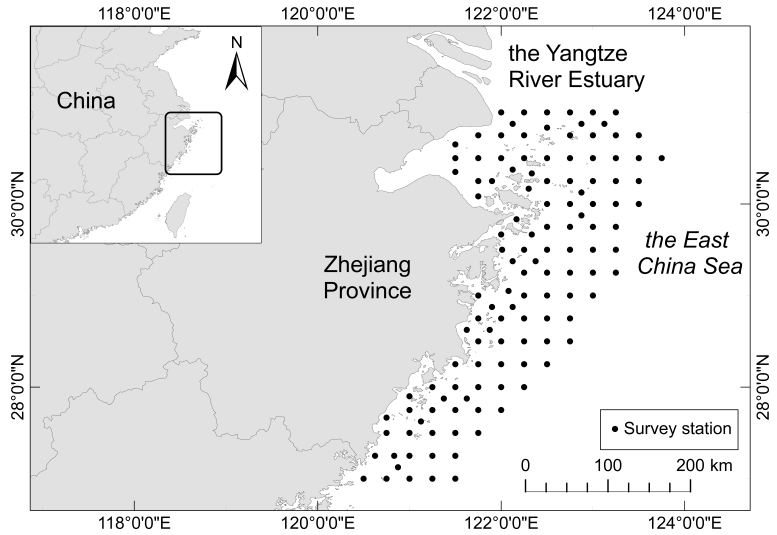


FIGURE 1
Survey locations of *H. nehereus* for all survey years.

TABLE 1 Statistical summary of predictor variables.

| Variable | Description | Range (Mean) | | | |
|---|---|---|---|---|---|
| | | 2017 | 2018 | 2019 | 2020 |
| Lon | Longitude | 120.5–123.75 | 120.5–123.75 | 120.5–123.75 | 120.5–123.75 |
| Lat | Latitude | 27–31 | 27–31 | 27–31 | 27–31 |
| Depth | Depth of water (m) | 3.32–70.48 (31.72) | 4.35–75.36 (32.58) | 3.42–73.45 (31.75) | 7.40–69.94 (34.62) |
| SST | Sea surface temperature (°C) | 12.92–19.61 (15.88) | 12.41–21.15 (15.96) | 13.43–21.51 (16.77) | 13.52–20.09 (15.62) |
| BST | Sea bottom temperature (°C) | 12.97–19.75 (15.80) | 12.84–19.33 (15.88) | 13.30–20.72 (16.75) | 13.58–19.92 (15.85) |
| SSS | Sea surface salinity (PSS) | 8.40–32.63 (26.89) | 6.39–34.14 (28.66) | 1.33–34.21 (26.81) | 8.37–34.23 (27.65) |
| BSS | Sea bottom salinity (PSS) | 10.81–39.59 (28.95) | 7.38–34.48 (30.28) | 6.93–34.61 (28.56) | 11.91–34.52 (27.43) |
| Sch.a | Sea surface chlorophyll a (μg/L) | 0.45–43.54 (7.08) | 0.02–58.37 (4.69) | 0.03–23.74 (2.78) | 0.08–87.23 (8.04) |
| Bch.a | Sea bottom chlorophyll a (μg/L) | 0.169–42.51 (9.21) | 0.06–62.74 (6.72) | 0.03–83.79 (11.74) | 0.01–89.42 (7.26) |
| SDO | Sea surface dissolved oxygen (mg/L) | 7.85–12.94 (9.37) | 7.24–11.88 (8.93) | 7.03–13.52 (8.88) | 8.01–11.75 (9.26) |
| BDO | Sea bottom dissolved oxygen (mg/L) | 2.81–9.17 (7.35) | 1.71–9.22 (7.14) | 2.83–9.92 (7.12) | 2.08–9.71 (7.32) |

### 2.3.1 Generalized additive models

Generalized additive models (GAM) (Hastie and Tibshirani, 1990) are universal and convenient statistical algorithms in traditional regression methods and are often used for standardizing catch data. GAMs are an extension of generalized linear models (GLMs), and both are based on the statistical distribution of response variables for data analysis (Li et al., 2017). GLMs assume that the predictive function between the response variable and the explanatory variable is a linear relationship, whereas GAMs consider a non-linear relationship (Wang et al., 2019). Data analysis is based on the additive predictive function, which ensures that the model has some non-parametric characteristics. The formula of GAM is as follows:

$$g(y) = a + \sum_{i=1}^{i} f_i(x_i) + \epsilon \quad (1)$$

where $g$ is the differentiable and monotonic link function, $y$ is the response variable, $\alpha$ is the function intercept, $f_i$ is a smooth function, $x_i$is the predictor variable, and $\epsilon$ is a random error term.

Owing to the unique geographical location of the marine environment, some environmental variables may have strong correlations. To reduce the influence of predictor variables with multicollinearity on the model fitting results, we first performed a correlation analysis on the predictor variables and conducted preliminary screening of the predictor variables added to the model. Thus, we only considered removing the predictor variables with strong collinearity in the process of constructing the GAM.

### 2.3.2 Random forests

Random forest (RF) (Breiman, 2001) is an improved method for bagged trees, and has the advantage of combining many randomly constructed decision trees to reduce the influence of outliers and redundant data on the prediction results. RF can quantify complex nonlinear relationships without obvious overfitting. According to the RF algorithm summarized by Liaw et al. (Liaw and Wiener, 2002), the operation of the model is mainly controlled by two model parameters, $n_{tree}$ and $m_{try}$; $n_{tree}$ determines the number of decision trees and $m_{try}$ determines the number of random features. The $n_{tree}$ value is generally determined by the relationship between the result and error, and $m_{try}$ defaults to 1/3 of the number of predictors. In this study, we determined that $n_{tree}$ was 1000 according to the stable trend, and that $m_{try}$ was 4.

We can also sort the relative importance of predictors using RF and the relative importance score calculation formula is as follows:

$$V_i = \frac{1}{n_{tree}} \sum v \in S_{X_i} G(X_i, v) \quad (2)$$

where $V_i$represents the explanatory rate of the predictor variable $X_i$ to the model, $S_{Xi}$ represents the set of nodes split by $X_i$ in the random forest of $n_{tree}$ trees, and $G$ ($X_i$, $v$) represents the

Gini information gain of $X_i$ at the split node $v$, which is used to select the explanatory variable of the maximum information gain.

## 2.4 Model evaluation

To ensure that the model has high accuracy and to add fewer predictor variables, we usually use the Akaike information criterion (AIC) as an index to filter the model (Akaike, 1998). However, owing to algorithm differences, this may not be applicable to tree-based regression (Li et al., 2015). This study combined AIC and mean absolute deviation (MAD) to screen the predictor variables added to the GAM, whereas the predictor screening of the RF model was completely based on MAD. Smaller values of the AIC and MAD are considered to indicate a higher accuracy of the model. In the fitting process, a backward selection regression method was used to substitute the predictor variables into the model, and the optimal model was selected based on AIC and MAD, as described previously (Li et al., 2015).

The AIC can be computed as follows:

$$\mathrm{AIC} = 2k - 2lnL \tag{3}$$

where $k$ is the number of parameters, $L$ is the likelihood function.

MAD can be computed as follows:

$$\mathrm{MAD} = \frac{1}{N}\sum_{i=1}^{N}|y_i - \hat{y}_i| \tag{4}$$

where $N$ is the number of samples,$\hat{y}_i$is the estimated value (the predicted value) from the model for the th observation, and is the actual value.

K-fold cross-validation is a common method for comparing different types of models and their prediction performance (Arlot and Celisse, 2010; Li et al., 2015). Therefore, we used it to evaluate the prediction performance of the RF and GAM. We used 80% of the dataset as the training set and the remaining 20% as the test set. Further, to facilitate the subset method for replacing a single model, we performed independent repeated sampling on the subset. The entire process was repeated 100 times. To quantitatively evaluate the prediction performance of the model, performance was mainly based on the root mean square error (RMSE) of the predicted value of the model (Hyndman and Koehler, 2006), the degree of linear regression between the predicted value, and the actual value in the test set.

To understand the distribution of suitable habitats for *H. nehereus* in different years using the two models, we divided the research water area into a grid size of 0.1° × 0.1° and obtained the coordinates of the center point of each grid. According to the environmental survey data of each site from 2017 to 2020, the conventional Kriging interpolation method was used to calculate the environmental data of the center point for each grid. The relative resource density of each center point was obtained based on the GAM and RF model, and the habitat suitability index (HSI) was calculated as follows:

$$HSI_{i,t} = \frac{\hat{y}_{i,t} - \hat{y}_{min,t}}{\hat{y}_{max,t} - \hat{y}_{min,t}} \tag{5}$$

here $HSI_{i,t}$ is the habitat suitability index of the ith grid point in year t, $\hat{y}_{i,t}$is the predicted value of the ith grid point in year t predicted by the model. $\hat{y}_{max,t}$ and $\hat{y}_{min,t}$are the highest and lowest values for the predicted value of year t, respectively.

# 3 Results

## 3.1 Distribution of *harpadon nehereus*

There were more high-value biomass stations in 2018 than in the previous years (Figure 2). By comparing the number of high-density stations in the surveyed sea area, *H. nehereus* biomass in the sea area near 30°N was found to be significantly higher than that at 28°N (t test $p$<0.05), and the center of gravity of *H. nehereus* resources in different years was basically the same.

## 3.2 Analysis and screening of the influence of factors

Habitat is an important factor that affects species distribution. By constructing a Spearman correlation matrix, we preliminarily understood the relationship between *H. nehereus* population resources and different non-biological variables and analyzed the correlation strength between two different predictor variables (Figure 3). Pearson's $R$ was used as the correlation coefficient between various predictor variables. The larger the color block, the greater was the correlation. The color of the block represents the size of the coefficient. Mantel's $R$ and Mantel's $P$ respectively represent the correlation coefficient and the significance of the degree of correlation between the resource density of *H. nehereus* and predictor variables. The results show that the amount of *H. nehereus* resources is significantly correlated with depth, sea surface temperature (SST), and Sea bottom temperature (BST) ($P < 0.01$), and that the correlation coefficient with SST was the highest among them. Further, the resources were also significantly correlated with the Longitude, Latitude, and sea surface salinity (SSS) ($P < 0.05$).

Among the predictor variables, there was a strong correlation between Depth, Longitude, BST, and sea bottom salinity (BSS); the correlation coefficient between longitude and latitude was the largest, and that between SST and BST was higher than that of other variables. To reduce the influence of collinearity on the fitting effect of the GAM, we performed a multicollinearity test on the predictor variables based on the variance inflation factor (VIF); as Longitude and other variables (Longitude VIF value > 4) have the dramback of multicollinearity, Longitude was not considered a predictor variable when constructing the GAM.

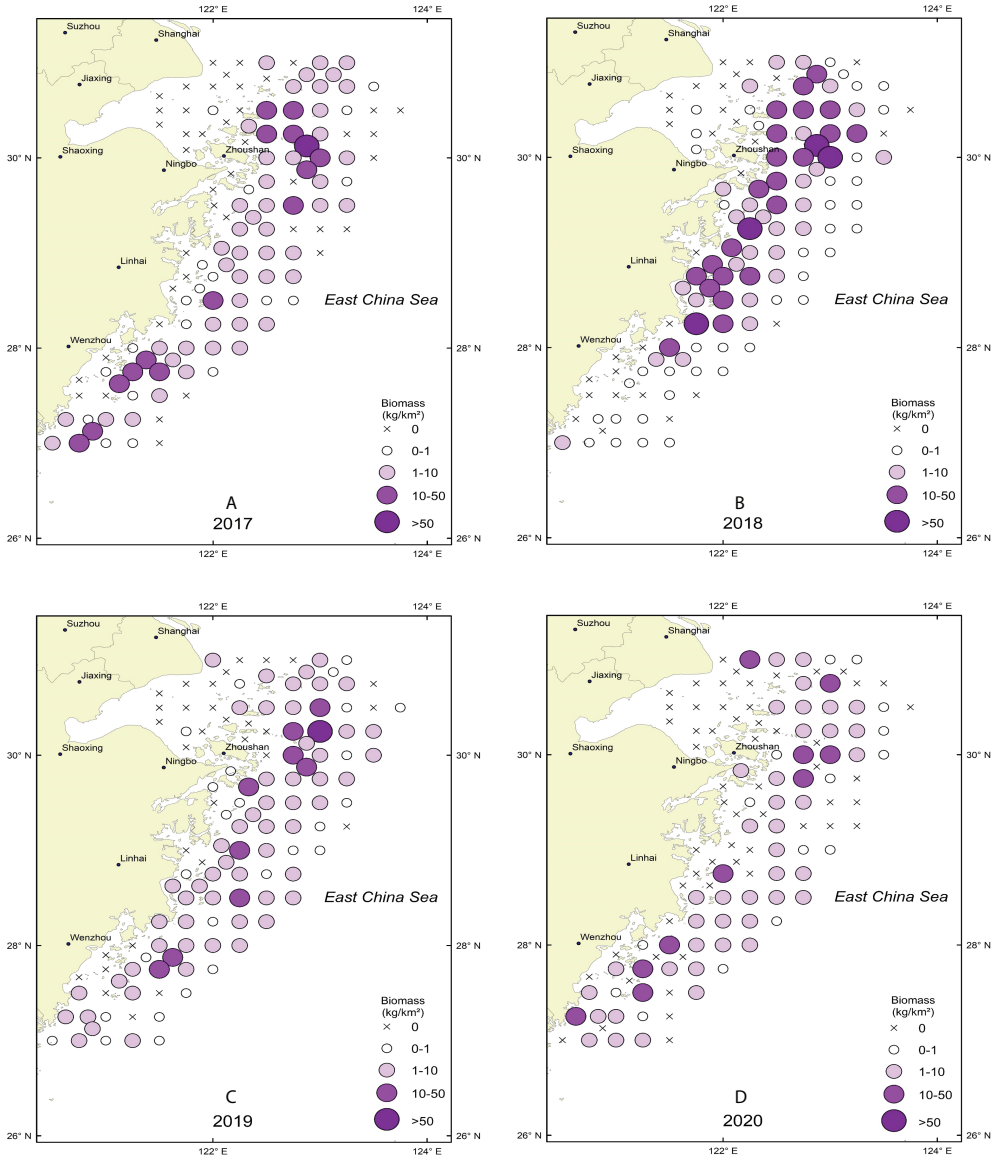


FIGURE 2
Spatial distribution of *H. nehereus* from 2017 to 2020. (**A**: 2017. **B**: 2018. **C**: 2019. **D**:2020).

Simultaneously, one of the predictor variables with strong correlation was selected as an explanatory variable and added to the GAM.

## 3.3 Model fitting results

In the model fitting process, we logarithmized the response variables and biomass data of *H. nehereus* at each station to reduce the influence of some maximum values on the model fitting effect. Table 2 shows the best model results for the GAM and RF after stepwise screening. The explained deviation between the two models is small, and several predictor variables have a significant effect on the response variable. We calculated the relative importance scores of predictors based on the RF model (Figure 4); SSS, BSS, and depth are the three most important predictor variables for the distribution of *H. nehereus* (relative importance scores > 30%).

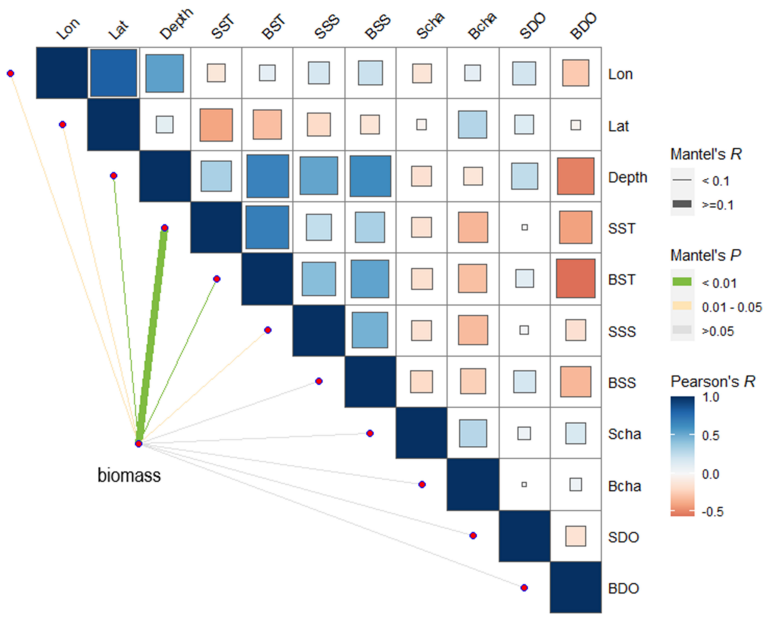


FIGURE 3
Correlation matrix for the relative biomass of *H. nehereus* and predictor variables. Pearson's *R* was used as the correlation coefficient between various predictor variables. The larger the color block, the greater was the correlation. The color of the block represents the size of the coefficient. Mantel's *R* and Mantel's *P* respectively represent the correlation coefficient and the significance of the degree of correlation between the resource density of *H. nehereus* and predictor variables.

## 3.4 The influence of different factors on the resource density of *H. nehereus*

In the best GAM and RF models (Figures 5, 6), the influence of different predictors on *H. nehereus* resource fluctuations indicated that, the year had little effect on the changes in the resources of *H. nehereus* (Figures 5A, 6A). In the fitting results of the two models, different predictors showed a nonlinear relationship with the density of *H. nehereus*. Under the same predictor, the trends of changes in the resources of *H. nehereus* fitted with the two models were similar (for example, in the RF model fitting results, the trend of relative biomass with SSS was similar to the lower limit of the 95% confidence interval in the GAM).

TABLE 2 Summary of the optimal fitted results of the models.

| **Models** | | **GAM** | | **RF** | |
|---|---|---|---|---|---|
| Explanation % | | 39.50 | | 40.85 | |
| AIC | | 444.65 | | \ | |
| MAD | | 0.28 | | 0.12 | |
| | | Added variables | Significance level | Added variables | Significance level |
| variables | Year | + | | + | |
| | Lon | \ | \ | + | ** |
| | Lat | + | ** | + | ** |
| | Depth | + | * | + | ** |
| | SST | \ | \ | + | ** |
| | BST | \ | \ | + | ** |
| | SSS | + | * | + | ** |
| | BSS | + | ** | + | ** |
| | BDO | + | ** | + | ** |

+ indicates the explanatory variable of the optimal model after screening, ** indicates that the predictor variable has a very significant influence on the response variable ($P < 0.01$); *indicates that the predictor variable has a significant influence on the response variable ($P < 0.05$).

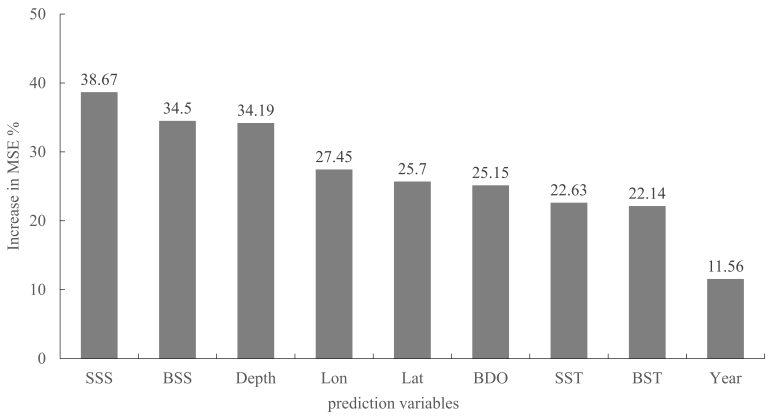


FIGURE 4
Relative importance of predictor variables for determining the distribution of *H. nehereus*. The relative importance score of the predictor variables was calculated based on RF; the higher the score, the more important the predictor variables are in explaining the distribution of *H. nehereus*.

Fluctuations in *H. nehereus* resources mainly occurred in high-salinity waters. When SSS > 25, there was an obvious trend of first increasing and then decreasing resource density, and the maximum resources appeared at SSS 30 (Figures 5B, 6B). At BSS > 15, the amount of *H. nehereus* resources increased with an increase in BSS (Figures 5D, 6D). The suitable SSS range was 25–32 and the suitable BSS range was 27–34. The resource density of *H. nehereus* presented a trend of first increasing and then decreasing with a change in water depth (Figures 5C, 6C). When the BDO concentration was less than 7 mg/L, the resource density of *H. nehereus* did not decrease significantly (Figure 5E, 6E). The areas with a high density of *H. nehereus* resources were mainly distributed between 28°N–30° N (Figures 5F, 6F) and 122°E–123°E (Figure 6G). An impact of water temperature on *H. nehereus* resources was mainly observed at SST < 16°C (Figure 6I), and the changing trend of resources with BST was not obvious (Figure 6H).

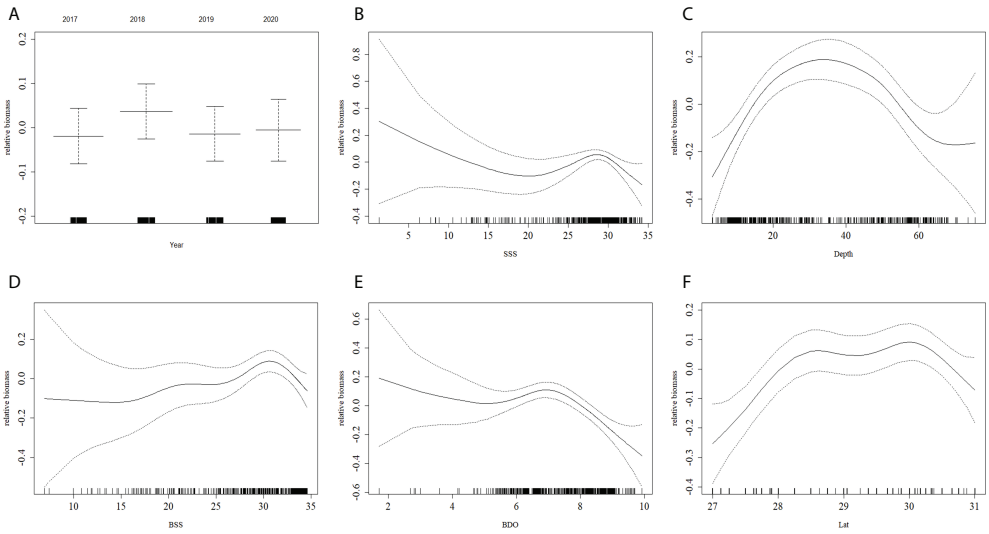


FIGURE 5
Effects of factors from GAM on the relative biomass of *H. nehereus*. (**A**: Year. **B**: SSS. **C**: Depth. **D**: BSS. **E**: BDO. **F**: Lat).

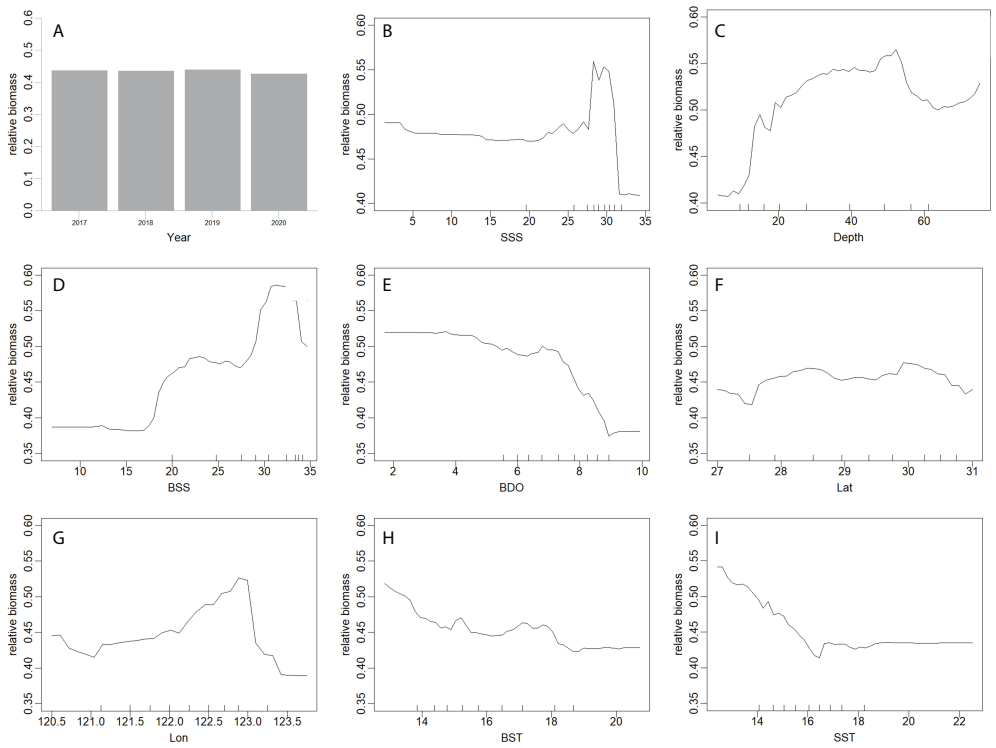


FIGURE 6
Effects of factors from RF on the relative biomass of *H. nehereus*. (**A**: Year. **B**: SSS. **C**: Depth. **D**:BSS. **E**: BDO. **F**: Lat. **G**: Lon. **H**: BST. **I**: SST).

## 3.5 Model prediction performance evaluation and display

Each group of data in the table represents the mean and range of the statistical results (Figure 7). In the cross-validation results, the average RMSE of the RF model (0.10) was less than that of GAM (0.23). In the linear regression results of the true and predicted values, the statistical results of the slope and the intercept of the two models had relatively small differences. The average coefficient of determination for RF cross-validation was 0.73, which was higher than that of GAM at 0.30 (Table 3). Overall, RF was better than GAM in terms of the model prediction performance.

The habitat suitability index (HSI) was used to predict the suitable habitat of *H. nehereus* based on the two models (Figure 7). A HSI with a numerical value from 0 to 1 represents a range from an unsuitable area (HSI value is 0) to the most suitable area (HSI value is 1). The highly suitable area for *H. nehereus* based on GAM fitting was wider than that obtained with the RF model. The central and northern waters of the study area were found to be highly suitable areas for *H. nehereus*. The eastern sea area of Zhoushan Islands was found to be the most suitable area for the distribution of *H. nehereus*. Further, the distribution areas of highly suitable habitats of *H. nehereus* also varied in different years.

# 4 Discussion

## 4.1 The influence of environmental variables

The oceanographic environment is a direct factor that stimulates fish to spawn and migrate. Consequently, factors such as water temperature and salinity affect the distribution of fish spawning grounds (Ciannelli et al., 2015). *H. nehereus* spawn over a prolonged time period ranging from summer to autumn, under the influence of coastal currents and the Kuroshio Current. The adult *H. nehereus* begin to swim from wintering waters (e.g., the East China Sea, the Yellow Sea) to nearshore waters in spring (Luo et al., 2012). Under the right conditions, the spawning brood stock of *H. nehereus* migrates to the offshore areas and estuaries to spawn (Taqwa et al., 2020; Wang et al., 2021). Salinity and depth were the most powerful predictors for *H. nehereus* distribution in spring. These patterns may be attributed to the seasonal migratory habits of *H.*

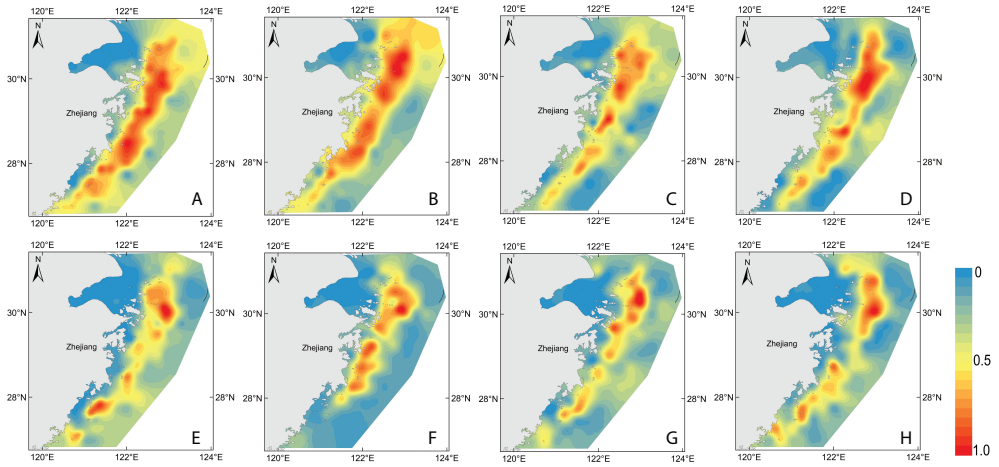


FIGURE 7
Maps of 2017–2020 model-based habitats suggested to be suitable for *H. nehereus*. **(A–D)**: 2017–2020 GAM model-based habitats, **(E–H)**: 2017–2020 RF model-based habitats.

*nehereus*, including spawning and overwintering migration. Furthermore, predation, starvation, or abnormal diffusion processes can limit the change in the habitat that fish experience from year to year (Jørgensen et al., 2008).

In this study, sea salinity had a significant influence on the distribution of *H. nehereus* in spring, which could be attributed to its selection of suitable habitats (Wang et al., 2019). The species was heavily concentrated in estuaries and offshore areas, indicating that it has a wide salinity tolerance range. Furthermore, *H. nehereus* has also been reported to be highly abundant in other coastal hypersaline habitats due to its ecological tolerance. (Nooralabettu, 2008; Liu et al., 2021; Wang et al., 2021) However, for coastal fish, the osmoregulatory mechanism in different life stages may differ. (Allen et al., 2014; Thomas et al., 2021) For example, *Pomatoschistus microps* is a widespread small-sized fish occurring in temperate estuaries, which has a relatively wide tolerance for salinity variation. However, juveniles display better physiological performances at low levels of salinity. (Souza et al., 2018) During the course of this study, 70% of *H. nehereus* samples captured in spring were adults with a body length greater than 160 mm. Compared with juveniles, adults have stronger swimming capability and can choose more suitable habitats for survival.

The salinity of the East China Sea was generally > 30‰ (Luo et al., 2012), and living in waters with similar salinity can ensure that *H. nehereus* will not experience a strong acute stress response (Ciannelli et al., 2015). Therefore, it would be able to meet osmoregulation and ionoregulation needs with lower energy expenditure. Additionally, the higher biomass of *H. nehereus* in high salinity waters may be related to the distribution of prey organisms. *Benthosema pterotum* and *Apogon lineantus* are the main prey organisms for *H. nehereus* in spring, and the optimum seawater salinities for the two species are 29.7-34‰ and 31.4-32‰, respectively (Liu et al., 2021; Tang et al., 2021). *H. nehereus* swim to the area where the prey organisms are located to forage, despite the increased energetic costs of living at higher salinities. Consequently, the distribution of the prey organisms may be one of the influencing factors of sea salinity on the distribution of *H. nehereus*.

Shallow waters have long been assumed to afford small fish protection from piscivorous fish; large piscivores enjoy a metabolic benefit by occupying deeper waters. In the Tsitsikamma National Park marine protected area, South Africa, the shallow reef (water depth of 11–25 m) assemblages were dominated by juveniles and low trophic level species, while deep reef (water depth of 45–75 m) assemblages were characterized by large, sexually mature, and predatory fish.

TABLE 3 Cross-validation comparison between the GAM and RF models.

| Model | RMSE | Slope (a) | Intercept (b) | Coefficient of determination ($r^2$) |
|---|---|---|---|---|
| GAM | 0.23 (0.18-0.28) | 0.30 (0.21-0.45) | 0.30 (0.22-0.38) | 0.28 (0.11-0.44) |
| RF | 0.10 (0.08-0.12) | 0.73 (0.69-0.77) | 0.12 (0.09-0.14) | 0.93 (0.88-0.96) |

(Heyns et al., 2016). In relevant research in this field, bottom water temperature and depth are considered important environmental variables affecting the habitat and distribution of *H. nehereus* (Wang et al., 2021).Changes in the water depth gradient can directly affect the bottom water environment, thereby altering the distribution of fish populations (McLean et al., 2016; Whitfield, 2017). Some bottom environmental variables (sea temperature, salinity) in this study showed a strong positive correlation with water depth. With the increase in depth, the resources of *H. nehereus* first increased and then decreased, which could explain the migration behavior of *H. nehereus* as a result of the bottom water environment change in this season. For example, cod (*Gadus morhua*) is a cold-water species, and their optimum water temperature for growth ranges between 9 and 15°C; sea surface temperatures that are too high or too low can prompt them to swim to deeper areas (Freitas et al., 2021). In addition, Funk et al. (2020) found that the inhabitation of different water depths by cods was associated with spawning behavior in the Baltic Sea. In the case of *H. nehereus*, April coincides with the pre-spawning time. At this time, *H. nehereus* uses deeper, more saline waters, to potentially maximize food availability, temperature preferences, and egg development. Besides, the seabed sediments at depths of 40–70 m consist of silty mud and fine argillaceous sand in the survey area, and adult *H. nehereus* prefers deep waters and sand-mud bottoms to resist high temperatures and light (Li et al., 2017).

Differences in dissolved oxygen (DO) in the water environment affect the classification and size of the zooplankton community, affecting the foraging and growth of fish and altering the spatial ecology and population dynamics of the water area. DePasquale et al. (2015) found that early life estuarine fish were more sensitive to low DO concentrations than to water acidification. Low DO has been reported to reduce the scope for activity, such as swimming and feeding, of Atlantic cod (*Gadus morhua*), resulting in reduced foraging success and increased predation risk (Chabot and Claireaux, 2008). However, potential lethality and avoidance has been observed in fish inhabiting areas with high DO concentrations. A fish kill in Lake Waubesa was thought to have been caused by supersaturation of DO, produced by a dense bloom of *Chlamydomonas* sp. (Nordlie, 2006). Low DO areas are believed to be unsuitable for the survival of benthic organisms (Gong et al., 2017), and hypoxia-tolerant organisms may use hypoxic waters as refuges to avoid predation (Roman et al., 2019). In this study, the amount of *H. nehereus* resources and bottom DO showed a non-linear negative correlation; the resources decreased with an increase in water temperature and bottom DO concentration in spring. When the bottom DO concentration was lower than 7 mg/l, the extent of resource fluctuation was small, and it showed a significantly reduced trend when the bottom DO was greater than 7 mg/L. This may be related to the distribution of regional population structure caused by changes in DO concentration. Breitburg et al. (2001) proposed that DO concentration has an important effect on the distribution of estuarine biological resources. Oxygen depletion can induce vertical or horizontal displacement of fish and this movement may render the individual more vulnerable to predation (Long and Seitz, 2008). Ocean deoxygenation is an important cause of increase in *H. nehereus* resources, as reported in a new study (Kang et al., 2021). High water content in the muscle and other tissues of *H. nehereus* can greatly reduce the demand for oxygen, giving *H. nehereus* an advantage when competing with other fish in the shallow sea. However, at higher DO concentrations, *H. nehereus* faces an increased risk of predation; therefore, the resources show a downward trend.

Water temperature was considered the most important factor affecting the geographical distribution pattern of offshore organisms (Snickars et al., 2010; Bučas et al., 2013; McLean et al., 2016). Wang et al. (2021) analyzed the impact of future climate change on the distribution of *H. nehereus* in the coastal waters of China and indicated that the annual average benthic water temperature was the most important environmental variable affecting *H. nehereus* distribution. In this study, water temperature had a negative impact on the *H. nehereus* distribution in spring. The thermal tolerance of fish that live in a highly variable environment for long durations is generally considered to be higher than that of fish living in a thermally stable environment. For individuals, there are significant differences in the width of thermal tolerance windows at different developmental stages (Pörtner and Peck, 2010). For example, in adult *Solea*, due to the need to provide oxygen for egg or sperm masses, the oxygen supply capacity gradually decreases relative to the demand, making larger individuals more heat sensitive and less tolerant to extreme temperatures (Rijnsdorp et al., 2009). The results of a study on glass eels *Anguilla anguilla* showed that lower water temperatures can significantly reduce eels' migration behavior from higher salinity seawater to lower salinity freshwater to reduce migration-related energy expenditure, thereby increasing the success rate of spawning reproduction (Edeline et al., 2006).

The complex water environment provides diverse habitats for marine life. The study area has a tropical monsoon climate, and its unique ocean conditions are suitable for various marine organisms to thrive. The coastal waters of Zhejiang Province exhibit typical spatial heterogeneity (Jiang et al., 2019); there are spatial differences in the resource and environment utilization and in the similarity and adaptability among species (Zhang et al., 2020), causing suitable habitats to often be distributed in patches. The suitable habitat of *H. nehereus* is narrow, the central and northern parts of the study area are greatly affected by Taiwan's warm, saline current, which maintains the salinity and water temperature in this sea area at a relatively high level. Simultaneously, the northern area is an estuary of the Yangtze River (Robinson et al., 2011; Sun et al., 2015; Gong et al., 2017),

where the fresh water and abundant food provides a better prey environment for *H. nehereus*. Consequently, the density of *H. nehereus* resources was significantly higher in this area than in the southern seas. Owing to the strong adaptability of *H. nehereus* (Kang et al., 2021; Wang et al., 2021), its population has an advantage in the fierce competition for suitable habitats. Simultaneously, short-distance migration habits allow *H. nehereus* to be widely distributed in the surveyed seas (Lin, 2009). In recent years, the increasing fishing intensity has severely reduced the resources of fish, such as *Trichiuridae*, occupying higher trophic levels, thus reducing the number of small fish. (Whitfield, 2017; Liu et al., 2021). Furthermore, the peak breeding season of *H. nehereus* in the coastal waters of Zhejiang is mainly during the summer closing season mandated by the management policy in the East China Sea. Consequently, the recruitment cohort is less affected by anthropogenic disturbances; thus, the recruitment of *H. nehereus* can be effectively recovered during the breeding season.

## 4.2 Model performance evaluation

Compared with other traditional regression models such as GLM, the advantage of GAM is that it adopts an additive method to comprehensively analyze the influence of different predictor variables on response variables and can optimize the expression of nonlinear relationships between variables (Park et al., 2020). In fact, many predictive variables used to analyze marine environmental variables may have strong collinearity issues (such as water depth and other variables used in this study). To reduce the deviation of fitting results caused by collinearity, a traditional regression model is usually used to screen the predictor variables, which may cause important predictors to be ignored (Wood and Augustin, 2002). Unlike traditional regression methods, machine learning methods, such as RF, can reduce the influence of discrete values on regression results without considering the collinearity of predictors. Relying on the advantages of the model, the correlation and interaction between variables can be effectively resolved. Based on the results of this study, we conclude that GAM can provide a good fitting effect based on fewer predictors (Yu et al., 2013). Machine learning methods, such as RF, can use the advantages of model algorithms to solve the problem of strong collinearity between predictor variables, which can further improve the predictive performance of the model, and simultaneously reflect the influence of more predictive variables on response variables (Reiss et al., 2011; Rinde et al., 2014). However, one of the main problems of machine learning is that it cannot provide clear statistical principles.

Various methods, including machine learning, have been widely used in environmental assessment, species distribution prediction, and other fields. In recent years, these have been gradually used in marine fish ecology-related research (Bučas et al., 2013; Smoliński and Radtke, 2017). We used two models to analyze the distribution of *H. nehereus* spawning stock in the study area, to fully understand the environmental factors that affect the fluctuations in their resources (Li et al., 2015). In this study, the gap between GAM, which is based on traditional regression methods, and RF, which is based on machine learning methods, was smaller in the model interpretation rate. However, RF was performed better than GAM in the model prediction performance and provided details of the habitat distribution upon suitable habitat prediction. The suitable habitat area for *H. nehereus* predicted by the GAM was wider than that predicted by RF. This difference may be attributed to the different descriptions of the basic and actual niches of the species in different models (Liu et al., 2020).

Species' distributions are affected by processes operating in both environmental and geographical space (Barry and Elith, 2006). The final prediction performance of the two models is not particularly high, which may be related to the small amount of data used in the experiment, key environmental variables may be undescribed. We suggested that when using different models to analyze suitable habitat characteristics of species to reduce the impact of data source constraints, the model should be matched with ecological knowledge, so that the information obtained through the model will be more abundant, and even raise new questions about ecology by elucidating subtle relationships in the model results.

# 5 Conclusion

Our results indicated that seawater salinity was an important environmental factor affecting the distribution of *H. nehereus*, followed by depth, whereas a change in water temperature had no obvious effect on *H. nehereus* distribution. In spring, *H. nehereus* mainly inhabited deep water areas with high salinity, which are characterized by lower dissolved oxygen and water temperature. The model-based prediction results indicated that the suitable habitat of *H. nehereus* mainly encompasses the region near Zhoushan Islands to the north of the fishing grounds, owing to the abundant nutrients and complex habitats brought and sustained by the Yangtze River. These results add to our understanding of the environmental factors affecting *H. nehereus* migration and spawning in the sea areas of interest and provide reference and theoretical basis for analyzing the habitat characteristics of other key nearshore species.

# Data availability statement

The raw data supporting the conclusions of this article will be made available by the authors, without undue reservation.

## Author contributions

RJ and HS contributed to methodology, writing–original draft, writing–review and editing. XL contributed to project administration, conceptualization, and methodology. YZ contributed to supervision, project administration, conceptualization, methodology, resources, and writing–review and editing. FC contributed to data curation and investigation. KX contributed to project administration. PL contributed to conceptualization. HZ contributed to data curation. All authors contributed to the article and approved the submitted version.

## Funding

This study was supported financially by funds from the National Key R&D Program of China (2020YFD0900804, 2019YFD0901204, 2018YFD0900904) and the Key R&D Program of Zhejiang Province (2019C02056).

## Acknowledgments

The authors express their gratitude to the staff of the Zhejiang Marine Fisheries Research Institute, Scientific Observing and Experimental Station of Fishery Resources for Key Fishing Grounds, Ministry of Agriculture, and Key Laboratory of Sustainable Utilization of Technology Research for Fishery Resources of Zhejiang Province for help with conducting the experiments.

## Conflict of interest

The authors declare that the research was conducted in the absence of any commercial or financial relationships that could be construed as a potential conflict of interest.

## Publisher's note



## References

Akaike, H. (1998). *Information Theory and an Extension of the Maximum Likelihood Principle. Selected Papers of Hirotugu Akaike*, 199–213. doi: 10.1007/978-1-4612-1694-0_15

Allen, P. J., Mitchell, Z. A., DeVries, R. J., Aboagye, D. L., Ciaramella, M. A., Ramee, S. W., et al. (2014). Salinity effects on Atlantic sturgeon (*Acipenser oxyrinchus* mitchil) growth and osmoregulation. *J. Appl. Ichthyol.* 30 (6), 1229–1236. doi: 10.1111/jai.12542

Arlot, S., and Celisse, A. (2010). A survey of cross-validation procedures for model selection. *Stat. Surv.* 4 (0), 40–79. doi: 10.1214/09-ss054

Barry, S., and Elith, J. (2006). Error and uncertainty in habitat models. *J. Appl. Ecol.* 43, 413–423. doi: 10.1111/j.1365-2664.2006.01136.x

Botsford, L. W., Castilla, J. C., and Peterson, C. H. (1997). The management of fisheries and marine ecosystems. *Science* 277, 509–515. doi: 10.1126/science.277.5325.509

Breiman, L. (2001). Random forests. *Mach. Learn.* 45 (1), 5–32. doi: 10.1023/A:1010933404324

Breitburg, D. L., Pihl, L., and Kolesar, S. E. (2001). Effects of low dissolved oxygen on the behavior, ecology and harvest of fishes: A comparison of the Chesapeake bay and Baltic-kattegat systems. *Coast. Hypoxia: Consequences living Resour. Ecosyst.* 58, 241–267. doi: 10.1029/CE058p0241

Brownscombe, J. W., Griffin, L. P., Gagne, T. O., Haak, C. R., Cooke, S. J., Finn, J. T., et al. (2019). Environmental drivers of habitat use by a marine fish on a heterogeneous and dynamic reef flat. *Mar. Biol.* 166 (2), 1–13. doi: 10.1007/s00227-018-3464-2

Bučas, M., Bergström, U., Downie, A. L., Sundblad, G., Gullström, M., Von Numers, M., et al. (2013). Empirical modelling of benthic species distribution, abundance, and diversity in the Baltic Sea: evaluating the scope for predictive mapping using different modelling approaches. *ICES J. Mar. Sci.* 70 (6), 1233–1243. doi: 10.1093/icesjms/fst036

Chabot, D., and Claireaux, G. (2008). Environmental hypoxia as a metabolic constraint on fish: the case of Atlantic cod, gadus morhua. *Mar. pollut. Bull.* 57 (6-12), 287–294. doi: 10.1016/j.marpolbul.2008.04.001

Chen, D. G., and Zhang, M. Z. (2015). *Marine fishes of China* (Qingdao, Shandong: China Ocean University Press), 416–418.

Ciannelli, L., Bailey, K., and Olsen, E. M. (2015). Evolutionary and ecological constraints of fish spawning habitats. *ICES J. Mar. Sci.* 72, 285–296. doi: 10.1093/icesjms/fsu145

Costa, L. D. F., Miranda-Filho, K. C., Severo, M. P., and Sampaio, L. A. (2008). Tolerance of juvenile pompano trachinotus marginatus to acute ammonia and nitrite exposure at different salinity levels. *Aquaculture* 285 (1-4), 270–272. doi: 10.1016/j.aquaculture.2008.08.017

DePasquale, E., Baumann, H., and Gobler, C. J. (2015). Vulnerability of early life stage Northwest Atlantic forage fish to ocean acidification and low oxygen. *Mar. Ecol. Prog. Ser.* 523, 145–156. doi: 10.3354/meps11142

Edeline, E., Lambert, P., Rigaud, C., and Elie, P. (2006). Effects of body condition and water temperature on Anguilla anguilla glass eel migratory behavior. *J. Exp. Mar. Biol. Ecol.* 331 (2), 217–225. doi: 10.1016/j.jembe.2005.10.011

Florin, A. B., Sundblad, G., and Bergström, U. (2009). Characterisation of juvenile flatfish habitats in the Baltic Sea. *Estuar. Coast. Shelf Sci.* 82 (2), 294–300. doi: 10.1016/j.ecss.2009.01.012

Freitas, C., Villegas-Ríos, D., Moland, E., and Olsen, E. M. (2021). Sea Temperature effects on depth use and habitat selection in a marine fish community. *J. Anim. Ecol.* 90, 1787–1800. doi: 10.1111/1365-2656.13497

Funk, S., Krumme, U., Temming, A., and Möllmann, C. (2020). Gillnet fishers' knowledge reveals seasonality in depth and habitat use of cod (Gadus morhua) in the Western Baltic Sea. *ICES J. Mar. Sci.* 77 (5), 1816–1829. doi: 10.1093/icesjms/fsaa071

Gong, S. B., Gao, A. G., Ni, G. T., Zhu, X. X., Zhang, Y. P., and Hou, Y. T. (2017). Progress in research of hypoxia in estuaries and coastal areas in China. *Water Resour. Prot.* 33 (4), 62–69. doi: 10.3880/jissn.1004-6933.2017.04.010

Gordó-Vilaseca, C., Pennino, M. G., Albo-Puigserver, M., Wolff, M., and Coll, M. (2021). Modelling the spatial distribution of sardina pilchardus and engraulis encrasicolus spawning habitat in the NW Mediterranean Sea. *Mar. Environ. Res.* 169, 105381. doi: 10.1016/j.marenvres.2021.105381

Hastie, T., and Tibshirani, R. J. (1990). "Generalized additive models," in *In monographs on statistics and applied probability* (London: Chapman and Hall), 335.

Heyns, E. R., Bernard, A. T. F., Richoux, N. B., Parker, D., Langlois, T. J., Harvey, E. S., et al. (2016). Depth and habitat determine assemblage structure of south

africa's warm-temperate reef fish. *Mar. Biol.* 163 (7), 1–17. doi: 10.1007/s00227-016-2933-8

Hyndman, R. J., and Koehler, A. B. (2006). Another look at measures of forecast accuracy. *Int. J. Forecast.* 22 (4), 679–688. doi: 10.1016/j.ijforecast.2006.03.001

Jiang, R., Zhang, L., Xu, K., Li, P., Xiao, Y., Fan, Z, et al (2019). Characteristics and diversity of nekton functional groups in the coastal waters of south-central Zhejiang Province. *Biodiv Sci.* 27 (12), 1330–1338. doi: 10.17520/biods.2019281

Jørgensen, C., Dunlop, E. S., Opdal, A. F., and Fiksen, Ø. (2008). The evolution of spawning migrations: state dependence and fishing-induced changes. *Ecology* 89, 3436–3448. doi: 10.1890/07-1469.1

Jury, S. H., and Watson, W. H. (2013). Seasonal and sexual differences in the thermal preferences and movements of American lobsters. *Can. J. Fish. Aquat.* 70, 1650–1657. doi: 10.1139/cjfas-2013-0061

Kang, B., Bakun, A., Lin, L., and Pauly, D. (2021). Increase of a hypoxia-tolerant fish, *Harpadon nehereus* (Synodontidae), as a result of ocean deoxygenation off southwestern China. *Environ. Biol. Fish.*, 1–5. doi: 10.1007/s10641-021-01130-7

Kasai, A., Kurikawa, Y., Ueno, M., Robert, D., and Yamashita, Y. (2010). Salt-wedge intrusion of seawater and its implication for phytoplankton dynamics in the yura estuary, Japan. *Estuar. Coast. Shelf Sci.* 86 (3), 408–414. doi: 10.1016/j.ecss.2009.06.001

Kir, M., and Sunar, M. (2018). Acute toxicity of ammonia and nitrite to Sea bream, sparus aurata (Linnaeu), in relation to salinity. *J. World Aquacult. Soc* 49, 516–522. doi: 10.1111/jwas.12448

Kir, M., Sunar, M., and Gök, M. (2019). Acute ammonia toxicity and the interactive effects of ammonia and salinity on the standard metabolism of European sea bass (*Dicentrarchus labrax*) aquaculture. *Aquaculture* 511, 734273. doi: 10.1016/j.aquaculture.2019.734273

Kume, M., Lavergne, E., Ahn, H., Terashima, Y., Kadowaki, K., Ye, F., et al. (2021). Factors structuring estuarine and coastal fish communities across Japan using environmental DNA metabarcoding. *Ecol. Indic.* 121, 107216.

Liaw, A., and Wiener, M. (2002). Classification and regression by randomForest. *R News.* 2, 18–22.

Lin, L. S. (2009). Spatial distribution and environmental characteristics of harpodon nehereus in the East China Sea region. *J. Shanghai Univ.* 18, 66–71.

Liu, Z., Yang, L., Yuan, X., Jin, Y., Yan, L., and Cheng, J. (2020). Overwintering distribution and its environmental determinants of small yellow croaker based on ensemble habitat suitability modeling. *Chinese Journal of Applied Ecology* 31 (6), 2076–2086. doi: 10.13287/j.1001-9332.202006.034

Liu, Z. H., Han, D. Y., Gao, C. X., and Ye, S. (2021). Feeding habits of Bombay ducks (*Harpadon nehereus*) in the offshore waters of southern zhejiang, based on predator CPUE weighting. *J. Fish. Sci. China.* 28 (04), 482–492. doi: 10.12264/JFSC2020-0249

Li, Z., Ye, Z., Wan, R., and Zhang, C. (2015). Model selection between traditional and popular methods for standardizing catch rates of target species: a case study of Japanese Spanish mackerel in the gillnet fishery. *Fish. Res.* 161, 312–319. doi: 10.1016/j.fishres.2014.08.021

Li, M., Zhang, C., Xu, B., Xue, Y., and Ren, Y. (2017). Evaluating the approaches of habitat suitability modelling for whitespotted conger (*Conger myriaster*) fish. *Res* 195, 230–237. doi: 10.1016/j.fishres.2017.07.024

Long, W. C., and Seitz, R. D. (2008). Trophic interactions under stress: hypoxia enhances foraging in an estuarine food web. *Mar. Ecol. Prog. Ser.* 362, 59–68. doi: 10.3354/meps07395

Luo, H. Z., Zhang, H. D., Li, P. F., and Zhou, Y. D. (2012). Analysis of the current situation of fishery biology of *Harpodon nehereus* in the East China Sea. *J. Zhejiang Ocean Univ. Nat. Sci.* 31 (3), 202–205,233.

McLean, D. L., Langlois, T. J., Newman, S. J., Holmes, T. H., Birt, M. J., Bornt, K. R., et al. (2016). Distribution, abundance, diversity and habitat associations of fishes across a bioregion experiencing rapid coastal development. *Estuar. Coast. Shelf Sci.* 178, 36–47. doi: 10.1016/j.ecss.2016.05.026

Nooralabettu, K. P. (2008). Effect of sun drying and artificial drying of fresh, salted Bombay duck (*Harpodon neherius*) on the physical characteristics of the product. *J. Aquat. Food Prod. Technol.* 17 (2), 99–116. doi: 10.1080/10498850801936994

Nordlie, F. G. (2006). Physicochemical environments and tolerances of cyprinodontoid fishes found in estuaries and salt marshes of eastern north America. *Rev. Fish. Biol. Fish.* 16, 51–106. doi: 10.1007/s11160-006-9003-0

Park, S. Y., Sur, C., Lee, J. H., and Kim, J. S. (2020). Ecological drought monitoring through fish habitat-based flow assessment in the gam river basin of Korea. *Ecol. Indic.* 109, 105830. doi: 10.1016/j.ecolind.2019.105830

Pasquaud, S., Vasconcelos, R. P., França, S., Henriques, S., Costa, M. J., and Cabral, H. (2015). Worldwide patterns of fish biodiversity in estuaries: Effect of global vs. *local factors. Estuar. Coast. Shelf Sci.* 154, 122–128. doi: 10.1016/j.ecss.2014.12.050

Perry, D., Staveley, T. A. B., and Gullström, M. (2018). Habitat connectivity of fish in temperate shallow-water seascapes. *Front. Mar. Sci.* 4. doi: 10.3389/fmars.2017.00440

Pörtner, H. O., and Peck, M. A. (2010). Climate change effects on fishes and fisheries: towards a cause-and-effect understanding. *J. Fish. Biol.* 77, 1745–1779. doi: 10.1111/j.1095-8649.2010.02783.x

Potter, I. C., Tweedley, J. R., Elliott, M., and Whitfield, A. K. (2015). The ways in which fish use estuaries: a refinement and expansion of the guild approach. *Fish Fish.* 16, 230–239. doi: 10.1111/faf.12050

Reiss, H., Cunze, S., König, K., Neumann, H., and Kröncke, I. (2011). Species distribution modelling of marine benthos: A north Sea case study. *Mar. Ecol. Prog. Ser.* 442, 71–86. doi: 10.3354/meps09391

Rice, J. C. (2005). Understanding fish habitat ecology to achieve conservation. *J. Fish Biol.* 67, 1–22. doi: 10.1111/j.0022-1112.2005.00933.x

Rijnsdorp, A., Peck, M. A., Engelhard, G. H., Möllmann, C., and Pinnegar, J. K. (2009). Resolving the effect of climate change on fish populations. *ICES J. Mar. Sci.* 66, 1570–1583. doi: 10.1093/ICESJMS/FSP056

Rinde, E., Christie, H., Fagerli, C. W., Bekkby, T., Gundersen, H., Norderhaug, K. M., et al. (2014). The influence of physical factors on kelp and sea urchin distribution in previously and still grazed areas in the NE Atlantic. *PLoS One* 9 (6), e100222. doi: 10.1371/journal.pone.0100222

Robinson, L. M., Elith, J., Hobday, A. J., Pearson, R. G., Kendall, B. E., Possingham, H. P., et al. (2011). Pushing the limits in marine species distribution modelling: Lessons from the land present challenges and opportunities. *Glob. Ecol. Biogeogr.* 20, 789–802. doi: 10.1111/j.1466-8238.2010.00636.x

Roman, M. R., Brandt, S. B., Houde, E. D., and Pierson, J. J. (2019). Interactive effects of hypoxia and temperature on coastal pelagic zooplankton and fish. *Front. Mar. Sci.* 6. doi: 10.3389/fmars.2019.00139

Seitz, R. D., Wennhage, H., Bergström, U., Lipcius, R. N., and Ysebaert, T. (2014). Ecological value of coastal habitats for commercially and ecologically important species. *ICES J. Mar. Sci.* 71 (3), 648–665. doi: 10.1093/icesjms/fst152

Shelford, V. E. (1911). Physiological animal geography. *J. Morphol.* 22, 551–618. doi: 10.1002/jmor.1050220303

Smoliński, S., and Radtke, K. (2017). Spatial prediction of demersal fish diversity in the Baltic Sea: comparison of machine learning and regression-based techniques. *ICES J. Mar. Sci.* 74 (1), 102–111. doi: 10.1093/icesjms/fsw136

Snickars, M., Sundblad, G., Sandström, A., Ljunggren, L., Bergström, U., Johansson, G., et al. (2010). Habitat selectivity of substrate-spawning fish: modelling requirements for the Eurasian perch perca fluviatilis. *Mar. Ecol. Prog. Ser.* 398, 235–243. doi: 10.3354/meps08313

Souza, A. T., Ilarri, M. I., Timóteo, S., Marques, J. C., and Martins, I. (2018). Assessing the effects of temperature and salinity oscillations on a key mesopredator fish from European coastal systems. *Sci. Total Environ.* 640, 1332–1345. doi: 10.1016/j.scitotenv.2018.05.348

Staveley, T., Jacoby, D., Perry, D., Meijs, F., Lagenfelt, I., and Gullström, M. (2019). Sea Surface temperature dictates movement and habitat connectivity of Atlantic cod in a coastal fjord system. *Ecol. Evol.* 9, 9076–9086. doi: 10.1002/ece3.5453

Sun, P. F., Dai, F. Q., Chen, Y. L., Shan, X., and Jin, X. (2015). Seasonal variations in structure of fishery resource in the Yangtze river estuary and its adjacent waters. *Prog. Fish. Sci.* 36, 8–16. doi: 10.11758/yykxjz.20150602

Su, J. L., and Yuan, Y. L. (2005). Hydrology in China Sea. *Ocean Beijing Chinese.* 35–62.

Tang, L., Zhang, Y. L., Xu, B. D., Zhang, C. L., Ren, Y. P., and Xue, Y. (2021). Habitat suitability analysis of *Apogon lineatus* during autumn in haizhou bay. *Periodical Ocean Univ. China.* 51 (S1), 154–160. doi: 10.16441/j.cnki.hdxb.20200268

Taqwa, A., Burhanuddin, A. I., Niartiningsih, A., and Nessa, M. N. (2020). Nomei fish (*Harpadon nehereus*, ham. 1822) reproduction biology in tarakan waters. *Conf. Ser.: Earth Environ. Sci.* 473 (1), 12012. doi: 10.1088/1755-1315/473/1/012012

Thomas, D., Rekha, M. U., Angel, J. R. J., Sreekanth, G. B., Thiagarajan, G., Subburaj, R., et al. (2021). Effects of salinity amendments on the embryonic and larval development of a tropical brackishwater ornamental silver moony fish. *Monodactylus argenteus (Linnaeus 1758) Aquaculture* 544, 737073. doi: 10.1016/j.aquaculture.2021.737073

Wang, G., and Fan, Z. (2004). Marine mammals and their distributions in coastal waters of zhejiang. *Chin. J. @ Zool.* 39 (1), , 60–, 63. doi: 10.13859/j.cjz.2004.01.012

Wang, L., Wang, X., Li, C., and Jia, X. (2019). Seasonal distribution and habitat preferences of crimson seabream parargyrops edita: Implications for a marine protected area in beibu gulf, northern south China Sea. *Mar. Coast. Fish.* 11 (3), 258–270. doi: 10.1002/mcf2.10075

Wang, S. C., Yang, R., Gao, C. X., Han, D. Y., and Ye, S. (2022). Keystone species of fish community in the offshore waters of southern zhejiang: Insight from

ecological network. *J. Fish. Sci. China.* 29 (01), 118–129. doi: 10.12264/JFSC2021-0140

Wang, L., Zhang, Z., Lin, L., Peng, X., Lin, L., and Kang, B. (2021). Redistribution of the lizardfish *Harpadon nehereus* in coastal waters of China due to climate change. *Hydrobiologia* 848 (20), 4919–4932. doi: 10.1007/s10750-021-04682-y

Whitfield, A. K. (2017). The role of seagrass meadows, mangrove forests, salt marshes and reed beds as nursery areas and food sources for fishes in estuaries. *Rev. Fish Biol. Fish.* 27, 75–110. doi: 10.1007/s11160-016-9454-x

Wood, S. N., and Augustin, N. H. (2002). GAMs with integrated model selection using penalized regression splines and applications to environmental modelling. *Eco. Model.* 157 (2-3), 157–177. doi: 10.1016/s0304-3800(02)00193-x

Yuan, H. R., Chen, P. M., Qin, C. X., Li, X. G., Zhou, Y. B., Feng, X., et al. (2017). Seasonal variation of fish community structure in zhelin bay, the south China Sea. *South China Fish. Sci.* 13, 26–35. doi: 10.3969/j.issn.2095–0780.2017.02.004

Yu, H., Jiao, Y., and Carstensen, L. W. (2013). Performance comparison between spatial interpolation and GLM/GAM in estimating relative abundance indices through a simulation study. *Fish. Res.* 147, 186–195. doi: 10.1016/j.fishres.2013.06.002

Zhang, L., Zhou, Y, Jiang, R., Li, Z., Fan, Z., Yin, R, et al (2020). Spatial niche of major fish species in spring in the coastal waters of central and southern Zhejiang Province, China. *Chinese Journal of Applied Ecology* 31 (2), 659–666. doi: 10.13287/j.1001-9332.202002.040

frontiers | Frontiers in Marine Science

TYPE Original Research
PUBLISHED 12 September 2022
DOI 10.3389/fmars.2022.936028



OPEN ACCESS

EDITED BY
Binhe Gu,
University of Florida, United States

REVIEWED BY
Tianming Wang,
Zhejiang Ocean University, China
Qiang Xu,
Hainan University, China
Yuan-Wei Du,
Ocean University of China, China

*CORRESPONDENCE
Zhongxin Wu
wuzhongxin@dlou.edu.cn
Tao Tian
tian2007@dlou.edu.cn

†These authors have contributed equally to this work and share first authorship

SPECIALTY SECTION
This article was submitted to Marine Ecosystem Ecology, a section of the journal Frontiers in Marine Science

RECEIVED 04 May 2022
ACCEPTED 16 August 2022
PUBLISHED 12 September 2022

CITATION
Wang Z, Feng J, Lozano-Montes HM, Loneragan NR, Zhang X, Tian T, and Wu Z (2022) Estimating ecological carrying capacity for stock enhancement in marine ranching ecosystems of Northern China. *Front. Mar. Sci.* 9:936028. doi: 10.3389/fmars.2022.936028



# Estimating ecological carrying capacity for stock enhancement in marine ranching ecosystems of Northern China

Zhaoguo Wang[1†], Jie Feng[2†], Hector M. Lozano-Montes[3], Neil R. Loneragan[3], Xiumei Zhang[4], Tao Tian[1,5*] and Zhongxin Wu[1,5*]

[1]Center for Marine Ranching Engineering Science Research of Liaoning, Dalian Ocean University, Dalian, China, [2]Key Laboratory of Marine Ecology and Environmental Sciences, Institute of Oceanology, Chinese Academy of Sciences, Qingdao, China, [3]Environmental and Conservation Sciences and Harry Butler Institute, Murdoch University, Perth, Australia, [4]College of Fisheries, Zhejiang Ocean University, Zhoushan, China, [5]Key Laboratory of Environment Controlled Aquaculture, Ministry of Education, Dalian Ocean University, Dalian, China

Marine ranching has been proposed as a promising solution to manage the depleted coastal fishery ecosystem in recent decades across China. Marine ranching integrates the practices of artificial habitat-based with aquaculture-based enhancement. Assessing the ecological carrying capacity of target species for enhancement is a precondition for determining the optimal numbers for release, particularly for those species whose habitat restrictions have been eliminated through the construction of artificial habitats in the marine ranch. A responsible approach to stock enhancement aims not only to increase total yield and stock abundance but also to consider any potential effects on ecosystem structure and function. A time-dynamic, ecosystem model was constructed using Ecopath with Ecosim for the Laizhou Bay (Bohai Sea) marine ranching ecosystem in the nearshore waters of northern China. Two sedentary target species with potential for stock enhancement, i.e., the carnivorous red snail *Rapana venosa* and the detritivorous sea cucumber *Apostichopus japonicus*, were selected to simulate and estimate their ecological carrying capacities and project their overall effects on the ecosystem. Ecological carrying capacity was defined as the maximum standing stocks of the target species that would not cause "unacceptable" impacts on the ecosystem function and resilience, i.e., not cause any other group's biomass to fall below 10% of its original biomass. The ecological carrying capacities estimated for *R. venosa* and *A. japonicus* were 623.46 and 200.57 t·km$^{-2}$, respectively, corresponding to 7.8 and 5.0 times higher than their current standing stocks. Simulations of *R. venosa* enhancement showed distinct effects of increased target species abundance on other functional groups and ecosystem properties. An increase in red snail biomass caused negative impacts on the biomass of most other functional groups and ecosystem indicators, such as Finn's cycling index, transfer efficiency, and Kempton's Q index. In contrast, the simulated *A. japonicus* enhancement had relatively few impacts, and the biomasses of most other functional groups and

ecosystem indicators did not change or changed very slightly (<5%). The current model framework provides a means of estimating the ecological carrying capacity in commercial-scale stock enhancement practices and avoiding potential ecological risks for marine ranching in northern China.

KEYWORDS

*Rapana venosa*, *Apostichopus japonicus*, Laizhou Bay, artificial habitats, aquaculture-based enhancement, ecosystem effects, ecological risk

## Introduction

The accelerating species extinction and the loss of biodiversity in the global marine environment have severely diminished the function of marine ecosystem services (Solan et al., 2004; Worm et al., 2006). The conservation and restoration of marine living resources are becoming increasingly important for maintaining marine systems (Worm et al., 2009; Stier et al., 2016). Marine stock enhancement, as a set of management approaches involving the release of cultured organisms to enhance or restore fisheries, has been practiced to implement marine biological resource conservation. Furthermore, it plays an increasingly important role in food security and developing and enhancing recreational fisheries (Lorenzen et al., 2010; Kitada, 2020; Lorenzen et al., 2021).

The implementation of stock enhancement programs in open waters nowadays still often lacks the necessary scientific evidence to be carried out effectively due to a lack of knowledge of the environment, target species, and release locations. This makes it difficult to identify any potential negative ecological impacts of stocking such as a reduction in genetic diversity, negative effects on wild stock growth and survival, and impacts on ecosystem functioning (Cudmore-Vokey and Crossman, 2000; Taylor et al., 2005; Townsend, 2010; Taylor et al., 2017; Lorenzen et al., 2021). For example, the introduction of salmon into Lake Michigan resulted in significant changes in the food web structure, causing the planktivorous fish ratio to fall from 8:1 in the 1930s to 1.3:1 at the end of the 20th century (Cudmore-Vokey and Crossman, 2000). In addition, the release of Brown Trout *Salmo trutta* into rivers in New Zealand drove the Whitebait *Galaxias* spp., which had the same niche as brown trout, to the brink of extinction (Townsend, 2010). In contrast, Khan et al. (2015) compared changes in the food web pre- and post-stocking of the carps, *Catla catla* (Hamilton), *Labeo rohita* (Hamilton), and *Cirrhinus mrigala* (Hamilton), in a tropical reservoir ecosystem in India, and showed that after stock enhancement, the reservoir ecosystem was more resilient and healthier based on ecological network indicators' analyses. Therefore, evaluating the potential effects of stocking strategies on other fish species and aquatic communities before stocking is important for informing the stakeholders and fisheries managers and for avoiding any unanticipated consequences of stocking.

A responsible approach to stock enhancement has been advocated internationally since the concept was first developed in 1995 and then later revised in 2010 (Blankenship and Leber, 1995; Lorenzen et al., 2010). This approach recommends considering the effects of stock enhancement on the structure and function of the target aquatic ecosystem such as biodiversity and ecosystem properties (Blankenship and Leber, 1995; FAO, 2005; Zhang et al., 2009; Lorenzen et al., 2010; Jiang et al., 2014; Taylor et al., 2017).

Assessing the ecological carrying capacity of target species is a precondition to determining the optimal number of individuals for stocking. In order to make effective use of juveniles reared or collected for stock enhancement, an understanding of the carrying capacity of the habitat is needed. Overstocking will have detrimental effects on wild populations of the species and the released individuals in terms of growth and survival, and understocking will not maximize the returns from stocking (Munro and Bell, 1997). The risk of overstocking remains a concern, particularly because of adverse ecological consequences, including the displacement of wild populations and other competitors (Taylor et al., 2013).

Carrying capacity is defined as the limiting biomass of a specific population that the ecosystem can support under specific environmental conditions, such as food and habitat (Cooney and Brodeur, 1998; Taylor et al., 2005; Filgueira et al., 2021). According to the relationship between population size and the availability of resources, carrying capacity can be classified into four broad categories: physical, production, ecological, and social carrying capacities (Inglis et al., 2000; McKindsey et al., 2006). The ecological carrying capacity describes the maximum standing stock of target species that does not cause "unacceptable" impacts on the species or the ecosystem (Inglis et al., 2000; Kluger et al., 2016). Recent advances in ecosystem modeling provide the means to estimate ecological carrying capacity, given sufficient data on biological processes (Byron et al., 2011; Kluger et al., 2016).

Kluger et al. (2016) introduced the definition of stock collapse (after Worm et al., 2009), i.e., any group biomass that falls below 10% of its original biomass, as an approach to define "unacceptable" impact thresholds and further to estimate the ecological carrying capacity for the target stocking species.

Laizhou Bay (LZB) in the Bohai Sea of north China is an important spawning and feeding ground and nursery area for many economically important fish and shrimp, such as the Chinese shrimp *Fenneropenaeus chinensis* and small yellow croaker *Larimichthys polyactis* (Jin and Deng, 2000; Jin et al., 2013). The LZB ecosystem has deteriorated severely in recent years as a result of overfishing and environmental pollution (Jin et al., 2013; Wei et al., 2022). Moreover, the fisheries resources and ecosystem structure of the LZB have changed dramatically (Jin and Deng, 2000; Jin et al., 2013). Since the 1990s, a series of fishery resource management approaches have been widely adopted in LZB to restore the productivity of the ecosystem (Shen and Heino, 2014). One of these initiatives has been the construction of marine ranches by deploying artificial reefs and releasing target species such as Japanese Flounder, *Paralichthys olivaceus*, and Chinese shrimp (Zhang et al., 2009). By the end of 2021, three national marine ranching demonstration zones had been built in LZB (Ministry of Agriculture and Rural Affairs of the People's Republic of China, 2022). Following the deployment of the artificial reefs, the reef surfaces were colonized by a large number of Pacific oysters *Crassostrea gigas*, forming oyster reefs and even oyster mountains (Xu et al., 2019). These provide important food and habitat foundation for enhancing reef-associated species such as the red snail *Rapana venosa* and sea cucumber *Apostichopus japonicus*, which are commercially important, local species for stock enhancement. The landings of *R. venosa* and *A. japonicus* in 2020 were 4.2 and 1.65 $t{\cdot}km^{-2}{\cdot}year^{-1}$, respectively, according to the statistics from the Blue Ocean Company.

In this study, we first build an Ecopath model (https://ecopath.org/) to represent the current trophic flows of the LZB marine ranching system. The base model for the system was set as 2020–2021, following an annual survey of the biological resources in the region. We then further developed the model with Ecosim (Christensen and Walters, 2004) to simulate the biomass increases of two resident target species, *R. venosa* and *A. japonicus*, following stock enhancement. The simulated increases in biomass following different levels of enhancement were used to estimate the ecological carrying capacity for each species (Kluger et al., 2016) and then to determine the indicators of ecosystem properties from the models. These ecosystem properties were compared for the different levels of enhancement with the pre-enhancement state to determine the potential impacts of different stocking levels. The results for estimating ecological carrying capacity from the dynamic ecosystem model (EwE) were compared with those from a static Ecopath model (Byron et al., 2011).

# Materials and methods

## Study area

Laizhou Bay, located in the southern region of the Bohai Sea, is the largest bay in Shandong Peninsula (Figure 1). It stretches from the northern corner of Qimu Cape in the east, to the estuary of the Yellow River in the west, with a natural coastline of 319 km. Its total area is 6,966 $km^2$, accounting for approximately 10% of the Bohai Sea, with a mean depth of 8 m and a maximum depth of ~15 m at the eastern mouth of the bay. The first marine ranch in LZB (37°15′–37°22′N, 119°38′–119°46′E) was built in 2010 by Shandong Blue Ocean Technology Co., Ltd. This marine ranch occupies a total area of 107.95 $km^2$ with an artificial reef area of 33.3 $km^2$ in the core area (Figure 1). The types of artificial reefs deployed in this marine ranch include stone reefs, derelict vessels, and artificial shell reefs. The core area of the ranch is used primarily for the stock enhancement of benthic, reef-associated species including *R. venosa* and *A. japonicus* (Xu et al., 2019), and the remaining zone of 74.6 $km^2$ is the zone of marine ranching outside the area for stock enhancement (Figure 1). No artificial reefs are deployed in this latter area.

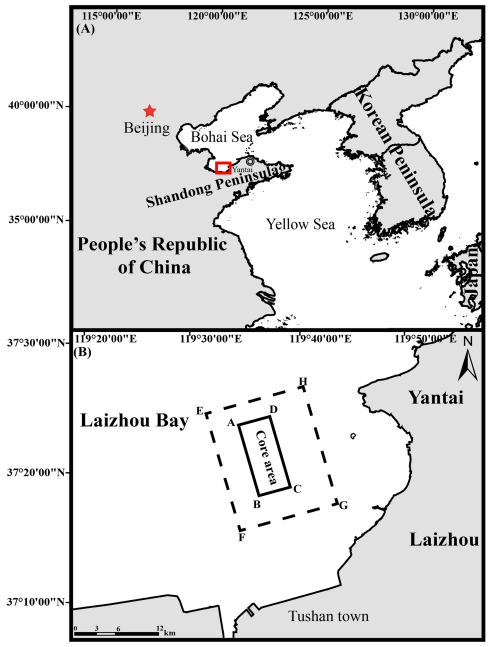


FIGURE 1
Map showing the location of **(A)** Laizhou Bay (dashed square) in the People's Republic of China and **(B)** the model domain of Laizhou Bay marine ranching area (EFGH—dashed rectangle) and the core area for implementing stock enhancement (ABCD—solid rectangle).

## The Ecopath model—functional groups and data sources

Ecopath with Ecosim (EwE version 6.6) was used to first construct the Ecopath model of LZB marine ranching. Based on the ecological habits, economic values, and ecological roles of the species in the area, we defined 27 functional groups in the model (Table 1), which covered the main trophic flows in LZB marine ranching ecosystem. Considering their important roles played in supporting fishery catch and ecosystem function, 10 single-species functional groups were established: four teleost groups (*Sebastes schlegelii*, *Hexagrammos otakii*, *Lateolabrax japonicus*, and *Sparus macrocephalus*); and six macroinvertebrate groups (*A. japonicus* (Sea Cucumber), *R. venosa* (Rea Snail), *Charybdis japonica* (Asian Paddle Crab), *Oratosquilla oratoria* (Japanese Mantis Shrimp), *C. gigas* (Pacific Oyster), and *Aurelia aurita* (Moon Jellyfish) (Table 1).

The biomass inputs for macroinvertebrates and fish in the Ecopath model were primarily based on the resource survey data. The biomasses of fish and macroinvertebrates in the modeled area were estimated by sampling using trawls, gillnets, long fishing traps, and SCUBA quadrats during 2020–2021. Phytoplankton biomass in terms of chlorophyll-*a* was first measured using a Turner fluorometer according to standard procedure (Parsons et al., 1984), and biomass was estimated by transforming the chlorophyll-*a* concentration ($mg/m^3$) using the following relationships: the ratio of organic carbon:chlorophyll-*a* = 43:1 (Wang et al., 1998), the organic carbon:dry weight ratio = 35:100 (Ning et al., 1995), and the dry weight:wet weight ratio = 1:2.86 (Su and Tang, 2002). The biomass of the macrobenthos and small zoobenthos were sampled *in situ* using grab samplers. The biomasses of water column bacteria and benthic bacteria were obtained from field experimental measurements, and the biomass of detritus (in water and sediment) was calculated with reference to the linear model proposed by Pauly and Bartz (1993), as follows:

$$\lg D = 2.41 + 0.954\lg PP + 0.863\lg E \quad (1)$$

where $D$ [$g(C)/m^2$] is detritus biomass, $PP$ [$g(C)/(m^2 \cdot a)$] is the primary production, and $E$ (m) is the euphotic depth.

In the Ecopath model, the fish Production : Biomass ratio (P/B) and Consumption to Biomass ratio (Q/B) values were calculated by empirical formula or using reported values of similar ecological characteristics (Palomares and Pauly, 1989; Pauly and Bartz, 1993; Wu et al., 2013). The P/B, Q/B, and additional unknown parameters of other functional groups are mainly based on the reported data in the Ecopath model in LZB (Lin et al., 2009; Lin et al., 2013; Yang et al., 2016). The diet composition was based mainly on the gut content analyses for *S. schlegelii*, *H. otakii*, and *C. japonica*, as well as the literature for other species (see Supplementary Material Table S1). However, for the *A. aurita* and Spatangoida functional groups, the two abundant taxa in this area, few or even no predators were observed or reported. Thus, they were not in the diet composition of any functional group. Data on landings of fished species (*S. schlegelii*, *L. japonicus*, *S. macrocephalus*, *C. japonica*, *O. oratoria*, *R. venosa*, and *A. japonicus*) were obtained from Shandong Blue Ocean Technology Co., Ltd (see Supplementary Material Table S2). No commercial landings on *H. otakii* were available, but it is a commercial interest species.

## Ecopath model tuning and quality analysis

Prior to balancing the model, a pre-balanced diagnostic (PREBAL) analysis was performed to evaluate the validity of the input parameters. The PREBAL diagnostics offered a series of tuning techniques to analyze the slope of the relationships for biological ratio, vital ratio, and production ratio, relative to the trophic level for each functional group (Link, 2010). According to the PREBAL criteria, as well as "rules of thumb", the biomass estimated by the model should span 5–7 orders of magnitude, where >7 indicates that there are too many taxonomic or age-structured taxa in the model, and <5 indicates that the model might be focused on specific trophic levels and not representative of the broader food web (Link, 2010; Heymans et al., 2016). In addition, the biomass (on a logarithmic scale) should decrease by 5%–10% with increasing trophic levels across all functional groups, based on PREBAL diagnostics. Likewise, P/Q and Q/B were subjected to the same biomass PREBAL criteria (Link, 2010; Heymans et al., 2016).

After completion of the PREBAL diagnostics, a preliminary Ecopath model that met the ecological and fishing principles was developed. The Ecopath model was balanced, and the model quality was evaluated using the second law of thermodynamics to check that it was maintained (Link, 2010). The indicators included are the respiration and assimilation ratio (R/A ratio) and the gross efficiency (GE) of each functional group. The dimensionless R/A ratio cannot exceed 1, because respiration cannot exceed assimilation. The GE indicates the value for the P/Q ratio should be between 0.1 and 0.3 (Darwall et al., 2010).

The pedigree index (referred to as the P index) was used to analyze the uncertainty of the Ecopath model input parameters. The P index quantifies the overall quality of the data and model (Christensen and Walters, 2004). The quality of the input data source was ranked in the following order: direct measurement, empirical relationship, other models, and other references. The confidence intervals of the input parameters (B, P/B, Q/B, Landing, and diet composition) were between 0 and 1. The P index of each functional group was used to evaluate the overall quality indicator of the model. A higher value of the pedigree index indicates a higher credibility of the model. The P index was

TABLE 1 Functional groups and main species comprising the different model compartments for the steady-state model of the Laizhou Bay marine ranching ecosystem.

| Number | Functional group | Rationale | Species |
|---|---|---|---|
| 1 | *Sebastes schlegelii* | Commercial and recreational fishing | *S. schlegelii* |
| 2 | *Hexagrammos otakii* | Commercial and recreational fishing | *H. otakii* |
| 3 | *Lateolabrax japonicus* | Commercial and recreational fishing | *L. japonicus* |
| 4 | *Sparus macrocephalus* | Commercial and recreational fishing | *S. macrocephalus* |
| 5 | Gobiidae | Aggregate group | *Synechogobius ommaturus*, *Acanthogobius flavimanus*, *Symechogobius hasta*, etc. |
| 6 | Other demersal fishes | Aggregate group | *Arelicus joyneri* Günther, *Paralichthys olivaceus*, *Kareius bicoloratus*, etc. |
| 7 | Pelagic fishes | Aggregate group | *Setipinna tenuifilis*, *Callionymus curvicornis*, *Thryssa kammalensis*, *Thryssa mystax*, etc. |
| 8 | Octopodidae | Aggregate group | *Octopus variabilis*, *Octopus ocellatus*, etc. |
| 9 | *Charybdis japonica* | Commercial fishing | *C. japonica* |
| 10 | *Oratosquilla oratoria* | Commercial fishing | *O. oratoria* |
| 11 | *Rapana venosa* | Stock enhancement/ commercial fishing | *R. venosa* |
| 12 | *Apostichopus japonicus* | Stock enhancement/ commercial fishing | *A. japonicus* |
| 13 | *Crassostrea gigas* | Habitat forming species | *C. gigas* |
| 14 | *Aurelia aurita* | Ecological importance | *A. aurita* |
| 15 | Spatangoida | Ecological importance | Spatangoida |
| 16 | Other shrimps and crabs | Aggregate group | *Matuta planip*, *Arcania undecimspinosa*, *Dorippe japonica*, *Eucrate crenata*, *Pyrhila pisum*, *Alpheus distinguendus*, etc. |
| 17 | Annelida | Aggregate group | *Nephtys oligobranchia*, *Nephtys polybranchia*, *Scoloplos rubra*, *Scoloplos armiger*, *Scoloplos marsupoalis*, *Sternaspis scutata*, etc. |
| 18 | Other Mollusca | Aggregate group | *Mytilus edulis*, *Alvenius ojianus*, *Moerella rutila*, *Ruditapes philippinarum*, etc. |
| 19 | Other macro-zoobenthos | Aggregate group | *Amphioplus japonicus*, *Ophiura kinbergi*, *Cleantiella*, *Leptochela gracilis*, etc. |
| 20 | Small zoobenthos | Aggregate group | Polychaete, Copepods, Gastrotricha, Nematoda, Amphipoda, Ostracoda, Cladoceran, etc. |
| 21 | Zooplankton | Secondary production | *Eurytemora pacifica*, *Centropages dorsispinatus*, *Labibocera bipinnata*, *Labibocera euchaeta*, *Acartia pacifica*, *Sagittacrassa*, *Macrura larvae*, *Ophiopluteus larvae*, *Polychaete larvae*, etc. |
| 22 | Bacterioplankton | Secondary production | Proteobacteria, Firmicutes, Bacteroidetes, Actinobacteria, Cyanobacteria, etc. |
| 23 | Sediment bacteria | Secondary production | Heterotrophic Bacteria |
| 24 | Phytoplankton | Primary production | *Achnanthes brevipes*, *Bacteriastrum hyalinum*, *Chaetoceros*, *Cocconeis*, *Coscinodiscus asteromphalus*, *Coscinodiscus oculusiridis*, *Coscinodiscus* spp., *Ceratium fusus*, Dinophyceae cyst, *Noctiluca scintillans*, *Protoperidinium* sp., etc. |
| 25 | Microphytobenthos | Primary production | Pyrrophyta, Bacillariophyta, etc. |
| 26 | Detritus in water column | Energy cycling | Detritus in water |
| 27 | Detritus in sediment | Energy cycling | Detritus in sediment |

calculated using the following formula:

$$P = \sum_{i=1}^{n} \frac{I_{ij}}{n} \quad (2)$$

where $I_{ij}$ represents the pedigree index value for functional group $i$, n represents the total number of functional groups in the ecosystem, and $j$ represents B, P/B, Q/B, Landing, and diet composition.

## The Ecopath with Ecosim model (Ecosim model)

The Ecosim model is a time scale-based dynamic model based on the Ecopath model (Walters et al., 1997; Christensen and Walters, 2004). It drives the time-dynamic model by changing the initial food web model (Ecopath) over time steps

and can simulate changes in the response of the system in a time series. The Ecosim model is used to simulate management behavior or environmental change to "experiment" with ecosystems and subsequently analyze how the ecosystem responds to changes, based on the different scenarios simulated.

The core equations of the Ecosim model are based on a series of differential equations, as follows:

$$\frac{dB_i}{dt} = g_i \sum Q_{ji} - \sum Q_{ij} + I_i - (F_i + Mo_i + e_i) * B_i \quad (3)$$

where the subscripts are as mentioned for equation (2), $dB_i/dt$ is the rate of change in biomass, $g_i$ is the net growth efficiency, $Q_{ji}$ is the consumption of function group $i$ by functional group $j$, $Mo_i$ is the non-predation natural mortality rate, $F_i$ is the fishing mortality rate, $e_i$ is emigration rate, $I_i$ is the immigration rate, and $B_i$ is the biomass of group $i$ (Christensen and Walters, 2004). The flow of biomass between functional groups in the Ecosim model is based on the "foraging arena" concept (Walters et al., 1997). The biomass of each function group was divided into two parts: vulnerable and invulnerable to predation. The vulnerability index is the transfer rate ($v_{ij}$) between the two states, and $Q_{ji}$ is based on the following:

$$Q_{ij} = \frac{a_{ij} v_{ij} B_i B_j}{v_{ij} + v'_{ij} + a_{ij} B_j} \quad (4)$$

Where $a_{ij}$ is the effective search efficiency of predator $j$ for prey organism $i$, $B_i$ is the biomass of prey organism $i$, $B_j$ is the biomass of predator organism $j$, $v_{ij}$ is the transfer rate between "vulnerable" and "invulnerable" components, and conversely ($v'_{ij}$), with the assumption $v_{ij}=v'_{ij}$ (Christensen et al., 2005).

The value of the vulnerability index in Ecosim determines whether the trophic control between predator and prey is a top-down, bottom-up, or intermediate effect. An empirical formula was applied to calculate the vulnerability index for each functional group in the present study following Cheung et al. (2002):

$$v_i = 0.1515 \times TL_i + 0.0485 \quad (5)$$

where $TL_i$ is the trophic level corresponding to functional group $i$. Vulnerability settings ranging from 0 to 1, with 0.0–0.3 representing a bottom-up control, 0.3 representing the mixed control, and 0.3–1.0 describing a top-down impact (Christensen and Walters, 2004). The $v_i$ was then transformed to derive $v_{new}$ for Ecosim input, which ranged from 1 to ∞:

$$\log(v_{new}) = 2.301985 \times v_i + 0.001051 \quad (6)$$

## Enhancement simulations and estimations of ecological carrying capacity

Different levels of stock enhancement were modeled by gradually increasing the individual density (e.g., 2, 3, and 4 inds·m$^{-2}$) in the core area to represent the actual biomass of an increase in each target species, *R. venosa* and *A. japonicus*, because of stock enhancement. During this process, we referred to the reported largest biomasses for *R. venosa* and *A. japonicus* in natural waters as the possible upper limit reference for biomasses of target species in the simulation (Xu et al., 2016; Shalovenkov, 2017) (Table 2). As the Ecosim simulation needs the biomass of target species as input data, the individual density was first multiplied by the mean individual weight (measured *in situ* during the resource surveys) to obtain the biomass of target species in the zone of stock enhancement, and the final biomass ($B_{final}$) (t/km$^2$) for the entire simulation area under different stock scenarios was calculated as follows:

$$B_{final} = (B_{enhancement} \times A_{enhancement}) + (B_{non\text{-}enhancement} \times A_{non\text{-}enhancement}) \quad (7)$$

where $B_{enhancement}$ is the biomass of the target species in the enhancement simulation, $B_{non\text{-}enhancement}$ is the original biomass from the Ecopath model, and $A_{enhancement}$ and $A_{non\text{-}enhancement}$ represent the proportion areas for stock enhancement and non-enhancement, respectively. Stock enhancement was implemented only in the core area (33.3 km$^2$), while the biomass in the non-enhancement area (74.6 km$^2$) during the simulation maintained the original biomass (Table 2).

We applied the criteria of stock collapse to estimate the ecological carrying capacity for two target species; i.e., when the relative biomass of any other functional groups fell below 10% of their original biomasses during the simulation of stepwise-increasing biomass of target species, the resulting biomass at the breakthrough points was identified as the ecological carrying capacity of target species (Kluger et al., 2016). Lastly, we selected four representative enhancement densities as the modeled scenarios of ecological carrying capacity, i.e., slightly increasing, intermediate increasing, approaching ecological carrying capacity, and exceeding ecological carrying capacity (Table 2).

Target species stocking expansion was simulated for a period of 30 years under scenarios of differing final enhancement biomass, which was implemented through a linear increase in stock from 2 to 6 years and then held constant for the remaining 24 years. The time series of changes in relative biomass of a single simulation scenario were extracted when all simulations finished.

## Ecological network analysis indicators

To explore the ecosystem effects under different stocking scenarios for the target species, ecological network analysis indicators were extracted and analyzed through the Ecopath and Ecosim output (network analysis). These indicators were divided into four categories in terms of **Ecosystem Size**—Total

TABLE 2 Simulation scenarios for different enhancement densities of the target species, red snail *Rapana venosa* and sea cucumber *Apostichopus japonicus*, in Laizhou Bay marine ranching using the Ecopath with Ecosim model.

| Target species | Enhancement density (inds·m$^{-2}$) | Enhancement biomass (t·km$^{-2}$) | Proportion of marine ranch for enhancement | Original biomass (t·km$^{-2}$) | Proportion of marine ranch for non-enhancment | Final biomass (t·km$^{-2}$) | Reference biomass (t·km$^{-2}$) |
|---|---|---|---|---|---|---|---|
| *R. venosa* | 10 | 800 | 0.31 | 80 | 0.69 | 302.33 | 6,032.942 (Shalovenkov, 2017) |
| | 20 | 1,600 | | | | 549.35 | |
| | 23 | 1,840 | | | | 623.46 | |
| | 24 | 1,920 | | | | 648.16 | |
| *A. japonicus* | 5 | 200 | | 40 | | 89.41 | 793 (Xu et al., 2016) |
| | 10 | 400 | | | | 151.16 | |
| | 14 | 560 | | | | 200.57 | |
| | 15 | 600 | | | | 212.92 | |

Reference biomass is the greatest biomass density recorded in similar waters from the literature.

system throughput (TST), Total system biomass (B), Primary production (PP), Total system respiration (R), and Total production (P); **Ecosystem Stability and Maturity**—Entropy (H), Average mutual information (AMI), Ascendancy (A), Capacity (C), and Finn's cycling index (FCI); **Ecosystem Efficiency**—Trophic transfer efficiency (TE); and **Ecosystem Biodiversity**—Kempton's Q (Q) (Table 3). The changes in ecological network indicators across the stocking levels were compared with their initial values using radar plots.

# Results

## Evaluating Ecopath model quality

The biomass magnitude span of the taxa in the Ecopath model estimated by the PREBAL diagnostics was 6, and the slope of the biomass (on a logarithmic scale) from the highest to the lowest TL declined by 8.5%, which indicates that the model is providing a realistic representation of the system (Link, 2010; Heymans et al., 2016). Moreover, the P/B and the Q/B magnitude span was in the order of 6 and 4, and the P/B and Q/B ratios showed an increasing trend from high to low trophic levels, indicating that these vital ratios of prey species were generally higher than those of predators (see Supplementary Material Figure S1). The thermodynamic consistency law test revealed that the distribution of R/A among trophic levels exhibited a positive slope (a = 0.074) (see Supplementary Material Figure S2). The gross efficiency test revealed that the model generally conformed to thermodynamic constraints, with the exception of the *O. oratoria* functional group (0.329) and other shrimp and crabs (0.321) with high GE (see Supplementary Material Figure S3). Subsequent to calibrating the Ecopath model, we obtained an ecologically significant mass-balanced model. The Ecopath model Pedigree (P index) was 0.602, indicating that a reasonable amount of the input data were from the local area and have relatively good reliability and credibility. The trophic levels of the functional groups in LZB ranged from 1 to 4.183 (Table 4 and Figure 2). The trophic levels of the target species for enhancement, *R. venosa*, and *A. japonicus*, were 2.62 and 2.27, respectively.

## Ecological carrying capacity estimation

When the simulated stocking density of the red snail *R. venosa* was maintained at 10, 20, and 23 inds·m$^{-2}$, the relative biomass of some functional groups (such as *S. schlegelii*, *L. japonicus*, *S. macrocephalus*, Gobiidae, *C. japonica*, *O. oratoria*, *A. japonicus*, *C. gigas*, other Mollusca, and small zoobenthos) declined by different proportions ranging from 10% for other Mollusca to ~75% for *A. japonicus* for different levels of stocking (Figure 3). The biomasses of some functional groups were predicted to increase greatly by up to three times, e.g., *H. otakii* and Octopodidae (Figure 3). However, no functional group fell below 10% of the original biomass, indicating that level of enhancement scales did not exceed the ecological carrying capacity of *R. venosa*. When the enhancement density was set at the greatest density of 24 *R. venosa*·m$^{-2}$, the relative change in the biomass of other Mollusca functional groups decreased by 93% in the 17th year of the simulation. This was lower than the assessment threshold of the ecological carrying capacity (Figure 3); thus, the estimated ecological carrying capacity of *R. venosa* was 623.46 t·km$^{-2}$, equivalent to a density of 23 inds·m$^{-2}$.

For the stocking scenarios of the sea cucumber *A. japonicus*, when the simulated individual densities were enhanced to 5, 10, and 14 inds·m$^{-2}$, respectively, the biomass of *H. otakii*, Gobiidae, and *R. venosa* declined by only ~10%, while small zoobenthos declined to as low as ~10% to 35% of the original biomass, depending on the enhancement scenario (Figure 4). When the enhancement density increased to 15 A. *japonicus*·m$^{-2}$, the relative change in the biomass of small

TABLE 3 Description of ecological network analysis indicators used in Laizhou Bay marine ranching ecosystem model.

| Indicators | Description |
|---|---|
| ***Ecosystem Size*** | |
| Total system throughput (TST) | The sum of all flows through the ecosystem, measure of system size (Ulanowicz, 1986) |
| Total system biomass (B) | Total biomass of the community excluding detritus (Christensen et al., 2005) |
| Primary production (PP) | The summed primary production from all producers (Christensen et al., 2005) |
| Total system respiration (R) | The part of the consumption that is not used for production or recycled as feces or urine (Christensen et al., 2005) |
| Total production (P) | The difference between total primary production and total respiration (Christensen et al., 2005) |
| ***Ecosystem Stability and Maturity*** | |
| Entropy (H) | The measurement of the number of interactions and evenness of flows in the food web (Baird et al., 2007) |
| Average mutual information (AMI) | The inherent organization and degree of specialization of flows in the ecological network (Ulanowicz, 2004) |
| Ascendancy (A) | The product of TST and AMI of the system, the key indicator of ecosystem development and maturity (Ulanowicz, 1986; Ulanowicz, 2004) |
| Capacity (C) | The product of TST and H represents the upper limit to the ascendency (Heymans et al., 2007) |
| Finn's cycling index (FCI) | The ratio of the recycled flow to ecosystem throughput, is a measure of system maturity (Finn, 1976) |
| ***Ecosystem Efficiency*** | |
| Trophic transfer efficiency (TE) | For a given trophic level (TL), the ratio between the sum of the exports and the flow transferred to the next TL, and the throughput on the TL (Christensen and Walters, 2004); in this study, the mean TE for TL > 2 is used |
| ***Ecosystem Biodiversity*** | |
| Kempton's Q (Q) | The measurement of the biomass of species with trophic levels greater than 3, where an increase in the index indicates an increase in upper-level biomass diversity (Kempton and Taylor, 1976; Shannon et al., 2009) |

zoobenthos functional groups decreased by 90.3% in the 12th year of the simulation, slightly lower than the evaluation threshold of the ecological carrying capacity (Figure 4). Thus, the estimated ecological carrying capacity of *A. japonicus* was 200.57 t·km$^{-2}$, equivalent to an individual density of 14 inds·m$^{-2}$.

## Overall ecosystem effects of enhancement

The ecological network analyses showed that the stock enhancement of two target species under four simulation scenarios caused different responses in the ecosystem size (TST, B, PP, R, and P), ecosystem stability, and maturity (H, AMI, C, A, and FCI), ecosystem efficiency (TE), and ecosystem biodiversity (Q). The maximum positive response was that the total system biomass increased by 102% after the stock enhancement of *R. venosa*, while the maximum negative effect was a 35% reduction in FCI for *R. venosa* enhancement (Figure 5). The variability of ecosystem property indicators to the *R. venosa* enhancement scenarios was more obvious than that for *A. japonicus* enhancement (Figure 5). For example, Kempton's Q, a measure of ecosystem biodiversity, was approximately 30% lower for *R. venosa* stocking than that for *A. japonicus* (Figure 5).

# Discussion

## Effects of simulated stock enhancement on other functional groups

Stocking target species may affect the structure and functioning of the ecosystem through direct and indirect trophic interactions in the food web (Pauly et al., 2000; Eby et al., 2006). Two sedentary benthic species, the red snail *R. venosa* and the sea cucumber *A. japonicus*, from different trophic levels were selected as the target species for stock enhancement in the LZB marine ranching ecosystem. We assessed the ecosystem effects of their stocking by evaluating different stocking densities in Ecopath with Ecosim. The simulations from these models showed that the effects of stocking were greater when releasing the benthic carnivorous *R. venosa* than for the benthic detritivore *A. japonicus*. When the stocking density for *R. venosa* reached 24 inds·m$^{-2}$, other Mollusca functional groups fell below the collapse threshold of 10% of their initial biomass, resulting from the direct feeding of *R. venosa* on bivalves.

The enhancement scenario for *A. japonicus* indicated that the biomass of the small zoobenthic functional group fell just below the threshold for collapse when the *A. japonicus* enhancement density reached 15 inds·m$^{-2}$. The detritivorous *A. japonicus* mainly preyed on microphytobenthos, detritus, and

TABLE 4 Summary of the input and output parameters for functional groups as estimated by the EwE model of Laizhou Bay stocking marine ranching ecosystem.

| No. | Functional group | Biomass ($t \cdot km^{-2}$) | P/B (year) | Q/B (year) | Unassimilation consumption | Detritus import ($t \cdot km^{-2} \cdot year^{-1}$) | EE | Catch ($t \cdot km^{-2} \cdot year^{-1}$) | Trophic level |
|---|---|---|---|---|---|---|---|---|---|
| 1 | *Sebastes schlegelii* | 2.8 | 0.9 | 5.62 | 0.2 | – | **0.540** | 0.6 | **4.183** |
| 2 | *Hexagrammos otakii* | 0.52 | 0.82 | 7.28 | 0.2 | – | **0.985** | – | **3.533** |
| 3 | *Lateolabrax japonicus* | 0.25 | 0.37 | 4.77 | 0.2 | – | **0.649** | 0.06 | **4.156** |
| 4 | *Sparus macrocephalus* | 0.41 | 0.75 | 6.67 | 0.2 | – | **0.195** | 0.06 | **3.804** |
| 5 | Gobiidae | 0.8 | 2.33 | 9.31 | 0.2 | – | **0.964** | – | **3.420** |
| 6 | Other demersal fishes | 0.5 | 0.743 | 6.975 | 0.2 | – | **0.892** | – | **3.761** |
| 7 | Pelagic fishes | 1.01 | 2.851 | 28.51 | 0.2 | – | **0.063** | – | **2.788** |
| 8 | Octopodidae | 0.38 | 3.3 | 11 | 0.2 | – | **0.901** | – | **3.792** |
| 9 | *Charybdis japonica* | 6.57 | 3.2 | 11.3 | 0.2 | – | **0.861** | 2.25 | **3.287** |
| 10 | *Oratosquilla oratoria* | 0.92 | 1.5 | 4.56 | 0.2 | – | **0.719** | 0.05 | **3.217** |
| 11 | *Rapana venosa* | 80 | 1.37 | 5.31 | 0.2 | – | **0.065** | 4.2 | **2.617** |
| 12 | *Apostichopus japonicus* | 40 | 0.6 | 3.37 | 0.2 | – | **0.069** | 1.65 | **2.273** |
| 13 | *Crassostrea gigas* | 268.1 | 4.31 | 16.63 | 0.4 | – | **0.574** | – | **2.333** |
| 14 | *Aurelia aurita* | 4.05 | 5.01 | 25.05 | 0.2 | – | **0.000** | – | **2.050** |
| 15 | Spatangoida | 10.79 | 2.25 | 7.85 | 0.2 | – | **0.000** | – | **2.000** |
| 16 | Other shrimps and crabs | 2.55 | 3 | 9.3551 | 0.2 | – | **0.995** | – | **2.543** |
| 17 | Annelida | 3.26 | 1.6875 | 5.625 | 0.2 | – | **0.696** | – | **2.322** |
| 18 | Other Mollusca | 14.75 | 5 | 20 | 0.2 | – | **0.777** | – | **2.200** |
| 19 | Other macro-zoobenthos | 6.63 | 0.7873 | 9.62 | 0.2 | – | **0.862** | – | **2.050** |
| 20 | Small zoobenthos | 0.97 | 11.18 | 44.7 | 0.35 | – | **0.589** | – | **2.250** |
| 21 | Zooplankton | 20.43 | 38.3041 | 127.6802 | 0.4 | – | **0.803** | – | **2.000** |
| 22 | Bacterioplankton | 3.46 | 174.51 | 580.16 | 0.2 | – | **0.580** | – | **2.000** |
| 23 | Sediment bacteria | 1.78 | 277.22 | 924 | 0.2 | – | **0.117** | – | **2.000** |
| 24 | Phytoplankton | 29.93 | 134.49 | – | – | – | **0.589** | – | **1.000** |
| 25 | Microphytobenthos | 12.38 | 72.43 | – | – | – | **0.562** | – | **1.000** |
| 26 | Detritus in water column | 399 | – | – | – | 320 | **0.873** | – | **1.000** |
| 27 | Detritus in sediment | 2962.96 | – | – | – | – | **0.925** | – | **1.000** |

Values in bold were estimated by Ecopath. "-" represents no data.

bacteria in the sediment (Mao et al., 2009; Wang et al., 2019), competing for food sources with the small zoobenthos functional group, which had a similar diet. The increasing biomass of *A. japonicus* following enhancement resulted in a reduction in their food resources and indirect competition with the small zoobenthos group, leading to a simulated decline in the biomass of small zoobenthos below the threshold.

*R. venosa* and *A. japonicus* are the typical reef-associated commercially important species on the northern coast of China, and the deployment of artificial reefs throughout the region provides an increase in settlement habitat for oysters and mussels (Xu et al., 2019; Xu et al., 2021). These species efficiently filter suspended particulate organic matter (POM) in the water column and provide food for higher trophic levels. Additionally, the feces and pseudo-feces excreted by filter-feeding oysters and mussels are removed by the detritivorous *A. japonicus*, which improves the utilization rate of organic detritus in the ecosystem and increases the energy recycling efficiency in the system (Molly et al., 1998; Kang et al., 2003; Zhou et al., 2006).

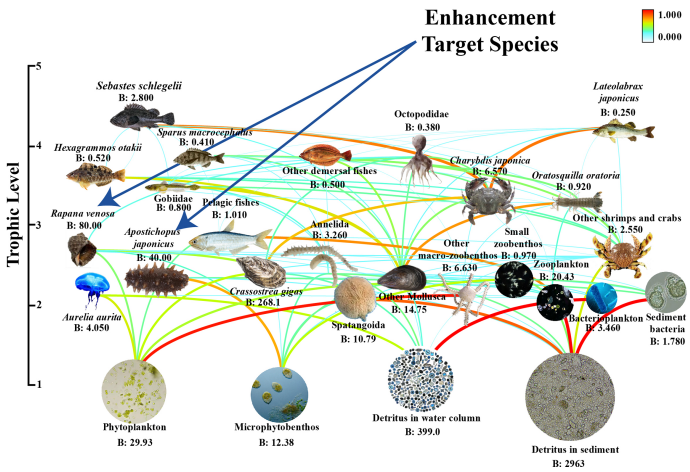


FIGURE 2
Functional groups and their biomass (B) in the food web of the Laizhou Bay stocking marine ranching ecosystem. Curved line shows prey–predator relationships. Blue arrows show target species for stock enhancement.

## Overall ecosystem-level effects

The ecological network analyses showed the ecosystem size increased proportionally in response to increased levels of stocking of the target species. However, the rate of increase was greater for the *R. venosa* scenarios than *A. japonicus*. This is possibly related to the higher biomass of the carnivorous *R. venosa*, more diverse diet, and more complex trophic connections than those for the detritivorous *A. japonicus*.

The values of total system biomass (B) and total system respiration (R) also increased as the level of stock enhancement increased. In fact, given the microbial cycling mechanisms, the actual oxygen consumption of the community may be much higher than the model estimates (Nizzoli et al., 2005). The total

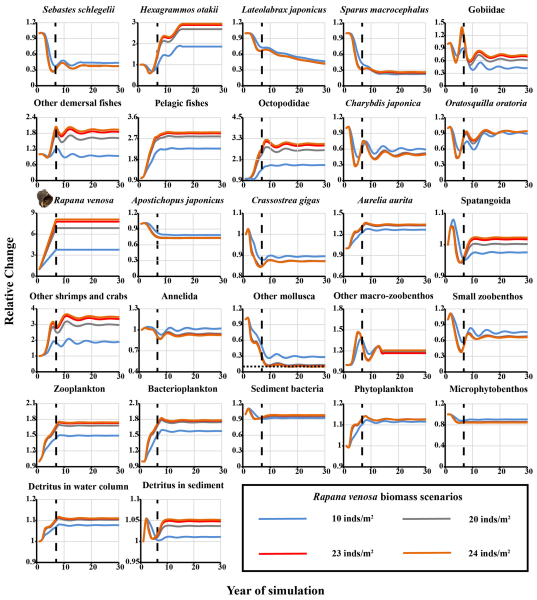


FIGURE 3
Predicted relative changes in biomass of each functional group in the Ecopath Model of Laizhou Bay marine ranching area for the selected four representative scenarios of the red snail *Rapana venosa* stock enhancement. Vertical dashed line, time after which the biomass level of *R. venosa* remained constant; horizontal dashed line, 10% threshold of initial biomass.

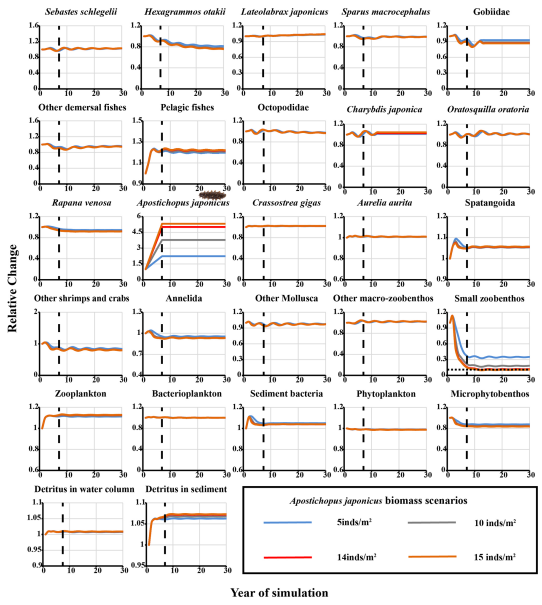


FIGURE 4
Predicted relative changes in biomass of each functional group for the selected four representative scenarios of the sea cucumber *Apostichopus japonicus* stock enhancement in the Ecopath Model of Laizhou Bay marine ranching area. Dashed black line, time after which the biomass level of *A. japonicus* remained constant; horizontal black dotted line, 10% threshold of initial biomass.

system respiration can also be considered as a limiting indicator through long-term monitoring of oxygen concentration in the future. The estimation of ecological carrying capacity presented in this study focused on the trophic interactions; however, other biotic and abiotic limiting factors (e.g., space, disease) for a population to grow might result in a change in the carrying capacity of the system. The TST, representing the sum of all flows through the ecosystem, under the stocking scenarios of *R. venosa* and *A. japonicus* (41,699 and 31,711 t·km$^{-2}$·year$^{-1}$, respectively), were far higher than the base value (25,110 t·km$^{-2}$·year$^{-1}$).

A distinct difference in ecosystem development and maturity indicators between the two target species' stocking was also detected. Expanding the enhancement scale of *R. venosa* facilitated the ecosystem capacity (C) and ascendancy (A), while ecosystem entropy (H) and average mutual information (AMI) gradually decreased. In contrast to *R. venosa*, enhancing *A. japonicus* to different levels resulted in an increase in all ecosystem development and maturity indicators i.e., C, A, H, and AMI, suggesting an increase in the trophic flow interactions among functional groups and a relative mature ecosystem, and a lower degree of unevenness and variability in the flow structure (Odum, 1969; Baird et al., 2007). Ulanowicz et al. (2004) proposed that AMI is more indicative of the developmental status of an ecosystem than H. With the biomass of *A. japonicus* growing through enhancement, the diversity of flows increased in the system. Furthermore, the increased AMI signifies that the system is channeling flows along more specific pathways. As a consequence, using the practices of appropriate stocking

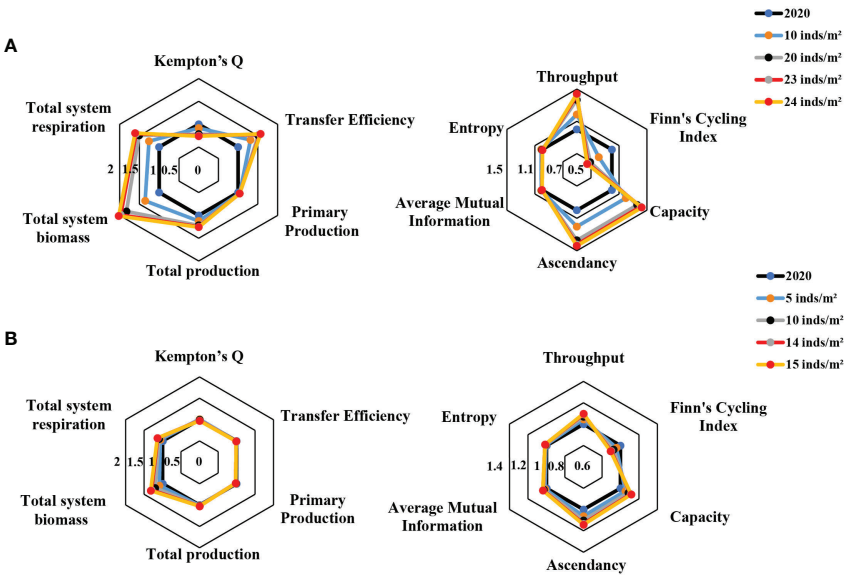


FIGURE 5
Radar plots showing the relative changes in ecological network analysis indicators predicted from the Ecopath model for the Laizhou Bay marine ranching areas under four stock enhancement scenarios for **(A)** the red snail *Rapana venosa* and **(B)** and the sea cucumber *Apostichopus japonicus*. 2020 = pre-enhancement values.

numbers, *A. japonicus* enhancement facilitates the maturity, stability, and resilience of LZB marine ranching.

Finn's cycling index (FCI), which describes the ratio of the recycled throughput to the total throughput, declined by different degrees as the scale of stocking increased but responded differently for *R. venosa* compared with *A. japonicus*. The FCI of *R. venosa* decreased by 35.1%, whereas it decreased by only 10.7% for *A. japonicus*, suggesting that the effects of the enhancement on ecosystems varied between these two species and that stocking *R. venosa* would impair the ecosystem maturity more than stocking *A. japonicus*. The stocked *R. venosa* increased the consumption of oysters and other filter-feeding bivalves greatly, which reduced the energy flow of the ecosystem and limited the production of some potential food sources like feces and pseudo-feces for detritivores such as *A. japonicus* and likely also greatly decreased the system cycling efficiency.

Kempton's Q index(Q), which measures the biomass diversity of species with trophic levels greater than 3 (Kempton and Taylor, 1976; Shannon et al., 2009), decreased significantly as the enhancement density of *R. venosa* increased. This indicates that the introduction of a large numbers of *R. venosa* through stocking reduced the biomass diversity of upper trophic levels in the Laizhou Bay marine ranching area. Kluger et al. (2016) and Gao et al. (2020) reported a similar trend in Q with the increasing culture biomass of the Peruvian bay scallop (*Argopecten purpuratus*) in Sechura Bay, Peru, and the Oyster (*C. gigas*) in Sanggou Bay, China, respectively. Conversely, Q changed by only −2.7% in the *A. japonicus* enhancement scenarios. The increase in single target species is likely to exert increased predation pressure on prey and even lead to the collapse of the prey functional group, decreasing biodiversity and disrupting the ecosystem balance (Beck et al., 2011; Camp et al., 2013). Empirical observations of the red snail have shown that when a large number of *R. venosa* invaded the Black Sea, significant changes in the benthic community were recorded, including a decline in biodiversity in the northern part of the continental shelf of the Black Sea (Janssen et al., 2014; Shalovenkov, 2017; Kasapoglu, 2021).

## Ecological carrying capacity

In the present study, the Ecopath-based method was also employed to estimate the ecological carrying capacity for the same target species (Byron et al., 2011). The resulting estimates for *A. japonicus* and *R. venosa* (148.9 and 90.89 t·km$^{-2}$, respectively) were only 45.3% and 23.9% of the prior Ecosim-based estimates, respectively. The discrepancies in estimates of carrying capacity are attributed to the different approaches in the estimations. The Ecopath method is based on a steady-state model that describes the constant energy flow between functional groups and assumes that the biomass of other functional groups remains unchanged when simulating the biomass increase of the target species (Jiang and Gibbs, 2005; Srithong et al., 2021). In comparison, in the dynamic Ecosim models, the biomasses of all functional groups vary over time, and thus, this approach provides a more realistic representation of the ecosystem changes. It shows the potential impact of increasing levels of stocking on a time scale and describes the responses of biomass and ecological network indicators over time (Kluger et al., 2016; Gao et al., 2020).

Most prior studies have focused on the ecological carrying capacity estimates of suspended particulate-feeding bivalves (Kluger et al., 2016; Gao et al., 2020), and we know of no other studies using Ecopath with Ecosim for evaluating the effects of enhancing target species in a marine ranching ecosystem. The current model framework provides an approach for estimating the ecological carrying capacity of marine ranching ecosystems along the coast of China, where the combination of habitat-based enhancement using artificial reefs, and releasing target species, is practiced on a very large scale. For example, in 2015, 190 marine ranches had been built in China, and an estimated 619.8 km$^2$ of coastal waters was covered with artificial reefs with a volume of 60.94 million m$^3$ along the coast of China (Chen, 2020). Meanwhile, 167 billion cultured juveniles (e.g., sea cucumber *A. japonicus* and abalone *Haliotis discus hannai*) were released by the government and private industry along the Chinese coast over the last two decades (Liu et al., 2022). The results of our study highlight the different ecosystem consequences of stocking two different species at different densities and the importance to managers of taking this information into account when designing their enhancement practices. This knowledge will help determine the optimal target species for enhancement and the densities for enhancement and reduce the possible ecological risks of enhancements. Our findings show that *A. japonicus* is an ideal potential target species for stocking because the simulated ecosystem responses in the Laizhou Bay marine ranching area after stocking were relatively small. When considering the implementation of stocking for commercially important carnivorous species, it is essential to strengthen the evaluation and monitoring of target species and their prey in the stock enhancement. Furthermore, a more realistic estimation of ecological carrying capacity in marine ranching is likely to be obtained if spatial processes are taken into account. This can be done by collecting information on different habitats and the distribution of species within the ranch and developing an Ecospace model to evaluate the ecological carrying capacity. This approach recognizes the spatial heterogeneity within the sea ranching ecosystem in estimating its potential ecological carrying capacity.

## Conclusion

The ecological carrying capacities of red snail *R. venosa* and sea cucumber *A. japonicus*, two sedentary and reef-associated target species with potential for stock enhancement in the marine ranching waters of northern China, were estimated to be 623.46 and 200.57 $t{\cdot}km^{-2}$, respectively. These estimated carrying capacities are 7.8 and 5.0 times higher than the current standing stocks of *R. venosa* and *A. japonicus*. The ecosystem consequences of stocking different species are species-specific and relevant to their trophic position in the food web and differ between the carnivorous gastropod *R. venosa* and the detritivorous *A. japonicus*. The simulated enhancement for *R. venosa* showed a stronger negative impact on most other functional groups and ecosystem properties of marine ranching, such as system maturity and stability and biodiversity, than that for *A. japonicus*, which had relatively benign impacts. The current dynamic model framework provides an alternative means of estimating the ecological carrying capacity for stock enhancement practices in the development of marine ranching in northern China.

## Data availability statement

The original contributions presented in the study are included in the article/Supplementary Material. Further inquiries can be directed to the corresponding authors.

## Author contributions

ZWu and ZWa conceptualized this paper. JF, ZWa, and ZWu organized the database and constructed the model. ZWa and ZWu wrote the first draft of the manuscript. All authors contributed to the manuscript revision and approved the submitted version. ZWa and JF share the first authorship of this manuscript

## Funding

This work was funded by the National Key Research and Development Program of China (Grant Number: 2019YFD0901304), the National Natural Science Foundation of China (Grant Number: 41906125), Dalian innovation and entrepreneurship project for high-level talents (Grant Number: 2020RQ112), and Dalian Science and Technology Innovation Fund (Grant Number: 2021JJ11CG001).

## Conflict of interest

The authors declare that the research was conducted in the absence of any commercial or financial relationships that could be construed as a potential conflict of interest.

The reviewer TW declared a shared affiliation with the author ZX to the handling editor at the time of review.

## Publisher's note



## Supplementary material

The Supplementary Material for this article can be found online at: https://www.frontiersin.org/articles/10.3389/fmars.2022.936028/full#supplementary-material

## References

Baird, D., Asmus, H., and Asmus, R. (2007). Trophic dynamics of eight intertidal communities of the sylt-rømø bight ecosystem, northern wadden Sea. *Mar. Ecol.: Prog. Ser.* 351, 25–41. doi: 10.3354/meps07137

Beck, M. W., Brumbaugh, R. D., Airoldi, L., Carranza, A., Coen, L. D., Crawford, C., et al. (2011). Oyster reefs at risk and recommendations for conservation, restoration, and management. *BioScience* 61, 107–116. doi: 10.1525/bio.2011.61.2.5

Blankenship, H. L., and Leber, K. M. (1995). A responsible approach to marine stock enhancement. *Am. Fish. Soc Symp.* 15, 67–175.

Byron, C., Link, J., Costa-Pierce, B., and Bengtson, D. (2011). Calculating ecological carrying capacity of shellfish aquaculture using mass-balance modeling: Narragansett bay, Rhode island. *Ecol. Modell.* 222, 1743–1755. doi: 10.1016/j.ecolmodel.2011.03.010

Camp, E. V., Lorenzen, K., Ahrens, R. N. M., Barbieri, L., and Leber, K. M. (2013). Potentials and limitations of stock enhancement in marine recreational fisheries systems: An integrative review of florida's red drum enhancement. *Rev. Fish. Sci.* 21, 388–402. doi: 10.1080/10641262.2013.83807

Chen, Y. (2020). Research and construction of modern marine ranching in China: A review. *J. Dalian Ocean Univ.* 35, 147–154. doi: 10.16535/j.cnki.dlhyxb.2019–260

Cheung, W. L., Watson, R., and Pitcher, T. J. (2002). Policy simulation of fisheries in the Hong Kong marine ecosystem. *N. Z. J. Mar. Freshw. Res.* 10, 46–54. doi: 10.1080/00288330.2014.901232

Christensen, V., and Walters, C. J. (2004). Ecopath with ecosim: Methods, capabilities and limitations. *Ecol. Modell.* 172, 109–139. doi: 10.1016/j.ecolmodel.2003.09.003

Christensen, V., Walters, C. J., and Pauly, D. (2005). *Ecopath with ecosim: a user's guide* Vol. 154 (Vancouver, British Columbia: University of British Columbia, Fisheries Centre, Canada and ICLARM, Penang, Malaysia), 31.

Cooney, R. T., and Brodeur, R. D. (1998). Carrying capacity and north pacific salmon production: Stock-enhancement implications. *Bull. Mar. Sci.* 62, 443–464. doi: 10.1029/98JC00121

Cudmore-Vokey, B., and Crossman, E. J. (2000). Checklists of the fish fauna of the laurentian great lakes and their connecting channels. *Victoria: MS. Rpt. Fish. Aquat. Sci* 2250:v+39p.

Darwall, W., Allison, E. H., Turner, G. F., and Irvine, K. (2010). Lake of flies, or lake of fish? A trophic model of lake Malawi. *Ecol. Model.* 221, 713–727. doi: 10.1016/j.ecolmodel.2009.11.001

Eby, L. A., Roach, W. J., Crowder, L. B., and Stanford, J. A. (2006). Effects of stocking-up freshwater food webs. *Trends Ecol. Evol.* 21, 576–584. doi: 10.1016/j.tree.2006.06.016

FAO (2005). *A review of stock enhancement practices in the inland water fisheries of Asia* (Bangkok: Asia Pacific Fishery Commission), 93.

Filgueira, R., Guyondet, T., Thupaki, P., Sakamaki, T., and Grant, J. (2021). The effect of embayment complexity on ecological carrying capacity estimations in bivalve aquaculture sites. *J. Cleaner Prod.* 288, 125739. doi: 10.1016/j.jclepro.2020.125739

Finn, J. T. (1976). Measures of ecosystem structure and function derived from analysis of flows. *J. Theor. Biol.* 56, 363–380. doi: 10.1016/S0022-5193(76)80080-X

Gao, Y. P., Fang, J. G., Lin, F., Li, F. X., Li, W. H., and Wang, X. Q. (2020). Simulation of oyster ecological carrying capacity in sanggou bay in the ecosystem context. *Aquacult. Int.* 28, 2059–2079. doi: 10.1007/s10499-020-00576-3

Heymans, J. J., Coll, M., Link, J. S., Link, J. S., Mackinson, S., Steenbeek, J., et al. (2016). Best practice in ecopath with ecosim food-web models for ecosystem-based management. *Ecol. Modell.* 331, 173–184. doi: 10.1016/j.ecolmodel.2015.12.007

Heymans, J. J., Guenette, S., and Christensen, V. (2007). Evaluating network analysis indicators of ecosystem status in the gulf of Alaska. *Ecosystems* 10, 488–502. doi: 10.1007/s10021-007-9034-y

Inglis, G. J., Hayden, B. J., and Ross, A. H. (2000). *An overview of factors affecting the carrying capacity of coastal embayments for mussel culture* Vol. 69 (Christchurch: National Institute of Water & Atmospheric Research), vi + 31p.

Janssen, R., Knudsen, S., Todorova, V., and Hosgor, A. G. (2014). Managing *Rapana* in the black Sea: Stakeholder workshops on both sides. *Ocean Coast. Manage.* 87, 75–87. doi: 10.1016/j.ocecoaman.2013.10.015

Jiang, W., and Gibbs, M. T. (2005). Predicting the carrying capacity of bivalve shellfish culture using a steady, linear food web model. *Aquaculture* 244, 171–185. doi: 10.1016/j.aquaculture.2004.11.050

Jiang, Y. Z., Lin, N., Yang, L. L., and Cheng, J. Y. (2014). The ecological risk of stock enhancement and the measures for prevention and control. *J. Fish. Sci. China* 21, 413–422. doi: 10.3724/SP.J.1118.2014.00413

Jin, X. S., and Deng, J. Y. (2000). Variations in community structure of fishery resources and biodiversity in the laizhou bay, Shandong. *Chin. Biodiversity* 8, 65–72. doi: 10.17520/biods.2000009

Jin, X. S., Shan, X. J., Xiansen, L. I., Wang, J., Cui, Y., and Zuo, T. (2013). Long-term changes in the fishery ecosystem structure of laizhou bay, China. *Sci. China: Earth Sci.* 56, 366–374. doi: 10.1007/s11430-012-4528-7

Kang, K. H., Kwon, J. Y., and Kim, Y. M. (2003). A beneficial coculture: Charm abalone *Haliotis discus hannai* and sea cucumber. *Stichopus japonicus*. *Aquaculture* 216, 87–93. doi: 10.1016/S0044-8486(02)00203-X

Kasapoglu, N. (2021). Population structure and shell dimension of the invasive veined whelk (*Rapana venosa*). *J. Fish.* 9, 91205–91205. doi: 10.17017/j.fish.256

Kempton, R. A., and Taylor, L. R. (1976). Models and statistics for species diversity. *Nature* 262, 818–820. doi: 10.1038/262818a0

Khan, M. F., Preetha, P., and Sharma, A. P. (2015). Modelling the food web for assessment of the impact of stock supplementation in a reservoir ecosystem in India. *Fish. Manage. Ecol.* 22, 359–370. doi: 10.1111/fme.12134

Kitada, S. (2020). Lessons from Japan marine stock enhancement and sea ranching programmes over 100 years. *Rev. Aquacul.* 12, 1944–1969. doi: 10.1111/raq.12418

Kluger, L. C., Taylor, M. H., Mendo, J., Tam, J., and Wolff, M. (2016). Carrying capacity simulations as a tool for ecosystem-based management of a scallop aquaculture system. *Ecol. Modell.* 331, 44–55. doi: 10.1016/j.ecolmodel.2015.09.002

Lin, Q., Jin, X. S., Zhang, B., and Gu, X. W. (2009). Comparative study on the changes of the bohai Sea ecosystem structure based on ecopath model between ten years. *Acta Ecol. Sin.* 29, 3613–3620. doi: 10.3321/j.issn:1000-0933.2009.07.020

Link, J. S. (2010). Adding rigor to ecological network models by evaluating a set of pre-balance diagnostics: A plea for PREBAL. *Ecol. Modell.* 221, 1580–1591. doi: 10.1016/j.ecolmodel.2010.03.012

Lin, Q., Li, X. S., Li, Z. Y., and Jin, X. S. (2013). Ecological carrying capacity of Chinese shrimp stock enhancement in laizhou bay of East China based on ecopath model. *Chin. J. Appl. Ecol.* 24, 1131–1140. doi: 10.13287/j.1001-9332.2013.0269

Liu, S. R., Zhou, X. J., Zeng, C., Frankstone, T., and Cao, L. (2022). Characterizing the development of Sea ranching in China. *Rev. Fish. Biol. Fisheries.* 32, 1–21. doi: 10.1007/s11160-022-09709-8

Lorenzen, K., Leber, K. M., and Blankenship, H. L. (2010). Responsible approach to marine stock enhancement: an update. *Rev. Fish. Sci.* 18, 189–210. doi: 10.1080/10641262.2010.491564

Lorenzen, K., Leber, K. M., Loneragan, N. R., Schloesser, R. W., and Taylor, M. D. (2021). Developing and integrating enhancement strategies to improve and restore fisheries. *Bull. Mar. Sci.* 97, 475–487. doi: 10.5343/bms.2021.0036

Mao, Y., Yang, H., Zhou, Y., Ye, N., and Fang, J. (2009). Potential of the seaweed *Gracilaria lemaneiformis* for integrated multi-trophic aquaculture with scallop *Chlamys farreri* in north China. *J. Appl. Phycol.* 21, 649–656. doi: 10.1007/s10811-008-9398-1

McKindsey, C. W., Thetmeyer, H., Landry, T., and Silvert, W. (2006). Review of recent carrying capacity models for bivalve culture and recommendations for research and management. *Aquaculture* 261, 451–462. doi: 10.1016/j.aquaculture.2006.06.044

Ministry of Agriculture and Rural Affairs of the People's Republic of China (2022). Notice of ministry of agriculture and rural affairs of the people's republic of China, (No. 115, 2321, 2476). http://www.moa.gov.cn/gk/tzgg_1/gg/ (Accessed by Apr 20, 2022)

Molly, O. A. (1998). Consumption and assimilation of salmon net pen fouling debris by the red Sea cucumber *Parastichopus californicus*: Implications for polyculture. *J. World Aquacult. Soc* 29, 133–139. doi: 10.1111/j.1749-7345.1998.tb00972.x

Munro, J. L., and Bell, J. D. (1997). Enhancement of marine fisheries resources. *Rev. Fish. Sci.* 5, 185–222. doi: 10.1080/10641269709388597

Ning, X. R., Liu, Z. L., and Shi, J. X. (1995). Assessment of potential fishery production and primary productivity in pohai, huanghai and dongha. *Acta Oceanol. Sin.* 17, 72–84. doi: 10.1088/0256-307X/12/7/010

Nizzoli, D., Welsh, D. T., Bartoli, M., and Viaroli, P. (2005). Impacts of mussel (*Mytilus galloprovincialis*) farming on oxygen consumption and nutrient recycling in a eutrophic coastal lagoon. *Hydrobiologia* 550, 183–198. doi: 10.1007/s10750-005-4378-9

Odum, E. P. (1969). The strategy of ecosystem development. *Science* 164, 262–270. doi: 10.5822/978-1-61091-491-8-20

Palomares, M. L., and Pauly, D. (1989). A multiple regression model for prediction the food consumption of marine fish populations. *Mar. Freshw. Res.* 40, 259–273. doi: 10.1071/MF9890259

Parsons, T. R., Maita, Y., and Lalli, C. M. (1984). *A manual of chemical and biological methods for seawater analysis* (Oxford: Pergamon Press).

Pauly, D., and Bartz, M. L. S. (1993). "Improved construction, parametrization and interpretation of steady-state ecosystem models," in *Trophic models of aquatic ecosystems*. Eds. V. Christensen and D. Pauly (Manila: ICLARM Conference Proceedings), 1–13.

Pauly, D., Christensen, V., and Walters, C. J. (2000). Ecopath, ecosim, and ecospace as tools for evaluating ecosystem impact of fisheries. *ICES J. Mar.* 57, 697–706. doi: 10.1006/jmsc.2000.0726

Shalovenkov, N. N. (2017). Non-native zoobenthic species at the Crimean black Sea coast. *Med. Mar. Sci.* 18, 260–270. doi: 10.12681/mms.1925

Shannon, L. J., Coll, M., and Neira, S. (2009). Exploring the dynamics of ecological indicators using food web models fitted to time series of abundance and catch data. *Ecol. Indic.* 9, 1078–1095. doi: 10.1016/j.ecolind.2008.12.007

Shen, G. M., and Heino, M. (2014). An overview of marine fisheries management in China. *Mar. Policy.* 44, 265–272. doi: 10.1016/j.marpol.2013.09.012

Solan, M., Cardinale, B. J., Downing, A. L., Engelhardt, K. A. M., Ruesink, J. L., and Srivastava, D. S. (2004). Extinction and ecosystem function in the marine benthos. *Science* 306, 1177–1180. doi: 10.1126/science.1103960

Srithong, N., Jensen, K. R., and Jarernpornnipat, A. (2021). Application of the ecopath model for evaluation of ecological structure and function for fisheries management: A case study from fisheries in coastal Andaman Sea, Thailand. *Reg. Stud. Mar. Sci.* 47, 101972. doi: 10.1016/j.rsma.2021.101972

Stier, A. C., Samhouri, J. F., Novak, M., Marshall, K. N., Ward, E. J., Holt, R. D., et al. (2016). Ecosystem context and historical contingency in apex predator recoveries. *Sci. Adv.* 2, e1501769. doi: 10.1126/sciadv.1501769

Su, J. L., and Tang, Q. S. (2002). *Study on ecosystem dynamics in costal ocean II processes of the bohai Sea ecosystem dynamics* (Beijing: Science Press).

Taylor, M. D., Brennan, N. P., Lorenzen, K., and Leber, K. M. (2013). Generalized predatory impact model: A numerical approach for assessing trophic limits to hatchery releases and controlling related ecological risks. *Rev. Fish. Sci.* 21, 341–353. doi: 10.1080/10641262.2013.796815

Taylor, M. D., Chick, R. C., Lorenzen, K., Agnalt, A. L., Leber, K. M., Blankenship, H. L., et al. (2017). Fisheries enhancement and restoration in a changing world. *Fish. Res.* 186, 407–412. doi: 10.1016/j.fishres.2016.10.004

Taylor, M. D., Palmer, P. J., Fielder, D. S., and Suthers, I. M. (2005). Responsible estuarine finfish stock enhancement: an Australian perspective. *J. Fish. Biol.* 67, 299–331. doi: 10.1111/j.0022-1112.2005.00809.x

Townsend, C. R. (2010). Individual, population, community, and ecosystem consequences of a fish invader in new Zealand streams. *Conserv. Biol.* 17, 38–47. doi: 10.1046/j.1523-1739.2003.02017.x

Ulanowicz, R. E. (1986). Growth and development: Ecosystems phenomenology. *Estuaries* 11, 73–74. doi: 10.2307/1351721

Ulanowicz, R. E. (2004). Quantitative methods for ecological network analysis. *Comput. Biol. Chem.* 28, 321–339. doi: 10.1016/j.compbiolchem.2004.09.001

Walters, C., Christensen, V., and Pauly, D. (1997). Structuring dynamic models of exploited ecosystems from trophic mass-balance assessments. *Rev. Fish. Biol. Fish.* 7, 139–172. doi: 10.1023/A:1018479526149

Wang, R., Chaolun, L. I., Wang, K. E., and Zhang, W. (1998). Feeding activities of zooplankton in the bohai Sea. *Fish. Ocean.* 7, 265–271. doi: 10.1046/j.1365-2419.1998.00067.x

Wang, B., Tian, J. S., Dong, Y., Chen, Z., Zhou, Z. C., Song, G., et al. (2019). Using carbon and nitrogen stable isotopes to evaluate feeding habits of Sea cucumber *Apostichopus japonicus* in aquaculture ponds in liaodong bay. *Fish. Sci.* 38, 236–240. doi: 10.16378/j.cnki.1003-1111.2019.02.014

Wei, Y. Q., Cui, H. W., Hu, Q. J., Bai, Y., Qu, K. M., Sun, J., et al. (2022). Eutrophication status assessment in the laizhou bay, bohai Sea: Further evidence for the ecosystem degradation. *Mar. pollut. Bull.* 181, 113867. doi: 10.1016/j.marpolbul.2022.113867

Worm, B., Barbier, E. B., Beaumont, N., Duffy, E., Folke, C., Halpern, B. S., et al. (2006). Impacts of biodiversity loss on ocean ecosystem services. *Science* 314, 787–790. doi: 10.1126/science.1132294

Worm, B., Hilborn, R., Baum, J. K., Branch, T. A., Collie, J. S., Costello, C., et al. (2009). Rebuilding global fisheries. *Science* 325, 578–585. doi: 10.1126/science.1173146

Wu, Z. X., Zhang, X. M., Zhang, L., Tong, F., and Liu, H. J. (2013). Predicting the ecological carrying capacity of lidao artificial reef zone of Shandong province for the sea cucumber, *Apostichopus japonicus*, (Selenck) and the abalone, *Haliotis discus hannai*, using a linear food web model. *J. Fish. Sci. China* 20, 327–337. doi: 10.3724/SP.J.1118.2013.00327

Xu, M., Qi, L., Zhang, L. B., Zhang, T., Yang, H. S., and Zhang, Y. L. (2019). Ecosystem attributes of trophic models before and after construction of artificial oyster reefs using ecopath. *Aquacult. Env. Interac.* 11, 111–127. doi: 10.3354/aei00284

Xu, M., Yang, X. Y., Song, X. J., Xu, K. D., and Yang, L. L. (2021). Seasonal analysis of artificial oyster reef ecosystems: implications for sustainable fisheries management. *Aquacult. Int.* 29, 167–192. doi: 10.1007/s10499-020-00617-x

Yang, C. J., Wu, Z. X., Liu, H. Y., Zhang, P. D., Li, W. T., Zeng, X. Q., et al. (2016). The fishing strategy of charybdis japonica and *Rapana venosa* and the carrying capacity of *Apostichopus japonucus* in zhuwang, laizhou artificial reef ecosystem based on ecopath model. *Period. Ocean Univ. China* 46, 168–177. doi: 10.16441/j.cnki.hdxb.20160112

Zhang, X. M., Wang, X. J., Tu, Z., Zhang, P. D., Wang, Y. Z., Gao, T. X., et al. (2009). Current status and prospect of fisheries resource enhancement in Shandong province. *Chin. Fish. Eco.* 27, 51–58. doi: 10.3969/j.issn.1009-590X.2009.02.008

Zhou, Y., Yang, H., Liu, S., Yuan, X., Mao, Y., Liu, Y., et al. (2006). Feeding and growth on bivalve biodeposits by the deposit feeder *Stichopus japonicus selenka* (Echinodermata: Holothuroidea) co-cultured in lantern nets. *Aquaculture* 256, 510–520. doi: 10.1016/j.aquaculture.2006.02.005

frontiers | Frontiers in Marine Science

TYPE Original Research
PUBLISHED 23 September 2022
DOI 10.3389/fmars.2022.970218



OPEN ACCESS

EDITED BY
Angel Borja,
Technology Center Expert in Marine and Food Innovation (AZTI), Spain

REVIEWED BY
Guanqiong Ye,
Zhejiang University,China
Cui Liang,
Institute of Oceanology (CAS), China

*CORRESPONDENCE
Min Zhang
zhm7875@mail.hzau.edu.cn
Peiyu Zhang
zhangpeiyu@ihb.ac.cn

SPECIALTY SECTION
This article was submitted to Marine Ecosystem Ecology, a section of the journal Frontiers in Marine Science

RECEIVED 15 June 2022
ACCEPTED 09 September 2022
PUBLISHED 23 September 2022

CITATION
Zhao K, He Y, Su G, Xu C, Xu X, Zhang M and Zhang P (2022) Implications for functional diversity conservation of China's marine fisheries.
*Front. Mar. Sci.* 9:970218.
doi: 10.3389/fmars.2022.970218



# Implications for functional diversity conservation of China's marine fisheries

Kangshun Zhao[1,2,3,4], Yuhan He[5], Guohuan Su[6,7], Congjun Xu[1,2,3], Xiaoqi Xu[1,2,3], Min Zhang[8]* and Peiyu Zhang[1,2]*

[1]Donghu Experimental Station of Lake Ecosystems, State Key Laboratory of Freshwater Ecology and Biotechnology of China, Institute of Hydrobiology, Chinese Academy of Sciences, Wuhan, China, [2]Laboratory for Marine Fisheries Science and Food Production Processes, Qingdao National Laboratory for Marine Science and Technology, Qingdao, China, [3]College of Advanced Agricultural Sciences, University of Chinese Academy of Sciences, Beijing, China, [4]Bren School of Environmental Science & Management, University of California, Santa Barbara, Santa Barbara, CA, United States, [5]Organismal and Evolutionary Biology, University of Helsinki, Helsinki, Finland, [6]Center for Advanced Systems Understanding (CASUS), Görlitz, Germany, [7]Helmholtz-Zentrum Dresden-Rossendorf (HZDR), Dresden, Germany, [8]College of Fisheries, Huazhong Agricultural University, Hubei Provincial Engineering Laboratory for Pond Aquaculture, Freshwater Aquaculture Collaborative Innovation Center of Hubei Province, Wuhan, China

Functional diversity is critical to ecosystem stability and resilience to disturbances as it supports the delivery of ecosystem services on which human societies rely. However, changes in functional diversity over space and time, as well as the importance of particular marine fish species to functional space are less known. Here, we reported a temporal change in the functional diversity of marine capture fisheries from all coastal provinces in China from 1989 to 2018. We suggested that both functional evenness (FEve) and functional divergence (FDiv) changed substantially over time, especially with considerable geographic variation in FEve in the detected patterns. Even within the same sea, the relative contributions of fishes with various water column positions and trophic levels in different waters have different patterns. Together these results underline the need of implementing specific climate-adaptive functional diversity conservation measures and sustainable fisheries management in different waters.

KEYWORDS

**functional diversity, biodiversity conservation, fisheries management, marine ecosystem, sustainable development**

## 1 Introduction

Marine fisheries and ecosystems are threatened by climate change and human activities worldwide, rising issues such as habitat degradation or resource overexploitation (Brierley and Kingsford, 2009; Halpern et al., 2015; Hilborn, 2016; Hughes et al., 2017). Despite conservation efforts to restore habitat and resources,

biodiversity loss continues at regional and global scales in diverse ecosystems (Vitousek et al., 1997; Cardinale et al., 2006; Maclean and Wilson, 2011; Worm and Tittensor, 2011; Mouillot et al., 2013). As a critical part of biodiversity, functional diversity indices have been increasingly applied to fish communities to explore the connection between biodiversity and ecosystem function, indicate the community structure changes, and assess the effect of multiple pressures (Villéger et al., 2010; Mouillot et al., 2013; Stuart-Smith et al., 2013; Belley and Snelgrove, 2016; Villéger et al., 2017; Rolim et al., 2022; Zhao et al., 2022). However, only a few studies so far report the functional diversity of marine fish communities.

China is the world's largest producer of capture fisheries, accounting for approximately 15% of total global captures in 2018 (FAO, 2020). Thus, China's sustainable marine capture fishery industry is critical to the global seafood supply, food security, and seafood trade (Smith et al., 2010; Blomeyer et al., 2012; Su et al., 2020). Zhao et al. (2022) recently used China's reported marine catch data and a comprehensive set of functional traits to explore how the functional diversity of commercial fish communities responds to climate change and changes in fishing pressure. They showed that climate warming and fishing significantly and oppositely affect the functional diversity (i.e.,FEve and FDiv), partly causing functional diversity fluctuations in China's seas. FEve describes the regularity of species abundance distribution in the functional space and reflects the overall utilization of resources by species. FDiv measures how species abundances diverge from the center of the functional space and reflects the competitive pressures among species in communities (Mason et al., 2005; Villéger et al., 2008). Functional diversity is a crucial facet of biodiversity, but how it changes over space and time is less known than taxonomic diversity (Trindade-Santos et al., 2020).

In recent years, Chinese government has invested extensive efforts into curbing overfishing and developing sustainable fisheries, and prioritized fishery resource conservation in marine fishery management (Han et al., 2018; Su et al., 2020; Zhao et al., 2021). Zhao et al., 2021 indicated that China's aquaculture is transforming into a sustainable development pattern with low input and high output, reducing its dependence on marine wild fishery resources. Along with the development of Chinese sustainable capture fisheries and increasing climate change in recent decades, an enhanced understanding of how biodiversity changes in space and time could improve decision-making about establishing protected areas, sustainable fishery management, etc. Here, China's marine catch data and functional traits reported by Zhao et al. (2022) were used to explore the temporal characteristics of functional diversity changes in fish communities caught by each province and the patterns of species' contributions to the functional space. This study could help guide targeted biodiversity conservation policies and marine fishery management under multiple pressures across various provinces and seas.

# 2 Materials and methods

## 2.1 Data set

### 2.1.1 Catch data

Marine catch data of 11 coastal province administrative regions (Tianjin, Hebei, Liaoning, Shanghai, Jiangsu, Zhejiang, Fujian, Shandong, Guangdong, Guangxi, and Hainan) from 1989 to 2018 were collated from the National Fishery Statistics Yearbook (Ministry of Agriculture and Rural Affairs of the People's Republic of China, 1990-2019). From 1989, 16 species or species groups (four individual species and 12 species groups) have been reported continuously and account for more than 84% of the total reported fish catch (Supplementary Table S1). In the present study, all catches in coastal regions were from the Bohai Sea, Yellow Sea, East China Sea, and South China Sea. Catch data for all seas were obtained by combining provincial catches based on their main fishing waters (Supplementary Table S2). Although the catch data for Chinese fisheries have been a subject of scrutiny for many years, the main concern is that China may over-report its catch (Watson and Pauly, 2001; Pauly et al., 2014; Pauly and Zeller, 2016). However, scaling up or down the reported catch should not introduce bias into FEve and FDiv estimation (Zhao et al., 2022), and we used relative catch data to calculate them.

Starting from the time records began in 2003, the proportions of power between different fishing methods remain relatively stable with no drastic overall changes in all provinces (Supplementary Figure S1). Over the past three decades, trawls, gillnets, and stow nets represent the three major fishing gears, accounting for approximately 81% of the total catch in China. Despite some variations in power proportions of trawling and gillnet vessels in Tianjin, Hebei, Jiangsu, and Shanghai, the poor selectivity of trawls and gillnet characterizes Chinese fishing activities indicates that the catch comprises many species and a large yield of bycatch without specific bias towards any species. In general, China's marine fishing practices have been exhaustive and largely nonselective, with minimal discard over the past decades (Costello et al., 2016; Costello, 2017; Szuwalski et al., 2017; Zhang et al., 2020; Zhao et al., 2021). Moreover, the proportions of China's annual catch from different fishing methods remained relatively stable from 1989 to 2018, suggesting that no single fishing method changed disproportionately in catch over the past three decades (Zhao et al., 2022). Thus, relative catch could represent a good proxy for the compositional community changes occurring in the ocean.

### 2.1.2 Functional traits

The selection of traits to be incorporated into functional analyses depends on the research question. This study focused on the functional diversity characteristics of commercial marine fish communities in all coastal provinces under multiple environmental pressures. Thus, the functional trait database, which encompasses seven traits (water column position, mouth position, diet, mean preferred temperature, trophic level, maximum body length, and body shape) was obtained from Zhao et al. (2022) for four individual species and 12 species groups (species–group mean quantitative traits were used), including food acquisition, locomotion, ecological adaptation, and population dynamics (Supplementary Tables S2, S3). China's fisheries record lumps a group of species with similar characteristics into one category. Many fish species occupy a large range, lacking differentiation between the communities according to the sea boundaries. In general, selected species that are similar in the ecological niche for each species group (Zhao et al., 2022). Thus, it is still appropriate to calculate functional diversity indices with the species–group mean quantitative traits. An underlying assumption of using a single estimate for each trait for a species or species group is that trait values are fixed and do not change for a particular species in time, space, or as individuals grow.

Subsequently, we followed the procedure described by Laliberté and Legendre (2010). First, a trait matrix for the complete set of species and species groups was constructed and then converted into a Gower dissimilarity matrix, which is a non-Euclidean measure appropriate for datasets comprising a combination of categorical and continuous traits with missing values. Then, principal coordinate analysis (PCoA) was performed on the dissimilarity matrix, and the first four axes of PCoA were selected as the new traits in accordance with Zhao et al. (2022).

## 2.2 Functional diversity indices

Different functional metrics provide distinct and often complementary perspectives on functional diversity (Villéger et al., 2008; Mouillot et al., 2013). Here, two complementary indices (FEve and FDiv) were calculated to assess the functional diversity of commercial marine fish communities for each province. The ecological effects of a species were well-documented to be generally proportional to its abundance or biomass (Grime, 1998). Compared to diversity metrics based on a simple count or inventory of species present within a broader geographic region, abundance-weighted functional diversity more accurately reflects community functional structure (Stuart-Smith et al., 2013). In the present study, the functional diversity indices were calculated based on the new traits (i.e., four axes of PCoA on Gower dissimilarity matrix) and the relative catch of species or species groups (Zhao et al., 2022). All functional diversity metrics were computed using the "FD" package in R.

## 2.3 Statistical analysis

First, locally estimated scatterplot smoothing regression was used to assess each province's temporal nonlinearity in functional diversity indices. Then, relative contribution of each species or species group was calculated by sequentially removing species or species groups from the dataset and then recalculating the functional diversity indices and computing the percent change in diversity value before and after species disappear (Pool et al., 2014). Here, the fishing water of each province's fishing fleets was assumed to have not changed over the past three decades. All commercial species or species groups have been reported in the Bohai and Yellow Seas, the East China Sea and the South China Sea. Thus, several species or species groups were unreported in some years, which should be too little in catches. Relative catches for unreported species or species groups were counted as 0. As the four axes of PCoA was used to construct the trait space, unreported species or species groups could still affect the relative positions of all species or species groups in the functional space when removed. Here, the relative contributions of species or species groups with catch count of 0 were generally small but still retained. Besides, FEve and FDiv were related to changes in species abundance rather than richness. Counting the catch of unreported species or species groups as 0 would cause little bias, and we didn't consider them here. Interquartile range method was used to detect outliers in the resulting relative contribution dataset (Rousseeuw and Hubert, 2011; Vinutha et al., 2018). The "wilcox.test" function from the "stats" package (R Development Core Team, 2020) was used to conduct Wilcoxon rank-sum tests and compare the relative contributions of fish species or species groups with different water column positions (demersal and pelagic) and trophic levels (with 3.5 as the threshold) to FD. All statistical analyses were performed using R version 4.1.1 for Windows (R Development Core Team, 2020).

# 3 Results

## 3.1 Dynamics of functional diversity across all provinces

Across all provinces, FEve fluctuated stronger than FDiv over the past three decades, except for the Guangdong (Figure 1).

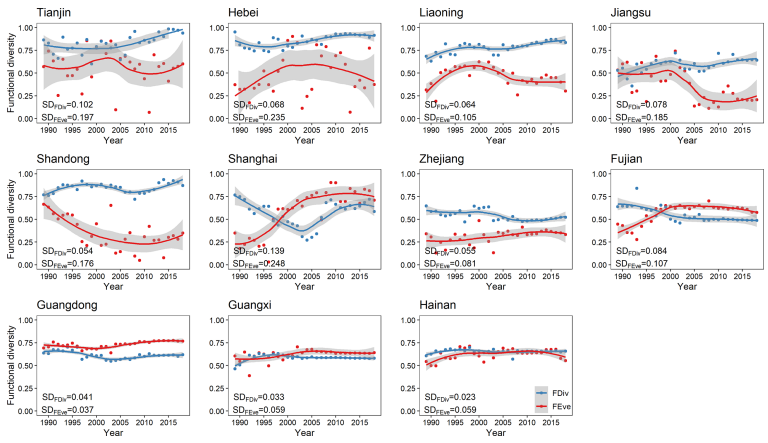


FIGURE 1
Locally estimated scatterplot smoothing regression curves of functional diversity for each coastal province from 1989 to 2018. The shaded gray column indicates 95% confidence interval. $SD_{FEve}$, standard deviation of functional evenness; $SD_{FDiv}$, standard deviation of functional divergence. (FEve, functional evenness; FDiv, functional divergence).

The functional diversity indices of five provinces (Tianjin, Hebei, Liaoning, Jiangsu, and Shandong) that mainly fished in the Bohai and Yellow Seas were the most unstable, followed by three provinces (Shanghai, Zhejiang, and Fujian) that mainly fished in the East China Sea. Three provinces (Guangdong, Guangxi, and Hainan) that mainly fished in the South China Sea exhibited a considerably stable functional diversity over time for both functional diversity indices.

## 3.2 Relative contribution of fishes to functional space

The relative contributions of fishes in the Bohai and Yellow Seas and the South China Sea were more concentrated than that in the East China Sea (Figure 2). The relative contributions of fishes in the South China Sea to both functional diversity indices were lower than that in the Bohai and Yellow Seas and East China Sea, except for FDiv in the Bohai and Yellow Seas (Figure 2). In most provinces, the relative contributions of fishes with different trophic levels to both functional diversity indices varied greatly. Only few provinces had significant differences in the relative contributions of fishes with different water column positions (Figures 3, 4). In all provinces, the contribution of low-trophic-level fish to functional diversity was higher than that of high-trophic-level fish, except for Shanghai and Guangxi (Figure 3). In Liaoning, Shandong, Fujian, and Hainan, demersal fish contributed more to FEve, while pelagic fish contributed more to FDiv in Guangdong, Guangxi, and Hainan (Figure 4).

# 4 Discussion

Functional diversity is a key facet of biodiversity that accounts for the diversity of biological and ecological features

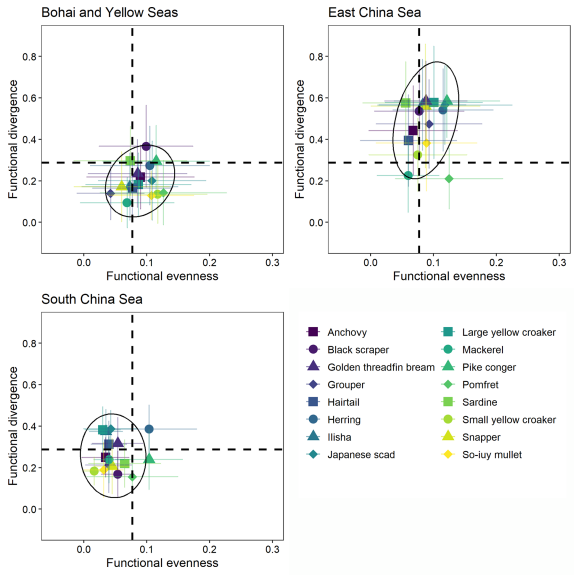


FIGURE 2
Contribution of 16 species or species groups to functional diversity in different seas. The dashed line indicates the average contribution of all species across three seas. The black circle is 95% confidence level ellipse for a multivariate t-distribution.

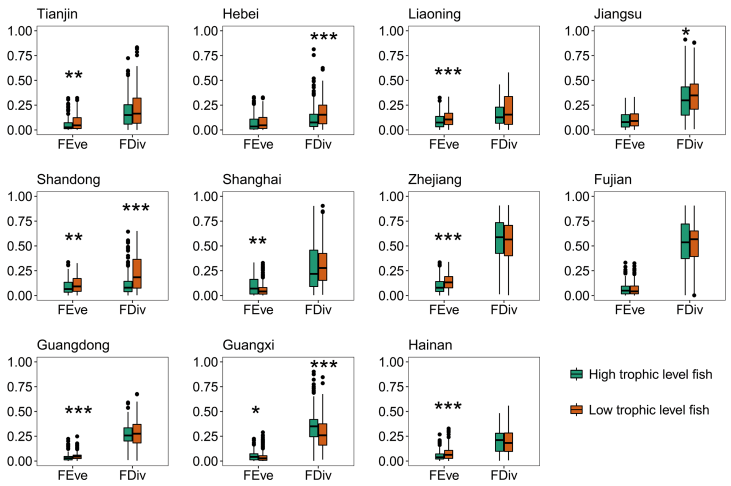


FIGURE 3
Comparison of relative contributions of fishes with different trophic levels to functional diversity for 11 provinces. The results of Wilcoxon rank-sum tests are shown upon each plotted item (*$p$ < 0.05; **$p$ < 0.01; ***$p$ < 0.001; Supporting Information Table S5 shows the complete Wilcoxon rank-sum tests. FEve, functional evenness; FDiv, functional divergence).

of organisms related to their responses to the environment and their effects on ecosystem processes (Su et al., 2022). The functional diversity of marine fish communities is facing pressure from habitat degradation, human activities, climate change, and overfishing (Villéger et al., 2010; D'Agata et al., 2014; Brandl et al., 2016; Zhao et al., 2022). In China, marine fishery resources and functional diversity have been affected by various factors, such as overfishing and climate change (Blasiak et al., 2017; Costello, 2017; Zhao et al., 2022). However, evaluating the functional diversity of marine fish communities and the influencing factors is insufficient. The results of the present study showed that the functional diversity of different provinces had different performance characteristics under multiple disturbances, and the most considerable temporal

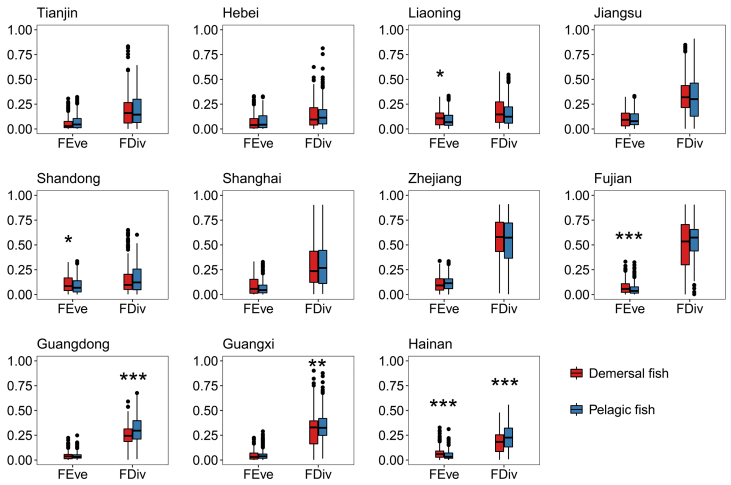


FIGURE 4
Comparison of relative contributions of fishes with different water column positions to functional diversity for 11 provinces. The results of Wilcoxon rank-sum tests are shown upon each plotted item (*$p$ < 0.05; **$p$ < 0.01; ***$p$ < 0.001; Supporting Information Table S5 shows the complete Wilcoxon rank-sum tests. FEve, functional evenness; FDiv, functional divergence).

fluctuations were found in provinces that fished in the Bohai and Yellow Seas and East China Sea (Figure 1). This finding indicated that the structure of the fish communities fished by Tianjin, Hebei, Liaoning, Jiangsu, and Shanghai fluctuated wildly, and these communities were probably more vulnerable in terms of resistance to external multiple pressures than those fished by Guangdong, Guangxi, and Hainan.

Our results showed that the relative contributions of fish species in the Bohai and Yellow Seas and the East China Sea were generally higher than that in the South China Sea (Figure 2 and Supplementary Figure S2). Moreover, in the past three decades, the functional diversity of provinces that fished in the Bohai and Yellow Seas and the East China Sea fluctuated greatly (Figure 1). If a particular species disappears [e.g., redistribution following the gradients of habitat suitability by their temperature preferences and limits or even local disappearance as temperature limits are exceeded (Cheung et al., 2010; Jones and Cheung, 2015; Cheung et al., 2016)] in the Bohai and Yellow Seas and the East China Sea, it would lead to more remarkable changes in the functional space and increased vulnerability to external environmental disturbance. Moreover, fish and other animals have already moved poleward and such movements are expected to continue or accelerate (Poloczanska et al., 2013; Cheung et al., 2016; Pinsky et al., 2020; Melbourne-Thomas et al., 2021). Thus, even in the South China Sea, where functional diversity is more stable, fish communities structure may change greatly in the future.

Meanwhile, low-trophic-level fish generally showed greater relative contributions to functional diversity (Figures 3, 4). This finding could be supported laterally by the substantial changes in the domestic marine catch composition, from the predominance of a few medium to relatively large-sized, high-valued, high-trophic-level demersal species to multiple small, low-valued, short-lived, low-trophic-level ones over the past six decades (Liu and De Mitcheson, 2008; Shen and Heino, 2014; Cao et al., 2017; Zhang et al., 2020). This phenomenon also happens worldwide, fishing down the marine food webs (Pauly et al., 1998). The extensive reduction in low-trophic-level forage fish (e.g., anchovy, sardine, and herring) generate concerns that commercial forage fish resources have not been merely overharvested but caused severe effects on the diversity of marine fish communities (Zhang et al., 2020; Zhao et al., 2022; Zhao et al., 2021; Zheng et al., 2014). Moreover, even within the same sea, no fixed pattern of the relative contributions of fishes existed with different water column positions and trophic levels in different waters (Figures 3, 4). Thus, designating climate-adaptive conservation schemes in accordance with different fish community features are necessary to improve functional diversity conservation.

At present, the Chinese government is vigorous in controlling marine overfishing (Han et al., 2018; Su et al., 2020; Zhao et al., 2021), but climate change could be difficult to control in the short term. Meanwhile, controlling overfishing alone will not conserve functional diversity of commercial marine fish communities under climate change (Zhao et al., 2022). Along with the increasing climate warming, the productivity of fish stocks is predicted to decrease in tropical and temperate regions and increase towards the poles (Lotze et al., 2019). A shifting fish stock exacerbates existing fisheries and sustainable management challenges need to be more concerned, and all coastal provinces should strengthen cooperation. Cooperation should extend beyond data sharing to inform genuinely collaborative management, which demands an emphasis on periodically acquiring reliable assessment of species shifts and changes in community structures. Finally, China should develop specific climate-adaptive sustainable fishery management in different waters, which is necessary to consider functional diversity.

## Data availability statement

The original contributions presented in the study are included in the article/Supplementary Material, further inquiries can be directed to the corresponding author/s.

## Author contributions

PZ and KZ conceived the study. PZ, MZ, and KZ collected and analyzed the data. KZ and MZ drafted the manuscript. All authors checked and edited the final manuscript. All authors contributed to the article and approved the submitted version.

## Funding

This research was also supported by the International Cooperation Project of the Chinese Academy of Sciences (Grant No. 152342KYSB20190025) and the National Natural Science Foundations of China (Grant No. 31872687).

## Acknowledgments

A special thanks to Professor Jun Xu, Jorge García Molinos and Steven D. Gaines for the suggestions to some earlier data processing.

## Conflict of interest

The authors declare that the research was conducted in the absence of any commercial or financial relationships that could be construed as a potential conflict of interest.

## Publisher's note

All claims expressed in this article are solely those of the authors and do not necessarily represent those of their affiliated organizations, or those of the publisher, the editors and the reviewers. Any product that may be evaluated in this article, or claim that may be made by its manufacturer, is not guaranteed or endorsed by the publisher.

## Supplementary material

The Supplementary Material for this article can be found online at: https://www.frontiersin.org/articles/10.3389/fmars.2022.970218/full#supplementary-material

## References


Belley, R., and Snelgrove, P. V. (2016). Relative contributions of biodiversity and environment to benthic ecosystem functioning. *Front. Mar. Sci.* 3, 242. doi: 10.3389/fmars.2016.00242

Blasiak, R., Spijkers, J., Tokunaga, K., Pittman, J., Yagi, N., and Österblom, H. (2017). Climate change and marine fisheries: Least developed countries top global index of vulnerability. *PLoS One* 12, e0179632. doi: 10.1371/journal.pone.0179632

Blomeyer, R., Goulding, I., Pauly, D., Sanz, A., and Stobberup, K. (2012). "The role of China in world fisheries," in *Directorate general for internal policies. policy department b* (European Union: Structural and Cohesion Policies. European Parliament).

Brandl, S. J., Emslie, M. J., Ceccarelli, D. M., and Z.T., R. (2016). Habitat degradation increases functional originality in highly diverse coral reef fish assemblages. *Ecosphere* 7, e01557. doi: 10.1002/ecs2.1557

Brierley, A. S., and Kingsford, M. J. (2009). Impacts of climate change on marine organisms and ecosystems. *Curr. Biol.* 19, R602–R614. doi: 10.1016/j.cub.2009.05.046

Cao, L., Chen, Y., Dong, S., Hanson, A., Huang, B., Leadbitter, D., et al. (2017). Opportunity for marine fisheries reform in China. *Proc. Natl. Acad. Sci.* 114, 435–442. doi: 10.1073/pnas.1616583114

Cardinale, B. J., Srivastava, D. S., Duffy, J. E., Wright, J. P., Downing, A. L., Sankaran, M., et al. (2006). Effects of biodiversity on the functioning of trophic groups and ecosystems. *Nature* 443, 989–992. doi: 10.1038/nature05202

Cheung, W. W., Lam, V. W., Sarmiento, J. L., Kearney, K., Watson, R., Zeller, D., et al. (2010). Large-Scale redistribution of maximum fisheries catch potential in the global ocean under climate change. *Global Change Biol.* 16, 24–35. doi: 10.1111/j.1365-2486.2009.01995.x

Cheung, W. W., Reygondeau, G., and Frölicher, T. L. (2016). Large Benefits to marine fisheries of meeting the 1.5 c global warming target. *Science* 354, 1591–1594. doi: 10.1126/science.aag2331

Costello, C. (2017). Fish harder; catch more? *Proc. Natl. Acad. Sci.* 114, 1442–1444. doi: 10.1073/pnas.1620731114

Costello, C., Ovando, D., Clavelle, T., Strauss, C. K., Hilborn, R., Melnychuk, M. C., et al. (2016). Global fishery prospects under contrasting management regimes. *Proc. Natl. Acad. Sci.* 113, 5125–5129. doi: 10.1073/pnas.1520420113

D'Agata, S., Mouillot, D., Kulbicki, M., Andrefouet, S., Bellwood, D. R., Cinner, J. E., et al. (2014). Human-mediated loss of phylogenetic and functional diversity in coral reef fishes. *Curr. Biol.* 24, 555–560. doi: 10.1016/j.cub.2014.01.049

FAO (2020). *The state of world fisheries and aquaculture* (Rome Italy: Food and Agriculture Organization of the United Nations), 40–41.

Grime, J. (1998). Benefits of plant diversity to ecosystems: immediate, filter and founder effects. *J. Ecol.* 86, 902–910. doi: 10.1046/j.1365-2745.1998.00306.x

Halpern, B. S., Frazier, M., Potapenko, J., Casey, K. S., Koenig, K., Longo, C., et al. (2015). Spatial and temporal changes in cumulative human impacts on the world's ocean. *Nat. Commun.* 6, 1–7. doi: 10.1038/ncomms8615

Han, D., Shan, X. J., Zhang, W. B., Chen, Y. S., Wang, Q. Y., Li, Z. J., et al. (2018). A revisit to fishmeal usage and associated consequences in Chinese aquaculture. *Rev. Aquaculture.* 10, 493–507. doi: 10.1111/raq.12183

Hilborn, R. (2016). Policy: Marine biodiversity needs more than protection. *Nature* 535, 224–226. doi: 10.1038/535224a

Hughes, T. P., Barnes, M. L., Bellwood, D. R., Cinner, J. E., Cumming, G. S., Jackson, J. B. C., et al. (2017). Coral reefs in the anthropocene. *Nature* 546, 82–90. doi: 10.1038/nature22901

Jones, M. C., and Cheung, W. W. (2015). Multi-model ensemble projections of climate change effects on global marine biodiversity. *ICES. J. Mar. Sci.* 72, 741–752. doi: 10.1093/icesjms/fsu172

Laliberté, E., and Legendre, P. (2010). A distance-based framework for measuring functional diversity from multiple traits. *Ecology* 91, 299–305. doi: 10.1890/08-2244.1

Liu, M., and De Mitcheson, Y. S. (2008). Profile of a fishery collapse: why mariculture failed to save the large yellow croaker. *Fish. Fisheries.* 9, 219–242. doi: 10.1111/j.1467-2979.2008.00278.x

Lotze, H. K., Tittensor, D. P., Bryndum-Buchholz, A., Eddy, T. D., Cheung, W. W., Galbraith, E. D., et al. (2019). Global ensemble projections reveal trophic amplification of ocean biomass declines with climate change. *Proc. Natl. Acad. Sci.* 116, 12907–12912. doi: 10.1073/pnas.1900194116

Maclean, I. M., and Wilson, R. J. (2011). Recent ecological responses to climate change support predictions of high extinction risk. *Proc. Natl. Acad. Sci.* 108, 12337–12342. doi: 10.1073/pnas.1017352108

Mason, N. W. H., Mouillot, D., Lee, W. G., and Wilson, J. B. (2005). Functional richness, functional evenness and functional divergence: the primary components of functional diversity. *Oikos* 111, 112–118. doi: 10.1111/j.0030-1299.2005.13886.x

Melbourne-Thomas, J., Audzijonyte, A., Brasier, M.J., et al. Poleward bound: adapting to climate-driven species redistribution. *Rev Fish Biol Fisheries* 32, 231–251 (2022). doi: 10.1007/s11160-021-09641-3

Ministry of Agriculture and Rural Affairs of the People's Republic of China (1990-2019). *Chinese National fishery statistics yearbook* (China Agriculture Press).

Mouillot, D., Graham, N. A. J., Villéger, S., Mason, N. W. H., and Bellwood, D. R. (2013). A functional approach reveals community responses to disturbances. *Trends Ecol. Evol.* 28, 167–177. doi: 10.1016/j.tree.2012.10.004

Pauly, D., Belhabib, D., Blomeyer, R., Cheung, W., Cisneros-Montemayor, A. M., Copeland, D., et al. (2014). China's distant-water fisheries in the 21st century. *Fish. Fisheries.* 15, 474–488. doi: 10.1111/faf.12032

Pauly, D., Christensen, V., Dalsgaard, J., Froese, R., and Torres, F. (1998). Fishing down marine food webs. *Science* 279, 860. doi: 10.1126/science.279.5352.860

Pauly, D., and Zeller, D. (2016). Catch reconstructions reveal that global marine fisheries catches are higher than reported and declining. *Nat. Commun.* 7, 10244. doi: 10.1038/ncomms10244

Pinsky, M. L., Selden, R. L., and Kitchel, Z. J. (2020). Climate-driven shifts in marine species ranges: Scaling from organisms to communities. *Annu. Rev. Mar. Sci.* 12, 153–179. doi: 10.1146/annurev-marine-010419-010916

Poloczanska, E. S., Brown, C. J., Sydeman, W. J., Kiessling, W., Schoeman, D. S., Moore, P. J., et al. (2013). Global imprint of climate change on marine life. *Nat. Climate Change* 3, 919–925. doi: 10.1038/nclimate1958

Pool, T. K., Grenouillet, G., Villéger, S., and Ricciardi, A. (2014). Species contribute differently to the taxonomic, functional, and phylogenetic alpha and beta diversity of freshwater fish communities. *Diversity Distributions.* 20, 1235–1244. doi: 10.1111/ddi.12231

R Development Core Team (2020). *R: A language and environment for statistical computing, 3.6.3* (Vienna, Austria: R Foundation for Statistical Computing).

Rolim, F. A., Langlois, T., Motta, F., Castro, G., Abieri, M. L., Gadig, O. B. F., et al. (2022). Habitat and marine reserve status drive reef fish biomass and functional diversity in the largest south Atlantic coral reef system (Abrolhos, Brazil). *Front. Mar. Sci.* 9, 678. doi: 10.3389/fmars.2022.701244

Rousseeuw, P. J., and Hubert, M. (2011). Robust statistics for outlier detection. Wiley interdisciplinary reviews. *Data Min. Knowledge. Discovery* 1, 73–79. doi: 10.1002/widm.2

Shen, G., and Heino, M. (2014). An overview of marine fisheries management in China. *Mar. Policy* 44, 265–272. doi: 10.1016/j.marpol.2013.09.012

Smith, M. D., Roheim, C. A., Crowder, L. B., Halpern, B. S., Turnipseed, M., Anderson, J. L., et al. (2010). Sustainability and global seafood. *Science* 327, 784–786. doi: 10.1126/science.1185345

Stuart-Smith, R. D., Bates, A. E., Lefcheck, J. S., Duffy, J. E., Baker, S. C., Thomson, R. J., et al. (2013). Integrating abundance and functional traits reveals new global hotspots of fish diversity. *Nature* 501, 539–542. doi: 10.1038/nature12529

Su, S., Tang, Y., Chang, B., Zhu, W., and Chen, Y. (2020). Evolution of marine fisheries management in China from 1949 to 2019: How did China get here and where does China go next? *Fish. Fisheries.* 21, 435–452. doi: 10.1111/faf.12439

Su, G., Tedesco, P. A., Toussaint, A., Villéger, S., and Brosse, S. (2022). Contemporary environment and historical legacy explain functional diversity of freshwater fishes in the world rivers. *Global Ecol. Biogeography.* 31, 700–713. doi: 10.1111/geb.13455

Szuwalski, C. S., Burgess, M. G., Costello, C., and Gaines, S. D. (2017). High fishery catches through trophic cascades in China. *Proc. Natl. Acad. Sci. United. States America* 114, 717–721. doi: 10.1073/pnas.1612722114

Trindade-Santos, I., Moyes, F., and Magurran, A. E. (2020). Global change in the functional diversity of marine fisheries exploitation over the past 65 years. *Proc. R. Soc. B.* 287, 20200889. doi: 10.1098/rspb.2020.0889

Villéger, S., Brosse, S., Mouchet, M., Mouillot, D., and Vanni, M. J. (2017). Functional ecology of fish: current approaches and future challenges. *Aquat. Sci.* 79, 783–801. doi: 10.1007/s00027-017-0546-z

Villéger, S., Mason, N. W., and Mouillot, D. (2008). New multidimensional functional diversity indices for a multifaceted framework in functional ecology. *Ecology* 89, 2290–2301. doi: 10.1890/07-1206.1

Villéger, S., Miranda, J. R., Hernández, D. F., and Mouillot, D. (2010). Contrasting changes in taxonomic vs. functional diversity of tropical fish communities after habitat degradation. *Ecol. Appl.* 20, 1512–1522. doi: 10.1890/09-1310.1

Vinutha, H., Poornima, B., and Sagar, B. (2018). Detection of outliers using interquartile range technique from intrusion dataset, information and decision sciences. *Springer* pp, 511–518. doi: 10.1007/978-981-10-7563-6_53

Vitousek, P. M., Mooney, H. A., Lubchenco, J., and Melillo, J. M. (1997). Human domination of earth's ecosystems. *Science* 277, 494–499. doi: 10.1126/science.277.5325.494

Watson, R., and Pauly, D. (2001). Systematic distortions in world fisheries catch trends. *Nature* 414, 534–536. doi: 10.1038/35107050

Worm, B., and Tittensor, D. P. (2011). Range contraction in large pelagic predators. *Proc. Natl. Acad. Sci.* 108, 11942–11947. doi: 10.1073/pnas.1102353108

Zhang, W. B., Liu, M., de Mitcheson, Y. S., Cao, L., Leadbitter, D., Newton, R., et al. (2020). Fishing for feed in China: Facts, impacts and implications. *Fish. Fisheries.* 21, 47–62. doi: 10.1111/faf.12414

Zhao, K., Gaines, S. D., García Molinos, J., Zhang, M., and Xu, J. (2022). Climate change and fishing are pulling the functional diversity of the world's largest marine fisheries to opposite extremes. *Global Ecol. Biogeography.*doi: 10.1111/geb.13534

Zhao, K., Zhang, M., Wang, K., Zhu, K., Xu, C., Xie, J., et al. (2021). Aquaculture impacts on china's marine wild fisheries over the past 30 years. *Front. Mar. Sci.* 31 (8):1616–1629. 10.3389/fmars.2021.710124

Zheng, Y., Li, J., Zhang, Q., and Hong, W. (2014). Research progresses of resource biology of important marine pelagic food fishes in China. *J. Fisheries. China* 38, 149–160. doi: 10.3724/SP.J.1231.2014.48799

# Frontiers in Marine Science

**Explores ocean-based solutions for emerging global challenges**

The third most-cited marine and freshwater biology journal, advancing our understanding of marine systems and addressing global challenges including overfishing, pollution, and climate change.

---

## Discover the latest Research Topics

See more →

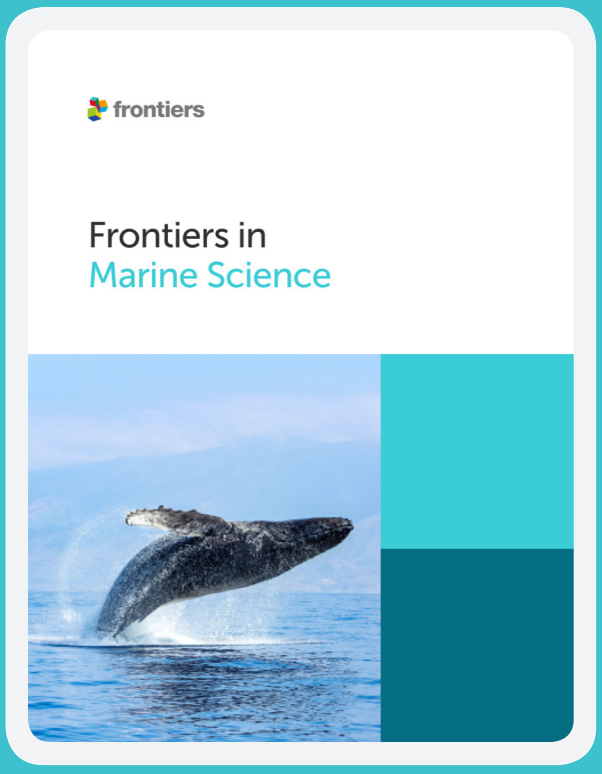


**Frontiers**

Avenue du Tribunal-Fédéral 34
1005 Lausanne, Switzerland
frontiersin.org

**Contact us**

+41 (0)21 510 17 00
frontiersin.org/about/contact